

**SYSTEMS ANALYSES OF ADVANCED BRAYTON CYCLES  
FOR  
HIGH EFFICIENCY ZERO EMISSION PLANTS**

**FINAL REPORT**

**PRINCIPAL AUTHORS**

**Dr. A. D. Rao  
D. J. Francuz  
J. D. Maclay  
Dr. J. Brouwer  
A. Verma  
M. Li  
Dr. G. S. Samuelsen**

**December 24, 2008**

**Award No. DE-FC26-05NT42652**

**PREPARED BY**

**Advanced Power and Energy Program  
University of California  
Irvine, California 92697-3550**

## **ACKNOWLEDGMENT**

This material is based upon work supported by the Department of Energy under Award Number DE-FC26-05NT42652.

## **DISCLAIMER**

This report was prepared as an account of work sponsored by an agency of the United States Government. Neither the United States Government nor any agency thereof, nor any of their employees, makes any warranty, express or implied, or assumes any legal liability or responsibility for the accuracy, completeness, or usefulness of any information, apparatus, product, or process disclosed, or represents that its use would not infringe privately owned rights. Reference herein to any specific commercial product, process, or service by trade name, trademark, manufacturer, or otherwise does not necessarily constitute or imply its endorsement, recommendation, or favoring by the United States Government or any agency thereof. The views and opinions of authors expressed herein do not necessarily state or reflect those of the United States Government or any agency thereof.

## TABLE OF CONTENTS

<b>LIST OF TABLES .....</b>	<b>10</b>
<b>LIST OF ILLUSTRATIONS.....</b>	<b>13</b>
<b>LIST OF ACRONYMS AND ABBREVIATIONS .....</b>	<b>27</b>
<b>EXECUTIVE SUMMARY .....</b>	<b>29</b>
OBJECTIVES .....	29
SCOPE OF PROJECT .....	29
SUMMARY OF RESULTS .....	30
Task 1.1 Milestone.....	30
Task 1.2 Milestone.....	30
Task 1.3 Milestone.....	31
Task 1.4.1 Milestone.....	31
Task 1.4.2 Milestone.....	32
Task 2.1 Milestone.....	33
Task 2.2.1 Milestone.....	34
Task 2.2.2 Milestone.....	34
Task 2.2.3 Milestone.....	35
Task 2.2.4 Milestone.....	36
Task 2.3 Milestone.....	36
<b>APPROACH.....</b>	<b>37</b>
TASK 1.1 – SET SYSTEM STUDY METHODOLOGIES.....	37
TASK 1.2 – IDENTIFY BASELINE CYCLE CONFIGURATION .....	37
TASK 1.3 - FIRST DETAILED SYSTEMS STUDY ANALYSIS .....	37
TASK 1.4 - SUBSEQUENT DETAILED SYSTEMS STUDY ANALYSES.....	38
TASK 2 - ADDITIONAL SYSTEMS STUDIES .....	39
<b>RESULTS AND DISCUSSION .....</b>	<b>40</b>
TASK 1.1 – SET SYSTEM STUDY METHODOLOGIES.....	40
TASK 1.2 – IDENTIFY BASELINE CYCLE CONFIGURATION .....	40
TASK 1.3 - FIRST DETAILED SYSTEMS STUDY ANALYSIS – BASELINE CASE .....	40
Low NOx Sensitivity Case .....	42
TASK 1.4.1: SCREENING ANALYSIS OF ADVANCED BRAYTON CYCLES .....	42
TASK 1.4.2: DETAILED ANALYSIS OF ADVANCED BRAYTON CYCLES .....	43
Simple Cycle Gas Turbine based IGCC with Increased Firing Temperature.....	43
Intercooled Gas Turbine based IGCC with Increased Firing Temperature .....	45
Intercooled-Reheat Gas Turbine based IGCC with Increased Firing Temperature.....	47
Intercooled Closed Circuit Air Cooled Gas Turbine based IGCC with Increased Firing Temperature .....	48
Air Partial Oxidation Topping Cycle.....	50
Selection of Advanced Brayton Cycle.....	51
Sensitivity Analysis of Selected Advanced Brayton Cycle .....	52
Gas Turbine Compressor Efficiency.....	52
Gas Turbine Expander Efficiency.....	53
High Efficiency Exhaust Diffuser.....	53
Application of Superconductivity Technology.....	54
Low NOx Strategies.....	54
Increased Diluent Nitrogen Addition.....	54
Reduced Firing Temperature .....	55

Air (Film) Cooled 1 <sup>st</sup> Stage Turbine .....	55
Economic Analysis .....	55
Development Needs .....	56
Combustor Needs .....	57
Compressor Needs .....	59
Turbine Needs .....	60
Development Costs and Time .....	61
TASK 2.1 - EVALUATION OF IMPACT OF RAMGEN COMPRESSION TECHNOLOGY ON IGCC PLANT PERFORMANCE .....	61
TASK 2.2 - DYNAMIC SIMULATION OF FUEL CELL / GAS TURBINE SYSTEM .....	62
Steady State Modeling .....	62
Dynamic Modeling .....	63
TASK 2.3: PERFORMANCE COMPARISON OF OXY-COMBUSTION AND IGCC PLANTS .....	66
<b>CONCLUSIONS .....</b>	<b>75</b>
TASK 1.2 – IDENTIFY BASELINE CYCLE CONFIGURATION .....	75
TASK 1.3 - FIRST DETAILED SYSTEMS STUDY ANALYSIS – BASELINE CASE .....	75
TASK 1.4.1 – SCREENING ANALYSIS OF ADVANCED BRAYTON CYCLES .....	75
Promising Cycles .....	76
TASK 1.4.2: DETAILED ANALYSIS OF ADVANCED BRAYTON CYCLES .....	76
Simple Cycle Gas Turbine based IGCC with Increased Firing Temperature .....	76
Intercooled Gas Turbine based IGCC with Increased Firing Temperature .....	77
Intercooled-Reheat Gas Turbine based IGCC with Increased Firing Temperature .....	78
Intercooled Closed Circuit Air Cooled Gas Turbine based IGCC with Increased Firing Temperature .....	78
Air Partial Oxidation Topping Cycle .....	79
Selection of Advanced Brayton Cycle .....	79
Sensitivity Analysis of Selected Advanced Brayton Cycle .....	80
Gas Turbine Compressor Efficiency .....	80
Gas Turbine Expander Efficiency .....	81
High Efficiency Exhaust Diffuser .....	81
Application of Superconductivity Technology .....	81
Low NOx Strategies .....	81
Air (Film) Cooled 1 <sup>st</sup> Stage Turbine .....	82
Economic Analysis .....	82
Development Needs .....	82
TASK 2.1 - EVALUATION OF IMPACT OF RAMGEN COMPRESSION TECHNOLOGY ON IGCC PLANT PERFORMANCE .....	85
TASK 2.2 - DYNAMIC SIMULATION OF FUEL CELL / GAS TURBINE SYSTEM .....	85
TASK 2.3: PERFORMANCE COMPARISON OF OXY-COMBUSTION AND IGCC PLANTS .....	87
<b>COST AND SCHEDULE STATUS .....</b>	<b>88</b>
<b>APPENDIX – COMPREHENSIVE SUMMARY OF WORK SINCE PROJECT INCEPTION .....</b>	<b>92</b>
<b>TASK 1.1: SET SYSTEMS STUDY METHODOLOGY .....</b>	<b>93</b>
INTRODUCTION .....	93
PROCESS DESIGN PROCEDURE .....	93
Site Conditions and Feedstock Characteristics .....	93
Coal .....	94

Natural Gas .....	94
Limestone.....	94
ADVANCED BRAYTON CYCLE TECHNOLOGY PROJECTIONS .....	97
SOFC / GT DESIGN GUIDELINES.....	98
OVERALL PLANT DESIGN CRITERIA.....	99
MATERIAL AND ENERGY BALANCES.....	100
Advanced Power Systems Analysis Tool (APSAT).....	101
Gas Turbine.....	102
Humidifier Model .....	103
Compressor and Steam Turbine Models.....	103
SPECIFICATIONS FOR UNIQUE EQUIPMENT AND PLANT UNITS .....	108
THIRD PARTY VALIDATION .....	108
REFERENCES .....	108
<b>TASK 1.2: IDENTIFY OVERALL BASELINE CYCLE CONFIGURATION.....</b>	<b>109</b>
SUMMARY .....	109
Gasifier Technology.....	109
Advanced Transport Reactor .....	109
GE Gasifier .....	110
Shell Gasifier .....	111
E-Gas Gasifier.....	111
Air Separation Technology.....	112
High Temperature Membrane Technology.....	112
Cryogenic Technology.....	113
Acid Gas Removal Technology.....	114
Warm Gas Cleanup.....	114
Cold Gas Cleanup.....	115
Power Generation Technology .....	117
Fuel Cell Hybrids.....	117
Gas Turbine based Cycles.....	118
Conclusions - Technology Selection – Baseline Case.....	125
REFERENCES .....	125
<b>TASK 1.3: FIRST DETAILED SYSTEMS STUDY ANALYSIS - BASELINE CASE....</b>	<b>135</b>
SUMMARY .....	135
PROCESS DESCRIPTIONS.....	135
Air Separation Unit, Gas Turbine Air Extraction and N <sub>2</sub> Preheat .....	135
Coal Receiving and Handling Unit.....	137
Gasification Unit.....	137
CO Shift / Low Temperature Gas Cooling Unit.....	138
Acid Gas Removal Unit (Selexol®) .....	139
Syngas Humidification Unit .....	140
CO <sub>2</sub> Compression / Dehydration Unit .....	141
Sulfur Recovery / Tail Gas Treating Unit.....	141
Power Block.....	144
General Facilities .....	147
<b>TASK 1.4.1: SCREENING ANALYSIS OF ADVANCED BRAYTON CYCLES.....</b>	<b>189</b>
EXECUTIVE SUMMARY .....	189
APPROACH .....	189
Selection of Cases for Detailed Analysis.....	189
Cases Proposed for Consideration in Screening Analysis .....	190

Increased Firing Temperature / Blade Surface Temperature .....	190
Pressure Gain Combustor .....	190
Inlet Air Fogging.....	190
Inverse Cycle .....	191
Intercooled Gas Turbine .....	191
Reheat Gas Turbine.....	191
Intercooled and Reheat Gas Turbine.....	192
Supercritical Rankine Bottoming Cycle .....	192
Chemical Recuperation.....	193
Humid Air Cooling of Gas Turbine Blades .....	193
Closed Circuit Air Cooled Gas Turbine.....	194
Air Partial Oxidation Topping Gas Turbine .....	194
HAT Cycle.....	194
High Efficiency Exhaust Diffuser.....	195
Oxy Combustion Gas Turbine .....	195
NOx Reduction Options.....	195
RESULTS AND DISCUSSION.....	196
Gas Turbine Cycle Configurations .....	196
Pressure Gain Combustor .....	196
Inlet Air Fogging.....	197
Inverse Cycle .....	198
Reheat Gas Turbine.....	198
Intercooled Gas Turbine .....	198
Intercooled and Reheat Gas Turbine.....	199
Chemical Recuperation.....	199
Humid Air Cooling of Gas Turbine Blades .....	200
Closed Circuit Air Cooled Gas Turbine.....	200
Air Partial Oxidation Topping Gas Turbine .....	200
HAT Cycle.....	201
Oxy Combustion Gas Turbine .....	201
Advanced Materials Technology .....	202
Increased Firing Temperature .....	202
Supercritical Rankine Bottoming Cycle .....	203
Enhanced Performance Gas Turbine Components .....	203
High Efficiency Exhaust Diffuser.....	203
Advanced Low NOx Combustors.....	204
CONCLUSIONS.....	206
Promising Cycles .....	206
BIBLIOGRAPHY.....	206
<b>TASK 1.4.2: ADVANCED BRAYTON CYCLE DETAILED ANALYSIS .....</b>	<b>219</b>
SUMMARY .....	219
<b>SIMPLE CYCLE GAS TURBINE IGCC WITH INCREASED FIRING TEMPERATURE</b>	<b>219</b>
.....	<b>219</b>
APPROACH .....	219
PROCESS DESCRIPTION .....	221
Air Separation Unit and N <sub>2</sub> Preheat .....	221
Coal Receiving and Handling Unit.....	222
Gasification Unit.....	222
CO Shift / Low Temperature Gas Cooling Unit .....	222

Acid Gas Removal Unit (Selexol®)	222
Syngas Humidification Unit	222
CO <sub>2</sub> Compression / Dehydration Unit	222
Sulfur Recovery / Tail Gas Treating Unit	223
Power Block	223
General Facilities	226
RESULTS AND DISCUSSION	226
CONCLUSIONS	227
<b>INTERCOOLED GAS TURBINE IGCC WITH INCREASED FIRING TEMPERATURE</b>	<b>227</b>
APPROACH	227
PROCESS DESCRIPTION	229
Air Separation Unit and N <sub>2</sub> Preheat	229
Coal Receiving and Handling Unit	230
Gasification Unit	230
CO Shift / Low Temperature Gas Cooling Unit	230
Acid Gas Removal Unit (Selexol®)	230
Syngas Humidification Unit	230
CO <sub>2</sub> Compression / Dehydration Unit	230
Sulfur Recovery / Tail Gas Treating Unit	231
Power Block	231
General Facilities	234
RESULTS AND DISCUSSION	234
CONCLUSIONS	235
<b>INTERCOOLED-REHEAT GAS TURBINE IGCC WITH INCREASED FIRING TEMPERATURE</b>	<b>235</b>
APPROACH	235
PROCESS DESCRIPTION	236
Air Separation Unit and N <sub>2</sub> Preheat	236
Coal Receiving and Handling Unit	237
Gasification Unit	237
CO Shift / Low Temperature Gas Cooling Unit	237
Acid Gas Removal Unit (Selexol®)	237
Syngas Humidification Unit	237
CO <sub>2</sub> Compression / Dehydration Unit	238
Sulfur Recovery / Tail Gas Treating Unit	238
Power Block	238
General Facilities	241
RESULTS AND DISCUSSION	241
CONCLUSIONS	242
<b>INTERCOOLED CLOSED CIRCUIT AIR COOLED GAS TURBINE</b>	<b>242</b>
APPROACH	242
PROCESS DESCRIPTION	243
Air Separation Unit and N <sub>2</sub> Preheat	243
Coal Receiving and Handling Unit	244
Gasification Unit	245
CO Shift / Low Temperature Gas Cooling Unit	245
Acid Gas Removal Unit (Selexol®)	245
Syngas Humidification Unit	245

CO <sub>2</sub> Compression / Dehydration Unit .....	245
Sulfur Recovery / Tail Gas Treating Unit.....	245
Power Block.....	245
General Facilities .....	248
RESULTS AND DISCUSSION .....	248
CONCLUSIONS.....	249
<b>AIR PARTIAL OXIDATION TOPPING CYCLE .....</b>	<b>249</b>
APPROACH .....	249
PROCESS DESCRIPTION .....	250
Air Separation Unit and N <sub>2</sub> Preheat.....	250
Coal Receiving and Handling Unit.....	251
Gasification Unit.....	252
CO Shift / Low Temperature Gas Cooling Unit.....	252
Acid Gas Removal Unit (Selexol®) .....	252
Syngas Humidification Unit .....	252
CO <sub>2</sub> Compression / Dehydration Unit .....	252
Sulfur Recovery / Tail Gas Treating Unit.....	253
Power Block.....	253
General Facilities .....	256
RESULTS AND DISCUSSION .....	256
CONCLUSIONS.....	256
<b>SELECTION OF ADVANCED BRAYTON CYCLE.....</b>	<b>257</b>
<b>SENSITIVITY ANALYSIS OF SELECTED ADVANCED BRAYTON CYCLE.....</b>	<b>258</b>
APPROACH .....	258
RESULTS AND DISCUSSION .....	259
Gas Turbine Compressor Efficiency.....	259
Gas Turbine Expander Efficiency.....	259
High Efficiency Exhaust Diffuser.....	260
Application of Superconductivity Technology .....	261
Low NO <sub>x</sub> Strategies.....	261
Increased Diluent Nitrogen Addition.....	261
Reduced Firing Temperature .....	261
Air (Film) Cooled 1 <sup>st</sup> Stage Turbine .....	262
<b>ECONOMIC ANALYSIS .....</b>	<b>262</b>
<b>DEVELOPMENT NEEDS.....</b>	<b>263</b>
COMBUSTOR NEEDS .....	264
Materials .....	265
COMPRESSOR NEEDS .....	266
Intercooler .....	266
TURBINE NEEDS .....	267
Cooling Technology.....	267
Turbine Blade Materials .....	267
DEVELOPMENT COSTS AND TIME .....	268
BIBLIOGRAPHY .....	268
<b>TASK 2.1 - EVALUATION OF IMPACT OF RAMGEN COMPRESSION</b>	
<b>TECHNOLOGY ON IGCC PLANT PERFORMANCE .....</b>	<b>362</b>
SUMMARY .....	362
APPROACH .....	363
RESULTS AND DISCUSSION .....	364

Ramgen Turbomachinery.....	364
LP and IP CO <sub>2</sub> Compressors.....	364
Non-Intercooled HP CO <sub>2</sub> Compressor.....	364
Intercooled HP CO <sub>2</sub> Compressor.....	368
Application of Ramgen Technology to Other Turbomachinery.....	369
CONCLUSIONS.....	370
<b>TASK 2.2: GAS TURBINE OPERATING REQUIREMENTS FOR GASIFICATION BASED FUEL CELL / GAS TURBINE SYSTEM.....</b>	<b>386</b>
EXECUTIVE SUMMARY .....	386
OBJECTIVE .....	387
SCOPE OF WORK.....	387
APPROACH .....	388
RESULTS AND DISCUSSION.....	390
SOFC-GT Hybrid System Model Development.....	390
Solid Oxide Fuel Cell Model .....	394
Gas Turbine Model .....	401
Cathode Ejector Model .....	407
Cathode BLOWER MODEL .....	417
Hybrid System Steady State Analyses.....	418
HYBRID SYSTEM DYNAMIC ANALYSES .....	428
Model Utilizing A Cathode Ejector .....	428
Model Utilizing a Cathode Blower.....	454
Comparison of Control Strategies #1 and #2.....	534
CONCLUSIONS.....	536
ATTACHMENT .....	538
REFERENCES .....	541
<b>TASK 2.3: PERFORMANCE COMPARISON OF OXY-COMBUSTION AND IGCC PLANTS.....</b>	<b>543</b>
SUMMARY .....	543
APPROACH .....	544
Process Configurations .....	545
IGCC Cases.....	546
Oxy-combustion Cases .....	547
RESULTS AND DISCUSSIONS.....	548
CONCLUSIONS.....	548
REFERENCES .....	549

## LIST OF TABLES

Table 1: Plant Performance Summary – Baseline and Sensitivity Case.....	68
Table 2: Auxiliary (In-Plant) Power Consumption Summary – Baseline and Sensitivity Cases .	69
Table 3: Main Features of the Power Cycle – High RIT Simple Cycle Gas Turbine.....	70
Table 4: Main Features of the Power Cycle – High RIT Intercooled Gas Turbine .....	71
Table 5: Main Features of the Power Cycle – High RIT Intercooled-Reheat Gas Turbine.....	72
Table 6: Main Features of the Power Cycle –Intercooled Closed Circuit Air Cooled Gas Turbine .....	73
Table 7: Main Features of the Power Cycle –Air Partial Oxidation Topping Cycle.....	74
Table 8: Project Milestones .....	90
Table 9: Summary of Budget and Costs .....	91
Table A1.1 - 1: Site Conditions .....	93
Table A1.1 - 2: Coal Analysis.....	95
Table A1.1 - 3: Natural Gas Composition .....	96
Table A1.1 - 4: Greer Limestone Analysis .....	96
Table A1.1 - 5: Overall Plant Design Criteria .....	100
Table A1.1 - 6: List of Modules in APSAT.....	104
Table A1.1 - 7: Comparison between APSAT and ASPEN .....	107
Table A1.2 - 1: Syngas Contaminants .....	131
Table A1.3 - 1: Plant Performance Summary.....	149
Table A1.3 - 2: Auxiliary (In-Plant) Power Consumption Summary.....	150
Table A1.3 - 3: Stream Data .....	167
Table A1.3 - 4: ASU Functional Specifications - General .....	175
Table A1.3 - 5: ASU Functional Specifications - Storage Requirements.....	175
Table A1.3 - 6: ASU Functional Specifications - Ambient Air Composition.....	175
Table A1.3 - 7: Coal Receiving And Handling Unit Functional Specifications.....	176
Table A1.3 - 8: Gasification Unit Functional Specifications - Coal Grinding and Slurry Preparation Subsystem .....	178
Table A1.3 - 9: Gasification Unit Functional Specifications - Gasifier Subsystem .....	178
Table A1.3 - 10: Gasification Unit Functional Specifications - Syngas Scrubber Subsystem...	179
Table A1.3 - 11: Gasification Unit Functional Specifications - Slag Recovery and Handling Subsystem.....	179
Table A1.3 - 12: Gasification Unit Functional Specifications - Black Water, Grey Water and Waste Water Handling Subsystem .....	180
Table A1.3 - 13: Selexol AGR Functional Specification – Feed Gas Definition.....	181
Table A1.3 - 14: Selexol AGR Functional Specification – Product Specifications .....	181
Table A1.3 - 15: Equipment List Unit 21 - Sour Shift / LT Gas Cooling .....	182

Table A1.3 - 16: Equipment List Unit 23 - Claus Sulfur Recovery Unit .....	183
Table A1.3 - 17: Equipment List Unit 24 - CO <sub>2</sub> Compression.....	185
Table A1.3 - 18: Equipment List Unit 25 - Humidification .....	186
Table A1.3 - 19: Equipment List Units 50/51 - Power Block .....	187
Table A1.4.1 - 1: Supercritical Steam Cycles.....	193
Table A1.4.1 - 2: Effect of Raising Firing Temperature on IGCC Performance.....	202
Table A1.4.2 - 1: Stream Data – Simple Cycle Gas Turbine.....	285
Table A1.4.2 - 2: Plant Performance Summary – Simple Cycle Gas Turbine .....	292
Table A1.4.2 - 3: Auxiliary (In-Plant) Power Consumption Summary – Simple Cycle Gas Turbine .....	293
Table A1.4.2 - 4: Main Features of the Power Cycle –Simple Cycle Gas Turbine.....	294
Table A1.4.2 - 5: Stream Data – Intercooled Gas Turbine .....	300
Table A1.4.2 - 6: Plant Performance Summary – Intercooled Gas Turbine.....	307
Table A1.4.2 - 7: Auxiliary (In-Plant) Power Consumption Summary – Intercooled Gas Turbine .....	308
Table A1.4.2 - 8: Main Features of the Power Cycle – Intercooled Gas Turbine .....	309
Table A1.4.2 - 9: Stream Data – Intercooled-Reheat Gas Turbine.....	320
Table A1.4.2 - 10: Plant Performance Summary – Intercooled-Reheat Gas Turbine .....	328
Table A1.4.2 - 11: Auxiliary (In-Plant) Power Consumption Summary – Intercooled-Reheat Gas Turbine .....	329
Table A1.4.2 - 12: Main Features of the Power Cycle – Intercooled-Reheat Gas Turbine.....	330
Table A1.4.2 - 13: Stream Data – Intercooled Closed Circuit Air Cooled Gas Turbine .....	334
Table A1.4.2 - 14: Plant Performance Summary – Intercooled Closed Circuit Air Cooled Gas Turbine .....	341
Table A1.4.2 - 15: Auxiliary (In-Plant) Power Consumption Summary – Intercooled Closed Circuit Air Cooled Gas Turbine .....	342
Table A1.4.2 - 16: Main Features of the Power Cycle – Intercooled Closed Circuit Air Cooled Gas Turbine .....	343
Table A1.4.2 - 17: Stream Data – Air Partial Oxidation Topping Cycle.....	351
Table A1.4.2 - 18: Plant Performance Summary – Air Partial Oxidation Topping Cycle .....	358
Table A1.4.2 - 19: Auxiliary (In-Plant) Power Consumption Summary – Air Partial Oxidation Topping Cycle .....	359
Table A1.4.2 - 20: Main Features of the Power Cycle – Air Partial Oxidation Topping Cycle.	360
Table A2.1 - 1: Stream Data – Baseline Case CO <sub>2</sub> Compression.....	373
Table A2.1 - 2: Stream Data – Baseline Case ASU and Gas Turbine Air Extraction.....	376
Table A2.1 - 3: Ramgen LP and IP CO <sub>2</sub> Compression Technology Characteristics.....	379
Table A2.1 - 4: Ramgen HP CO <sub>2</sub> Compression Technology Characteristics.....	379
Table A2.1 - 5: Impact on Plant Performance with Ramgen CO <sub>2</sub> Compression (LP + IP + HP) Technology .....	380

Table A2.1 - 6: Ramgen Air Expander Technology Characteristics .....	381
Table A2.1 - 7: Ramgen ASU Compressor Technology Characteristics.....	381
Table A2.1 - 8: Stream Data – Baseline Case ASU and Gas Turbine Air Extraction .....	384
Table A2.2 - 1: SOFC/GT fuel stream specifications.....	391
Table A2.2 - 2: Percent error in energy conservation for fuel cell components.....	392
Table A2.2 - 3: One-dimensional isentropic compressible-flow functions for an ideal gas with constant specific heats and molar mass, $\gamma = 1.4$ (Truncated version, adapted from Fluid Mechanics, Frank M White Table B-1).....	409
Table A2.2 - 4: Gas turbine and fuel cell design parameters used for steady state operation. ...	419
Table A2.2 - 5: Gas turbine and fuel cell steady state performance values (cathode ejector)....	423
Table A2.2 - 6: Hybrid system steady state values for various cycle pressures using a cathode blower.....	425
Table A2.2 - 7: Hybrid system steady state values for various cycle pressures using a cathode ejector. ....	426
Table A2.2 - 8: Percent error between Simulink and ASPEN results for steady state power (using cathode blower). ....	428
Table A2.2 - 9: Percent error between Simulink and ASPEN results for steady state power (using cathode ejector). ....	428
Table A2.2 - 10: Results of map perturbation on steady state operation point stability.....	450
Table A2.3- 1: CO <sub>2</sub> Composition / Conditions.....	553
Table A2.3- 2: Case Matrix .....	554
Table A2.3- 3: Shift Reactors in IGCC Cases with Total Quench Heat Recovery .....	566
Table A2.3- 4: Shift Reactors in IGCC Cases with Radiant Quench Heat Recovery .....	567
Table A2.3- 5: Overall Plant Performance Summaries - GT RIT = 1392°C.....	568
Table A2.3- 6: Overall Plant Performance Summaries - GT RIT = 1734°C.....	569
Table A2.3- 7: Overall Plant Performance Summaries - SO <sub>2</sub> Co-sequestration - GT RIT = 1392°C.....	570

## LIST OF ILLUSTRATIONS

Figure 1: Project Schedule.....	89
Figure A1.1 - 1: SOFC / GT System for Dynamic Simulations.....	99
Figure A1.1 - 2: Variation of Power Output with Compressor Inlet Temperature.....	107
Figure A1.2 - 1: Advanced Transport Reactor.....	127
Figure A1.2 - 2: GE Total Quench Gasifier.....	128
Figure A1.2 - 3: Shell Gasifier.....	129
Figure A1.2 - 4: E-Gas Gasifier.....	130
Figure A1.2 - 5: HAT Cycle.....	132
Figure A1.2 - 6: Partial Oxidation Cycle.....	132
Figure A1.2 - 7: Impact of Firing / Blade Temperatures on Efficiency.....	133
Figure A1.2 - 8: Reheat Gas Turbine Cycle.....	133
Figure A1.2 - 9: Overall Block Flow Diagram – Baseline Case IGCC with CO <sub>2</sub> Capture.....	134
Figure A1.3 - 1: Overall Block Flow Diagram – Baseline Case IGCC with CO <sub>2</sub> Capture – IP ASU.....	151
Figure A1.3 - 2: Block Flow Diagram - Air Separation Unit, Gas Turbine Air Extraction and N <sub>2</sub> Preheat.....	152
Figure A1.3 - 3: Block Flow Diagram - Gasification Unit and Coal Slurry Preparation.....	153
Figure A1.3 - 4: Process Flow Diagram - CO Shift / Low Temperature Gas Cooling Unit.....	154
Figure A1.3 - 5: Block Flow Diagram - Acid Gas Removal Unit (Selexol®).....	156
Figure A1.3 - 6: Process Flow Diagram - Syngas Humidification Unit.....	157
Figure A1.3 - 7: Process Flow Diagram - CO <sub>2</sub> Compression / Dehydration Unit.....	158
Figure A1.3 - 8: Process Flow Diagram - Sulfur Recovery / Tail Gas Treating Unit.....	159
Figure A1.3 - 9: Process Flow Diagram – Power Block.....	162
Figure A1.3 - 10: Steam Balance Diagram.....	163
Figure A1.3 - 11: Gas Turbine Cycle Diagram - Syngas Case.....	164
Figure A1.3 - 12: Gas Turbine Cycle Diagram - Natural Gas Case.....	165
Figure A1.3 - 13: Overall IGCC Plant Water Balance.....	166
Figure A1.4.1 - 1: Effect of Increasing Firing and 1 <sup>st</sup> Stage Stator Blade Temperatures.....	209
Figure A1.4.1 - 2: Reheat Gas Turbine Cycle.....	210
Figure A1.4.1 - 3: Intercooled - Reheat Gas Turbine Cycle.....	211
Figure A1.4.1 - 4: Steam Rankine Cycle Thermal Efficiencies.....	212
Figure A1.4.1 - 5: Air POx Cycle.....	213
Figure A1.4.1 - 6: HAT-Combined Cycle.....	214
Figure A1.4.1 - 7: Pressure Gain and Compressor Discharge Conditions in a Pressure Gain Combustor.....	215

Figure A1.4.1 - 8: Ox Gas Turbine.....	216
Figure A1.4.1 - 9: POx Gas Turbine.....	217
Figure A1.4.1 - 10: Heat Rate Improvement due to Firing Temperature and Other Changes....	218
Figure A1.4.1 - 11: Heat Rate Improvement due to Radically New Approaches .....	218
Figure A1.4.2 - 1: Effect of Increasing Firing and 1 <sup>st</sup> Stage Stator Blade Temperatures.....	269
Figure A1.4.2 - 2: Overall Block Flow Diagram – IGCC with CO <sub>2</sub> Capture – Simple Cycle GT / PR=37 / IP ASU .....	270
Figure A1.4.2 - 3: Overall Block Flow Diagram – IGCC with CO <sub>2</sub> Capture – Simple Cycle GT / PR=37 / HP ASU.....	271
Figure A1.4.2 - 4: Overall Block Flow Diagram – IGCC with CO <sub>2</sub> Capture – Simple Cycle GT / PR=37 / No Air Extraction.....	272
Figure A1.4.2 - 5: Overall Block Flow Diagram – IGCC with CO <sub>2</sub> Capture – Simple Cycle GT / PR=50 / IP ASU .....	273
Figure A1.4.2 - 6: Overall Block Flow Diagram – IGCC with CO <sub>2</sub> Capture – Simple Cycle GT / PR=50 / HP ASU.....	274
Figure A1.4.2 - 7: Overall Block Flow Diagram – IGCC with CO <sub>2</sub> Capture – Simple Cycle GT / PR=50 / No Air Extraction.....	275
Figure A1.4.2 - 8: Process Flow Diagram – Air Separation Unit - Simple Cycle GT with PR=50, Intercooled Cycle GT with PR=50 & Intercooled Closed Circuit Air Cooled Gas Turbine	276
Figure A1.4.2 - 9: Process Flow Diagram – CO Shift / Low Temperature Gas Cooling Unit - Simple Cycle GT with PR=50, Intercooled Cycle GT with PR=50 & Intercooled Closed Circuit Air Cooled GT.....	277
Figure A1.4.2 - 10: Process Flow Diagram – Syngas Humidification Unit - Simple Cycle GT with PR=50, Intercooled Cycle GT with PR=50 & Intercooled Closed Circuit Air Cooled GT.....	279
Figure A1.4.2 - 11: Process Flow Diagram – Sulfur Recovery / Tail Gas Treating Unit - Simple Cycle GT with PR=50, Intercooled Cycle GT with PR=50 & Intercooled Closed Circuit Air Cooled GT .....	280
Figure A1.4.2 - 12: Process Flow Diagram – Power Block - Simple Cycle GT with PR=50 ....	283
Figure A1.4.2 - 13: Steam Balance Diagram –Simple Cycle GT with PR=50.....	284
Figure A1.4.2 - 14: Spray vs Shell and Tube Intercooler .....	295
Figure A1.4.2 - 15: Overall Block Flow Diagram – IGCC with CO <sub>2</sub> Capture – Intercooled GT / PR=50 / HP ASU.....	296
Figure A1.4.2 - 16: Overall Block Flow Diagram – IGCC with CO <sub>2</sub> Capture – Intercooled GT / PR=50 & 70 / No Air Extraction.....	297
Figure A1.4.2 - 17: Process Flow Diagram – Power Block - Intercooled GT with PR=50 .....	298
Figure A1.4.2 - 18: Steam Balance Diagram – Intercooled GT with PR=50.....	299
Figure A1.4.2 - 19: Overall Block Flow Diagram – IGCC with CO <sub>2</sub> Capture – Intercooled-Reheat GT.....	310
Figure A1.4.2 - 20: Process Flow Diagram – Air Separation Unit – Intercooled-Reheat GT....	311
Figure A1.4.2 - 21: Process Flow Diagram – CO Shift / Low Temperature Gas Cooling Unit - Intercooled-Reheat GT .....	312

Figure A1.4.2 - 22: Process Flow Diagram – Syngas Humidification Unit - Intercooled-Reheat GT.....	314
Figure A1.4.2 - 23: Process Flow Diagram – Sulfur Recovery / Tail Gas Treating Unit - Intercooled Reheat GT & Air POX Topping Cycle GT.....	315
Figure A1.4.2 - 24: Process Flow Diagram – Power Block - Intercooled-Reheat GT .....	318
Figure A1.4.2 - 25: Steam Balance Diagram — Intercooled-Reheat GT.....	319
Figure A1.4.2 - 26: Overall Block Flow Diagram – IGCC with CO <sub>2</sub> Capture – Intercooled Closed Circuit Air Cooled GT.....	331
Figure A1.4.2 - 27: Process Flow Diagram – Power Block – Intercooled Closed Circuit Air Cooled GT .....	332
Figure A1.4.2 - 28: Steam Balance Diagram — Intercooled Closed Circuit Air Cooled GT.....	333
Figure A1.4.2 - 29: Overall Block Flow Diagram – IGCC with CO <sub>2</sub> Capture – Air POx Topping Cycle.....	344
Figure A1.4.2 - 30: Process Flow Diagram – Air Separation Unit – Air POx Topping Cycle ..	345
Figure A1.4.2 - 31: Process Flow Diagram – CO Shift / Low Temperature Gas Cooling Unit - Air POx Topping Cycle.....	346
Figure A1.4.2 - 32: Process Flow Diagram – Syngas Humidification Unit - Air POx Topping Cycle.....	348
Figure A1.4.2 - 33: Process Flow Diagram – Power Block - Air POx Topping Cycle.....	349
Figure A1.4.2 - 34: Steam Balance Diagram – Air POx Topping Cycle.....	350
Figure A1.4.2 - 35: Effect of Firing Temperature on Net Plant Heat rate and NO <sub>x</sub> Emission (using Short Combustor) .....	361
Figure A2.1 - 1: Process Flow Diagram – Baseline Case CO <sub>2</sub> Compression / Dehydration Unit .....	372
Figure A2.1 - 2: Process Flow Diagram – Baseline Case ASU and Gas Turbine Air Extraction .....	374
Figure A2.1 - 3: Process Flow Diagram – CO <sub>2</sub> Compression / Dehydration Unit with Ramgen Non-intercooled HP Compressor .....	378
Figure A2.1 - 4: Power from a Rankine Cycle .....	382
Figure A2.1 - 5: Power from a Hypothetical Working Fluid with Variable Evaporation and Condensing Temperatures.....	382
Figure A2.1 - 6: Process Flow Diagram – ASU and Gas Turbine Air Extraction with Ramgen Air Expander and Air Compressors .....	383
Figure A2.2 - 1. Diagram of the pressurized 100 MW SOFC/GT hybrid power block utilizing an ejector for cathode recirculation.....	388
Figure A2.2 - 2. Diagram of the pressurized 100 MW SOFC/GT hybrid power block utilizing a blower for cathode recirculation.....	389
Figure A2.2 - 3. Diagram of the pressurized 220 kW SOFC/GT hybrid system.....	390
Figure A2.2 - 4: SOFC/GT hybrid efficiencies vs. percent fuel recirculation of coal syngas (Fuel utilization set to 80%).....	393
<b>Figure A2.2 - 5: SOFC/GT hybrid anode and cathode temperatures vs. percent fuel recirculation.</b> .....	394

Figure A2.2 - 6: Voltage vs. current density for Siemens Westinghouse 220 kW SOFC-GT hybrid system.....	395
Figure A2.2 - 7: SOFC stack performance for various SECA participants (2004 data).....	396
Figure A2.2 - 8: Extrapolated voltage vs. current density based on 2004 SECA participant data. ....	397
Figure A2.2 - 9: Voltage vs. current density based on ultimate SECA targets.....	398
Figure A2.2 - 10: Power density vs. current density based on ultimate SECA targets. ....	399
Figure A2.2 - 11: Voltage vs. current density based on 2004 literature and ultimate SECA targets. ....	400
Figure A2.2 - 12: Total cell conductivity density vs. reciprocal temperature for Siemens Westinghouse 220 kW and SECA target SOFC.....	401
Figure A2.2 - 13: Empirical axial compressor pressure ratio vs. corrected mass flow for various corrected speeds (in black). Red line is surge line and blue lines represent efficiency islands (Source: GSP).....	402
Figure A2.2 - 14: Empirical axial turbine corrected mass flow vs. pressure ratio for various corrected speeds (Source: GSP). ....	403
Figure A2.2 - 15: Axial compressor pressure ratio vs. mass flow for various speeds using equation 2. ....	404
Figure A2.2 - 16: Compressor isentropic efficiency (normalized to maximum design value) vs. mass flow.....	405
Figure A2.2 - 17: Axial turbine mass flow vs. pressure ratio for various speeds using equation 3. ....	406
Figure A2.2 - 18: Turbine isentropic efficiency (normalized to maximum design value) vs. pressure ratio. ....	407
Figure A2.2 - 19: Fuel cell cathode ejector.....	408
Figure A2.2 - 20: Cathode ejector primary nozzle. ....	409
Figure A2.2 - 21: Area ratio vs. Mach number for isentropic flow of an ideal gas with $k = 1.4$ (Air).....	410
Figure A2.2 - 22: Mach number vs. ejector location for primary and secondary streams.....	415
Figure A2.2 - 23: Pressure vs. ejector location for primary and secondary streams. ....	415
Figure A2.2 - 24: Temperature vs. ejector location for primary and secondary streams. ....	416
Figure A2.2 - 25: Ejector exit temperature and entrainment ratio vs. primary stream pressure. ....	417
Figure A2.2 - 26: Average fuel cell cathode operating temperature vs. multiple parameters. ....	420
Figure A2.2 - 27: Fuel cell power density vs. multiple parameters.....	421
Figure A2.2 - 28: Ejector pressure drop vs. multiple parameters. ....	422
Figure A2.2 - 29: Fuel cell oxygen utilization and air-to-fuel stoichiometry vs. cathode temperature rise. ....	424
Figure A2.2 - 30: Compressor dynamic response to a fuel cell load decrease from 100% (blue) to 50% (red) design state using weak controller parameters. PID control is applied to shaft RPM.....	429
Figure A2.2 - 31: Compressor dynamic response to a fuel cell load increase from 50% (red) to 100% (blue) design state using weak controller parameters. PID control is applied to shaft RPM.....	430

Figure A2.2 - 32: Compressor dynamic response to a fuel cell load decrease from 100% (blue) to 50% (red) design state using robust controller parameters. PID control is applied to shaft RPM.....	431
Figure A2.2 - 33: Compressor dynamic response to a fuel cell load increase from 50% (red) to 100% (blue) design state using robust controller parameters. PID control is applied to shaft RPM.....	432
Figure A2.2 - 34: Compressor dynamic response to a 50% decrease in fuel hydrogen balanced with nitrogen. Initial state A (blue) to final state B (red). PID control is applied to shaft RPM.....	433
Figure A2.2 - 35: Compressor dynamic response to a 50% decrease in fuel hydrogen balanced with steam. Initial state A (blue) to final state B (red). PID control is applied to shaft RPM.....	434
Figure A2.2 - 36: Compressor dynamic response to a fuel cell load decrease from 100% (blue) to 90% (red) design state when cascade PID control is applied to fuel cell temperature and shaft RPM.....	435
Figure A2.2 - 37: Compressor dynamic response to a fuel cell load decrease from 100% (blue) to 75% (red) design state when cascade PID control is applied to fuel cell temperature and shaft RPM.....	436
Figure A2.2 - 38: Compressor dynamic response to a fuel cell load decrease from 100% (blue) to 50% (red) design state when cascade PID control is applied to fuel cell temperature and shaft RPM.....	437
Figure A2.2 - 39: Compressor dynamic response to a 10% decrease in fuel hydrogen balanced with nitrogen. Initial state A (blue) to final state B (red) when cascade PID control is applied to fuel cell temperature and shaft RPM.....	438
Figure A2.2 - 40: Compressor dynamic response to a 25% decrease in fuel hydrogen balanced with nitrogen. Initial state A (blue) to final state B (red) when cascade PID control is applied to fuel cell temperature and shaft RPM.....	439
Figure A2.2 - 41: Compressor dynamic response to a 50% decrease in fuel hydrogen balanced with nitrogen. Initial state A (blue) to final state B (red) when cascade PID control is applied to fuel cell temperature and shaft RPM.....	440
Figure A2.2 - 42: Compressor dynamic response to a 10% decrease in fuel hydrogen balanced with steam. Initial state A (blue) to final state B (red) when cascade PID control is applied to fuel cell temperature and shaft RPM.....	441
Figure A2.2 - 43: Compressor dynamic response to a 25% decrease in fuel hydrogen balanced with steam. Initial state A (blue) to final state B (red) when cascade PID control is applied to fuel cell temperature and shaft RPM.....	442
Figure A2.2 - 44: Compressor dynamic response to a 50% decrease in fuel hydrogen balanced with steam. Initial state A (blue) to final state B (red) when cascade PID control is applied to fuel cell temperature and shaft RPM.....	443
Figure A2.2 - 45: Compressor dynamic response to a fuel cell load decrease from 100% (blue) to 75% (red) design state when plenum volume is increased by a factor of 10 compared to Figure A2.2 - 37. ....	444
Figure A2.2 - 46: Compressor dynamic response to a fuel cell load decrease from 100% (blue) to 75% (red) design state when plenum volume is decreased by a factor of 16 compared to Figure A2.2 - 37. ....	445

Figure A2.2 - 47: Compressor dynamic response to a fuel cell load decrease from 100% (blue) to 75% (red) design state when rotating moment of inertia is increased by a factor of 1000 compared to Figure A2.2 - 37.....	446
Figure A2.2 - 48: Compressor dynamic response to a fuel cell load decrease from 100% (blue) to 75% (red) design state when rotating moment of inertia is decreased by a factor of 1,000 compared to Figure A2.2 - 37.....	447
Figure A2.2 - 49: Compressor dynamic response to a fuel cell load decrease from 100% (blue) to 75% (red) design state when fuel cell electrolyte set-point temperature is increased from 1,100 K in Figure A2.2 - 37 to 1,125 K. ....	448
Figure A2.2 - 50: Perturbation of 0.96 NRPM speed line by changing the individual coefficients in equation 26. ....	449
Figure A2.2 - 51: Compressor dynamic response to a fuel cell load decrease from 100% (blue) to 75% (red) design state when equation 27 is used to calculate compressor speed lines vs. equation 26 in the base case of Figure A2.2 - 37. ....	451
Figure A2.2 - 52: Compressor dynamic response to a fuel cell load decrease from 100% (blue) to 75% (red) design operating conditions when design mass flow rate is decreased relative to the base case of Figure A2.2 - 37. ....	452
Figure A2.2 - 53: Compressor dynamic response to a fuel cell load decrease from 100% (blue) to 75% (red) design state when design pressure ratio is increased relative to the base case of Figure A2.2 - 37. ....	453
Figure A2.2 - 54: Compressor dynamic response to a fuel cell load decrease from 100% (blue) to 75% (red) design state when both design mass flow rate is decreased and design pressure ratio is increased relative to the base case of Figure A2.2 - 37. ....	454
Figure A2.2 - 55: Compressor dynamic response to a fuel cell load decrease from 100% (blue) to 90% (red) of design state. Gas turbine shaft speed controlled at 3,600 RPM and primary control of blower/compressor mixture temperature at 800 K and secondary control of blower speed.....	455
Figure A2.2 - 56: Compressor dynamic response to a fuel cell load decrease from 100% (blue) to 75% (red) of design state. Gas turbine shaft speed controlled at 3,600 RPM and primary control of blower/compressor mixture temperature at 800 K and secondary control of blower speed.....	456
Figure A2.2 - 57: Dynamic anode-cathode inlet pressure difference response to a fuel cell load decrease from 100% to 75% of design point. Gas turbine speed controlled at 3,600 RPM and primary control of blower/compressor mixture temperature at 800 K with secondary control of recycle blower speed. ....	457
Figure A2.2 - 58: Dynamic anode inlet-outlet temperature difference response to a fuel cell load decrease from 100% to 75% of design point. Gas turbine speed controlled at 3,600 RPM and primary control of blower/compressor mixture temperature at 800 K with secondary control of recycle blower speed. ....	458
Figure A2.2 - 59: Dynamic cathode inlet-outlet temperature difference response to a fuel cell load decrease from 100% to 75% of design point. Gas turbine speed controlled at 3,600 RPM and primary control of blower/compressor mixture temperature at 800 K with secondary control of recycle blower speed. ....	459
Figure A2.2 - 60: Dynamic average fuel cell temperature response to a fuel cell load decrease from 100% to 75% of design point. Gas turbine speed controlled at 3,600 RPM and primary	

control of blower/compressor mixture temperature at 800 K with secondary control of recycle blower speed. ....	460
Figure A2.2 - 61: Dynamic tri-layer temperature response to a fuel cell load decrease from 100% to 75% of design point. Gas turbine speed controlled at 3,600 RPM and primary control of blower/compressor mixture temperature at 800 K with secondary control of recycle blower speed. ....	461
Figure A2.2 - 62: Dynamic gas turbine shaft speed response to a fuel cell load decrease from 100% to 75% of design point. Gas turbine speed controlled at 3,600 RPM and primary control of blower/compressor mixture temperature at 800 K with secondary control of recycle blower speed. ....	462
Figure A2.2 - 63: Compressor dynamic response to a fuel cell load decrease from 100% (blue) to 50% (red) of design state. Gas turbine shaft speed controlled at 3,600 RPM and primary control of blower/compressor mixture temperature at 800 K and secondary control of blower speed. ....	463
Figure A2.2 - 64: Compressor dynamic response to a fuel cell load increase from 100% (blue) to 125% (red) of design state. Gas turbine shaft speed controlled at 3,600 RPM and primary control of blower/compressor mixture temperature at 800 K and secondary control of blower speed. ....	464
Figure A2.2 - 65: Dynamic anode-cathode inlet pressure difference response to a fuel cell load increase from 100% to 125% of design point. Gas turbine speed controlled at 3,600 RPM and primary control of blower/compressor mixture temperature at 800 K with secondary control of recycle blower speed. ....	465
Figure A2.2 - 66: Dynamic anode inlet-outlet temperature difference response to a fuel cell load increase from 100% to 125% of design point. Gas turbine speed controlled at 3,600 RPM and primary control of blower/compressor mixture temperature at 800 K with secondary control of recycle blower speed. ....	466
Figure A2.2 - 67: Dynamic cathode inlet-outlet temperature difference response to a fuel cell load increase from 100% to 125% of design point. Gas turbine speed controlled at 3,600 RPM and primary control of blower/compressor mixture temperature at 800 K with secondary control of recycle blower speed. ....	467
Figure A2.2 - 68: Dynamic average fuel cell temperature response to a fuel cell load increase from 100% to 125% of design point. Gas turbine speed controlled at 3,600 RPM and primary control of blower/compressor mixture temperature at 800 K with secondary control of recycle blower speed. ....	468
Figure A2.2 - 69: Dynamic tri-layer temperature response to a fuel cell load increase from 100% to 125% of design point. Gas turbine speed controlled at 3,600 RPM and primary control of blower/compressor mixture temperature at 800 K with secondary control of recycle blower speed. ....	469
Figure A2.2 - 70: Dynamic gas turbine shaft speed response to a fuel cell load increase from 100% to 125% of design point. Gas turbine speed controlled at 3,600 RPM and primary control of blower/compressor mixture temperature at 800 K with secondary control of recycle blower speed. ....	470
Figure A2.2 - 71: Compressor dynamic response to a fuel cell load increase from 100% (blue) to 150% (red) of design state. Gas turbine shaft speed controlled at 3,600 RPM and primary control of blower/compressor mixture temperature at 800 K and secondary control of blower speed. ....	471

Figure A2.2 - 72: Compressor dynamic response to a decrease in fuel hydrogen balanced with nitrogen from 100% (blue) to 90% (red) of design state. Gas turbine shaft speed controlled at 3,600 RPM and primary control of blower/compressor mixture temperature at 800 K and secondary control of blower speed. ....	472
Figure A2.2 - 73: Compressor dynamic response to a decrease in fuel hydrogen balanced with nitrogen from 100% (blue) to 75% (red) of design state. Gas turbine shaft speed controlled at 3,600 RPM and primary control of blower/compressor mixture temperature at 800 K and secondary control of blower speed. ....	473
Figure A2.2 - 74: Dynamic anode-cathode inlet pressure difference response to a decrease in fuel hydrogen balanced with nitrogen from 100% to 75% of design point. Gas turbine speed controlled at 3,600 RPM and primary control of blower/compressor mixture temperature at 800 K with secondary control of recycle blower speed. ....	474
Figure A2.2 - 75: Dynamic anode inlet-outlet temperature difference response to a decrease in fuel hydrogen balanced with nitrogen from 100% to 75% of design point. Gas turbine speed controlled at 3,600 RPM and primary control of blower/compressor mixture temperature at 800 K with secondary control of recycle blower speed. ....	475
Figure A2.2 - 76: Dynamic cathode inlet-outlet temperature difference response to a decrease in fuel hydrogen balanced with nitrogen from 100% to 75% of design point. Gas turbine speed controlled at 3,600 RPM and primary control of blower/compressor mixture temperature at 800 K with secondary control of recycle blower speed. ....	476
Figure A2.2 - 77: Dynamic average fuel cell temperature response to a decrease in fuel hydrogen balanced with nitrogen from 100% to 75% of design point. Gas turbine speed controlled at 3,600 RPM and primary control of blower/compressor mixture temperature at 800 K with secondary control of recycle blower speed. ....	477
Figure A2.2 - 78: Dynamic tri-layer temperature response to a decrease in fuel hydrogen balanced with nitrogen from 100% to 75% of design state. Gas turbine speed controlled at 3,600 RPM and primary control of blower/compressor mixture temperature at 800 K with secondary control of recycle blower speed. ....	478
Figure A2.2 - 79: Dynamic gas turbine shaft speed response to a decrease in fuel hydrogen balanced with nitrogen from 100% to 75% of design point. Gas turbine speed controlled at 3,600 RPM and primary control of blower/compressor mixture temperature at 800 K with secondary control of recycle blower speed. ....	479
Figure A2.2 - 80: Compressor dynamic response to a decrease in fuel hydrogen balanced with nitrogen from 100% (blue) to 50% (red) of design state. Gas turbine shaft speed controlled at 3,600 RPM and primary control of blower/compressor mixture temperature at 800 K and secondary control of blower speed. ....	480
Figure A2.2 - 81: Compressor dynamic response to a decrease in fuel hydrogen balanced with steam from 100% (blue) to 90% (red) of design state. Gas turbine shaft speed controlled at 3,600 RPM and primary control of blower/compressor mixture temperature at 800 K and secondary control of blower speed. ....	481
Figure A2.2 - 82: Compressor dynamic response to a decrease in fuel hydrogen balanced with steam from 100% (blue) to 75% (red) of design state. Gas turbine shaft speed controlled at 3,600 RPM and primary control of blower/compressor mixture temperature at 800 K and secondary control of blower speed. ....	482
Figure A2.2 - 83: Compressor dynamic response to a decrease in fuel hydrogen balanced with steam from 100% (blue) to 50% (red) of design state. Gas turbine shaft speed controlled at	

3,600 RPM and primary control of blower/compressor mixture temperature at 800 K and secondary control of blower speed. ....	483
Figure A2.2 - 84: Compressor dynamic response to a decrease in fuel hydrogen balanced with methane from 100% to 75% of design point. Gas turbine speed controlled at 3,600 RPM and primary control of blower/compressor mixture temperature at 800 K with secondary control of recycle blower speed. ....	484
Figure A2.2 - 85: Dynamic anode-cathode inlet pressure difference response to a decrease in fuel hydrogen balanced with methane from 100% to 75% of design point. Gas turbine speed controlled at 3,600 RPM and primary control of blower/compressor mixture temperature at 800 K with secondary control of recycle blower speed. ....	485
Figure A2.2 - 86: Dynamic anode inlet-outlet temperature difference response to a decrease in fuel hydrogen balanced with methane from 100% to 75% of design point. Gas turbine speed controlled at 3,600 RPM and primary control of blower/compressor mixture temperature at 800 K with secondary control of recycle blower speed. ....	486
Figure A2.2 - 87: Dynamic cathode inlet-outlet temperature difference response to a decrease in fuel hydrogen balanced with methane from 100% to 75% of design point. Gas turbine speed controlled at 3,600 RPM and primary control of blower/compressor mixture temperature at 800 K with secondary control of recycle blower speed. ....	487
Figure A2.2 - 88: Dynamic average fuel cell temperature response to a decrease in fuel hydrogen balanced with methane from 100% to 75% of design point. Gas turbine speed controlled at 3,600 RPM and primary control of blower/compressor mixture temperature at 800 K with secondary control of recycle blower speed. ....	488
Figure A2.2 - 89: Dynamic tri-layer temperature response to a decrease in fuel hydrogen balanced with methane from 100% to 75% of design point. Gas turbine speed controlled at 3,600 RPM and primary control of blower/compressor mixture temperature at 800 K with secondary control of recycle blower speed. ....	489
Figure A2.2 - 90: Dynamic gas turbine shaft speed response to a decrease in fuel hydrogen balanced with methane from 100% to 75% of design point. Gas turbine speed controlled at 3,600 RPM and primary control of blower/compressor mixture temperature at 800 K with secondary control of recycle blower speed. ....	490
Figure A2.2 - 91: Compressor dynamic response to a fuel cell load decrease from 100% (blue) to 90% (red) of design state. Primary control of fuel cell temperature at 1,100 K and secondary control of gas turbine shaft speed and primary control of blower/compressor mixture temperature at 800 K and secondary control of blower speed. ....	491
Figure A2.2 - 92: Compressor dynamic response to a fuel cell load decrease from 100% (blue) to 75% (red) of design state. Primary control of fuel cell temperature at 1,100 K and secondary control of gas turbine shaft speed and primary control of blower/compressor mixture temperature at 800 K and secondary control of blower speed. ....	492
Figure A2.2 - 93: Dynamic anode-cathode inlet pressure difference response to a fuel cell load decrease from 100% to 75% of design point. Primary control of fuel cell temperature at 1,100 K and secondary control of gas turbine speed and primary control of blower/compressor mixture temperature at 800 K with secondary control of recycle blower speed. ....	493
Figure A2.2 - 94: Dynamic anode inlet-outlet temperature difference response to a fuel cell load decrease from 100% to 75% of design point. Primary control of fuel cell temperature at 1,100 K and secondary control of gas turbine speed and primary control of	

blower/compressor mixture temperature at 800 K with secondary control of recycle blower speed.....	494
Figure A2.2 - 95: Dynamic cathode inlet-outlet temperature difference response to a fuel cell load decrease from 100% to 75% of design point. Primary control of fuel cell temperature at 1,100 K and secondary control of gas turbine speed and primary control of blower/compressor mixture temperature at 800 K with secondary control of recycle blower speed.....	495
Figure A2.2 - 96: Dynamic average fuel cell temperature response to a fuel cell load decrease from 100% to 75% of design point. Primary control of fuel cell temperature at 1,100 K and secondary control of gas turbine speed and primary control of blower/compressor mixture temperature at 800 K with secondary control of recycle blower speed. ....	496
Figure A2.2 - 97: Dynamic tri-layer temperature response to a fuel cell load decrease from 100% to 75% of design point. Primary control of fuel cell temperature at 1,100 K and secondary control of gas turbine speed and primary control of blower/compressor mixture temperature at 800 K with secondary control of recycle blower speed.....	497
Figure A2.2 - 98: Dynamic gas turbine shaft speed response to a fuel cell load decrease from 100% to 75% of design point. Primary control of fuel cell temperature at 1,100 K and secondary control of gas turbine speed and primary control of blower/compressor mixture temperature at 800 K with secondary control of recycle blower speed. ....	498
Figure A2.2 - 99: Compressor dynamic response to a fuel cell load decrease from 100% (blue) to 50% (red) of design state. Primary control of fuel cell temperature at 1,100 K and secondary control of gas turbine shaft speed and primary control of blower/compressor mixture temperature at 800 K and secondary control of blower speed. ....	499
Figure A2.2 - 100: Dynamic tri-layer temperature response to a fuel cell load decrease from 100% to 50% of design point. Primary control of fuel cell temperature at 1,100 K and secondary control of gas turbine speed and primary control of blower/compressor mixture temperature at 800 K with secondary control of recycle blower speed. ....	500
Figure A2.2 - 101: Dynamic gas turbine shaft speed response to a fuel cell load decrease from 100% to 50% of design point. Primary control of fuel cell temperature at 1,100 K and secondary control of gas turbine speed and primary control of blower/compressor mixture temperature at 800 K with secondary control of recycle blower speed. ....	501
Figure A2.2 - 102: Compressor dynamic response to a fuel cell load increase from 100% (blue) to 150% (red) of design state. Primary control of fuel cell temperature at 1,100 K and secondary control of gas turbine shaft speed and primary control of blower/compressor mixture temperature at 800 K and secondary control of blower speed. ....	502
Figure A2.2 - 103: Dynamic tri-layer temperature response to a fuel cell load increase from 100% to 125% of design point. Primary control of fuel cell temperature at 1,100 K and secondary control of gas turbine speed and primary control of blower/compressor mixture temperature at 800 K with secondary control of recycle blower speed. ....	503
Figure A2.2 - 104: Dynamic gas turbine shaft speed response to a fuel cell load increase from 100% to 125% of design point. Primary control of fuel cell temperature at 1,100 K and secondary control of gas turbine speed and primary control of blower/compressor mixture temperature at 800 K with secondary control of recycle blower speed. ....	504
Figure A2.2 - 105: Dynamic tri-layer temperature response to a fuel cell load increase from 100% to 97.5% of design point. Primary control of fuel cell temperature at 1,100 K and secondary control of gas turbine speed and primary control of blower/compressor mixture temperature at 800 K with secondary control of recycle blower speed. ....	505

Figure A2.2 - 106: Dynamic gas turbine shaft speed response to a fuel cell load increase from 100% to 97.5% of design point. Primary control of fuel cell temperature at 1,100 K and secondary control of gas turbine speed and primary control of blower/compressor mixture temperature at 800 K with secondary control of recycle blower speed. .... 506

Figure A2.2 - 107: Compressor dynamic response to a decrease in fuel hydrogen balanced with nitrogen from 100% (blue) to 90% (red) of design state. Primary control of fuel cell temperature at 1,100 K and secondary control of gas turbine shaft speed and primary control of blower/compressor mixture temperature at 800 K and secondary control of blower speed. .... 507

Figure A2.2 - 108: Compressor dynamic response to a decrease in fuel hydrogen balanced with nitrogen from 100% (blue) to 75% (red) of design state. Primary control of fuel cell temperature at 1,100 K and secondary control of gas turbine shaft speed and primary control of blower/compressor mixture temperature at 800 K and secondary control of blower speed. .... 508

Figure A2.2 - 109: Dynamic anode-cathode inlet pressure difference response to a decrease in fuel hydrogen balanced with nitrogen from 100% to 75% of design point. Primary control of fuel cell temperature at 1,100 K and secondary control of gas turbine speed and primary control of blower/compressor mixture temperature at 800 K with secondary control of recycle blower speed. .... 509

Figure A2.2 - 110: Dynamic anode inlet-outlet temperature difference response to a decrease in fuel hydrogen balanced with nitrogen from 100% to 75% of design point. Primary control of fuel cell temperature at 1,100 K and secondary control of gas turbine speed and primary control of blower/compressor mixture temperature at 800 K with secondary control of recycle blower speed ..... 510

Figure A2.2 - 111: Dynamic cathode inlet-outlet temperature difference response to a decrease in fuel hydrogen balanced with nitrogen from 100% to 75% of design point. Primary control of fuel cell temperature at 1,100 K and secondary control of gas turbine speed and primary control of blower/compressor mixture temperature at 800 K with secondary control of recycle blower speed. .... 511

Figure A2.2 - 112: Dynamic average fuel cell temperature response to a decrease in fuel hydrogen balanced with nitrogen from 100% to 75% of design point. Primary control of fuel cell temperature at 1,100 K and secondary control of gas turbine speed and primary control of blower/compressor mixture temperature at 800 K with secondary control of recycle blower speed..... 512

Figure A2.2 - 113: Dynamic tri-layer temperature response to a decrease in fuel hydrogen balanced with nitrogen from 100% to 75% of design point. Primary control of fuel cell temperature at 1,100 K and secondary control of gas turbine speed and primary control of blower/compressor mixture temperature at 800 K with secondary control of recycle blower speed..... 513

Figure A2.2 - 114: Dynamic gas turbine shaft speed response to a decrease in fuel hydrogen balanced with nitrogen from 100% to 75% of design point. Primary control of fuel cell temperature at 1,100 K and secondary control of gas turbine speed and primary control of blower/compressor mixture temperature at 800 K with secondary control of recycle blower speed..... 514

Figure A2.2 - 115: Compressor dynamic response to a decrease in fuel hydrogen balanced with nitrogen from 100% (blue) to 50% (red) of design state. Primary control of fuel cell temperature at 1,100 K and secondary control of gas turbine shaft speed and primary control

of blower/compressor mixture temperature at 800 K and secondary control of blower speed. .....	515
Figure A2.2 - 116: Compressor dynamic response to a decrease in fuel hydrogen balanced with steam from 100% (blue) to 90% (red) of design state. Primary control of fuel cell temperature at 1,100 K and secondary control of gas turbine shaft speed and primary control of blower/compressor mixture temperature at 800 K and secondary control of blower speed. .....	516
Figure A2.2 - 117: Compressor dynamic response to a decrease in fuel hydrogen balanced with steam from 100% (blue) to 75% (red) of design state. Primary control of fuel cell temperature at 1,100 K and secondary control of gas turbine shaft speed and primary control of blower/compressor mixture temperature at 800 K and secondary control of blower speed. .....	517
Figure A2.2 - 118: Compressor dynamic response to a decrease in fuel hydrogen balanced with steam from 100% (blue) to 50% (red) of design state. Primary control of fuel cell temperature at 1,100 K and secondary control of gas turbine shaft speed and primary control of blower/compressor mixture temperature at 800 K and secondary control of blower speed. .....	518
Figure A2.2 - 119: Compressor dynamic response to a decrease in fuel hydrogen balanced with methane from 100% to 75% of design point. Primary control of fuel cell temperature at 1,100 K and secondary control of gas turbine speed and primary control of blower/compressor mixture temperature at 800 K with secondary control of recycle blower speed. ....	519
Figure A2.2 - 120: Dynamic anode-cathode inlet pressure difference response to a decrease in fuel hydrogen balanced with methane from 100% to 75% of design point. Primary control of fuel cell temperature at 1,100 K and secondary control of gas turbine speed and primary control of blower/compressor mixture temperature at 800 K with secondary control of recycle blower speed. ....	520
Figure A2.2 - 121: Dynamic anode inlet-outlet temperature difference response to a decrease in fuel hydrogen balanced with methane from 100% to 75% of design point. Primary control of fuel cell temperature at 1,100 K and secondary control of gas turbine speed and primary control of blower/compressor mixture temperature at 800 K with secondary control of recycle blower speed. ....	521
Figure A2.2 - 122: Dynamic cathode inlet-outlet temperature difference response to a decrease in fuel hydrogen balanced with methane from 100% to 75% of design point. Primary control of fuel cell temperature at 1,100 K and secondary control of gas turbine speed and primary control of blower/compressor mixture temperature at 800 K with secondary control of recycle blower speed. ....	522
Figure A2.2 - 123: Dynamic average fuel cell temperature response to a decrease in fuel hydrogen balanced with methane from 100% to 75% of design point. Primary control of fuel cell temperature at 1,100 K and secondary control of gas turbine speed and primary control of blower/compressor mixture temperature at 800 K with secondary control of recycle blower speed. ....	523
Figure A2.2 - 124: Dynamic tri-layer temperature response to a decrease in fuel hydrogen balanced with methane from 100% to 75% of design point. Primary control of fuel cell temperature at 1,100 K and secondary control of gas turbine speed and primary control of blower/compressor mixture temperature at 800 K with secondary control of recycle blower speed. ....	524

Figure A2.2 - 125: Dynamic gas turbine shaft speed response to a decrease in fuel hydrogen balanced with methane from 100% to 75% of design point. Primary control of fuel cell temperature at 1,100 K and secondary control of gas turbine speed and primary control of blower/compressor mixture temperature at 800 K with secondary control of recycle blower speed. ....	525
Figure A2.2 - 126: Compressor dynamic response to a fuel cell shutdown over 8 hours. Primary control of fuel cell temperature at 1,100 K and secondary control of gas turbine speed and primary control of blower/compressor mixture temperature at 800 K with secondary control of recycle blower speed. ....	526
Figure A2.2 - 127: Dynamic anode-cathode inlet pressure difference response to a fuel cell shutdown over 8 hours. Primary control of fuel cell temperature at 1,100 K and secondary control of gas turbine speed and primary control of blower/compressor mixture temperature at 800 K with secondary control of recycle blower speed.....	527
Figure A2.2 - 128: Dynamic anode inlet-outlet temperature difference response to a fuel cell shutdown over 8 hours. Primary control of fuel cell temperature at 1,100 K and secondary control of gas turbine speed and primary control of blower/compressor mixture temperature at 800 K with secondary control of recycle blower speed.....	528
Figure A2.2 - 129: Dynamic cathode inlet-outlet temperature difference response to a fuel cell shutdown over 8 hours. Primary control of fuel cell temperature at 1,100 K and secondary control of gas turbine speed and primary control of blower/compressor mixture temperature at 800 K with secondary control of recycle blower speed.....	529
Figure A2.2 - 130: Dynamic average fuel cell temperature response to a fuel cell shutdown over 8 hours. Primary control of fuel cell temperature at 1,100 K and secondary control of gas turbine speed and primary control of blower/compressor mixture temperature at 800 K with secondary control of recycle blower speed. ....	530
Figure A2.2 - 131: Dynamic tri-layer temperature response to a fuel cell shutdown over 8 hours. Primary control of fuel cell temperature at 1,100 K and secondary control of gas turbine speed and primary control of blower/compressor mixture temperature at 800 K with secondary control of recycle blower speed. ....	531
Figure A2.2 - 132: Dynamic gas turbine shaft speed response to a fuel cell shutdown over 8 hours. Primary control of fuel cell temperature at 1,100 K and secondary control of gas turbine speed and primary control of blower/compressor mixture temperature at 800 K with secondary control of recycle blower speed. ....	532
Figure A2.2 - 133: Compressor dynamic response to a fuel cell shutdown over 8 days. Primary control of fuel cell temperature at 1,100 K and secondary control of gas turbine speed and primary control of blower/compressor mixture temperature at 800 K with secondary control of recycle blower speed. ....	533
Figure A2.2 - 134: Integrated Gasification Fuel Cell Power Plant.....	539
Figure A2.2 - 135: Section of the Plant for Dynamic Analysis.....	540
Figure A2.3- 1: Thermal Performance – H Class (1392°C RIT) GT Cases .....	550
Figure A2.3- 2: Thermal Performance – Advanced (1734°C RIT) GT Cases.....	550
Figure A2.3- 3: Specific O <sub>2</sub> Consumption – H Class (1392°C RIT) GT Cases .....	551
Figure A2.3- 4: Specific O <sub>2</sub> Consumption – Advanced (1734°C RIT) GT Cases.....	551

Figure A2.3- 5: Economic Worth of Additional CO <sub>2</sub> Capture – H Class (1392°C RIT) GT Cases .....	552
Figure A2.3- 6: Economic Worth of Additional CO <sub>2</sub> Capture – Advanced (1734°C RIT) GT Cases.....	552
Figure A2.3- 7: Block Flow Diagram - TQ IGCC Cases with 80% and 90% CO <sub>2</sub> Capture, GT RIT = 1392°C .....	555
Figure A2.3- 8: Block Flow Diagram - TQ IGCC Cases with 90% and 99%+ CO <sub>2</sub> Capture, GT RIT = 1392°C .....	556
Figure A2.3- 9: Block Flow Diagram – R+Q IGCC Cases with 80% and 90% CO <sub>2</sub> Capture, GT RIT = 1392°C .....	557
Figure A2.3- 10: Block Flow Diagram – R+Q IGCC Cases with 90% and 99%+ CO <sub>2</sub> Capture, GT RIT = 1392°C.....	558
Figure A2.3- 11: Block Flow Diagram - TQ IGCC Cases with 80% and 90% CO <sub>2</sub> Capture, GT RIT = 1734°C .....	559
Figure A2.3- 12: Block Flow Diagram - TQ IGCC Cases with 90% and 99%+ CO <sub>2</sub> Capture, GT RIT = 1734°C .....	560
Figure A2.3- 13: Block Flow Diagram – R+Q IGCC Cases with 80% and 90% CO <sub>2</sub> Capture, GT RIT = 1734°C .....	561
Figure A2.3- 14: Block Flow Diagram – R+Q IGCC Cases with 90% and 99%+ CO <sub>2</sub> Capture, GT RIT = 1734°C .....	562
Figure A2.3- 15: Block Flow Diagram - Oxy-combustion Cycle based Cases .....	563
Figure A2.3- 16: Block Flow Diagram - TQ IGCC SO <sub>2</sub> Co-sequestration Case with 90% CO <sub>2</sub> Capture, GT RIT = 1392°C .....	564
Figure A2.3- 17: Block Flow Diagram - Oxy-combustion Cycle based SO <sub>2</sub> Co-sequestration Case, GT RIT = 1392°C .....	565

## LIST OF ACRONYMS AND ABBREVIATIONS

AC	Alternating Current
AGRU	Acid Gas Removal Unit
ASU	Air Separation Unit
Atm	Atmosphere (Pressure)
CES	Clean Energy Systems
BarA	Bar Absolute (Pressure)
DOE	U.S. Department of Energy
EP	Elevated Pressure
FC	Fuel Cell
GE	General Electric
GJ	Giga Joules
GJ/hr	Giga Joules per hour
GSP	Gas Turbine Simulation Program
GT	Gas Turbine
HHV	Higher Heating Value
HP	High Pressure
HRSG	Heat Recovery Steam Generator
IGCC	Integrated Gasification Combined Cycle
IP	Intermediate Pressure
kg/s	Kilograms per Second
kJ	Kilo Joules
kPa	Kilo Pascal (Pressure)
kW	Kilowatt
LHV	Lower Heating Value
LP	Low Pressure
MATLAB	Matrix Laboratory (Mathworks, Inc.)
MF	Moisture Free
MJ	Mega Joule
MMBtu	Million British Thermal Units
MW	Megawatt
mW	Milliwatt
NASA	National Aeronautics and Space Administration
NETL	National Energy Technology Laboratory
NO <sub>x</sub>	Oxides of Nitrogen
O/C	Oxygen to Carbon Ratio
PID	Proportional Integral Derivative (Controller)
ppmVd	Parts per Million by Volume on a Dry Basis
psi	Pounds per Square Inch (Pressure)
RIT	Rotor Inlet Temperature
RPM	Revolutions per Minute
SCR	Selective Catalytic Reduction
SECA	Solid State Energy Conversion Alliance
SOFC	Solid Oxide Fuel Cell
SO <sub>x</sub>	Oxides of Sulfur
SRU	Sulfur Removal Unit
ST	Short Ton
Tonne/D	Metric Ton (1000 kg) per Day

TBC  
Vol %  
\$

Thermal Barrier Coating  
Percentage by Volume  
United States Dollar

## EXECUTIVE SUMMARY

### OBJECTIVES

The main objective is to identify and assess advanced improvements to the Brayton Cycle (such as but not limited to firing temperature, pressure ratio, combustion techniques, intercooling, fuel or combustion air augmentation, enhanced blade cooling schemes) that will lead to significant performance improvements in coal based power systems. This assessment is conducted in the context of conceptual design studies (systems studies) that advance state-of-art Brayton cycles and result in coal based efficiencies equivalent to 65% + on natural gas basis (LHV), or approximately an 8% reduction in heat rate of an IGCC plant utilizing the H class steam cooled gas turbine. H class gas turbines are commercially offered by General Electric and Mitsubishi for natural gas based combined cycle applications with 60% efficiency (LHV) and it is expected that such machine will be offered for syngas applications within the next 10 years.

The studies are being sufficiently detailed so that third parties will be able to validate portions or all of the studies. The designs and system studies are based on plants for near zero emissions (including CO<sub>2</sub>). Also included in this program is the performance evaluation of other advanced technologies such as advanced compression concepts and the fuel cell based combined cycle. The objective of the fuel cell based combined cycle task is to identify the desired performance characteristics and design basis for a gas turbine that will be integrated with an SOFC in Integrated Gasification Fuel Cell (IGFC) applications.

### SCOPE OF PROJECT

The goal is the conceptualization of near zero emission (including CO<sub>2</sub> capture) integrated gasification power plants producing electricity as the principle product. The capability of such plants to coproduce H<sub>2</sub> is qualitatively addressed. Since a total systems solution is critical to establishing a plant configuration worthy of a comprehensive market interest, a baseline IGCC plant scheme is developed and used to study how alternative process schemes and power cycles might be used and integrated to achieve higher systems efficiency. To achieve these design results, the total systems approach is taken requiring creative integration of the various process units within the plant.

Advanced gas turbine based cycles for Integrated gasification Combined cycle (IGCC) applications are identified by a screening analysis and the more promising cycles recommended for detailed systems analysis.

In the case of the IGFC task, the main objective is met by developing a steady-state simulation of the entire plant and then using dynamic simulations of the hybrid Solid Oxide Fuel Cell (SOFC) / Gas Turbine sub-system to investigate the turbo-machinery performance. From these investigations the desired performance characteristics and a basis for design of turbo-machinery for use in a fuel cell gas turbine power block is developed.

## **SUMMARY OF RESULTS**

### **Task 1.1 Milestone**

1. **Title:** Set System Study Methodologies for Advanced Brayton Cycle Study
2. **Brief Description of what is to be Accomplished:** This task is to provide an explanation of the systems study procedures to be used to evolve the conceptual gasification based plant designs.
3. **Planned start date:** October 1, 2005
4. **Actual Start Date:** October 1, 2005
5. **Planned End Date:** December 31, 2005
6. **Actual End Date:** March 31, 2006 (due to revised study approach)
7. **Brief Description of Results:** This systems study procedure established the following:
  - site conditions and feedstock characteristics
  - advanced Brayton cycle technology projections
  - SOFC / GT design guidelines
  - overall plant design criteria
  - procedure for executing material and energy balances
  - procedure for setting equipment specifications where required
  - third party validation of a detail or the entire study is addressed.

### **Task 1.2 Milestone**

1. **Title:** Identify Baseline Cycle Configuration for Advanced Brayton Cycle Study
2. **Brief Description of what is to be Accomplished:** This task is to identify the overall plant configuration for the Baseline Cycle that will be used for comparing the advanced Brayton cycle concepts to be developed in subsequent tasks.
3. **Planned start date:** November 1, 2005
4. **Actual Start Date:** November 1, 2005
5. **Planned End Date:** December 31, 2005
6. **Actual End Date:** March 31, 2006 (due to revised study approach)
7. **Brief Description of Results:** The selected plant scheme for the defined Baseline Cycle consists of a cryogenic air separation unit supplying 95% purity O<sub>2</sub> to GE type high pressure quench gasifiers. The raw gas after scrubbing is treated in a sour shift unit to react the CO with H<sub>2</sub>O to form H<sub>2</sub> and CO<sub>2</sub>. The gas is further treated to remove Hg in a sulfided activated carbon bed. The syngas is desulfurized and decarbonized in a Selexol<sup>®</sup>

acid gas removal unit and the decarbonized syngas after humidification and preheat is fired in a GE 7H type steam-cooled gas turbine. Intermediate pressure N<sub>2</sub> from the air separation unit (ASU) is also supplied to the combustor of the gas turbine as additional diluent for NO<sub>x</sub> control. A portion of the air required by the ASU is extracted from the gas turbines. An ultra low NO<sub>x</sub> (2 ppmvd, 15% O<sub>2</sub> basis) sensitivity case is identified that includes an SCR in the heat recovery steam generator.

### **Task 1.3 Milestone**

1. **Title:** First Detailed Systems Study Analysis – Baseline Case for Advanced Brayton Cycle Study
2. **Brief Description of what is to be Accomplished:** This task is to perform a detailed analysis of the Baseline Cycle configured in the previous Task 1.2 to develop the overall plant performance.
3. **Planned start date:** January 2, 2006
4. **Actual Start Date:** April 1, 2006 (due to revised study approach which delayed completion of Task 1.2)
5. **Planned End Date:** June 30, 2006
6. **Actual End Date:** June 30, 2006
7. **Brief Description of Results:** The simulation of the plant outside the power block for the Baseline Case IGCC facility was developed on Aspen Plus while that for the power block was developed on Thermoflex. The net power output of this IGCC facility utilizing a single train GE 7H type gas turbine while gasifying Pittsburgh No. 8 coal and capturing 90% of the carbon present in the syngas as gaseous compounds (CO<sub>2</sub> leaving the plant battery limits at 138.9 bara or 2015 psia), is 383.2 MW at ISO conditions. The net plant heat rate is 10,305 kJ/kWh (HHV) which is about 5 to 10% lower than an IGCC plant also designed for 90% carbon capture but utilizing GE 7FA+e gas turbines. A sensitivity case over the Baseline Case was developed to assess the impact of limiting the NO<sub>x</sub> emissions to 2 ppmVd (15% O<sub>2</sub> basis) by installing an SCR in the HRSG downstream of the gas turbine. The IGCC plant performance was insignificantly affected. The sulfur content of the decarbonized syngas is insignificant to cause any problems associated with formation of ammonium salts. A catalytic NH<sub>3</sub> oxidation unit may be installed in the HRSG downstream of the SCR if the NH<sub>3</sub> slippage from the SCR is cause for concern from an environmental emissions standpoint. The effect on the overall plant heat rate of this additional catalytic unit is expected to be similar to that of the SCR.

### **Task 1.4.1 Milestone**

1. **Title:** Screening Analysis of Advanced Brayton Cycles

2. **Brief Description of what is to be Accomplished:** This task is to identify advanced Brayton cycle concepts for Screening Analysis and then to perform an analysis at a screening level in order to select promising cycles for detailed analysis in the subsequent task.
3. **Planned start date:** June 1, 2006
4. **Actual Start Date:** June 1, 2006
5. **Planned End Date:** September 30, 2006
6. **Actual End Date:** September 30, 2006
7. **Brief Description of Results:** The following lists the advanced Brayton cycle concepts identified for Screening Analysis. This analysis included identifying changes to the basic cycle configuration and / or conditions.
  - 1) Increased Firing Temperature / Blade Surface Temperature
  - 2) Intercooled Gas Turbine
  - 3) Intercooled and Reheat Gas Turbine
  - 4) Humid Air Cooling of Gas Turbine Blades
  - 5) Closed Circuit Air Cooling of Gas Turbine Blades
  - 6) Pressure Gain Combustor
  - 7) Air Partial Oxidation Topping Cycle
  - 8) Oxy Combustion Gas Turbine including the Partial Oxidation (POx) Gas Turbine
  - 9) Humid Air Turbine Cycle
  - 10) Supercritical Rankine Bottoming Cycle
  - 11) Chemical Recuperation
  - 12) Inlet Air Fogging
  - 13) Inverse Cycle

This screening analysis identified the following promising cycles for the next detailed analysis task:

  - 1) Steam-cooled Simple Cycle Gas Turbine based Combined Cycle
  - 2) Steam-cooled Intercooled Gas Turbine based Combined Cycle
  - 3) Steam-cooled Intercooled and Reheat Gas Turbine based Combined Cycle
  - 4) Air POx Topping Cycle added to a Steam-cooled Gas Turbine based Combined Cycle
  - 5) Closed Circuit Air-cooled Gas Turbine based Combined Cycle.

#### **Task 1.4.2 Milestone**

1. **Title:** Detailed Analysis of Advanced Brayton Cycles
2. **Brief Description of what is to be Accomplished:** This task is to identify the most promising advanced Brayton cycle concept by performing a detailed analysis of the five cycles identified in the previous screening analysis task. Also included in this task is the development of rough order of magnitude cost estimates of the most promising cycle identified by this task relative to the Baseline Case.

3. Planned start date: October 1, 2006
4. Actual Start Date: October 1, 2006
5. Planned End Date: September 30, 2007
6. Actual End Date: December 31, 2007
7. **Brief Description of Results:** The closed circuit steam-cooled intercooled gas turbine (with a rotor inlet temperature of 1734°C or 3153°F) was selected as the most promising cycle by performing a detailed analysis of the five advanced cycles identified in the previous task. This cycle requires a pressure ratio of 50 which is not significantly higher than that of a commercially proven aero-engine while limiting the exhaust temperature to a reasonable value. It incorporates spray intercooling which has been proven in a commercial land-based aero-engine derived gas turbine and has the advantage of lowering compressor discharge temperature resulting in savings in materials of construction, lower NOx emission and higher specific power output. Steam cooling, another feature of this cycle has been proven in the H class machines. Sensitivity analysis conducted to measure the impact of increasing the component efficiencies of this advanced gas turbine showed that the individual contributions are not very significant but the sum total is, justifying research and development in these areas. The rough order of magnitude plant cost and cost of electricity of the selected advanced Brayton cycle are about 8% lower than those of the Baseline Case. The greatest technological challenge for the development of this advanced gas turbine is in the area of combustor and turbine materials required to withstand the very high firing temperature.

### **Task 2.1 Milestone**

1. Title: Evaluation of Impact of Ramgen Compression Technology on IGCC Plant Performance
2. Brief Description of what is to be Accomplished: This task is to evaluate the impact of incorporating Ramgen compression technology in a near zero emission IGCC plant from an overall plant performance standpoint in order to quantify the advantages this technology may be able to offer in such applications.
3. Planned start date: June 1, 2006
4. Actual Start Date: June 1, 2006
5. Planned End Date: December 31, 2007
6. Actual End Date: March 31, 2008
7. **Brief Description of Results:** From an overall plant thermal efficiency standpoint, the Ramgen high efficiency intercooled CO<sub>2</sub> compressor technology is more promising than their non-intercooled compressor. The net increase in power output over the Baseline Case of utilizing the Ramgen low pressure, intermediate pressure and intercooled high

pressure compressors for CO<sub>2</sub> compression is 1.61 MW for this 380 MW IGCC plant. By applying the Ramgen technology to the gas turbine extraction air expander, the ASU air and nitrogen compressors in addition to the CO<sub>2</sub> compressors, the net power output over the Baseline Case is increased by as much as 5.92 MW for this 380 MW IGCC plant. Thus, the high efficiency intercooled Ramgen compressors can play a significant role in improving the efficiency of IGCC plants, especially in zero emission plants where CO<sub>2</sub> capture is required, subject to verification of the compressor efficiencies by test work.

### **Task 2.2.1 Milestone**

1. **Title:** Overall Plant Design Basis for “GT Requirements for Gasification based FC / GT System” Study
2. **Brief Description of what is to be Accomplished:** This task is to establish the overall plant design basis for the study to define the GT requirements for gasification based FC / GT systems.
3. **Planned start date:** June 1, 2006
4. **Actual Start Date:** June 1, 2006
5. **Planned End Date:** June 30, 2006
6. **Actual End Date:** June 30, 2006
7. **Brief Description of Results:** The gasification plant configuration and technology as well as the design basis for the SOFC (geometry, fuel utilization, maximum anode and cathode gas temperature rises, power density, operating pressures, etc) and the gas turbine cycle were established.

### **Task 2.2.2 Milestone**

1. **Title:** SOFC/GT System I/O Stream Specifications at Steady State Operation for “GT Requirements for Gasification based FC / GT System” Study
2. **Brief Description of what is to be Accomplished:** This task is to establish steady state I/O stream specifications for the SOFC/GT subsystem in the gasification based plant.
3. **Planned start date:** July 1, 2006
4. **Actual Start Date:** July 1, 2006
5. **Planned End Date:** July 31, 2006
6. **Actual End Date:** July 31, 2006

7. **Brief Description of Results:** The SOFC/GT subsystem input stream specifications consisting of the syngas composition and temperature were developed at steady state in order to develop the SOFC/GT performance estimates which in turn defined the SOFC/GT subsystem output stream specifications to complete the balance of plant energy integration.

### **Task 2.2.3 Milestone**

1. **Title:** Dynamic Simulation of FC/GT System for “GT Requirements for Gasification based FC / GT System” Study
2. **Brief Description of what is to be Accomplished:** This task is to identify the desired performance characteristics and design basis for a gas turbine that will be integrated with an SOFC in IGCC applications.
3. **Planned start date:** August 1, 2006
4. **Actual Start Date:** August 1, 2006
5. **Planned End Date:** June 30, 2007
6. **Actual End Date:** December 31, 2007
7. **Brief Description of Results:** The main objective was met by developing a steady-state simulation of the entire plant and then using dynamic simulations of the hybrid SOFC/GT sub-system to investigate the turbo-machinery performance. From these investigations the desired performance characteristics and a basis for design of turbo-machinery for use in a fuel cell gas turbine power block were developed. The major findings are:
  - a cathode blower is preferred to an ejector for cathode gas recycle for efficiency and control purposes
  - perturbations that could lead to compressor surge could damage the fuel cell
  - load-shed perturbations are especially challenging for avoidance of compressor surge
  - special turbo-machinery designs and control strategies have been developed and tested to show how compressor surge can be avoided during perturbations
  - design of turbo-machinery with larger surge margin is recommended for SOFC/GT systems
  - minimizing the fuel cell plenum volume is important to address dynamic operation during perturbations
  - design of the system with additional actuators (e.g., bleed valves, fuel injection) is desirable for controlling the system during perturbations.The major recommendations are:
  - study of additional control strategies for SOFC/GT systems
  - development of matched turbo-machinery with larger surge margins
  - study of axial versus radial turbo-machinery for these applications
  - development and use of additional actuators that can be manipulated with fast dynamic response (e.g., bleed, bypass, control valves).

### **Task 2.2.4 Milestone**

1. **Title:** Integration of SOFC/GT into Gasification Plant for IGFC Steady State Performance for “GT Requirements for Gasification based FC / GT System” Study
2. **Brief Description of what is to be Accomplished:** This task is to identify the desired performance characteristics and design basis for a gas turbine that will be integrated with an SOFC in IGCC applications.
3. **Planned start date:** July 1, 2007
4. **Actual Start Date:** July 1, 2007
5. **Planned End Date:** September 30, 2007
6. **Actual End Date:** September 30, 2007
7. **Brief Description of Results:** The steady state performance estimates for the IGFC plants with 90% CO<sub>2</sub> capture (CO<sub>2</sub> leaving the plant battery limits at 138.9 bara or 2015 psia) utilizing currently proven technologies for balance of plant subsystems showed that the net plant thermal efficiency can range from 39.5 to 41.6% (HHV basis) with the SOFC operating pressure varying from 5 to 10 atm.

### **Task 2.3 Milestone**

- **Title:** Performance Comparison of Oxy-combustion and IGCC Plants
- **Brief Description of what is to be Accomplished:** This task is to compare the oxy-combustion cycle being developed by Clean Energy Systems (CES) with the down-selected advanced Brayton cycle based combined cycle in integrated coal gasification plants.
- **Planned start date:** July 1, 2008
- **Actual Start Date:** July 1, 2008
- **Planned End Date:** September 30, 2008
- **Actual End Date:** September 30, 2008
- **Brief Description of Results:** Unless there is a substantial reduction in the cost for the oxy-combustion based plant which appears to be unlikely due to its significantly higher O<sub>2</sub> consumption, the oxy-combustion based cycle in coal gasification plants appears to show no efficiency nor economic advantage over the IGCC.

## **APPROACH**

Technical barriers and issues as well as R&D needed to overcome these issues were identified as the tasks described under this section were being performed. Insights as they occurred were documented and discussed in Quarterly Progress Reports and Project Review Meetings, and are summarized in this Final Report. In the process of completing a module or element of a system model as part of the systems analysis, the technical barriers and issues if any, that must be overcome in order to satisfy the requirements of the system are identified. The following describe the various tasks undertaken sequentially to reach the overall program goals.

### **TASK 1.1 – SET SYSTEM STUDY METHODOLOGIES**

Before subsequent tasks were started, a detailed explanation of the systems study procedure to be used to evolve the conceptual IGCC plant design was submitted to the COR. The procedure explained the rationale or approach for choosing plant size, for arranging and interconnecting major equipment items and plant units, for executing materials and energy balances and for setting unique equipment specifications where required.

The procedure was meant to simplify, to the degree practical, a third party validating a detail or the entire study. A goal of the procedure used was the documentation to minimize the study validation process by third parties.

The procedure also included the identification as appropriate of technical barriers / issues and the technical approach(s) that would be applied: (1) in order to resolve these technical issues and (2) to estimate order of magnitude costs required for the development of the technology or technologies.

### **TASK 1.2 – IDENTIFY BASELINE CYCLE CONFIGURATION**

Before engaging in detailed energy balance analysis, an assessment of alternative flow sheet "schemes" was made in order to select one for establishing the Baseline Case in order to provide a basis for comparing the advanced Brayton cycle technologies developed and studied under this program such that a comparison of technologies to be available during similar time frames was facilitated and the incentives if any, for developing the advanced Brayton cycle technologies (hardware wise) could be quantified.

### **TASK 1.3 - FIRST DETAILED SYSTEMS STUDY ANALYSIS**

A detailed thermodynamic analysis of the plant scheme identified in Task 1.2 was performed to determine the preferred (or first best guess) IGCC plant equipment and streams configuration to accommodate the Baseline Brayton Cycle. Every attempt was made to set up this first conceptual plant systems design as a model that was amenable to easy (requiring minimal resources) sensitivity analysis to aid discovery of process improvements or for gaining insights to establish a superior and dramatically different or unique IGCC plant scheme in the subsequent tasks.

## TASK 1.4 - SUBSEQUENT DETAILED SYSTEMS STUDY ANALYSES

The following lists the initial activities that were included in this task to select promising cycles for inclusion in the systems analysis:

- Based on previous experience with advanced cycle concepts and by performing a literature search, identify gas turbine based cycles that have a potential for high efficiency in IGCC applications.
- Conduct brainstorming sessions in order to identify those gas turbine based cycles that have a potential to meet the objectives of this program. Improvements to these cycles as well as the evolution of new cycle configurations by synergistically combining aspects of other cycles are also brainstormed.
- Perform a screening analysis to select the more promising cycles for detailed systems analysis.

As part of the identification process, the literature search where required was documented by UC Irvine as well as the findings through the work of the previous task utilized, in order to show the basis for choices made in configuring the plants. The COR approval was requested by UC Irvine to proceed with the systems analysis and design of the proposed unique Brayton Cycle schemes.

Some of the technological advances being made or being investigated to improve the Brayton cycle included the following:

- Rotor inlet temperature of 1700°C (3100°F) or higher which would require the development and use of advanced materials including advanced thermal barrier coatings and turbine cooling techniques including closed loop steam cooling.
- High blade surface temperature in the neighborhood of ~1040°C (1900°F) while limiting coolant amount would again require the development and use of the advanced materials including advanced thermal barrier coatings.
- Improvements to the aerodynamic and mechanical design such as pressure gain combustion, improved compressor and / or turbine isentropic efficiencies.
- Advanced gas turbine combustor concepts to limit the combustor diluent addition to a value which optimizes the overall plant thermal efficiency while minimizing the NO<sub>x</sub> emissions.
- High pressure ratio compressor (greater than 30 to take full advantage of higher firing temperature).
- Catalytic combustors (such as that being developed by Precision Combustion, Inc).

- Cycle changes such as air humidification and recuperation, inlet air fogging, in-situ reheating and intercooling.
- Oxy combustion.

The balance of plant configuration and technology were selected in order to synergistically integrate with the particular Advanced Brayton cycle under investigation such that the overall plant performance was optimized. The effect of incorporating the various advanced technology concepts were studied methodically such that any gain in performance realized could be associated with the particular change in cycle condition or configuration made.

## **TASK 2 - ADDITIONAL SYSTEMS STUDIES**

Additional Systems Studies as needed were performed upon mutual agreement of UC Irvine and COR and dependent upon funding availability. Three such studies conducted were:

- Task 2.1 – Evaluation of Advanced Compression Technology in IGCC Applications: This task evaluated the impact of Ramgen technology on IGCC plant performance.
- Task 2.2 – Gas Turbine Operating Requirements for Gasification based Fuel Cell / Gas Turbine System: This task developed the dynamic simulation of a SOFC / Gas Turbine system to obtain gas turbine operating requirements including steady state performance in order to fix system geometry. Specifically, the following were developed in addition to the overall IGFC plant performance:
  - Determine SOFC /Gas Turbine power block configuration of interest
  - Develop dynamic SOFC / Gas Turbine power block model
  - Use dynamic power block model to determine how and under what operating conditions the turbomachinery fails
  - Manipulate compressor and turbine maps in a reasonable manner to improve performance
  - Provide modified maps and guidance on map characteristics that are best suited to robust SOFC / Gas Turbine dynamic performance.
- Task 2.3 - Performance Comparison of Oxy-combustion and IGCC Plants: This task compared the oxy-combustion cycle being developed by Clean Energy Systems (CES) with the down-selected advanced Brayton cycle based combined cycle in integrated coal gasification plants.

## RESULTS AND DISCUSSION

### TASK 1.1 – SET SYSTEM STUDY METHODOLOGIES

The system study methodologies established for this study are included in this report in the Appendix. It provides an explanation of the systems study procedure to be used to evolve the conceptual gasification based plant designs. This systems study procedure provides the following:

- site conditions and feedstock characteristics
- advanced Brayton cycle technology projections
- SOFC / GT design guidelines
- overall plant design criteria
- procedure for executing material and energy balances
- procedure for setting equipment specifications where required
- a procedure for third party validation of a detail or the entire study such that the study validation process by third parties is minimized.

### TASK 1.2 – IDENTIFY BASELINE CYCLE CONFIGURATION

The identification of Baseline Cycle configuration established for this study are included in this report in the Appendix. It provides a discussion of the various process options available or under development for an IGCC facility and a description of the qualitative technology evaluation conducted in order to identify those options that may be suitable for incorporation in the Baseline Case design.

The selected plant scheme consists of a cryogenic air separation unit supplying 95% purity O<sub>2</sub> to GE type HP total quench gasifiers. The raw gas after scrubbing is treated in a sour shift unit to react the CO with H<sub>2</sub>O to form H<sub>2</sub> and CO<sub>2</sub>. The gas is further treated to remove Hg in a sulfided activated carbon bed. The syngas is desulfurized and decarbonized in a Selexol acid gas removal unit and the decarbonized syngas after humidification and preheat is fired in a GE 7H type steam cooled gas turbine. IP N<sub>2</sub> from the ASU is also supplied to the combustor of the gas turbine as additional diluent for NO<sub>x</sub> control. A portion of the air required by the ASU is extracted from the gas turbines.

An ultra low NO<sub>x</sub> (2 ppmvd, 15% O<sub>2</sub> basis) sensitivity case is identified that includes an SCR in the heat recovery steam generator.

### TASK 1.3 - FIRST DETAILED SYSTEMS STUDY ANALYSIS – BASELINE CASE

The simulation of the plant outside the power block for the Baseline Case IGCC facility was developed on Aspen Plus while that for the power block was developed on Thermoflex. Process

descriptions of these various units along with the process flow diagrams and the corresponding stream data are provided in the Appendix section of this report.

The overall plant scheme consists of a cryogenic air separation unit supplying 95% purity O<sub>2</sub> to GE type high pressure (HP) total quench gasifiers. The raw gas after scrubbing is treated in a sour shift unit to react the CO with H<sub>2</sub>O to form H<sub>2</sub> and CO<sub>2</sub>. The gas is further treated to remove Hg in a sulfided activated carbon bed. The syngas is desulfurized and decarbonized in a Selexol acid gas removal unit and the decarbonized syngas after humidification and preheat is fired in a GE 7H type steam cooled gas turbine. Intermediate pressure (IP) N<sub>2</sub> from the ASU is also supplied to the combustor of the gas turbine as additional diluent for NO<sub>x</sub> control. A portion of the air required by the ASU is extracted from the gas turbines. The overall block flow diagram is presented in Figure A1.3 – 1 of the Appendix.

The plant consists of the following major process units:

- Air Separation Unit (ASU)
- Coal Receiving and Handling Unit
- Gasification Unit
- CO Shift / Low Temperature Gas Cooling (LTGC) Unit
- Acid Gas Removal Unit (AGR) Unit
- Fuel Gas Humidification Unit
- Carbon Dioxide Compression / Dehydration Unit.
- Claus Sulfur Recovery / Tail Gas Treating Unit (SRU / TGTU)
- Power Block.

The overall plant performance is summarized in Table 1 while the in-plant power consumption summary is presented in Table 2. The net power output of this IGCC facility utilizing a single train GE 7H type gas turbine while gasifying Pittsburgh No. 8 coal and capturing 90% of the carbon present in the syngas as gaseous compounds, is 383.2 MW at ISO conditions. The net plant heat rate is 10,305 kJ/kWh (HHV) which is about 5 to 10% lower than an IGCC plant also designed for 90% carbon capture but utilizing GE 7FA+e gas turbines.

Air is extracted from the gas turbine to limit the increase in its pressure ratio while firing the lower heating value syngas (current gas turbines such as the GE 7H are designed for optimal operation on natural gas fuel). Since the air extracted from the gas turbine is at a significantly higher pressure than the typical supply pressure of an elevated pressure (EP) ASU cryogenic unit, the air pressure is let down through a power recovery turbo-expander (resulting in the “IP ASU Case”). As the operating pressure of the cold box is increased, the relative volatility between O<sub>2</sub> and N<sub>2</sub> approaches unity increasing the number of distillation stages in the cold box. If the extraction air is to be utilized in the EP ASU without first letting down its pressure, an additional distillation column may have to be added in the cryogenic cold box unit. The trade-off between extraction air expansion while using a more conventional (proven) EP ASU cold box design versus not letting the extraction air pressure down (thus eliminating the turbo-expander) and utilizing a cold box with an additional column should be established in a more detailed study with the involvement of the ASU vendor. The overall IGCC plant performance developed as a sensitivity case utilizing an estimated performance of the ASU operating at the higher pressure

(“HP ASU Case”), i.e., without the extraction air expander, showed that the gain would be quite small (results presented in Table 1).

### **Low NO<sub>x</sub> Sensitivity Case**

A sensitivity case over the Baseline Case was developed to assess the impact of limiting the NO<sub>x</sub> emissions to 2 ppmVd (15% O<sub>2</sub> basis) by installing an SCR in the HRSG downstream of the gas turbine. The gas turbine back pressure was increased in order to accommodate pressure drop across the SCR. Pressure drops ranging from by 2 to 5 In W.C. were investigated (the catalyst requirement and thus the cost of the SCR unit being reduced as the allowable pressure drop is increased). The IGCC plant performance was insignificantly affected. The heat rate increased from 10,305 kJ/kWh (Baseline Case) to 10,319 kJ/kWh with 2 In W.C. to 10,331 kJ/kWh with 5 In W.C. A catalytic NH<sub>3</sub> oxidation unit may be installed in the HRSG downstream of the SCR if the NH<sub>3</sub> slippage from the SCR is cause for concern from an environmental emissions standpoint. The pressure drop of this additional catalytic unit is expected to be similar to that of the SCR.

Problems associated with salt deposition in the HRSG equipped with an SCR when combusting a sulfur bearing fuel in the gas turbine have been experienced but in the present case the sulfur content of the decarbonized syngas is insignificant since the plant includes the following process steps:

- sour shift upstream of the acid gas removal unit
- acid gas removal unit to capture the CO<sub>2</sub> and also perform desulfurization of the syngas.

Most of the COS is hydrolyzed to H<sub>2</sub>S in the shift reactors, while due to the very large solvent circulation rate maintained in the acid gas removal unit to capture the CO<sub>2</sub>, the sulfur content of the treated syngas is very low. In such cases, the incremental cost penalties associated with producing low sulfur syngas suitable for firing in a gas turbine equipped with an SCR are not significant either.

### **TASK 1.4.1: SCREENING ANALYSIS OF ADVANCED BRAYTON CYCLES**

The following lists the advanced Brayton cycle concepts identified for Screening Analysis as part of the Task 1.4.1 activity. This analysis consists of identifying changes to the basic cycle configuration and / or conditions. Details of the work accomplished under this task are provided in the Appendix section of this report.

1. Increased Firing Temperature / Blade Surface Temperature
2. Intercooled Gas Turbine
3. Intercooled and Reheat Gas Turbine
4. Humid Air Cooling of Gas Turbine Blades
5. Closed Circuit Air Cooling of Gas Turbine Blades
6. Pressure Gain Combustor
7. Air Partial Oxidation Topping Cycle

8. Oxy Combustion Gas Turbine including the Partial Oxidation Gas Turbine
9. HAT Cycle
10. Supercritical Rankine Bottoming Cycle
11. Chemical Recuperation
12. Inlet Air Fogging
13. Inverse Cycle

Among these various advanced technology concepts screened, increased firing and blade surface temperatures, as well as reheat and pressure gain combustion showed promise of significant efficiency improvement.

Based on the results of this screening analysis task, the cycles listed below are identified as promising cycles recommended for evaluation in the next detailed analysis task.

1. Steam-cooled Simple Cycle Gas Turbine based Combined Cycle
2. Steam-cooled Intercooled Gas Turbine based Combined Cycle
3. Steam-cooled Intercooled and Reheat Gas Turbine based Combined Cycle
4. Air POx Topping Cycle added to a Steam-cooled Gas Turbine based Combined Cycle
5. Closed Circuit Air-cooled Gas Turbine based Combined Cycle.

#### **TASK 1.4.2: DETAILED ANALYSIS OF ADVANCED BRAYTON CYCLES**

The goal of this detailed analysis task is to further narrow down the cycles to the most promising cycle or cycles. Sensitivity analysis is then conducted on the selected most promising cycle of incorporating higher compressor and turbine efficiencies, high efficiency exhaust diffuser, application of superconductivity technology to transformers and generators as well as the impact of increasing the diluent nitrogen addition to the gas turbine combustor in order to lower NOx emission. Thermoflex is used to simulate the power block and Aspen Plus the balance of plant. Details of the work accomplished under this task are provided in the Appendix section of this report.

##### **Simple Cycle Gas Turbine based IGCC with Increased Firing Temperature**

The first set of these advanced cases consisting of a steam-cooled gas turbine combined cycle with increased rotor inlet temperature (RIT) and blade surface temperature. The gas turbine itself has the simple cycle configuration as in the Baseline Case, i.e., without intercooling or reheat. The gas turbine firing temperature (1<sup>st</sup> rotor inlet temperature) required to realize about 8% improvement in heat rate over the Baseline Case is 1734°C or 3153°F (which is 342°C or 615°F above the Baseline Case) while increasing the blade surface temperatures by about the same amount over the Baseline Case (342°C or 615°F). This increase in the blade surface temperature is consistent with the projected values for advanced firing temperature and materials presented in Figure A1.4.2 – 1 of the Appendix section. The corresponding pressure ratio of the

gas turbine while maintaining an exhaust temperature in the neighborhood of 650°C<sup>a</sup> or 1200°F is 50. The pressure ratio of 50 is significantly higher than what has been currently demonstrated but such a high pressure ratio has been proposed for an advanced aero engine (Pratt & Whitney's baseline engine proposed for Boeing's 787 transport plane). The maximum pressure ratio for a commercial land based gas turbine engine without intercooling is 36 (Rolls-Royce's Trent 60 with water injection). A lower pressure ratio case is thus also investigated (a pressure ratio of 37 which is close to that of the Trent 60) while letting the turbine exhaust temperature rise significantly above the 650°C constraint. Significantly higher steam superheat and reheat temperatures are required than those in the 50 pressure ratio case in order to limit the irreversibility in heat transfer and keep it similar to that in the Baseline Case.

Performances for cases utilizing higher operating pressure air separation units consistent with the higher pressure ratio gas turbines are also developed. In addition, configurations where no air is extracted from the gas turbines ("syngas gas turbines") are investigated to quantify the incentive for developing gas turbines specifically designed for IGCC applications (i.e., unlike the currently offered gas turbines which are designed for natural gas and distillate fuels. Such "natural gas / distillate fuel gas turbines" are operated in off-design mode in IGCC applications such that air extraction is required to limit the increase in the gas turbine pressure ratio to stay within the surge margin of its compressor). The required air extraction expressed as a fraction of the compressor inlet air is increased as the gas turbine firing temperature is raised since the syngas fuel to air ratio to the combustor is higher. Thus, for these advanced firing temperature cases utilizing a "natural gas gas-turbine," as much as 20% of the air (expressed as a percentage of the compressor inlet air) is extracted while only 14% is extracted in the Baseline Cases.

The following lists the various cases investigated:

- Gas turbine with a pressure ratio of 37
  - No air extraction.
  - Air extraction Sensitivity Case while utilizing an ASU operating at a pressure currently demonstrated (Intermediate Pressure or IP ASU).
  - Air extraction Sensitivity Case while utilizing a HP ASU such that the extracted air is supplied to the cryogenic unit at full pressure, i.e., without first reducing its pressure in a turboexpander.
  
- Gas turbine with a pressure ratio of 50
  - No air extraction.
  - Air extraction Sensitivity Case while utilizing an ASU operating at a pressure currently demonstrated (IP ASU).
  - Air extraction Sensitivity Case while utilizing a HP ASU such that the extracted air is supplied to the cryogenic unit at full pressure, i.e., without first reducing its pressure in a turboexpander.

---

<sup>a</sup> such that strength in the roots of the long and uncooled last stage blades is maintained. Furthermore, use of advanced superheat and reheat steam temperatures of 613°C or 1135°F for the bottoming cycle is facilitated without having very large temperature differences between the gas turbine exhaust and the steam such that the irreversibility in heat transfer is similar to that in the Baseline Case.

Table 3 shows the overall system efficiency, coal (HHV) to power for these above described cases along with those for the Baseline Cases. The main features of the power cycle for these various cases are also included in this table. The following summarizes the results:

- The advanced firing temperature cases show a 7 to 9% improvement in overall plant heat rate over the Baseline Case.
- The improvement in plant heat rate utilizing a HP ASU over an IP ASU is quite small, less than 1% (subject to verification of the HP ASU performance estimates by an ASU vendor).
- The improvement in plant heat rate utilizing a “syngas gas turbine” is more significant, especially for the 50 pressure ratio gas turbine case. This result is to be expected since as the gas turbine pressure ratio is increased, there is also an increase in the irreversibility associated with (1) adiabatic compression and (2) cooling before the air can be used in the ASU.
- Comparing the performance of the 37 and 50 pressure ratio gas turbine cases, the plant heat rates are quite similar when extracting air from the gas turbine for the ASU. The difference in overall plant heat rate becomes significant, however, for the syngas turbine cases (i.e., without air extraction), the 50 pressure ratio case showing a better overall plant performance.

The estimated NO<sub>x</sub> emissions for the 37 and 50 pressure ratio gas turbine cases are 183 and 251 ppmVd (15% O<sub>2</sub> basis) respectively while that estimated for the Baseline Case is 18 ppmVd (15% O<sub>2</sub> basis) when utilizing combustors of the non-premixed type and maintaining a residence time of 30 ms in the dilution zone. These significant increases in the NO<sub>x</sub> emissions are primarily due to (1) the increase in the flame temperature caused by the increase in the combustion air temperature which increases as the gas turbine pressure ratio increases as well as due to (2) temperatures remaining high in the quench section of the combustor caused by the low air to fuel ratio which is required to achieve the higher firing. The estimated NO<sub>x</sub> emissions for the 37 and 50 pressure ratio gas turbine cases are 50 and 67 ppmVd (15% O<sub>2</sub> basis) respectively when the residence time is reduced to 5 ms in the dilution zone. Physically, this entails constructing a very short combustor. The combustor efficiency with a 5 ms residence time remained essentially unchanged, the fuel being mostly H<sub>2</sub>. A short residence time combustor, however, will pose a problem if natural gas firing is required either at startup or as a backup fuel and other means of NO<sub>x</sub> control would be preferred.

### **Intercooled Gas Turbine based IGCC with Increased Firing Temperature**

This case investigates the effect of including an intercooler in the high firing temperature / high pressure ratio gas turbines. The advantages of intercooling are:

- Lower compressor discharge temperature

- Savings in materials of construction
- Lower NO<sub>x</sub>
- Higher specific power output
  - Reduced compressor work (in a simple cycle gas turbine, approximately half of turbine power is used in compression)
- But more complex turbomachinery
  - Multi-spool engine

There are two choices for the type of intercooler:

- Shell and tube
- Spray type (as used in the GE LM6000 SPRINT engine)

The following lists the cases investigated:

- Gas turbine with a pressure ratio of 50
  - No air extraction.
  - Air extraction Sensitivity Case while utilizing a HP ASU such that the extracted air is supplied to the cryogenic unit at full pressure, i.e., without first reducing its pressure in a turboexpander.
- Gas turbine with a pressure ratio of 70 (and no air extraction) to determine if a significant advantage exists for the overall plant performance at this very high pressure ratio.

An evaluation of the two type of intercoolers along with its location in the compressor from a cycle thermal efficiency standpoint was made for the gas turbine case with overall pressure ratio of 50. Listed below are other advantages of the spray type intercooler over the shell and tube type, in addition to having an efficiency advantage:

- Lower equipment cost
- Spray adds motive fluid for expansion in the turbine and thermal diluent for reducing the NO<sub>x</sub> formation

The spray intercooler does need high quality spray water and the spray system needs to be carefully designed to minimize any large droplet carryover into the HP compressor in order to the compressor blades from impingement.

The compression pressure ratio (i.e., that of the low pressure compressor) chosen for locating this intercooler is 2.75. The thermal efficiency is increased but only slightly as this pressure ratio is decreased but the other advantages of spray intercooling listed above are compromised.

These advanced cycles again consist of the steam-cooled gas turbine combined cycle with the increased rotor inlet temperature (RIT) and blade surface temperature similar to the previous advanced case except for the intercooler. The direct contact intercooling utilizes steam condensate sprayed into the air stream at an intermediate pressure. The corresponding gas turbine exhaust temperature is 660°C (1220°F) for the pressure ratio of 50 gas turbine while that for 70 overall pressure ratio case has an exhaust temperature of 597°C (1170°F).

Table 4 shows the overall system efficiency, coal (HHV) to power for this advanced case along with those for the Baseline Cases. The main features of the power cycle for these cases are also included in this table. The following summarizes the results:

- The overall plant heat rates for these advanced firing temperature cases with intercooling are similar to those of the previous advanced cases without intercooling and show similar improvements in overall plant heat rate over the Baseline Case.
- The efficiency gain for the intercooled case with an overall pressure ratio of 70 is very small over the case with the 50 pressure ratio.
- The penalty associated with extracting air (for an HP ASU) from the 50 pressure ratio intercooled case is not as significant as in the corresponding non-intercooled cases. This result is to be expected since the intercooler makes the compression process more efficient by reducing the required work.
- Comparing the intercooled case to the previous non-intercooled case at an overall pressure ratio of 50, a substantial decrease in the compressor discharge temperature of 136°C (or 246°F) is realized for the intercooled case.
- The estimated NO<sub>x</sub> emissions for the 50 and 70 pressure ratio gas turbine cases are 166 and 231 ppmVd (15% O<sub>2</sub> basis) respectively while that estimated for the Baseline Case is 18 ppmVd (15% O<sub>2</sub> basis) when utilizing combustors of the non-premixed type and maintaining a residence time of 30 ms in the dilution zone. These NO<sub>x</sub> emissions are lower than the previous advanced non-intercooled case due to (1) the lower the flame temperature caused by the decrease in the combustion air temperature, a result of intercooling, and due to (2) additional thermal diluent being introduced via the spray intercooler. The estimated NO<sub>x</sub> emissions for the 50 and 70 pressure ratio gas turbine cases are 42 and 56 ppmVd (15% O<sub>2</sub> basis) respectively when the residence time is reduced to 5 ms in the dilution zone.

### **Intercooled-Reheat Gas Turbine based IGCC with Increased Firing Temperature**

This advanced cycle investigates the addition of reheat to the intercooled gas turbine with an overall pressure ratio of 70. This higher pressure ratio is chosen in order to limit the exhaust temperature while obtaining a reasonable pressure ratio for the HP turbine located between the HP and reheat combustors. The direct contact spray intercooler is selected due to its advantages over a shell and tube intercooler as discussed in the previous section. The gas turbine firing temperatures (1<sup>st</sup> rotor inlet temperature of the HP and the LP turbines downstream of the HP and the reheat combustors, respectively) are increased above the Baseline Case just enough to meet the heat rate improvement target set for this study. The following summarizes the main features of this gas turbine:

- Pressure ratio of 70

- Spray intercooled
- Reheat combustion
- No air extraction
- N<sub>2</sub> returned from an IP ASU.

Table 5 shows the overall system efficiency, coal (HHV) to power for this advanced case along with those for the Baseline Cases. The main features of the power cycle for these cases are also included in this table. The following summarizes the results:

- The gas turbine firing temperatures (1<sup>st</sup> rotor inlet temperature of the HP and the LP turbines downstream of the HP and the reheat combustors, respectively) required to realize the target improvement goal in heat rate over the Baseline Case is 1592°C or 2898°F (which is 200°C or 360°F above the Baseline Case but is 142°C or 255°F lower than all of the previous increased firing temperature cases) while increasing the blade surface temperatures by about the same amount over the Baseline Case (200°C or 360°F).
- The estimated NO<sub>x</sub> emissions for this reheat case is 42 ppmVd (15% O<sub>2</sub> basis) while that estimated for the Baseline Case is 18 ppmVd (15% O<sub>2</sub> basis) when utilizing combustors of the non-premixed type and maintaining a residence time of 30 ms in the dilution zone. These NO<sub>x</sub> emission is lower than the previous advanced cases due to the substantially lower flame temperature in the reheat combustor and consequently a significantly lower to the total NO<sub>x</sub> emission from the gas turbine. The estimated NO<sub>x</sub> emissions for the reheat case is 39 ppmVd (15% O<sub>2</sub> basis) when the residence time is reduced to 5 ms in the dilution zone.

### **Intercooled Closed Circuit Air Cooled Gas Turbine based IGCC with Increased Firing Temperature**

This case investigates the effect of utilizing closed loop air cooling (instead of closed loop steam cooling) in the HP sections of the gas turbine. An air compressor boosts the pressure of the cooling air leaving the turbine blades (to compensate for the pressure drops in the closed circuit air flow path) and returns the air to the combustor of the gas turbine. The following summarizes the main features of this gas turbine:

- Pressure ratio of 50
- Spray intercooled gas turbine air compressor
- Closed circuit air cooled gas turbine
- Addition of an air compressor to boost pressure of the cooling air to compensate for the pressure drops in the closed circuit air flow path while returning the air to the combustor of the gas turbine
- No air extraction
- N<sub>2</sub> returned from an IP ASU.

The advantages / disadvantages of closed loop air intercooling are:

- An advantage of this method as compared to the closed circuit steam cooling method is that the cooling air recuperates heat removed from the working fluid in the gas turbine by recycling it back to the combustor of the gas turbine whereas in the case of steam cooling the heat removed from the fluid within the turbine enters the steam cycle, i.e. heat is removed from the topping cycle and introduced into the bottoming cycle.
- Reduced rotor inlet temperature as compared to the previous advanced cases while realizing the same heat rate advantage over the Baseline Case.
- On the other hand, the reliability of the cooling air compressor is a concern. A possible solution in the event that this compressor trips is to open a fast acting relief valve upstream of the compressor to allow the free flow of cooling air. Thus it may be important to locate this compressor downstream of the turbine blades. The resulting increase in the plant heat rate is quite small due to the increase in the power consumption of the compressor in this location where the air stream being compressed is hotter.

The direct contact intercooling utilizes steam condensate sprayed into the air stream. The gas turbine exhaust temperature for this case with a pressure ratio of 50 is limited to 620°C (1148°F) at the ISO operating point.

Table 6 shows the overall system efficiency, coal (HHV) to power for this advanced case along with those for the Baseline Cases. The main features of the power cycle for these cases are also included in this table. The following summarizes the results:

The following summarizes the results:

- The required gas turbine firing temperature for this closed circuit air cooled gas turbine case with intercooling is 1678°C or 3053°F to obtain an overall plant heat rate similar to those of the previous advanced steam cooled cases, i.e., similar improvement in overall plant heat rate over the Baseline Case. This firing temperature as well as the turbine blade temperatures are 56°C or 100°F lower than the previous advanced cases.
- The combustor inlet air which is a mixture of the returned cooling air (leaving the booster compressor) and the remainder of gas turbine compressor discharge air is only slightly hotter (7°C or 13°F) than that in the previous steam cooled intercooled case at the same overall pressure ratio of 50.
- The estimated NO<sub>x</sub> emissions for this case is 115 ppmVd (15% O<sub>2</sub> basis) while that estimated for the Baseline Case is 18 ppmVd (15% O<sub>2</sub> basis) when utilizing combustors of the non-premixed type and maintaining a residence time of 30 ms in the dilution zone. This NO<sub>x</sub> emission is lower than the previous advanced intercooled (non-reheat) case with steam cooling and an overall pressure ratio of 50 due to the lower firing temperature. The estimated NO<sub>x</sub> emissions for the 50 pressure ratio gas turbine closed circuit air cooled gas turbine case is 35 ppmVd (15% O<sub>2</sub> basis) when the residence time is reduced to 5 ms in the dilution zone.

## **Air Partial Oxidation Topping Cycle**

This advanced cycle investigates the addition of an air partial oxidation (POx) topping cycle to an advanced steam cooled gas turbine. The partially oxidized syngas after partial expansion in a turbo-generator (POx turbine) and heat exchange is supplied to the advanced gas turbine (Ox turbine). The POx unit is operated at a pressure of 70 atm while the Ox turbine integrated with this POx unit has a pressure ratio of about 37. A high operating pressure is chosen for the POx unit and a moderate pressure ratio is chosen for the Ox turbine in order to limit the POx turbine exhaust temperature while obtaining a reasonable pressure ratio across the POx turbine.

The advanced gas turbine (Ox turbine) includes a direct contact spray intercooler which is selected due to its advantages over a shell and tube intercooler as discussed in the previous section. Humidified, preheated, decarbonized syngas is combusted with less than the stoichiometric amount of air in the POx unit followed by complete combustion with excess air in the oxidizing combustor. IP nitrogen supplied by the ASU is added to the combustor as a thermal dilution for NOx control as well as to increase the amount of motive fluid for expansion. The following summarizes the main features of this gas turbine:

- POx topping cycle operating at a pressure of 70 atm
- Spray intercooled advanced steam cooled gas turbine (Ox turbine) with pressure ratio of 37
- Air extraction from the Ox turbine to provide air for the POx unit but none supplied to the ASU
- N<sub>2</sub> returned from an IP ASU.

The advantages of utilizing this air POx topping cycle are:

- Reduction in firing temperature of the Ox turbine while achieving the heat rate reduction goal for this study.
- Potential for lower NOx due to lower heating value of the syngas fired in the advanced gas turbine since the syngas is partially oxidized and due to the lower firing temperature in the advanced gas turbine.

There are certain challenges, however, with respect to implementation of this air POx topping cycle:

- Concerns with POx turbine seals.
- Control issues as discussed in a previous section.
- H<sub>2</sub> embrittlement and corrosion due to loss of oxide protective layer, especially in the POx turbine.
- Carbonyl formation and metal dusting when utilized in “un-decarbonized” syngas applications.

Table 7 shows the overall system efficiency, coal (HHV) to power for this advanced case along with those for the Baseline Cases. The main features of the power cycle for these cases are also included in this table. The following summarizes the results:

The following summarizes the results:

- The gas turbine firing temperatures (1<sup>st</sup> rotor inlet temperature) of the advanced steam cooled gas turbine (Ox turbine) firing the partially oxidized syngas required to realize the target improvement goal in heat rate over the Baseline Case is 1699°C or 3090°F (which is 307°C or 553°F above the Baseline Case but is only 35°C or 63°F lower than the first two advanced cases investigated. The difference in the blade surface temperatures of the advanced gas turbine between this case and the previous cases is consistent with the firing temperature, i.e., higher or lower by the same amount as the firing temperature (see Figure A1.4.2 - 1 in the Appendix section).
- The estimated NOx emissions for this air POx based case is 117 ppmVd (15% O<sub>2</sub> basis) while that estimated for the Baseline Case is 18 ppmVd (15% O<sub>2</sub> basis) when utilizing combustors of the non-premixed type and maintaining a residence time of 30 ms in the dilution zone. The estimated NOx emissions for the air POx based case is 32 ppmVd (15% O<sub>2</sub> basis) when the residence time is reduced to 5 ms in the dilution zone.

### **Selection of Advanced Brayton Cycle**

It may be concluded from the results obtained by this detailed analysis of the above discussed advanced Brayton cycles that the more promising advanced Brayton cycles are the high pressure ratio intercooled gas turbines employing either closed circuit steam or air cooling. The following summarizes the attributes of these two advanced cycles:

- Required gas turbine pressure ratio of 50 is close to that of a commercially proven aero-engine while limiting the exhaust temperature to a reasonable value.
- Spray intercooling which has been proven in a commercial aero-engine derived gas turbine has the following advantages:
  - Lower compressor discharge temperature than that in a non-intercooled gas turbine with the same pressure ratio
    - Savings in materials of construction may be realized
    - Produces lower NOx emission not only due to lower compressor discharge temperature (or combustor inlet air temperature) but also due to the higher humidity of this air stream (caused by using the spray intercooler)
  - Higher specific power output
    - Reduced compressor work (in a simple cycle gas turbine, approximately half of turbine power is used in compression)
    - Spray water increases the motive fluid for expansion in the turbine.

Next, comparing these two advanced cycles:

- The required firing and blade surface temperatures for the closed circuit air cooled case are a bit lower (by about 56°C or 100°F) along with NOx emissions as compared to the corresponding closed circuit steam cooled case.
- However, closed circuit air cooling has not been demonstrated while the reliability of the cooling air compressor is a concern.
- On the other hand, start-up and shutdown procedures for the closed circuit air cooled case may be simpler than those for the closed circuit steam cooled case.

- The steam cooled case however, incorporates proven cooling technology and H class combined cycles (utilizing the steam cooled gas turbines) have been operated successfully in commercial applications which include startup and shutdown operations.

Based on these above attributes of these two advanced cycles, the most promising cycle for further analysis appears to be the steam cooled case, i.e., an advanced Brayton cycle employing a high pressure ratio gas turbine with spray intercooling, closed circuit steam cooling and an advanced firing temperature. Sensitivity analysis is conducted on this selected cycle as described in the following.

### **Sensitivity Analysis of Selected Advanced Brayton Cycle**

Since the most technological challenge in the development of the advanced Brayton cycle is its advanced firing temperature (requiring advanced materials), the approach taken in this sensitivity analysis is to quantify the reduction in the firing temperature made possible by incorporating improvements in the other areas (Items 1 through 4 listed in the following) while realizing the same improvement in overall plant efficiency over the Baseline Case.

The sensitivity analysis also prioritizes the development needs of the advanced Brayton cycle. Low NO<sub>x</sub> strategies are also investigated (Item 5 below) as well as use of air cooling as an alternate to closed circuit steam cooling of the turbine 1<sup>st</sup> stage (Item 6 below) which has very high operating temperature, the film of air forming on the outside surface of the blade providing an additional insulating layer (i.e., in addition to thermal barrier coatings to protect the metal).

1. Increasing the gas turbine air compressor efficiency
2. Increasing the gas turbine expander
3. High efficiency exhaust diffuser
4. Application of superconductivity technology to transformers and generators
5. Low NO<sub>x</sub> strategy
  - a. Increased diluent nitrogen addition
  - b. Reduction in firing temperature
6. Air (film) cooled 1<sup>st</sup> stage turbine.

### **Gas Turbine Compressor Efficiency**

The LP and HP compressor polytropic efficiencies for the baseline case are 92% and 91.3%, respectively. By increasing the polytropic efficiency of both the LP and HP compressors by 1 percentage point (i.e., to 93% for the LP Air compressor and to 92.3% for the HP compressor), only a 11°C or 19 °F reduction in the firing temperature may be realized (while maintaining the same overall plant efficiency).

Next, by increasing the polytropic efficiency of both the LP and HP compressors by 2 percentage points (i.e., to 94% for the LP Air compressor and to 93.3% for the HP compressor), a 20°C or 36°F reduction in the firing temperature may be realized (again while maintaining the same overall plant efficiency).

The results of this analysis thus indicate that very substantial aerodynamic design improvements are required to the gas turbine compressor to realize a significant reduction in the required firing temperature. The need for very high firing temperature is not diminished by a significant amount however, and shows that major emphasis should be placed on technology developments required to realize the very high firing temperature identified by this study.

### **Gas Turbine Expander Efficiency**

The uncooled isentropic stage efficiencies for the baseline case are:

Baseline Case	Uncooled Isentropic Efficiency
Stage 1	89.5
Stage 2	90.5
Stage 3	90.5
Stage 4	92
Stage 5	92

By increasing each of these stage efficiencies by 1 percentage point, only a 20°C or 36°F reduction in the firing temperature may be realized (while maintaining the same overall plant efficiency). The resulting stage efficiencies are listed below:

Stage Efficiency Increased by 1% Point	Uncooled Isentropic Efficiency
Stage 1	90.5
Stage 2	91.5
Stage 3	91.5
Stage 4	93
Stage 5	93

The results of this analysis are similar to the previous compressor efficiency analysis, i.e., indicate that very substantial aerodynamic design improvements are required to the gas turbine expander to realize a significant reduction in the required firing temperature. The need for very high firing temperature is not diminished by a significant amount however, and shows that major emphasis should be placed on technology developments required to realize the very high firing temperature identified by this study.

### **High Efficiency Exhaust Diffuser**

The coefficient of performance for a conventional diffuser is typically around 0.6. According to Meruit Inc. as mentioned previously in the Screening Analysis, the gas turbine exhaust diffuser

can be designed to have a coefficient of performance as high as 0.9 utilizing their proprietary design consisting of an Annular Recirculating Diffuser. With an increase in the diffuser coefficient of performance to 0.9, about 30°C or 54°F reduction in the firing temperature may be realized (while maintaining the same overall plant efficiency).

Once again the need for very high firing temperature is not diminished by a significant amount however, and shows that major emphasis should be placed on technology developments required to realize the very high firing temperature identified by this study.

### **Application of Superconductivity Technology**

Superconductivity technology offers higher efficiency electrical equipment such as generators and transformers. The efficiencies of these equipment for the Baseline Case are listed below:

Baseline Case	Uncooled Isentropic Efficiency
Gas Turbine Generator	98.6
Transformer Efficiency (24/345 kV)	0.997
Transformer Efficiency (24/4.16 kV)	0.995
Transformer Efficiency (4,160/480 V)	0.995

As seen from the above data, the efficiencies are already quite high and the application of the more efficient electrical equipment is not expected to make a significant improvement in the overall plant performance or conversely a significant reduction in the required firing temperature of the gas turbine for a targeted overall plant performance.

### **Low NOx Strategies**

As discussed previously, a partial solution to reducing the NOx emission may be to limit the residence time in the dilution zone of the combustor by constructing a short combustor (reducing the residence time from 30 ms to 5 ms reduced the NOx by as much as ~ 70% for the very high rotor inlet cases while the burnout of H<sub>2</sub>, CO and CH<sub>4</sub> was not affected significantly, the fuel being decarbonized syngas contains only small concentrations of CO and CH<sub>4</sub>). As mentioned previously, a short residence time combustor, however, will pose a problem if natural gas firing is required either at startup or as a backup fuel and other means of NOx control would be preferred. Thus, other strategies are considered as follows.

### **Increased Diluent Nitrogen Addition**

Increasing the diluent addition to the syngas is a strategy investigated in this sensitivity analysis which may be done in addition to installing an SCR. In the Baseline Case, the combined LHV of the humidified syngas and diluent N<sub>2</sub> (provided by the ASU) is 4,720 kJ/nm<sup>3</sup> or 120 Btu/scf. The ASU can be designed to provide additional nitrogen for syngas dilution. With an ASU designed to provide the maximum amount of N<sub>2</sub>, the resulting (lowest) combined LHV of the humidified syngas and diluent N<sub>2</sub> is 3,980 kJ/nm<sup>3</sup> or 101 Btu/scf. The increased nitrogen dilution reduces the NOx significantly, from 42 ppmvd to 10 ppmvd (at 15% O<sub>2</sub> concentration)

with the shorter combustors, i.e., corresponding to a residence time of 5 ms in the 2<sup>nd</sup> PSR. However, the firing temperature of gas turbine is also reduced, by about 22°C or 40°F resulting in an increase in the net plant heat rate by about 2.2%.

### **Reduced Firing Temperature**

The trade-off between heat rate and NO<sub>x</sub> emission by reducing the firing temperature is investigated in this sensitivity analysis. The results of this analysis show that a 56°C or 100°F reduction in firing temperature from the initial 1734°C or 3153°F results in approximately 1.5% increase in heat rate while the NO<sub>x</sub> reduces from 42 ppmvd to 28 ppmvd (at 15% O<sub>2</sub> concentration) with the shorter combustors, i.e., corresponding to a residence time of 5 ms in the 2<sup>nd</sup> PSR. A further 56°C or 100°F reduction in firing temperature (i.e. 93°C or 200°F reduction from the initial 1734°C or 3153°F) results in an additional 1.5% or total of 3% increase in heat rate while the NO<sub>x</sub> reduces from 42 ppmvd to 20 ppmvd (at 15% O<sub>2</sub> concentration).

### **Air (Film) Cooled 1<sup>st</sup> Stage Turbine**

Open-circuit film-cooling of the blades has the advantage of forming a protective layer on the outside surface of the blade, i.e., by creating an additional insulating layer in addition to thermal barrier coatings to protect the metal. The effect on plant performance of utilizing air (film) cooling of the 1<sup>st</sup> stage turbine stationary and rotating blades instead of closed circuit steam cooling is investigated in this sensitivity analysis performed on the selected advanced case. The 2<sup>nd</sup> and 3<sup>rd</sup> stages of the turbine employ closed circuit steam cooling while the 4<sup>th</sup> and 5<sup>th</sup> stages employ open circuit air cooling as in the selected advanced case. Note that the gas temperature entering the 2<sup>nd</sup> stage at about 1500°C or 2740°F is much lower. The results of this analysis show that the heat rate penalty of utilizing air (film) cooling for the 1<sup>st</sup> stage instead of closed circuit steam cooling is about 0.8%, quantifying the trade-off between plant performance and the need for developing the required more advanced materials required with closed circuit steam cooling of the 1<sup>st</sup> stage.

### **Economic Analysis**

Rough order of magnitude (ROM) plant cost estimates, operating and maintenance cost estimates, and levelized cost of electricity are developed for the Baseline Case and the selected advanced Brayton cycle case consisting of the intercooled gas turbine in order to assess the economic incentive for funding the development of such an advanced engine. The ROM plant cost estimate for the Baseline Case is \$2,285/kW while that for the Advanced Brayton cycle is \$2,107/kW (on a 4<sup>th</sup> quarter 2007 basis) which is a 7.8% reduction in cost. This significant reduction in the total plant cost on a per kW basis is primarily due to:

1. the higher efficiency of the advanced Brayton cycle which increases the plant power output for a given coal throughput and consequently decreases the associated capital charges
2. and due to the higher specific power output of the advanced combined cycle which reduces the relative equipment sizes in the power block.

The plant section costs were factored primarily from the costs estimates presented in the DOE / NETL report titled, “Cost and Performance Baseline for Fossil Energy Plants,” Report No. DOE / NETL - 2007/1282, dated May 2007. The relative cost of the advanced intercooled gas turbine was developed using methodology presented for aero-derivative gas turbines in the Final Report prepared for Gas Research Institute by Fluor titled, “Evaluation of Advanced Gas Turbine Cycles,” Report No. GRI-93/0250, dated August 1993. The operating and maintenance costs as well as the 20-year period levelized cost of electricity were estimated utilizing methodology consistent with that used in the above cited DOE / NETL report.

The levelized cost of electricity for the Baseline Case was estimated at \$85.72/MWhr while that for the Advanced Brayton cycle case was estimated at \$79.08/MWhr (at a capacity factor of 80% and with the Pittsburgh No. 8 coal priced at \$1.73/MM Btu, HHV) which is almost an 8% reduction over the Baseline Case. If a cost penalty of \$30/ST CO<sub>2</sub> emitted is assigned to the two cases, then the levelized cost of electricity of the Baseline Case is increased to \$89.08/MWhr while that for the Advanced Brayton cycle case is increased to \$82.19/MWhr.

Next, with respect to the impact of including an SCR to reduce NO<sub>x</sub> emissions to an ultra low value (2 ppmvd, 15% O<sub>2</sub> basis) on the cost of electricity, a previous study conducted for the DOE / NETL under contract DE-FC26-00NT40845 determined that it was insignificant.

### **Development Needs**

The promising advanced Brayton cycle identified to meet the efficiency objectives of this project has the following characteristics:

Type Brayton cycle	Intercooled high pressure ratio
Overall Compression Ratio	50
LP Compressor Pressure Ratio	2.75
HP Compressor Pressure Ratio	18.8
Intercooler Type	Spray
Gas Turbine Specific Power	1,630 kW/(kg/s) or 740 kW/(lb/s)
Net Plant Specific Power	1,639 kW/(kg/s) or 743 kW/(lb/s) <sup>b</sup>
Gas Turbine Exhaust Mass Flow Rate to Inlet Mass Flow Rate Ratio	1.457 <sup>c</sup>
Firing Temperature (1 <sup>st</sup> Stage Rotor Inlet)	1734°C or 3153°F
Turbine Cooling	Closed circuit steam cooling of HP stages and open circuit air cooling of LP stages
Shaft Arrangement	HP compressor driven by HP turbine. LP compressor and generator driven by LP turbine, operating at 3600 RPM.

<sup>b</sup> Corresponds to about 340 MW net IGCC output with the inlet air flow of a GE LMS100PA gas turbine.

<sup>c</sup> This ratio is significantly higher than current engines operating on natural gas or distillate because of (1) spray intercooling, (2) syngas firing with diluent addition and (3) no air extraction for the ASU.

Bottoming Rankine Cycle, Superheat Pressure / Superheat Temperature / Reheat temperature	166.5 barA / 618°C / 618°C or 2415 psia / 1145°F / 1145°F
--	---

The greatest technological challenge for the development of this gas turbine is in the area of advanced materials required to withstand the very high firing temperature. Thus, the sensitivity analysis performed and discussed in a previous section on this cycle measured the reduction in the firing temperature that may be made possible (and thus the required advanced turbine materials to meet the overall plant thermal efficiency goal) by making performance enhancements in other areas such as gas turbine component aerodynamic improvements and the electrical equipment. Their individual contributions are summarized in the following table. As discussed previously, the individual contributions are not highly significant but the data shows that the sum total contribution can be significant, as much as 70°C or 126°F reduction in the firing temperature. A reduction of 70°C or 126°F in the firing temperature has the additional benefit of reducing NO<sub>x</sub> emission. Based on data developed in the previous sensitivity analysis of the effect of firing temperature on NO<sub>x</sub>, a significant reduction in the NO<sub>x</sub> from 42 ppmvd to 26 ppmvd (at 15% O<sub>2</sub> concentration) may be realized (while utilizing the shorter combustors, i.e., corresponding to a residence time of 5 ms in the 2<sup>nd</sup> PSR) with the 70°C or 126°F decrease in firing temperature. The data presented in this table also helps prioritize these other areas of research.

	<b>Contribution to Reduction in Firing Temperature</b>
Increasing the gas turbine air compressor efficiency by 2% points	20°C or 36°F
Increasing the gas turbine expander by 1% point	20°C or 36°F
High efficiency exhaust diffuser (C <sub>p</sub> = 0.9)	30°C or 54°F
Application of superconductivity technology to transformers and generators	Insignificant
<b>Combined Contribution</b>	<b>70°C or 126°F</b>

### Combustor Needs

The table below summarizes the main features of the combustor required by this advanced Brayton cycle.

Combustor	
Inlet Air Temperature	523°C (973°F)
Discharge Temperature	1781°C (3237°F)
Inlet Air O <sub>2</sub> Concentration, Volume %	19.9
Discharge O <sub>2</sub> Concentration, Volume %	1.6
Decarbonized Syngas Adiabatic Flame Temperature	1875°C (3407°F)

As seen from this data, a combustor to withstand the very high temperatures is required while the relatively small amount of excess air used to increase the firing temperature further exacerbates

the technological challenge for the development of such a combustor. As discussed previously, the NO<sub>x</sub> continues to form in the dilution zone of the combustors because of the very high combustor discharge temperature. Thus, the current approaches to low NO<sub>x</sub> combustor designs described under Task 1.4.1 may not suffice since the air to fuel ratio is too small to cause rapid quenching of the flame within the combustor to limit the formation of NO<sub>x</sub>.

If a short combustor is utilized to minimize the residence time and thus limit the NO<sub>x</sub> formation, then natural gas as a backup fuel or startup cannot be considered. The gasification island will have to be started up first while flaring the syngas and then the gas turbine will have to be brought online.

As discussed in the sensitivity analysis where the ASU is designed to provide the maximum amount of N<sub>2</sub>, the resulting (lowest) combined LHV of the humidified syngas and diluent N<sub>2</sub> is 3,980 kJ/nm<sup>3</sup> or 101 Btu/scf. The increased nitrogen dilution does reduce the NO<sub>x</sub> significantly, from 42 ppmvd to 10 ppmvd (at 15% O<sub>2</sub> concentration) with the shorter combustors, i.e., corresponding to a residence time of 5 ms in the 2<sup>nd</sup> PSR. However, the firing temperature of gas turbine is also reduced, by about 22°C or 40°F resulting in an increase in the net plant heat rate by as much as 2.2%. Furthermore, increasing the diluent addition may increase the challenge for the combustor design since the O<sub>2</sub> content of the combustor exhaust gas is already very low at 1.6%.

SCRs would be required to limit the NO<sub>x</sub> emissions to the desired 2 ppmVd (15% O<sub>2</sub> basis) value. Higher SCR catalyst volume would be required for these advanced firing temperature cases, however, since the amount of NO<sub>x</sub> generated within the combustor is substantially higher than that in the Baseline Case.

### Materials

Materials that can withstand a combination of creep, pressure loading, high cycle and thermal fatigue at these temperatures are required. Materials presently used such as wrought, sheet-formed nickel-based super-alloys provide good thermo-mechanical fatigue; creep and oxidation resistance for static parts and can be formed into the required shapes (combustor barrels and transition pieces), weldability and suitability to repair and overhaul operations. The severe temperatures require that large portions of the combustor be protected using thermal barrier coatings. These coatings are applied over the surface of existing materials to provide protection against wear, erosion, oxidation / hot corrosion, as well as for improving and maintaining the surface finish.

Materials technology for the combustor should be aimed at replacement of conventional wrought nickel-based products with:

- More suitable Ni-based alloys
- Oxide dispersion strengthened metallic systems
- Ceramic matrix composites.

Thermal barrier coatings for combustor applications is currently based primarily on systems comprising of a bondcoat of MCrAlY (where M is the base metal such as Ni and / or Co) and a

topcoat of ceramic material. Developments aimed at applying thicker coatings to enable the higher firing temperature as well as increasing the phase stability and resistance to sintering of the ceramic topcoat at higher temperatures are required. Furthermore, thermal barrier coatings that can withstand an environment containing water vapor at a high partial pressure are required.

## **Compressor Needs**

The overall pressure ratio of 50 for this advanced Brayton cycle is significantly higher than what has been currently demonstrated but such a high pressure ratio has been proposed for an advanced aero engine (Pratt & Whitney's baseline engine proposed for Boeing's 787 transport plane) and is close to that of the aero-derivative GE LMS100 intercooled gas turbine which has a pressure ratio of 41 at ISO conditions.

The advanced Brayton cycle design will thus have to be based on modifying an existing aero-derivative engine such as the GE LMS100; by adding stages at the front-end of the LP compressor<sup>d</sup> and / or at the back-end of the HP compressor depending on the existing Mach number limitations. An added advantage of utilizing the GE LMS100 engine is that it is configured with an intercooler. The suction air flow of this engine is 208 kg/s or 458 lb/s at ISO conditions. With a plant specific power output of 1,639 kW/(kg/s) or 743 kW/(lb/s) for the advanced Brayton cycle IGCC, the net plant output on a per gas turbine basis would be 1,639 kW/(kg/s) X 208 kg/s or 340 MW; or for a two gas turbine based plant, the net output would be 680 MW, a reasonable (i.e., economically viable) plant size.

If an aircraft engine is modified instead, the major mechanical changes from aircraft to this ground-based engine involves replacing the turbofan and installing a new LP compressor using lower cost materials, combustor changes, HP turbine changes to handle increased flow and to reduce cost, and a new, lower cost LP turbine to expand to atmospheric pressure. Additional shaft length to accommodate scrolls for the intercooler would also be needed. The key to keeping development costs to a minimum is keeping gas path the same, thereby allowing the compressors, especially the high pressure compressor to remain unchanged, except for materials.

In either case, the development of the advanced Brayton cycle which requires an aero-frame engine should be based on the use of existing compressor gas path designs. This would significantly reduce the cost of development.

Finally, it must be stated that in general, the challenge facing the compressor is to provide improved cycle efficiency, operability and reduced costs by optimizing the work done by each stage. The need to maintain compressor performance and integrity through life, while reducing parts costs and the use of more effective manufacturing processes is paramount, as is the need to achieve operational lifetimes in excess of 100,000 hours. Many of these targets are dependent upon improved design and aero-thermal analysis methods.

### Intercooler

---

<sup>d</sup> Addition of front-end stages increases the suction air flow.

Spray intercooling has been commercially practiced in the GE LM6000 SPRINT engine for a number of years. Presence of any water droplets in the intercooler discharge would lead to erosion of the HP compressor blading and erosion resistant coatings for existing materials or development of erosion resistant materials may be required. Proper design of the spray system is essential to minimize droplet carryover into the HP compressor. A demister pad installed at the discharge end of the intercooler with low pressure drop characteristics would be very desirable.

## **Turbine Needs**

### Cooling Technology

The 1<sup>st</sup>, 2<sup>nd</sup> and 3<sup>rd</sup> stages of the turbine employ closed circuit steam cooling while the 4<sup>th</sup> and 5<sup>th</sup> stages employ open circuit air cooling. Steam with its very high specific heat is an excellent cooling medium while the advantage with closed circuit cooling is that the momentum and dilution losses which are incurred in open circuit cooling are avoided. On the other hand, open circuit film cooling of the blades (utilizing air) has the advantage of forming a protective layer on the outside surface of the blade, i.e., by creating an additional insulating layer (i.e., in addition to thermal barrier coatings to protect the metal).

The effect on plant performance of utilizing air (film) cooling of the 1<sup>st</sup> stage turbine stationary and rotating blades (where the temperatures are highest) instead of closed circuit steam cooling was discussed in sensitivity analysis of this cycle. The 2<sup>nd</sup> and 3<sup>rd</sup> stages of the turbine employed closed circuit steam cooling while the 4<sup>th</sup> and 5<sup>th</sup> stages employ open circuit air cooling as in the selected advanced case. Note that the gas temperature entering the 2<sup>nd</sup> stage at about 1500°C or 2740°F is much lower than that in the 1<sup>st</sup> stage. The results of this analysis as discussed previously showed that the heat rate penalty of utilizing air (film) cooling for the 1<sup>st</sup> stage instead of closed circuit steam cooling was about 0.8%, quantifying the trade-off between plant performance and the need for developing the necessary more advanced materials required with closed circuit steam cooling of the 1<sup>st</sup> stage.

### Turbine Blade Materials

A main consideration in the design of blades is to avoid creep failure due to the combined effect of high stresses and temperatures with target lifetime being in excess of 50,000 operating hours. Turbine blades are subjected to severe thermal stresses caused by the many start-up / shutdown operations and unexpected trips. Furthermore, the rotating blades are subjected to high frequency excitations as they pass through the wake of the upstream combustor and the stationary blades. These excitations can lead to fatigue failure.

To meet these requirements while the turbine firing temperatures are being increased, conventionally cast nickel-based super-alloys are being replaced by directional solidification blades as well as single crystal blades which provide even more significant benefits. However, alloys with greater defect tolerance need to be developed and demonstrated. Development of alloys having improved castability, higher corrosion resistance and reduced heat treatment times are required.

In order to achieve increased creep strength, higher levels of alloying with Al, Ti, Ta, Re, W have been used. Cr additions had to be reduced to offset the increased tendency to form topologically close-packed phases which limit ductility and reduced strength. Lower Cr concentrations reduce the corrosion resistance of the alloys which in turn has led to the development of protective coatings. Coatings are applied over the surface of existing materials to provide protection against wear, erosion, oxidation / hot corrosion, as well as for improving and maintaining the surface finish. The coating process includes aluminizing, chromizing and application of the MCrAlY (M = Ni / Co). Ceramic coatings provide thermal barrier protection to reduce metal temperatures. These thermal barrier coatings need to be able to withstand an environment containing water vapor at a high partial pressure are required.

Development of ceramic matrix composites may also be required for the very hot components or sections of the turbine. Ceramic composites employing silicon carbide fibers in a ceramic matrix such as silicon carbide or alumina are commercially available while single crystal oxide fibers are under consideration.

### **Development Costs and Time**

Based on the development costs and timeline for advanced gas turbines as documented in a previous study conducted for the DOE / NETL under contract DE-FC26-00NT40845, the design and component test phase may take approximately 40 to 42 months. Initial build could commence with long lead items about half way through the first phase and last 24 to 27 months. At the end of the approximately 54 months, test of the initial unit could begin and could last approximately 15 months. Cost for such a program can be between \$250 and \$275 million, the program being predicated on a minimum commitment of 8 engines.

### **TASK 2.1 - EVALUATION OF IMPACT OF RAMGEN COMPRESSION TECHNOLOGY ON IGCC PLANT PERFORMANCE**

This study task consists of a thermodynamic assessment of the Ramgen turbomachinery technology for pressurizing the captured CO<sub>2</sub> to sequestration pressure in a coal based near zero emission IGCC power plant. The study also includes an assessment of the application of these technologies to the other major turbomachinery within the plant.

The Ramgen compressor technology is substituted into the Baseline Case which utilizes the current state-of-the-art compression technology as defined under Tasks 1.2 and 1.3 is of this contract. Options evaluated in this advanced compression study include compression with intercooling, and without intercooling with various options for recovery of the low temperature heat contained in the compressed stream.

Results of this study indicate the following (subject to verification of the turbomachinery efficiencies as quoted by Ramgen by test work):

- The Ramgen LP and IP CO<sub>2</sub> compressors with their higher efficiencies can save about 0.5 MW in in-plant electric power consumption for a 380 MW IGCC near zero emission power plant.
- Among the various practical heat recovery options evaluated for the Ramgen HP CO<sub>2</sub> non-intercooled compressor, use of a LiBr absorption refrigeration system provides the most efficient route for conversion of this low temperature heat. The chilled water produced by the absorption refrigeration unit is utilized for chilling the Selexol solvent in the AGR unit, thereby reducing the mechanical refrigeration load. The net IGCC plant output is reduced, however, even with the reduction in the mechanical refrigeration load and with a higher HP compressor efficiency.
- The Ramgen HP CO<sub>2</sub> compressor with intercooling provides greater advantage. The net result of utilizing this Ramgen compressor which has a significantly higher efficiency than that of the Baseline Case compressor is that the plant output is increased by 1.1 MW over the Baseline Case. This increment is only slightly lower (0.3 MW) than that obtained by utilizing the Ramgen high efficiency non-intercooled HP compressor with the conversion of the exhaust heat by a hypothetical working fluid (with variable evaporation and condensing temperatures) which represents an upper limit for this heat conversion process. Thus, from an overall plant thermal efficiency standpoint, the Ramgen high efficiency intercooled compressor technology is more promising. The net increase in power output over the Baseline Case of utilizing the Ramgen LP, IP and intercooled HP compressors is 1.61 MW for this 380 MW IGCC plant.
- Next, by applying the Ramgen technology to other major turbomachinery in the IGCC plant in addition to the CO<sub>2</sub> compressors (i.e., to the gas turbine extraction air expander, the ASU air and nitrogen compressors), the net power output over the Baseline Case is increased significantly, by as much as 6 MW for this 380 MW IGCC plant.

## **TASK 2.2 - DYNAMIC SIMULATION OF FUEL CELL / GAS TURBINE SYSTEM**

Details of the work accomplished under this task are provided in the Appendix section of this report.

### **Steady State Modeling**

Two SOFC-GT hybrid cycles that meet DOE criteria were numerically modeled and their dynamic performance simulated as part of a perturbation and response analyses. The main difference between the two cycles is the means by which cathode recycle is accomplished; initially via an ejector and ultimately via a blower during the evolution of the study. Models of these two subsystems were built specifically to assist in these studies. The dynamic models of the entire system stem from the 220 kW Siemens Westinghouse hybrid system model that was developed at the National Fuel Cell Research Center and validated with experimental data. These correlations between the model and experiment have been described in numerous journal publications. The main changes to the 220 kW model were to scale up the power block to 100

MW, replace tubular fuel cell geometry with planar geometry, replace centrifugal turbo-machinery with axial design and adjust overpotential parameters in the SOFC to match SECA target performance goals of  $500 \text{ mW/cm}^2$  at 80% fuel utilization. Since experimental data at the 100 MW system level is unavailable, model performance was compared and validated against ASPEN, industry standard software used in plant design. Very good correlation was found between the models described in this work and that of ASPEN.

Using a cathode blower in place of an ejector was found to increase steady state cycle efficiency by approximately three percentage points for the three different cycle pressure scenarios investigated resulting in an overall plant heat rate improvement of approximately three percent. It is unknown whether currently available blowers can operate at the temperatures required or whether blowers could maintain the pressure rises required in the current cycles.

## **Dynamic Modeling**

These studies primary focused on the impact of perturbations to the steady state design operating point that led to gas turbine failure in the form of compressor surge and design and operational strategies to avoid this phenomenon. The pressure fluctuations associated with compressor surge will likely damage if not destroy the fuel cell before the turbo-machinery if pressure regulators are not placed between the fuel cell stack and the turbo-machinery. The main perturbations investigated that lead to surge were load shed and dilution of syngas hydrogen content with nitrogen or steam. Fuel cell shutdowns also led to surge. The design strategies that were found to help in avoiding surge include designing the turbine and compressor to allow greater surge margin under steady state operation, minimizing the plenum volume between the fuel cell outlet and turbine inlet, minimizing gas turbine rotational moment of inertia and designing for compressor speed lines that are more vertical in nature. Modification of the turbo-machinery design pressure ratio and mass flow to achieve more stable dynamic response to load shed and fuel dilution perturbations usually comes with an efficiency penalty. But, the efficiency penalty associated with these design modifications may be worth the increase in stability. This argument is further supported if the gas turbine is mainly seen as a means of feeding air to the fuel cell.

The dynamic response of the fuel cell was studied for the above mentioned perturbations. These responses include anode-cathode inlet pressure difference, anode and cathode inlet-outlet temperature differences, average fuel cell cathode temperature, tri-layer (electrolyte) temperature and gas turbine shaft speed. In many cases the perturbation investigated did not lead to compressor surge but these other failure mechanisms were observed.

Two separate control strategies were employed in this study; the first controls gas turbine shaft speed at 3,600 RPM, assuming a synchronous generator and the second (cascade controller) primarily controls fuel cell temperature and secondarily controls gas turbine shaft speed, assuming an asynchronous generator. Careful tuning of the controls is necessary in order to avoid dynamic operational paths taken between initial and final steady state operating points that tend towards surge.

## Comparison of Control Strategies #1 and #2

Comparing the two control strategies reveals the very dramatic impact that control strategy has on compressor dynamics and surge avoidance. When control strategy #1 is used there is very little impact on the compressor steady state operating point and thus surge is relatively easily avoided. There are two main reasons for this. First, the fuel cell tri-layer temperature is allowed to vary during the dynamic and therefore the compressor is not required to respond in any way to changes in fuel cell operating temperature. However, large variations in fuel cell stack operating temperature can lead to stack degradation, which should be avoided. Second, the blower is primarily being used to control cathode inlet temperature by varying exhaust recycle ratios and this is done by using electrical power that is independent of the compressor. This is contrasted with the case when a cathode recycle ejector is used and cathode inlet temperature is controlled by the exhaust recycle ratio, which must be driven directly by the compressor. The ejector case thus leads to much more dynamic compressor response requirements to meet system operating conditions.

In contrast, there is a very strong impact on compressor dynamics and the potential for surge when control strategy #2 is used. This is because the compressor is being manipulated to maintain fuel cell tri-layer temperature at a constant and safe condition. This will likely be necessary to protect the high cost fuel cell stack in such hybrid systems. The trade off is that compressor surge can become difficult to avoid when the system is subjected to some of the more significant perturbations. It should be noted that there is very little difference in the initial and final states or the dynamic path of the compressor when a cathode blower is used instead of a cathode ejector in the case that fuel cell operating temperature is the primary control strategy (#2).

## Strategies for Improved Dynamic Performance of Gas Turbines in Hybrid Systems

One of the most damaging gas turbine responses to perturbations is compressor surge. Compressor surge is also challenging to avoid while maintaining the system within all operating constraints. This is especially the case when the turbo-machinery is integrated into a hybrid fuel cell gas turbine system. As a result, the bulk of the dynamic system analyses conducted to-date have focused upon this formidable challenge to the dynamic operation and control of gas turbines as integrated into hybrid systems.

Many of strategies for avoiding compressor surge have been described in previous sections. This section of the current report outlines all of the major turbo-machinery design and control strategies investigated over the course of these studies to-date followed by a listing of some approaches that warrant further investigation.

## Turbo-machinery Design and Control Strategies for Improved Dynamic Performance in Hybrid Systems Studied To-Date

- Decrease the compressor's design mass flow. This allows operation in a region that avoids surge but is associated with a penalty in compressor efficiency.
- A similar means of moving operation away from surge is to increase the design pressure ratio but again this comes with an efficiency penalty.
- Surge avoidance is substantially improved with the combined effects of reducing design mass flow and increasing design pressure ratio.
- Minimizing the volume between the gas turbine and the compressor helps in avoiding surge. This approach has been suggested by others (e.g., Hill & Peterson, 1992).
- Minimizing gas turbine rotational moment of inertia was found to help avoid surge during load sheds.
- Operating the compressor in the vertical region of the speed line was found to help avoid surge since there is little mass flow dependence on pressure ratio in this region. This is especially true for systems being controlled to operate at constant speed. Steep speed lines are desired in general compressor design philosophy to enhance compressor flow distortion tolerance (Greitzer, 1980).
- In general, one should design the compressor such that mass flow will not decrease faster than the pressure ratio can decrease as suggested by Kurz & White, 2004.
- When a PID controller is used, careful tuning of the controller is necessary to avoid dynamic operation paths that can lead to surge. Assuming the PID controller is effective at reaching its set points, there is very little if any effect that tuning has on final and initial states of the transient response to perturbations that may occur in the region associated with surge.
- Surge was found to be much less of a concern when fuel cell temperature is not a control parameter than when it was. This is because the compressor mass flow is the main manipulated variable for controlling fuel cell temperature. The fuel cell temperature control strategy should be designed to accept some delays in mass flow response (which the fuel cell should be able to handle due to large thermal mass) so that the hybrid system will have better surge avoidance.
- When fuel cell temperature *is not* a control parameter, cathode recycle blowers were found to lead to less compressor operating point fluctuation than when an ejector is used for the same purpose. Thus, a blower is preferred for surge avoidance and superior dynamic response to perturbations with this control strategy.
- When fuel cell temperature *is* a control parameter, there was very little difference in surge avoidance between systems that used a cathode blower or an ejector.
- Lower fuel cell set point temperatures were found to aid in avoiding surge since higher mass flow rates are required to achieve the lower temperature. However, this control strategy incurs a system efficiency penalty.
- Some of the dynamics found to lead to surge, especially in the case when fuel cell temperature was a control parameter, were: (1) large decreases in fuel cell load current, and (2) decreases in syngas hydrogen content.
- In general, it was found that machines driving synchronous generators were less likely to experience surge but were unable to effectively control fuel cell temperature for all the perturbations studied. The converse of this is true for asynchronous machines.

### Turbo-machinery Design and Control Strategies for Improved Dynamic Performance in Hybrid Systems that Merit Further Investigation

- Compressor bleed and bypass flow
- Variable inlet guide vanes
- New control strategies and feedback/feedforward control loops
- Effect of compressor inlet area
- Effect of number of compressor stages
- Centrifugal vs. axial compressor design
- Impact of turbine inlet temperature
- Impact of turbine design size on compressor operating point
- Impact of the magnitude of various pressure drops within the cycle on compressor operating point
- Other dynamic perturbations that may lead to surge should also be investigated

### **TASK 2.3: PERFORMANCE COMPARISON OF OXY-COMBUSTION AND IGCC PLANTS**

This task consists of comparing the Oxy-combustion cycle being developed by Clean Energy Systems (CES) with the down-selected advanced Brayton cycle based combined cycle in integrated coal gasification plants. Details of the work accomplished under this task are provided in the Appendix section of this report. Pittsburgh No. 8 coal is utilized in both types of plants. In an IGCC system which consists of pre-combustion carbon capture, the percentage of CO<sub>2</sub> capture is limited by the thermodynamic penalty required to shift the raw syngas to a H<sub>2</sub> and CO<sub>2</sub> mixture and the performance of the acid gas removal unit to separate the CO<sub>2</sub>. As the percentage of carbon capture is pushed beyond 80 to 90%, a point of diminishing return can be reached. The oxy-fuel cycle may provide an advantage over the pre-combustion decarbonization cycle since the water gas shift reaction is not required, less duty is placed on the acid gas removal system (if pre-combustion desulfurization is utilized) while nearly 100% of the carbon (as CO<sub>2</sub>) is captured. Thus as a first step, a study is required to compare the thermal performance of the two types of plants. Maintaining consistency in the design basis with respect to coal characteristics, site conditions, mode of heat rejection, etc. between the two cases is essential to obtain meaningful results.

The following lists the appropriate gasifier and / or its operating pressure for each of the cycles:

- For the IGCC cases, General Electric slurry feed entrained bed type gasifiers with two alternate heat recovery options as specified in the Statement of Work with operating pressures of:
  - Operating pressure of < 8.7 MPa (1260 psia) for Total Quench (TQ) Heat Recovery option
  - Operating pressure of 5.62 MPa (815 psia) for Radiant Syngas Cooler Plus Quench (R+Q) Heat Recovery option
- For the oxy-combustion cycle, a gasifier of the E-STR type offered by Conoco Phillips also slurry fed while operating at a pressure of 8.38 MPa (1215 psia).

The following summarize the results (for more details, see the Appendix section of this report):

The performance summaries for both the IGCC and the oxy-combustion cycle cases as presented in Appendix section of this report show that the oxy-combustion cycle based plants are less efficient than IGCC cases which have the slightly lower CO<sub>2</sub> capture at both firing temperatures studied and with the two heat recovery options used in the IGCC cases.

The relative economic worth of capturing additional CO<sub>2</sub> as measured by subtracting the CO<sub>2</sub> emission penalty cost (assumed at \$30/tonne) from the revenue stream associated with the sale of electricity (assumed at \$50/MWhr) at constant coal throughput (3,078 tonne/d of Pittsburgh No. 8 coal) show that there does not appear to be any advantage for the oxy-combustion based cases even with the assumed significantly high penalty of \$30/tonne for CO<sub>2</sub> emission and the assumed low sale price for electricity of \$50/MWhr.

**Table 1: Plant Performance Summary – Baseline and Sensitivity Case  
(ISO Ambient Conditions)**

	<b>IP ASU &amp; Air Extraction</b>	<b>HP ASU &amp; Air Extraction</b>
Fuel Feed Rate, ST/D (MF)	3,392	
MMBtu/hr (HHV)	3,744	
Fuel Feed Rate, Tonne/D (MF)	3,078	
GJ/hr (HHV)	3,949	
Power Generation, kW		
Gas Turbine	318,378	318,323
Steam Turbine	157,600	159,033
Clean Syngas Expander	2,320	2,320
Gas Turbine Extraction Air Expander	4,745	0
Auxiliary Power Consumption, kW	99,795	93,924
Net Plant Output, kW	383,247	385,753
Generation Efficiency (HHV)		
Net Heat Rate, Btu/kWh	9,769	9,706
Net Heat Rate, kJ/kWh	10,305	10,238
% Fuel to Power	34.94	35.16
Estimated NOx, ppmVd (15% O2 Basis)	18	
Raw Water Makeup, m3/kWh	0.0026	0.0026

**Table 2: Auxiliary (In-Plant) Power Consumption Summary – Baseline and Sensitivity Cases**

	<b>IP ASU &amp; Air Extraction</b>	<b>HP ASU &amp; Air Extraction</b>
	kW	kW
Coal Handling	401	401
Coal Milling	802	802
Coal Slurry Pumps	274	274
Slag Handling and Dewatering	155	155
Miscellaneous Syngas Plant Equipment	380	380
Air Separation Unit Air Compressors	14,778	15,788
Air Separation Auxiliaries	1,290	1,290
Oxygen Compressor	12,522	11,122
Nitrogen Compressor	22,007	16,415
CO <sub>2</sub> Compressor	19,368	19,368
Tail Gas Recycle Compressor	998	998
Boiler Feedwater Pumps	4,047	4,054
Cooling Tower and Pumps	7,242	7,340
Steam Condensate Pump	42	44
Selexol Acid Gas Removal	11,788	11,788
Syngas Humidification	214	214
Claus Plant Auxilliaries	100	100
Gas Turbine Auxiliaries	517	517
Steam Turbine Auxiliaries	517	517
General Makeup and Demineralized Water	322	322
Miscellaneous Balance-of-Plant and Lighting	1,000	1,000
Transformer Losses	1,031	1,034
<b>Total Auxiliary Power Consumption</b>	<b>99,795</b>	<b>93,924</b>

**Table 3: Main Features of the Power Cycle – High RIT Simple Cycle Gas Turbine**

	BASELINE CASE		High RIT Case with PR=37			High RIT Case with PR=50		
	<i>IP ASU &amp; Air Extraction</i>	<i>HP ASU &amp; Air Extraction</i>	<i>IP ASU &amp; Air Extraction</i>	<i>HP ASU &amp; Air Extraction</i>	<i>IP ASU &amp; No Extraction Air</i>	<i>IP ASU &amp; Air Extraction</i>	<i>HP ASU &amp; Air Extraction</i>	<i>IP ASU &amp; No Extraction Air</i>
<b>Gas Turbine</b>								
Power Output, kW	318,378	318,323	349,031	349,491	392,709	363,997	363,967	413,402
Rotor Inlet Temperature	1392°C (2538°F)		1734°C (3153°F)			1734°C (3153°F)		
Pressure Ratio	24		37			50		
Combustor								
Inlet Air Temperature	487°C (908°F)		583°C (1081°F)			659°C (1219°F)		
Discharge Temperature	1433°C (2611°F)		1781°C (3237°F)			1780°C (3236°F)		
Inlet Air Flow, kg/s	421.8 kg/s (930 lb/s)		258.2 kg/s (569.3 lb/s)			274.2 kg/s (604.5 lb/s)		
Discharge O2 Concentration, Vol %	7.8		2.7			3.4		
Exhaust Temperature	582°C (1079°F)		718°C (1325°F)			656°C (1213°F)		
Air Extracted, % of Inlet Air	14		20	20	0	20	20	0
<b>Steam Cycle</b>								
Power Output, kW	157,600	159,033	153,362	154,966	145,633	138,341	139,790	134,435
HP Steam Pressure	166.5 bara (2415 psia)		166.5 bara (2415 psia)			166.5 bara (2415 psia)		
Superheat & Reheat Temperatures	538°C (1000°F)		675°C (1247°F)			613°C (1135°F)		
<b>Overall Plant Performance</b>								
Fuel Feed Rate, Tonne/D (MF)	3,078		3,078			3,078		
GJ/hr (HHV)	3,949		3,949			3,949		
Net Plant Output, kW	383,247	385,753	411,254	414,136	414,807	411,579	414,028	420,451
Net Heat Rate, Btu/kWh	9,769	9,706	9,104	9,041	9,026	9,097	9,043	8,905
kJ/kWh	10,305	10,238	9,603	9,536	9,521	9,595	9,539	9,393
% Fuel to Power	34.94	35.16	37.49	37.75	37.81	37.52	37.74	38.33
Estimated NOx, ppmVd (15% O2 Basis)	15		31			55		
Raw Water Makeup, m3/kWh	0.0026	0.0026	0.0023	0.0023	0.0023	0.0023	0.0023	0.0022

**Table 4: Main Features of the Power Cycle – High RIT Intercooled Gas Turbine**

	Baseline Case		Intercooled High RIT GT		
	IP ASU & Air Extraction	HP ASU & Air Extraction	HP ASU & Air Extraction	IP ASU & No Air Extraction	IP ASU & No Air Extraction
<b>Gas Turbine</b>					
Power Output, kW	318,378	318,323	374,664	414,531	436,825
Rotor Inlet Temperature	1392°C (2538°F)		1734°C (3153°F)		1734°C (3153°F)
Pressure Ratio	24		50		70
<b>Combustor</b>					
Inlet Air Temperature	487°C (908°F)		523°C (973°F)		590°C (1094°F)
Discharge Temperature	1433°C (2611°F)		1781°C (3237°F)		1780°C (3236°F)
Inlet Air Flow, kg/s	421.8 kg/s (930 lb/s)		240.7 kg/s (530.6 lb/s)		252.2 kg/s (556.1 lb/s)
Inlet Air O2 Concentration, Vol %	20.74		19.90		19.81
Discharge O2 Concentration, Vol %	7.8		1.6		2.1
Adiabatic Flame Temperature	1891°C (3435°F)		1877°C (3410°F)		1901°C (3454°F)
Estimated NOx (15% O2 Dry Basis)	0		0		0
Exhaust Temperature	582°C (1079°F)		660°C (1220°F)		597°C (1107°F)
Air Extracted, % of Inlet Air	14		20	0	0
<b>Steam Cycle</b>					
Power Output, kW	157,600	159,033	132,820	129,254	112,891
HP Steam Pressure	166.5 bara (2415 psia)		166.5 bara (2415 psia)		166.5 bara (2415 psia)
Superheat & Reheat Temperatures	538°C (1000°F)		620°C (1147°F)		552°C (1025°F)
<b>Overall Plant Performance</b>					
Fuel Feed Rate, MT/D (MF)	3,078		3,078		3,078
GJ/hr (HHV)	3,949		3,949		3,949
Net Plant Output, kW	383,247	385,753	414,443	416,665	417,351
Net Heat Rate, Btu/kWh	9,769	9,706	9,034	8,986	8,971
kJ/kWh	10,305	10,238	9,529	9,478	9,463
% Fuel to Power	34.94	35.16	37.78	37.98	38.04
Estimated NOx, ppmVd (15% O2 Basis)					
Raw Water Makeup, m3/kWh	0.0026	0.0026	0.0023	0.0023	0.0023

**Table 5: Main Features of the Power Cycle – High RIT Intercooled-Reheat Gas Turbine**

	Baseline Case		Intercooled-Reheat High RIT GT	
	IP ASU & Air Extraction	HP ASU & Air Extraction	IP ASU & No Air Extraction	
<b>Gas Turbine</b>				
Power Output, kW	318,378	318,323	412,147	
Rotor Inlet Temperature	1392°C (2538°F)		1592°C (2898°F)	
			<b>HP</b>	<b>LP</b>
Pressure Ratio	24		70	27
<b>Combustor</b>				
Inlet Air Temperature	487°C (908°F)		590°C (1094°F)	1302°C (2375°F)
Discharge Temperature	1433°C (2611°F)		1636°C (2977°F)	1607°C (2924°F)
Inlet Air Flow, kg/s	421.8 kg/s (930 lb/s)		215.8 kg/s (475.8 lb/s)	292.2 kg/s (644.3 lb/s)
Inlet Air O2 Concentration, Vol %	20.74		19.81	4.76
Discharge O2 Concentration, Vol %	7.8		4.6	0.5
Adiabatic Flame Temperature	1891°C (3435°F)		1901°C (3454°F)	1639°C (2982°F)
Estimated NOx (15% O2 Dry Basis)			0	
Exhaust Temperature	582°C (1079°F)		704°C (1299°F)	
Air Extracted, % of Inlet Air	14		0	
<b>Steam Cycle</b>				
Power Output, kW	157,600	159,033	130,891	
HP Steam Pressure	166.5 bara (2415 psia)		166.5 bara (2415 psia)	
Superheat & Reheat Temperatures	538°C (1000°F)		661°C (1222°F)	
<b>Overall Plant Performance</b>				
Fuel Feed Rate, MT/D (MF)	3,078		3,078	
GJ/hr (HHV)	3,949		3,949	
Net Plant Output, kW	383,247	385,753	416,102	
Net Heat Rate, Btu/kWh	9,769	9,706	8,998	
kJ/kWh	10,305	10,238	9,491	
% Fuel to Power	34.94	35.16	37.93	
Raw Water Makeup, m3/kWh	0.0026	0.0026	0.0023	

**Table 6: Main Features of the Power Cycle –Intercooled Closed Circuit Air Cooled Gas Turbine**

	<b>Baseline Case</b>	<b>Intercooled - Closed-Circuit Air Cooled Gas Turbine</b>
<b>Gas Turbine</b>		
Pressure Ratio	24	50
ASU	IP	IP
Air Extraction	Yes	No
Power Output, kW	318,378	425,808
Rotor Inlet Temperature	1392°C (2538°F)	1678°C (3053°F)
<b>Combustor</b>		
Inlet Air Temperature	487°C (908°F)	530°C (986°F)
Discharge Temperature	1433°C (2611°F)	1712°C (3114°F)
Inlet Air Flow, kg/s	421.8 kg/s (930	288 kg/s (634 lb/s)
Inlet Air O <sub>2</sub> Concentration, Vol %	20.74	19.90
Discharge O <sub>2</sub> Concentration, Vol %	7.8	3.5
Adiabatic Flame Temperature	1891°C (3435°F)	1919°C (3486°F)
<b>Estimated NO<sub>x</sub> (15% O<sub>2</sub> Dry Basis)</b>		
2nd PSR Residence Time = 30 ms <sup>1</sup>	18	115
2nd PSR Residence Time = 5 ms <sup>2</sup>	17	35
Exhaust Temperature	582°C (1079°F)	620°C (1148°F)
Air Extracted, % of Inlet Air	14	0
<b>Steam Cycle</b>		
Power Output, kW	157,600	118,289
HP Steam Pressure	166.5 bara (2415	166.5 bara (2415 psia)
Superheat & Reheat Temperatures	538°C (1000°F)	577°C (1070°F)
<b>Overall Plant Performance</b>		
Fuel Feed Rate, MT/D (MF)	3,078	3,078
GJ/hr (HHV)	3,949	3,949
Net Plant Output, kW	383,247	417,249
Net Heat Rate, Btu/kWh	9,769	8,973
kJ/kWh	10,305	9,465
% Fuel to Power	34.94	38.03
Raw Water Makeup, m <sup>3</sup> /kWh	0.0026	0.0022

**Table 7: Main Features of the Power Cycle –Air Partial Oxidation Topping Cycle**

	<b>Baseline Case</b>	<b>Air POX Gas Turbine</b>	
<b>Gas Turbine</b>			
Pressure Ratio	24	70	37
ASU	IP	IP	
Air Extraction	Yes	No	
Power Output, kW	318,378	21,237	380,040
Rotor Inlet Temperature	1392°C (2538°F)	1699°C (3090°F)	
<b>Combustor</b>			
Inlet Air Temperature	487°C (908°F)	514°C (958°F)	583°C (1081°F)
Discharge Temperature	1433°C (2611°F)	927°C (1700°F)	1954°C (3550°F)
Inlet Air Flow, kg/s	421.8 kg/s (930	17.8 kg/s (39.2 lb/s)	239.3 kg/s (527.5 lb/s)
Inlet Air O <sub>2</sub> Concentration, Vol %	20.74	18.70	20.74
Discharge O <sub>2</sub> Concentration, Vol %	7.8	0	2.96
Adiabatic Flame Temperature	1891°C (3435°F)		1880°C (3416°F)
<b>Estimated NO<sub>x</sub> (15% O<sub>2</sub> Dry Basis)</b>			
2nd PSR Residence Time = 30 ms <sup>1</sup>	18	117	
2nd PSR Residence Time = 5 ms <sup>2</sup>	17	32	
Exhaust Temperature	582°C (1079°F)	698°C (1289°F)	
Air Extracted, % of Inlet Air	14	0	
<b>Steam Cycle</b>			
Power Output, kW	157,600	141,692	
HP Steam Pressure	166.5 bara (2415	166.5 bara (2415 psia)	
Superheat & Reheat Temperatures	538°C (1000°F)	655°C (1211°F)	
<b>Overall Plant Performance</b>			
Fuel Feed Rate, MT/D (MF)	3,078	3,078	
GJ/hr (HHV)	3,949	3,949	
Net Plant Output, kW	383,247	415,660	
Net Heat Rate, Btu/kWh	9,769	9,008	
kJ/kWh	10,305	9,501	
% Fuel to Power	34.94	37.89	
Raw Water Makeup, m3/kWh	0.0026	0.0023	

1. NO<sub>x</sub> values are predicted using a Chemkin 2 PSR model with a 0.44 millisecond residence time in the first reactor and a 30 millisecond residence time in the second reactor.
2. NO<sub>x</sub> values are predicted using a Chemkin 2 PSR model with a 0.44 millisecond residence time in the first reactor and a 5 millisecond residence time in the second reactor.

## CONCLUSIONS

Details of the work accomplished under each of the tasks below are provided in the Appendix section of this report.

### **TASK 1.2 – IDENTIFY BASELINE CYCLE CONFIGURATION**

The plant scheme consisting of a cryogenic air separation unit supplying 95% purity O<sub>2</sub> to GE type HP total quench gasifiers is suitable for these zero emission IGCCs when gasifying bituminous coal such as the Pittsburgh No. 8. The raw gas after scrubbing is treated in a sour shift unit to react the CO with H<sub>2</sub>O to form H<sub>2</sub> and CO<sub>2</sub>. The gas is further treated to remove Hg in a sulfided activated carbon bed. The syngas is desulfurized and decarbonized in a Selexol acid gas removal unit and the decarbonized syngas after humidification and preheat is fired in a GE 7H type steam cooled gas turbine. IP N<sub>2</sub> from the ASU is also supplied to the combustor of the gas turbine as additional diluent for NO<sub>x</sub> control. A portion of the air required by the ASU is extracted from the gas turbines.

### **TASK 1.3 - FIRST DETAILED SYSTEMS STUDY ANALYSIS – BASELINE CASE**

The Baseline Case consisting of an IGCC facility utilizing a single train GE 7H type gas turbine while gasifying Pittsburgh No. 8 coal and capturing 90% of the carbon present in the syngas as gaseous compounds, generates 383.2 MW at ISO conditions on a net basis. The corresponding net plant heat rate is 10,305 kJ/kWh (HHV) which is about 5 to 10% lower than an IGCC plant also designed for 90% carbon capture but utilizing GE 7FA+e gas turbines.

The impact on overall plant performance of limiting the NO<sub>x</sub> emissions to 2 ppmVd (15% O<sub>2</sub> basis) by installing an SCR in the HRSG downstream of the gas turbine was found to be insignificant. The gas turbine back pressure was increased in order to accommodate pressure drop across the SCR. Pressure drops ranging from by 2 to 5 In W.C. were investigated (the catalyst requirement and thus the cost of the SCR unit being reduced as the allowable pressure drop is increased). The IGCC plant performance was insignificantly effected. The heat rate increased from 10,305 kJ/kWh (Baseline Case) to 10,319 kJ/kWh with 2 In W.C. to 10,331 kJ/kWh with 5 In W.C. A catalytic NH<sub>3</sub> oxidation unit may be installed in the HRSG downstream of the SCR if the NH<sub>3</sub> slippage from the SCR is cause for concern from an environmental emissions standpoint. The pressure drop of this additional catalytic unit is expected to be similar to that of the SCR.

### **TASK 1.4.1 – SCREENING ANALYSIS OF ADVANCED BRAYTON CYCLES**

Based on the results of this screening study, the cycles in the order listed under “Promising Cycles” in the following are selected for the Task 1.4.2, “Advanced Brayton Cycle Detailed

Analysis.” Analysis of each of these selected cycles in an integrated gasification based power plant is performed in order to quantify the required firing temperature (along with the corresponding blade metal / TBC temperatures and pressure ratio) to meet the ultimate goal of achieving the efficiency target of this program. Sensitivity to cycle pressure ratio and letting the gas turbine exhaust temperature rise above the 650°C or 1200°F constraint used in the Screening Study is also required. Appropriate advanced steam cycle conditions will be utilized corresponding to the higher gas turbine exhaust temperatures.

### **Promising Cycles**

The promising cycles selected for the detailed analysis task are listed below. The results of this detailed analysis task further narrow down the cycles to the most promising cycle or cycles. Sensitivity analysis is performed on the selected most promising cycle of incorporating higher compressor and turbine efficiencies, high efficiency exhaust diffuser, application of superconductivity technology to transformers and generators as well as the impact of increasing the diluent nitrogen addition to the gas turbine combustor in order to lower NO<sub>x</sub> emission.

1. Steam-cooled Simple Cycle Gas Turbine based Combined Cycle
2. Steam-cooled Intercooled Gas Turbine based Combined Cycle
3. Steam-cooled Intercooled and Reheat Gas Turbine based Combined Cycle
4. Air PO<sub>x</sub> Topping Cycle added to a Steam-cooled Gas Turbine based Combined Cycle
5. Closed Circuit Air-cooled Gas Turbine based Combined Cycle.

## **TASK 1.4.2: DETAILED ANALYSIS OF ADVANCED BRAYTON CYCLES**

### **Simple Cycle Gas Turbine based IGCC with Increased Firing Temperature**

Based on the results developed for the first of the advanced cases which consists of a steam-cooled gas turbine combined cycle with increased firing and blade surface temperatures, it may be concluded that a substantial increases in both firing temperature and blade surface temperature are required over the Baseline Case, about 342°C or 615°F to meet the performance improvement goals of this study. Significant increases in gas turbine pressure ratio are also required to limit the exhaust temperature. Incorporation of aero-derivative compressor design including materials to withstand the higher air temperatures within the compressor would be required for such high pressure ratio gas turbines.

For these very high firing temperature cases advanced low NO<sub>x</sub> combustor designs described under Task 1.4.1 may not suffice since the air to fuel ratio is too small to cause rapid quenching of the flame within the combustor to limit the formation of NO<sub>x</sub>. More diluent addition and/or SCRs would be required to limit the NO<sub>x</sub> emissions to the desired 2 ppmVd (15% O<sub>2</sub> basis) value. Higher SCR catalyst volume would be required for these advanced firing temperature cases, however, since the amount of NO<sub>x</sub> generated within the combustor is substantially higher than that in the Baseline Case. A correspondingly higher pressure drop across the SCR would

result making the heat rate penalty a little more significant than that seen in the sensitivity case developed for the Baseline Case in Task 1.3.

In addition to the NO<sub>x</sub> being higher for the gas turbine with a pressure ratio of 50 as compared to the gas turbine with a pressure ratio of 37, a major challenge associated with developing such a gas turbine with a pressure ratio of 50 is the design of the compressor and its materials. On the other hand, in the case of a gas turbine operating at a pressure ratio of 37 and with the required advanced firing temperature, major challenges are associated with the design of the last section of the turbine since this section of the turbine operates at significantly higher temperatures. Furthermore, a steam turbine also capable of operating at significantly high temperatures is required. More expensive superheater and reheater coils in the HRSG and the piping between the HRSG and the steam turbine would be required due to the higher grade metallurgical requirements.

### **Intercooled Gas Turbine based IGCC with Increased Firing Temperature**

Based on the results developed for this advanced case which consists of an intercooled steam cooled gas turbine combined cycle, it may be concluded that incorporation of intercooling into these very high pressure ratio gas turbines is a very desirable feature although challenges associated with developing the gas turbine with the required high firing temperature and pressure ratio remain. Similar to the previous non-intercooled advanced case, substantial increases in both firing temperature and blade surface temperature are required over the Baseline Case, about 342°C or 615°F to meet the performance improvement goals of this study. Incorporation of aero-derivative compressor design would be required for such high pressure ratio gas turbines.

Again, advanced low NO<sub>x</sub> combustor designs described under Task 1.4.1 may not suffice since the air to fuel ratio is too small to cause rapid quenching of the flame within the combustor to limit the formation of NO<sub>x</sub>. More diluent addition may be a challenge for the combustor design since the O<sub>2</sub> content of the combustor exhaust gas is already very low at 1.6% for the 50 pressure ratio case and slightly higher at 2.1% for the 70 pressure ratio case. SCRs would be required to limit the NO<sub>x</sub> emissions to the desired 2 ppmVd (15% O<sub>2</sub> basis) value. Higher SCR catalyst volume would be required for these advanced firing temperature cases, however, since the amount of NO<sub>x</sub> generated within the combustor is substantially higher than that in the Baseline Case. A correspondingly higher pressure drop across the SCR would result making the heat rate penalty a little more significant than that seen in the sensitivity case developed for the Baseline Case in Task 1.3.

The developmental challenges of this intercooled advanced gas turbine are similar to the previous case with respect to the need for very high firing and blade surface temperatures. The next set of advanced cases to be evaluated consist of a reheat gas turbine in order to reduce the firing temperature as explained under Task 1.4.1 while maintaining a similar heat rate improvement goal over the Baseline Case.

## **Intercooled-Reheat Gas Turbine based IGCC with Increased Firing Temperature**

Based on the results developed for this advanced case which consists of an intercooled-reheat steam cooled gas turbine combined cycle, it may be concluded that much lower increases in both firing temperature and blade surface temperature (as compared to the previous non-reheat cases with advanced firing temperatures) are required over the Baseline Case to achieve the heat rate improvement goal set for this study. On the other hand, significant increase in gas turbine pressure ratio is required to limit the exhaust temperature.

Again, advanced low NO<sub>x</sub> combustor designs described under Task 1.4.1 may not suffice since the air to fuel ratio is too small. More diluent addition may be a challenge for the combustor design since the O<sub>2</sub> content of the combustor exhaust gas is already very low at 0.5%. SCR's would be required to limit the NO<sub>x</sub> emissions to the desired 2 ppmVd (15% O<sub>2</sub> basis) value. Higher SCR catalyst volume would be required for this advanced firing temperature case, however, since the amount of NO<sub>x</sub> generated within the combustor is substantially higher than that in the Baseline Case. A correspondingly higher pressure drop across the SCR would result making the heat rate penalty a little more significant than that seen in the sensitivity case developed for the Baseline Case in Task 1.3.

In addition, a major challenge associated with developing a gas turbine for this cycle is the need for a very high pressure ratio of 70. Even with this very high pressure ratio the gas turbine exhaust remained high at 704°C or 1299°F. The required steam superheat and reheat temperatures for this case had to be consequently increased to 661°C or 1222°F in order to minimize the irreversibility in heat transfer. A steam turbine capable of operating at significantly high temperatures is thus required. More expensive superheater and reheater coils in the HRSG and the piping between the HRSG and the steam turbine are also required due to the higher grade metallurgical requirements.

## **Intercooled Closed Circuit Air Cooled Gas Turbine based IGCC with Increased Firing Temperature**

Based on the results developed for this advanced case, it may be concluded that incorporation of closed circuit air cooling of the blades in the HP sections of the gas turbine allows a significant reduction in the firing temperature and the blade surface temperatures while achieving similar overall plant heat rate. Incorporation of aero-derivative compressor design would be required for this intercooled and high pressure ratio gas turbine.

Again, advanced low NO<sub>x</sub> combustor designs described under Task 1.4.1 may not suffice since the air to fuel ratio is too small to cause rapid quenching of the flame within the combustor to limit the formation of NO<sub>x</sub>. More diluent addition to the combustor may be a partial solution. The O<sub>2</sub> content of the combustor exhaust gas at 3.5% is higher than the previous advanced cases leaving room for some additional diluent addition. SCR may also be required to limit the NO<sub>x</sub> emission to the desired 2 ppmVd (15% O<sub>2</sub> basis) value. Higher SCR catalyst volume would be required for this advanced firing temperature case, however, since the amount of NO<sub>x</sub> generated within the combustor is substantially higher than that in the Baseline Case. A correspondingly

higher pressure drop across the SCR would result making the heat rate penalty a little more significant than that seen in the sensitivity case developed for the Baseline Case in Task 1.3.

### **Air Partial Oxidation Topping Cycle**

Based on the results developed for this advanced case, it may be concluded that only slight reductions in firing temperature and blade surface temperature may be realized for the advanced gas turbine (Ox turbine) when integrated with the POx system as compared to the first two advanced cases investigated while achieving the required heat rate improvement goal set for this study. On the other hand, this firing temperature is higher than both the reheat and the closed circuit air cooled gas turbine cases. The pressure ratio for the advanced gas turbine is modest at 37 but the exhaust temperature is much higher than the desired value of 649°C or 1200°F.

Again, advanced low NO<sub>x</sub> combustor designs described under Task 1.4.1 may not suffice since the air to fuel ratio is quite small. More diluent addition may be a partial solution since the O<sub>2</sub> content of the combustor exhaust gas is already quite low at 2.96%. SCRs would be required to limit the NO<sub>x</sub> emissions to the desired 2 ppmVd (15% O<sub>2</sub> basis) value. Higher SCR catalyst volume would be required for this advanced case, however, since the amount of NO<sub>x</sub> generated within the combustor is substantially higher than that in the Baseline Case. A correspondingly higher pressure drop across the SCR would result making the heat rate penalty a little more significant than that seen in the sensitivity case developed for the Baseline Case in Task 1.3.

In addition, major challenges are associated with the development of the POx turbine such as concerns with its seals, H<sub>2</sub> embrittlement and corrosion due to loss of oxide protective layer as well as the overall fuel control issues. The advanced gas turbine (Ox turbine) exhaust temperature is high at 698°C or 1289°F<sup>c</sup>. The required steam superheat and reheat temperatures for this case had to be consequently increased to 655°C or 1211°F in order to minimize the irreversibility in heat transfer. A steam turbine capable of operating at significantly high temperatures is thus required. More expensive superheater and reheater coils in the HRSG and the piping between the HRSG and the steam turbine are also required due to the higher grade metallurgical requirements. The heat exchange equipment and piping within the POx unit will also cause a significant increase in the plant cost.

### **Selection of Advanced Brayton Cycle**

It may be concluded from the results obtained by this detailed analysis of the above discussed advanced Brayton cycles that the more promising advanced Brayton cycles are the high pressure ratio intercooled gas turbines employing either closed circuit steam or air cooling. The following summarizes the attributes of these two advanced cycles:

- Required gas turbine pressure ratio of 50 is close to that of a commercially proven aero-engine while limiting the exhaust temperature to a reasonable value.

---

<sup>c</sup> Note that this exhaust temperature may be reduced by increasing the pressure ratio across the Ox turbine. However, this will then require a further increase in the operating pressure of the POx unit, i.e., beyond the already high 70 atm in order to maintain a reasonable pressure ratio across the POx turbine.

- Spray intercooling which has been proven in a commercial aero-engine derived gas turbine has the following advantages:
  - Lower compressor discharge temperature than that in a non-intercooled gas turbine with the same pressure ratio
    - Savings in materials of construction may be realized
    - Produces lower NO<sub>x</sub> emission not only due to lower compressor discharge temperature (or combustor inlet air temperature) but also due to the higher humidity of this air stream (caused by using the spray intercooler)
  - Higher specific power output
    - Reduced compressor work (in a simple cycle gas turbine, approximately half of turbine power is used in compression)
    - Spray water increases the motive fluid for expansion in the turbine.

Next, comparing these two advanced cycles:

- The required firing and blade surface temperatures for the closed circuit air cooled case are a bit lower (by about 56°C or 100°F) along with NO<sub>x</sub> emissions as compared to the corresponding closed circuit steam cooled case.
- However, closed circuit air cooling has not been demonstrated while the reliability of the cooling air compressor is a concern.
- On the other hand, start-up and shutdown procedures for the closed circuit air cooled case may be simpler than those for the closed circuit steam cooled case.
- The steam cooled case however, incorporates proven cooling technology and H class combined cycles (utilizing the steam cooled gas turbines) have been operated successfully in commercial applications which include startup and shutdown operations.

Based on these above attributes of these two advanced cycles, the most promising cycle for further analysis appears to be the steam cooled case, i.e., an advanced Brayton cycle employing a high pressure ratio gas turbine with spray intercooling, closed circuit steam cooling and an advanced firing temperature. Sensitivity analysis is conducted on this selected cycle as described in the following.

### **Sensitivity Analysis of Selected Advanced Brayton Cycle**

The sensitivity analysis which quantifies the reduction in the firing temperature made possible by incorporating improvements in the other areas while realizing the same overall improvement in plant efficiency over the Baseline Case prioritizes the development needs of the advanced Brayton cycle. Low NO<sub>x</sub> strategies are also investigated as well as use of air cooling as an alternate to closed circuit steam cooling of the turbine 1<sup>st</sup> stage which has very high operating temperature, the film of air forming on the outside surface of the blade providing an additional insulating layer (i.e., in addition to thermal barrier coatings to protect the metal).

### **Gas Turbine Compressor Efficiency**

The results of this analysis indicate that very substantial aerodynamic design improvements are required to the gas turbine compressor to realize a significant reduction in the required firing

temperature. The need for very high firing temperature is not diminished by a significant amount however, and shows that major emphasis should be placed on technology developments required to realize the very high firing temperature identified by this study.

### **Gas Turbine Expander Efficiency**

The results of this analysis are similar to the previous compressor efficiency analysis, i.e., indicate that very substantial aerodynamic design improvements are required to the gas turbine expander to realize a significant reduction in the required firing temperature. The need for very high firing temperature is not diminished by a significant amount however, and shows that major emphasis should be placed on technology developments required to realize the very high firing temperature identified by this study.

### **High Efficiency Exhaust Diffuser**

By increasing the coefficient of performance (for a conventional diffuser it is typically around 0.6) to 0.9, about 30°C or 54°F reduction in the firing temperature may be realized. Once again the need for very high firing temperature is not diminished by a significant amount however, and shows that major emphasis should be placed on technology developments required to realize the very high firing temperature identified by this study.

### **Application of Superconductivity Technology**

Superconductivity technology offers higher efficiency electrical equipment such as generators and transformers but the efficiencies are already quite high and the application of the more efficient electrical equipment is not expected to make a significant improvement in the overall plant performance or conversely a significant reduction in the required firing temperature of the gas turbine for a targeted overall plant performance.

### **Low NO<sub>x</sub> Strategies**

As discussed previously, a partial solution to reducing the NO<sub>x</sub> emission may be to limit the residence time in the dilution zone of the combustor by constructing a short combustor (reducing the residence time from 30 ms to 5 ms reduced the NO<sub>x</sub> by as much as ~ 70% for the very high rotor inlet cases while the burnout of H<sub>2</sub>, CO and CH<sub>4</sub> was not affected significantly, the fuel being decarbonized syngas contains only small concentrations of CO and CH<sub>4</sub>). As mentioned previously, a short residence time combustor, however, will pose a problem if natural gas firing is required either at startup or as a backup fuel and other means of NO<sub>x</sub> control would be preferred. Thus, other strategies are considered as follows.

#### Increased Diluent Nitrogen Addition

Increasing the diluent addition to the syngas is a strategy investigated in this sensitivity analysis which may be done in addition to installing an SCR. In the Baseline Case, the combined LHV of

the humidified syngas and diluent N<sub>2</sub> (provided by the ASU) is 4,720 kJ/nm<sup>3</sup> or 120 Btu/scf. The ASU can be designed to provide additional nitrogen for syngas dilution. With an ASU designed to provide the maximum amount of N<sub>2</sub>, the resulting (lowest) combined LHV of the humidified syngas and diluent N<sub>2</sub> is 3,980 kJ/nm<sup>3</sup> or 101 Btu/scf. The increased nitrogen dilution reduces the NO<sub>x</sub> significantly, from 42 ppmvd to 10 ppmvd (at 15% O<sub>2</sub> concentration) with the shorter combustors, i.e., corresponding to a residence time of 5 ms in the 2<sup>nd</sup> PSR. However, the firing temperature of gas turbine is also reduced, by about 22°C or 40°F resulting in an increase in the net plant heat rate by about 2.2%.

### Reduced Firing Temperature

The trade-off between heat rate and NO<sub>x</sub> emission by reducing the firing temperature is investigated in this sensitivity analysis. The results of this analysis show that a 56°C or 100°F reduction in firing temperature from the initial 1734°C or 3153°F results in approximately 1.5% increase in heat rate while the NO<sub>x</sub> reduces from 42 ppmvd to 28 ppmvd (at 15% O<sub>2</sub> concentration) with the shorter combustors, i.e., corresponding to a residence time of 5 ms in the 2<sup>nd</sup> PSR. A further 56°C or 100°F reduction in firing temperature (i.e. 93°C or 200°F reduction from the initial 1734°C or 3153°F) results in an additional 1.5% or total of 3% increase in heat rate while the NO<sub>x</sub> reduces from 42 ppmvd to 20 ppmvd (at 15% O<sub>2</sub> concentration).

### **Air (Film) Cooled 1<sup>st</sup> Stage Turbine**

The effect on plant performance of utilizing air (film) cooling of the 1<sup>st</sup> stage turbine stationary and rotating blades instead of closed circuit steam cooling show that the heat rate penalty of utilizing air (film) cooling for the 1<sup>st</sup> stage instead of closed circuit steam cooling is about 0.8%, quantifying the trade-off between plant performance and the need for developing the necessary more advanced materials required with closed circuit steam cooling of the 1<sup>st</sup> stage.

### Economic Analysis

The ROM plant cost estimate for the Baseline Case is \$2,285/kW while that for the selected advanced Brayton cycle consisting of the spray intercooled gas turbine with the advanced firing temperature is \$2,107/kW (on a 4<sup>th</sup> quarter 2007 basis) which is a 7.8% reduction in cost.

The levelized cost of electricity for the Baseline Case was estimated at \$85.72/MWhr while that for the Advanced Brayton cycle case was estimated at \$79.08/MWhr (at a capacity factor of 80% and with the Pittsburgh No. 8 coal priced at \$1.73/MM Btu, HHV) which is almost an 8% reduction over the Baseline Case. If a cost penalty of \$30/ST CO<sub>2</sub> emitted is assigned to the two cases, then the levelized cost of electricity of the Baseline Case is increased to \$89.08/MWhr while that for the Advanced Brayton cycle case is increased to \$82.19/MWhr.

### Development Needs

The greatest technological challenge for the development of this advanced intercooled gas turbine is in the area of materials required to withstand the very high firing temperature. Thus,

the sensitivity analysis performed and discussed in a previous section on this cycle measured the reduction in the firing temperature that may be made possible (and thus the required advanced turbine materials to meet the overall plant thermal efficiency goal) by making performance enhancements in other areas, specifically gas turbine component aerodynamics. Their individual contributions are not highly significant but the data shows that the sum total contribution can be significant, as much as 70°C or 126°F reduction in the firing temperature. A reduction of 70°C or 126°F in the firing temperature has the additional benefit of reducing NO<sub>x</sub> emission. Based on data developed in the previous sensitivity analysis of the effect of firing temperature on NO<sub>x</sub>, a significant reduction in the NO<sub>x</sub> from 42 ppmvd to 26 ppmvd (at 15% O<sub>2</sub> concentration) may be realized (while utilizing the shorter combustors, i.e., corresponding to a residence time of 5 ms in the 2<sup>nd</sup> PSR) with the 70°C or 126°F decrease in firing temperature. Thus development in these other areas should also be pursued in tandem with advanced materials. Following summarizes specific development areas:

- Apart from the need for a short combustor to minimize the residence time to limit NO<sub>x</sub>, a combustor to withstand the very high temperatures is required. The relatively small amount of excess air used to increase the firing temperature further exacerbates the technological challenge for the development of such a combustor. SCRs would be required to limit the NO<sub>x</sub> emissions to the desired 2 ppmVd (15% O<sub>2</sub> basis) value. Higher SCR catalyst volume would be required for these advanced firing temperature cases, however, since the amount of NO<sub>x</sub> generated within the combustor is substantially higher than that in the Baseline Case.
- Combustor materials that can withstand a combination of creep, pressure loading, high cycle and thermal fatigue at these temperatures are required. Materials technology for the combustor should be aimed at replacement of conventional wrought nickel-based products with:
  - More suitable Ni-based alloys
  - Oxide dispersion strengthened metallic systems
  - Ceramic matrix composites.

Developments aimed at applying thicker coatings to enable the higher firing temperature as well as increasing the phase stability and resistance to sintering of the ceramic topcoat at higher temperatures are required.

- The overall pressure ratio of 50 for the advanced Brayton cycle is significantly higher than what has been currently demonstrated but such a high pressure ratio has been proposed for an advanced aero engine (Pratt & Whitney's baseline engine proposed for Boeing's 787 transport plane) and is close to that of the aero-derivative GE LMS100 intercooled gas turbine which has a pressure ratio of 41 at ISO conditions. The advanced Brayton cycle design will thus have to be based on modifying an existing aero-derivative engine such as the GE LMS100; by adding stages at the front-end of the LP compressor<sup>f</sup> and / or at the back-end of the HP compressor depending on the existing Mach number limitations. An added advantage of utilizing the GE LMS100 engine is

---

<sup>f</sup> Addition of front-end stages increases the suction air flow.

that it is configured with an intercooler. The suction air flow of this engine is 208 kg/s or 458 lb/s at ISO conditions. With a plant specific power output of 1,639 kW/(kg/s) or 743 kW/(lb/s) for the advanced Brayton cycle IGCC, the net plant output on a per gas turbine basis would be 1,639 kW/(kg/s) x 208 kg/s or 340 MW; or for a two gas turbine based plant, the net output would be 680 MW, a reasonable (i.e., economically viable) plant size. If an aircraft engine is modified instead, the major mechanical changes from aircraft to this ground-based engine involves replacing the turbofan and installing a new LP compressor using lower cost materials, combustor changes, HP turbine changes to handle increased flow and to reduce cost, and a new, lower cost LP turbine to expand to atmospheric pressure. Additional shaft length to accommodate scrolls for the intercooler would also be needed. The key to keeping development costs to a minimum is keeping gas path the same, thereby allowing the compressors, especially the high pressure compressor to remain unchanged, except for materials. In either case, the development of the advanced Brayton cycle which requires an aero-frame engine should be based on the use of existing compressor gas path designs. This would significantly reduce the cost of development.

- Spray intercooling has been commercially practiced in the GE LM6000 SPRINT engine for a number of years. Presence of any water droplets in the intercooler discharge would lead to erosion of the HP compressor blading and erosion resistant coatings for existing materials or development of erosion resistant materials may be required. Proper design of the spray system is essential to minimize droplet carryover into the HP compressor. A demister pad installed at the discharge end of the intercooler with low pressure drop characteristics would be very desirable.
- The 1<sup>st</sup>, 2<sup>nd</sup> and 3<sup>rd</sup> stages of the turbine employ closed circuit steam cooling while the 4<sup>th</sup> and 5<sup>th</sup> stages employ open circuit air cooling. Steam with its very high specific heat is an excellent cooling medium while the advantage with closed circuit cooling is that the momentum and dilution losses which are incurred in open circuit cooling are avoided. On the other hand, open circuit film cooling of the blades (utilizing air) has the advantage of forming a protective layer on the outside surface of the blade, i.e., by creating an additional insulating layer (i.e., in addition to thermal barrier coatings to protect the metal). The effect of utilizing air (film) cooling of the 1<sup>st</sup> stage turbine stationary and rotating blades (where the temperatures are highest) instead of closed circuit steam cooling is that the heat rate is increased by about 0.8%, quantifying the trade-off between plant performance and the need for developing the necessary more advanced materials required with closed circuit steam cooling of the 1<sup>st</sup> stage.
- As the turbine firing temperatures are being increased, conventionally cast nickel-based super-alloys are being replaced by directional solidification blades as well as single crystal blades which provide even more significant benefits. However, alloys with greater defect tolerance need to be developed and demonstrated. Development of alloys having improved castability, higher corrosion resistance and reduced heat treatment times are required. A holistic approach is required to include coatings, liding and repair while development of multilayer coatings and application methods are required to improve

reliability and reduce cost. Development of ceramic matrix composites may also be required for the very hot components or sections of the turbine.

- Based on the development costs and timeline for advanced gas turbines as documented in a previous study conducted for the DOE / NETL under contract DE-FC26-00NT40845, the design and component test phase may take approximately 40 to 42 months. Initial build could commence with long lead items about half way through the first phase and last 24 to 27 months. At the end of the approximately 54 months, test of the initial unit could begin and could last approximately 15 months. Cost for such a program can be between \$250 and \$275 million, the program being predicated on a minimum commitment of 8 engines.

## **TASK 2.1 - EVALUATION OF IMPACT OF RAMGEN COMPRESSION TECHNOLOGY ON IGCC PLANT PERFORMANCE**

The Ramgen LP and IP CO<sub>2</sub> compressors with their higher efficiencies can save about 0.5 MW in in-plant electric power consumption for this 380 MW IGCC near zero emission power plant. The Ramgen HP CO<sub>2</sub> compressor with intercooling provides the greatest advantage. The net result of utilizing this higher efficiency compressor is that the plant output is increased by 1.1 MW over the Baseline Case. This increment is only slightly lower (0.3 MW) than that obtained by utilizing the Ramgen high efficiency non-intercooled HP CO<sub>2</sub> compressor with the conversion of the exhaust heat by a hypothetical working fluid (with variable evaporation and condensing temperatures) which represents an upper limit for this heat conversion process. Thus, from an overall plant thermal efficiency standpoint, the Ramgen high efficiency intercooled compressor technology is more promising. The net increase in power output over the Baseline Case of utilizing the Ramgen LP, IP and intercooled HP compressors for CO<sub>2</sub> compression is 1.61 MW for this 380 MW IGCC plant.

Next, by applying the Ramgen technology to the gas turbine extraction air expander, the ASU air and nitrogen compressors in addition to the CO<sub>2</sub> compressors, the net power output over the Baseline Case is increased significantly, by as much as 5.92 MW for this 380 MW IGCC plant.

Thus, the high efficiency intercooled Ramgen compressors can play a significant role in improving the efficiency of IGCC plants, especially in zero emission plants where CO<sub>2</sub> capture is required, subject to verification of the compressor efficiencies by test work.

## **TASK 2.2 - DYNAMIC SIMULATION OF FUEL CELL / GAS TURBINE SYSTEM**

These studies primary focused on the impact of perturbations to the steady state design operating point that led to gas turbine failure in the form of compressor surge and design and operational strategies to avoid this phenomenon. The pressure fluctuations associated with compressor surge will likely damage if not destroy the fuel cell before the turbo-machinery if pressure regulators are not placed between the fuel cell stack and the turbo-machinery. The main perturbations investigated that lead to surge were load shed and dilution of syngas hydrogen content with nitrogen or steam. Fuel cell shutdowns also led to surge. The design strategies that were found

to help in avoiding surge include designing the turbine and compressor to allow greater surge margin under steady state operation, minimizing the plenum volume between the fuel cell outlet and turbine inlet, minimizing gas turbine rotational moment of inertia and designing for compressor speed lines that are more vertical in nature. Modification of the turbo-machinery design pressure ratio and mass flow to achieve more stable dynamic response to load shed and fuel dilution perturbations usually comes with an efficiency penalty. But, the efficiency penalty associated with these design modifications may be worth the increase in stability. This argument is further supported if the gas turbine is mainly seen as a means of feeding air to the fuel cell.

The dynamic response of the fuel cell was studied for the above mentioned perturbations. These responses include anode-cathode inlet pressure difference, anode and cathode inlet-outlet temperature differences, average fuel cell cathode temperature, tri-layer (electrolyte) temperature and gas turbine shaft speed. In many cases the perturbation investigated did not lead to compressor surge but these other failure mechanisms were observed.

Two separate control strategies were employed in this study; the first controls gas turbine shaft speed at 3,600 RPM, assuming a synchronous generator and the second (cascade controller) primarily controls fuel cell temperature and secondarily controls gas turbine shaft speed, assuming an asynchronous generator. Careful tuning of the controls is necessary in order to avoid dynamic operational paths taken between initial and final steady state operating points that tend towards surge. The main difference between the two control strategies is that when RPM is the only control parameter, surge is more easily avoided but fuel cell temperature can vary dramatically. The cascade controller is very effective at controlling fuel cell temperature but because this parameter is controlled by varying gas turbine shaft speed, surge becomes a factor. The fuel cell temperature strategy should be designed to accept some delays in mass flow response (which the fuel cell should be able to handle due to its large thermal mass) so that the hybrid system will have better surge avoidance. When fuel cell temperature *is not* a control parameter, cathode recycle blowers were found to lead to less compressor operating point fluctuation than when an ejector is used for the same purpose. Thus, a blower is preferred for surge avoidance and superior dynamic response to perturbations with this control strategy. When fuel cell temperature *is* a control parameter, there was very little difference in surge avoidance between systems that used a cathode blower or an ejector. In general, it was found that machines driving synchronous generators were less likely to experience surge but were unable to effectively control fuel cell temperature for all the perturbations studied. The converse of this is true for asynchronous machines. Using the cathode blower in place of the ejector was found to increase steady state cycle efficiency by approximately three percentage points for the three different cycle pressure scenarios investigated. It is unknown whether currently available blowers can operate at the temperatures required or whether blowers could maintain the pressure ratios required in the current cycles.

Many studies that merit further investigation are suggested.

### **TASK 2.3: PERFORMANCE COMPARISON OF OXY-COMBUSTION AND IGCC PLANTS**

The calculated plant thermal efficiencies show that the efficiency of the oxy-combustion cycle based cases is lower than both the Total Quench Heat Recovery option and the Radiant Syngas Cooler Plus Quench Heat Recovery option IGCC cases with the slightly lower CO<sub>2</sub> capture.

Unless there is a substantial reduction in the cost for the oxy-combustion based plant which appears to be unlikely due to its significantly higher O<sub>2</sub> consumption, the oxy-combustion based cycle in coal gasification plants appears to show no efficiency nor economic advantage over the IGCC.

The Radiant Syngas Cooler Plus Quench Heat Recovery option IGCC is more efficient than the Total Quench Heat Recovery option IGCC even in applications where CO<sub>2</sub> capture is required. The total plant cost, however, for the IGCCs with the radiant syngas coolers will be significantly higher.

## **COST AND SCHEDULE STATUS**

The project schedule based on the information flow among the proposed tasks is shown in Figure 1 while the project milestones are presented in Table 8. The various activities / tasks completed under this contract, along with the time for the accomplishment of these activities / tasks are identified. These tasks are listed below.

- Task 1.1 – Set System Study Methodologies
- Task 1.2 – Identify baseline cycle Configuration
- Task 1.3 - First Detailed Systems Study Analysis – Baseline Case
- Task 1.4.1 – Screening Analysis of Advanced Brayton Cycles
- Task 1.4.2 - Detailed Analysis of Advanced Brayton Cycles
- Task 2.1 - Evaluation of Impact of Ramgen Compression Technology on IGCC Plant Performance
- Task 2.2 - Gas Turbine Operating Requirements for Gasification based Fuel Cell / Gas Turbine System.
- Task 2.3 - Performance Comparison of Oxy-combustion and IGCC Plants

A summary of budget and costs is presented in Table 9.

**Figure 1: Project Schedule**

Month Ending	1	2	3	4	5	6	7	8	9	10	11	12	13	14	15	16	17	18	19	20	21	22	23	24	25	26	27	28	29	30	28	29	30			
	O	N	D	J	F	M	A	M	J	J	A	S	O	N	D	J	F	M	A	M	J	J	A	S	O	N	D	J	F	M	A	M	J	J	A	S
Task 1.1 – Set System Study Methodologies			(1)			(3)																														
Task 1.2 – Identify Overall Baseline Cycle Configuration			(2)			(4)																														
Task 1.3 - First Detailed Systems Study Analysis – Baseline Case						(5)																														
Task 1.4 - Subsequent Systems Study - Advanced Brayton Cycle Cases																																				
Task 1.4.1 - Screening Analysis												(10)																								
Task 1.4.2 - Detailed Analysis														(12)	(13)	(14)	(16)																			
Task 2.1 - Impact of Ramgen Advanced Compression on IGCC Performance									(7)			(11)																								
Task 2.2 - GT Operating Requirements for Gasification based Fuel Cell / GT System																																				
Task 2.2.1 - Overall Plant Design Basis												(8)																								
Task 2.2.2 - SOFC/GT System I/O Stream Specifications - Steady State (SS) Operation												(9)																								
Task 2.2.3 - SOFC/GT SS & Dynamic Performance, GT Design Basis																																				
Task 2.2.4 - Integration of SOFC/GT into Gasification Plant for IGFC SS Performance																																				
Task 2.3 - Performance Comparison of Oxy-combustion and IGCC Plants																																				(18)
Reporting (Including R&D Requirements)																																				

 = Original Plan

 = Actual

**Table 8: Project Milestones**

(1) Issue report documenting System Study Methodologies	
(2) Complete concept characterizations	
(3) Issue revised Systems Study Methodologies	
(4) Issue revised concept characterizations and issue BFD along with narrative for recommending the overall configuration for Baseline IGCC Case	
(5) Set up Balance of Plant Simulation (i.e., exclusive of Gas Turbine) for Baseline Case and issue Process Descriptions	
(6) Complete plant simulation of Baseline Case (issue process flow sketches along with stream data and overall plant performance in Quarterly Report)	
(7) Issue Compressor Functional Specifications to Ramgen	
(8) Establish Overall Plant Design Basis for Gasification based Fuel Cell /GT Case	
(9) Establish SOFC/GT System I/O Stream Specifications for SS Operation	
(10) Complete screening analysis of Advanced Cycles (issue findings in Quarterly Report)	
(11) Complete simulations of IGCC incorporating Ramgen Advanced Compression Technology	
(12) Complete Process Flow Sketches along with stream data and overall plant performances for Advanced Brayton Cycle based Case developed during this quarter (issue in Progress Report)	
(13) Complete Process Flow Sketches along with stream data and overall plant performances for Advanced Brayton Cycle based Case developed during this quarter (issue in Progress Report)	
(14) Complete Process Flow Sketches along with stream data and overall plant performances for Advanced Brayton Cycle based Case developed during this quarter (issue in Progress Report)	
(15) Complete SOFC/GT SS & Dynamic Performance & establish GT Design Basis	
(16) Complete Process Flow Sketches along with stream data and overall plant performances for Advanced Brayton Cycle based Case developed during this quarter (issue in Progress Report)	
(17) Complete Integration of SOFC/GT into Gasification Plant for IGFC SS Performance (issue results of completed Task 2.2 in Quarterly Report)	
(18) Complete Process Flow Sketches along with stream data and overall plant performances for Advanced Brayton Cycle based Case developed during this quarter (issue in Progress Report)	

**Table 9: Summary of Budget and Costs**

<b>Fiscal Period</b>	<b>QTR</b>	<b>DOE Budget</b>	<b>Cost Share Budget</b>	<b>Combined Budget</b>	<b>DOE Cost</b>	<b>University Cost</b>	<b>Total Cost</b>	<b>Difference</b>
Q1FY06	1	\$ 50,000	\$ 31,863	\$ 81,863	\$ 8,285.87	\$ 28,628.22	\$ 36,914.09	\$ 44,948.91
Q2FY06	2	\$ 62,800	\$ 31,863	\$ 94,663	\$ 85,642.28	\$ 29,636.83	\$ 115,279.11	\$ (20,616.11)
Q3FY06	3	\$ 62,711	\$ 31,863	\$ 94,574	\$ 78,275.94	\$ 18,850.51	\$ 97,126.45	\$ (2,552.45)
Q4FY06	4	\$ 120,000	\$ 6,600	\$ 126,600	\$ 115,420.63	\$ 6,530.49	\$ 121,951.12	\$ 4,648.88
Q1FY07	5	\$ 120,000	\$ 31,863	\$ 151,863	\$ 119,657.44	\$ 43,061.83	\$ 162,719.27	\$ (10,856.27)
Q2FY07	6	\$ 120,000	\$ 31,863	\$ 151,863	\$ 125,034.92	\$ 56,873.64	\$ 181,908.56	\$ (30,045.56)
Q3FY07	7	\$ 125,000	\$ 31,863	\$ 156,863	\$ 170,049.06	\$ 34,495.58	\$ 204,544.64	\$ (47,681.64)
Q4FY07	8	\$ 120,000	\$ 6,000	\$ 126,000	\$ 110,087.99	-	\$ 110,087.99	\$ 15,912.01
Q1FY08	9	\$ 62,600	\$ 12,000	\$ 74,600	\$ 29,819.44	-	\$ 29,819.44	\$ 44,780.56
Q2FY08	10	\$ 62,500	\$ 10,625	\$ 73,125	\$ 51,878.61	\$ 8,931.50	\$ 60,810.11	\$ 12,314.89
Q3FY08	11	\$ 72,215	\$ 18,055	\$ 90,269	\$ 28,927.48	\$ 25,305.88	\$ 54,233.36	\$ 36,035.64
Q1FY08	12	\$ 29,715	\$ 7,430	\$ 37,144	\$ 84,460.34	-	\$ 84,460.34	\$ (47,316.34)
<b>Total:</b>		<b>\$1,007,540.00</b>	<b>\$ 251,887.00</b>	<b>\$ 1,259,427.00</b>	<b>\$ 1,007,540.00</b>	<b>\$ 252,314.48</b>	<b>\$ 1,259,854.48</b>	<b>\$ 427.48</b>

## **APPENDIX – COMPREHENSIVE SUMMARY OF WORK SINCE PROJECT INCEPTION**

The following pages include a comprehensive summary of the following tasks accomplished under this study:

- Task 1.1 – Set System Study Methodologies
- Task 1.2 – Identify baseline cycle Configuration
- Task 1.3 - First Detailed Systems Study Analysis – Baseline Case
- Task 1.4.1 – Screening Analysis of Advanced Brayton Cycles
- Task 1.4.2: Detailed Analysis of Advanced Brayton Cycles
- Task 2.1: Evaluation of Impact of Ramgen Compression Technology on IGCC Plant Performance
- Task 2.2 - Gas Turbine Operating Requirements for Gasification based Fuel Cell / Gas Turbine System.
- Task 2.3 - Performance Comparison of Oxy-combustion and IGCC Plants

## TASK 1.1: SET SYSTEMS STUDY METHODOLOGY

### INTRODUCTION

This document provides an explanation of the systems study procedure to be used to evolve the conceptual gasification based plant designs. It is the intent to adhere to the “Quality Guidelines for Energy System Studies” established by the DOE / NETL wherever possible.

This systems study procedure provides the following:

- site conditions and feedstock characteristics
- advanced Brayton cycle technology projections
- SOFC / GT design guidelines
- overall plant design criteria
- procedure for executing material and energy balances
- procedure for setting equipment specifications where required
- third party validation of a detail or the entire study is addressed.

### PROCESS DESIGN PROCEDURE

#### Site Conditions and Feedstock Characteristics

Table A1.1 - 1 summarizes the site conditions to be used in this systems analysis study.

**Table A1.1 - 1: Site Conditions**

Dry Bulb Temperature	15° C <sup>1</sup>
Relative Humidity	60% <sup>1</sup>
Elevation	sea level <sup>1</sup>
Air Composition by Volume	
O <sub>2</sub>	20.77%
N <sub>2</sub>	77.22%
CO <sub>2</sub>	0.003%
H <sub>2</sub> O	1.04%
Ar	0.94%
Plant Make-up Water	Fresh Water
Plant Site	Level Greenfield without any Piling Requirement

<sup>1</sup> International Standards Organization (ISO) conditions.

**Coal**

Pittsburgh No. 8 coal will be utilized for this study. Table A1.1 - 2 shows its ultimate, proximate, and sulfur analyses along with that of Illinois No. 6 coal for Sensitivity Analysis, taken from the “Quality Guidelines for Energy System Studies.”

**Natural Gas**

The composition shown in Table A1.1 - 3 taken from the “Quality Guidelines for Energy System Studies,” which is based on the mean of over 6,800 samples of pipeline quality natural gas taken in 26 major metropolitan areas of the United States will be used.

**Limestone**

Limestone if required (e.g., as a flux) having the composition shown in Table A1.1 - 4 (taken from the “Quality Guidelines for Energy System Studies”) will be utilized.

**Table A1.1 - 2: Coal Analysis**

<b>Rank</b>	<b>Medium-volatile Bituminous</b>		<b>High-volatile Bituminous</b>	
<b>Seam</b>	Pittsburgh No. 8		Illinois #6 (Herrin)	
<b>Sample Location</b>	PA		St. Clair Co., IL	
<b>PROXIMATE ANALYSIS</b>	As Received	Dry	As Received	Dry
<b>Moisture</b>	6.00	0	7.97	0
<b>Ash</b>	9.94	10.57	14.25	15.48
<b>Volatile Matter</b>	35.94	38.23	41.31	44.88
<b>Fixed Carbon</b>	48.12	51.20	36.47	39.64
<b>HHV</b>				
<b>kJ/kg</b>	28,959	30,806	25,584	27,798
<b>Btu/lb</b>	12,450	13,244	10,999	11,951
<b>ULTIMATE ANALYSIS</b>				
<b>Carbon</b>		73.79		65.65
<b>Hydrogen</b>		4.81		4.23
<b>Nitrogen</b>		1.29		1.16
<b>Chlorine</b>		0.10		0.05
<b>Sulfur</b>		3.07		4.83
<b>Ash</b>		10.57		15.48
<b>Oxygen</b>		6.37		8.60
<b>SULFUR SPECIES</b>				
<b>Pyritic</b>		-		2.81
<b>Sulfate</b>		-		0.01
<b>Organic</b>		-		2.01
<b>ASH FUSION TEMPERATURE</b>	<b>Reducing Atmosphere, °C (°F)</b>	<b>Oxidizing Atmosphere, °C (°F)</b>	<b>Reducing Atmosphere, °C (°F)</b>	<b>Oxidizing Atmosphere, °C (°F)</b>
Initial Deformation	1,102 (2,015)	1,410 (2,570)	-	-
Spherical	1,168 (2,135)	1,434 (2,614)	-	-
Hemispherical	1,218 (2,225)	1,442 (2,628)	-	-
Fluid	1,343 (2,450)	1,474 (2,685)	-	-

**Table A1.1 - 3: Natural Gas Composition**

<b>Component</b>	<b>Volume Percentage</b>	
Methane, CH <sub>4</sub>	93.1	
Ethane, C <sub>2</sub> H <sub>6</sub>	3.2	
Propane, C <sub>3</sub> H <sub>8</sub>	0.7	
<i>n</i> -Butane, C <sub>4</sub> H <sub>10</sub>	0.4	
Carbon Dioxide, CO <sub>2</sub>	1.0	
Nitrogen, N <sub>2</sub>	1.6	
	<b>LHV</b>	<b>HHV</b>
MJ/nm <sup>3</sup>	36.69	40.63
Btu/scf	932	1032

Notes:

1. The reference data reported the mean volume percentage of higher hydrocarbons (C<sub>4</sub> +) to be 0.4%. For simplicity, the above composition represents all the higher hydrocarbons as *n*-butane (C<sub>4</sub>H<sub>10</sub>).
2. The reference data reported the mean volume percentage of CO<sub>2</sub> and N<sub>2</sub> (combined) to be 2.6%. The above composition assumes that the mean volume percentage of CO<sub>2</sub> is 1.0%, with the balance (1.6%) being N<sub>2</sub>.
3. LHV = lower heating value; HHV = higher heating value

**Table A1.1 - 4: Greer Limestone Analysis**

<b>Component</b>	<b>Dry Basis %</b>
Calcium Carbonate, CaCO <sub>3</sub>	80.40
Magnesium Carbonate, MgCO <sub>3</sub>	3.50
Silica, SiO <sub>2</sub>	10.32
Aluminum Oxide, Al <sub>2</sub> O <sub>3</sub>	3.16
Iron Oxide, Fe <sub>2</sub> O <sub>3</sub>	1.24
Sodium Oxide, Na <sub>2</sub> O	0.23
Potassium Oxide, K <sub>2</sub> O	0.72
Balance	0.43

## ADVANCED BRAYTON CYCLE TECHNOLOGY PROJECTIONS

Some of the technological advances being made or being investigated to improve the Brayton cycle include the following:

- Rotor inlet temperature of 1700°C (3100°F) or higher which would require the development and use of advanced materials including advanced thermal barrier coatings and turbine cooling techniques including closed loop steam cooling.
- High blade surface temperature in the neighborhood of ~1040°C (1900°F) while limiting coolant amount would again require the development and use of the advanced materials including advanced thermal barrier coatings.
- Improvements to the aerodynamic and mechanical design such as pressure gain combustion, improved compressor and / or turbine isentropic efficiencies.
- Advanced gas turbine combustor concepts to limit the combustor diluent addition to a value which optimizes the overall plant thermal efficiency while minimizing the NO<sub>x</sub> emissions.
- High pressure ratio compressor (greater than 30 to take full advantage of higher firing temperature).
- Catalytic combustors (such as that being developed by Precision Combustion, Inc).
- Cycle changes such as air humidification and recuperation, inlet air fogging, in-situ reheating and intercooling.

The balance of plant configuration and technology will be selected in order to synergistically integrate with the particular Advanced Brayton cycle under investigation such that the overall plant performance is optimized. The effect of incorporating the various advanced technology concepts will be studied methodically such that any gain in performance realized can be associated with the particular change in cycle condition or configuration made.

A myriad of gas turbine based cycles have been proposed in the past but the majority of these cycles have been for natural gas applications. Thus, it is important to identify only those cycles that have a potential for success in coal based gasification plants also and the following lists the initial activities included in this task to select promising cycles for inclusion in the systems analysis:

- Based on a literature search, identify gas turbine based cycles that have a potential for high efficiency.

- Conduct brainstorming sessions in order to identify those gas turbine based cycles that have a potential to meet the objectives of this program. Improvements to these cycles as well as the evolution of new cycle configurations by synergistically combining aspects of other cycles will also be brainstormed.

After the selection of the advanced cycles, a narrative accompanying the recommended cycles as well as the integration scheme with the remainder of the plant for each of the cases will be made to the COR. Upon COR approval, UC Irvine will proceed with detailed systems analysis and design for these cases. Three or more systems studies will be conducted in the second year which integrate these advanced technologies upon mutual agreement of UC Irvine and COR (the exact number of cases dependent upon funding availability).

## **SOFC / GT DESIGN GUIDELINES**

The following lists the design guidelines that will be adhered to in developing the steady state and dynamic simulations of the SOFC / GT based system. The overall plant steady state simulation will be developed while the dynamic simulations will be limited to the SOFC / GT system as depicted in Figure A1.1-1.

1. Overall Plant:
  - a. General Design Basis same as Baseline IGCC case for the Advanced Brayton Cycle study [CO<sub>2</sub> Capture = 90% of Gasified Carbon (leaving gasifier as gaseous components)]
  - b. Size of each FC / GT Power Block or Train = 100 MW (plant will consist of multiple 100 MW trains to take advantage of a larger gasification plant)
  - c. HRSG pressure drop for the dynamic simulations will be estimated by assuming flow through a non-choked orifice.
2. SOFC:
  - a. Planar SOFC
  - b. Non-Internal Reforming
  - c. Hydrocarbon Content of Syngas < 1%
  - d. Average Operating Temp = 750°C (±25°C)
  - e. Power Density = 500 mW/cm<sup>2</sup>
  - f. Fuel Utilization = 80%
  - g. Max Temp. Rise on Anode Side ≤ 100°C
  - h. Max Temp. Rise on Cathode Side ≤ 100°C
  - i. Air Preheat within Stack: 100 to 150°C Temperature Rise
  - j. Fuel Preheat within Stack: as required based on supplying the syngas to the power block at around 300°C
  - k. Operating pressure: 5 atm (two other pressures considered, steady-state only)
  - l. Syngas pressure at power block: 120 to 140 psi above SOFC Operating Pressure

3. Gas Turbine:
  - a. Dynamic simulations to aid in identifying and specifying the ideal (or optimal) turbine and compressor characteristics to accommodate the SOFC and allow for control during transient operation
  - b. Non-recuperated cycle with cathode recycle gas to preheat the cathode air
  - c. Simplified eductor model
    - i. Low design pressure drop that varies linearly with flow-rate squared
    - ii. Fixed eductant flow curve (function of pressure drop)
    - iii. Instantaneous dynamic response
  - d. Ideal (“mixing cup”) temperature achieved with 3% heat loss.

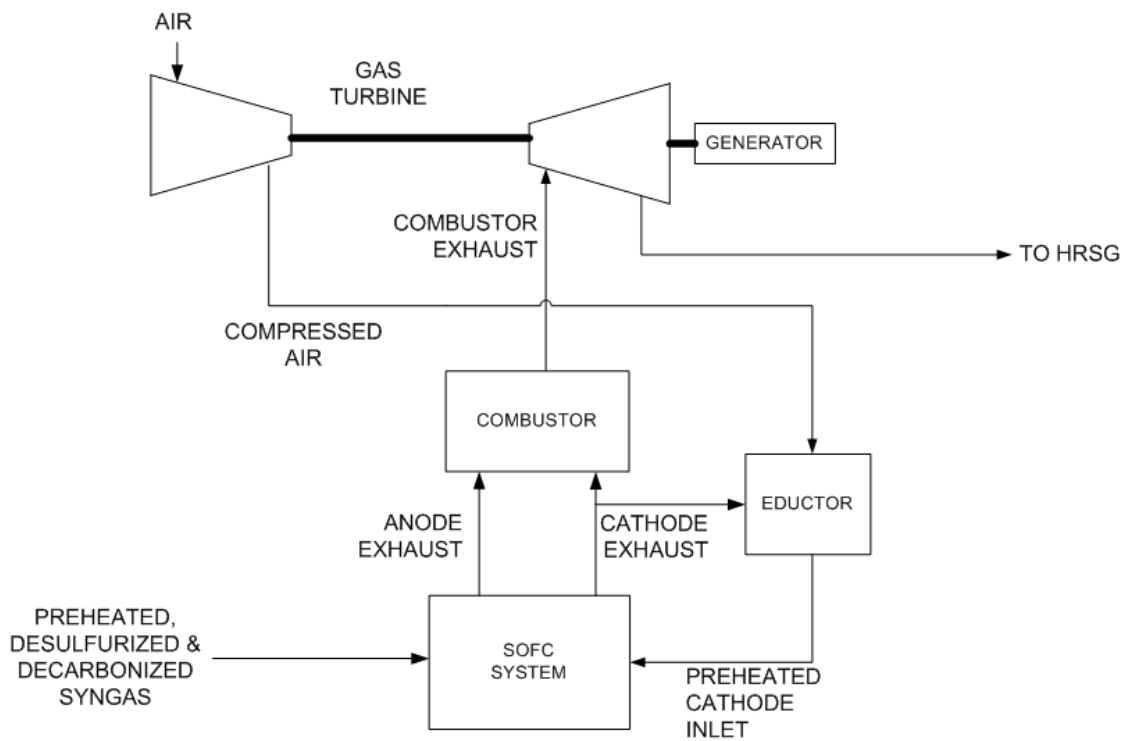


**Figure A1.1 - 1: SOFC / GT System for Dynamic Simulations**

## OVERALL PLANT DESIGN CRITERIA

Table A1.1 - 5 summarizes the design criteria for the Cases 1.1 through 2.0 as defined in the following.

**Table A1.1 - 5: Overall Plant Design Criteria**

Location	Midwest U.S.
ASU-GT Integration	GT Air Extraction and N <sub>2</sub> Injection into GT
Hydrogen Export	None (only Qualitatively Discussion)
CO <sub>2</sub> Capture	90% of Carbon in Coal less Carbon in Slag, Producing > 95% CO <sub>2</sub> Purity Stream with H <sub>2</sub> S < 22 ppmV, Dew Point ≤ -40°C (-40°F) and at Pressure = 138 barg or 2000 psig
NO <sub>x</sub> Emission Limit	15 ppmVd for Baseline Case and 2 ppmVd (15% O <sub>2</sub> Basis) for Ultra Low NO <sub>x</sub> Sensitivity Case
Liquid Wastes	Treated Wastes (Non-Zero Discharge)
Plant Heat Rejection	Mechanical Draft Cooling Towers

## **MATERIAL AND ENERGY BALANCES**

The material and energy balances will be developed utilizing a predictive computer simulation technique. The following lists the tools that will be utilized:

- Advanced Power Systems Analysis Tool (APSAT)
- Aspen Plus®
- Thermoflex
- Matlab-Simulink(R)

The capabilities of APSAT, a simulation tool developed by UC Irvine are described later in this section and is useful for high level evaluations of alternative schemes while the primary heat and mass balance code will be the Aspen Plus® simulator. Thermoflex which is a Thermoflow Suite product will be utilized primarily in developing the performance for the steam cooled H class gas turbine on syngas as well as the Advanced Brayton cycles identified for analysis in this project.

The SOFC/GT dynamic simulations will utilize the Matlab-Simulink(R) framework. This effort will include modifying and applying verified dynamic simulation techniques and models to the system design(s) of interest. These existing dynamic models that have been developed in the Matlab-Simulink(R) framework take into account the dynamic physical, chemical and electrochemical equations that govern fuel cell, gas turbine, and other component technology performance. Some degree of geometric resolution is captured in each of the significant component models (e.g., fuel cell, compressor, heat exchanger), albeit in a simplified (usually one- or two-dimensional) manner. Since the performance of fuel cells, reformers and even simple heat exchangers depends upon local conditions and properties (temperature, pressure, species concentrations) it is important to capture some of the geometrical features of major system components for accurate predictions and insight. However, full three-dimensional and dynamic resolution of the concurrent processes (e.g., chemistry and electrochemistry, heat transfer, mass transfer, momentum) that apply to each of the components in a complex system model is too

computationally intensive. The current approach captures essential geometrical features in a simplified manner allowing solution of the dynamic equations that govern heat and mass transfer, momentum and energy conservation, chemistry and electrochemistry in complex fuel cell systems. The current effort leverages earlier work funded by the California Energy Commission, the U.S. Department of Energy, and the U.S. Department of Defense Fuel Cell Program that supported the development of generic dynamic SOFC and other system component models. The capabilities of these dynamic simulation tools have been demonstrated many publications [e.g., Gemmen et al., 2000; Roberts, et al., 2004; Roberts and Brouwer, 2005; Mueller, Brouwer, and Samuelsen, 2005; Freeh, Pratt, and Brouwer, 2004; Yuan, Brouwer, and Samuelsen, 2004].

The following specific modeling guidelines will be applied to the overall energy system:

- Process models will generate sufficient information to generate a complete process flow diagram and a stream property table.
- Heat loss, blowdown amount, pressure drop, mechanical efficiency, auxiliary and miscellaneous power and cooling water requirements will be taken into account for each piece of equipment or plant section.
- All major streams appearing in the flow diagram will be labeled with an accompanying table that will provide stream compositions, flowrates and conditions of pressure and temperature.
- Overall performance summaries will be developed showing the power generation by each equipment and the power consumed by the plant. The “plant” will include all necessary facilities for a stand alone operation and will include the coal and limestone receiving and processing, raw water and boiler feed water treating, condensate handling, general facilities such as waste water treating, cooling water system and instrument air.

### **Advanced Power Systems Analysis Tool (APSAT)**

Existing models for analysis of systems such as power plants may be divided into two types (1) those developed for simulating chemical process plants (e.g. commercially available Hysis, Aspen, Pro II) and (2) those developed for simulating power plants (e.g. commercially available Thermoflex and GATE/Cycle). Models in the first category have the capability for predicting the performance of typical process equipment and the thermodynamic properties of non-ideal systems but do not include the proper models for power cycle equipment such as gas turbines, steam turbines and fuel cells. The models in the second category have the capability of modeling gas and steam turbines in detail but do not handle rigorously the modeling of process equipment such as gasifiers or partial oxidation units, shift reactors and humidifiers which are playing an important role in IGCC plant designs, nor the properties of non-ideal gases except for pure steam.

Non-ideal gas behavior is quite important in thermodynamic analyses, as there are many processes where such behavior is critical. Two examples of where non-ideal properties for a gas stream need to be accounted for are: (1) predicting the Joule-Thompson cooling of natural gas when its pressure is reduced from typical pipeline pressure to the pressure required by say a heavy frame gas turbine which typically operates at a pressure-ratio in the neighborhood of 15, and (2) the recovery and compression of the carbon dioxide to supercritical pressures (which is typically required for sequestration with greenhouse gas emissions becoming a more global concern). Predicting the saturated vapor content of water vapor in a gas stream at high pressure, which is important in determining the correct heat release curve for syngas cooling, also requires the proper accounting of the non-ideal behavior of the vapor phase.

After years of piecing together the chemical process models with the power plant models, it was obvious that an overall fuel-in to kW-out simulation capability was needed especially in complex multi working fluid/multi power generating component cycles that are becoming more attractive. Beginning in 1997 development began on Advanced Power Systems Analysis Tool (APSAT). This modeling system is based on more than 30 years of process industry and power plant experience with gasification licensors and process/power plant engineering firms. APSAT is a C-based (C++) simulation tool that runs on a PC. Components are described in a series of modules (e.g., see below) and the thermodynamic and flow properties from one module feeds into the following module(s). A series of balances are calculated and convergence obtained. Molar properties are tracked for each stream. APSAT has been successfully used in a number of studies for the DOE and other energy industry members. It is an organic modeling capability and additional modules are added as new technology requires.

Table A1.1 - 6 lists the major modules available in APSAT along with brief descriptions. Note that each of these modules consist of a number of subroutines that calculate the thermodynamic and flow system parameters that are then sent along to the next module.

### **Gas Turbine**

Two types of gas turbine models are included, one that may be configured by the user to include multiple compression stages with intercooling between the stages and multiple expansion stages with reheat (with combustors) between the stages, and the second consisting of a fixed geometry simple cycle (or conventional Brayton cycle) with no intercooling of the compressor or reheat during expansion.

In the user-defined gas turbine model, the efficiency of the compressor and expander and the air required for cooling the blades of the turbine as well as its purge air requirements are calculated by first calibrating a simple cycle engine based on data published by the gas turbine manufacturer, and then applying adjustments to the values determined for the "base-line engine." The program determines internally the necessary parameters for the base-line engine and for use with the user-defined model (as well as with the "fixed geometry" model).

The fixed geometry model assumes that the gas turbine has the same geometry as the gas turbine used for calibrating the engine. The firing temperature and pressure-ratio of the gas turbine are adjusted for variations in flow rate and composition of the working fluid. The firing temperature is adjusted in order to maintain the same surface temperature of the first-stage blades as that for the base-line engine since the turbine cooling flows are not controlled in an engine. A correlation derived from published performance data for the Nuovo Pignone gas turbine (Model PGT 5B/1) which has an output of 5.4 MW at ISO conditions is utilized to adjust the polytropic efficiency of the compressor for changes in the pressure-ratio. The small Nuovo Pignone gas turbine is utilized since it is in the size range being considered by industry for fuel cell based hybrid applications.

The performance curves generated by the model for a large industrial gas turbine (General Electric MS 7001EA model with output of 85 MW at ISO conditions) are presented along with data published by General Electric in Figure A1.1 - 2. As can be seen, the agreement between the model predictions and published data are in excellent agreement despite the more than an order of magnitude scale-up in the size of the gas turbine.

A comparison of the combustor outlet temperature as developed by APSAT for a syngas fuel is compared to that calculated by ASPEN in Table A1.1 - 7. As can be seen, the outlet temperatures are in close agreement validating the thermodynamic basis used.

### **Humidifier Model**

The humidifier is modeled rigorously by accounting for the simultaneous heat and mass transfer rate-controlled processes occurring within this contact device rather than modeling it simplistically as a series of equilibrium stages.

### **Compressor and Steam Turbine Models**

APSAT has the advantage of predicting the isentropic efficiency using relationships that take into account the capacity of the unit in the case of a compressor (Gas Research Institute Report, 1993), while in the case of steam turbines, correlations developed by Spencer et. al. (1974) may be utilized to predict the isentropic efficiency for each of the sections (high pressure, intermediate pressure and condensing). A comparison of the compressor outlet temperature as predicted by APSAT is compared to that calculated by ASPEN in Table A1.1 - 7 while utilizing the isentropic efficiency as predicted by APSAT in ASPEN. As can be seen, the outlet temperatures are in close agreement validating the thermodynamic basis used.

**Table A1.1 - 6: List of Modules in APSAT**

<b>Module Name</b>	<b>Description</b>
Combine	Combines two streams adiabatically to give the mixture temperature at pressure equal to the lower of the two streams being combined
Combust	Calculates effluent composition & conditions for a combustor with specified $Q_{loss}$ and pressure drop
CombustT	Calculates effluent composition & conditions & heat release for a combustor with given outlet temperature and pressure drop
Compress	Calculates the power and outlet temperature of a compressor for a given outlet pressure (the isentropic efficiency may either be specified or can be calculated by module)
Controller	Adjusts variable upstream to make desired variable match target value (while simulating a flowsheet with iterations to satisfy a specified design criteria)
COSHyd	Adiabatic COS hydrolysis reactor to calculate effluent composition and conditions
Deaer	Calculates the effluent conditions from & heat required by a boiler feed water deaerator
Decant	Decanter to separate a solid from water for a specified moisture content in separated solid
ExchQ	Calculates outlet temperature for a specified heat duty and pressure drop
ExchT	Calculates heat duty for a specified outlet temperature and pressure drop
Expand	Calculates the power and outlet temperature of a gas expander for a given outlet pressure (the isentropic efficiency may either be specified or can be calculated by module)
GTcalib	Calibrates gas turbine (for use in below Gas Turbine modules)
GasTurb	Gas turbine of geometry same as that specified in GTcalib
GTcombEXP	Combustor/Expander of a gas turbine consistent with GTcalib (used in configuring a new cycle)
GTcomp	Compressor of a gas turbine consistent with GTcalib (used in configuring a new cycle)
GTsplit	Splits for cooling air of gas turbine consistent with that specified in Gtcalib. Cooling air is taken just upstream of combustor specified in GTcombEXP. (used in configuring a new cycle)

---

HPstmTurb	Calculates the power and outlet temperature of a steam turbine – HP section (the isentropic efficiency may either be specified or as a default, it is calculated using the Spencer-Cotton Correlations)
Humid	Calculates gas & water streams leaving a Humidifier or Dehumidifier (composition of gas as well as flowrate, temperature & pressure) by solving simultaneous heat and mass transfer equations using nodal analysis.
IPstmTurb	Calculates the power and outlet temperature of a steam turbine – IP section (the isentropic efficiency may either be specified or as a default, it is calculated using the Spencer-Cotton Correlations)
LPstmTurb	Calculates the power and outlet temperature of a steam turbine – condensing section (the isentropic efficiency may either be specified or as a default, it is calculated using the Spencer-Cotton Correlations)
Membrane	Calculates the outlet streams while taking into account the partial pressure gradients
Pipe	Calculates outlet conditions for specified pressure and temperature drops
Pox	Calculates adiabatic POx effluent composition and conditions
PoxH2	Calculates adiabatic H2 POx effluent composition and conditions
PoxH2Temp	Calculates H2 POx effluent composition and conditions & qloss for a given outlet temperature
PoxTemp	Calculates POx effluent composition and conditions & heat loss for a given outlet temperature
Pump	Calculates power required and outlet temperature for a pump for a given discharge pressure and isentropic efficiency
Recycler	Iterates till two streams match or their temperatures maintain a specified delta T
Reform	Calculates reformer effluent composition and conditions and absorbed duty
Results	Shows results with stream composition, temperature and pressure, elemental flow rates (for quick check of the elemental balance), energy and exergy contents (for cycle analysis), physical properties (for equipment specs), overall plant thermal efficiency.
SatStmHP	Calculates energy (enthalpy above 60 deg F) of saturated steam/BFW mixture for given pressure
SatStmHT	Calculates energy (enthalpy above 60 deg F) of saturated steam/BFW mixture for given temperature
Separate	Separates water condensate & liquid/solid from a stream
SepComp	Removes a specific vapor component (by %) from a stream

---

---

Shift	Adiabatic shift reactor to calculate effluent composition and conditions
ShiftTemp	Non-adiabatic shift reactor to calculate effluent composition and conditions & duty in shift reaction for a specified outlet temperature
SOFC	Performance (depleted fuel and oxidant composition and conditions and power) and sizing of Solid Oxide Fuel Cell
SplitFlo	Splits a stream into two streams for a given kg/s (or lb/s)
SplitPer	Splits a stream into two streams for a given % Split
SteamGenM	Steam generator (calculates steam produced, blowdown, heat duty for a specified steam pressure and BFW flowrate)
SteamGenQ	Steam generator (calculates steam generated, blowdown, BFW required for a specified heat duty and pressure)
SteamCon	Steam consumer (calculates steam required, condensate produced for specified heat duty and pressure)
Substitute	Substitutes or duplicates a stream
Valve	Calculates outlet conditions including any phase change for a specified pressure drop

---

**Table A1.1 - 7: Comparison between APSAT and ASPEN**

<b>Syngas Combustor</b>	<b>Air Compressor</b>
Inlet Air Conditions = 404 °C, 15.85 atm Inlet Syngas Composition = 38.4% H <sub>2</sub> , 1.2% CO, 0.06% CH <sub>4</sub> , 1.63% CO <sub>2</sub> , 31.1% H <sub>2</sub> O, 26.76% N <sub>2</sub> , 0.81% Ar, 0.04% H <sub>2</sub> S Outlet Pressure = 15.29 atm Calculated Outlet Temperature: ASPEN = 1233 °C APSAT = 1235 °C	Inlet Conditions = 15 °C, 1 atm Outlet Pressure = 15.85 atm Isentropic Efficiency = 85.7% Calculated Outlet Temperature: ASPEN = 404.4 °C APSAT = 404.2 °C

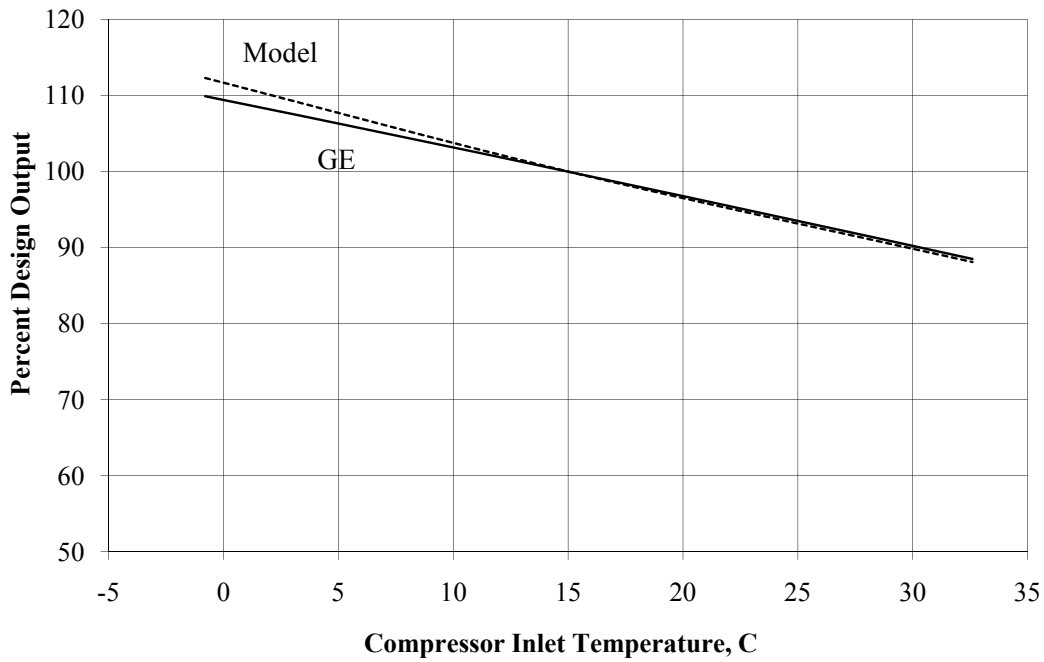


**Figure A1.1 - 2: Variation of Power Output with Compressor Inlet Temperature**

## **SPECIFICATIONS FOR UNIQUE EQUIPMENT AND PLANT UNITS**

Duty / functional specifications will be developed where necessary for unique equipment and plant units.

## **THIRD PARTY VALIDATION**

The flow diagrams along with the overall performance summaries as described previously will form the basis for a third party validation if the DOE so chooses. Any additional information not included in the quarterly progress reports or final report issued to the DOE will be provided when requested by the DOE for this purpose. The plant cost estimates where developed will be broken down by major process units so that a third party may be able to assess the reasonableness of the cost estimate while the study basis and assumptions will be clearly identified.

## **REFERENCES**

1. Freeh, J.E., Pratt, J.W., and Brouwer, J., (2004). "Development of a Solid-Oxide Fuel Cell / Gas Turbine Hybrid System Model for Aerospace Applications," ASME Paper Number GT2004-53616.
2. Gas Research Institute Report, "Evaluation of Advanced Gas Turbine Cycles," GRI-93/0250, August 1993.
3. Gemmen, R. S., Liese, E., Rivera, J. G., Jabbari, F. and Brouwer, J. (2000). "Development of dynamic modeling tools for solid oxide and molten carbonate hybrid fuel cell gas turbine systems." American Society of Mechanical Engineers 2000-GT-554.
4. Mueller, F., Brouwer, J., and Samuelsen, G.S., (2005). "Dynamic Simulation of an Integrated Solid Oxide Fuel Cell System Including Current-Based Fuel Flow Control," ASME Journal of Fuel Cell Science and Technology, accepted, March, 2005.
5. Roberts, R.A., and Brouwer, J., (2005). "Dynamic Simulation of a 220kW Solid Oxide Fuel Cell Gas Turbine Hybrid System with Comparison to Data," ASME Journal of Fuel Cell Science and Technology, accepted, April, 2005.
6. Roberts, R.A., Brouwer, J., Liese, E., Gemmen, R.S., (2004). "Dynamic Simulation of Carbonate Fuel Cell-Gas Turbine Hybrid Systems," ASME Paper Number GT2004-53653.
7. Spencer, R.C. et al., "A Method for Predicting the Performance of Steam Turbine-Generators," General Electric Technical Bulletin GER -2007C, July 1974.
8. Yuan, L., Brouwer, J., and Samuelsen, G.S., (2004). "Dynamic Simulation of an Autothermal Methane Reformer," 2nd International Conference on Fuel Cell Science, Engineering and Technology, American Society of Mechanical Engineers, June, 2004.

## TASK 1.2: IDENTIFY OVERALL BASELINE CYCLE CONFIGURATION

### SUMMARY

This document discusses the various process options available or under development for an IGCC facility and a qualitative technology evaluation is conducted in order to identify those options that may be suitable for incorporation in the Baseline Case design.

The selected plant scheme consists of a cryogenic air separation unit (ASU) supplying 95% purity O<sub>2</sub> to GE type HP total quench gasifiers. The raw gas after scrubbing is treated in a sour shift unit to react the CO with H<sub>2</sub>O to form H<sub>2</sub> and CO<sub>2</sub>. The gas is further treated to remove Hg in a sulfided activated carbon bed. The syngas is desulfurized and decarbonized in a Selexol acid gas removal unit and the decarbonized syngas after humidification and preheat is fired in a GE 7H type steam cooled gas turbine. IP N<sub>2</sub> from the ASU is also supplied to the combustor of the gas turbine as additional diluent for NO<sub>x</sub> control. A portion of the air required by the ASU is extracted from the gas turbines.

An ultra low NO<sub>x</sub> (2 ppmvd, 15% O<sub>2</sub> basis) sensitivity case is developed by the inclusion of an SCR in the heat recovery steam generator (HRSG).

### Gasifier Technology

Current-state-of-the-art (commercially proven) and near-term gasification technologies for large scale applications are listed below:

- 1) Advanced Transport Reactor
- 2) General Electric (GE)
- 3) Shell
- 4) ConocoPhillips (E-Gas)

The four gasifier types are depicted in Figures A1.2 - 1 through 4 and their major attributes and their suitability are discussed below. This analysis and the results concluded with respect to the gasifier technology selection are specific to the high rank bituminous coal feedstocks chosen for this study (Pittsburgh No. 8 and Illinois No. 6 coal).

### **Advanced Transport Reactor**

This type of gasifier is depicted in Figure A1.2 - 1 and its main features along with its status are summarized below:

- Bottom-mounted Injectors
- Dry Solid Feeds and Low Operating Temperature
  - Potential for High Cold Gas Efficiency if High Carbon Conversion can be Maintained
  - O<sub>2</sub> Consumption Similar to Previous Gasifier

- Dried Solids Conveyed by N<sub>2</sub> or Syngas
- Convective Waste Heat Boilers
- ~ 50 Tonne/d Process Demonstration Unit (PDU) Operated
- Company & Orlando Utilities Commission to build 285 MW IGCC in Florida.

This gasifier is very suitable for low rank reactive coals where high carbon conversion may be achieved while maintaining a relatively low gasifier operating temperature, i.e., less than 1000°C. The cold gas efficiency can thus be increased while the specific O<sub>2</sub> or air consumption can be kept low. However, in the case of bituminous coals (such as Pittsburgh No. 8 chosen for this study) which tend to be less reactive as compared to the lower rank coals, the PDU experience has shown that the carbon conversion is limited to about 90% while operating in the neighborhood of 1000°C. Based on current operating experience, the carbon conversion is expected to be limited to about 95% by increasing the operating temperature of the gasifier by as much as 50°C.

In light of the above, this gasifier is not chosen for use in the Baseline Case.

### **GE Gasifier**

This type of gasifier is depicted in Figure A1.2 - 2 and its main features and its status are summarized below:

- Top-mounted feed injector
- Solid feeds fed as water slurry
- Syngas with high H<sub>2</sub>/CO ratio
- Total Quench (TQ) design
  - Lower capital cost
  - Suitable for sour shift (H<sub>2</sub> production/CO<sub>2</sub> Capture)
- Syngas cooler available for higher efficiency (more suitable in power only applications)
- Commercially proven up to ~ 80 bar operating pressure on oil feed.

The two main characteristics of this type of gasifier which are slurry feed and high operating temperature (in the neighborhood of 1300°C) give it the flexibility to operate at very high pressures and gasify relatively unreactive feedstocks while achieving high carbon conversion especially when recycle of the unconverted carbon is included in the design. On the other hand, these same attributes limit the cold gas efficiency of the gasifier (defined as the ratio of the HHV of the net syngas produced by the gasifier to the HHV of the feedstock) while increasing the specific O<sub>2</sub> consumption.

Three options are available for heat recovery from the raw syngas leaving the gasifier and before it is scrubbed with water: (1) a radiant cooler followed by a convective cooler, (2) only the radiant cooler, and (3) quenching the gas with water by direct contact while eliminating the costly syngas coolers as depicted in Figure A1.2 - 2. For applications involving a high degree of shifting of the syngas to convert most of the CO into CO<sub>2</sub> for capture, the following steps are utilized: (1) shift the raw gas leaving the particulate scrubber utilizing a sour shift catalyst after preheating to the required temperature and (2) remove the CO<sub>2</sub> in the acid gas removal unit used

for desulfurization of the syngas, after syngas cleanup / heat recovery. This sour shift configuration integrates especially well with the GE gasifier incorporating the direct contact cooling of the gasifier effluent (“total quench” design). Steam injection into the raw gas upstream of the shift unit is not required, since the moisture present in the scrubber outlet gas is sufficient. It also simplifies the design of a physical solvent-based acid gas removal unit (required to remove the sulfur compounds and the CO<sub>2</sub>) as explained later. This type of gasifier is highly suitable for zero emission IGCC plants but for IGCC plants without CO<sub>2</sub> recovery where high efficiency is a primary goal, this type of gasifier may not be the optimum choice.

In light of the above, this type of gasifier is chosen for use in the Baseline Case.

### **Shell Gasifier**

This type of gasifier is depicted in Figure A1.2 - 3 and its main features are summarized below:

- Horizontally opposed injectors near bottom for solid feeds
- Dry solid feeds
  - Potential for higher cold gas efficiency
  - Lower O<sub>2</sub> consumption
  - Dry solids conveyed by N<sub>2</sub>
  - Convective waste heat boilers
- Membrane wall gasifier for solid feeds
- Reduction of waste heat boiler inlet temperature by gas recycle
- Candle filters remove dry solids from syngas
- Pressure limited to ~ 40 bar.

The Shell gasifier is offered with syngas coolers as depicted in Figure A1.2 - 3 which tends to maximize the heat recovery. The Shell gasifier with its dry feed system has a lower O<sub>2</sub> demand, typically about 5 to 6% lower than the GE gasifier. The lower O<sub>2</sub> demand does reduce the cost of the air separation unit but the cost savings are typically largely off-set by the higher cost of the gasifier and its high temperature syngas coolers as compared to the GE gasifier system with the total quench design. Also, the dry feed system with its drier and other special equipment, has greater power consumption, higher costs and limits the operating pressure of the gasifier as compared to a gasification system using a slurry feed. The Baseline Case as well as the more advanced Brayton cycles to be investigated under Task 2 of this program as explained later, will require the gasifier to operate at a pressure in excess of 40 bar in order to supply the syngas at a pressure consistent with the requirement of the high pressure ratio advanced gas turbines.

In light of the above, this gasifier is not chosen for use in the Baseline Case.

### **E-Gas Gasifier**

This type of gasifier is depicted in Figure A1.2 - 4 and its main features are summarized below:

- Horizontally opposed bottom injectors with upward flow of syngas
- Feed injected in top section (2<sup>nd</sup> stage) also but without O<sub>2</sub>

- Evaporation of slurry water and endothermic reactions help cool syngas to limit temperature in syngas cooler
- Increases cold gas efficiency
- Candle filters for recovery of entrained ash and unconverted carbon for recycle directly to gasifier (i.e., without slurring)
- Commercially proven at ~ 30 bar operating pressure but higher operating pressure conceptualized.

The E-Gas gasifier with its two stages has a lower O<sub>2</sub> demand, typically about 5% lower than the GE gasifier. The lower O<sub>2</sub> demand reduces the cost of the air separation unit. The lower O<sub>2</sub> demand results in increasing the cold gas efficiency of the E-Gas gasifier over the GE gasifier. The CO/H<sub>2</sub> ratio and the CH<sub>4</sub> content in the syngas both tend to be higher than those for the GE gasifier which are disadvantages for a plant incorporating CO<sub>2</sub> capture. The higher CO/H<sub>2</sub> ratio increases the load on the downstream shift unit while the higher CH<sub>4</sub> content limits the amount of CO<sub>2</sub> capture.

The overall efficiency of the IGCC utilizing this type of gasifier has been shown to be similar to that of a Shell gasifier based plant but a proposed design improvement consisting of increasing the amount of slurry fed to the E-Gas gasifier 2<sup>nd</sup> stage would increase its cold gas efficiency significantly. When a greater fraction of the slurry is fed to the 2<sup>nd</sup> stage however, the temperature within the gasifier in this 2<sup>nd</sup> stage is reduced which may result in a lower destruction of the tars and oils and CH<sub>4</sub> formed during the pyrolysis step within the 2<sup>nd</sup> stage. The presence of tars and oils in the raw syngas will pose special challenges to their gas cleanup process while the higher concentration of CH<sub>4</sub> will further limit the amount of carbon capture.

In light of the above, this gasifier is not chosen for use in the Baseline Case.

## **Air Separation Technology**

The largest consumer of parasitic power in an IGCC is the ASU. ASU power consumption constitutes more than half of the total power consumed by the plant or 10 to 20 percent of the total power produced by the plant. Thus, technologies are being developed as well as various studies have been performed with the intent to minimize this parasitic power consumption of the plant.

## **High Temperature Membrane Technology**

Praxair as well as Air Products are developing membranes (semi-conductor materials) that operate at temperatures in the neighborhood of 800°C to 900°C (1500°F to 1600°F) for air separation. This technology promises reduction in both power consumption and capital cost by about 30%. Praxair, however, points out that for this technology to be economical, it will require the integration of the membrane unit with a gas turbine capable of roughly 50% of the total gas turbine inlet air (i.e., air entering the gas turbine compressor) being available for extraction. The integrated system consists of providing hot pressurized air extracted from the gas turbine compressor to the membrane unit which separates a portion of the O<sub>2</sub> by transferring the O<sub>2</sub> as

ions through the membrane wall while the depleted air is returned to the gas turbine. Thus the gas turbine must also be capable of receiving the depleted air from the membrane unit which is typically at 800°C to 900°C (around 1500°F to 1600°F), the operating temperature of the membrane unit. Note that the air supplied to the membrane unit is preheated to the operating temperature of the membrane unit by directly firing syngas into the air stream. The depleted air exiting the membrane unit consists of a stream that has an O<sub>2</sub> content that is lower than that of fresh air; a portion of the O<sub>2</sub> being separated from the air stream by the membrane.

Air Products has stated at the Gasification Technologies Council Annual Meeting [Armstrong, 2006] that a large scale ITM unit with a capacity of 2,000 ST/D (1800 Tonne/D) will be available for demonstration in 2012. The challenge still remains that a gas turbine with the above stated 50% extraction rate is required and such gas turbines are not expected to be available in the near-term.

In light of the above, this technology is not chosen for use in the Baseline Case but may be considered for the Advanced Brayton Cycles to be investigated under Task 2 of this program.

### **Cryogenic Technology**

The optimum O<sub>2</sub> purity for IGCC applications with low pressure (LP) or EP cryogenic ASUs is 95% based on internal studies made by both Praxair and Air Products for the Demkolec IGCC plant. The number of distillation stages decreases steeply as the purity is reduced from 99.5% to 95%, but remains quite insensitive as the purity is further reduced. The O<sub>2</sub> compression costs (both capital and operating) continue to increase as purity is decreased below 95%. Note that the size of equipment downstream of the ASU also increases (slightly) while the efficiency of the gasification unit decreases as the purity is reduced.

A paper published by Linde [Baker, 1981] supports the above stated relationship between the number of stages and the O<sub>2</sub> purity although the results are for an LP ASU. The separation energy according to the Linde paper also tends to flatten off at purity levels below 95%.

Thus 95% purity O<sub>2</sub> will be utilized for all the cases incorporating a Cryogenic ASU, i.e., including the Baseline case.

For IGCC applications, EP ASUs are preferred over LP ASUs since the oxygen and nitrogen product can be used at elevated pressures, and air extraction from the gas turbine for the ASU is possible. The operating pressure of the ASU distillation operation affects the bubble point of the liquid being distilled in the cold box. The higher the pressure, the less severe the cold box temperature is, which results in a reduced pressure ratio of the incoming air to that of the outgoing streams (O<sub>2</sub> and N<sub>2</sub>). If the O<sub>2</sub> and the N<sub>2</sub> leaving the cold box can be utilized within the gasification plant at the product supply pressure or higher, then a net increase in the overall IGCC plant efficiency is realized. The N<sub>2</sub> produced by the cold box operating at an elevated pressure is further compressed and fed to the gas turbine for increased power output and NO<sub>x</sub> reduction.

Results from previous studies have indicated that about 2% reduction in both the plant heat rate and plant cost may be realized by installing the EP ASU over the LP ASU. Both the Demkolec IGCC and the Polk County IGCC utilize an EP ASU (with 95% purity O<sub>2</sub> in the Demkolec plant and 96% purity O<sub>2</sub> in the Polk County plant).

### EP versus LP ASU and Gas Turbine Air Extraction

The feed air pressure for an LP ASU is in the range of 350 to 600 kPag (50 to 90 psig) while the feed air pressure for an EP ASU is typically set based on the pressure of the air extracted from the gas turbine which corresponds to the discharge pressure of the gas turbine compressor. Note that extraction of air from the gas turbine compressor discharge increases the commonality for the gas turbine design for both IGCC and natural gas applications. When the feed air pressure is very high, a partial expansion step may be required in order to limit the operating pressure of the cold box such that the relative volatility between O<sub>2</sub> and N<sub>2</sub> is not too close to unity in order to limit the number of stages required in the distillation operation. The advanced Brayton cycle as explained later is expected to have a high pressure ratio (in excess of 30) and thus a partial expansion step is foreseen. The other option consisting of mid-compressor air extraction may not be practical from a gas turbine design standpoint since such a design would limit the versatility and fuel flexibility of the gas turbine.

Based on the above considerations, an EP ASU will be utilized with partial air and full N<sub>2</sub> integration with the gas turbine in the Baseline case.

### **Acid Gas Removal Technology**

The various impurities that may be present in raw syngas are listed in Table A1.2-1. Conventional (proven) technology for cleanup consists of “Cold Gas Cleanup,” i.e., cleanup of the syngas near ambient temperatures. “Warm Gas Cleanup” technology is being developed to treat syngas in the temperature range of 300° to 400°C with the potential for increasing the thermal efficiency of the plant while minimizing the generation of a waste water stream (condensate stream formed during cooling of the raw syngas below its water dew point). The two types of technologies are described in the following along with the justification for recommending the Cold Gas Cleanup technology for the Baseline Case.

#### **Warm Gas Cleanup**

The first required step in this process is the removal of particulates from the syngas. Barrier filters are required with the requirement to remove over 99.99% of the particulates entrained in the syngas to protect the downstream cleanup units. The syngas may then be treated in a nahcolite bed to remove chlorides as well as the other halides. This will have to be followed by another barrier filter after which it may be treated with ZnO. This treatment process with the ZnO may be accomplished in a transport desulfurizer in order to make the process continuous since the ZnO is converted to ZnS which has to be regenerated. The regeneration may be accomplished using air extracted from the gas turbine to release the sulfur as SO<sub>2</sub> from which the saleable product H<sub>2</sub>SO<sub>4</sub> may be made.

Warm gas mercury removal processes are also being developed and one such process is that being developed by ADA technologies (funded by the EPA and the DOE) that operates around 300° to 400°C [Butz 2003] and uses a fixed bed reactor containing an Amended Silicates™ sorbent where the mercury is chemisorbed from the syngas.

Most (~90%) of the nitrogen containing compounds such as NH<sub>3</sub> and HCN if present in the syngas fed to the gas turbine will form NO<sub>x</sub> and thus removal of these components is essential for a “Clean Coal” plant. Technologies are being investigated for this cleanup step but are at a very preliminary stage of development.

Warm gas cleanup technologies to capture components such as the metal carbonyls as well as the very fine particulates formed by the condensation of the volatile alkali salts are also required to meet the very stringent specifications expected for the advanced Brayton cycle gas turbine operating at elevated temperatures. Based on the current status of this technology, it will not be used in the baseline Baseline Case but will be considered for application in the Advanced Cases to be investigated under Task 2 of the project.

## **Cold Gas Cleanup**

The selection of the acid gas removal process for desulfurization and decarbonization of the syngas is described next followed by a description of the processes recommended for the removal of metal carbonyls and mercury (as well as arsenic, cadmium and selenium).

### Acid Gas Removal

The proposed scheme for controlling the carbon emissions consists of the following steps: (1) shifting of the raw syngas leaving the particulate scrubber utilizing a sour shift catalyst after preheating to the required temperature, (2) heat recovery and gas cleanup to remove trace components, and (3) capture of the CO<sub>2</sub> in the acid gas removal unit used for desulfurization of the syngas.

The following five acid gas removal technologies are considered:

1. Amine Scrubbing
2. Rectisol
3. Benfield (licensed by UOP)
4. Morphysorb (licensed by Thyssen Krupp)
5. Selexol™ (licensed by UOP)

The amine scrubbing process with additives to improve the selectivity between H<sub>2</sub>S and CO<sub>2</sub> absorption does not produce an acid gas suitable for even a Selectox sulfur recovery unit, as a minimum of 5% H<sub>2</sub>S concentration is required in its feed gas for stable operation. An acid enrichment unit is required and in addition to this enrichment step, another amine unit to remove additional CO<sub>2</sub> that slips through the primary amine unit is required. The equivalent power consumption (net electric power + thermal energy of low pressure steam converted to electric power using an appropriate conversion efficiency) of the amine-based unit is significantly higher than the Selexol-based unit.

With respect to the Benfield process, it is found that it is unable to meet the sulfur specifications in the product gases, and cannot demonstrate selectivity between H<sub>2</sub>S and CO<sub>2</sub>, which is critical to this application. The modest incremental back pressure of the Regenerator does not overcome its serious deficiencies for this application.

Since the sulfur specification for the fuel gas is not too stringent, it is not necessary to install a Rectisol unit, the Rectisol unit tends to be relatively expensive, and its use is typically justified when the treated gas suitable for chemical synthesis is required (< 0.1 ppmV sulfur).

The Morphysorb process which utilizes a physical solvent is a potential candidate especially suitable to IGCC applications where large amounts of sour gas components have to be removed. The solvent has already been used for the sour gas removal from natural gas in a plant located in Kwoon, British Columbia, Canada and has proven to be a safe and reliable process for more than two years. However, little experience if any exists with treating of coal derived syngas in the Morphysorb process, the first application to syngas was to be tested at the FlexFuel facility in Des Plaines by the Gas Technologies Institute. The licensor of this process is not willing to provide any performance information at the current time and wants to wait till they have obtained significant data from field testing. This technology will be considered for application in the Advanced Cases to be investigated under Task 2 of the project contingent upon the availability of licensor data, while for the Baseline case, the Selexol™ process will be utilized since it does not suffer from the disadvantages pointed out for the first three processes listed above.

### Metal Carbonyls

Metal carbonyls that may be present in the raw gas, such as those of nickel and iron, deposit as nickel sulfide at elevated temperatures (such as those in the shift reactors) in the presence of a catalyst in the top layers of the first-stage shift reactor catalyst bed. It has been found that the top 0.5 meters (1 to 2 ft) of the shift catalyst needs to be replaced approximately every two years due to increased pressure drop caused by the sulfide deposition. The impact on the annual operating cost of replacing the top section of the bed at a greater frequency (2 years instead of the normal 3 years) is not expected to have a very significant effect on the overall economics of the plant.

### Mercury, Arsenic, Cadmium and Selenium

These metals typically volatilize within the gasifier and leave the gasifier along with the raw syngas. Sulfided activated carbon has been used to remove mercury and arsenic from coal derived syngas at the Tennessee Eastman gasification plant. Calgon offers this type of activated carbon for removal of mercury, reducing its concentration to as low as 0.01 to 0.1 µg/Nm<sup>3</sup> Hg in the syngas depending on the operating temperature and moisture content. Mercury is captured predominantly as a sulfide, but some of it is captured in its elemental form. The spent carbon has to be disposed of as a hazardous waste although attempts are being made to recover elemental Mercury. Mercury capture by sulfided carbon beds is unaffected by pressure of the syngas. The

capture efficiency is reduced, however, as the operating temperature is increased and as the relative humidity of the syngas is increased.

Experience at the Tennessee Eastman plant indicates that activated carbon is even more effective in capturing the arsenic. Calgon's experience has shown that arsenic if present in the form of an arsine, is captured by this sulfided carbon. SudChemie offers the activated carbons for removal of arsenic and its compounds. A copper impregnated carbon is offered to capture arsenic if present as an organic compound.

Other volatile metal compounds that may be present in coal derived syngas are those of cadmium and selenium. Capture of these species by the activated carbon is yet to be ascertained. Any metal (Ni and Fe) carbonyls that may remain in the syngas may be expected to be captured by the sulfided activated carbon bed.

## **Power Generation Technology**

### **Fuel Cell Hybrids**

Higher conversion efficiencies are achievable with a fuel cell when compared to heat engines; the chemical energy is directly converted into electricity, the intermediate step of conversion into heat as in a heat engine is eliminated, and thus without being constrained by temperature limitations of the materials as in the case with heat engines. A fuel cell based hybrid cycle consists of combining a fuel cell with a heat engine to maximize the overall system efficiency. Overall system efficiencies greater than 60% on natural gas on an LHV basis may be achieved (cycles approaching 75% efficiency on natural gas on an LHV basis have been identified [example: Rao and Samuelsen, 2003]). High temperature fuel cells such as solid oxide and molten carbonate fuel cells are most suitable for such applications. In the case of a high pressure fuel cell based hybrid, the combustor of the gas turbine is replaced by the fuel cell system [Litzinger, et. al., 2005; Agnew, G., et. al., 2005; Schonewald, 2005] while in the case of a low pressure fuel cell based hybrid [Ghezal-Ayagh, 2004], the heat rejected by the fuel cell may be transferred to the working fluid of the gas turbine through a heat exchanger (indirect cycle).

The fraction of the total power produced by the fuel cell in a Solid Oxide Fuel Cell (SOFC) hybrid based power plant is approximately 70%. Thus, for a central station power plant producing nominally 250 MW gross, the SOFC would have to generate as much as 175 MW. This represents a scale up of orders of magnitude over the currently demonstrated units, which have been limited to less than a MW size. Even if the power block is split up into four modules, the size of each SOFC stack module would still require a very large scale-up. In addition to scale-up, another challenge consists of developing materials that allow much higher current densities, orders of magnitude higher than the current values, in order to reduce the physical size to something more manageable from a plot space and piping standpoint. Note that for a 50 MW SOFC, the estimated required cross-sectional area for oxygen ion transport or flow of current within the cells is greater than 10,000 m<sup>2</sup> with today's current densities.

For the reasons mentioned above, fuel cells will not be employed in the Baseline Case.

## Gas Turbine based Cycles

A conventional gas turbine cycle consists of pressurizing a working fluid (air) by compression, followed by combustion of the fuel; the energy thus released from the fuel is absorbed into the working fluid as heat. The working fluid with the absorbed energy is then expanded in a turbine to produce mechanical energy, which may in turn be used to drive a generator to produce electrical power. Unconverted energy is exhausted in the form of heat which may be recovered for producing additional power. The efficiency of the engine is at a maximum when the temperature of the working fluid entering the expansion step is also at a maximum. This occurs when the fuel is burned in the presence of the pressurized air under stoichiometric conditions.

When natural gas is burned with air under stoichiometric conditions, however, the resulting temperature is greater than 1940°C (3500°F) depending on the temperature of the combustion air. It is therefore necessary to utilize a large excess of air in the combustion step, which acts as a thermal diluent and reduces the temperature of the combustion products, this temperature being dependent on the gas turbine firing temperature which in turn is set by the materials used in the turbine parts exposed to the hot gas, and the cooling medium (its temperature and physical properties) as well as the heat transfer method employed for cooling the hot parts. A fraction of the air from the compressor is bled off as cooling air when air is utilized for cooling, the air being extracted from the compressor at appropriate pressures depending upon where it is utilized in the turbine. From a cycle efficiency and engine specific power output (kW per kg/s of suction air flow) standpoint, it is important to minimize the amount of cooling air as well as the excess combustion air.

The necessity to use a large excess of pressurized air in the combustor as well as for turbine cooling when air cooling is employed creates a large parasitic load on the cycle, since compression of the air requires mechanical energy and this reduces the net power produced from the system, as well as reducing the overall efficiency of the system.

Some of the more promising cycle configurations and technology advancements being pursued are discussed in the following directed at increasing the performance of the basic Brayton cycle.

### Humid Air Turbine (HAT) Cycle

The mechanical energy required for air compression in the Brayton cycle can be reduced by utilizing interstage cooling. However, from an overall cycle efficiency standpoint, interstage cooling can be utilized advantageously if the heat removed from the compressed air in the intercooler can be efficiently recovered for conversion to power. If the entire heat is simply rejected to the atmosphere, the overall cycle efficiency may actually decrease depending upon the cycle pressure ratio, since it results in the consumption of more fuel to compensate for the energy lost through the intercooler. Only at very high pressure ratios can intercooling be justified in most cycles.

In the HAT cycle [Rao, 1989] a significant portion of the excess air that is required as thermal diluent in a gas turbine, is replaced with water vapor (see Figure A1.2 - 5). The water vapor is introduced into the system in an efficient manner, by pumping of a liquid followed by low

temperature evaporation. Pumping a liquid requires less mechanical energy compared to gas (air) compression. Evaporation of the water into the compressed air stream is accomplished using low temperature heat, in a counter-current multistage humidification column, rather than generating steam in a boiler. This method of humidification permits the use of low temperature heat for accomplishing the evaporation of water. For example, water which boils at 100°C (212°F) at atmospheric pressure may be made to evaporate at room temperature when exposed to a stream of relatively dry air.

The process also reduces the parasitic load of compressing the combustion air by intercooling the compressor, while recovering most of the heat removed in the intercooler for the humidification operation. Thus, a more thermally efficient power cycle is achieved. Humidification of the compressed air also leads to a reduction of NO<sub>x</sub> emissions. The humid air is preheated by heat exchange with the turbine exhaust in a recuperator to recycle the exhaust energy to the combustor, thereby eliminating the expensive steam bottoming cycle required in a combined cycle.

The advantages of the HAT cycle are:

- Less than 5 ppmV NO<sub>x</sub> without post-combustion treatment
- High efficiency without a steam bottoming cycle
- Excellent part-load performance, efficiency essentially constant down to 60% of full load
- Performance quite insensitive to ambient temperature
- Water usage less than that for a combined cycle employing wet cooling tower and if desired, water may be recovered from HAT exhaust
- High specific power output
- Integrates synergistically with reliable low-cost “Total Quench” gasifier
- In coal based Zero Emission plants, the “Total Quench Gasifier” option is of choice
- In natural gas Zero Emission based plants where CO<sub>2</sub> is recovered from exhaust, CO<sub>2</sub> concentration is higher (dry basis).

Despite the HAT cycle’s potential advantages, the development of the required turbo-machinery is occurring at a very slow pace, mainly due to the very high development costs for developing the required large intercooled gas turbine. Studies sponsored by EPRI have found that the costs of developing the engine could be as high as \$700 to 800 million. Based on the current status of this technology, it will not be used in the Baseline Case but will be considered for application in the Advanced Cases to be investigated under Task 2 of the project.

### Oxy-Fuel Cycles

Another promising approach is oxy-fuel combustion for ultra high temperature and high pressure “steam turbines” [Jericha, et. al., 1995; Smith et. al., 2000]. In these systems, the fuel is combusted utilizing a relatively pure O<sub>2</sub> stream to create a working fluid for the turbine composed mostly of water, and CO<sub>2</sub>. The design of these systems would facilitate the capture of essentially all of the CO<sub>2</sub> and all of the Clean Air Act criteria pollutants such as NO<sub>x</sub> and SO<sub>x</sub> and other unregulated pollutants depending on the purity constraints set for the product CO<sub>2</sub> stream for sequestration. The syngas cleanup system will be simplified significantly resulting in

efficiency and capital cost benefits if these criteria pollutants are allowed to be contained in the captured CO<sub>2</sub> stream leaving the plant. Only particulate cleanup would be required in the syngas cleanup process.

These cycles do not require a shift unit upstream of the power block as is done in the other cycles that consist of pre-combustion CO<sub>2</sub> recovery in Zero Emission power plant applications. Thus, from a thermal performance standpoint such cycles have the advantage of not by-passing the thermal energy produced during the exothermic shift reaction around the topping cycle as is done in the other cycles consisting of pre-combustion CO<sub>2</sub> recovery. In the pre-combustion CO<sub>2</sub> recovery based cases, the thermal energy generated in the shift unit enters the bottoming steam cycle directly. In Oxy-Fuel cycles, the CO<sub>2</sub> is captured from the exhaust of the turbine in the condenser. The disadvantage, however, is that the CO<sub>2</sub> is recovered at low pressure (at sub-atmospheric pressure) and requires a significant amount of compression power to pressurize the CO<sub>2</sub> before it may be transported for sequestration. Alternate schemes to extract the CO<sub>2</sub> at higher pressure should be investigated as well as system configurations that produce excess hydrogen for export.

A large amount of O<sub>2</sub> is also required as compared to the pre-combustion CO<sub>2</sub> recovery schemes. An Ion Transport Membrane (ITM) unit would be required to produce the O<sub>2</sub> for both the gasifiers and the power cycle in order to limit the negative effects on plant performance and cost due to the demand for a large quantity of O<sub>2</sub>.

Development needs include the design of the combustor as well as the “steam turbine” which has many of the features of a gas turbine. An organization with significant involvement in the development of such a system in the U.S. is Clean Energy Systems, Inc.

Based on the current status of this technology, it will not be used in the Baseline Case but will be considered for application in the Advanced Cases to be investigated under Task 2 of the project.

### Partial Oxidation Cycles

One form of this cycle is depicted in Figure A1.2 - 6. This concept is similar to a reheat cycle except that the first combustor is operated under sub-stoichiometric or partial oxidation conditions [Korobitsyn, Kers and Hirs, 1998; Newby et. al., 1997]. Following the sub-stoichiometric stage, oxidation of the fuel is completed in the second combustor after expansion in the high pressure turbine. This is an alternative scheme that may be used to limit the firing temperature while gaining efficiency. The absence of excess O<sub>2</sub> in the first stage combustor decreases NO<sub>x</sub> formation. Potential challenges are (1) due to the metallurgical issues such as H<sub>2</sub> embitterment and metal dusting within the partial oxidation combustor as well as the high pressure turbine, (2) soot formation within the partial oxidation combustor and (3) design of the high pressure turbine seals to contain the CO and H<sub>2</sub> at the high temperature and pressure. A large addition of steam may be required to circumvent Concerns 1 and 2 while a buffer gas such as N<sub>2</sub> (supplied by the ASU) may be required for the seals (Concern 3). Humidification of the syngas or of the oxidant (as in the case of the HAT cycle described previously) could be used to replace some or all of the steam required by the partial oxidation combustor while utilizing low temperature heat for the humidification operation in order to enhance the overall plant efficiency.

The oxidant may consist of O<sub>2</sub> instead of air in the case of a Zero Emission plant that utilizes an Oxy-Fuel Cycle described previously.

Based on the current status of this technology, it will not be used in the Baseline Case but will be considered for application in the Advanced Cases to be investigated under Task 2 of the project.

### Advanced Brayton Cycles

Some of the technological advances being made or being investigated to improve the basic Brayton cycle include the following, in addition to the changes in the basic cycle configuration such as the inclusion of reheat combustion, intercooling (which is justified for very high pressure ratio cycles) and fogging of the compressor inlet air:

- Rotor inlet temperature of 1700°C (3100°F) or higher which would require the development and use of advanced materials including advanced thermal barrier coatings and turbine cooling techniques including closed loop steam cooling
- Advanced combustor liner (combustion air and combustion products being hotter) required due to increases in rotor inlet temperatures
- High blade surface temperature in the neighborhood of ~1040°C (1900°F) while limiting coolant amount would again require the development and use of the advanced materials including advanced thermal barrier coatings
- Pressure gain combustor
- Cavity or trapped vortex combustor to reduce NO<sub>x</sub> formation
- High pressure ratio compressor (greater than 30 to take full advantage of higher firing temperature)
- Integration capability with high temperature ion transport membrane air separation in IGCC applications.

Addition of novel bottoming cycles is yet another approach to improving the overall plant (combined cycle) performance. Overall cycle efficiencies approaching 65% on natural gas on an LHV basis may be expected (see Figure A1.2 - 7) utilizing these advanced technology gas turbines. Some of these developments and challenges are described in the following and then a recommendation is made regarding the selection of the power technology for the Baseline Case.

### Gas Turbine Firing Temperature

Current-state-of-the-art gas turbines for land-based applications have firing temperatures (rotor inlet temperatures) that are as high as about 1430°C (2600°F) on natural gas base-loaded operation. This increase in firing temperature has been made possible by being able to operate the turbine components (that come into contact with the hot gasses) at higher temperatures while at the same time utilizing closed circuit steam cooling. In a state-of-the-art air-cooled gas turbine with firing temperature close to 1320°C (2400°F), as much as 25% of the compressor air may be used for turbine cooling, which results in a large parasitic load of air compression. In air cooled gas turbines, as the firing temperature is increased, the demand for cooling air is further increased. Closed circuit steam cooling of the gas turbine provides an efficient way of increasing the firing temperature without having to use a large amount of cooling air. Furthermore, steam

with its very large heat capacity is an excellent coolant. Closed circuit cooling also minimizes momentum and dilution losses in the turbine while the turbine operates as a partial reheater for the steam cycle. Another major advantage with closed circuit cooling is that the combustor exit temperature and thus the NO<sub>x</sub> emissions are reduced for a given firing temperature; the temperature drop between the combustor exit gas and the turbine rotor inlet gas is reduced since the coolant used in the first stage nozzles of the turbine does not mix with the gasses flowing over the stationary vanes. Note that control of NO<sub>x</sub> emissions at such high firing temperatures becomes a major challenge. The GE H series gas turbines as well as the Siemens and Mitsubishi G series gas turbines incorporate steam cooling although the GE turbine includes closed circuit steam cooling for the rotors of the high pressure stages.

Taking the firing temperature beyond 1430°C (2600°F) poses challenges for the materials in the turbine hot gas path. Single crystal blading has been utilized successfully in advanced turbines but in addition to this, development of advanced thermal barrier coatings would be required. Extensive use of ceramics may be predicated for firing temperature near 1700°C (3100°F).

Use of a reheat or sequential combustor in a gas turbine is an alternative scheme that may be used to limit the firing temperature while gaining efficiency. Such a scheme as depicted in Figure A1.2 - 8 has been commercialized by Alstom in their GT 24 and 26 engines. For a given firing temperature, the gain in combined cycle heat rate is approximately 2% with the use of a reheat combustor. Another advantage is the reduced NO<sub>x</sub> emission due to both the lower firing temperature and the destruction of some of the NO<sub>x</sub> that is formed in the first combustor by the reheat combustor. The challenges associated with the design of the reheat combustor are due to the combustion air that consists of a hot (> 650°C or 1200°F) vitiated (< 15% O<sub>2</sub> by volume) stream.

### Gas Turbine Pressure Ratio

The optimum pressure ratio for a given cycle configuration increases with the firing temperature of the gas turbine. Thus to take full advantage of the higher firing temperature of the gas turbine with firing temperature greater than 1700°C (3100°F) the required pressure ratio may be in excess of 30. Another constraint to also consider is the temperature of the last stage buckets in the turbine. This temperature may have to be limited to about 650°C (1200°F) from a strength of materials standpoint since the last stage buckets in large scale gas turbines tend to be very long and a certain minimum pressure ratio would be required to limit this temperature. Development of a compressor with such a high pressure ratio may require the adoption of the aero-engine technology including twin-spools in order maintain a fuel flexible design. Note that the pressure ratio of the gas turbine increases when firing syngas as compared to natural gas operation (syngas being a much lower heat content gas than natural gas). The increase in pressure ratio is dependent upon the amount and nature of the diluent added to the syngas for NO<sub>x</sub> control and the degree to which the compressor inlet guide vanes are closed. Air extraction from the compressor (while supplying the extracted air to the ASU) will help in order to limit the increase in the engine pressure ratio but an upper limit exists for the fraction of air that may be extracted without affecting the amount of air remaining for combustor liner cooling purposes.

## Combustor Developments

**Pressure Gain Combustor.** A pressure gain combustor produces an end-state stagnation pressure that is greater than the initial state stagnation pressure. An example of such a system is the constant volume combustion in an ideal spark ignited engine. Such systems produce a greater available energy in the end state than constant pressure systems. It has been shown that the heat rate of a simple cycle gas turbine with a pressure ratio of 10 and a turbine inlet temperature of  $\sim 1200^{\circ}\text{C}$  ( $2200^{\circ}\text{F}$ ) can be decreased by more than 10% utilizing such a constant volume combustion system [Gemmen, Richards and Janus, 1994]. Pulse combustion which relies on the inherent unsteadiness of resonant chambers can be utilized as a pressure gain combustor. Research continues at the U.S. DOE and at NASA for the development of pressure gain combustors. Based on the current status of this technology, it will not be used in the Baseline Case but will be considered for application in the Advanced Cases to be investigated under Task 2 of the project.

**Trapped Vortex Combustor.** The Trapped Vortex Combustor (TVC) has the potential for numerous operational advantages over current gas turbine engine combustors [Hsu, Gross and Trump, 1995]. These include lower weight, lower pollutant emissions, effective flame stabilization, high combustion efficiency, and operation in the lean burn modes of combustion. The TVC concept grew out of fundamental studies of flame stabilization and is a radical departure in combustor design using swirl cups to stabilize the flame. Swirl stabilized combustors have somewhat limited combustion stability and can blow out under certain operating conditions. On the other hand, the TVC maintains a high degree of flame stability because the vortex trapped in a cavity provides a stable recirculation zone that is protected from the main flow in the combustor. The second part of a TVC is a bluff body dome which distributes and mixes the hot products from the cavity with the main air flow. Fuel and air are injected into the cavity in a way that it reinforces the vortex that is naturally formed within it.

The TVC may be considered a staged combustor with two pilot zones and a single main zone, the pilot zones being formed by cavities incorporated into the liners of the combustor [Burrus et al., 2001]. The cavities operate at low power as rich pilot flame zones achieving low CO and unburned hydrocarbon emissions, as well as providing good ignition and the lean blowout margins. At higher power conditions (above 30% power) the additional required fuel is staged from the cavities into the main stream while the cavities are operated at below stoichiometric conditions. Experiments have demonstrated an operating range that is 40% wider than conventional combustors with combustion efficiencies of 99%+. Use of the TVC combustor holds special promise as an alternate option for suppressing the NO<sub>x</sub> emissions in syngas applications where pre-mixed burners may not be employed. Research continues in this area and based on the current status of this technology, it will not be used in the baseline Baseline Case but will be considered for application in the Advanced Cases to be investigated under Task 2 of the project. Organizations actively involved in the development of such combustors include GE and Ramgen.

**Catalytic Combustor.** Lean stable combustion can be obtained by catalytically reacting the fuel-air mixture with a potential for simultaneous low NO<sub>x</sub>, CO and unburned hydrocarbons. It also has the potential for improving lean combustion stability and reducing

combustion-induced pressure oscillations. The catalytic combustor can play a special role in IGCC applications to reduce NO<sub>x</sub> emissions but such a combustor for the large scale applications with commercial guarantees is not expected to be available in the near term. Based on the current status of this technology, it will not be used in the Baseline Case but will be considered for application in the Advanced Cases to be investigated under Task 2 of the project.

#### Recommendation of Gas Turbine Technology for the Baseline Case

- Based on the developmental status of the above described technologies, it is recommended that for the Baseline Case, the steam cooled “H” technology gas turbine as represented by the GE 7H machine be utilized.

#### Other Considerations

**Inlet Air Fogging.** An alternate approach to reducing the parasitic load of air compression in a gas turbine is to introduce liquid water into the suction air [Bhargava and Meher-Homji, 2002]. The water droplets will have to be extremely small in size and be in the form of a fog to avoid impingement on the blades of the compressor causing erosion. As the water evaporates within the compressor from the heat of compression, the air being compressed is cooled which in turn causes a reduction in the compressor work. Note that the compression work is directly proportional to the absolute temperature of the fluid being compressed.

A benefit in addition to increasing the specific power output of the engine is the reduction in the NO<sub>x</sub> due to the presence of the additional water vapor in the combustion air. A number of gas turbines have been equipped with such a fogging system operating on natural gas. Care should be taken, however, in specifying the water treatment equipment since high quality demineralized water is required as well as in the design of the fogging system to avoid impingement of the compressor blades with water droplets.

This technology has been proven in a number of natural gas based plants and will be considered for incorporation in the Baseline Case as a sensitivity.

**NO<sub>x</sub> Control.** The name plate NO<sub>x</sub> emission from the GE Frame 7FB gas turbine which is being offered for IGCC applications, on syngas with massive N<sub>2</sub> and/or moisture addition is 15 ppmV (dry, 15% O<sub>2</sub> basis). To achieve lower NO<sub>x</sub> emissions, a selective catalytic reduction (SCR) unit would be required. The unreacted ammonia leaving the SCR, however, reacts with any SO<sub>3</sub> present to form ammonium salts that can (1) deposit in the low temperature sections of the HRSG causing fouling, and (2) result in particulate emissions. In order to limit the number of HRSG washes to one per year to remove these salt deposits, the total equivalent sulfur concentration in the gas turbine exhaust should be limited to 2 ppmV, which is roughly equivalent to 10 to 15 ppmV total sulfur in the syngas. The SO<sub>3</sub> is formed by (1) oxidation within the gas turbine combustor of the H<sub>2</sub>S and COS present in the syngas, and (2) oxidation of the SO<sub>2</sub> within the SCR containing a vanadium catalyst.

If an SCR is required, then the following design option may be required:

- Utilize a low vanadium content SCR catalyst.
- Install a NH<sub>3</sub> oxidation catalyst (developed by Engelhard) downstream of the SCR to oxidize the NH<sub>3</sub> slipping through the SCR catalyst into N<sub>2</sub> and H<sub>2</sub>O in order to minimize the NH<sub>3</sub> emissions. The catalyst can reduce the incoming concentration of NH<sub>3</sub> from 1 - 20 ppmV to less than 0.5 ppmV (the NH<sub>3</sub> oxidation catalyst itself produces some SO<sub>3</sub>, however).
- Limit the concentration of the sulfur compounds in the fuel gas to 10 ppmV. This will not be a problem for an IGCC plant designed for producing a decarbonized syngas utilizing a sour shift and an acid gas removal unit to capture the CO<sub>2</sub> while performing desulfurization of the syngas because most of the COS is hydrolyzed to H<sub>2</sub>S in the shift reactors, while a very large solvent circulation rate is maintained in the acid gas removal unit to capture the CO<sub>2</sub> resulting in very low sulfur content in the treated syngas.

This approach will be considered for incorporation in the Baseline Case as a sensitivity for the ultra low NO<sub>x</sub> IGCC.

### **Conclusions - Technology Selection – Baseline Case**

The overall plant configuration proposed for the Baseline Case is depicted in Figure A1.2 - 9. The plant scheme consists of high pressure (EP) cryogenic air separation unit (ASU) supplying 95% purity O<sub>2</sub> to GE type HP total quench gasifiers. The raw gas after scrubbing is treated in a sour shift unit to react the CO with H<sub>2</sub>O to form H<sub>2</sub> and CO<sub>2</sub>. The gas is further treated to remove Hg in a sulfided activated carbon bed. The syngas is desulfurized and decarbonized in a Selexol acid gas removal unit and the decarbonized syngas after humidification and preheat is fired in a GE 7H type steam cooled gas turbine. IP N<sub>2</sub> from the ASU is also supplied to the combustor of the gas turbine as additional diluent for NO<sub>x</sub> control. A portion of the air required by the ASU is extracted from the gas turbines.

An ultra low NO<sub>x</sub> (2 ppmvd, 15% O<sub>2</sub> basis) sensitivity case is developed by the inclusion of an SCR in the heat recovery steam generator (HRSG).

### **REFERENCES**

1. Agnew, G., et. al., "The Design and Integration of the Rolls-Royce Fuel Cell Systems 1 MW SOFC," *Proceedings of the ASME Turbo Expo Conference*, Reno-Nevada, June 2005.
2. Armstrong, P. A., "ITM Oxygen: The New Oxygen Supply for the New IGCC Market," *Presented at the Gasification Technologies Conference*, San Francisco, October, 2005.
3. Baker, C. R., "Low Purity O<sub>2</sub> Saves Energy in Coal Conversion," *Hydrocarbon Processing*, July 1981.
4. Bhargava, R. and C. B. Meher-Homji, "Parametric Analysis of Existing Gas Turbines with Inlet Evaporative and Overspray Fogging," *Proceedings of the ASME IGTI Turbo-Expo Conference*, Amsterdam, June 2002.
5. Burrus, D. L., A. W. Johnson and W. M. Roquemore, and D. T. Shouse, "Performance Assessment of a Prototype Trapped Vortex Combustor for Gas Turbine Application," *Proceedings of the ASME IGTI Turbo-Expo Conference*, New Orleans, June 2001.

6. Butz, J. R., J. S. Lovell, T. E. Broderick, R. W. Sidwell, C. S. Turchi and A. K. Kuhn, "Evaluation of Amended Silicates™ Sorbents for Mercury Control," Proceedings of the Mega Symposium, Washington DC, May 2003.
7. Gemmen, R. S., G. A. Richards and M. C. Janus, "Development of a Pressure Gain Combustor for Improved Cycle Efficiency," *Proceedings of the ASME Cogen Turbo Power Congress and Exposition*, 1994.
8. Ghezel-Ayagh, H., "Hybrid Controls," *Presented at the ICEPAG Conference*, Irvine, California, September 2004.
9. Hsu, K. Y., Gross, L. P. and Trump, D. D., "Performance of a Trapped Vortex Combustor," *J. of Propulsion and Power*, Paper No. 95-0810, AIAA 33<sup>rd</sup> Aerospace Sciences Meeting and Exhibit, Reno, Nevada, Jan 9-12, 1995.
10. Jericha H., Sanz W., Woisetschläger J., Fesharaki M., "CO<sub>2</sub>-Retention Capability of CH<sub>4</sub>/O<sub>2</sub>-Fired Graz Cycle", CIMAC Paper G07, CIMAC Conference Interlaken, Switzerland, 1995.
11. Korobitsyn, M.A., Kers, P.W., Hirs, G.G., "Analysis of a gas turbine cycle with partial oxidation," (ASME Paper 98-GT-33), Presented at the 43rd ASME International Gas Turbine & Aeroengine Congress, Stockholm, Sweden, June 2-5, 1998.
12. Litzinger, K., et. al., "Comparative Evaluation of SOFC Gas Turbine Hybrid System Options," *Proceedings of the ASME Turbo Expo Conference*, Reno-Nevada, June 2005
13. Rao, A. D., "Process for Producing Power," U.S. Patent No. 4,289,763 dated May 16, 1989.
14. Rao, A. D. and G. S. Samuelsen, "A Thermodynamic Analysis of Tubular SOFC based Hybrid Systems," *ASME J. of Engineering for Gas Turbines and Power*, Vol. 125, January 2003.
15. Schonewald, R., "Turbo-Machinery Requirements for Practical SOFC-Gas Turbine Hybrid Systems," *Proceedings of the ASME Turbo Expo Conference*, Reno-Nevada, June 2005.

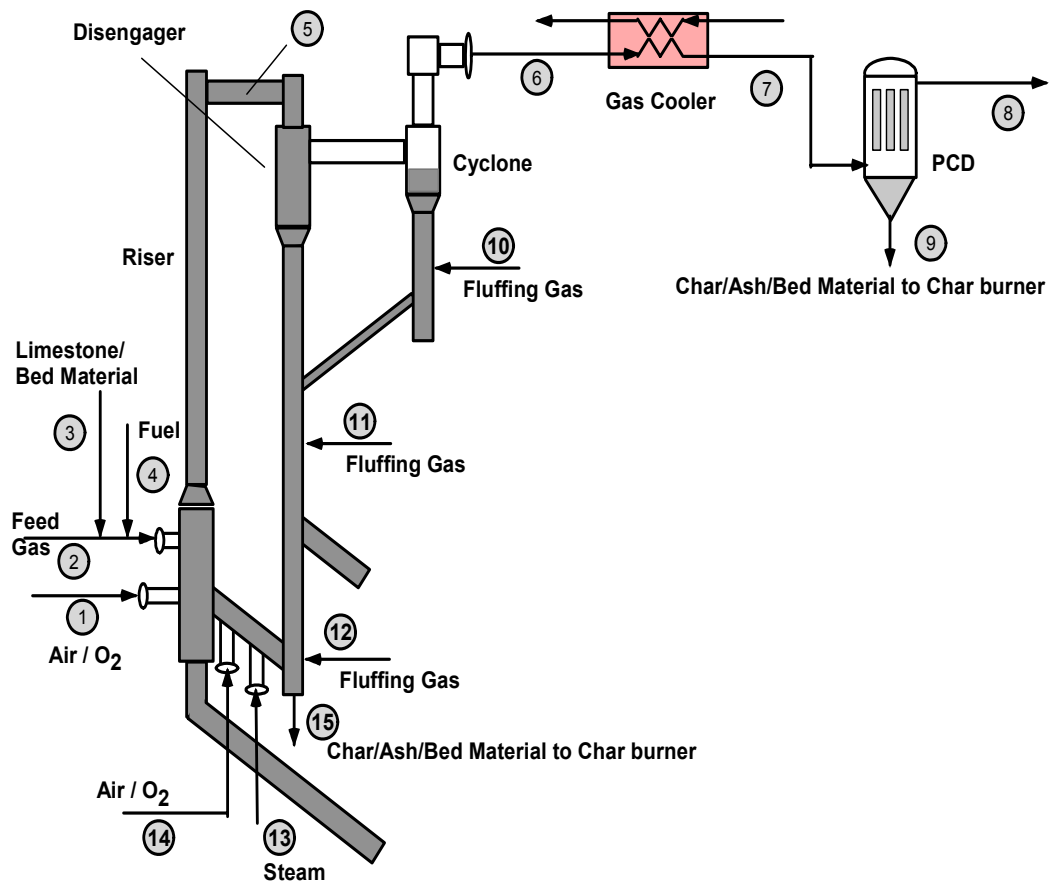


**Figure A1.2 - 1: Advanced Transport Reactor**

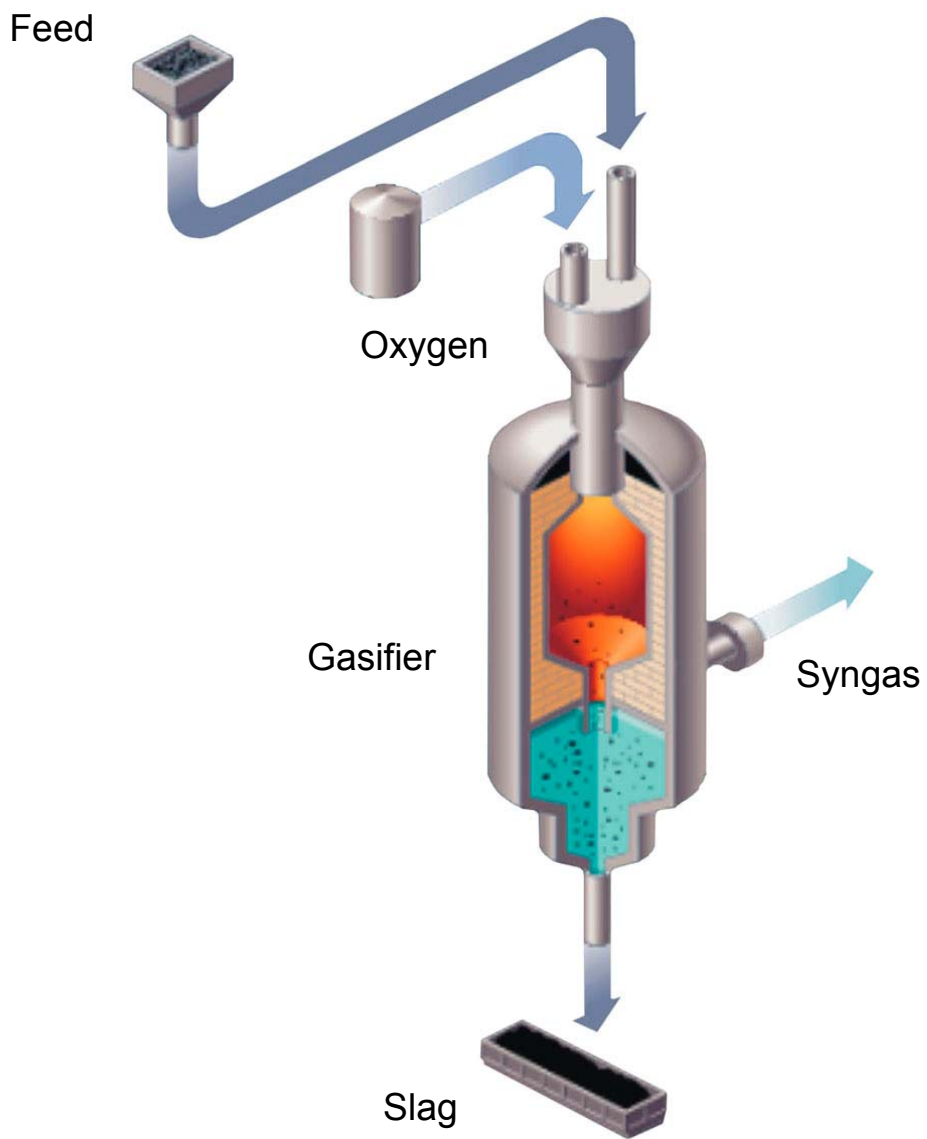


**Figure A1.2 - 2: GE Total Quench Gasifier**

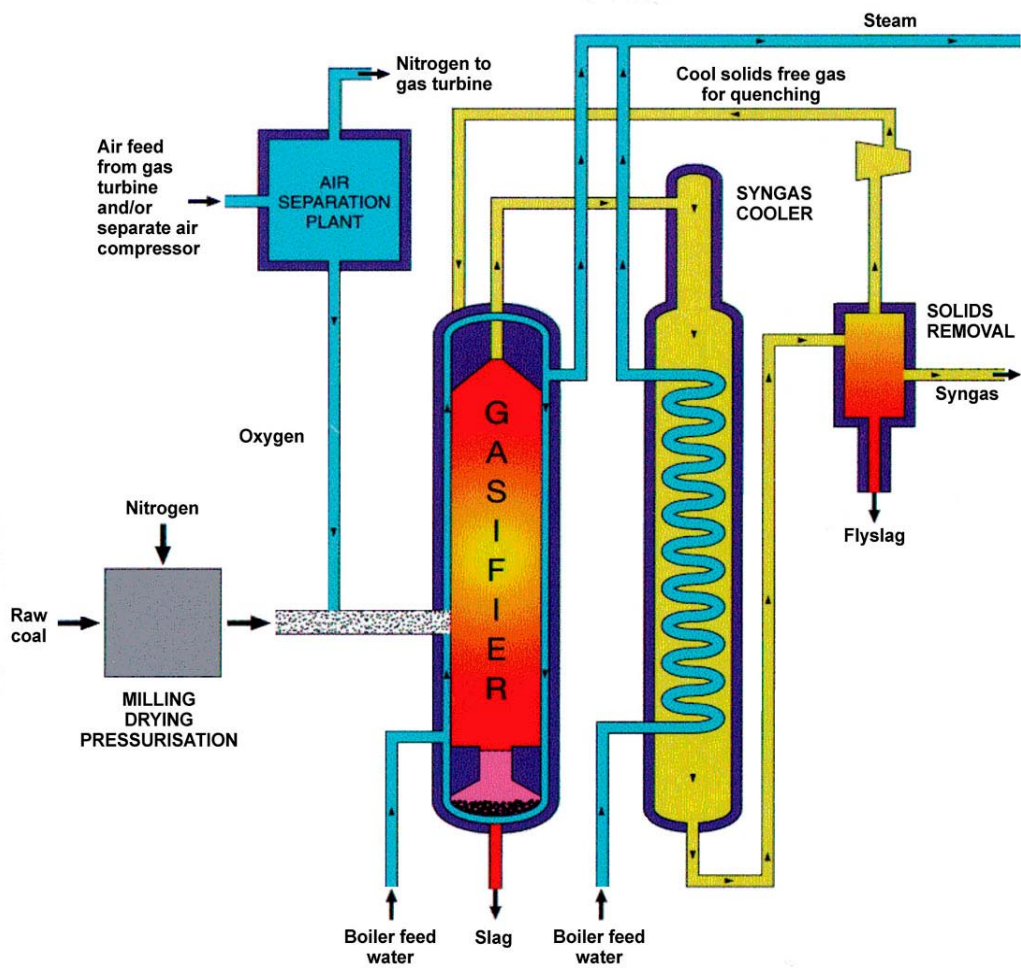


Figure A1.2 - 3: Shell Gasifier

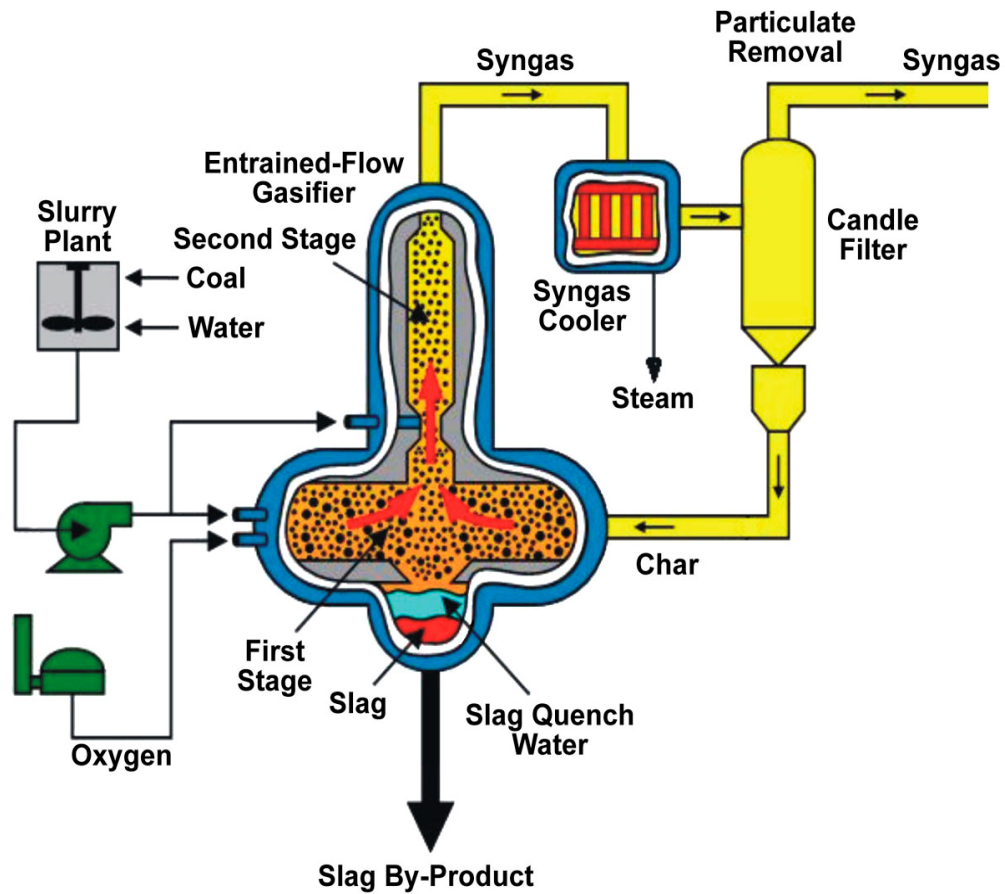


Figure A1.2 - 4: E-Gas Gasifier<sup>g</sup>

<sup>g</sup> Recycle quench gas not shown (see Report titled, “Cost and Performance Baseline for Fossil Energy Plants,” DOE/NETL-2007/1281, Revision 1, August 2007 for more details).

**Table A1.2 - 1: Syngas Contaminants<sup>h</sup>**

Contaminant	Concentration (ppmV)	Comments
Arsenic, as AsH <sub>3</sub>	<0.04	Kingsport gasification stream
	0.150-0.578	Kingsport gasification feed conc.
	0.2	UND-EERC highest vaporization
Halogens {Cl & F}	~0	Kingsport gasification stream
Chlorine	120	UND-EERC highest vaporization
CH <sub>3</sub> F	2.55	Kingsport gasification feed conc.
CH <sub>3</sub> Cl	2.01	Kingsport gasification feed conc.
HCl	<1	Kingsport gasification stream
Fe(CO) <sub>5</sub>	0.05-0.01	Kingsport gasification stream
	5.63	Kingsport gasification feed conc.
Ni(CO) <sub>4</sub>	0.025-0.001	Kingsport gasification stream
HCN	<1	Kingsport gasification stream
CH <sub>3</sub> SCN	2.14	Kingsport gasification feed conc.
Acetonitrile	<0.5	Kingsport gasification stream
PH <sub>3</sub>	1.91	Kingsport gasification feed conc.
Antimony	<0.025	Kingsport gasification stream
	0.07	UND-EERC highest vaporization
Cadmium	0.011	UND-EERC highest vaporization
Beryllium	<0.025	Kingsport gasification stream
Chromium	<0.025	Kingsport gasification stream
	6.0	UND-EERC highest vaporization
Mercury	<0.025	Kingsport gasification stream
	0.0015	UND-EERC highest vaporization
Nickel	3.0	UND-EERC highest vaporization
Potassium	512	UND-EERC highest vaporization
Selenium	<0.15	Kingsport gasification stream
	0.17	UND-EERC highest vaporization
Sodium	320	UND-EERC highest vaporization
Thiophene	1.61	Kingsport gasification stream
Vanadium	<0.025	Kingsport gasification stream
Lead	0.26	UND-EERC highest vaporization
Zinc	9.0	UND-EERC highest vaporization

<sup>h</sup> In addition to H<sub>2</sub>S, COS, Possibly CS<sub>2</sub>, NH<sub>3</sub>, HCN.

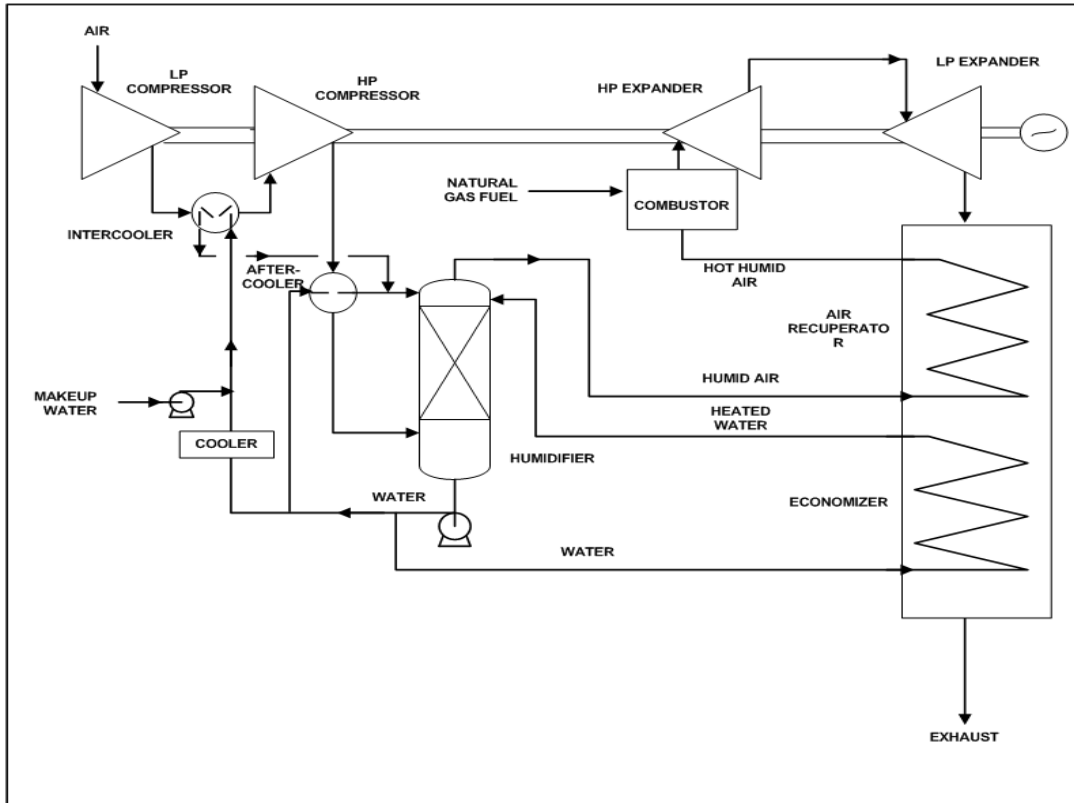


Figure A1.2 - 5: HAT Cycle

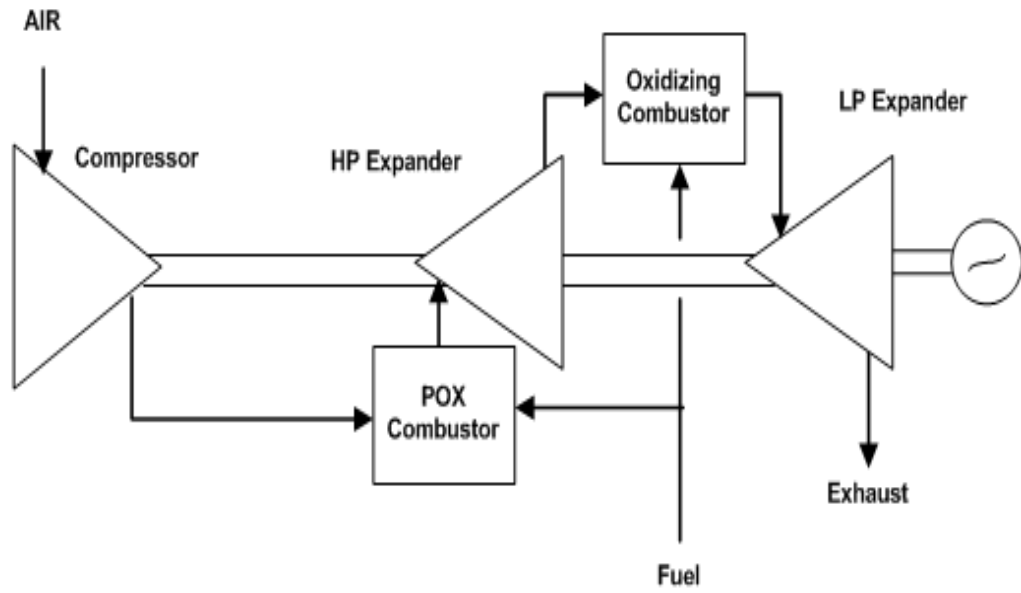


Figure A1.2 - 6: Partial Oxidation Cycle

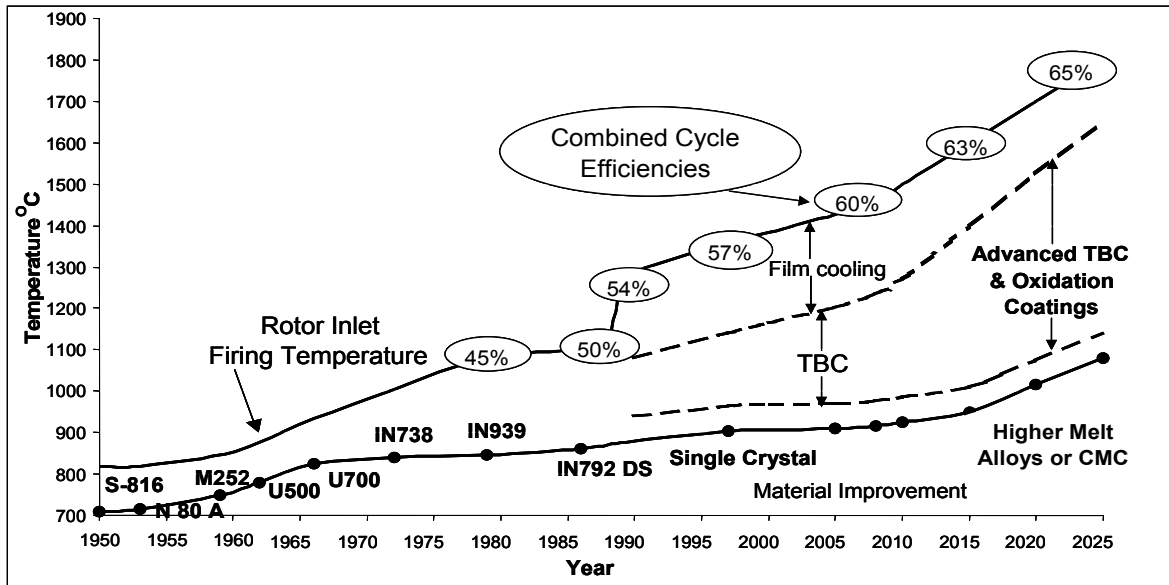


Figure A1.2 - 7: Impact of Firing / Blade Temperatures on Efficiency

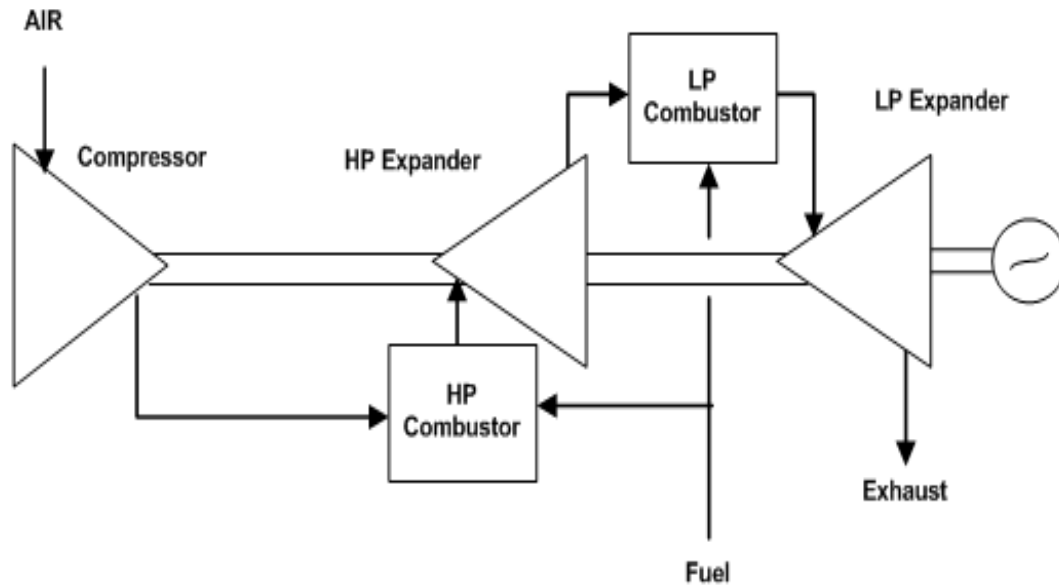


Figure A1.2 - 8: Reheat Gas Turbine Cycle

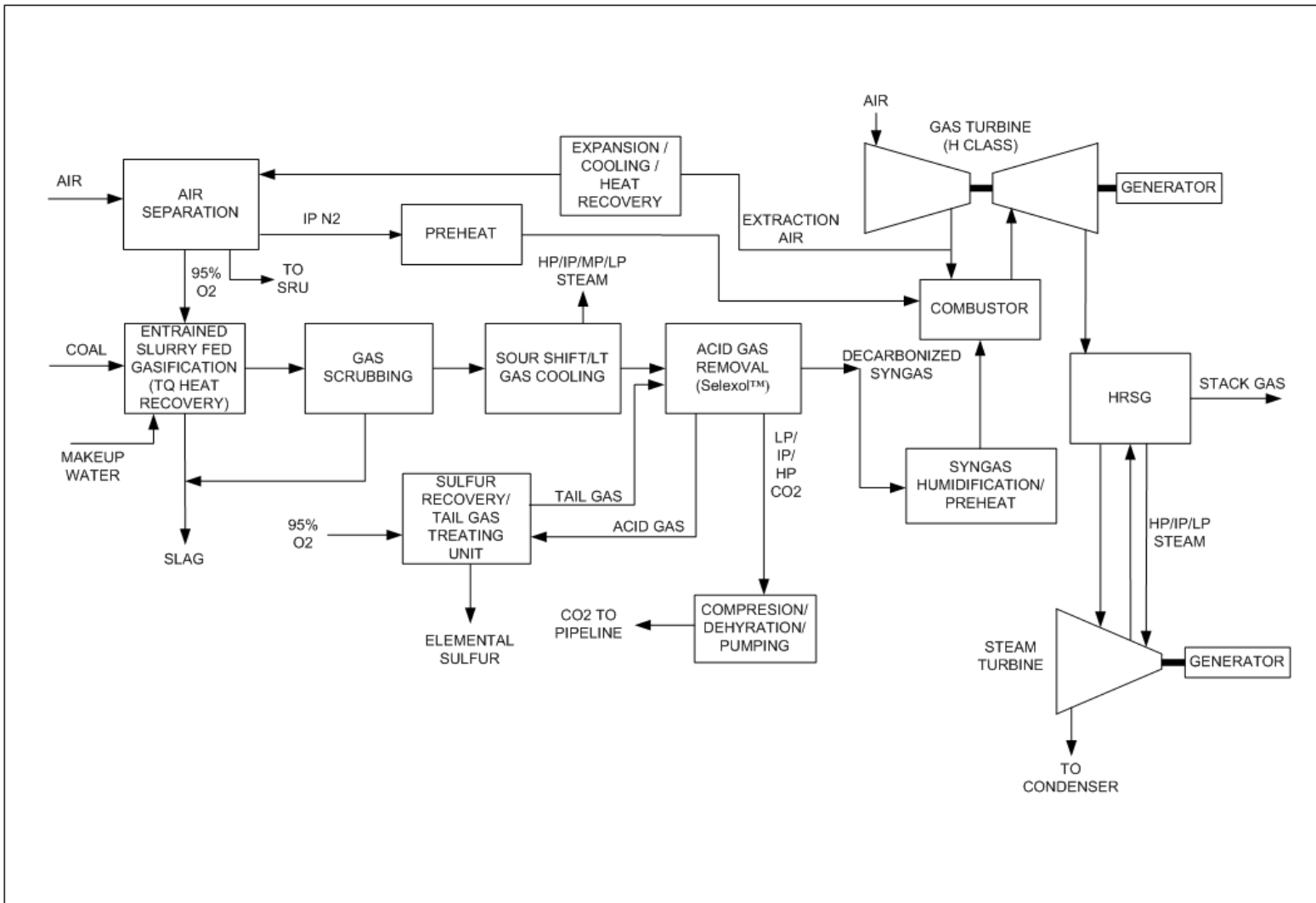


Figure A1.2 - 9: Overall Block Flow Diagram – Baseline Case IGCC with CO<sub>2</sub> Capture

## TASK 1.3: FIRST DETAILED SYSTEMS STUDY ANALYSIS - BASELINE CASE

### SUMMARY

Table A1.3-1 shows that the overall system efficiency, coal (HHV) to power, is 35% for the Baseline Case. The table also summarizes the performance of a Sensitivity Case to assess the performance advantage of utilizing air extracted from the gas turbine without pressure reduction in a turbo-expander and an Air Separation Unit (ASU) operating at a significantly higher pressure (than what has been demonstrated in an IGCC plant). As can be seen from these results, the performance gain with this higher pressure ASU is quite small. Table A1.3-2 summarizes the auxiliary power consumption within the plant for these two cases.

The overall block flow diagram is presented in Figure A1.3 - 1 and the key unit process flow diagrams are shown in subsequent figures. Stream data are given in Table A1.3-3. Equipment function specifications are provided in Tables A1.3 - 4 through 19.

The overall plant scheme consists of a cryogenic air separation unit supplying 95% purity O<sub>2</sub> to GE type high pressure (HP) total quench gasifiers. The raw gas after scrubbing is treated in a sour shift unit to react the CO with H<sub>2</sub>O to form H<sub>2</sub> and CO<sub>2</sub>. The gas is further treated to remove Hg in a sulfided activated carbon bed. The syngas is desulfurized and decarbonized in a Selexol acid gas removal unit and the decarbonized syngas after humidification and preheat is fired in a GE 7H type steam cooled gas turbine. Intermediate pressure (IP) N<sub>2</sub> from the ASU is also supplied to the combustor of the gas turbine as additional diluent for NO<sub>x</sub> control. A portion of the air required by the ASU is extracted from the gas turbines.

The plant consists of the following major process units:

- Air Separation Unit
- Gasification Unit
- CO Shift / Low Temperature Gas Cooling (LTGC) Unit
- Acid Gas Removal Unit (AGR) Unit
- Fuel Gas Humidification Unit
- Carbon Dioxide Compression / Dehydration Unit.
- Claus Sulfur Recovery / Tail Gas Treating Unit (SRU / TGTU)
- Power Block.

### PROCESS DESCRIPTIONS

#### **Air Separation Unit, Gas Turbine Air Extraction and N<sub>2</sub> Preheat**

The primary purpose of the ASU is to supply high pressure, high purity O<sub>2</sub> (at a nominal 95 mole %) to the Gasification unit. Figure A1.3 - 2 depicts the main features of this unit. For the purpose of computer simulation, the ASU has been modeled as two separate sections: An elevated pressure (EP) section which provides compressed air to the cold box operating at elevated pressure, and a low pressure (LP) section which provides compressed air to the cold box

operating at lower pressure. This ASU set up with an EP and LP section provides a valid approximation for the performance of an ASU providing oxygen and nitrogen to an IGCC facility in which only a fraction of the entire amount of N<sub>2</sub> available from the ASU is required at pressure for gas turbine injection. The actual design of the ASU will be determined by the ASU vendor. The EP section produces the N<sub>2</sub> which is sent to the gas turbine. The Sulfur Recovery unit also consumes a small quantity of O<sub>2</sub>. O<sub>2</sub> and N<sub>2</sub> in air are separated by means of cryogenic distillation. Approximately 60% of the N<sub>2</sub> separated from the air leaves the distillation unit at pressure and is compressed and injected into the gas turbines for NO<sub>x</sub> emissions control as well as providing additional motive fluid.

For both the EP and LP section, ambient air is sent through a filter to remove dust and other particulate matter and then compressed before providing the air to the “cold box.” Interstage cooling and after-cooling of the compressor is accomplished with cooling water. For the EP section, air extracted from the gas turbine compressor discharge is also provided to the “cold box” after expansion, heat recovery, and cooling, while a portion of the N<sub>2</sub> stream produced in the cold box is compressed, preheated and provided to the gas turbine to provide the thermal diluent for NO<sub>x</sub> control within the combustor of the gas turbine as well as provide extra motive fluid for expansion in the turbine.

The compressed air is treated to remove moisture, CO<sub>2</sub> and any hydrocarbons present. This air pretreatment system consists of two molecular sieve vessels. The vessels are operated in a staggered cycle: while one vessel is being used to filter the compressed air, the other is regenerated with the waste N<sub>2</sub> stream from the distillation columns. The waste N<sub>2</sub> is heated to the required regeneration temperature with medium pressure (MP) steam. The clean, dry air is liquefied utilizing a combination of chilling, feed/effluent heat exchange, compression and turbo-expansion. The expander may be compressor loaded or generator loaded. A multi-column system separates the liquefied air into a high purity N<sub>2</sub> stream and a high purity O<sub>2</sub> stream. This cold box is modeled as a separator such that the inlet and outlet stream conditions are consistent with data provided by an air separation unit vendor in the past. Current designs for the cold box consist of pumped liquid O<sub>2</sub> systems to avoid buildup of hydrocarbons within the cold box which could lead to a hazardous situation. The overall performance of the ASU consisting of a pumped liquid O<sub>2</sub> system, however, is similar to that of the system modeled in Aspen for this study.

The O<sub>2</sub> stream required by the gasifier and the N<sub>2</sub> stream provided to the gas turbine are compressed in multistage intercooled compressors. The N<sub>2</sub> serves the purpose of a thermal diluent in the gas turbine combustor for NO<sub>x</sub> control and it also increases the motive fluid for expansion. It is preheated to a temperature of 288°C against HP and high temperature boiler feed water (BFW) extracted from the HRSG located in the power block before it is injected into the gas turbine combustor. The resulting cooler HP BFW is pumped back to the power block.

Since the air extracted from the gas turbine is at a significantly higher pressure than the typical supply pressure of an EP ASU cryogenic unit, the air pressure is let down through a power recovery turbo-expander. As the operating pressure of the cold box is increased, the relative volatility between O<sub>2</sub> and N<sub>2</sub> approaches unity increasing the number of distillation stages in the cold box. If the extraction air is to be utilized in the EP ASU without first letting down its pressure, an additional distillation column may have to be added in the cryogenic cold box unit.

The trade-off between extraction air expansion while using a more conventional (proven) EP ASU cold box design (IP ASU Case) versus not letting the extraction air pressure down (thus eliminating the turbo-expander) and utilizing a cold box with an additional column should be established in a more detailed study with the involvement of the ASU vendor. The overall IGCC plant performance developed as a sensitivity case utilizing an estimated performance of the ASU operating at the higher pressure (“HP ASU Case”), i.e., without the extraction air expander, showed that the gain would be quite small (results presented in Table A1.3-1).

A second sensitivity case was developed consisting of cooling the extracted air after steam generation against cooling water to 27°C or 80°F and then expanding the air in the turbo-expander. The chilled air leaving the expander provided part of the refrigeration duty required for chilling the Selexol solvent in the AGR unit. The refrigeration duty available downstream of the expander was about 4 GJ/hr and saved about 0.25 MW of electric power in the mechanical refrigeration unit in the AGR unit while the reduction in the expander power due to the lower inlet temperature was about 0.61 MW. The net IGCC power output was thus actually decreased by about 0.36 MW over the Baseline Case.

### **Coal Receiving and Handling Unit**

Coal is received at the plant site by unit train. The coal is unloaded from bottom dump cars into an unloading hopper. Vibrating feeders withdraw the coal from these hoppers and place it on receiving conveyors. A belt scale measures the actual conveyor transport rate. After passing through a magnetic separator, the coal is transported to storage pile. Coal is reclaimed from the coal pile and supplied to day bins which supply coal on a continuous basis to the rod mills for the grinding operation. Coal dust recovered by dust collection systems in the coal storage areas is also sent to the grinding mills.

### **Gasification Unit**

The unit consists of the following sub-systems:

- Coal Grinding and Slurry Preparation
- Quench Gasifier and Slag Handling
- Syngas Scrubber
- Vacuum Flash System
- Soot Filtration
- Condensate Stripping
- Wastewater Pretreatment (WWPT)
- Miscellaneous Supporting Facilities

Figure A1.3 - 3 depicts the main features of this unit along with the coal grinding / slurry preparation. Slurrying water and additives are added to the grinding mill with a feed ratio controller to control the viscosity and produce the desired slurry concentration. This unit is modeled as a mixer to combine the coal with the water and a heater to model the heat added by the milling process. The coal slurry is pumped from a slurry holding tank to the gasifiers where

it reacts with the 95% purity O<sub>2</sub>. In this arrangement, the reaction chamber effluent is cooled by direct contact with water. The heat carried away by the raw syngas from the gasifier is ultimately recovered as medium pressure (MP) and low pressure (LP) steam downstream in the gas cooling unit.

A quench gasifier consists of a reaction chamber located above a quench chamber. The gasifier is a refractory-lined vessel capable of withstanding high temperature and pressure. The coal slurry and O<sub>2</sub> are fed via a feed injector mounted on top of the gasifier. The injector is cooled by circulating water in a closed-loop injector cooling water system. The coal and O<sub>2</sub> react in the reaction chamber and under conditions of partial oxidation to produce a syngas, which consists primarily of H<sub>2</sub> and CO with lesser amounts of H<sub>2</sub>O vapor, CO<sub>2</sub>, H<sub>2</sub>S, CH<sub>4</sub>, and N<sub>2</sub>. Traces of COS, HCl and NH<sub>3</sub> are also formed. A portion of the ash, which was present in the coal, and a portion of the unconverted carbon in the gasifier form a liquid melt called slag.

The hot syngas and slag flow downward from the reaction chamber into the quench chamber via a dip tube. The syngas and the slag are cooled by quench water at the bottom of the dip tube. The slag solidifies and is fractured by contact with the water.

The syngas exiting the quench chamber along with particulates which are predominantly carbon, is fed to the syngas scrubber. Syngas exits the top of the syngas scrubber and flows to the CO Shift unit and gas cooling unit. The scrubber removes the particulates and the HCl.

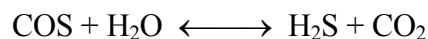
### **CO Shift / Low Temperature Gas Cooling Unit**

The purpose of this unit is to convert most of the CO in the syngas to H<sub>2</sub> by means of the water gas shift reaction:



This conversion step is crucial to the overall carbon capture of the IGCC plant.

The small amount of COS in the raw syngas is also converted into H<sub>2</sub>S via the following hydrolysis reaction:



Ammonia in the feed passes through the shift reactor unchanged and will not affect the catalyst performance. On the other hand, HCN will be hydrogenated to CH<sub>4</sub> and N<sub>2</sub>. The raw syngas from the Syngas Scrubber has sufficient water vapor to support the water gas shift reaction. Therefore, additional steam injection at the shift reactor is not required.

The heat evolved by the highly exothermic shift reaction is used to generate high and intermediate pressure steam as well as preheat the reactor feed. The remaining sensible heat is further recovered by generating steam at lower pressures and by heating several process streams to cool the shifted syngas down to a level suitable for the Acid Gas Removal unit. Thus the

proper design of this section is one of the key factors in determining the overall energy efficiency of the Near Zero Emission plant.

As depicted in Figure A1.3 - 4, scrubbed syngas from gasification is preheated in a feed/effluent exchanger before entering the first shift reactor (the reactor inlet temperature is maintained at start-of-run and at end-of-run by manipulating the scrubbed syngas bypass around the feed/effluent exchanger). The temperatures are set to limit the temperature rise of the syngas as it flows through the first shift reactor. An electric heater is utilized for startup.

The hot shifted syngas exiting this reactor is cooled first in two separate exchangers while producing HP steam (2575 psia) and IP steam (445 psia) and then in the feed/effluent exchanger. The syngas then enters the second shift reactor for additional conversion of the CO. The effluent from the second reactor is then successively cooled by generating steam in the first series of exchangers: the intermediate pressure (IP) steam generator (445 psia), the MP steam generator (120 psia) and then the shifted gas is used to heat up the circulating water streams from the fuel gas humidifier. The outlet temperature of the MP steam generator is set to support the clean syngas humidification processes. The water condensed out from the shifted gas is removed and collected in a process condensate return drum for recycle to the scrubber.

Next as depicted in Figure A1.3 - 5, the shifted gas is further cooled by heating the cold vacuum condensate from the surface condenser of the steam turbine. The shifted gas temperature then flows through a mercury removal bed where 95% of the mercury is captured. Arsenic, Cadmium and Selenium are also expected to be captured by this bed. The bed consists of sulfided activated carbon. The shifted gas is preheated upstream of the carbon bed using MP steam to avoid condensation within the bed.

The shifted gas exiting the mercury removal bed is finally cooled by cooling water and routed to the Acid Gas Removal unit. Condensed water collected in this second series of exchangers is sent to the NH<sub>3</sub> stripper and is then recycle to the particulate scrubber after combining with demineralized deaerated makeup provided by the BFW pump located in the power block.

### **Acid Gas Removal Unit (Selexol®)**

The AGR unit is modeled as a separator such that the component recoveries, the inlet and outlet stream conditions and the utility requirements are consistent with data provided by UOP previously for a study conducted by UC Irvine for the DOE under Award No. DE-FC26-00NT40845. The unit is depicted in Figure A1.3 - 6 where the Untreated Feed Gas enters the unit battery limits and is combined with a stream of concentrated CO<sub>2</sub> which has been stripped from the solvent in the solvent regeneration section as well as hydrogenated, compressed tail gas recycled from the Claus Sulfur Recovery / Tail Gas Recycle unit. This combined stream is sent to the H<sub>2</sub>S Absorber, where it contacts cold, loaded solvent. In the H<sub>2</sub>S absorber, H<sub>2</sub>S, COS, some CO<sub>2</sub> and low levels of other gases such as H<sub>2</sub>, are transferred from the gas phase to the liquid phase. The treated gas exits the H<sub>2</sub>S absorber and is then sent to the CO<sub>2</sub> absorber. The flow of the solvent exiting the H<sub>2</sub>S absorber is described below.

In the CO<sub>2</sub> absorber, the gas contacts chilled, flash-regenerated solvent. Co-absorbed H<sub>2</sub> recovered in the flash process is recompressed, cooled and recycled to the CO<sub>2</sub> absorber. In the CO<sub>2</sub> absorber, CO<sub>2</sub> and low levels of other gases are transferred from the gas phase to the liquid phase. The Treated Syngas exits the CO<sub>2</sub> absorber. The Treated Syngas is sent out of the Selexol unit battery limits to the Humidification unit. The flow of the solvent exiting the CO<sub>2</sub> absorber is described below.

The solvent exiting the H<sub>2</sub>S absorber is termed rich solvent, as it contains a significant amount of H<sub>2</sub>S, some CO<sub>2</sub> and other gases. The rich solvent exits the H<sub>2</sub>S absorber and is pumped through a heat exchanger where its temperature is increased by heat exchange with the lean solvent from the stripper. A portion of the CO<sub>2</sub>, CO, H<sub>2</sub> and other gases are selectively stripped from the rich solvent. This stream is mixed with the feed gas, as described above.

The rich solvent is sent to the stripper where the solvent is regenerated and the acid gases are transferred to the gas phase. The acid gases from the stripper are cooled and the condensate is removed. The acid gases are sent out of the Selexol unit battery limits to the Claus Sulfur Recovery Unit. The lean solvent exiting the bottom of the stripper is used to heat rich solvent as described above. The temperature of the lean solvent is further reduced and the lean solvent is then sent to the top of the CO<sub>2</sub> absorber.

The solvent exiting the CO<sub>2</sub> absorber is termed loaded solvent and contains some H<sub>2</sub> and other product gases, but only trace amounts of H<sub>2</sub>S. The loaded solvent is flashed and H<sub>2</sub> and other gases are transferred to the gas phase. These gases are separated from any condensate, compressed and are sent back to the CO<sub>2</sub> absorber. The solvent is further regenerated by decreasing its pressure in a series of flash drums. These flash drums are termed the HP, IP and LP Flash Drums. In these drums, large amounts of the absorbed gases, primarily CO<sub>2</sub>, are transferred from the liquid phase to the gas phase. The evolved gas exits its respective drum and exits the unit battery limits and are supplied to the CO<sub>2</sub> Compression/Dehydration unit.

The flash-regenerated solvent is chilled and sent back to the CO<sub>2</sub> Absorber. The pressure levels in the HP, IP, and LP Flash Drums are set to match the expected inlet pressures of various stages of a multi-stage compressor.

### **Syngas Humidification Unit**

One of the primary purposes of this humidification unit is to dilute the syngas to the gas turbines with moisture to meet the specification of no more than 65 mole% of H<sub>2</sub> as stipulated by GE for their 7FB gas turbines. This same specification is assumed for the H class gas turbine. The moisture acts as a thermal diluent in the combustor of the gas turbine and thus reduces the NO<sub>x</sub> formation. In addition, it increases the motive fluid for expansion in the gas turbine and thus the humidification operation provides a means for efficient recovery of low temperature waste heat in the plant. As depicted in Figure A1.3 - 7, fuel gas from the Acid Gas Removal unit is humidified in a packed column where it is contacted with circulating water in a counter-current manner. The circulating water is heated by shifted syngas in the low temperature gas cooling section. The makeup water to the humidifier is provided by IP BFW that is extracted from the

deaerator in the power block. The required amount of moisture can be controlled by resetting the recirculating water flow controller, based on the measurements of the H<sub>2</sub> content, flow rate, temperature and pressure of the feed gas, as well as the temperature and pressure of the humidified syngas. Blowdown from the humidifier to avoid solids buildup within the column is equivalent to 0.5% of the water evaporated in the column. The blowdown is routed to the primary wastewater treating unit. The humidified fuel gas is heated to a temperature of 288°C using high temperature HP BFW extracted from the HRSG. The resulting cooler HP BFW is pumped back to the power block.

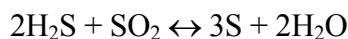
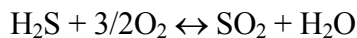
### **CO<sub>2</sub> Compression / Dehydration Unit**

As depicted in Figure A1.3 - 8, this unit receives CO<sub>2</sub> product streams from the Acid Gas Removal unit and raises its pressure. The CO<sub>2</sub> compression system is designed to raise the pressure of the CO<sub>2</sub> to a level just above the critical pressure. The CO<sub>2</sub> is then pumped as a supercritical fluid to the pipeline pressure before it leaves the plant battery limits. Inter-stage cooling is effected with cooling water. The unit also includes a dehydration unit (utilizing glycerol as the drying agent) to remove water vapor to meet the design dew point criteria. Any condensate collected in the compression process is routed to the solvent flash drum in the Acid Gas Removal unit.

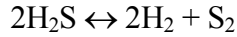
### **Sulfur Recovery / Tail Gas Treating Unit**

This combined unit is depicted in Figures A1.3 - 9, 10 and 11. The purpose of the unit is to convert sulfur compounds in the acid and sour gas streams to elemental sulfur using the Claus process. Ammonia present in the sour gas streams is converted into N<sub>2</sub> and H<sub>2</sub>O by oxidation. Any entrained liquid in the acid gas from the AGR unit is separated and sent to the WWPT NH<sub>3</sub> stripper feed drum.

The condensate stripper off gas is fed to a Knockout (KO) drum for removal of any entrained liquid. Liquid is evacuated from the drum and is also sent to the WWPT NH<sub>3</sub> stripper feed drum. A portion of the gas from the acid gas drum is combined with the overhead from the Sour Water Stripper (SWS) drum and fed to the main burner. Fuel gas and LP steam (both normally not required) are also provided to the burner to assist in the combustion of NH<sub>3</sub>. The sour gas streams are partially oxidized with O<sub>2</sub> from the Air Separation Unit according to the Claus reaction scheme as shown below:

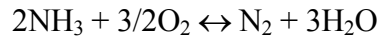


Hydrogen sulfide also dissociates at high temperatures, forming H<sub>2</sub> and elemental sulfur as shown below:



The bulk of the O<sub>2</sub> to the burner is controlled as a “main” stream of O<sub>2</sub> with a smaller, parallel O<sub>2</sub> stream for “trim control” and inputs to the combustion controllers include flow rates of the acid gases and H<sub>2</sub>S/SO<sub>2</sub> concentration in the tail gas.

The temperature of the burner is maintained at level required for complete thermal decomposition of the NH<sub>3</sub> into N<sub>2</sub> and H<sub>2</sub>O vapor as shown below:



The undesirable NO formation may result if an excess of O<sub>2</sub> is present; therefore, precise monitoring and control of the O<sub>2</sub> stream is necessary.

The stoichiometry of the Claus reaction scheme dictates that only one-third of the H<sub>2</sub>S should be combusted with O<sub>2</sub> to generate the required SO<sub>2</sub> for the Claus reaction. Any excess O<sub>2</sub> will lead to a stoichiometric imbalance of H<sub>2</sub>S and SO<sub>2</sub>, resulting in lower sulfur recovery.

The effluent from the main burner is combined with the remaining portion of the acid gas feed in the reaction furnace. The gas is then cooled by producing HP and IP Steam in the waste heat boiler. Elemental sulfur in the cooled gas is condensed by producing LP steam. The temperature of the cooled gas (which determines the level of steam produced) is set so that almost all the elemental sulfur is condensed; however, it is set high enough to avoid water condensation and sulfur viscosity issues. The condensed sulfur is separated from the gas in a coalescer section that is integral in the exchanger and is drained by gravity to the sulfur pit.

Because thermodynamic equilibrium limits the extent of conversion that can be achieved in the reaction furnace, two additional catalytic beds in series are supplied to recover the required overall sulfur. To allow for the sulfur conversion to proceed further in each subsequent bed, the elemental sulfur produced is condensed and removed from the gas stream.

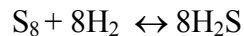
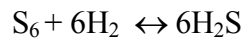
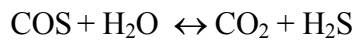
The effluent gas from the No. 1 Condenser is heated in the No. 1 Reheater with HP steam to avoid condensation of sulfur as the conversion reaction proceeds in the catalyst. The outlet temperature of the gas from the reheater is controlled by varying the HP steam rate. The heated acid gas is routed to the No. 1 Converter where residual H<sub>2</sub>S and SO<sub>2</sub> react over catalyst to form elemental sulfur and water in the vapor phase. As the Claus reaction is exothermic, a temperature rise develops across the catalyst bed. As in the previous stage, the elemental sulfur in the gas is condensed in the No. 2 Condenser by producing LP steam. The sulfur condensed in the exchanger is drained by gravity to the sulfur pit.

The last stage of conversion again heats the acid gas in the No. 2 Reheater with IP steam. The outlet temperature of the gas from the reheater is maintained by adjusting the IP steam rate. The heated acid gas is routed to the No. 2 Converter where residual H<sub>2</sub>S and SO<sub>2</sub> react over catalyst to form elemental sulfur and water in the vapor phase. The No. 1 and 2 converters are installed in one vessel with a partition separating the catalyst beds. The elemental sulfur in the gas is condensed in the No. 3 Condenser by cooling water. The sulfur condensed in the exchanger is drained by gravity to the sulfur pit.

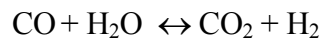
Air is swept across the sulfur pit and gases released from the molten sulfur in the sulfur pit are removed by the sulfur pit vent ejector using MP steam as a motive fluid and recycled to the reactor furnace. The molten sulfur is pumped to the Degassing and Granulation system.

The effluent gas from the last condenser, called tail gas, still contains small amounts of sulfur dioxide and elemental sulfur compounds and is routed to the Tail Gas Treating section of the unit where any unreacted sulfur dioxide, carbonyl sulfide (COS) and elemental sulfur vapor in the tail gas is converted to H<sub>2</sub>S by hydrogenation.

The tail gas is heated in the Reactor Feed Heater with HP steam. The inlet temperature to the hydrogenation reactor is controlled by adjusting the HP steam rate. An analyzer on the tail gas measures the H<sub>2</sub> content of the stream and, if required, treated fuel gas from the Acid Gas Removal unit is added to the reactor feed. The heated tail gas is hydrogenated where sulfur compounds are reduced at elevated temperature via the following reactions:



In addition, the following shift reaction occurs:



The effluent from the reactor is cooled by producing LP steam. The partially cooled gas is then further cooled in a contact condenser. The gas enters the condenser below the bottom trays and is contacted with caustic so that any sulfur dioxide remaining in the gas is captured. The column bottoms is recycled in a circulating loop and spent caustic is periodically removed from the loop and routed to the effluent bio-treatment unit.

The scrubbed gas then flows up the condenser for direct quenching with water. The water is removed from the chimney tray in the middle of the condenser and cooled in a water cooled heat exchanger. If required, sour water is removed from the system to maintain the water balance (flow rate is varied to control the liquid level on the chimney tray). A portion of the water from the cooling loop may also be diverted to the lower section of the condenser to maintain the liquid level in the bottom of the column. The contact condenser overhead gas is sent to the recycle compressor suction drum to remove entrained liquid. The compressed tail gas is recycled back to the Acid Gas Removal unit.

## **Power Block**

The process scheme for the combined-cycle power block consists of a gas turbine supporting a reheat steam turbine. The interface between the HRSG and the steam turbine also includes a reheat steam loop. This configuration has been demonstrated in the power industry to be an economical modular design. The process flow diagram for this unit is depicted in Figure A1.3-12. The overall integration of the steam system between the Power Block and the balance of the IGCC plant is shown on the Steam Balance Diagram, Figure A1.3-13.

The power block consists of the following major systems:

- Gas Turbine
- Heat Recovery Steam Generator (HRSG)
- Steam Turbine and the associated Vacuum Condensate System
- Integral Deaerator
- Blowdown System
- Miscellaneous Supporting Facilities:
  - boiler chemical injection
  - demineralized water package.

The gas turbine selected for this study is a steam cooled H class machine. The performance of the gas turbine on the decarbonized syngas was developed utilizing Thermoflex. A model was set up in Thermoflex utilizing published performance by General Electric (GE) for their 7H gas turbine on natural gas and then this model was “operated” in off-design mode to obtain an estimate of its performance on syngas while limiting the blade surface temperatures at the same value as that for the natural gas case. This resulted in a decrease in the firing temperature of the gas turbine: from 1428°C (2602°F) on natural gas to 1392°C (2538°F) on the syngas. Air was extracted from the compressor discharge of this machine while operating on the syngas in order to limit the engine output to 317.7 MWe. This output was assumed to be the torque limit of the gas turbine and was established as follows:

1. It was assumed that the upper limit for the net power output of the natural gas fired 7H combined cycle occurs at the lowest ambient temperature of -18°C (0°F) shown in the ambient temperature sensitivity performance curve published by GE for this combined cycle plant [the combined cycle net power and heat rate are shown as functions of ambient temperature all the way down to -18°C (0°F)].
2. Next, the natural gas combined cycle performance calibrated for the ISO conditions was operated in off-design mode at the -18°C (0°F) ambient temperature in Thermoflex while matching the corresponding power output and heat rate shown in the above described curve. The air flow to the gas turbine was determined utilizing the compressor map

published by GE (for the public domain the actual values of the pressure ratio were left out).

3. The results of the Thermoflex simulation then provided the portion of power developed by the gas turbine alone (which was 317.7 MWe). The relative increase in power over its ISO output (increase in output expressed as a percentage of the ISO power) was found to be similar to that for the GE 7FA+e gas turbine going from natural gas to syngas operation. Note that the gas turbine in the IGCC application will be “flat rated” at this output of 317.7 MWe.

Figures A1.3 -14 and 15 show the gas turbine cycle diagram for the syngas case and the natural gas case. The cooling steam inlet and outlet volumetric flow rates (and thus the velocities) are essentially the same for the two cases.

Ambient air is drawn into the gas turbine air compressor via a filter to remove air-borne particulates, especially those that are larger than 10 microns. The humidified fuel gas and compressed air are mixed and combusted in the turbine. The preheated nitrogen is injected into the turbine through separate nozzles for NO<sub>x</sub> control. The combined LHV of the humid syngas and diluent nitrogen is 4,720 kJ/nm<sup>3</sup> or 120 Btu/scf. The Baseline Case does not have any additional NO<sub>x</sub> abatement control such as an SCR. As a reference GE guarantees 15 ppmvd (15% O<sub>2</sub> basis) on syngas with moisture and nitrogen dilution to the same level as in the baseline case for their “F” technology gas turbines. A sensitivity case has been developed to reduce the NO<sub>x</sub> to 2 ppmvd (15% O<sub>2</sub> basis) utilizing an SCR.

The hot gas turbine exhaust flows through a customized Heat Recovery Steam Generator (HRSG). The HRSG consists basically of the following sub-systems:

- LP steam
- IP steam
- HP steam
- Reheat steam

In addition to these sub-systems, the HRSG is integrated with the rest of the IGCC plant. The HRSG has its own stack, which is equipped with a continuous emissions monitoring system (CEMS).

### LP Steam System

Low temperature heat is recovered from the syngas generation / processing units (Process) by heating the vacuum cold condensate from the surface condenser + makeup BFW. The makeup BFW is sprayed directly into the surface condenser and the combined stream of the cold vacuum condensate + makeup is drawn from the Surface Condenser by the Vacuum Condensate Pump and is sent to the vacuum condensate heaters in the Low Temperature Gas Cooling Unit and Black Water Flash section of the Gasification Unit to recover the low temperature heat. The hot vacuum condensate is further heated in the LP Economizer in the HRSG.

The hot vacuum condensate is combined with LP Condensate returning from the Gasification Unit and is supplied as BFW to the LP Steam Drum in the HRSG. The saturated steam from the LP Steam Drum is mixed with the saturated LP steam produced in the Process units. The combined flow is sent through the LP Superheater coils in the HRSG and then is fed to the LP section of the Steam Turbine.

The LP Feed Water Booster Pump sends heated BFW from the LP steam drum to the Process users in the Syngas plant.

### BFW Pump

The main BFW pump of the HRSG supplies both IP and HP BFW to the IP and HP steam systems as well as makeup to the CO Shift/LTGC unit. It is a multistage centrifugal pump, with intermediate bleeds to support the IP steam system and supply the makeup. The discharge pressure of the BFW pump is dictated by the design conditions set at the inlet of the steam turbine.

### IP Steam System

The IP BFW is taken from a bleed off of the main BFW Feed pump. The makeup water for the syngas humidifier is taken from the IP bleed before the economizer. The remaining IP boiler feed water flows through the IP Economizer in the HRSG. A portion of the preheated IP BFW is routed to the IP Steam Generators in the CO Shift/LTGC unit and the Sulfur Recovery Unit and the rest is fed to the IP Steam drum. Saturated IP steam generated in the IP steam drum mixes with surplus IP steam from other process units and merges with the reheat steam system.

### HP Steam System

The discharge from the main BFW Feed pump is mixed with the HP boiler feed water returning from the Fuel Gas and Nitrogen heaters before it flows through two HP Economizers in the HRSG. The HP BFW Circulating pump sends part of the preheated HP boiler feed water exiting the first HP Economizer to the Fuel Gas and Nitrogen heaters.

A portion of the preheated HP BFW is routed to the HP Steam Generator in the CO Shift/LTGC unit and the HP Waste Heat Boiler in the Sulfur Recovery Unit and the remainder is fed to the HP Steam drum. Saturated HP steam generated in the HP steam drum mixes with surplus HP steam from other process units and then is superheated in HP Superheater coils within the HRSG. The superheated HP steam from the HRSG is sent to the inlet of the steam turbine.

A small portion of the main BFW Feed pump discharge is used as attemperator water for the control of the temperature of the superheated steam.

### Reheat Steam System

To improve the efficiency of the combined-cycle, the exit steam from the HP section of the steam turbine is returned to the HRSG to raise its temperature by absorbing additional heat. This reheated steam is combined with the IP steam from the HRSG, superheated to the same temperature as the HP steam, and then is fed to the inlet of the IP section of the steam turbine.

## Gas Turbine Cooling

The 1<sup>st</sup> and 2<sup>nd</sup> stages of the gas turbine stator and rotating blades are cooled with steam taken from the HP steam turbine exhaust. The steam returning from this closed circuit cooling of the gas turbine is mixed with the IP steam before it enters the reheater coils in the HRSG.

## Deaerator

An integrated LP steam drum/deaerator is provided in the HRSG. This eliminates the need for an external deaerator. The deaerator removes any dissolved gases such as O<sub>2</sub> and CO<sub>2</sub> in the feed water by using LP steam in the steam drum as the stripping medium. The pressure in the LP Steam Drum is controlled by varying the amount of steam vented with the dissolved gases.

## Blowdown System

The steam drums of the HRSG are continuously purged to control the amount of built-up of dissolved solids. The continuous blowdown is cascaded from the HP steam drum to the IP steam drum. The blowdown is then drawn from the IP steam drum and routed to the Continuous Blowdown drum. Flash steam in the Continuous Blowdown drum is sent to the LP steam drum and the saturated water is letdown into the Intermittent Blowdown drum. Whenever required, blowdown from each steam drum in the HRSG system can be routed directly to the Intermittent Blowdown drum. Flash steam from the Intermittent Blowdown drum is vented to atmosphere and the liquid collected in Blowdown Sump.

## Steam Turbine

The inlet pressure of the HP section of the steam turbine is set at 166.5 bara. The exhaust from the LP section is set at a vacuum of 0.044 bara. The surface condenser uses circulating cooling water from the cooling towers as the cooling medium while the makeup water for the steam system is added to the well of the condenser.

## Demineralized Water System

Demineralized water system consists of mixed-bed exchangers, one in operation and one in stand-by, filled with cation/anion resins, with internal-type regeneration. The package includes facilities for resin bed regeneration, chemical storage and neutralization basin.

## **General Facilities**

The following is a listing of the various necessary support and general facilities that are required for a stand-alone plant. Any utility requirements by these facilities are accounted for in developing the plant performances.

- Natural gas supply – for start-up
- Cooling water system – includes mechanical draft cooling towers and the cooling water supply pumps
- Potable water system
- General makeup water supply system

- Oily water separator - oily water from all process units is collected in the oily water sump, which separates the oil from the water by a corrugated plate interceptor (oil/water separator). Contaminated storm water is also sent to the oily water sump for treatment.
- Drains and blowdowns
- Fire protection and monitoring systems – consist of general firewater system and specialized system for chemical fire protection
- Plant and instrument air system
- Wastewater treatment system – process wastewater is collected for treatment and the treated water is discharged from the plant. A sanitary wastewater treating unit is included in this system
- Flare – the flare system consists of collection headers for the process unit relief gases and a system of knockout drums prior to safe disposal in an elevated flare. A separate flare system is provided for the Sulfur Recovery unit.
- Miscellaneous materials (e.g. slag, fine slag, sulfur) handling (unloading and loading facilities)
- In-plant electric power distribution
- Uninterruptible power supply
- Generator step-up transformers
- Distributed control system
- Continuous emissions monitoring
- Process analyzers
- Hazardous gas detection system
- Communications
- Laboratory for inspection, certification and process control
- Maintenance, warehouse and administration facility
- Other supporting facilities (e.g. interconnecting piping; rail spur for construction materials access; roads, paving, parking, fencing and lighting; heating, ventilation and air conditioning systems).

The overall plant water balance is presented in Figure A1.3-16.

**Table A1.3 - 1: Plant Performance Summary  
(ISO Ambient Conditions)**

	IP ASU & Air Extraction	HP ASU & Air Extraction
Fuel Feed Rate, ST/D (MF)	3,392	
MMBtu/hr (HHV)	3,744	
Fuel Feed Rate, Tonne/D (MF)	3,078	
GJ/hr (HHV)	3,949	
Power Generation, kW		
Gas Turbine	318,378	318,323
Steam Turbine	157,600	159,033
Clean Syngas Expander	2,320	2,320
Gas Turbine Extraction Air Expander	4,745	0
Auxiliary Power Consumption, kW	99,795	93,924
Net Plant Output, kW	383,247	385,753
Generation Efficiency (HHV)		
Net Heat Rate, Btu/kWh	9,769	9,706
Net Heat Rate, kJ/kWh	10,305	10,238
% Fuel to Power	34.94	35.16
Estimated NOx, ppmVd (15% O2 Basis)	15	
Raw Water Makeup, m3/kWh	0.0026	0.0026

**Table A1.3 - 2: Auxiliary (In-Plant) Power Consumption Summary**

	<b>IP ASU &amp; Air Extraction</b>	<b>HP ASU &amp; Air Extraction</b>
	kW	kW
Coal Handling	401	401
Coal Milling	802	802
Coal Slurry Pumps	274	274
Slag Handling and Dewatering	155	155
Miscellaneous Syngas Plant Equipment	380	380
Air Separation Unit Air Compressors	14,778	15,788
Air Separation Auxiliaries	1,290	1,290
Oxygen Compressor	12,522	11,122
Nitrogen Compressor	22,007	16,415
CO <sub>2</sub> Compressor	19,368	19,368
Tail Gas Recycle Compressor	998	998
Boiler Feedwater Pumps	4,047	4,054
Cooling Tower and Pumps	7,242	7,340
Steam Condensate Pump	42	44
Selexol Acid Gas Removal	11,788	11,788
Syngas Humidification	214	214
Claus Plant Auxilliaries	100	100
Gas Turbine Auxiliaries	517	517
Steam Turbine Auxiliaries	517	517
General Makeup and Demineralized Water	322	322
Miscellaneous Balance-of-Plant and Lighting	1,000	1,000
Transformer Losses	1,031	1,034
<b>Total Auxiliary Power Consumption</b>	<b>99,795</b>	<b>93,924</b>



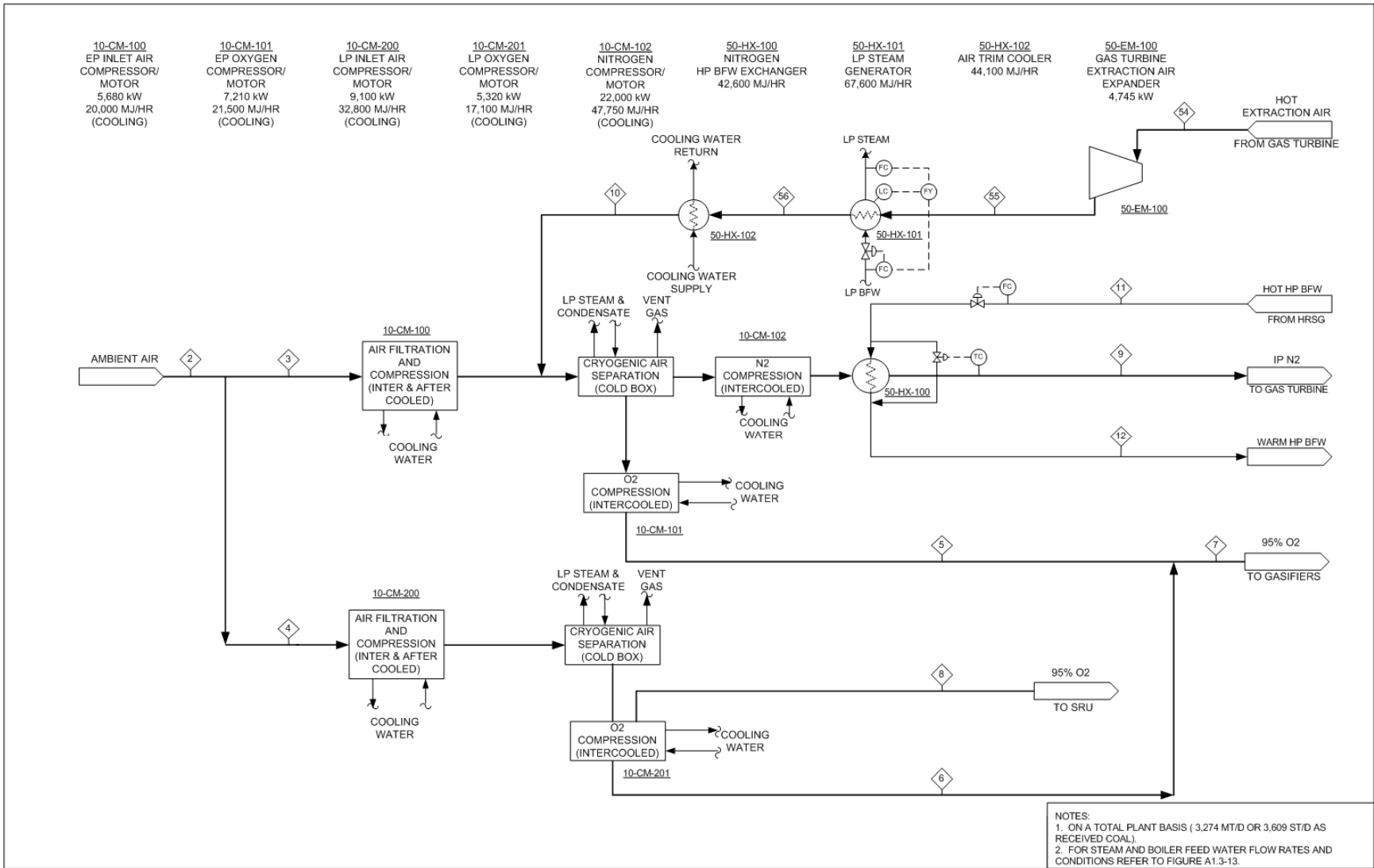


**Figure A1.3 - 2: Block Flow Diagram - Air Separation Unit, Gas Turbine Air Extraction and N<sub>2</sub> Preheat**



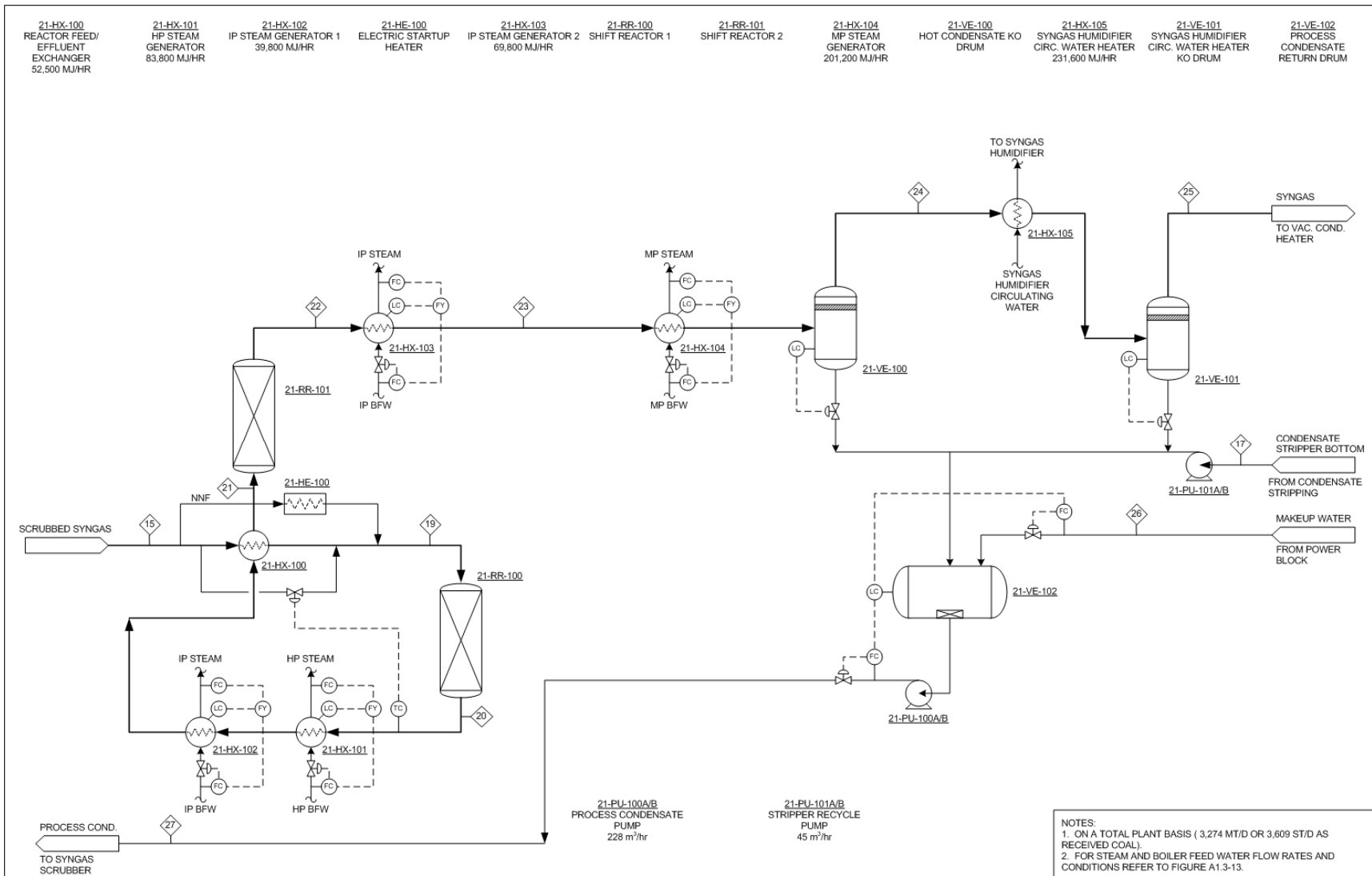


**Figure A1.3 - 4: Process Flow Diagram - CO Shift / Low Temperature Gas Cooling Unit**

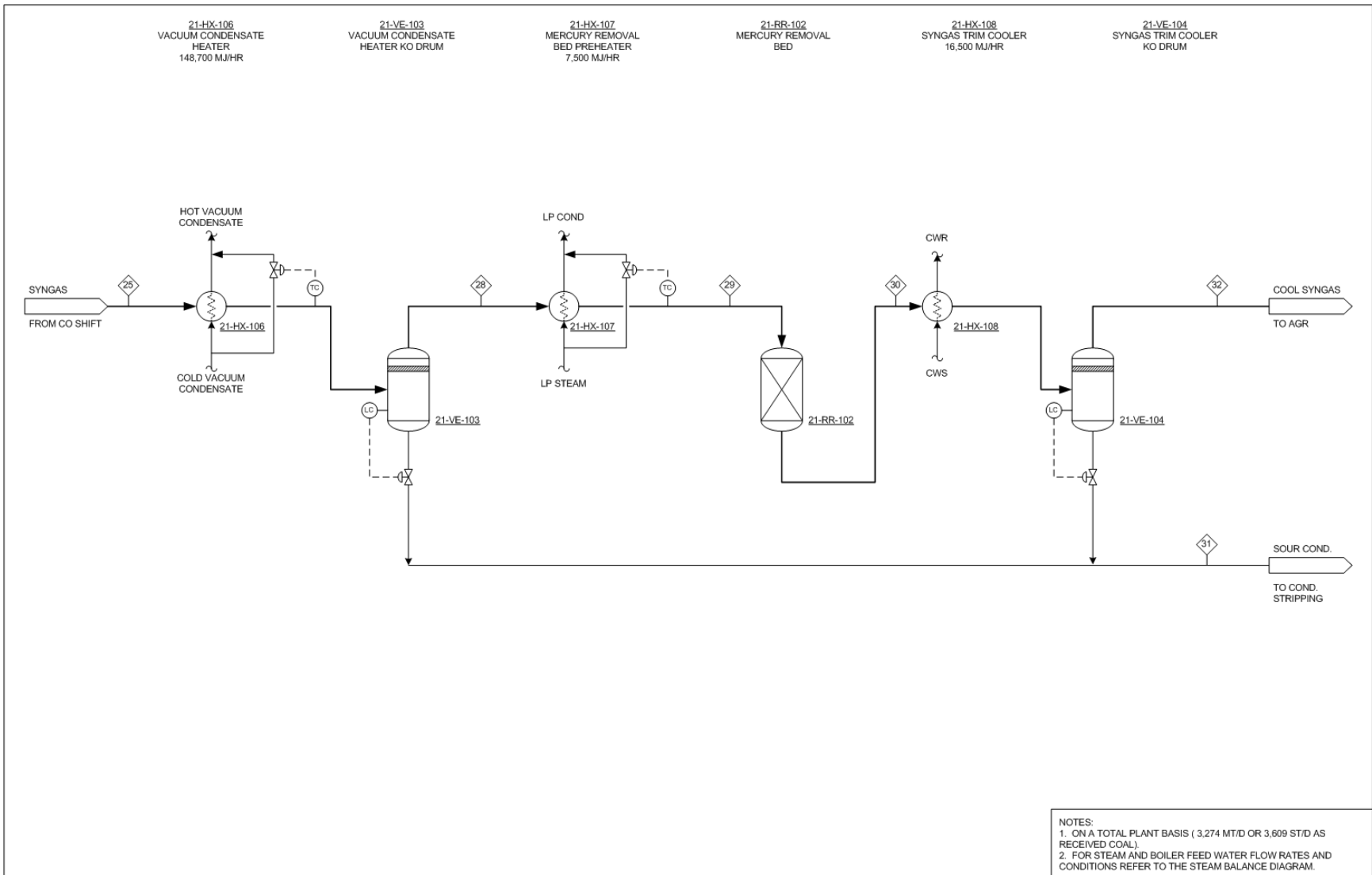


**Figure A1.3 -4: Process Flow Diagram - CO Shift / Low Temperature Gas Cooling Unit (Cont'd.)**

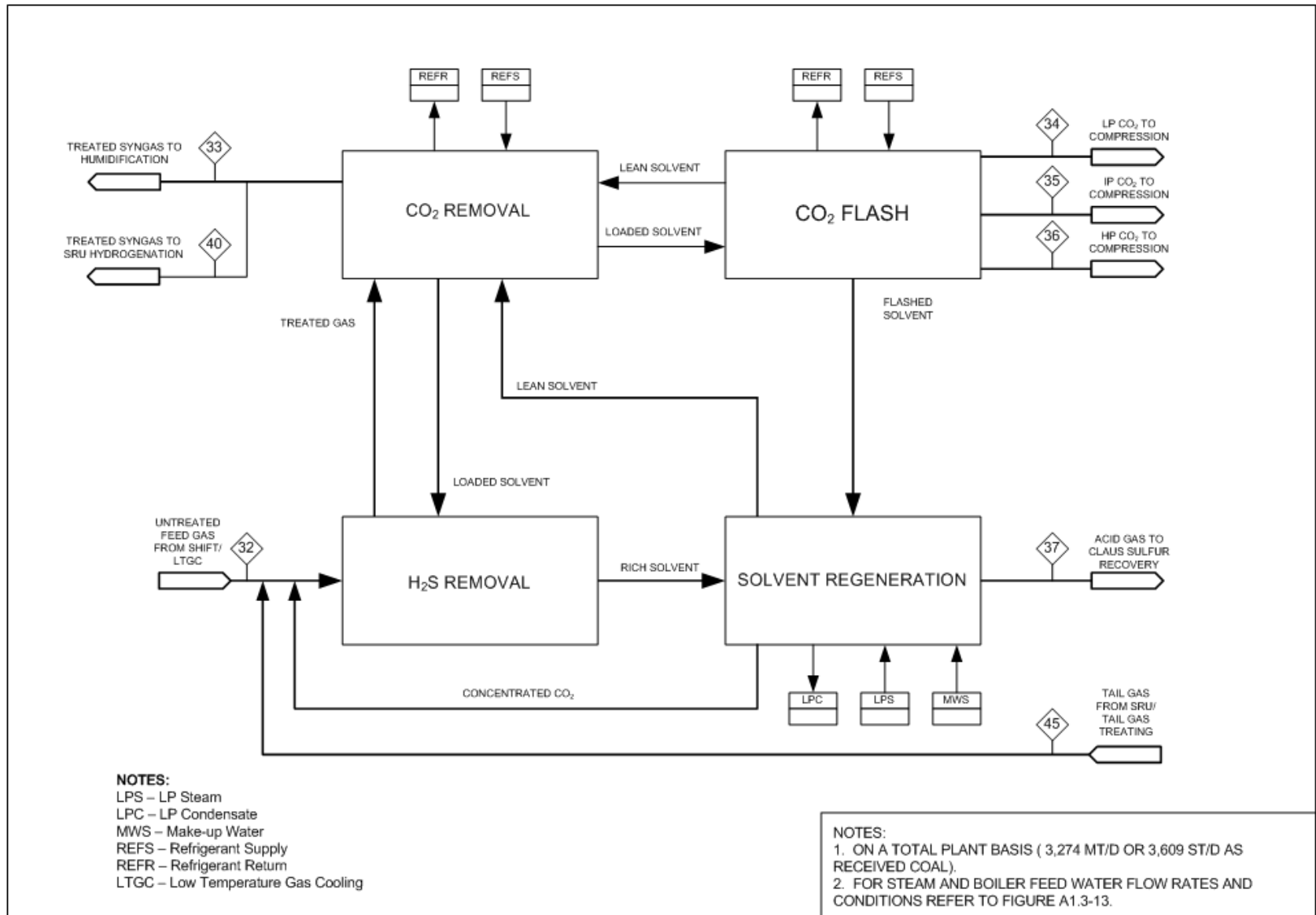


**Figure A1.3 - 5: Block Flow Diagram - Acid Gas Removal Unit (Selexol®)**

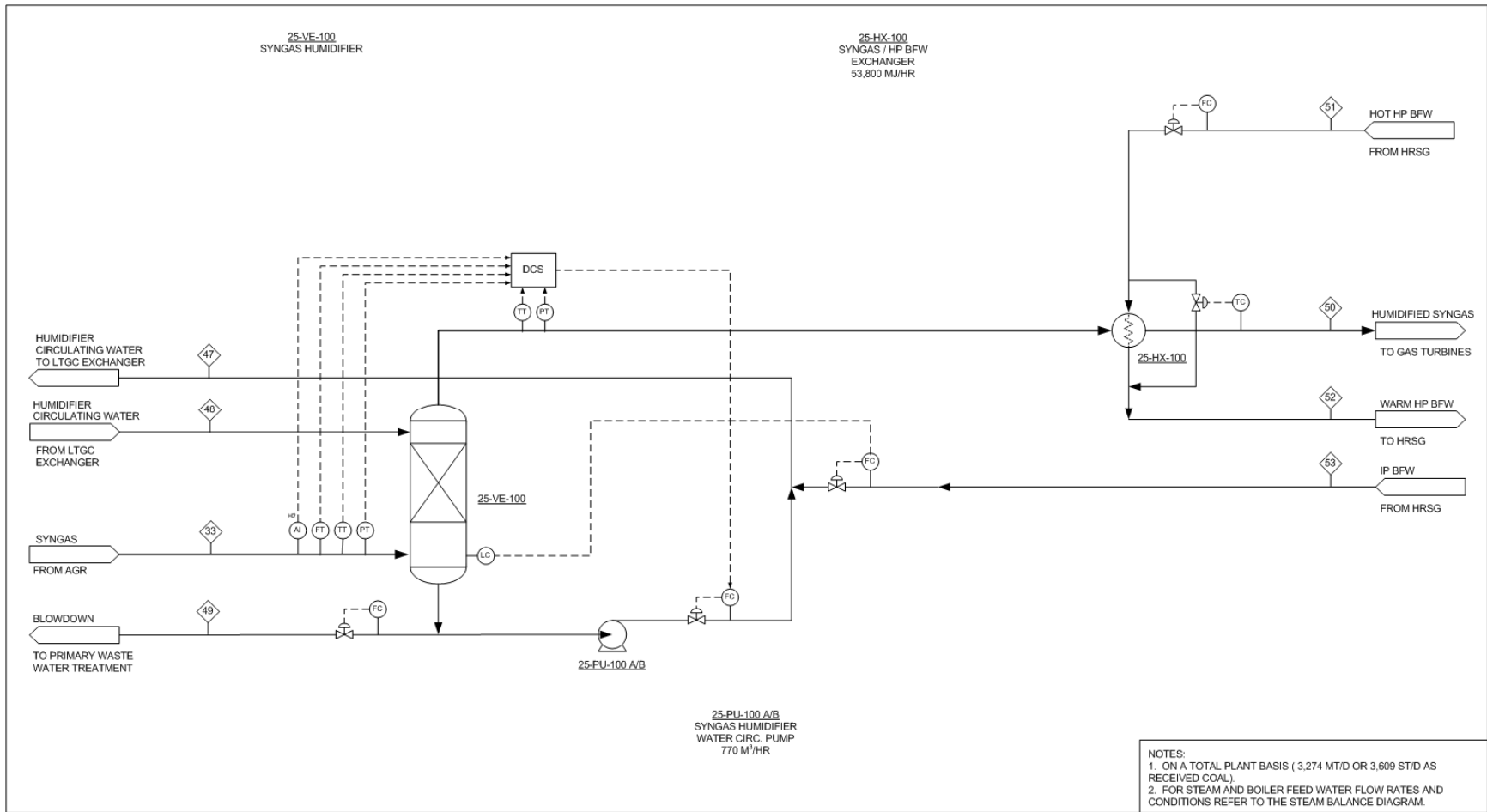


**Figure A1.3 - 6: Process Flow Diagram - Syngas Humidification Unit**

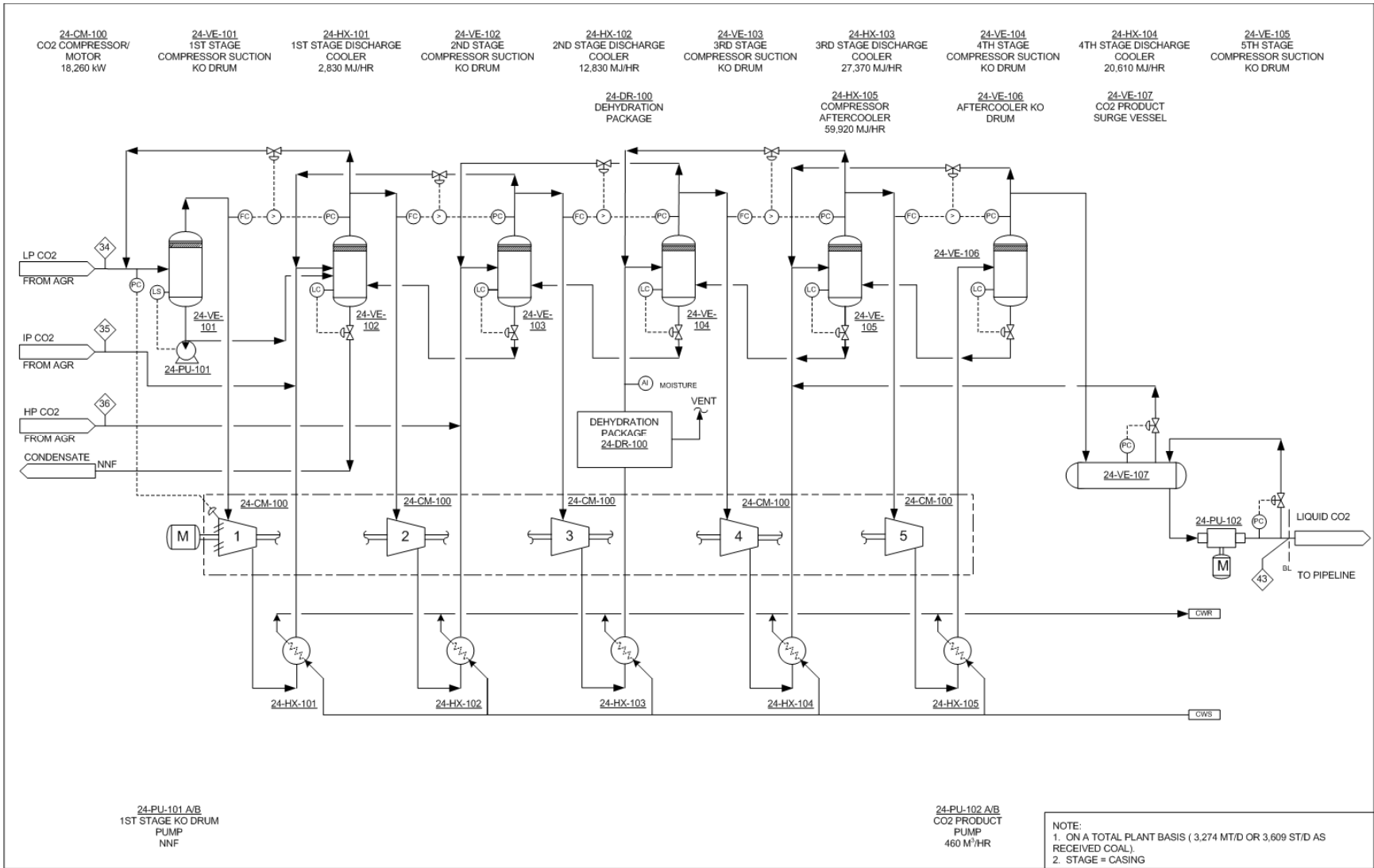


**Figure A1.3 - 7: Process Flow Diagram - CO<sub>2</sub> Compression / Dehydration Unit**

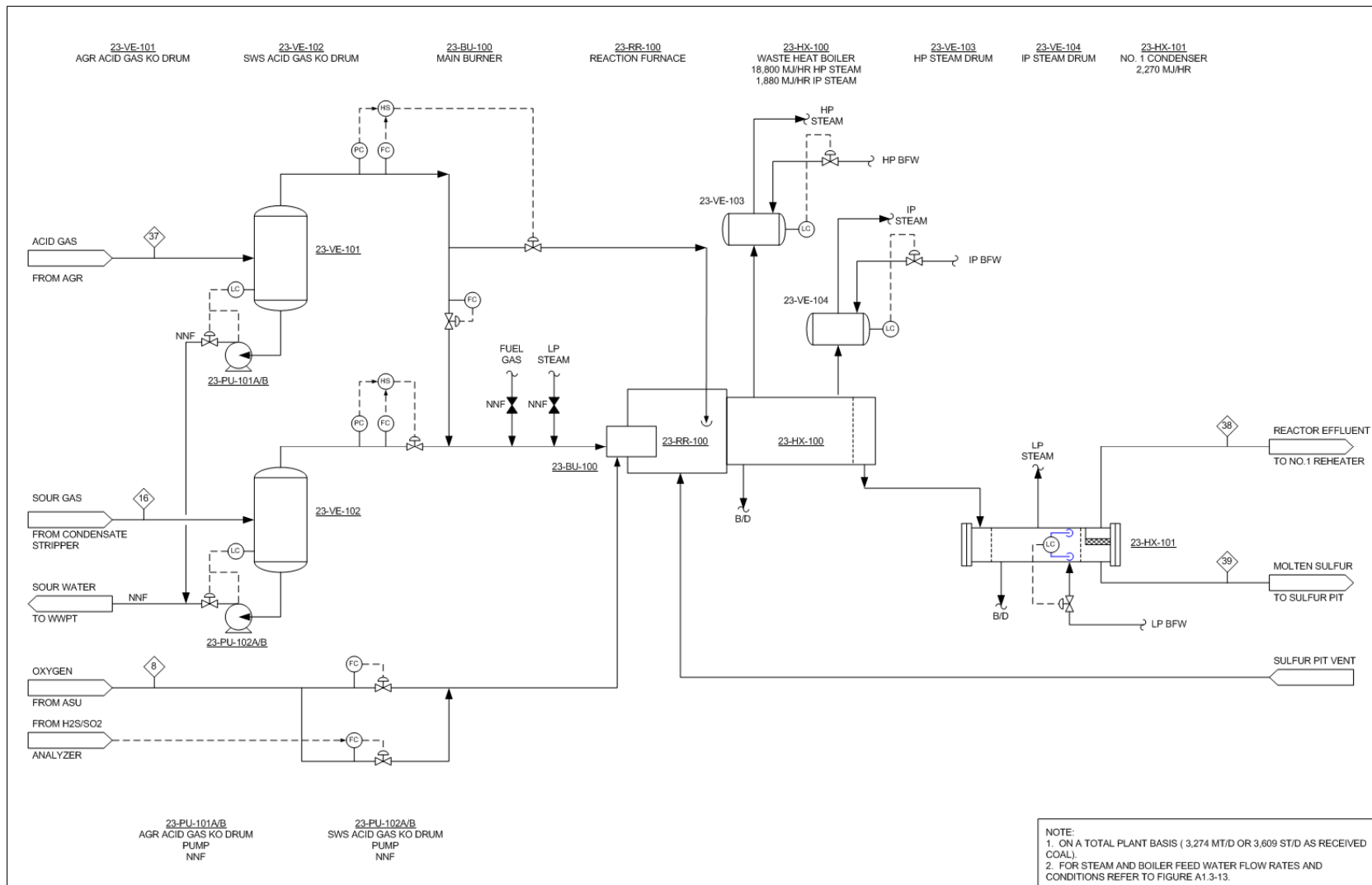


**Figure A1.3 - 8: Process Flow Diagram - Sulfur Recovery / Tail Gas Treating Unit**

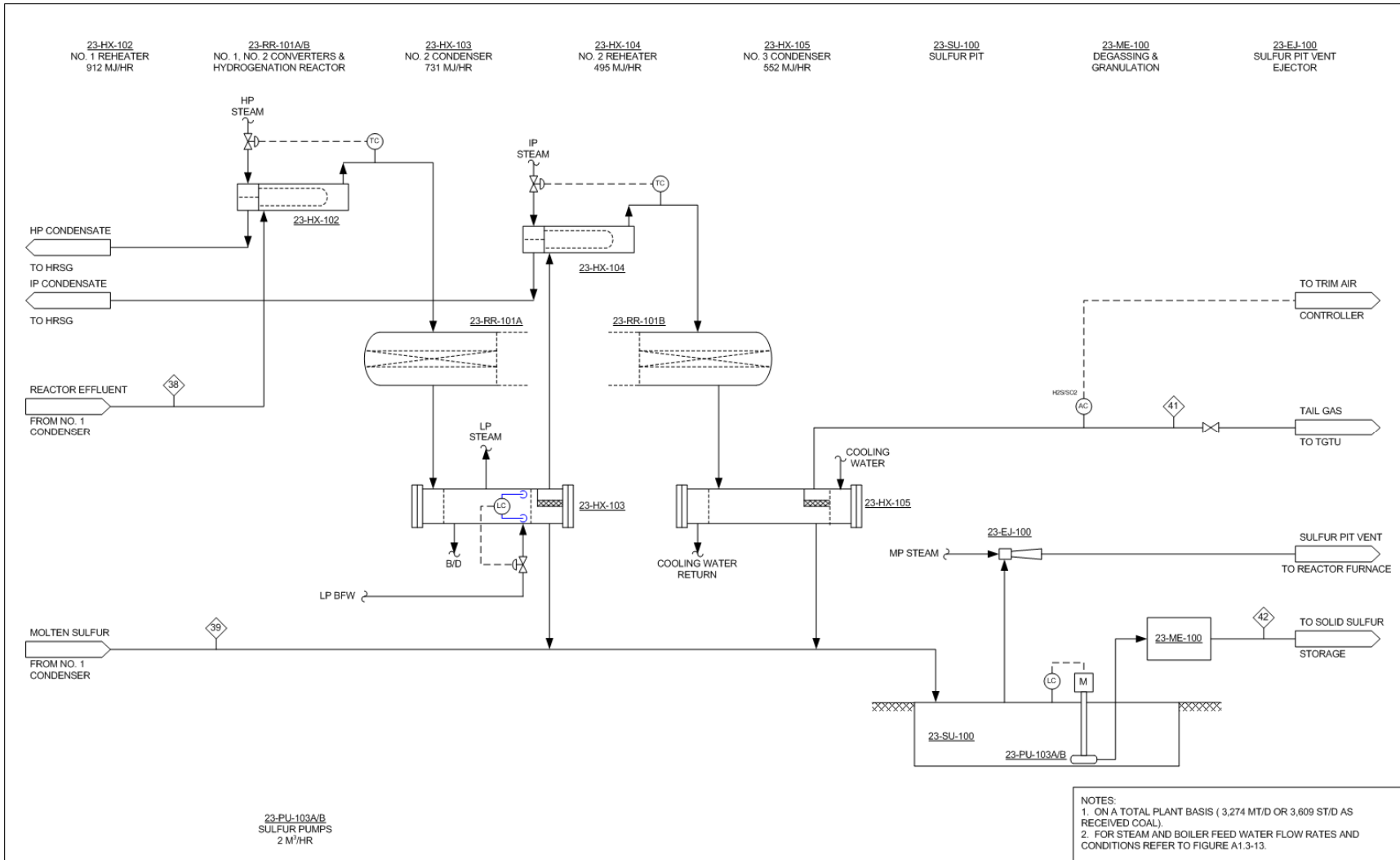


**Figure A1.3 -8: Process Flow Diagram - Sulfur Recovery / Tail Gas Treating Unit (Cont'd.)**

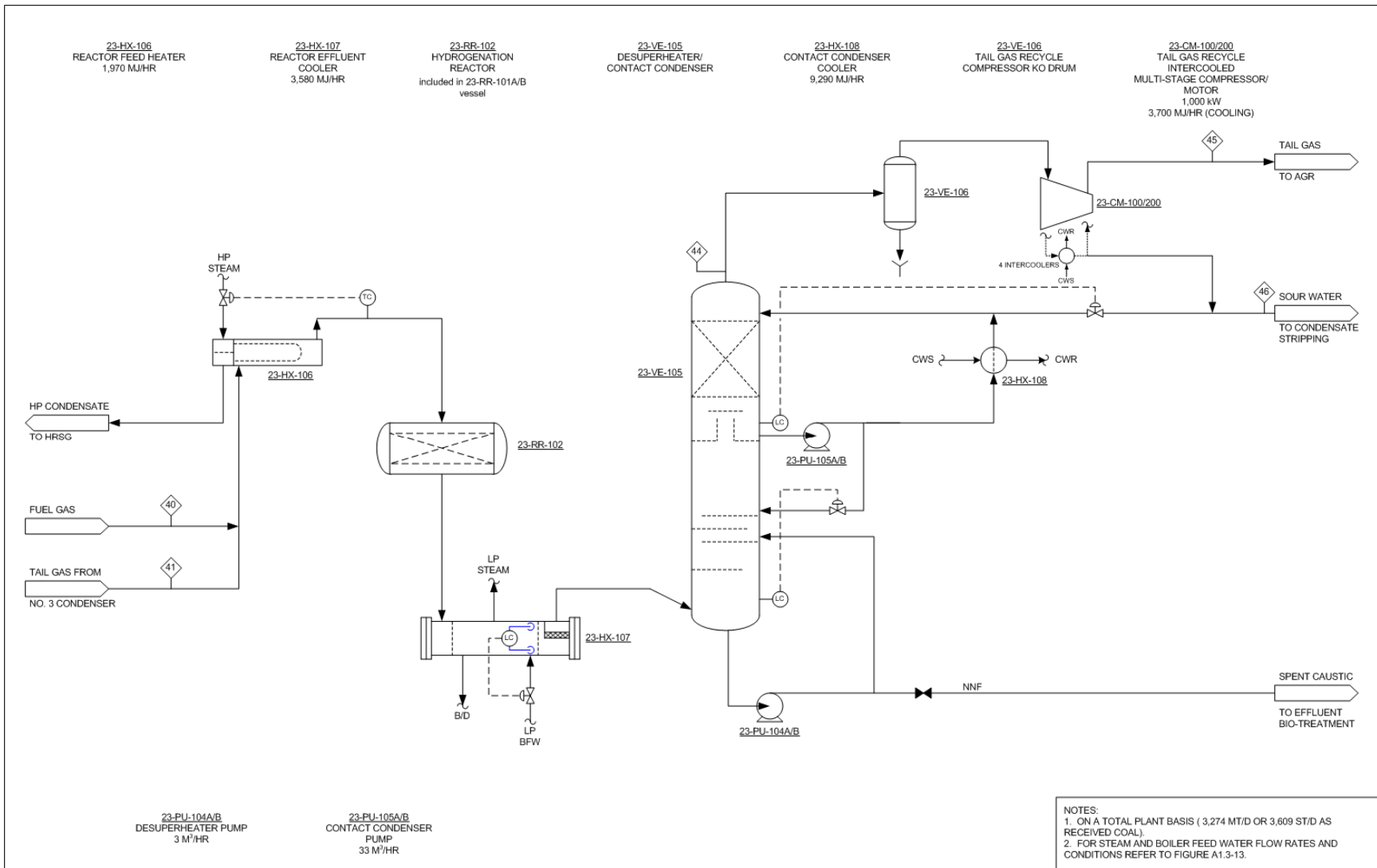


**Figure A1.3 -8: Process Flow Diagram - Sulfur Recovery / Tail Gas Treating Unit (Cont'd.)**

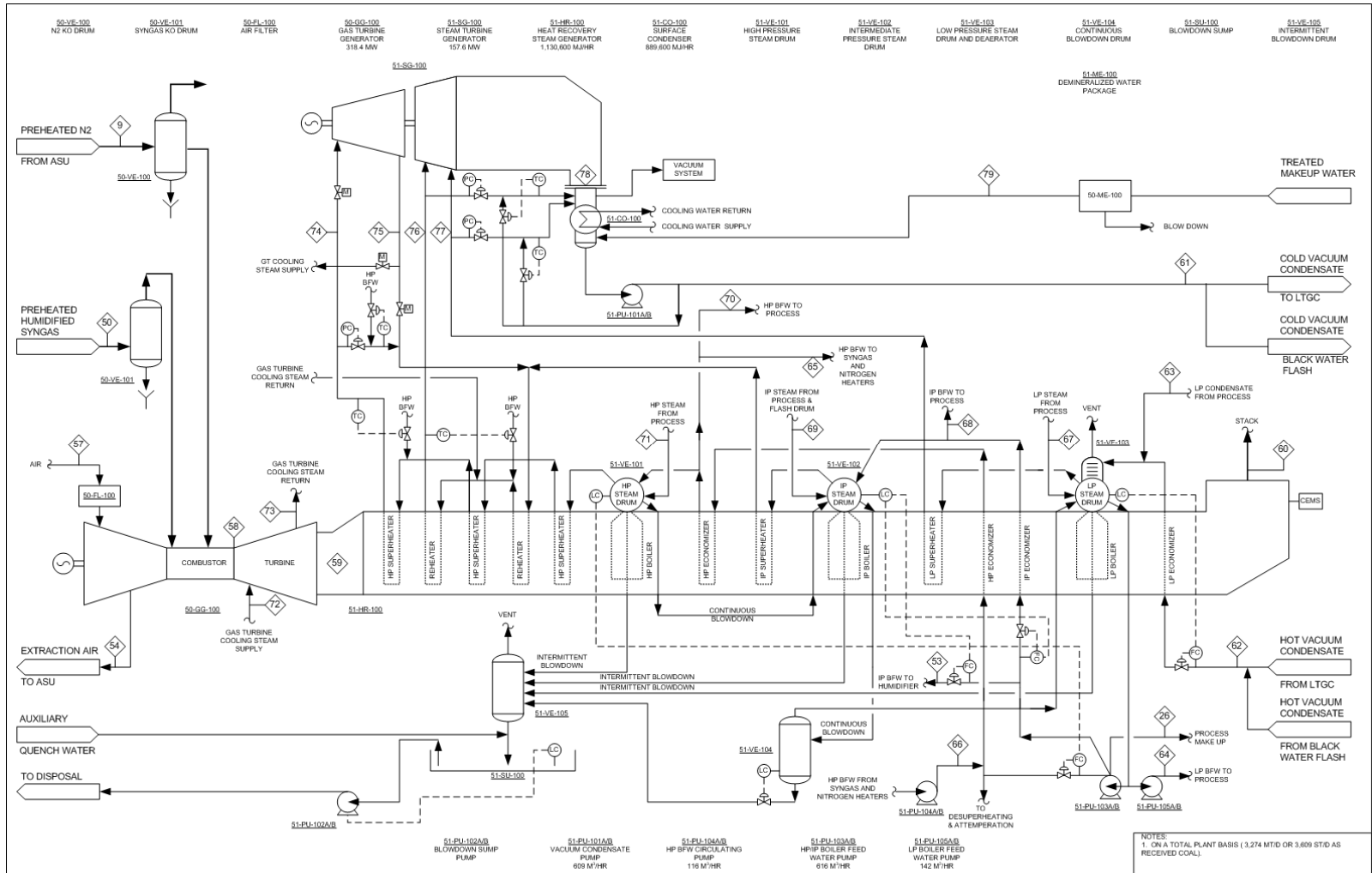


**Figure A1.3 - 9: Process Flow Diagram – Power Block**





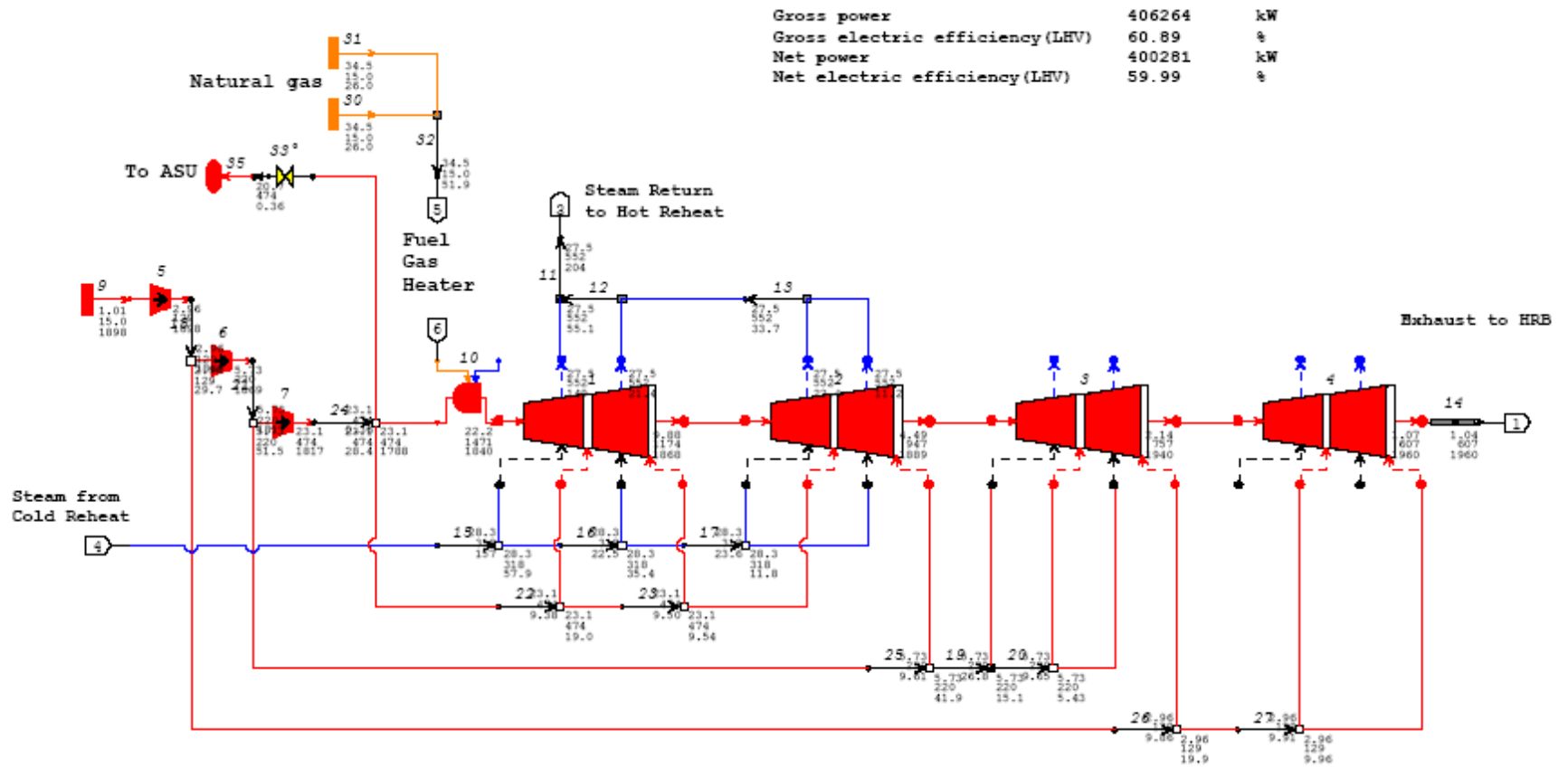
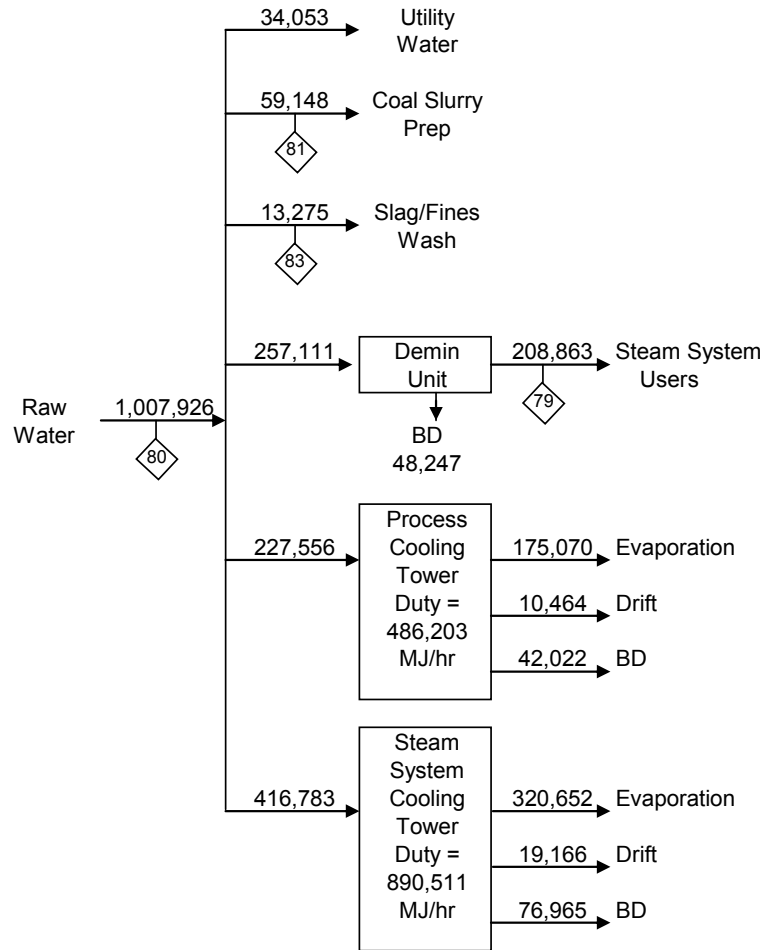


Figure A1.3 - 12: Gas Turbine Cycle Diagram - Natural Gas Case

# WATER BALANCE

Flows are in kg/hr.



**Figure A1.3 - 13: Overall IGCC Plant Water Balance**

**Table A1.3 - 3: Stream Data**

Basis: 3,274 Tonne/D (As Received) or 3,078 Tonne/D (Dry Basis) Pittsburgh No. 8 Coal

Mol Fraction	1	2	3	4	5	6	7	8	9	10	11	12
O2		0.2077	0.2077	0.2077	0.9504	0.9500	0.9502	0.9500	0.0062	0.2090		
N2		0.7722	0.7722	0.7722	0.0230	0.0176	0.0212	0.0176	0.9891	0.7788		
Ar		0.0094	0.0094	0.0094	0.0266	0.0324	0.0286	0.0324	0.0047	0.0093		
H2												
CO												
CO2		0.0003	0.0003	0.0003						0.0003		
H2O		0.0104	0.0104	0.0104						0.0026	1.0000	1.0000
CH4												
H2S												
SO2												
Cl2												
HCl												
NH3												
COS												
Total		1.0000	1.0000	1.0000	1.0000	1.0000	1.0000	1.0000	1.0000	1.0000	1.0000	1.0000
Coal (As Received), kg/hr	136,416											
kgmol/hr (w/o Solids)	-	8,734	2,311	6,423	2,426	1,291	3,717	82	8,780	9,009	2,260	2,260
kg/hr (w/o Solids)	-	252,016	66,689	185,327	77,921	41,563	119,484	2,635	246,663	260,681	40,717	40,717
Temp., C	15.0	15.0	15.0	15.0	91.5	80.6	87.7	19.4	287.8	26.7	349.1	140.6
Press., bar	1.01	1.01	1.01	1.01	82.94	82.94	82.94	3.04	35.09	15.34	180.96	177.47
Enthalpy, MJ/hr	-123,514	-25,616	-6,778	-18,838	3,567	1,435	5,003	-16	67,738	-7,311	67,203	24,584
See Note	1, 2	2	2	2	2	2	2	2	2	2	3	3

Note:

1. Enthalpy expressed as HHV = 3,949,275 MJ/hr.
2. The reference state for thermodynamic properties is the standard enthalpy of formation of ideal gas at 25°C and 1 atm.
3. Enthalpy corresponds to ASME Steam Tables Basis.

**Table A1.3 - 3: Stream Data – continued**

Basis: 3,274 Tonne/D (As Received) or 3,078 Tonne/D (Dry Basis) Pittsburgh No. 8 Coal

Mol Fraction	13	14	15	16	17	18	19	20	21	22	23	24
O2												
N2	0.0000		0.0042	0.0012			0.0042	0.0042	0.0042	0.0042	0.0042	0.0049
Ar	0.0000		0.0036	0.0024			0.0036	0.0036	0.0036	0.0036	0.0036	0.0043
H2	0.0003		0.1663	0.1154			0.1663	0.3284	0.3284	0.3497	0.3497	0.4085
CO	0.0003		0.1936	0.0323			0.1936	0.0315	0.0315	0.0103	0.0103	0.0120
CO2	0.0007		0.0687	0.1149	0.0000		0.0687	0.2310	0.2310	0.2523	0.2523	0.2945
H2O	0.9978	1.0000	0.5558	0.0172	0.9999	1.0000	0.5558	0.3935	0.3935	0.3722	0.3722	0.2670
CH4	0.0000		0.0020	0.0012			0.0020	0.0020	0.0020	0.0020	0.0020	0.0023
H2S	0.0002		0.0040	0.0345	0.0000		0.0040	0.0042	0.0042	0.0042	0.0042	0.0049
SO2												
Cl2												
HCl												
NH3	0.0006		0.0015	0.6801	0.0000		0.0015	0.0015	0.0015	0.0015	0.0015	0.0016
COS	0.0000		0.0002	0.0007			0.0002	0.0000	0.0000	0.0000	0.0000	0.0000
Total	1.0000	1.0000	1.0000	1.0000	1.0000	1.0000	1.0000	1.0000	1.0000	1.0000	1.0000	1.0000
kgmol/hr (w/o Solids)	290	447	29,165	44	2,342	1,160	29,165	29,165	29,165	29,165	29,165	24,961
kg/hr (w/o Solids)	5,363	8,062	561,932	857	42,186	20,896	561,932	561,930	561,930	561,930	561,930	486,041
kg/hr Solids	12,141	3,455										
kg/hr Total	17,504	11,516	561,932	857	42,186	20,896	561,932	561,930	561,930	561,930	561,930	486,041
Temp., C	<93.3	60.3	240.1	42.0	123.4	156.7	287.8	443.5	287.8	308.2	246.1	196.2
Press., bar	1.01	1.01	67.22	2.07	2.21	4.59	66.88	65.90	64.87	63.89	63.54	63.20
Enthalpy, MJ/hr	<-81,402	-140,029	-5,171,726	-3,725	-651,700	57,741	-5,119,197	-5,119,118	-5,294,885	-5,294,884	-5,364,972	-4,419,547
See Note	1	1	1	1	1	2	1	1	1	1	1	1

Note:

1. The reference state for thermodynamic properties is the standard enthalpy of formation of ideal gas at 25°C and 1 atm.
2. Enthalpy corresponds to ASME Steam Tables Basis.

**Table A1.3 - 3: Stream Data – continued**  
 Basis: 3,274 Tonne/D (As Received) or 3,078 Tonne/D (Dry Basis) Pittsburgh No. 8 Coal

Mol Fraction	25	26	27	28	29	30	31	32	33	34	35	36
O2												
N2	0.0061		0.0000	0.0067	0.0067	0.0067		0.0067	0.0124		0.0000	0.0002
Ar	0.0053		0.0000	0.0058	0.0058	0.0058	0.0000	0.0058	0.0096	0.0000	0.0000	0.0005
H2	0.5103		0.0000	0.5575	0.5575	0.5575	0.0000	0.5578	0.9090	0.0000	0.0006	0.0200
CO	0.0150		0.0000	0.0164	0.0164	0.0164		0.0164	0.0266	0.0000	0.0001	0.0016
CO2	0.3678		0.0007	0.4017	0.4017	0.4017	0.0003	0.4019	0.0375	0.9973	0.9980	0.9763
H2O	0.0851	1.0000	0.9983	0.0017	0.0017	0.0017	0.9824	0.0017	0.0001	0.0027	0.0012	0.0008
CH4	0.0029		0.0000	0.0031	0.0031	0.0031		0.0031	0.0049	0.0000	0.0000	0.0006
H2S	0.0061		0.0001	0.0066	0.0066	0.0066	0.0001	0.0066	0.0000	0.0000	0.0000	0.0000
SO2												
Cl2												
HCl												
NH3	0.0015		0.0009	0.0005	0.0005	0.0005	0.0171					
COS	0.0000		0.0000	0.0000	0.0000	0.0000		0.0000	0.0000	0.0000	0.0000	0.0000
Total	1.0000	1.0000	1.0000	1.0000	1.0000	1.0000	1.0000	1.0000	1.0000	1.0000	1.0000	1.0000
kgmol/hr	19,976	5,816	17,343	18,286	18,286	18,286	1,699	18,277	11,166	1,097	2,798	3,119
kg/hr	396,095	104,787	312,793	365,662	365,662	365,662	30,596	365,498	56,249	48,186	122,963	134,416
Temp., C	147.0	150.0	151.7	40.6	51.7	51.7	41.4	26.7	16.7	0.1	3.6	11.7
Press., bar	62.85	74.67	75.84	62.51	62.18	61.68	62.51	61.34	36.61	1.08	3.24	10.00
Enthalpy, MJ/hr	-3,270,758	-1,612,489	-4,800,591	-2,940,077	-2,932,596	-2,932,596	-479,927	-2,948,603	-205,038	-432,021	-1,101,962	-1,202,019
See Note	1	1	1	1	1	1	1	1	1	1	1	1

Note: 1. The reference state for thermodynamic properties is the standard enthalpy of formation of ideal gas at 25°C and 1 atm.

**Table A1.3 - 3: Stream Data – continued**

Basis: 3,274 Tonne/D (As Received) or 3,078 Tonne/D (Dry Basis) Pittsburgh No. 8 Coal

Mol Fraction	37	38	39	40	41	42	43	44	45	46	47	48
O2												
N2	0.0014	0.0438		0.0124	0.0452		0.0001	0.0791	0.0812	0.0001	0.0000	0.0000
Ar	0.0025	0.0090		0.0096	0.0092		0.0003	0.0166	0.0170	0.0000	0.0000	0.0000
H2	0.1621	0.1013		0.9089	0.1044		0.0091	0.3597	0.3694	0.0000	0.0001	0.0001
CO	0.0072	0.1101		0.0266	0.1134		0.0008	0.0232	0.0238	0.0000	0.0000	0.0000
CO2	0.3156	0.1526		0.0375	0.1572		0.9895	0.4462	0.4582	0.0080	0.0000	0.0000
H2O	0.0563	0.4671		0.0001	0.5425			0.0280	0.0019	0.9891	0.9999	0.9999
CH4	0.0030			0.0049			0.0003	0.0003	0.0003		0.0000	0.0000
H2S	0.4513	0.0770			0.0183		0.0000	0.0464	0.0476	0.0027		
SO2		0.0385			0.0091							
Cl2												
HCl												
NH3								0.0003	0.0003	0.0000		
COS	0.0006	0.0006			0.0006		0.0000	0.0002	0.0002	0.0000		
Total	1.0000	1.0000		1.0000	1.0000		1.0000	1.0000	1.0000	1.0000	1.0000	1.0000
Sulfur, kg/hr			2,827			3,927						
kgmol/hr	291	386	44	12	374	78	7,004	215	209	173	38,346	38,346
kg/hr	9,023	9,689	2,827	60	8,589	3,927	305,403	5,583	5,482	3,167	690,845	690,845
Temp., C	48.9	176.7	176.7	15.3	287.8	25.0	40.7	26.6	26.7	28.2	119.6	189.4
Press., bar	2.07	1.87	1.87	1.30	1.30	1.01	138.93	1.24	64.78	3.45	40.96	40.27
Enthalpy, MJ/hr	-42,939	-74,432	4,741	-217	-74,706	0	-2,790,575	-39,914	-38,746	-49,528	-10,730,342	-10,498,783
See Note	1	1	1	1	1	1	1	1	1	1	1	1

Note: 1. The reference state for thermodynamic properties is the standard enthalpy of formation of ideal gas at 25°C and 1 atm.

**Table A1.3 - 3: Stream Data – continued**

Basis: 3,274 Tonne/D (As Received) or 3,078 Tonne/D (Dry Basis) Pittsburgh No. 8 Coal

Mol Fraction	49	50	51	52	53	54	55	56	57	58	59	60
O2						0.2074	0.2074	0.2074	0.2074	0.0784	0.0848	0.0848
N2		0.0088				0.7728	0.7728	0.7728	0.7729	0.6899	0.6890	0.6890
Ar		0.0069				0.0092	0.0092	0.0092	0.0093	0.0083	0.0083	0.0083
H2	0.0000	0.6500										
CO		0.0190										
CO2	0.0000	0.0268				0.0003	0.0003	0.0003	0.0003	0.0109	0.0103	0.0103
H2O	0.9999	0.2850	1.0000	1.0000	1.0000	0.0103	0.0103	0.0103	0.0101	0.2125	0.2075	0.2075
CH4		0.0035										
H2S		0.0000										
SO2												
Cl2												
HCl												
NH3												
COS		0.0000										
Total	1.0000	1.0000	1.0000	1.0000	1.0000	1.0000	1.0000	1.0000	1.0000	1.0000	1.0000	1.0000
kgmol/hr	22	15,615	3,589	3,589	4,471	9,079	9,079	9,079	65,913	71,834	76,632	76,632
kg/hr	401	136,401	64,659	64,659	80,553	261,950	261,950	261,950	1,901,912	1,901,872	2,033,816	2,033,816
Temp., C	115.4	287.8	349.1	190.6	149.1	483.9	421.3	177.8	15.0	1,432.8	581.5	111.8
Press., bar	35.92	35.58	180.96	177.47	36.26	24.13	15.75	15.55	1.01	23.50	1.07	1.01
Enthalpy, MJ/hr	-6,233	-1,152,638	106,720	52,925	50,794	102,174	84,198	16,660	-188,413	-501,915	-2,807,013	-3,955,481
See Note	1	1	2	2	2	1	1	1	1	1,3	1,3	1,3

Note:

1. The reference state for thermodynamic properties is the standard enthalpy of formation of ideal gas at 25°C and 1 atm.
2. Enthalpy corresponds to ASME Steam Tables Basis.
3. For NOx see Performance Summary, Table 1.

**Table A1.3 - 3: Stream Data – continued**

Basis: 3,274 Tonne/D (As Received) or 3,078 Tonne/D (Dry Basis) Pittsburgh No. 8 Coal

Mol Fraction	61	62	63	64	65	66	67	68	69	70	71	72
H2O	1.0000	1.0000	1.0000	1.0000	1.0000	1.0000	1.0000	1.0000	1.0000	1.0000	1.0000	1.0000
Total	1.0000	1.0000	1.0000	1.0000	1.0000	1.0000	1.0000	1.0000	1.0000	1.0000	1.0000	1.0000
kgmol/hr	33,715	33,715	33,715	7,219	5,849	5,849	2,178	3,409	3,224	6,288	6,043	12,304
kg/hr	607,379	607,379	88,148	130,045	105,376	105,376	39,240	61,410	58,088	113,274	108,864	221,657
Temp., C	23.7	94.9	134.9	148.6	349.1	171.3	156.7	225.6	231.2	348.9	356.0	295.3
Press., bar	16.82	11.44	4.57	11.75	180.96	177.47	4.57	32.00	28.61	178.88	174.07	28.31
Enthalpy, MJ/hr	61,444	241,034	50,031	81,531	173,923	77,509	108,434	59,565	162,845	186,921	279,295	662,299
See Note	1	1	1	1	1	1	1	1	1	1	1	1

Note: 1. Enthalpy corresponds to ASME Steam Tables Basis.

**Table A1.3 - 3: Stream Data – continued**

Basis: 3,274 Tonne/D (As Received) or 3,078 Tonne/D (Dry Basis) Pittsburgh No. 8 Coal

Mol Fraction	73	74	75	76	77	78	79
H2O	1.0000	1.0000	1.0000	1.0000	1.0000	1.0000	1.0000
Total	1.0000	1.0000	1.0000	1.0000	1.0000	1.0000	1.0000
kgmol/hr	11,703	17,049	17,049	19,943	2,178	22,121	11,594
kg/hr	210,833	307,142	307,142	359,276	39,240	398,516	208,863
Temp., C	526.1	537.8	295.7	538.0	214.0	30.5	15.6
Press., bar	27.51	166.51	28.58	24.82	3.17	0.04	3.40
Enthalpy, MJ/hr	741,822	1,043,879	917,728	1,274,633	113,558	938,484	13,752
See Note	1	1	1	1	1	1	1

Note: 1. Enthalpy corresponds to ASME Steam Tables Basis.

**Table A1.3 - 3: Stream Data - continued**

Basis: 3,274 Tonne/D (As Received) or 3,078 Tonne/D (Dry Basis) Pittsburgh No. 8 Coal

Mol Fraction	80	81	82	83
O2				
N2				
Ar				
H2				
CO				
CO2				
H2O	1.0000	1.0000	0.9981	1.0000
CH4				
H2S				
SO2				
Cl2				
HCl			0.0016	
NH3			0.0003	
COS				
Total	1.0000	1.0000	1.0000	1.0000
kgmol/hr	55,948	3,283	2,279	737
kg/hr	1,007,926	59,148	41,128	13,275
Temp., C	15.6	15.6	26.7	15.6
Press., bar	1.014	1.014	1.4	1.0
Enthalpy, MJ/hr	66,132	3,881	-654,063	871
See Note	1	1	2	1

- Note:
1. Enthalpy corresponds to ASME Steam Tables Basis.
  2. The reference state for thermodynamic properties is the standard enthalpy of formation of ideal gas at 25°C and 1 atm.

**Table A1.3 - 4: ASU Functional Specifications - General**

	Units	Quantity	Requirements (See Notes Below)
<b>GT Air Extraction</b>			Temperature and pressure correspond to conditions at GT extraction point. Air may be either (1) cooled and utilized in the ASU or (2) expanded hot through a turboexpander and then cooled and utilized in the ASU.
Flow Rate	kg/hr	261,950	
Temperature		484	
Pressure	Bar	24.13	
<b>HP O<sub>2</sub></b>			95 mol% O <sub>2</sub> purity
Flow Rate (based on contained O <sub>2</sub> )	kg/hr	113,081	
Pressure	Bar	82.94	
<b>LP O<sub>2</sub></b>			95 mol% O <sub>2</sub> purity
Flow Rate (based on contained O <sub>2</sub> )	kg/hr	2,432	
Pressure	Bar	3.04	
<b>IP N<sub>2</sub> (GT Injection)</b>			O <sub>2</sub> Content < 1.0 mol%
Flow Rate	kg/hr	246,507	
Pressure	Bar	35.09	

**Notes:**

1. All compressors to be motor driven
2. Supply of utilities outside ASU scope
3. Cooling water available at 15.6°C or 60°F
4. Flow rates shown below are on total plant basis.

**Table A1.3 - 5: ASU Functional Specifications - Storage Requirements**

	Capacity	
Liquid O <sub>2</sub> (based on Contained O <sub>2</sub> )	Hr	8
Gaseous O <sub>2</sub> (please recommend)	Min	Approx. 3.5

**Table A1.3 - 6: ASU Functional Specifications - Ambient Air Composition**

Component	Mole %
O <sub>2</sub>	20.77
N <sub>2</sub>	77.22
CO <sub>2</sub>	0.03
H <sub>2</sub> O	1.04

**Table A1.3 - 7: Coal Receiving And Handling Unit Functional Specifications**

**General**

1. Coal handling sections include coal receiving, storage, stacking and reclaiming.
2. 3273 Tonne/D of “as received” Pittsburgh No.8 coal
3. Hardgrove grinding index = 50, size > 50.0 mm = 3%
4. Wed-western location.

**Facilities Description**

Facilities for transportation, storage and reclaiming of coal shall include the following:

- Truck unloading facilities
- Transfer of coal from the trucks to the coal storage area
- 14 days covered live coal storage
- Coal stacking
- Coal reclaiming (multiple units for increased availability)
- Coal transport from storage to the gasification battery limits
- Dust collection system in the storage as well as well transfer points in the conveying system
- Conveyers for transfer of coal
- Dust control and suppression via water / chemicals spraying
- Collection of run-off water and slag fines
- Transfer of the run-off water to water treatment section
- Fire protection
- Safety equipment
- Magnetic separators to remove tramp iron
- 20 day back-up dead coal storage with vegetation for dust control
- Noise control
- Covered conveyers
- Bin vibrators
- Weigh scales
- Conveying of coal from dead storage to covered storage
- Metal detectors
- Sampling systems
- Electrical systems
- Control and supervision system including programmable logic controller for maximizing automatic operations
- Control room
- Distribution of utilities (fire water, potable water, compressed air and electricity ) within the battery limits

### **Interface Definition**

The coal leaving the “Feed Receiving and Handling System” is fed to feed bins in gasification unit which provide the feed to wet rod mills. The scope of the “Feed Receiving and Handling System” should consist of providing the coal to these feed bins.

### **Emissions and Effluents**

All the coal handling systems (unloading, storage, conveying, reclaiming) except the dead coal storage are covered to minimize particulate emissions. The transfer bins and hoppers shall include bin vent filters to capture dust from displaced air. Induced air dust collectors shall be installed at all transfer points. The dumping of coal from incoming trippers associated with high impact velocity from free fall of over 60 feet shall be avoided to minimize coal degradation and segregation as well as dust emissions. The target design level of particulate (PM10 and PM25) is 5.9 mg/Nm<sup>3</sup>.

The aqueous effluents from the system (contaminated rain water, water used for dust control, melting snow, water used for fire protection) shall be routed to a sump to separate the coal fines using filters for recycle to the coal storage area. The aqueous effluent shall be routed to the waste water treatment section. The below ground system shall include trenches covered with grating to collect all coal contaminated wash water for recycle.

### **Fire Protection**

All the coal handling equipment shall include fire protection systems. Safety systems including temperature measurement, combustion gas analysis, alarms, safety showers and eye wash stations and others as needed shall be provided. Mobile fire equipment shall be provided as well.

### **Noise**

The noise limits shall be in compliance with EPA and OSHA regulations. Typically, the noise shall not exceed 85 dba at 3 feet from the source and 60 dba in the nighttime and 70 dba in the daytime at the plant fence line. The coal unloading operations shall be limited to 5 days per week and 8 hours per day. The transfer of coal to the plant shall be done 7 days per week and 16 hours per day.

**Table A1.3 - 8: Gasification Unit Functional Specifications - Coal Grinding and Slurry Preparation Subsystem**

Technology Type	Rod Mills -Wet Coal Grinding (See Notes)
Operating Conditions (Total Plant Basis)	
Inlet: Coal	136,416 kg/hr as received Pittsburgh #8 coal
Outlet: Coal Slurry	195,530 kg/hr with particle size consistent with GE Energy slurry feed, entrained bed oxygen blown gasifier
Slurry Strength	65.6% solids

**Table A1.3 - 9: Gasification Unit Functional Specifications - Gasifier Subsystem**

Technology Type	GE Energy Slurry Feed, Entrained Bed Oxygen Blown Gasifier (See Notes)
Gasifier Effluent Cooling	Total Quench (direct contact cooling with water)
Operating Conditions (Total Plant Basis)	
Inlet: Coal Slurry	195,530 kg/hr coal + water
Outlet: Raw Gas	299,480 kg/hr syngas (Prior to Quenching) at 72.6 bar and 1,371°C with H <sub>2</sub> + CO = 10,500 kg moles/hr

**Table A1.3 - 10: Gasification Unit Functional Specifications - Syngas Scrubber Subsystem**

Technology Type	Direct Contact Water Scrubber (See Notes)
Operating Conditions (Total Plant Basis)	
Inlet-Gas	577,570 kg/hr raw syngas at 69.6 bar, 243°C
Inlet Water	67,550 kg/hr at 76 bar and 153°C
Outlet-Gas	561,920 kg/hr scrubbed syngas at 67.2 bar, 240°C
Contaminant Removal, %	Particulate, 99.9%
Particulate Slurry Strength	4% solids

**Table A1.3 - 11: Gasification Unit Functional Specifications - Slag Recovery and Handling Subsystem**

Technology Type	Wet Lock Hopper System (See Notes)
Operating Conditions (Total Plant Basis)	
Inlet	Solids (coarse and fines) containing water
Outlet	12,140 kg/hr solids + 5,360 kg/hr water, near ambient conditions (1.01 bar, 15°C)
Dewatered Slag Moisture Content	≤ 30%

**Table A1.3 - 12: Gasification Unit Functional Specifications - Black Water, Grey Water and Waste Water Handling Subsystem**

Technology Type	Settling Tanks and Filtration (See Notes)
Operating Conditions (Total Plant Basis)	
Inlet	Solids (fines) containing water
Outlet-Treated Waste Water	27,720 kg/hr (quality compatible for bio-treatment unit)
Outlet-Filter Cake (Fine Slag)	3,460 kg/hr solids + 8,060 kg/hr water, near ambient conditions (1.01 bar, 15°C)
Filter Cake Moisture Content	≤ 70%

**Notes:**

1. All rotating equipment to be motor driven
2. Supply of utilities outside supplier scope
3. Cooling water available at 15.6°C or 60°F .

**Table A1.3 - 13: Selexol AGR Functional Specification – Feed Gas Definition**

Mol Fraction	
N <sub>2</sub>	0.00752663
Ar	0.00593841
H <sub>2</sub>	0.55533812
CO	0.01640200
CO <sub>2</sub>	0.40242082
H <sub>2</sub> O	0.00165392
CH <sub>4</sub>	0.00309023
H <sub>2</sub> S	0.00709379
NH <sub>3</sub>	0.00052234
COS	1.3698e-05
Total	1.000000
kgmol/hr	18,495
kg/hr	371,155
Temperature, °C	28
Pressure, bar	61.3

**Table A1.3 - 14: Selexol AGR Functional Specification – Product Specifications**

<b>Treated Syngas Stream</b>	
Total H <sub>2</sub> S + COS	≤ 10 ppmv
Pressure	36.61 bar (utilize a cold gas expander to recover power and generate refrigeration for solvent chilling)
<b>CO<sub>2</sub> Stream</b>	
Overall CO <sub>2</sub> Capture	90% total carbon removal (CO <sub>2</sub> + CO + CH <sub>4</sub> )
CO <sub>2</sub> Purity	Limit H <sub>2</sub> S to < 22 ppmV
Pressure of CO <sub>2</sub> Stream(s)	Leaving the AGR at maximum Pressure(s), the CO <sub>2</sub> being ultimately compressed to 138 barg or 2000 psig.
<b>Acid Gas Stream</b>	
Total H <sub>2</sub> S + COS	Acceptable to an O <sub>2</sub> blown Claus unit (20 mol % Minimum).
Pressure	Suitable to a Claus unit (2.07 bar)

**Notes:**

1. Feed gas includes tail gas recycle stream
2. All compressors to be motor driven
3. Supply of utilities outside AGR supplier scope
4. Cooling water available at 15.6°C or 60°F.

**Table A1.3 - 15: Equipment List Unit 21 - Sour Shift / LT Gas Cooling**

Basis: 3,274 Tonne/D (As Received) or 3,078 Tonne/D (Dry Basis) Pittsburgh No. 8 Coal

Equipment Number	Service	Number of Operating (spare)	Equipment Description (per Operating Train Basis)	Remarks
21-HE-100	Electric Startup Heater	1 (0)	2,639 GJ/hr	
21-HX-100	Reactor Feed/Effluent Exchanger	1 (0)	52,500 GJ/hr	
21-HX-101	HP Steam Generator	1 (0)	83,800 GJ/hr	
21-HX-102	IP Steam Generator 1	1 (0)	39,800 GJ/hr	
21-HX-103	IP Steam Generator 2	1 (0)	69,800 GJ/hr	
21-HX-104	MP Steam Generator	1 (0)	201,200 GJ/hr	
21-HX-105	Syngas Humidifier Circ. Water Heater	1 (0)	231,600 GJ/hr	
21-HX-106	Vacuum Condensate Heater	1 (0)	148,700 GJ/hr	
21-HX-107	Mercury Removal Bed Preheater	1 (0)	7,500 GJ/hr	
21-HX-108	Syngas Trim Cooler	1 (0)	16,500 GJ/hr	
21-PU-100	Process Condensate Pump	1 (1)	238 m3/hr	
21-PU-101	Stripper Recycle Pump	1 (1)	45 m3/hr	
21-RR-100	Shift Reactor 1	1 (0)	4,730 kg moles/hr of CO Converted	
21-RR-101	Shift Reactor 2	1 (0)	620 kg moles/hr of CO Converted	
21-RR-102	Mercury Removal Bed	1 (0)	18,290 kg moles/hr of Syngas Treated	
21-VE-100	Hot Condensate KO Drum	1 (0)	486,056 kg/hr of Saturated Syngas; 75,858 kg/hr Condensate	
21-VE-101	Syngas Humidifier Cric. Water KO Drum	1 (0)	396,122 kg/hr of Saturated Syngas; 89,934 kg/hr Condensate	
21-VE-102	Process Condensate Return Drum	1 (0)	207,898 kg/hr Condensate	
21-VE-103	Vacuum Condensate Heater KO Drum	1 (0)	365,677 kg/hr of Saturated Syngas; 30,445 kg/hr Condensate	
21-VE-104	Syngas Trim Cooler KO Drum	1 (0)	365,677 kg/hr of Saturated Syngas, NNF Condensate	

**Table A1.3 - 16: Equipment List Unit 23 - Claus Sulfur Recovery Unit**

Basis: 3,274 Tonne/D (As Received) or 3,078 Tonne/D (Dry Basis) Pittsburgh No. 8 Coal

Equipment Number	Service	Number of Operating (spare)	Equipment Description	Remarks
23-BU-100	Main Burner	1 (0)	108.6 kg moles/hr Acid + Sour gasses	
23-EJ-100	Sulfur Pit Vent Ejector	1 (0)		
23-HX-100	Waste Heat Boiler	1 (0)	18,800 MJ/hr, 178 bar (HP) Steam 1,880 MJ/hr, 31 bar (IP) Steam	
23-HX-101	No. 1 Condenser	1 (0)	2,270 MJ/hr	
23-HX-102	No. 1 Reheater	1 (0)	912 MJ/hr	
23-HX-103	No. 2 Condenser	1 (0)	731 MJ/hr	
23-HX-104	No. 2 Reheater	1 (0)	495 MJ/hr	
23-HX-105	No. 3 Condenser	1 (0)	552 MJ/hr	
23-HX-106	Reactor Feed Heater	1 (0)	1,970 MJ/hr	
23-HX-107	Reactor Effluent Cooler	1 (0)	3,580 MJ/hr	
23-HX-108	Contact Condenser Cooler	1 (0)	9,290 MJ/hr	
23-PU-101	AGR Acid Gas KO Drum Pump	1 (1)		Normally no flow
23-PU-102	SWS Acid Gas KO Drum Pump	1 (1)		Normally no flow

**Table A1.3 - 16: Equipment List – Unit 23 Claus Sulfur Recovery Unit - continued**

Basis: 3,274 Tonne/D (As Received) or 3,078 Tonne/D (Dry Basis) Pittsburgh No. 8 Coal

Equipment Number	Service	Number of Operating (spare)	Equipment Description	Remarks
23-PU-103	Sulfur Pumps	1 (1)	2 m3/hr	
23-PU-104	Desuperheater Pump	1 (1)	3 m3/hr	
23-PU-105	Contact Condenser Pump	1 (1)	33 m3/hr	
23-RR-100	Reaction Furnace	1 (0)	174 kg moles/hr of Reaction Products	
23-RR-101A	No. 1 Converter	1 (0)	386 kg moles/hr of Feed Gas	
23-RR-101B	No. 2 Converter	1 (0)	379 kg moles/hr of Feed Gas	
23-RR-102	Hydrogenation Reactor	1 (0)	385 kg moles/hr of Feed Gas	
23-SU-100	Sulfur Pit	1 (0)	94,200 kg Molten Sulfur	24 hr Storage
23-VE-101	AGR Acid Gas KO Drum	1 (0)	301 kg moles/hr of Feed Gas	
23-VE-102	SWS Acid Gas KO Drum	1 (0)	34 kg moles/hr of Feed Gas	
23-VE-103	HP Steam Drum	1 (0)	20,556 kg/hr, 178 bar Steam	Included in 23-HX-100
23-VE-104	IP Steam Drum	1 (0)	1,024 kg/hr, 31 bar Steam	Included in 23-HX-100
23-VE-105	Desuperheater / Contact Condenser	1 (0)	382 kg moles/hr of Feed Gas	
23-VE-106	Tail Gas Recycle Compressor KO Drum	1 (0)	214 kg moles/hr of Feed Gas	
23-CM-100	Tail Gas Recycle Compressor (Intercooled)	1 (1)	1,000 kW (3,700 MJ/hr Intercooling Duty)	Isentropic efficiency: Casing 1: 0.84, Casing 2: 0.79, Casing 3: 0.72, Casing 4: 0.62
23-ME-100	Degassing and Granulation	1 (0)	3,927 kg/h Sulfur	

**Table A1.3 - 17: Equipment List Unit 24 - CO<sub>2</sub> Compression**

Basis: 3,274 Tonne/D (As Received) or 3,078 Tonne/D (Dry Basis) Pittsburgh No. 8 Coal

Equipment Number	Service	Number of Operating (spare)	Equipment Description (per Operating Train Basis)	Remarks
24-CM-100 (24-VE-102, 103, 104, 105 and 24-HX-101, 102, 103, 104)	CO <sub>2</sub> Compressor (with Intercoolers and Suction KO Drums)	1 (0)	18,260 kW; 48,190 kg/hr of LP Inlet Gas at 1.08 bar and 0.1°C, 122,980 kg/hr of IP Gas Added at 3.24 bar and 3.6 °C, 134,430 kg/hr of HP Inlet Gas Added at 10.0 bar and 11.7°C 305,590 kg/hr of Discharge Gas at 81.4 bar	Isentropic efficiency: Casing 1: 0.831, Casing 2: 0.8313, Casing 3: 0.8376, Casing 4: 0.8376, Casing 5: 0.8189
24-HX-105	Compressor Aftercooler	1 (0)	59,920 GJ/hr	
24-PU-101	1st Compressor Suction KO Drum Pump	1 (1)		Normally no flow
24-PU-102	CO <sub>2</sub> Product Pump	1 (1)	410 m <sup>3</sup> /hr with inlet at 81.0 bar and Discharge at 138.9 bar	
24-VE-101	1st Stage Compressor Suction KO Drum	1 (0)	48,190 kg/hr of LP Inlet Gas at 1.08 bar and 0.1°C	
24-VE-106	Compressor Aftercooler KO Drum	1 (0)	305,440 kg/hr of Inlet Gas at 82.6 bar and 26.7°C	
24-VE-107	CO <sub>2</sub> Product Surge Vessel	1 (0)	305,440 kg/hr of Product CO <sub>2</sub>	
24-DR-107	Dehydration Package	1 (0)	305,610 kg/hr of CO <sub>2</sub> at 28.61 bar and 27°C (Moist = 0.13 mole %)	Product Dew Point ≤ -40°C



**Table A1.3 - 19: Equipment List Units 50/51 - Power Block**

Basis: 3,274 Tonne/D (As Received) or 3,078 Tonne/D (Dry Basis) Pittsburgh No. 8 Coal

Equipment Number	Service	Number of Operating (spare)	Equipment Description (per Operating Train Basis)	Remarks
50-EM-100	Gas Turbine Extraction Air Expander	1 (0)	4,745 kW	Isentropic efficiency: 0.775
50-HX-101	LP Steam Generator	1 (0)	67,600 MJ/hr	
50-HX-102	Air Trim Cooler	1 (0)	44,100 MJ/hr	
50-HX-100	N2 / HP BFW Exchanger	1 (0)	42,600 MJ/hr	
51-CO-100	Surface Condenser	1 (0)	889,600 MJ/hr	
50-FL-100	Air Filter	1 (0)	1,902,000 kg/hr Air Treated	Included with Gas Turbine
50-GG-100	Gas Turbine Generator	1 (0)	318.4 MW at Generator Terminals 1392 °C Rotor Inlet Temperature, Pressure Ratio: 24	Steam Cooled Gas Turbine
51-HR-100	Heat Recovery Steam Generator	1 (0)	1,130,600 MJ/hr	
51-ME-101	Boiler Chemical Injection Skid	1 (0)	697,730 kg/hr of BFW	Not shown
51-PU-105	LP Boiler Feedwater Pump	1 (1)	142 m <sup>3</sup> /hr	
51-PU-103	HP/IP Boiler Feed Water Pump	1 (1)	616 m <sup>3</sup> /hr	
51-PU-101	Vacuum Condensate Pump	1 (1)	609 m <sup>3</sup> /hr	
51-PU-102	Blowdown Sump Pump	1 (1)		
51-PU-104	HP BFW Circulating Pump	1 (1)	116 m <sup>3</sup> /hr	
51-SG-100	Steam Turbine Generator	1 (0)	157.6 MW at Generator Terminals	Isentropic efficiency: HP Section 0.8468, IP Section 0.9158, LP Section 0.8906

**Table A1.3 - 19: Equipment List Units 50/51 - Power Block - continued**

Basis: 3,274 Tonne/D (As Received) or 3,078 Tonne/D (Dry Basis) Pittsburgh No. 8 Coal

Equipment Number	Service	Number of Operating (spare)	Equipment Description (per Operating Train Basis)	Remarks
51-SU-100	Blowdown Sump	1 (0)		
51-SU-101	Water Wash Sump	1 (0)		Not shown
50-VE-100	N2 KO Drum	1 (0)	246,600 kg/hr N2	
50-VE-101	Syngas KO Drum	1 (0)	136,390 kg/hr Humid Syngas	
51-VE-101	High Pressure Steam Drum	1 (0)	307,140 kg/hr Total Steam	Included with HRSG
51-VE-102	Intermediate Pressure Steam Drum	1 (0)	62,930 kg/hr Total Steam	Included with HRSG
51-VE-103	Low Pressure Steam Drum / Deaerator	1 (0)	17,267 kg/hr Total Steam                      Integral Type	Included with HRSG
51-VE-104	Continuous Blowdown Drum	1 (0)	9,500 kg/hr Blowdown	
51-VE-105	Intermittent Blowdown Drum	1 (0)		
51-ME-100	Demineralizer Unit	1 (0)	208,860 kg/hr Treated Water	

## **TASK 1.4.1: SCREENING ANALYSIS OF ADVANCED BRAYTON CYCLES**

### **EXECUTIVE SUMMARY**

The ultimate goal of this program is to identify the power block cycle conditions and / or configurations which could increase the overall thermal efficiency of the Baseline IGCC by about 8% on a relative basis (i.e., 8% on a heat rate basis). This document presents the cycle conditions and / or the configurations for evaluation in an initial screening analysis. These cycle conditions and / or configurations for investigation in the screening analysis are identified by literature searches and brain storming sessions. The screening analysis in turn narrows down the number of promising cases for detailed analysis.

### **APPROACH**

Simulations of the power blocks (identified by the literature searches and brainstorming sessions of having a potential for increasing the thermal efficiency of the Baseline Case significantly) are performed on Thermoflex. The syngas composition as established in the Baseline Case is used in these simulations. The steam/BFW interchanges between the power block and the syngas generation (gasification) plant are taken into account in the bottoming cycle. The flow rates of the steam/BFW streams are adjusted in proportion to the fuel consumption of the power block. The net thermal efficiency of the overall plant is estimated by accounting for the power required both by the power block and by the gasification plant. Based on these results, cycle conditions and / or configurations are proposed for detailed analysis in the next step of this program that have a potential for significant improvement in the overall plant thermal efficiency (by about 8%) over the Baseline Case.

### **Selection of Cases for Detailed Analysis**

The following lists the proposed criteria for selecting the cycle conditions and / or configurations evaluated by the screening analysis for the detailed analysis of this program:

- Simplicity of configuration and controllability
- High overall IGCC plant thermal efficiency
- Minimum increase in pressure ratio over the Baseline Case while reaching the thermal efficiency goal
- Potential for lowering NOx

Cycle improvements or combinations of two or more of the improvements evaluated in the screening analysis are then selected for detailed analysis as described in the following section.

An example of combination of cycle improvements may be gas turbine compressor intercooling with turbine reheat.

### **Cases Proposed for Consideration in Screening Analysis**

The following describes the cycle conditions, configurations and / or component enhancements identified for the power block by the literature searches and brainstorming sessions of having a potential for increasing the thermal efficiency of the Baseline Case.

#### **Increased Firing Temperature / Blade Surface Temperature**

The effect of raising the firing temperature of the Baseline Case gas turbine is quantified for a given surface temperature of the 1<sup>st</sup> stage stator blades. Pressure ratio is varied to obtain the maximum plant thermal efficiency. A map of firing temperature (at the optimum pressure ratio) versus cycle efficiency is generated while adjusting the blade metal / TBC temperatures such that the coolant amounts to each set of blades remain at the same values as the Baseline Case gas turbine. This map is superimposed on to Figure A1.4.1- 1 (which shows projected increases in blade metal / TBC temperatures as increases in the firing temperature are realized in the future) to check for reasonableness of the blade metal / TBC temperatures used in this analysis. The minimum firing temperature along with the corresponding blade metal / TBC temperatures are then selected for use in the remainder of this screening analysis task with the goal of achieving the efficiency target of this program.

#### **Pressure Gain Combustor**

A pressure gain combustor produces an end-state stagnation pressure that is greater than the initial state stagnation pressure [Akbari, Baronia and Nalim, 2006; Venkat E., Rasheed and Dean, 2007]. An example of such a system is the constant volume combustion in an ideal spark ignited engine. Such systems produce a greater available energy in the end state than constant pressure systems. It was shown by Gemmen, Richards and Janus [1994] that the heat rate of a simple cycle gas turbine with a pressure ratio of 10 and a turbine inlet temperature of ~1200°C (2200°F) could be decreased by more than 10% utilizing such a constant volume combustion system. Pulse combustion which relies on the inherent unsteadiness of resonant chambers can be utilized as a pressure gain combustor. Research continues at the U.S. DOE and at NASA for the development of pressure gain combustors.

The impact on the plant thermal efficiency by utilizing a pressure gain combustor in the gas turbine is quantified.

#### **Inlet Air Fogging**

Roughly 50% of the power developed by the turbine in a gas turbine is used in its compressor. An approach to reducing this large parasitic load of air compression in a gas turbine is to introduce liquid water into the suction air [Utamara et. al., 1999; Bhargava and Meher-Homji, 2002]. The water droplets will have to be extremely small in size and be in the form of a fog to avoid impingement on the blades of the compressor causing erosion. As the water evaporates

within the compressor from the heat of compression, the air being compressed is cooled which in turn causes a reduction in the compressor work. Note that the compression work is directly proportional to the absolute temperature of the fluid being compressed.

A benefit in addition to increasing the specific power output of the engine is the reduction in the NO<sub>x</sub> due to the presence of the additional water vapor in the combustion air. A number of gas turbines have been equipped with such a fogging system. Care should be taken, however, in specifying the water treatment equipment since high quality demineralized water is required as well as in the design of the fogging system to avoid impingement of the compressor blades with water droplets.

The impact on the plant thermal efficiency by the addition of gas turbine inlet fogging is quantified.

### **Inverse Cycle**

The “inverse cycle” proposed by many investigators in the past ([http://www.energytech.at/kwk/portrait\\_kapitel-2\\_6.html#h4](http://www.energytech.at/kwk/portrait_kapitel-2_6.html#h4)) consists of reducing the back pressure on the gas turbine exhaust to sub-atmospheric pressure and utilizing a blower installed downstream of the HRSG to pressurize the flue gas to atmospheric pressure so that it may be discharged to the atmosphere. A cooler installed between the HRSG and the blower helps reduce the parasitic blower power consumption. Such a cycle has been touted for applications where a low calorific value fuel gas containing a significant fraction of hydrogen is available at a low pressure. In such cases, the gas turbine pressure ratio may be increased utilizing the flue gas blower to reduce the gas turbine exhaust pressure, instead of by increasing the turbine inlet pressure and having to compress the large volume of the low calorific value fuel gas to the correspondingly higher pressure required by the gas turbine combustor.

### **Intercooled Gas Turbine**

In simple cycle gas turbine approximately half of the power generated in the turbine is used by the compression. Intercooling can reduce this parasitic load of air compression while also reducing the compressor discharge temperature, an important consideration for high pressure ratio gas turbines. The lower air temperature results in lower NO<sub>x</sub> emissions. The machine specific power output is increased but more complex turbomachinery is required consisting of dual spools. A disadvantage of the intercooler in non-recuperative cycles is that the fuel required in the combustor for a given gas turbine firing temperature is increased due to the lower air temperature. At low pressure ratios, the intercooler may actually decrease the efficiency of the cycle.

### **Reheat Gas Turbine**

Gas turbine efficiency may be improved by incorporation of a reheat or sequential combustor. Figure A1.4.1-2 depicts the reheat gas turbine cycle. The following lists the main features of this cycle:

- Increased Cycle Efficiency

- Alstom's Approach while Maintaining Lower Firing Temperature
- Approximately 2% Improvement in Combined Cycle Heat Rate
- Other Gas Turbine Vendors Evaluating this Option
- Reduced NO<sub>x</sub> Emissions
  - Due to Lower Firing Temperature
  - NO<sub>x</sub> Destruction in Reheat (Sequential) Combustor

Because of the above listed advantages, evaluation of the reheat cycle is included in this screening study. The impact on the plant thermal efficiency by the addition of a reheater in the gas turbine is quantified. Included in this analysis is the optimum placement of the reheat combustor, i.e., the optimum pressure ratio of the high pressure turbine providing the vitiated air to the reheat combustor.

### **Intercooled and Reheat Gas Turbine**

Another approach to reducing the parasitic load of air compression in a gas turbine as discussed earlier is to incorporate intercooling. Intercooling is justified from an overall cycle thermal efficiency standpoint however at very high pressure ratios. Since the Advanced Brayton cycle with the high firing temperature in combination with reheat is expected to optimize at very high pressure ratio, intercooling of the compressor is included in this screening study. Figure A1.4.1-3 depicts the intercooled / reheat gas turbine cycle.

The impact on the plant thermal efficiency by the addition of an intercooler in the reheat gas turbine compressor is quantified.

### **Supercritical Rankine Bottoming Cycle**

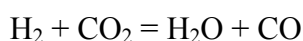
The bottoming cycle used by GE for the H class gas turbine based combined cycles consists of subcritical conditions. The bottom cycle as configured by UCIrvine utilizing literature data published by GE consists of a triple pressure superheat-reheat cycle with steam conditions at the throttle of the high pressure steam turbine of 165 bar / 566°C or 2400 psig / 1050°F and those of the reheated steam at the inlet of the steam turbine of 24 bar / 566°C or 345 psig / 1050°F. Use of supercritical steam cycle conditions in a high firing temperature gas turbine (with a correspondingly high exhaust temperature) may have a potential of increasing the overall combined cycle thermal efficiency significantly. Figure A1.4.1-4 presents the thermal efficiency of the steam Rankine cycle for various subcritical and supercritical conditions [Kitto, 1996]. A current State-of-the-Art steam cycle consists of 290 bar / 580°C / 600°C or 4200 psi / 1080°F / 1110°F while the European Thermie Project is scheduled to demonstrate in the year 2008, cycle conditions of 375 bar / 700°C or 5439 psi / 1292°F and the projected thermal efficiency (HHV) of > 45%. Table A1.4.1 - 1 summarizes some of the supercritical steam conditions being offered currently or being developed [Armstrong, Abe, Sasaki and Matsuda J., 2003; Ashmore, 2006; Kjaer (Elsam Engineering A/S); Retzlaff and Ruegger, 1996; Torre, 2003].

**Table A1.4.1 - 1: Supercritical Steam Cycles**

<b>Manufacturer/Study</b>	<b>Steam Conditions</b>	<b>Reheat</b>
Hitachi	248 barg / 600 °C / 610 °C (3600 psig / 1112°F / 1130 °F)	Single
Siemens	300 bar /600°C / 620°C (4350 psi / 1112°F / 1148°F)	Single
GE (1980s EPRI)	2482 bar / 593°C / 593C (4500 psi / 1100°F / 1100 °F)	Single
GE Philo 6 Plant	2482 bar / 621°C (4500 psi/1150 °F)	
THERMIE Program (Study)	375 bar / 700 °C (5439 psi / 1292 °F) 1 <sup>st</sup> Reheat: 120 bar/720 °C (1740 psi/1328 °F) 2 <sup>nd</sup> Reheat: 23.5 bar/720 °C (340 psi/1328 °F)	Double

### Chemical Recuperation

It may be possible to recover a portion of the high temperature heat available in the gas turbine exhaust to endothermally react the H<sub>2</sub> rich decarbonized syngas with the residual amounts of CO<sub>2</sub> also present in the syngas by the following “reverse shift” reaction:



It is expected that the reaction will move in the reverse shift direction since the concentration of the H<sub>2</sub> in the decarbonized syngas is very high while that of the CO is very low.

The impact on the plant thermal efficiency by the addition of chemical recuperation by which exhaust heat from the gas turbine is recycled to its combustor is quantified.

### Humid Air Cooling of Gas Turbine Blades

The advantages with steam cooling of the gas turbine blades over air cooling are:

- Gas turbine compression power is reduced
- Thermal dilution losses in the turbine are minimized when closed circuit cooling is utilized
- Momentum losses in the turbine are minimized again when closed circuit cooling is utilized.
- NOx emissions are reduced since the gas turbine combustor exit temperature is reduced for a given rotor inlet temperature.

A disadvantage of utilizing closed circuit steam cooling however, is that heat absorbed by the steam within the turbine enters the bottoming (steam) cycle by passes the topping (gas turbine) cycle. With open circuit air cooling of the turbine blades, the bypassing of the heat is avoided but this method of cooling does not have the above advantages listed for closed circuit steam

cooling. Humidification of the cooling air utilizing low temperature heat has the potential of reducing the major penalty associated with air cooling which is the increase in the parasitic air compression power requirement.

The impact on the plant thermal efficiency by utilizing an air cooled gas turbine with humidification of the cooling air utilized in the high pressure stages of the turbine is quantified. An SCR is included to reduce the NO<sub>x</sub> emissions since NO<sub>x</sub> emissions from the gas turbine would be higher due to the higher operating temperature of the combustor of this non-steam cooled gas turbine.

### **Closed Circuit Air Cooled Gas Turbine**

Another approach for cooling the blades in a gas turbine is to employ closed circuit air cooling [Chiesa and Macchi, 2002]. The air after performing the cooling function in the turbine is fed back to the combustor of the gas turbine. A compressor is included in the cooling air circuit to compensate for the various pressure drops in this flow circuit. An advantage of this method of cooling as compared to the closed circuit steam cooling is that the cooling air recycles or recuperates the heat removed from the fluid in the turbine (absorbed by the cooling air) back to the combustor of the gas turbine whereas in the case of steam cooling (as mentioned previously) the heat removed from the fluid within the turbine enters the steam cycle, i.e., heat is removed from the topping cycle and introduced into the bottoming cycle.

### **Air Partial Oxidation Topping Gas Turbine**

Another approach to introducing reheat in a gas turbine is to operate the high pressure combustor under fuel rich or partially oxidizing conditions while the lower pressure combustor completes the combustion or oxidation process [Newby et. al, 1997]. Apart from a potential for increased efficiency, there is a significant potential for lower NO<sub>x</sub> emissions. NO<sub>x</sub> formation within the high pressure combustor should be negligible, if any, due to the prevailing reducing conditions while the NO<sub>x</sub> formation in the lower pressure combustor should be low since the fuel entering this second combustor will have a very low heat content.

### **HAT Cycle**

A potential exists to synergistically combine the HAT cycle with the combined cycle to improve the overall thermal efficiency of an integrated gasification power plant. Figure A1.4.1-5 depicts the proposed cycle. The high pressure superheated steam generated in the gasification section of the plant is utilized in a back pressure steam turbine. The heat from the exhaust steam is recovered by condensing it in a high pressure condenser against HAT humidifier circulating water. The gas turbine consists of humid air cooling of the turbine blades rather than steam cooling since it is expected that the power block will be started up on natural gas without the gasification plant on-line which is the only source for the steam. The resulting overall plant thermal efficiency is quantified. Ultra low NO<sub>x</sub> emissions are expected for this HAT case based on results of previous work.

Cooling of the turbine blades with liquid water has been proposed in the past and a detailed theoretical analysis was performed by the National Advisory Committee for Aeronautics [Byron and Livingood, 1947]. Since the HAT cycle cannot take advantage of steam cooling, water

cooling with the subsequent use of the hot water exiting the turbine (after performing the blade cooling function) in the humidifier of the HAT cycle has the potential of raising the overall cycle thermal efficiency. The performance of the “HAT-Combined Cycle” may be improved by this liquid water cooling method. Another approach consists of utilizing closed circuit air cooling to HAT which also has the potential to improving the cycle efficiency.

### **High Efficiency Exhaust Diffuser**

Meruit Inc. [Fonda-Bonardi, 1996] has developed an Annular Recirculating Diffuser concept which is expected to improve the efficiency of a gas turbine engine by 3% by reducing the exhaust loss in the turbine section. In cycles employing exhaust heat recovery such as in combined cycle applications, the net overall cycle efficiency gain is expected to be lower however. The impact on the overall IGCC plant efficiency is quantified by incorporating this type of diffuser.

### **Oxy Combustion Gas Turbine**

Various cycles have been proposed where O<sub>2</sub> rather than air is utilized for the combustion of the fuel. Examples of such cycles are the (1) Graz cycle, (2) Partial Oxidation cycle (which resulted from study of fundamental Brayton cycle principles as put forth by Northwestern and improved upon by Gas Technology Institute), and (3) Clean Energy Systems cycle. A single oxy combustion cycle will be selected by this screening analysis task for the later detailed analysis.

### **NO<sub>x</sub> Reduction Options**

The combustion characteristics of the syngas, especially decarbonized syngas with its very high H<sub>2</sub> content are significantly different from natural gas precluding the use of current design premixed combustors for NO<sub>x</sub> control. Current approaches to reduce NO<sub>x</sub> emissions include addition of a thermal diluent in the form of moisture and / or N<sub>2</sub>, and / or installing an SCR. The following describes two alternate approaches for reducing NO<sub>x</sub> emissions.

#### Vortex Combustion

The Trapped Vortex Combustor (TVC) has the potential for numerous operational advantages over current gas turbine engine combustors. These include lower weight, lower pollutant emissions, effective flame stabilization, high combustion efficiency, and operation in the lean burn modes of combustion. The TVC concept grew out of fundamental studies of flame stabilization and is a radical departure in combustor design using swirl cups to stabilize the flame. Swirl stabilized combustors have somewhat limited combustion stability and can blow out under certain operating conditions. On the other hand, the TVC maintains a high degree of flame stability because the vortex trapped in a cavity provides a stable recirculation zone that is protected from the main flow in the combustor. The second part of a TVC is a bluff body dome which distributes and mixes the hot products from the cavity with the main air flow. Fuel and air are injected into the cavity in a way that it reinforces the vortex that is naturally formed within it.

The TVC may be considered a staged combustor with two pilot zones and a single main zone, the pilot zones being formed by cavities incorporated into the liners of the combustor [Burrus et al., 2001]. The cavities operate at low power as rich pilot flame zones achieving low CO and unburned hydrocarbon emissions, as well as providing good ignition and the lean blowout margins. At higher power conditions (above 30% power) the additional required fuel is staged from the cavities into the main stream while the cavities are operated at below stoichiometric conditions. Experiments have demonstrated an operating range that is 40% wider than conventional combustors with combustion efficiencies of 99%+. Use of the TVC combustor holds special promise as an alternate option for suppressing the NO<sub>x</sub> emissions in syngas applications where lean pre-mixed burners may not be employed. Organizations actively involved in the development of such combustors include General Electric and Ramgen. A semi-quantitative analysis will be made of the use of the TVC in an IGCC to assess if it has a significant impact on the plant thermal efficiency.

### Catalytic Combustion

Catalytic combustion is known to improve flame stability and can also reduce NO<sub>x</sub> emissions without excessive use of diluent. Precision Combustion, Inc. (PCI) has demonstrated the feasibility of achieving ultra-low NO<sub>x</sub> emissions on syngas utilizing a test rig under a DOE Contract (DE-FC26-03NT41721, "Ultra Low NO<sub>x</sub> Catalytic Combustion for IGCC Power Plants"). The following summarizes the milestones achieved so far:

- Tests performed in PCI's sub-scale combustion rig at 10 atm pressure with heated syngas over the planned range of operating conditions showed good operation (catalyst temperatures, catalytic conversion), confirming PCI's basic reactor design, catalysts, and substrate metallurgy for syngas operation.
- Successfully achieved 2.0 ppmvd NO<sub>x</sub> (15% O<sub>2</sub> basis) with near-zero CO emissions at 10 atm, sub-scale base-load conditions corresponding to Tampa Electric's Polk Power Station operation on 100% syngas.

## **RESULTS AND DISCUSSION**

### **Gas Turbine Cycle Configurations**

#### **Pressure Gain Combustor**

Figure A1.4.1-6 shows (1) the calculated pressure gain and (2) the calculated temperature of the compressor discharge air again as functions of the compressor discharge pressure. The fuel (syngas) to air ratio was varied to maintaining the same combustor exhaust temperature as that in the Baseline Case of 1433°C or 2611°F. Since the compressor discharge temperature changes as its discharge pressure changes, the fuel to air ratio varies with compressor pressure for a constant combustor discharge temperature. A 4% pressure loss was also assumed as in the Baseline Case. As can be seen from the data presented in the plots, the pressure gain expressed as the ratio of the

combustor discharge pressure to the compressor discharge pressure varies by as much as 2.3 to 3.0 as the compressor discharge pressure is varied from 5 bar to 20 bar.

The complete gas turbine cycle along with the steam bottoming cycle were next simulated for a compressor discharge pressure of 8.74 bar which provides a turbine inlet pressure same as in the Baseline Case gas turbine of 23.5 bar. The resulting net heat rate of the IGCC plant was significantly reduced, by as much as 7%. Next a sensitivity case was simulated to assess the impact on the overall IGCC plant heat rate if only half of this pressure gain could be actually realized due to much higher losses. The required compressor discharge pressure had to be increased to 17.4 bar to obtain the same turbine inlet pressure of 23.5 bar. The resulting net heat rate of the IGCC plant was still significantly impacted, reduced by almost 3%. Thus, the pressure gain combustor has the potential to make a significant positive impact on the IGCC plant performance. Major challenges exist, however, with respect to interfacing the pressure gain combustor which tends to be cyclic in operation with the gas turbine compressor and turbine which require steady flows.

Additionally, there is the concern of premature ignition when the fuel consists of syngas with a very high H<sub>2</sub> content. Although premature ignition should not occur on account of the air and fuel temperatures alone for the case when the compressor discharge pressure is limited to 8.74 bar [corresponding air temperature is near 300°C (570°F) while the diluted decarbonized syngas enters the combustor at 288°C (550°F)], the combustor walls will be hot from the previous combustion cycle and a potential exists for ignition before the air / fuel filling cycle is completed. If the pressure losses in this combustion system turn out to be significant, then a much higher firing temperature than that of the Baseline Case would be required to meet the efficiency target of this project. The compressor pressure ratio will have to be raised in order to increase the turbine expansion ratio to take full advantage of the higher firing temperature. Compressor discharge pressure much greater than 8.74 bar would then be required which would result in higher combustion air temperatures further exacerbating the premature ignition problem, limiting this cycle concept's use for such syngas applications. This type of combustion may be practical only for applications involving the less combustible fuels such as natural gas.

### **Inlet Air Fogging**

Using 0.5% overspray (expressed as % of saturated air flow) which is typically the maximum amount beyond which the gas turbine warranties do not hold, the overall plant performance is actually poorer. The compressor discharge temperature is reduced from 487°C or 908°F (for the Baseline Case) to 447°C or 836°F indicating a significant reduction in compression power but on the other hand, the fuel to air ratio is increased by 3.7% over the Baseline Case negating the savings in compression power. Secondary effects causing a further reduction in the efficiency of this Inlet Fogging Case are: (1) due to the higher moisture content of the air entering the combustor or the gas entering the turbine, a reduction the firing temperature from 1392°C or 2538°F (for the Baseline Case) to 1388°C or 2530°F to maintain the same 1<sup>st</sup> stage stator blade temperatures, (2) due to the lower compressor discharge temperature for the Inlet Fogging Case, a reduction from 4,747 kW generated by the extraction expander to 4,559 kW and also (3) a reduction of 9.5 GJ/hr or 9 MMBtu/hr of heat available for LP steam generation downstream of this expander. The net reduction in power generated by this Inlet Fogging Case over the Baseline Case is 1,361 kW or 0.36%.

## **Inverse Cycle**

A simulation was performed to quantify the performance improvement, if any, of the Baseline Case when equipped with a blower to draw a vacuum in the gas turbine exhaust such that HRSG exhaust. The exhaust pressure was reduced to 0.68 bar or 9.9 psia versus the 1.014 bar or 14.7 psia for the Baseline Case. The HRSG exhaust was first cooled to 27°C or 80°F using cooling water followed by the blower to compress the gas back up to the ISO atmospheric pressure. The net heat rate actually increased by almost 2% even after making the following optimistic assumptions: (1) 90% blower polytropic efficiency and (2) less than 7.6 cm or 3 in WC pressure drop for the flue gas cooler.

The Inverse Cycle may be useful in gas turbine based cycles where the flue gas contains a large fraction of water vapor (such as “wet cycles”). In such applications, the quantity of gas to be compressed in the blower would be much smaller than the working fluid within the gas turbine when the flue gas is cooled below its dew point upstream of the blower such that a significant fraction of the water vapor is condensed out.

## **Reheat Gas Turbine**

A reheat combustor is installed between the 1<sup>st</sup> and 2<sup>nd</sup> stages of the turbine. The pressure ratio is increased to 36 which is the highest for a commercially offered non-intercooled land-based gas turbine (Rolls Royce Trent 60 WLE, an aero engine) at ISO conditions. The reheat combustor outlet temperature is reduced in order to limit the temperature of the gas leaving the last stage to around 650°C or 1200°F (actual temperature obtained is 669°C or 1237°F) such that strength in the roots of the long and uncooled last stage blades is maintained. Furthermore, use of advanced superheat and reheat steam temperatures of 621°C or 1150°F for the bottoming cycle is facilitated without having very large temperature differences between the gas turbine exhaust and the steam such that the irreversibility in heat transfer is similar to that in the Baseline Case. The resulting reduced rotor inlet temperature for the 2<sup>nd</sup> stage turbine is 1345°C or 2453°F while the 1<sup>st</sup> stage rotor inlet temperature is kept close to that of the Baseline Case (1391°C or 2536°F versus 1392°C or 2538°F for the Baseline Case). The net increase in power generated by the plant over the Baseline Case (on a constant coal consumption basis) is significant, about 9 to 10 MW or more than 2%.

## **Intercooled Gas Turbine**

There are two types of intercoolers:

- Shell and Tube
- Spray Type (used in GE LM6000 SPRINT)

A shell and tube intercooler installed in the compressor can cool the air leaving the low pressure compressor against cooling water to as low a temperature of 27°C or 80°F at ISO conditions while in the case of a spray type intercooler, this temperature is limited to a much higher temperature, the adiabatic saturation temperature of the compressed air. Thus the spray intercooler does not reduce the compression power as much as a shell and tube intercooler does. On the other hand, the spray intercooler adds motive fluid which for expansion in the turbine. Other attributes of the spray intercooler include:

- Lower Equipment Cost
- Added moisture acts as a thermal diluent to reduce NO<sub>x</sub> formation in the combustor
- But needs High Quality Water
- Potential for droplet carryover and impingement on the high pressure compressor blades

A spray type intercooler was selected in this screening analysis to assess its impact on the overall cycle efficiency. It was found that the overall cycle efficiency remained essentially unchanged with the high pressure ratio gas turbines. At high pressure ratios intercooling may be desirable to limit the compressor discharge temperature which eases the challenges in the design of the compressor and the required materials of construction, as well as to reduce the formation of NO<sub>x</sub> within the combustor of the gas turbine.

The selection of the type of intercooler and its optimum placement, i.e., the optimum pressure ratio of the low pressure compressor providing the air to the intercooler will be evaluated in the detailed analysis Task of this study.

### **Intercooled and Reheat Gas Turbine**

A higher overall pressure ratio may be realized with intercooling without letting the compressor discharge temperature becoming excessive. Higher pressure ratio in turn allows raising the rotor inlet temperature of the 2<sup>nd</sup> stage turbine to that of the Baseline Case while limiting the gas turbine exhaust temperature to around 650°C or 1200°F (actual temperature obtained is 670°C or 1238°F) such that strength in the roots of the long and uncooled last stage blades is maintained. The reheat combustor is again installed between the 1<sup>st</sup> and 2<sup>nd</sup> stages of the turbine. The overall pressure ratio is increased to 42 which is close to that of the GE LMS100 intercooled gas turbine which has a pressure ratio of 41 at ISO conditions. Again, use of advanced superheat and reheat steam temperatures of 621°C or 1150°F for the bottoming cycle is facilitated without having very large temperature differences between the gas turbine exhaust and the steam such that the irreversibility in heat transfer is similar to that in the Baseline Case. The net increase in power generated by the gas turbine over the Reheat Case (on a constant syngas input basis) is insignificant however. Again at high pressure ratios intercooling may be desirable to limit the compressor discharge temperature which eases the challenges in the design of the compressor and the required materials of construction, as well as to reduce the formation of NO<sub>x</sub> within the combustor of the gas turbine.

### **Chemical Recuperation**

The amount of heat converted to chemical energy by adding a shift reactor downstream of the Selexol unit (and prior to syngas humidification) in the Baseline Case while operating this reactor at an isothermal temperature of 510°C is 12.35 GJ/hr. The net increase in electric power for the IGCC plant is estimated to be 0.5 MW which corresponds to only a 0.13% reduction in net heat rate. The heat reduction is too small to justify addition of the shift reactor and the associated heat exchange equipment.

## **Humid Air Cooling of Gas Turbine Blades**

The steam cooling of the 1<sup>st</sup> stage turbine blades of the Baseline Case was replaced with humid air cooling. The required amount of compressor discharge air was cooled, humidified, preheated against the air humidifier in-coming air and then used in the 1<sup>st</sup> stage turbine stator and rotor blades. The moisture content of the humid air was 40% (mass basis). The overall system performance did not change significantly over the Baseline Case. This type of cooling may be considered for applications where a steam cooled gas turbine is not preferred such as in simple cycle applications or where close coupling of the Brayton cycle and the bottoming Rankine cycles is not desirable.

## **Closed Circuit Air Cooled Gas Turbine**

The steam cooling of the 1<sup>st</sup> and the 2<sup>nd</sup> stage turbine blades of the Baseline Case was replaced with closed circuit air cooling. The cooling air leaving the turbine was then compressed and then introduced back into the combustor of the gas turbine. This location for the compressor was chosen in order to provide protection for the turbine blades in the event that this cooling air compressor trips. A relief valve located upstream of the compressor would then open up to allow the flow of the cooling air through the blades while the gas turbine shuts down.

The estimated overall plant heat rate is reduced by more than 1% over the Baseline Case.

## **Air Partial Oxidation Topping Gas Turbine**

The cycle arrangement as depicted in Figure A1.4.1-7 consists of extracting a portion of the air leaving the compressor of the gas turbine and boosting its pressure in a compressor after it is cooled in a recuperative exchanger followed by a spray cooler, and then preheating the compressed air in the recuperative exchanger before it is supplied to the POx combustor. The partially oxidized syngas leaving the partially oxidation (POx) combustor at a temperature of 927°C or 1700°F [Rabovitser et.al., 2007] is expanded in a turbo-expander to generate power, then cooled in a heat exchanger against the hot humid syngas and then supplied to the combustor of the gas turbine. The estimated overall plant heat rate is reduced by less than 1% over the Baseline Case but its major advantage is in reduction of NOx emissions.

A major challenge with this cycle, however, is its controllability. From a control stability standpoint, it is advisable not to have control valves in series. Thus a single valve installed on the fuel to the POx combustor will have to control the power output of the gas turbine while the air supplied to the POx combustor will have to control the temperature of the partially oxidized syngas entering the turbo-expander. This arrangement has the following disadvantages:

1. Large capacitance due to the large volume of gas between the fuel control valve and the gas turbine.
2. The air flow to the POx combustor will have to lag behind the fuel flow to this combustor which could lead to a dangerous situation during ramping down the fuel flow.

Other challenges include:

1. Metallurgical issues such as H<sub>2</sub> embitterment within the partial oxidation combustor as well as the turbo-expander
2. Turbo-expander seals to avoid leakage of the syngas. Buffer gas such as N<sub>2</sub> (supplied by the ASU) may be required for these seals.

## **HAT Cycle**

The HAT-Combined Cycle was simulated where the low temperature heat available from within the cycle as well as that available in the gasification island were recovered for humidification of the compressed air of the HAT cycle while the higher temperature heat was recovered to generate steam and utilized in a back pressure steam turbine. The results showed that the net overall plant efficiency of this plant was essentially the same as the Baseline Case consisting of the steam cooled gas turbine. When closed circuit air cooling was applied to HAT, the resulting plant efficiency was higher than that of the Baseline Case (while holding the same firing temperature) but the O<sub>2</sub> content of the combustor exhaust was low due to the large amount of water vapor introduced into the combustion air. This severely limits the firing temperature of the cycle and it cannot compete with cycles that can take advantage of high firing temperatures. Thus, the HAT cycle based case is dropped from the next detailed analysis task.

## **Oxy Combustion Gas Turbine**

Two types of oxy combustion cycles were screened, one consisting of the “Ox Gas Turbine” which has both the high pressure and reheat combustors operating under oxidizing conditions and the other consisting of the “POx Gas Turbine” which has the high pressure combustor operating under sub- stoichiometric conditions while the reheat combustor operates under oxidizing conditions. In the Ox Gas Turbine configuration shown in Figure A1.4.1-8, all of the oxygen required is sent through the first combustor and the syngas flow is split between these two combustors. In the POx Gas Turbine configuration shown in Figure A1.4.1-9, the entire syngas is supplied to the first combustor and the oxygen flow is split between the two combustors. In either case, the syngas is desulfurized but not decarbonized. These cycles involve post combustion carbon capture, the gas stream leaving the condenser of the cycle consisting mainly of CO<sub>2</sub>. The O<sub>2</sub> is supplied by an LP ASU since N<sub>2</sub> dilution in the combustor of the gas turbine (typically utilized for NO<sub>x</sub> control and power augmentation) is not desirable since the CO<sub>2</sub> is captured downstream of the gas turbine.

Screening analysis of these two types of oxy combustion cycles indicated that the partial oxidation cycle has a heat rate advantage of about 4% over the other Oxy Combustion cycle. The advantage of the POx Gas Turbine is due to the fact that it does not require all the O<sub>2</sub> to be compressed to the HP combustor pressure while the syngas is available at high pressure. This would also result in a reduction in the cost of the O<sub>2</sub> compressor which tends to be a costly machine. An added advantage of the POx Gas Turbine is that the HP combustor operating under sub-stoichiometric conditions minimizes the formation (if any) of NO<sub>x</sub>. On the other hand, the POx Gas Turbine requires the HP turbine in addition to the HP combustor to operate in partial oxidation mode. Potential challenges for the gas turbine are (1) due to the metallurgical issues such as H<sub>2</sub> embitterment and metal dusting within the partial oxidation combustor as well as the HP turbine, (2) soot formation within the partial oxidation combustor and (3) design of the high

pressure turbine seals to prevent leakage of the CO and H<sub>2</sub> at the high operating temperature and pressure. A large addition of steam may be required to circumvent Concerns 1 and 2 while a buffer gas such as N<sub>2</sub> (supplied by the ASU) may be required for the seals (Concern 3).

A challenge with Oxy Combustion cycles in general is due the cost penalty associated with the requirement for a very large amount of O<sub>2</sub> required by the cycle. This penalty is further exacerbated when the captured CO<sub>2</sub> stream is to meet the specifications required for enhanced oil recovery applications. In such cases, either an O<sub>2</sub> stream of greater than the standard 95% purity is required or a purification step to reduce the O<sub>2</sub>, N<sub>2</sub> and Ar content of the captured crude CO<sub>2</sub> stream is required. On the other hand, these Oxy Combustion cycles do have the advantage of capturing essentially all the carbon gasified.

Due to the above discussed technical hurdles and challenges, it is recommended that Oxy Combustion cycles be dropped from consideration for the next detailed analysis task.

## **Advanced Materials Technology**

### **Increased Firing Temperature**

Table A1.4.1 -2 summarizes the results of the screening analysis where the gas turbine firing temperature is increased over the Baseline Case in order to reduce the net heat rate of the IGCC. The firing temperature along with the blade surface temperatures were increased in nominal 100°C increments over those in the Baseline Case while the gas turbine pressure ratio was increased to maintain the exhaust temperature similar to that of the Baseline Case gas turbine while operating on natural gas (607°C or 1125°F). The steam bottoming cycle superheat and reheat temperatures for these higher firing temperature gas turbines were increased to the same values as those for this Baseline Case gas turbine operating on natural gas, i.e., 566°C or 1050°F (triple pressure subcritical steam cycle).

**Table A1.4.1 - 2: Effect of Raising Firing Temperature on IGCC Performance**

	<b>Baseline Case</b>	<b>Nominal 100°C Increase in Rotor Inlet</b>	<b>Nominal 200°C Increase in Rotor Inlet</b>	<b>Nominal 300°C Increase in Rotor Inlet</b>
<b>1<sup>st</sup> Stage Rotor Inlet Temperature</b>	1392°C (2538°F)	1502°C (2736°F)	1611°C (2932°F)	1722°C (3131°F)
<b>Combustor Outlet Temperature</b>	1433°C (2611°F)	1544°C (2811°F)	1655°C (3011°F)	1766°C (3211°F)
<b>Increase in Blade Surface Temperatures over Baseline Case</b>	-	108°C (195°F)	223°C (402°F)	342°C (615°F)
<b>Pressure Ratio</b>	24	30.4	44.4	63.5
<b>Compressor Discharge Temperature</b>	487°C (908°F)	538°C (1001°F)	630°C (1166°F)	724°C (1335°F)
<b>Increase in Net Plant Efficiency over Baseline Case</b>	-	3.6%	5.9%	8.0%

As can be seen, the required gas turbine firing temperature to realize an 8% decrease in the heat rate over the Baseline Case is as high as 1722°C or 3131°F (versus 1392°C or 2538°F for the Baseline Case) while the pressure ratio has to be increased to as high a value as 63.5 (versus 24 for the Baseline Case) while limiting the exhaust temperature. A combination of increased firing temperature along with cycle modifications such as intercooling (based on the previous results, intercooling does not hurt the cycle performance while limiting the discharge temperature of the air) and / or reheat may be desirable in order to limit the increase in firing and blade temperatures.

Next, a case is developed to reduce the pressure ratio of the 1722°C firing temperature gas turbine while allowing the exhaust temperature increase to around the 650°C or 1200°F constraint discussed previously (actual exhaust temperature for this case is 656°C or 1212°F). The corresponding pressure ratio for this case was 49.9. The steam bottoming cycle superheat and reheat temperatures were increased to 621°C or 1150°F to take full advantage of the higher gas turbine exhaust temperature. The net IGCC plant heat rate is essentially unaffected by reducing the gas turbine pressure ratio as long as the steam superheat and reheat temperatures are increased to limit the irreversibility in heat transfer in the HRSG.

### **Supercritical Rankine Bottoming Cycle**

An ultra supercritical steam cycle with double reheat forms the bottoming cycle of the 1722°C firing temperature gas turbine with the lower pressure ratio of 49.9 where the gas turbine exhaust temperature is around 650°C or 1200°F (actual exhaust temperature for this case is 656°C or 1212°F). The steam cycle consists of the following conditions:

- Supercritical HP at 376 bara / 621°C or 5455 psia / 1150°F
- 1st Reheat at 166.5 bara / 621°C or 2415 psia / 1150°F
- 2nd Reheat at 24.8 psia / 621°C or 360 psia / 1150°F
- LP Steam Induction at 3.17 bara or 46 psia

The results of the cycle analysis indicate that the net IGCC plant heat rate is essentially unaffected by installing an advanced steam bottoming cycle. Such advanced steam cycles show a significant advantage in lowering the heat rate in a boiler plant because the amount of high temperature heat is significantly higher than that available in the exhaust of a gas turbine.

### **Enhanced Performance Gas Turbine Components**

The enhancements discussed in the following may be incorporated to the most promising cycles identified in the detailed analysis task.

#### **High Efficiency Exhaust Diffuser**

According to Meruit Inc., the gas turbine exhaust diffuser can be designed to have a coefficient of performance ( $C_p$ ) as high as 0.9 utilizing their proprietary design. As a reference point, the  $C_p$  of a “conventional” diffuser is typically about 0.6. Before a detailed analysis of the diffuser

is conducted in order to verify Meruit's claim, a sensitivity case was developed to establish the upper limit for efficiency gain utilizing a diffuser approaching a Cp of 1.0. The results of this analysis indicated that the power output of the gas turbine is increased by as much as 3.5% but at the expense of a reduction of as much as 15°C or 27°F in the exhaust temperature. The steam turbine power output is consequently reduced with an overall combined cycle heat rate improvement of about 1% over the Baseline Case.

### **Advanced Low NOx Combustors**

A potential advantage for the advanced combustors such as the vortex or the catalytic combustors in an IGCC application is that the amount of thermal diluent addition to the combustor of the gas turbine for NOx control may be reduced while achieving ultra low NOx emissions. As explained in the following however, increasing the amount of diluent addition via syngas humidification (while utilizing only low temperature heat) and / or consisting of N<sub>2</sub> supplied by an EP ASU has the advantage of lowering the IGCC plant heat rate. The estimated NOx emission for the Baseline Case is 18 ppmVd (15% O<sub>2</sub> basis) with diluent addition and for lower NOx emission an SCR can be installed within the HRSG<sup>9</sup>. The SCR can reduce the NOx down to about 2 ppmVd (15% O<sub>2</sub> basis). The cost and heat rate penalty as explained under the "Low NOx Sensitivity Case" of "Task 1.3 - First Detailed Systems Study Analysis – Baseline Case" of the "Results and Discussion" section of this report, are quite small. The major advantage of the vortex and the catalytic combustors in such applications is that the SCR and the associated NH<sub>3</sub> handling system are eliminated. The advanced Brayton cycles with the much higher firing temperatures are expected to generate much higher amounts of NOx and a combination of advanced combustor concepts with increased diluent addition and SCR may be required.

In an IGCC with a gas turbine utilizing a "diffusion" type combustors, diluent addition is required to the syngas in order to reduce the NOx generation. Two types of diluents are available in an IGCC plant, water vapor introduced into the syngas stream by direct contact of the syngas with hot water in a counter-current column while recovering low temperature waste heat and / or N<sub>2</sub> supplied by an elevated pressure air separation unit. The choice of the diluent depends on a number of factors such as:

- amount of low temperature waste heat available for the humidification operation and
- amount of excess N<sub>2</sub> available from the air separation unit.

The amount of low temperature waste heat available in a gasification plant in turn depends primarily on the gasification heat recovery system employed (i.e., the extent to which cooling of the raw gasifier effluent is accomplished in a syngas cooler before the syngas is quenched / scrubbed with water). On the other hand, the amount of N<sub>2</sub> available as a diluent for the gas turbine depends on:

---

<sup>9</sup> Since the sulfur content is < 1 ppmV of the decarbonized syngas due to the very large circulation rate maintained in the acid gas removal unit (which also captures the CO<sub>2</sub>), formation of ammonium salts should be minimized keeping the required HRSG washes to a minimum. The expected NH<sub>3</sub> slip from the SCR is 10 ppmVd (15% O<sub>2</sub> basis). If NH<sub>3</sub> slip is a concern, then an NH<sub>3</sub> oxidation catalyst may be installed downstream of the SCR to convert it N<sub>2</sub>. The expected NH<sub>3</sub> concentration downstream of this catalyst is 0.5 ppmVd (15% O<sub>2</sub> basis).

- the specific O<sub>2</sub> consumption of the gasifier - the amount of N<sub>2</sub> produced by the air separation unit is lower when the specific O<sub>2</sub> consumption of the gasifier is lower and
- the type of gasifier feed system - dry feed systems utilize significant portions of the N<sub>2</sub> as lock hopper pressurization gas as well as in the drying and transport of the coal into the gasifier and only the remaining amount of N<sub>2</sub> is available for gas turbine injection.

In the case of the liquid slurry fed gasifier (GE type) selected for these near zero emission IGCC plants with pre-combustion carbon capture, the specific O<sub>2</sub> consumption tends to be high and so enough N<sub>2</sub> is available from the ASU for gas turbine combustor injection.

For IGCC applications, EP ASUs are preferred over LP ASUs when the oxygen and nitrogen product can be used at elevated pressures. The feed air pressure for an LP ASU is in the range of 3.5 to 6 bar (50 to 90 psig) while the feed air pressure for an EP ASU is set typically around 15 bar (200 psig). The operating pressure of the ASU distillation operation affects the bubble point of the liquid being distilled in the cold box. The higher the operating pressure, the less severe the cold box temperature is. Furthermore the cold box equipment pressure drops as a percentage of to inlet air pressure are also reduced as the cold box operating pressure is increased. The result is a reduced pressure ratio of the incoming air to that of the outgoing streams (O<sub>2</sub> and N<sub>2</sub>). If the O<sub>2</sub> and the N<sub>2</sub> leaving the cold box can be utilized within the gasification plant at the product supply pressure or higher, then a net increase in the overall IGCC plant efficiency is realized. When the N<sub>2</sub> after further compression is introduced into the combustor of the gas turbine provides extra motive fluid for expansion in the turbine in addition to reducing the NO<sub>x</sub> emissions. Results from previous studies have indicated that about 2% reduction in both the plant heat rate and plant cost may be realized by utilizing the EP ASU over the LP ASU.

Next, for the liquid slurry fed total quench gasifier (GE type) with shifting of the syngas as in these near zero emission IGCC plants with pre-combustion carbon capture, a large amount of low temperature waste heat is generated. The low temperature waste heat can be recovered for fuel gas humidification to provide both motive fluid and thermal diluent in the gas turbine. The humidification operation consists of counter-currently contacting the syngas with hot water in a packed column to simultaneously transfer heat and mass (water vapor) into the fuel gas stream from the water stream. The evaporation of water in the presence of syngas within the column occurs at a temperature much lower than the boiling point of water. Thus, the heat required for this evaporation process may be provided by circulating the water leaving the column through the low temperature waste heat recovery exchanger located downstream of the shift unit. Thus syngas humidification allows capture of waste heat and lowers the overall IGCC plant heat rate.

An evaluation of these advanced combustor concepts would therefore include determining the optimum amount of diluent addition (N<sub>2</sub> injection and syngas humidification) from an overall IGCC plant performance and cost standpoint.

## CONCLUSIONS

Figures A1.4.1-10 and A1.4.1-11 summarize the findings of this screening study. It can be seen that the bulk of the heat rate improvement has to come from increase in the gas turbine firing temperature unless radically new approaches such as the pressure gain combustor based gas turbine cycle are pursued.

The cycles in the order listed in the following under “Promising Cycles” are recommended for the Task 1.4.2, “Advanced Brayton Cycle Detailed Analysis.” Analysis of each of these selected cycles in an integrated gasification based power plant is recommended to quantify the effect of the cycle design parameters such that the ultimate goal of achieving the efficiency target for this study (8% improvement in heat rate over the Baseline Case which is equivalent to increasing the efficiency of a natural gas fired combined cycle from 60% to 65%) is met while minimizing the technological advancements required. The cycle conditions investigated during this screening analysis provide a bases and “starting points” for the next detailed study consisting of developing the performance of the integrated plants. Sensitivity to increasing the cycle pressure ratio while letting the gas turbine exhaust temperature rise above the 650°C or 1200°F constraint used in the Screening Study is also required on some of the cycle configurations. Appropriate advanced steam cycle conditions will be utilized corresponding to the higher gas turbine exhaust temperatures.

### Promising Cycles

The promising cycles recommended for evaluation in the detailed analysis task are listed below.

1. Steam-cooled Simple Cycle Gas Turbine based Combined Cycle
2. Steam-cooled Intercooled Gas Turbine based Combined Cycle
3. Steam-cooled Intercooled and Reheat Gas Turbine based Combined Cycle
4. Air POx Topping Cycle added to a Steam-cooled Gas Turbine based Combined Cycle
5. Closed Circuit Air-cooled Gas Turbine based Combined Cycle.

## BIBLIOGRAPHY

1. Akbari, P., D. Baronia and R. Nalim, “Single-Tube Simulation Of A Semi-Intermittent Pressure-Gain Combustor,” *Proceedings of the ASME Turbo Expo 2006: Power for Land, Sea and Air*, Barcelona, May 8-11, 2006.
2. Ashmore, C., “Steam Turbine Technology Goes Ultra Supercritical,” *Energy Focus*, March 30, 2006 (<http://www.energy-focus.com/pdfs/POWER/STEAM.pdf>)
3. Armstrong, P., Abe T., Sasaki T. and Matsuda J., “Design and Operating Experience of Supercritical Pressure Coal Fired Plant,” Presented to Electric Power 2003, March 4-6, 2003

<http://www.hitachi.us/Apps/hitachicom/content.jsp?page=powerequipment/TechnicalPublications/index.html&level=2&section=powerequipment&parent=TechnicalPublications&nav=left&path=jsp/hitachi/forbus/powerequipmentsystems/&nId=iD>

4. Bolland, O., "A Comparitive Evaluation of Advanced Combined Cycle Alternatives," *ASME J. of Engineering for Gas Turbines and Power*, Vol 113, pp 190-197, April 1991.
5. Bhargava, R. and C. B. Meher-Homji, "Parametric Analysis of Existing Gas Turbines with Inlet Evaporative and Overspray Fogging," *Proceedings of the ASME IGTI Turbo-Expo Conference*, Amsterdam, June 2002.
6. Burrus, D. L., A. W. Johnson and W. M. Roquemore, and D. T. Shouse, "Performance Assessment of a Prototype Trapped Vortex Combustor for Gas Turbine Application," *Proceedings of the ASME IGTI Turbo-Expo Conference*, New Orleans, June 2001.
7. Byron, B. and J. N. B. Livingood, "Cooling of Gas Turbines III – Analysis of Rotor and Blade Temperatures in Liquid Cooled Gas turbines," National Advisory Committee for Aeronautics Document (Unclassified), RM No. E7B11c, February 11, 1947.
8. Chambers, S. et. al., "The Influence of In Situ Reheat on Turbine-Combustor Performance," *Proceedings of ASME IGTI Gas Turbine Conference and Exhibition*, Vienna, Paper No. GT-2004-54071, 2004.
9. Chiesa, P. and E. Macchi, "A Thermodynamic Analysis of Different Options to Break 60% Electric Efficiency in Combined Cycle Power Plants," *Proceedings of ASME Turbo Expo Conference, Amsterdam*, Paper No. GT-2002-30663, 2002.
10. Fiaschi, D., L. Lombardi and L. Tapinassi, "The Recuperative Auto Thermal Reforming and Recuperative Reforming Gas Turbine Power Cycles with CO<sub>2</sub> Removal, Part I: The R-ATR Cycle," *Proceedings of ASME IGTI Gas Turbine Conference and Exhibition*, Amsterdam, Paper No. GT-2002-30116, 2002.
11. Fiaschi, D., L. Lombardi and L. Tapinassi, "The Recuperative Auto Thermal Reforming and Recuperative Reforming Gas Turbine Power Cycles with CO<sub>2</sub> Removal, Part II: The Recuperative Reforming Cycle," *ASME J. of Engineering for Gas Turbines and Power*, Vol 126, pp 62-68, January, 2004.
12. Fonda-Bonardi, G., "Theory, Design, and Test of an Efficient Subsonic Diffuser," *Proceedings of the ASME*, FED-Vol 238, Fluids Engineering Summer Meeting, pp 609-621, 1996.
13. Gemmen, R. S., G. A. Richards and M. C. Janus, "Development of a Pressure Gain Combustor for Improved Cycle Efficiency," presented at the 1994 ASME COGEN Turbo Power Congress and Exposition, IGTI Vol. 9.
14. Hsu, K. Y., Gross, L. P. and Trump, D. D., "Performance of a Trapped Vortex Combustor," *J. of Propulsion and Power*, Paper No. 95-0810, AIAA 33<sup>rd</sup> Aerospace Sciences Meeting and Exhibit, Reno, Nevada, Jan 9-12, 1995.
15. Ito, S., et. al., "Conceptual Design and Cooling Blade Development of 1700°C Class High-Temperature Gas Turbine," *ASME J. of Engineering for Gas Turbines and Power*, Vol 127, pp 358-368, April 2005.
16. Kjaer, S., "Advanced Super Critical Power Plant; Experiences of ELSAMPROJEKT," Elsam Engineering A/S (<http://www.elsamprojekt.com.pl/usc.html>)
17. Kitto, J. B., "Technology Development for Advanced Pulverized Coal-Fired Boilers," Presented at the Power-Gen International '96, Orlando, Florida, December 1996.
18. Moritsuka, H., "Proposal of Innovative Gas Turbine Combined Cycle Power Generation System," *Proceedings of ASME IGTI Gas Turbine Conference and Exhibition, Vienna*,

- Paper No. GT-2004-54177, 2004.
19. Naqvi, R. et. al., "Chemical Looping Combustion – Analysis of Natural Gas Fired Power Cycles with Inherent CO<sub>2</sub> Capture," *Proceedings of ASME IGTI Gas Turbine Conference and Exhibition*, Vienna, Paper No. GT-2004-53359, 2004.
  20. Newby et. al., "An Evaluation of a Partial Oxidation Concept for Combustion Turbine Power Systems," ASME paper 97-AA-24, 1997.
  21. Rabovitser, J., et. Al., "Development of a Partial Oxidation Gas Turbine (POGT) for Innovative Gas Turbine Systems," *Proceedings of ASME Turbo Expo 2007*, Montreal, May 14-17, 2007.
  22. Rao, A. D., "Process for Producing Power," U.S. Patent No. 4,289,763 dated May 16, 1989.
  23. Rao, A. D., M. Sander, J. Sculati, V. Francuz and E. West, "Evaluation of Advanced Gas Turbine Cycles," Final Report prepared for Gas Research Institute by Fluor, August 1993, Report No. GRI-93/0250.
  24. Rao, A. D., V. J. Francuz, L. C. Shen and E. W. West, "A Comparison of Humid Air Turbine (HAT) Cycle and Combined Cycle Power Plants," EPRI Report IE-7300, March 1991.
  25. Rao, A. D., V. J. Francuz, F. J. Mulato, B. Sng, E. W. West, J. Kana, G., Perkins and D. Podolski, "A Feasibility and Assessment Study for FT4000 Humid Air Turbine (HAT)," EPRI Report TR-102156, September 1993.
  26. Retzlaff, K.M. and Ruegger, W.A., "Steam Turbines for Ultrasupercritical Power Plants," GER3945-A, GE Power Systems, Schenectady, NY, August, 1996  
[http://www.gepower.com/prod\\_serv/products/tech\\_docs/en/downloads/ger3945a.pdf](http://www.gepower.com/prod_serv/products/tech_docs/en/downloads/ger3945a.pdf)
  27. Smith, L.L., DOE Contract DE-FC26-03NT41721 Topical Report , "Ultra Low NOx Catalytic Combustion for IGCC Power Plants," Precision Combustion, Inc., March 2004.
  28. Thien, V. and M. Oechsner, "Materials for Gas Turbines," presented at the Second International Gas Turbine Conference, Slovenia, April 29-30, 2004.
  29. Torre, M., "ASME to Honor Philo Unit 6 Power Plant," Press Release, New York, July 28, 2003  
[http://www.asme.org/NewsPublicPolicy/PressReleases/Honor\\_Philos\\_Unit\\_6\\_Power.cfm](http://www.asme.org/NewsPublicPolicy/PressReleases/Honor_Philos_Unit_6_Power.cfm)
  30. Utamara, M. et. al., "Effect of Intensive Evaporative Cooling on Performance Characteristics of Land-based Gas Turbine," *ASME J. of Engineering for Gas Turbines and Power*, Vol. 34, July 1999.
  31. Venkat E., A. Rasheed and A. J. Dean, "Performance of a Pulse Detonation Combustor-Based Hybrid Engine," *Proceedings of ASME Turbo Expo 2007: Power for Land, Sea and Air*, Montreal, May 14-17, 2007.

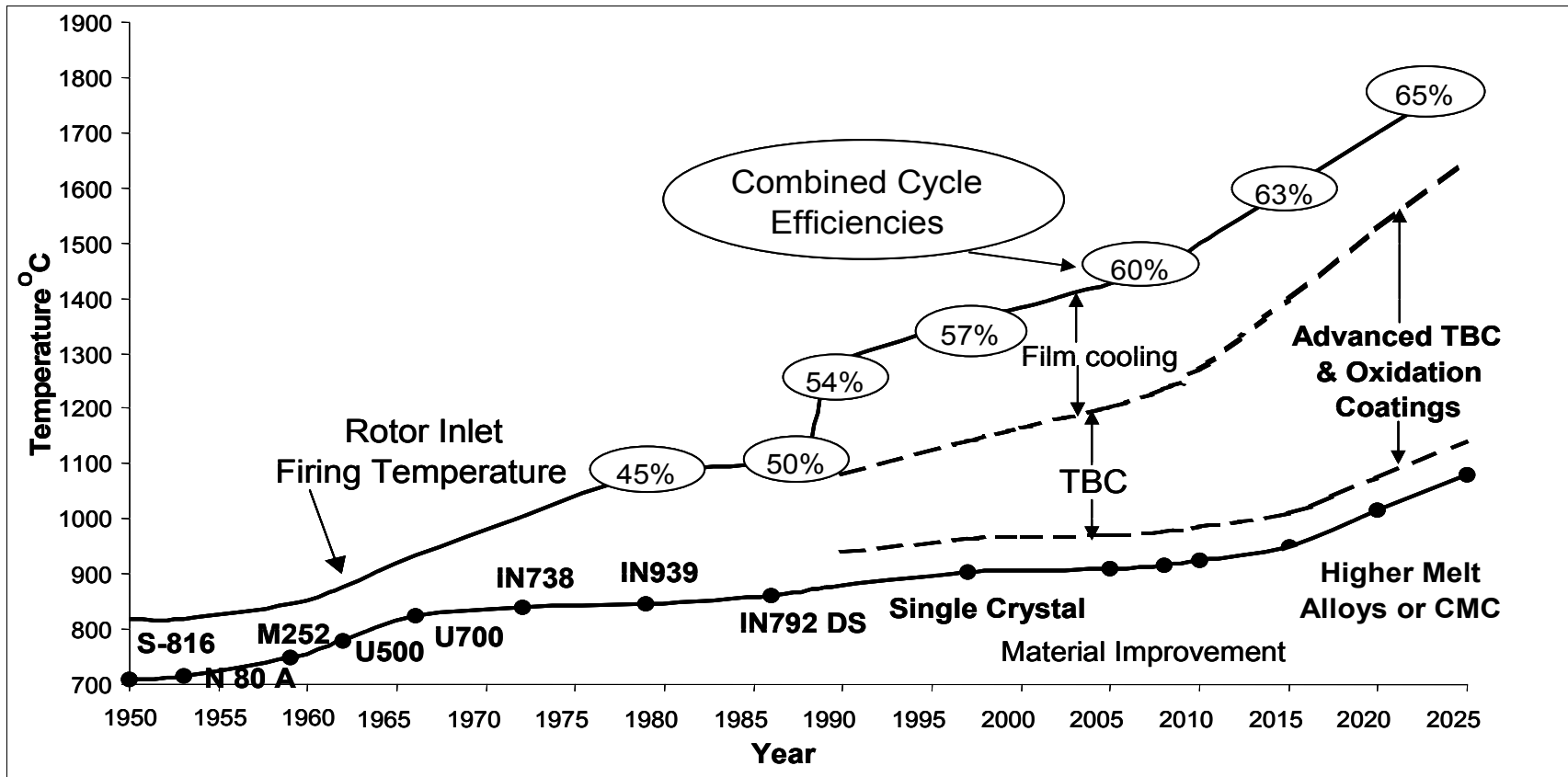


Figure A1.4.1 - 1: Effect of Increasing Firing and 1<sup>st</sup> Stage Stator Blade Temperatures

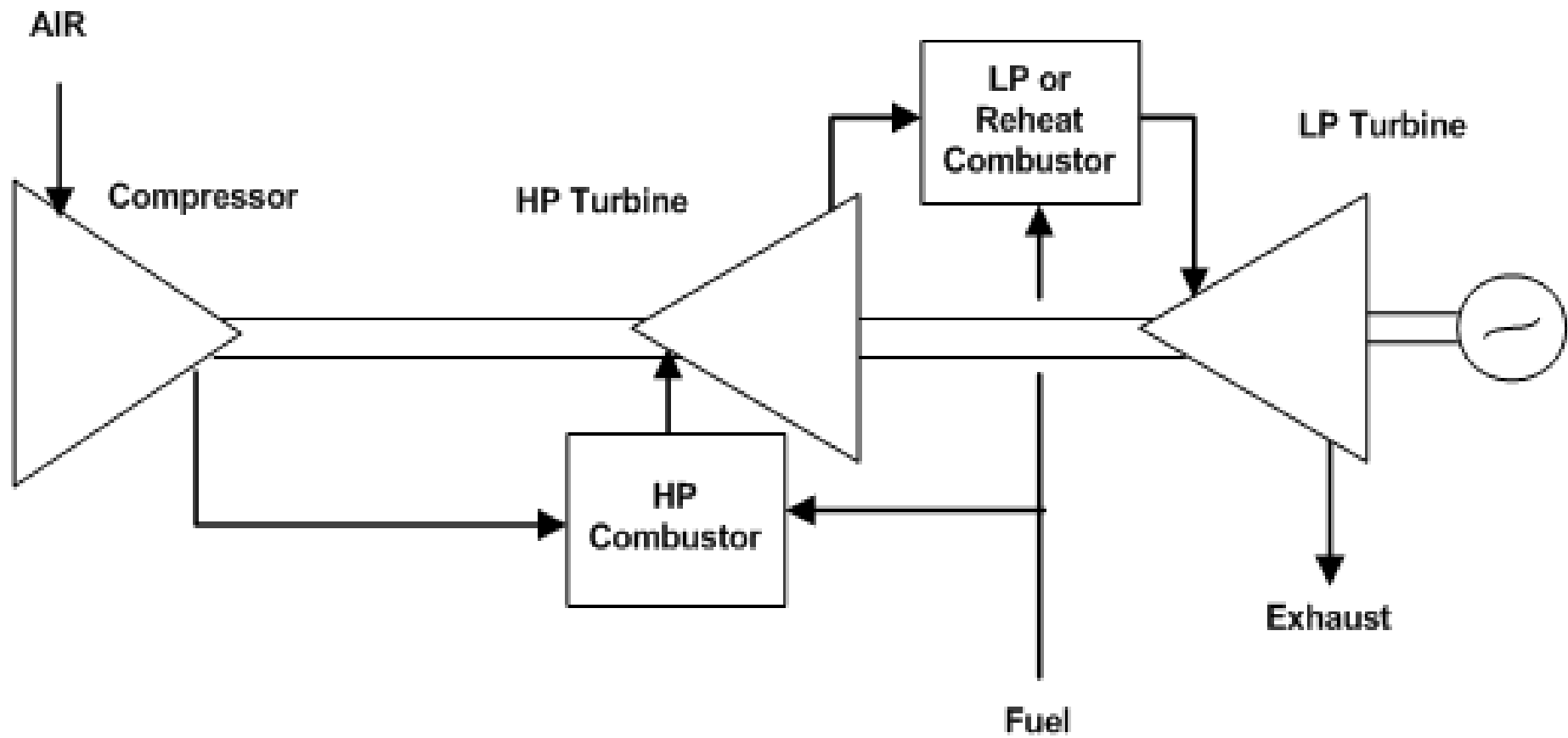
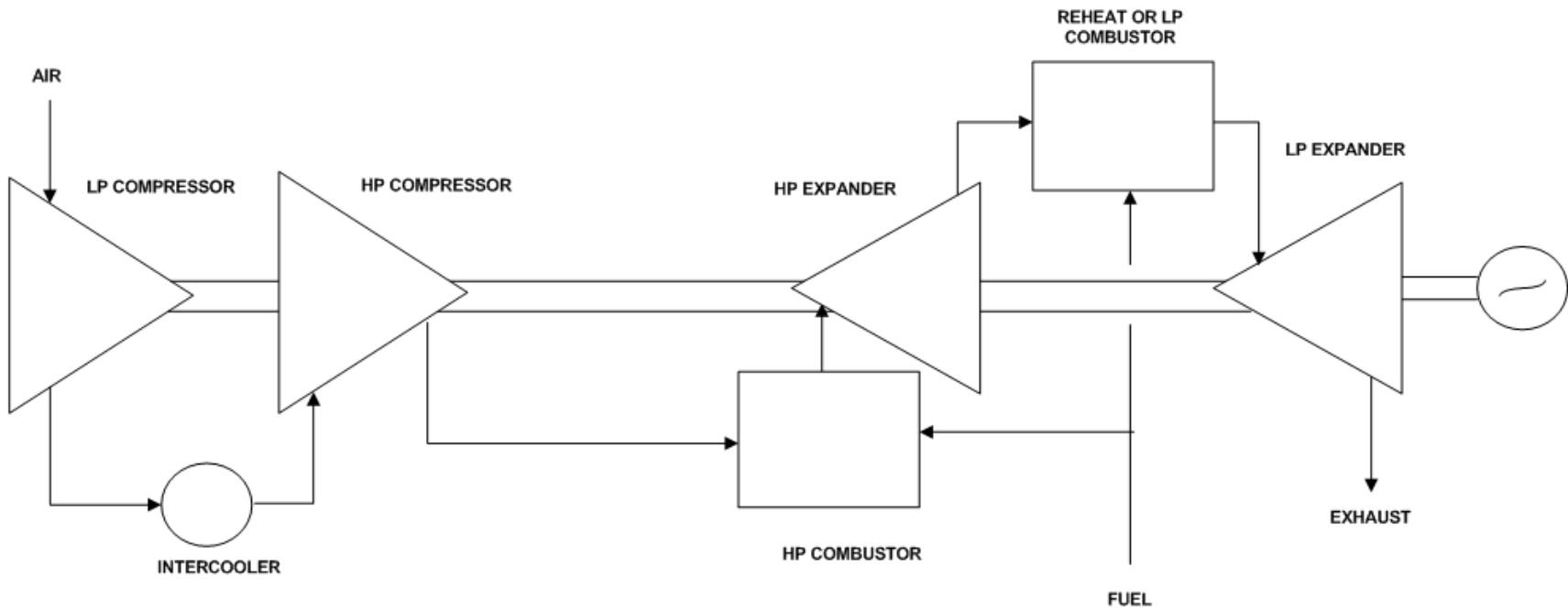
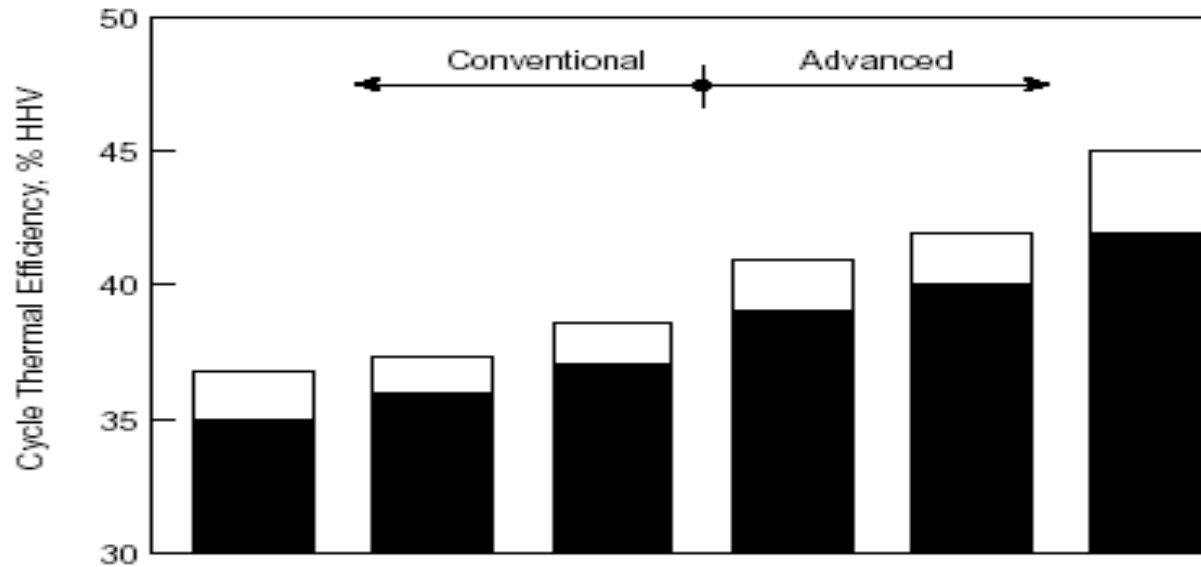


Figure A1.4.1 - 2: Reheat Gas Turbine Cycle



**Figure A1.4.1 - 3: Intercooled - Reheat Gas Turbine Cycle**



Pressure, psi	2400	3500	3500	4500*	4500*	6000*
SH Temp, F	1000	1000	1000	1050	1100	1200
RH Temp, F	1000	1000	1025	1050	1100	1200
2RH Temp, F	—	—	1050	1050	1100	1200
Pressure, bar	16.6	24.1	24.1	31.0	31.0	41.4
SH Temp, C	538	538	538	566	593	649
RH Temp, C	538	538	552	566	593	649
2RH Temp, C	—	—	566	566	593	649

Figure A1.4.1 - 4: Steam Rankine Cycle Thermal Efficiencies

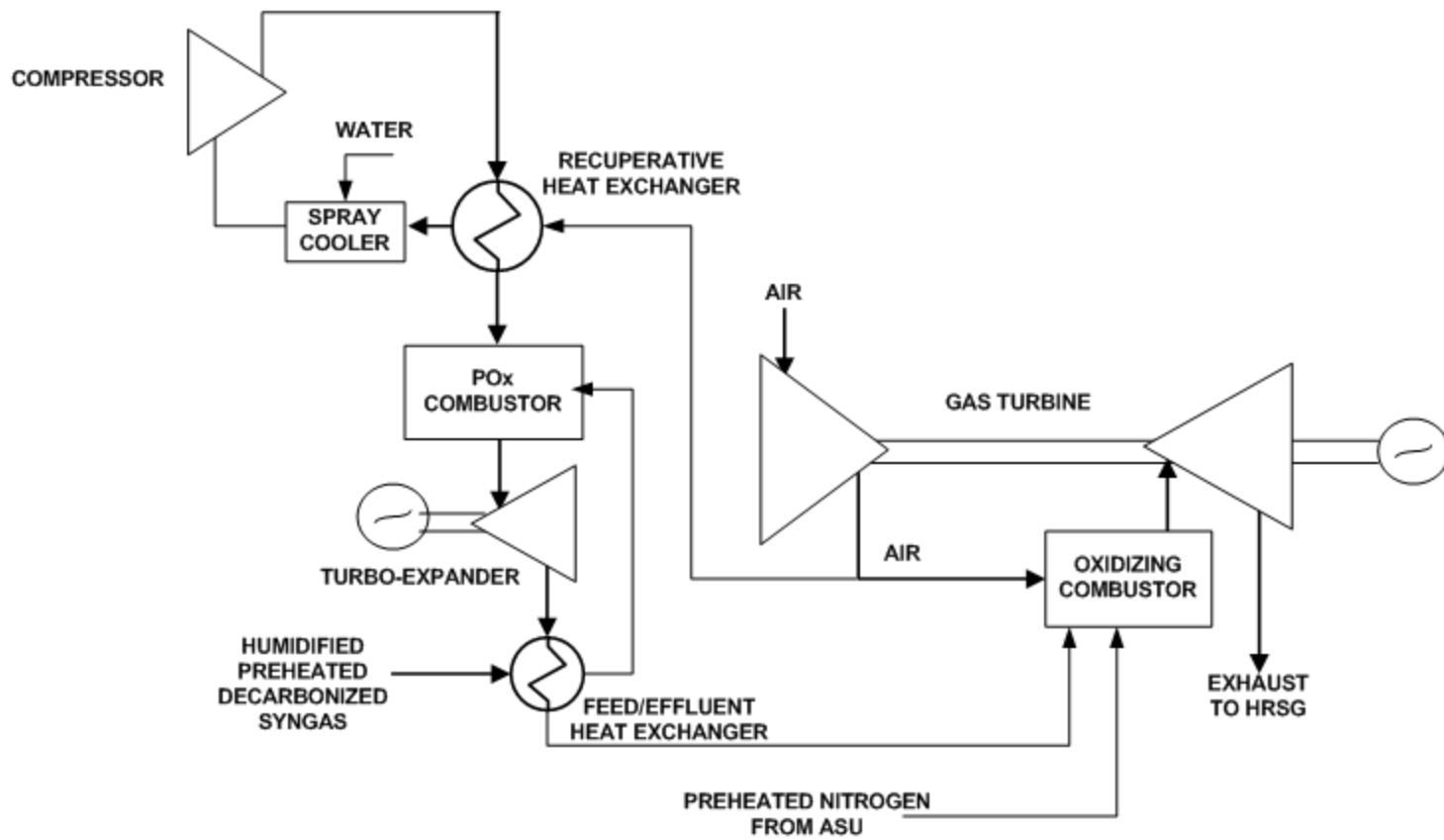


Figure A1.4.1 - 5: Air POx Cycle

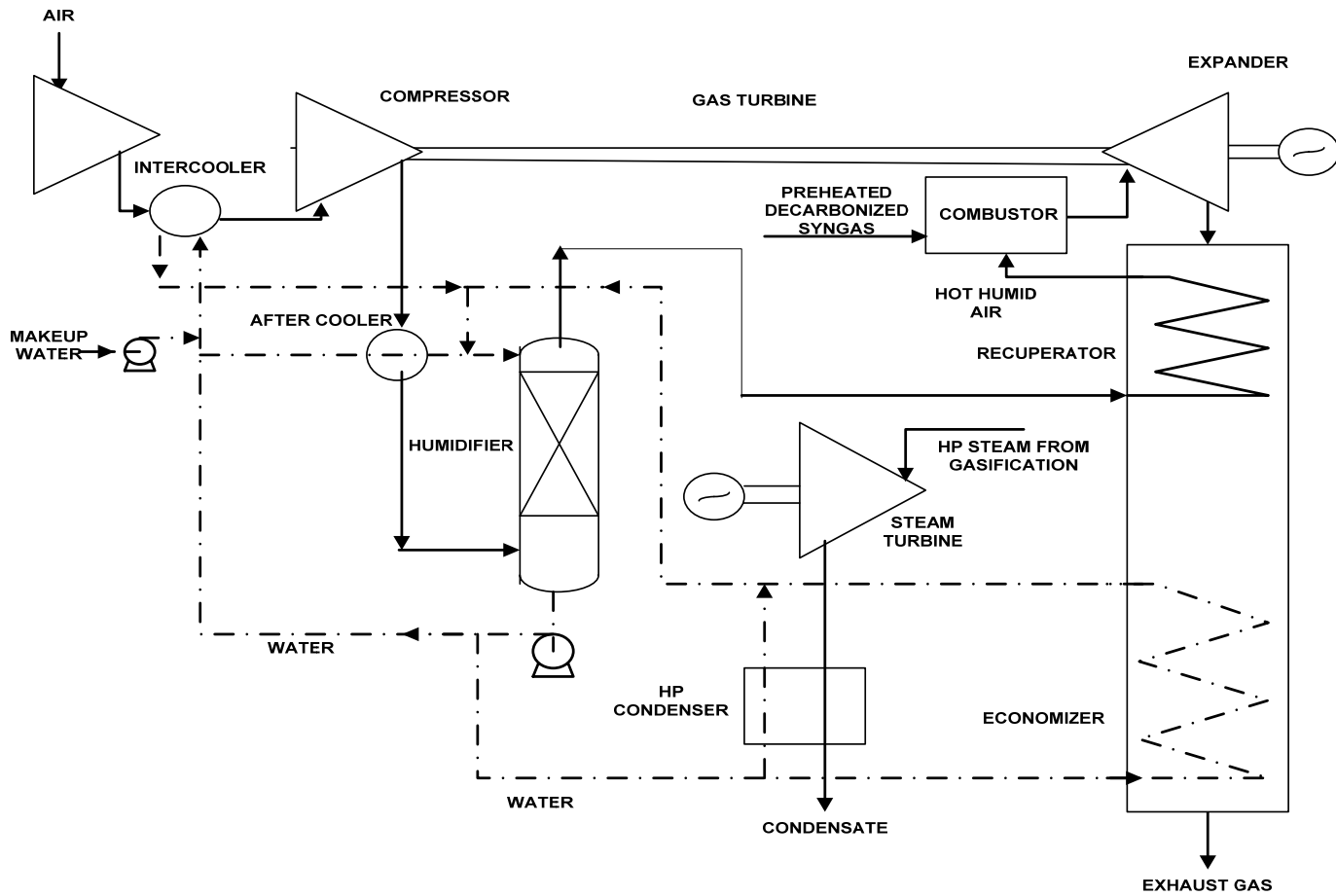
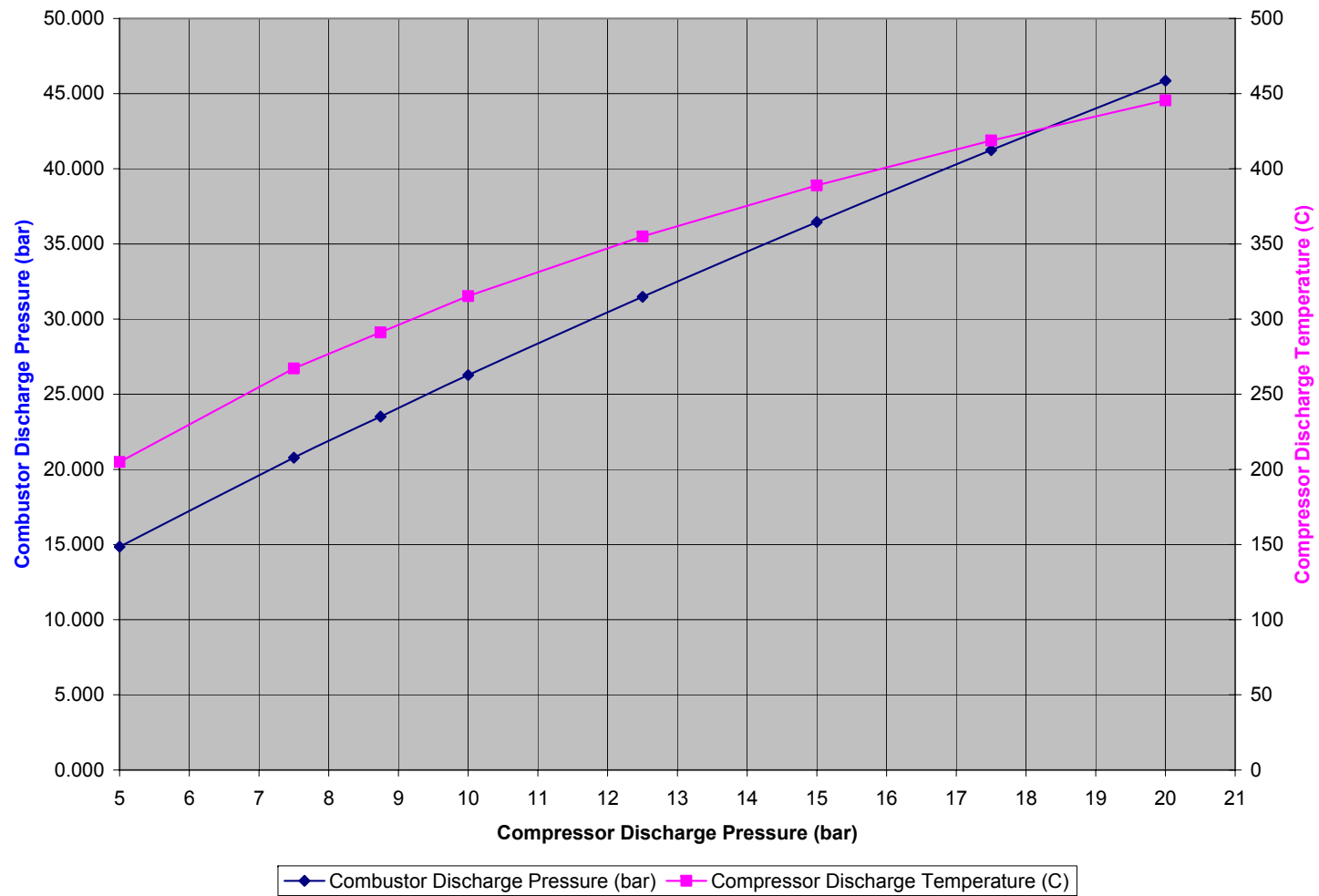
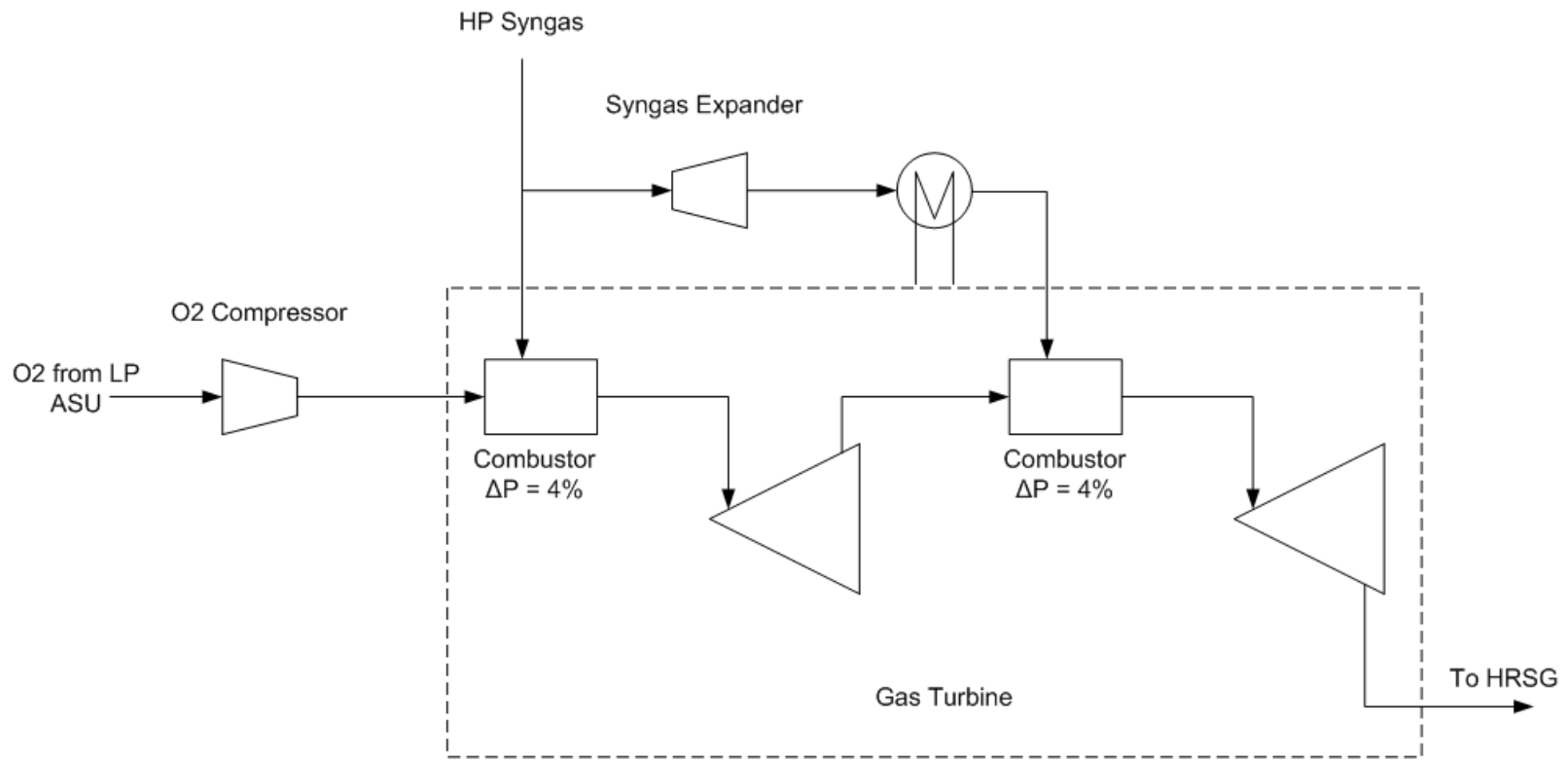


Figure A1.4.1 - 6: HAT-Combined Cycle



**Figure A1.4.1 - 7: Pressure Gain and Compressor Discharge Conditions in a Pressure Gain Combustor**



**Figure A1.4.1 - 8: Ox Gas Turbine**

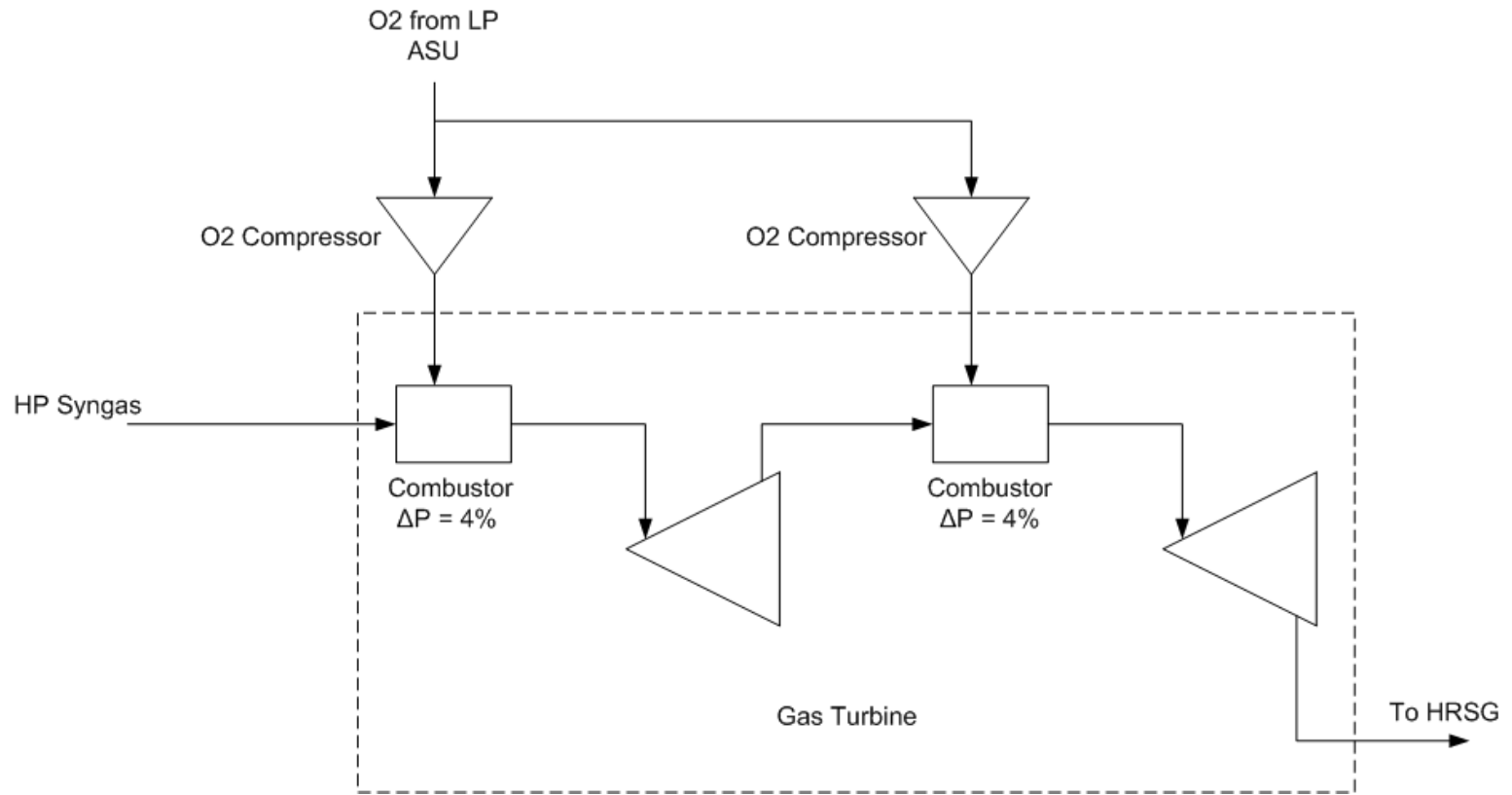


**Figure A1.4.1 - 9: POx Gas Turbine**

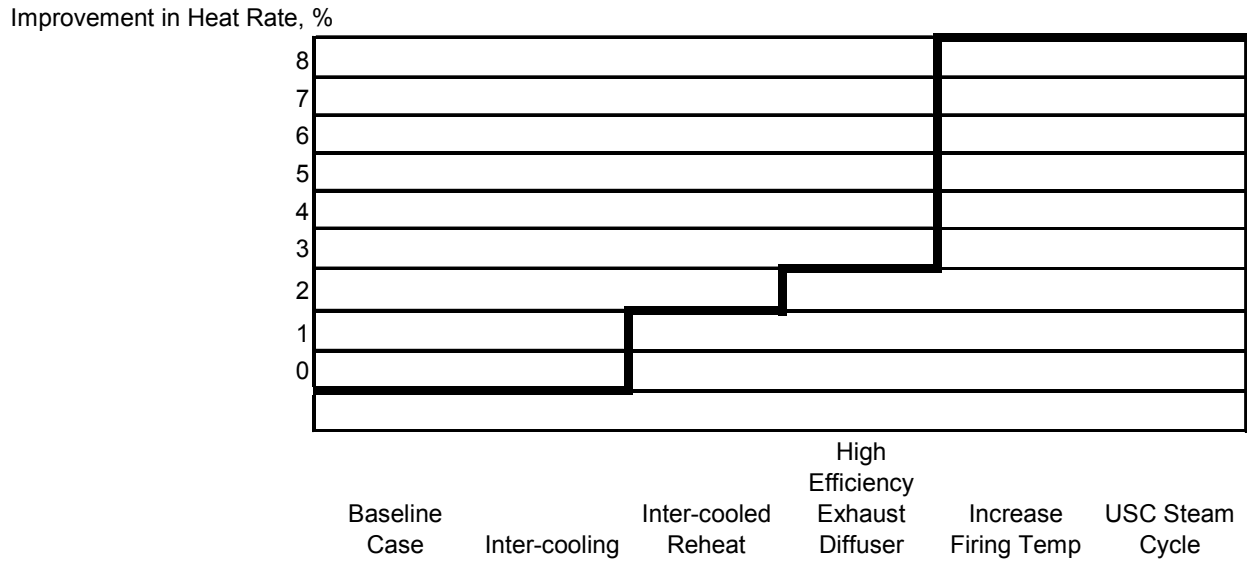


**Figure A1.4.1 - 10: Heat Rate Improvement due to Firing Temperature and Other Changes**

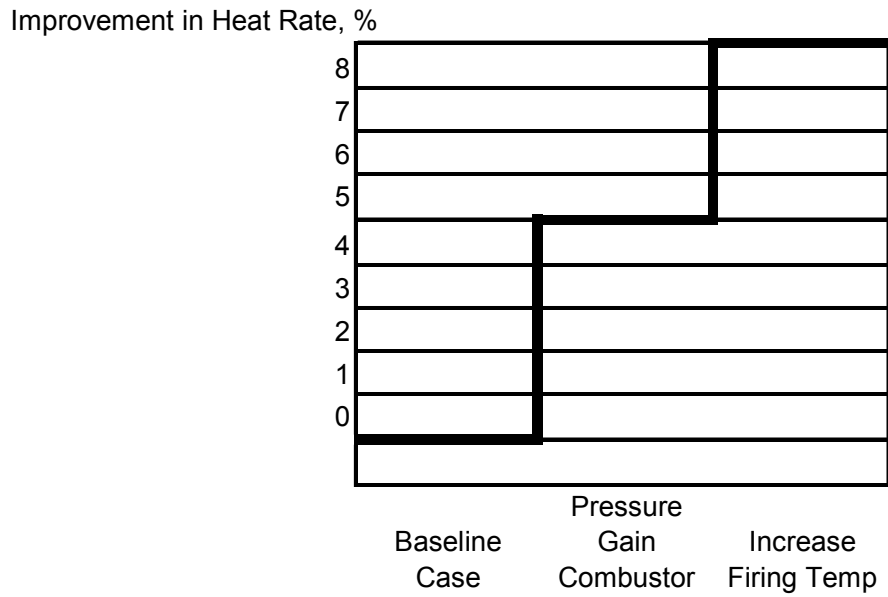


**Figure A1.4.1 - 11: Heat Rate Improvement due to Radically New Approaches**

## TASK 1.4.2: ADVANCED BRAYTON CYCLE DETAILED ANALYSIS

### SUMMARY

A detailed analysis is performed of the promising advanced cycles identified in the “Screening Analysis” Task 1.4.1. Sensitivity analysis is included for some of the cycles to quantify the effect of varying the cycle design parameters such that the ultimate goal of achieving the efficiency target for this study (about 8% improvement in heat rate over the Baseline Case which is equivalent to increasing the efficiency of a natural gas fired combined cycle from 60% to 65%) is met while minimizing the technological advancements required.

The following presents the performance summaries of the advanced cases developed up to this point in this study. Thermoflex was used to simulate the power block and Aspen Plus the balance of plant. The NO<sub>x</sub> estimates were developed for each case by modeling the primary and the dilution zones as Perfectly Stirred Reactors (PSRs) in series<sup>10</sup>. The Konnov Model<sup>11</sup> was utilized for the reaction mechanism and kinetics. It was determined that NO<sub>x</sub> continued to form at significant rate in the dilution zone due to the high temperatures for these advanced firing temperature cycles. A partial solution to reducing the NO<sub>x</sub> emission may be to limit the residence time in the dilution zone by constructing a short combustor. It was found that reducing the residence time from 30 ms to 5 ms reduced the NO<sub>x</sub> by as much as ~ 70% for the very high rotor inlet cases while the burnout of H<sub>2</sub>, CO and CH<sub>4</sub> was not affected significantly, the fuel being decarbonized syngas contains only small concentrations of CO and CH<sub>4</sub>. If a short combustor is utilized to minimize the residence time and thus limit the NO<sub>x</sub> formation, then natural gas as a backup fuel or startup cannot be considered. The gasification island will have to be started up first while flaring the syngas and then the gas turbine will have to be brought online.

### SIMPLE CYCLE GAS TURBINE IGCC WITH INCREASED FIRING TEMPERATURE

#### APPROACH

This is the first advanced cycle evaluated and consists of the steam-cooled gas turbine combined cycle with increased rotor inlet temperature (RIT) and blade surface temperature in a near zero emission gasification plant similar to the Baseline Case. The gas turbine itself has the simple cycle configuration as in the Baseline Case, i.e., without intercooling or reheat. The gas turbine firing temperature (1<sup>st</sup> rotor inlet temperature) required to realize about 8% improvement in heat rate over the Baseline Case is 1734°C or 3153°F (which is 342°C or 615°F above the Baseline Case) while increasing the blade surface temperatures by about the same amount over the Baseline Case (342°C or 615°F). This increase in the blade surface temperature is consistent

---

<sup>10</sup> Touchton, G. L., “An Experimentally Verified NO<sub>x</sub> Prediction Algorithm Incorporating the Effects of Steam Injection,” *Journal of Engineering for Gas Turbines and Power*, 1984, Vol. 106, 833-840.

<sup>11</sup> Konnov, A. A., “Detailed Reaction Mechanism for Small Hydrocarbons Combustion,” Release 0.5, <http://homepages.vub.ac.be/~akonnov/>, 2000.

with the projected values for advanced firing temperature and materials presented in Figure A1.4.2 - 1. The corresponding pressure ratio of the gas turbine while maintaining an exhaust temperature in the neighborhood of 650°C<sup>12</sup> or 1200°F is 50. The pressure ratio of 50 is significantly higher than what has been currently demonstrated but such a high pressure ratio has been proposed for an advanced aero engine (Pratt & Whitney's baseline engine proposed for Boeing's 787 transport plane). The maximum pressure ratio for a commercial land based gas turbine engine without intercooling is 36 (Rolls-Royce's Trent 60 with water injection). A lower pressure ratio case is thus also investigated (a pressure ratio of 37 which is close to that of the Trent 60) while letting the turbine exhaust temperature rise significantly above the 650°C constraint. Significantly higher steam superheat and reheat temperatures are required than those in the 50 pressure ratio case in order to limit the irreversibility in heat transfer to that in the Baseline Case.

Performances for cases utilizing higher operating pressure air separation units consistent with the higher pressure ratio gas turbines are also developed. In addition, configurations where no air is extracted from the gas turbine ("syngas gas turbine") are investigated to quantify the incentive for developing a gas turbine specifically designed for IGCC applications (i.e., unlike the currently offered gas turbines which are designed for natural gas and distillate fuels. Such "natural gas / distillate fuel gas turbines" are operated in off-design mode in IGCC applications such that air extraction is required to limit the increase in the gas turbine pressure ratio to stay within the surge margin of its compressor). The required air extraction expressed as a fraction of the compressor inlet air is increased as the gas turbine firing temperature is raised since the syngas fuel to air ratio to the combustor is higher. Thus, for these advanced firing temperature cases utilizing a "natural gas gas-turbine," as much as 20% of the air (expressed as a percentage of the compressor inlet air) is extracted while only 14% is extracted in the Baseline Cases.

The following lists the various cases investigated:

- Gas turbine with a pressure ratio of 37
  - No air extraction.
  - Air extraction Sensitivity Case while utilizing an ASU operating at a pressure currently demonstrated (Intermediate Pressure or IP ASU).
  - Air extraction Sensitivity Case while utilizing a HP ASU such that the extracted air is supplied to the cryogenic unit at full pressure, i.e., without first reducing its pressure in a turboexpander.
  
- Gas turbine with a pressure ratio of 50
  - No air extraction.
  - Air extraction Sensitivity Case while utilizing an ASU operating at a pressure currently demonstrated (IP ASU).

---

<sup>12</sup> such that strength in the roots of the long and uncooled last stage blades is maintained. Furthermore, use of advanced superheat and reheat steam temperatures of 613°C or 1135°F for the bottoming cycle is facilitated without having very large temperature differences between the gas turbine exhaust and the steam such that the irreversibility in heat transfer is limited to that in the Baseline Case.

- Air extraction Sensitivity Case while utilizing a HP ASU such that the extracted air is supplied to the cryogenic unit at full pressure, i.e., without first reducing its pressure in a turboexpander.

The overall block flow diagrams depicting the overall plant configuration for these cases are presented in Figure A1.4.2 - 2 through A1.4.2 – 7.

## **PROCESS DESCRIPTION**

Process description for the case with the 50 pressure ratio gas turbine, IP ASU and no extraction air is presented in the following.

### **Air Separation Unit and N<sub>2</sub> Preheat**

The primary purpose of the ASU is to supply high pressure, high purity O<sub>2</sub> (at a nominal 95 mole %) to the Gasification unit. Figure A1.4.2 - 8 depicts the main features of this unit. For the purpose of computer simulation, the ASU has been modeled as two separate sections: An elevated pressure (EP) section which provides compressed air to the cold box operating at elevated pressure, and a low pressure (LP) section which provides compressed air to the cold box operating at lower pressure. This ASU set up with an EP and LP section provides a valid approximation for the performance of an ASU providing oxygen and nitrogen to an IGCC facility in which only a fraction of the entire amount of N<sub>2</sub> available from the ASU is required at pressure for gas turbine injection. The actual design of the ASU will be determined by the ASU vendor. The EP section produces the N<sub>2</sub> which is sent to the gas turbine. The Sulfur Recovery unit also consumes a small quantity of O<sub>2</sub>. O<sub>2</sub> and N<sub>2</sub> in air are separated by means of cryogenic distillation. Approximately 60% of the N<sub>2</sub> separated from the air leaves the distillation unit at pressure and is compressed and injected into the gas turbines for NO<sub>x</sub> emissions control as well as providing additional motive fluid.

For both the EP and LP section, ambient air is sent through a filter to remove dust and other particulate matter and then compressed before providing the air to the “cold box.” Interstage cooling and after-cooling of the compressor is accomplished with cooling water. For the EP section, a portion of the N<sub>2</sub> stream produced in the cold box is compressed, preheated and provided to the gas turbine to provide the thermal diluent for NO<sub>x</sub> control within the combustor of the gas turbine as well as provide extra motive fluid for expansion in the turbine.

The compressed air is treated to remove moisture, CO<sub>2</sub> and any hydrocarbons present. This air pretreatment system consists of two molecular sieve vessels. The vessels are operated in a staggered cycle: while one vessel is being used to filter the compressed air, the other is regenerated with the waste N<sub>2</sub> stream from the distillation columns. The waste N<sub>2</sub> is heated to the required regeneration temperature with medium pressure (MP) steam. The clean, dry air is liquefied utilizing a combination of chilling, feed/effluent heat exchange, compression and turbo-expansion. The expander may be compressor loaded or generator loaded. A multi-column system separates the liquefied air into a high purity N<sub>2</sub> stream and a high purity O<sub>2</sub> stream. This cold box is modeled as a separator such that the inlet and outlet stream conditions are consistent with data provided by an air separation unit vendor in the past. Current designs for the cold box consist of pumped liquid O<sub>2</sub> systems to avoid buildup of hydrocarbons within the cold box which

could lead to a hazardous situation. The overall performance of the ASU consisting of a pumped liquid O<sub>2</sub> system, however, is similar to that of the system modeled in Aspen for this study.

The O<sub>2</sub> stream required by the gasifier and the N<sub>2</sub> stream provided to the gas turbine are compressed in multistage intercooled compressors. The N<sub>2</sub> serves the purpose of a thermal diluent in the gas turbine combustor for NO<sub>x</sub> control and it also increases the motive fluid for expansion. It is preheated to a temperature of 288°C against HP and high temperature boiler feed water (BFW) extracted from the HRSG located in the power block before it is injected into the gas turbine combustor. The resulting cooler HP BFW is pumped back to the power block.

### **Coal Receiving and Handling Unit**

Refer to the Baseline Case process description in section titled “Task 1.3: First Detailed Systems Study Analysis - Baseline Case” for the description and block flow diagram for this unit.

### **Gasification Unit**

Refer to the Baseline Case process description in section titled “Task 1.3: First Detailed Systems Study Analysis - Baseline Case” for the description and process flow diagram for this unit.

### **CO Shift / Low Temperature Gas Cooling Unit**

Refer to the Baseline Case process description in section titled “Task 1.3: First Detailed Systems Study Analysis - Baseline Case” for the description for this unit. The process flow diagram for this case is depicted in Figure A1.4.2 - 9.

### **Acid Gas Removal Unit (Selexol®)**

Refer to the Baseline Case process description in section titled “Task 1.3: First Detailed Systems Study Analysis - Baseline Case” for the description and block flow diagram for this unit.

### **Syngas Humidification Unit**

Refer to the Baseline Case process description in section titled “Task 1.3: First Detailed Systems Study Analysis - Baseline Case” for the description for this unit. The process flow diagram for this case is depicted in Figure A1.4.2 - 10.

### **CO<sub>2</sub> Compression / Dehydration Unit**

Refer to the Baseline Case process description in section titled “Task 1.3: First Detailed Systems Study Analysis - Baseline Case” for the description and process flow diagram for this unit.

## **Sulfur Recovery / Tail Gas Treating Unit**

Refer to the Baseline Case process description in section titled “Task 1.3: First Detailed Systems Study Analysis - Baseline Case” for the description for this unit. The process flow diagram for this case is depicted in Figure A1.4.2 - 11.

## **Power Block**

The process scheme for the combined-cycle power block consists of the advanced firing temperature gas turbine with the pressure ratio of 50 supporting a reheat steam turbine. The process flow diagram for this unit is depicted in Figure A1.4.2 - 12. The overall integration of the steam system between the Power Block and the balance of the IGCC plant is shown on the Steam Balance Diagram Figure A1.4.2 - 13.

The power block consists of the following major systems:

- Gas Turbine
- Heat Recovery Steam Generator (HRSG)
- Steam Turbine and the associated Vacuum Condensate System
- Integral Deaerator
- Blowdown System
- Miscellaneous Supporting Facilities:
  - boiler chemical injection
  - demineralized water package.

The performance of the advanced gas turbine operating on the decarbonized syngas was developed utilizing Thermoflex.

Ambient air is drawn into the gas turbine air compressor via a filter to remove air-borne particulates, especially those that are larger than 10 microns. The humidified fuel gas and compressed air are mixed and combusted in the turbine. The preheated nitrogen is injected into the turbine through separate nozzles for NO<sub>x</sub> control. The combined LHV of the humid syngas and diluent nitrogen is 4,720 kJ/nm<sup>3</sup> or 120 Btu/scf..

The hot gas turbine exhaust flows through a customized Heat Recovery Steam Generator (HRSG). The HRSG consists basically of the following sub-systems:

- LP steam
- HP steam
- Reheat steam

In addition to these sub-systems, the HRSG is integrated with the rest of the IGCC plant. The HRSG has its own stack, which is equipped with a continuous emissions monitoring system (CEMS).

### LP Steam System

Low temperature heat is recovered from the syngas generation / processing units (Process) by heating the vacuum cold condensate from the surface condenser + makeup BFW. The makeup BFW is sprayed directly into the surface condenser and the combined stream of the cold vacuum condensate + makeup is drawn from the Surface Condenser by the Vacuum Condensate Pump and is sent to the vacuum condensate heaters in the Low Temperature Gas Cooling Unit and Black Water Flash section of the Gasification Unit to recover the low temperature heat. The hot vacuum condensate is further heated in the LP Economizer in the HRSG.

The hot vacuum condensate is combined with LP Condensate returning from the Gasification Unit and is supplied as BFW to the LP Steam Drum in the HRSG. The saturated steam from the LP Steam Drum is mixed with the saturated LP steam produced in the Process units. The combined flow is sent through the LP Superheater coils in the HRSG and then is fed to the LP section of the Steam Turbine.

The LP Feed Water Booster Pump sends heated BFW from the LP steam drum to the Process users in the Syngas plant.

### BFW Pump

The main BFW pump of the HRSG supplies both IP and HP BFW to the IP and HP steam systems as well as makeup to the CO Shift/LTGC unit. It is a multistage centrifugal pump, with intermediate bleeds to support the IP steam system and supply the makeup. The discharge pressure of the BFW pump is dictated by the design conditions set at the inlet of the steam turbine.

### IP Steam System

The IP BFW is taken from a bleed off of the main BFW Feed pump. The makeup water for the syngas humidifier is taken from the IP bleed before the economizer. The IP BFW is routed to the IP Steam Generators in the CO Shift/LTGC unit and the Sulfur Recovery Unit. The surplus IP steam from other process units merges with the reheat steam system.

### HP Steam System

The discharge from the main BFW Feed pump is mixed with the HP boiler feed water returning from the Fuel Gas and Nitrogen heaters before it flows through two HP Economizers in the HRSG. The HP BFW Circulating pump sends part of the preheated HP boiler feed water exiting the first HP Economizer to the Fuel Gas and Nitrogen heaters.

A portion of the preheated HP BFW is routed to the HP Steam Generator in the CO Shift/LTGC unit and the HP Waste Heat Boiler in the Sulfur Recovery Unit and the remainder is fed to the HP Steam drum. Saturated HP steam generated in the HP steam drum mixes with surplus HP steam from other process units and then is superheated in HP Superheater coils within the HRSG. The superheated HP steam from the HRSG is sent to the inlet of the steam turbine.

A small portion of the main BFW Feed pump discharge is used as attemperator water for the control of the temperature of the superheated steam.

### Reheat Steam System

To improve the efficiency of the combined-cycle, the exit steam from the HP section of the steam turbine is returned to the HRSG to raise its temperature by absorbing additional heat. This reheated steam is combined with the IP steam from the syngas production plant, superheated to approximately the same temperature as the HP steam, and then is fed to the inlet of the IP section of the steam turbine.

### Gas Turbine Cooling

The 1<sup>st</sup> and 2<sup>nd</sup> stages of the gas turbine stator and rotating blades are cooled with steam taken from the HP steam turbine exhaust. The steam returning from this closed circuit cooling of the gas turbine is mixed with the IP steam before it enters the reheater coils in the HRSG.

### Deaerator

An integrated LP steam drum/deaerator is provided in the HRSG. This eliminates the need for an external deaerator. The deaerator removes any dissolved gases such as O<sub>2</sub> and CO<sub>2</sub> in the feed water by using LP steam in the steam drum as the stripping medium. The pressure in the LP Steam Drum is controlled by varying the amount of steam vented with the dissolved gases.

### Blowdown System

The steam drums of the HRSG are continuously purged to control the amount of built-up of dissolved solids. The continuous blowdown is routed to the Continuous Blowdown drum. Flash steam in the Continuous Blowdown drum is sent to the LP steam drum and the saturated water is letdown into the Intermittent Blowdown drum. Whenever required, blowdown from each steam drum in the HRSG system can be routed directly to the Intermittent Blowdown drum. Flash steam from the Intermittent Blowdown drum is vented to atmosphere and the liquid collected in Blowdown Sump.

### Steam Turbine

The inlet pressure of the HP section of the steam turbine is set at 166.5 bara. The exhaust from the LP section is set at a vacuum of 0.044 bara. The surface condenser uses circulating cooling water from the cooling towers as the cooling medium while the makeup water for the steam system is added to the well of the condenser.

### Demineralized Water System

Demineralized water system consists of mixed-bed exchangers, one in operation and one in stand-by, filled with cation/anion resins, with internal-type regeneration. The package includes facilities for resin bed regeneration, chemical storage and neutralization basin.

## **General Facilities**

Refer to the Baseline Case process descriptions in the section titled “Task 1.3: First Detailed Systems Study Analysis - Baseline Case” for the description and process flow diagram for this unit.

The stream data for this case are presented in Table A1.4.2 - 1.

## **RESULTS AND DISCUSSION**

The overall system performances for these above described cases along with that for the Baseline Case is presented in Table A1.4.2 -2. Table A1.4.2 - 3 summarizes the auxiliary power consumption within the plant while Table A1.4.2 - 4 summarizes the main features of the power cycle for these cases.

The following summarizes the results:

- The advanced firing temperature cases (342°C or 615°F above the Baseline Case) show a 7 to 9% improvement in overall plant heat rate over the Baseline Case.
- The improvement in plant heat rate utilizing a HP ASU over an IP ASU is quite small, less than 1% (subject to verification of the HP ASU performance estimates by an ASU vendor).
- The improvement in plant heat rate utilizing a “syngas gas turbine” is more significant, especially for the 50 pressure ratio gas turbine case. This result is to be expected since as the gas turbine pressure ratio is increased, there is also an increase in the irreversibility associated with (1) adiabatic compression and followed by (2) cooling before the air can be used in the ASU.
- Comparing the performance of the 37 and 50 pressure ratio gas turbine cases, the plant heat rates are quite similar when extracting air from the gas turbine for the ASU. The difference in overall plant heat rate becomes significant, however, for the syngas turbine cases (i.e., without air extraction), the 50 pressure ratio case showing a better overall plant performance.
- The estimated NO<sub>x</sub> emissions for the 37 and 50 pressure ratio gas turbine cases are 183 and 251 ppmVd (15% O<sub>2</sub> basis) respectively while that estimated for the Baseline Case is 18 ppmVd (15% O<sub>2</sub> basis) when utilizing combustors of the non-premixed type and maintaining a residence time of 30 ms in the dilution zone. These significant increases in the NO<sub>x</sub> emissions are primarily due to (1) the increase in the flame temperature caused by the increase in the combustion air temperature which increases as the gas turbine pressure ratio increases as well as due to (2) temperatures remaining high in the quench section of the combustor caused by the low air to fuel ratio which is required to achieve the higher firing. The estimated NO<sub>x</sub> emissions for the 37 and 50 pressure ratio gas

turbine cases are 50 and 67 ppmVd (15% O<sub>2</sub> basis) respectively when the residence time is reduced to 5 ms in the dilution zone.

## **CONCLUSIONS**

It may be concluded from the above results that substantial increases in both firing temperature and blade surface temperature are required over the Baseline Case, about 342°C or 615°F to meet the performance improvement goals of this study. Significant increases in gas turbine pressure ratio are also required to limit the exhaust temperature. Incorporation of aero-derivative compressor design including materials to withstand the higher air temperatures within the compressor would be required for such high pressure ratio gas turbines.

For these very high firing temperature cases advanced low NO<sub>x</sub> combustor designs described under Task 1.4.1 may not suffice since the air to fuel ratio is too small to cause rapid quenching of the flame within the combustor to limit the formation of NO<sub>x</sub>. More diluent addition and/or SCRs would be required to limit the NO<sub>x</sub> emissions to the desired 2 ppmVd (15% O<sub>2</sub> basis) value. Higher SCR catalyst volume would be required for these advanced firing temperature cases, however, since the amount of NO<sub>x</sub> generated within the combustor is substantially higher than that in the Baseline Case. A correspondingly higher pressure drop across the SCR would result making the heat rate penalty a little more significant than that seen in the sensitivity case developed for the Baseline Case in Task 1.3.

In addition to the NO<sub>x</sub> being higher for the gas turbine with a pressure ratio of 50 as compared to the gas turbine with a pressure ratio of 37, a major challenge associated with developing such a gas turbine with a pressure ratio of 50 is the design of the compressor and its materials. On the other hand, in the case of a gas turbine operating at a pressure ratio of 37 and with the required advanced firing temperature, major challenges are associated with the design of the last section of the turbine since this section of the turbine operates at significantly higher temperatures. Furthermore, a steam turbine also capable of operating at significantly high temperatures is required. More expensive superheater and reheater coils in the HRSG and the piping between the HRSG and the steam turbine would be required due to the higher grade metallurgical requirements.

## **INTERCOOLED GAS TURBINE IGCC WITH INCREASED FIRING TEMPERATURE**

### **APPROACH**

This case investigates the effect of including an intercooler in the high firing temperature / high pressure ratio gas turbines. The advantages / disadvantages of intercooling are:

- Lower compressor discharge temperature
  - Savings in materials of construction
  - Lower NO<sub>x</sub>
- Higher specific power output

- Reduced compressor work (in a simple cycle gas turbine, approximately half of turbine power is used in compression)
- But more complex turbomachinery
  - Multi-spool engine

The following lists the cases investigated:

- Gas turbine with a pressure ratio of 50
  - No air extraction.
  - Air extraction Sensitivity Case while utilizing a HP ASU such that the extracted air is supplied to the cryogenic unit at full pressure, i.e., without first reducing its pressure in a turboexpander..
- Gas turbine with a pressure ratio of 70 (and no air extraction) to determine if a significant advantage exists for the overall plant performance at this very high pressure ratio since advantages of intercooling from a cycle efficiency standpoint are realized at high pressure ratios.

There are two choices for the type of intercooler:

- Shell and tube
- Spray type (as used in the GE LM6000 SPRINT engine)

An evaluation of the two types of intercoolers along with its location in the compressor from a cycle thermal efficiency standpoint was made for the gas turbine case with overall pressure ratio of 50. As can be seen from the plots presented in Figure A1.4.2 - 14, the cycle efficiency is higher with the spray intercooler. Other advantages for the spray type intercooler over the shell and tube type are listed below:

- Lower equipment cost
- Lower equipment footprint
- Spray adds motive fluid for expansion in the turbine and thermal diluent for reducing the NO<sub>x</sub> formation

The spray intercooler does need high quality spray water and the spray system needs to be carefully designed to minimize any large droplet carryover into the HP compressor in order to avoid impingement and erosion of the compressor blades. The compression pressure ratio (i.e., that of the low pressure compressor) chosen for locating this intercooler is 2.75. The thermal efficiency is increased but only slightly as this pressure ratio is decreased below 2.75 but the other advantages of spray intercooling listed above are compromised.

These advanced cycles again consist of the steam-cooled gas turbine combined cycle with the increased rotor inlet temperature (RIT) and blade surface temperature similar to the previous advanced case except for the intercooler. The direct contact intercooling utilizes steam condensate sprayed into the air stream. The corresponding gas turbine exhaust temperature is 660°C (1220°F) for the pressure ratio of 50 while that for 70 overall pressure ratio case has an exhaust temperature of 597°C (1170°F) at the ISO operating point.

The overall block flow diagram depicting the overall plant configuration for these cases is presented in Figure A1.4.2 - 15 and Figure A1.4.2 - 16.

## **PROCESS DESCRIPTION**

Process description for the case with the intercooled 50 pressure ratio gas turbine, IP ASU and no extraction air is presented in the following.

### **Air Separation Unit and N<sub>2</sub> Preheat**

The primary purpose of the ASU is to supply high pressure, high purity O<sub>2</sub> (at a nominal 95 mole %) to the Gasification unit. Figure A1.4.2 - 8 depicts the main features of this unit. For the purpose of computer simulation, the ASU has been modeled as two separate sections: An elevated pressure (EP) section which provides compressed air to the cold box operating at elevated pressure, and a low pressure (LP) section which provides compressed air to the cold box operating at lower pressure. This ASU set up with an EP and LP section provides a valid approximation for the performance of an ASU providing oxygen and nitrogen to an IGCC facility in which only a fraction of the entire amount of N<sub>2</sub> available from the ASU is required at pressure for gas turbine injection. The actual design of the ASU will be determined by the ASU vendor. The EP section produces the N<sub>2</sub> which is sent to the gas turbine. The Sulfur Recovery unit also consumes a small quantity of O<sub>2</sub>. O<sub>2</sub> and N<sub>2</sub> in air are separated by means of cryogenic distillation. Approximately 60% of the N<sub>2</sub> separated from the air leaves the distillation unit at pressure and is compressed and injected into the gas turbines for NO<sub>x</sub> emissions control as well as providing additional motive fluid.

For both the EP and LP section, ambient air is sent through a filter to remove dust and other particulate matter and then compressed before providing the air to the “cold box.” Interstage cooling and after-cooling of the compressor is accomplished with cooling water. For the EP section, a portion of the N<sub>2</sub> stream produced in the cold box is compressed, preheated and provided to the gas turbine to provide the thermal diluent for NO<sub>x</sub> control within the combustor of the gas turbine as well as provide extra motive fluid for expansion in the turbine.

The compressed air is treated to remove moisture, CO<sub>2</sub> and any hydrocarbons present. This air pretreatment system consists of two molecular sieve vessels. The vessels are operated in a staggered cycle: while one vessel is being used to filter the compressed air, the other is regenerated with the waste N<sub>2</sub> stream from the distillation columns. The waste N<sub>2</sub> is heated to the required regeneration temperature with medium pressure (MP) steam. The clean, dry air is liquefied utilizing a combination of chilling, feed/effluent heat exchange, compression and turbo-expansion. The expander may be compressor loaded or generator loaded. A multi-column system separates the liquefied air into a high purity N<sub>2</sub> stream and a high purity O<sub>2</sub> stream. This cold box is modeled as a separator such that the inlet and outlet stream conditions are consistent with data provided by an air separation unit vendor in the past. Current designs for the cold box consist of pumped liquid O<sub>2</sub> systems to avoid buildup of hydrocarbons within the cold box which could lead to a hazardous situation. The overall performance of the ASU consisting of a pumped liquid O<sub>2</sub> system, however, is similar to that of the system modeled in Aspen for this study.

The O<sub>2</sub> stream required by the gasifier and the N<sub>2</sub> stream provided to the gas turbine are compressed in multistage intercooled compressors. The N<sub>2</sub> serves the purpose of a thermal diluent in the gas turbine combustor for NO<sub>x</sub> control and it also increases the motive fluid for expansion. It is preheated to a temperature of 288°C against HP and high temperature boiler feed water (BFW) extracted from the HRSG located in the power block before it is injected into the gas turbine combustor. The resulting cooler HP BFW is pumped back to the power block.

### **Coal Receiving and Handling Unit**

Refer to the Baseline Case process description in section titled “Task 1.3: First Detailed Systems Study Analysis - Baseline Case” for the description and block flow diagram for this unit.

### **Gasification Unit**

Refer to the Baseline Case process description in section titled “Task 1.3: First Detailed Systems Study Analysis - Baseline Case” for the description and process flow diagram for this unit.

### **CO Shift / Low Temperature Gas Cooling Unit**

Refer to the Baseline Case process description in section titled “Task 1.3: First Detailed Systems Study Analysis - Baseline Case” for the description for this unit. The process flow diagram for this case is depicted in Figure A1.4.2 - 9.

### **Acid Gas Removal Unit (Selexol®)**

Refer to the Baseline Case process description in section titled “Task 1.3: First Detailed Systems Study Analysis - Baseline Case” for the description and block flow diagram for this unit.

### **Syngas Humidification Unit**

Refer to the Baseline Case process description in section titled “Task 1.3: First Detailed Systems Study Analysis - Baseline Case” for the description for this unit. The process flow diagram for this case is depicted in Figure A1.4.2 - 10.

### **CO<sub>2</sub> Compression / Dehydration Unit**

Refer to the Baseline Case process description in section titled “Task 1.3: First Detailed Systems Study Analysis - Baseline Case” for the description and process flow diagram for this unit.

## **Sulfur Recovery / Tail Gas Treating Unit**

Refer to the Baseline Case process description in section titled “Task 1.3: First Detailed Systems Study Analysis - Baseline Case” for the description for this unit. The process flow diagram for this case is depicted in Figure A1.4.2 - 11.

## **Power Block**

The process scheme for the combined-cycle power block consists of the advanced firing temperature intercooled gas turbine with the pressure ratio of 70 supporting a reheat steam turbine. The process flow diagram for this unit is depicted in Figure A1.4.2 - 17. The overall integration of the steam system between the Power Block and the balance of the IGCC plant is shown on the Steam Balance Diagram, Figure A1.4.2 - 18.

The power block consists of the following major systems:

- Intercooled Gas Turbine
- Heat Recovery Steam Generator (HRSG)
- Steam Turbine and the associated Vacuum Condensate System
- Integral Deaerator
- Blowdown System
- Miscellaneous Supporting Facilities:
  - boiler chemical injection
  - demineralized water package.

The performance of the advanced gas turbine operating on the decarbonized syngas was developed utilizing Thermoflex.

Ambient air is drawn into the gas turbine air compressor via a filter to remove air-borne particulates, especially those that are larger than 10 microns. A direct contact spray cooler utilizing steam condensate provides intercooling. The humidified fuel gas and compressed air are mixed and combusted in the turbine. The preheated nitrogen is injected into the turbine through separate nozzles for NO<sub>x</sub> control. The combined LHV of the humid syngas and diluent nitrogen is 4,720 kJ/nm<sup>3</sup> or 120 Btu/scf.

The hot gas turbine exhaust flows through a customized Heat Recovery Steam Generator (HRSG). The HRSG consists basically of the following sub-systems:

- LP steam
- HP steam
- Reheat steam

In addition to these sub-systems, the HRSG is integrated with the rest of the IGCC plant. The HRSG has its own stack, which is equipped with a continuous emissions monitoring system (CEMS).

## LP Steam System

Low temperature heat is recovered from the syngas generation / processing units (Process) by heating the vacuum cold condensate from the surface condenser + makeup BFW. The makeup BFW is sprayed directly into the surface condenser and the combined stream of the cold vacuum condensate + makeup is drawn from the Surface Condenser by the Vacuum Condensate Pump and is sent to the vacuum condensate heaters in the Low Temperature Gas Cooling Unit and Black Water Flash section of the Gasification Unit to recover the low temperature heat. The hot vacuum condensate is further heated in the LP Economizer in the HRSG.

The hot vacuum condensate is combined with LP Condensate returning from the Gasification Unit and is supplied as BFW to the LP Steam Drum in the HRSG. The saturated steam from the LP Steam Drum is mixed with the saturated LP steam produced in the Process units. The combined flow is sent through the LP Superheater coils in the HRSG and then is fed to the LP section of the Steam Turbine.

The LP Feed Water Booster Pump sends heated BFW from the LP steam drum to the Process users in the Syngas plant.

### BFW Pump

The main BFW pump of the HRSG supplies both IP and HP BFW to the IP and HP steam systems as well as makeup to the CO Shift/LTGC unit. It is a multistage centrifugal pump, with intermediate bleeds to support the IP steam system and supply the makeup. The discharge pressure of the BFW pump is dictated by the design conditions set at the inlet of the steam turbine.

## IP Steam System

The IP BFW is taken from a bleed off of the main BFW Feed pump. The makeup water for the syngas humidifier is taken from the IP bleed before the economizer. The IP BFW is routed to the IP Steam Generators in the CO Shift/LTGC unit and the Sulfur Recovery Unit. The surplus IP steam from other process units merges with the reheat steam system.

## HP Steam System

The discharge from the main BFW Feed pump is mixed with the HP boiler feed water returning from the Fuel Gas and Nitrogen heaters before it flows through two HP Economizers in the HRSG. The HP BFW Circulating pump sends part of the preheated HP boiler feed water exiting the first HP Economizer to the Fuel Gas and Nitrogen heaters.

A portion of the preheated HP BFW is routed to the HP Steam Generator in the CO Shift/LTGC unit and the HP Waste Heat Boiler in the Sulfur Recovery Unit and the remainder is fed to the HP Steam drum. Saturated HP steam generated in the HP steam drum mixes with surplus HP steam from other process units and then is superheated in HP Superheater coils within the HRSG. The superheated HP steam from the HRSG is sent to the inlet of the steam turbine.

A small portion of the main BFW Feed pump discharge is used as attemperator water for the control of the temperature of the superheated steam.

### Reheat Steam System

To improve the efficiency of the combined-cycle, the exit steam from the HP section of the steam turbine is returned to the HRSG to raise its temperature by absorbing additional heat. This reheated steam is combined with the IP steam from the syngas production plant, superheated to approximately the same temperature as the HP steam, and then is fed to the inlet of the IP section of the steam turbine.

### Gas Turbine Cooling

The 1<sup>st</sup> and 2<sup>nd</sup> stages of the gas turbine stator and rotating blades are cooled with steam taken from the HP steam turbine exhaust. The steam returning from this closed circuit cooling of the gas turbine is mixed with the IP steam before it enters the reheater coils in the HRSG.

### Deaerator

An integrated LP steam drum/deaerator is provided in the HRSG. This eliminates the need for an external deaerator. The deaerator removes any dissolved gases such as O<sub>2</sub> and CO<sub>2</sub> in the feed water by using LP steam in the steam drum as the stripping medium. The pressure in the LP Steam Drum is controlled by varying the amount of steam vented with the dissolved gases.

### Blowdown System

The steam drums of the HRSG are continuously purged to control the amount of built-up of dissolved solids. The continuous blowdown is routed to the Continuous Blowdown drum. Flash steam in the Continuous Blowdown drum is sent to the LP steam drum and the saturated water is letdown into the Intermittent Blowdown drum. Whenever required, blowdown from each steam drum in the HRSG system can be routed directly to the Intermittent Blowdown drum. Flash steam from the Intermittent Blowdown drum is vented to atmosphere and the liquid collected in Blowdown Sump.

### Steam Turbine

The inlet pressure of the HP section of the steam turbine is set at 166.5 bara. The exhaust from the LP section is set at a vacuum of 0.044 bara. The surface condenser uses circulating cooling water from the cooling towers as the cooling medium while the makeup water for the steam system is added to the well of the condenser.

### Demineralized Water System

Demineralized water system consists of mixed-bed exchangers, one in operation and one in stand-by, filled with cation/anion resins, with internal-type regeneration. The package includes facilities for resin bed regeneration, chemical storage and neutralization basin.

## **General Facilities**

Refer to the Baseline Case process descriptions in the section titled “Task 1.3: First Detailed Systems Study Analysis - Baseline Case” for the description and process flow diagram for this unit.

The stream data for this case are presented in Table A1.4.2 – 5.

## **RESULTS AND DISCUSSION**

Table A1.4.2 - 6 shows the overall system efficiency, coal (HHV) to power for these above described cases along with those for the Baseline Case. Table A1.4.2 - 7 summarizes the auxiliary power consumption within the plant while Table A1.4.2 - 8 summarizes the main features of the power cycle for these cases.

The following summarizes the results:

- The overall plant heat rates for these advanced firing temperature cases with intercooling are similar to those of the previous advanced cases without intercooling and show similar improvements in overall plant heat rate over the Baseline Case.
- The efficiency gain for the intercooled case with an overall pressure ratio of 70 is very small over the case with the 50 pressure ratio.
- The penalty associated with extracting air (for an HP ASU) from the 50 pressure ratio intercooled case is not as significant as in the corresponding non-intercooled cases. This result is to be expected since the intercooler makes the compression process more efficient by reducing the required work.
- Comparing the intercooled case to the previous non-intercooled case at an overall pressure ratio of 50, a substantial decrease in the compressor discharge temperature of 136°C (or 246°F) is realized for the intercooled case.
- The estimated NO<sub>x</sub> emissions for the 50 and 70 pressure ratio gas turbine cases are 166 and 231 ppmVd (15% O<sub>2</sub> basis) respectively while that estimated for the Baseline Case is 18 ppmVd (15% O<sub>2</sub> basis) when utilizing combustors of the non-premixed type and maintaining a residence time of 30 ms in the dilution zone. These NO<sub>x</sub> emissions are lower than the previous advanced non-intercooled case due to (1) the lower the flame temperature caused by the decrease in the combustion air temperature, a result of intercooling, and due to (2) additional thermal diluent being introduced via the spray intercooler. The estimated NO<sub>x</sub> emissions for the 50 and 70 pressure ratio gas turbine cases are 42 and 56 ppmVd (15% O<sub>2</sub> basis) respectively when the residence time is reduced to 5 ms in the dilution zone.

## CONCLUSIONS

From the results of this analysis, it may be concluded that incorporation of intercooling into these very high pressure ratio gas turbines is a very desirable feature although challenges associated with developing the gas turbine with the required high firing temperature and pressure ratio remain. Similar to the previous non-intercooled advanced case, substantial increases in both firing temperature and blade surface temperature are required over the Baseline Case, about 342°C or 615°F to meet the performance improvement goals of this study. Incorporation of aero-derivative compressor design would be required for such high pressure ratio gas turbines.

Again, advanced low NO<sub>x</sub> combustor designs described under Task 1.4.1 may not suffice since the air to fuel ratio is too small to cause rapid quenching of the flame within the combustor to limit the formation of NO<sub>x</sub>. More diluent addition may be a challenge for the combustor design since the O<sub>2</sub> content of the combustor exhaust gas is already very low at 1.6% for the 50 pressure ratio case and slightly higher at 2.1% for the 70 pressure ratio case. SCRs would be required to limit the NO<sub>x</sub> emissions to the desired 2 ppmVd (15% O<sub>2</sub> basis) value. Higher SCR catalyst volume would be required for these advanced firing temperature cases, however, since the amount of NO<sub>x</sub> generated within the combustor is substantially higher than that in the Baseline Case. A correspondingly higher pressure drop across the SCR would result making the heat rate penalty a little more significant than that seen in the sensitivity case developed for the Baseline Case in Task 1.3.

The developmental challenges of this intercooled advanced gas turbine are similar to the previous case with respect to the need for very high firing and blade surface temperatures. The next set of advanced cases to be evaluated consist of a reheat gas turbine in order to reduce the firing temperature as explained under Task 1.4.1 while maintaining a similar heat rate improvement goal over the Baseline Case.

## INTERCOOLED-REHEAT GAS TURBINE IGCC WITH INCREASED FIRING TEMPERATURE

### APPROACH

This advanced cycle investigates the addition of reheat to the intercooled gas turbine with an overall pressure ratio of 70. This higher pressure ratio is chosen in order to limit the exhaust temperature while obtaining a reasonable pressure ratio for the HP turbine located between the HP and reheat combustors. The direct contact spray intercooler is selected due to its advantages over a shell and tube intercooler as discussed in the previous section. The gas turbine firing temperatures (1<sup>st</sup> rotor inlet temperature of the HP and the LP turbines downstream of the HP and the reheat combustors, respectively) are increased above the Baseline Case just enough to meet the heat rate improvement target set for this study. The following summarizes the main features of this gas turbine:

- Pressure ratio of 70
- Spray intercooled
- Reheat combustion
- No air extraction
- N<sub>2</sub> returned from an IP ASU.

The overall block flow diagram depicting the overall plant configuration for this case is presented in Figure A1.4.2 - 19.

## **PROCESS DESCRIPTION**

Process description for this case with the 70 pressure ratio intercooled-reheat gas turbine, IP ASU and no extraction air is presented in the following.

### **Air Separation Unit and N<sub>2</sub> Preheat**

The primary purpose of the ASU is to supply high pressure, high purity O<sub>2</sub> (at a nominal 95 mole %) to the Gasification unit. Figure A1.4.2 - 20 depicts the main features of this unit. For the purpose of computer simulation, the ASU has been modeled as two separate sections: An elevated pressure (EP) section which provides compressed air to the cold box operating at elevated pressure, and a low pressure (LP) section which provides compressed air to the cold box operating at lower pressure. This ASU set up with an EP and LP section provides a valid approximation for the performance of an ASU providing oxygen and nitrogen to an IGCC facility in which only a fraction of the entire amount of N<sub>2</sub> available from the ASU is required at pressure for gas turbine injection. The actual design of the ASU will be determined by the ASU vendor. The EP section produces the N<sub>2</sub> which is sent to the gas turbine. The Sulfur Recovery unit also consumes a small quantity of O<sub>2</sub>. O<sub>2</sub> and N<sub>2</sub> in air are separated by means of cryogenic distillation. Approximately 60% of the N<sub>2</sub> separated from the air leaves the distillation unit at pressure and is compressed and injected into the gas turbines for NO<sub>x</sub> emissions control as well as providing additional motive fluid.

For both the EP and LP section, ambient air is sent through a filter to remove dust and other particulate matter and then compressed before providing the air to the “cold box.” Interstage cooling and after-cooling of the compressor is accomplished with cooling water. For the EP section, a portion of the N<sub>2</sub> stream produced in the cold box is compressed to two different levels, preheated and provided to the gas turbine to provide the thermal diluent for NO<sub>x</sub> control within the initial combustor and the reheat combustor of the gas turbine as well as provide extra motive fluid for expansion in the turbine.

The compressed air is treated to remove moisture, CO<sub>2</sub> and any hydrocarbons present. This air pretreatment system consists of two molecular sieve vessels. The vessels are operated in a staggered cycle: while one vessel is being used to filter the compressed air, the other is regenerated with the waste N<sub>2</sub> stream from the distillation columns. The waste N<sub>2</sub> is heated to the required regeneration temperature with medium pressure (MP) steam. The clean, dry air is liquefied utilizing a combination of chilling, feed/effluent heat exchange, compression and turbo-expansion. The expander may be compressor loaded or generator loaded. A multi-column

system separates the liquefied air into a high purity N<sub>2</sub> stream and a high purity O<sub>2</sub> stream. This cold box is modeled as a separator such that the inlet and outlet stream conditions are consistent with data provided by an air separation unit vendor in the past. Current designs for the cold box consist of pumped liquid O<sub>2</sub> systems to avoid buildup of hydrocarbons within the cold box which could lead to a hazardous situation. The overall performance of the ASU consisting of a pumped liquid O<sub>2</sub> system, however, is similar to that of the system modeled in Aspen for this study.

The O<sub>2</sub> stream required by the gasifier and the N<sub>2</sub> streams provided to the gas turbine are compressed in multistage intercooled compressors. The N<sub>2</sub> serves the purpose of a thermal diluent in the gas turbine combustor for NO<sub>x</sub> control and it also increases the motive fluid for expansion. It is preheated to a temperature of 288°C against HP and high temperature boiler feed water (BFW) extracted from the HRSG located in the power block before it is injected into the gas turbine combustor. The resulting cooler HP BFW is pumped back to the power block.

### **Coal Receiving and Handling Unit**

Refer to the Baseline Case process description in section titled “Task 1.3: First Detailed Systems Study Analysis - Baseline Case” for the description and block flow diagram for this unit.

### **Gasification Unit**

Refer to the Baseline Case process description in section titled “Task 1.3: First Detailed Systems Study Analysis - Baseline Case” for the description and process flow diagram for this unit.

### **CO Shift / Low Temperature Gas Cooling Unit**

Refer to the Baseline Case process description in section titled “Task 1.3: First Detailed Systems Study Analysis - Baseline Case” for the description for this unit. The process flow diagram for this case is depicted in Figure A1.4.2 – 21.

### **Acid Gas Removal Unit (Selexol®)**

Refer to the Baseline Case process description in section titled “Task 1.3: First Detailed Systems Study Analysis - Baseline Case” for the description and block flow diagram for this unit.

### **Syngas Humidification Unit**

One of the primary purposes of this humidification unit is to dilute the syngas to the gas turbines with moisture to meet the specification of no more than 65 mole% of H<sub>2</sub> as stipulated by GE for their 7FB gas turbines. This same specification is assumed for the intercooled reheat pressure ratio 70 gas turbine. The moisture acts as a thermal diluent in the combustor of the gas turbine and thus reduces the NO<sub>x</sub> formation. In addition, it increases the motive fluid for expansion in the gas turbine and thus the humidification operation provides a means for efficient recovery of low temperature waste heat in the plant. As depicted in Figure A1.4.2 - 22, HP syngas from the Acid Gas Removal Unit is further compressed in an intercooled multistage compressor. The syngas is then humidified in a packed column where it is contacted with circulating water in a

counter-current manner. The circulating water is heated by shifted syngas in the low temperature gas cooling section.

The LP syngas from the Acid Gas Removal Unit is sent to a second packed, humidification column where it is contacted with circulating water in a counter-current manner. The circulating water is heated by shifted syngas in the low temperature gas cooling section.

The makeup water to the humidifier is provided by IP BFW that is extracted from the deaerator in the power block. The required amount of moisture can be controlled by resetting the recirculating water flow controller, based on the measurements of the H<sub>2</sub> content, flow rate, temperature and pressure of the feed gas, as well as the temperature and pressure of the humidified syngas. Blowdown from the humidifier to avoid solids buildup within the column is equivalent to 0.5% of the water evaporated in the column. The blowdown is routed to the primary wastewater treating unit. The humidified fuel gas is heated to a temperature of 288°C using high temperature HP BFW extracted from the HRSG. The resulting cooler HP BFW is pumped back to the power block.

### **CO<sub>2</sub> Compression / Dehydration Unit**

Refer to the Baseline Case process description in section titled “Task 1.3: First Detailed Systems Study Analysis - Baseline Case” for the description and process flow diagram for this unit.

### **Sulfur Recovery / Tail Gas Treating Unit**

Refer to the Baseline Case process description in section titled “Task 1.3: First Detailed Systems Study Analysis - Baseline Case” for the description for this unit. The process flow diagram for this case is depicted in Figure A1.4.2 – 23.

### **Power Block**

The process scheme for the combined-cycle power block consists of the advanced firing temperature intercooled-reheat gas turbine with the pressure ratio of 70 supporting a reheat steam turbine. The process flow diagram for this unit is depicted in Figure A1.4.2 - 24. The overall integration of the steam system between the Power Block and the balance of the IGCC plant is shown on the Steam Balance Diagram, Figure A1.4.2 – 25.

The power block consists of the following major systems:

- Intercooled-Reheat Gas Turbine
- Heat Recovery Steam Generator (HRSG)
- Steam Turbine and the associated Vacuum Condensate System
- Integral Deaerator
- Blowdown System
- Miscellaneous Supporting Facilities:
  - boiler chemical injection

- demineralized water package.

The performance of the advanced gas turbine operating on the decarbonized syngas was developed utilizing Thermoflex.

Ambient air is drawn into the gas turbine air compressor via a filter to remove air-borne particulates, especially those that are larger than 10 microns. A direct contact spray cooler utilizing steam condensate provides intercooling. A portion of the humidified syngas is mixed with the compressed air and combusted in the HP section of the turbine. The remaining syngas is mixed with the HP turbine exhaust and is combusted in the reheat combustor. The preheated nitrogen is injected into both of the combustors through separate nozzles for NO<sub>x</sub> control. The combined LHV of the humid syngas and diluent nitrogen is 4,720 kJ/nm<sup>3</sup> or 120 Btu/scf.

The hot gas turbine exhaust flows through a customized Heat Recovery Steam Generator (HRSG). The HRSG consists basically of the following sub-systems:

- LP steam
- HP steam
- Reheat steam

In addition to these sub-systems, the HRSG is integrated with the rest of the IGCC plant. The HRSG has its own stack, which is equipped with a continuous emissions monitoring system (CEMS).

### LP Steam System

Low temperature heat is recovered from the syngas generation / processing units (Process) by heating the vacuum cold condensate from the surface condenser + makeup BFW. The makeup BFW is sprayed directly into the surface condenser and the combined stream of the cold vacuum condensate + makeup is drawn from the Surface Condenser by the Vacuum Condensate Pump and is sent to the vacuum condensate heaters in the Low Temperature Gas Cooling Unit and Black Water Flash section of the Gasification Unit to recover the low temperature heat. The hot vacuum condensate is further heated in the LP Economizer in the HRSG.

The hot vacuum condensate is combined with LP Condensate returning from the Gasification Unit and is supplied as BFW to the LP Steam Drum in the HRSG. The saturated steam from the LP Steam Drum is mixed with the saturated LP steam produced in the Process units. The combined flow is sent through the LP Superheater coils in the HRSG and then is fed to the LP section of the Steam Turbine.

The LP Feed Water Booster Pump sends heated BFW from the LP steam drum to the Process users in the Syngas plant.

### BFW Pump

The main BFW pump of the HRSG supplies both IP and HP BFW to the IP and HP steam systems as well as makeup to the CO Shift/LTGC unit. It is a multistage centrifugal pump, with

intermediate bleeds to support the IP steam system and supply the makeup. The discharge pressure of the BFW pump is dictated by the design conditions set at the inlet of the steam turbine.

### IP Steam System

The IP BFW is taken from a bleed off of the main BFW Feed pump. The makeup water for the syngas humidifier is taken from the IP bleed before the economizer. The IP BFW is routed to the IP Steam Generators in the CO Shift/LTGC unit and the Sulfur Recovery Unit. The surplus IP steam from other process units merges with the reheat steam system.

### HP Steam System

The discharge from the main BFW Feed pump is mixed with the HP boiler feed water returning from the Fuel Gas and Nitrogen heaters before it flows through two HP Economizers in the HRSG. The HP BFW Circulating pump sends part of the preheated HP boiler feed water exiting the first HP Economizer to the Fuel Gas and Nitrogen heaters.

A portion of the preheated HP BFW is routed to the HP Steam Generator in the CO Shift/LTGC unit and the HP Waste Heat Boiler in the Sulfur Recovery Unit and the remainder is fed to the HP Steam drum. Saturated HP steam generated in the HP steam drum mixes with surplus HP steam from other process units and then is superheated in HP Superheater coils within the HRSG. The superheated HP steam from the HRSG is sent to the inlet of the steam turbine.

A small portion of the main BFW Feed pump discharge is used as attemperator water for the control of the temperature of the superheated steam.

### Reheat Steam System

To improve the efficiency of the combined-cycle, the exit steam from the HP section of the steam turbine is returned to the HRSG to raise its temperature by absorbing additional heat. This reheated steam is combined with the IP steam from the syngas production plant, superheated to the same temperature as the HP steam, and then is fed to the inlet of the IP section of the steam turbine.

### Gas Turbine Cooling

The 1<sup>st</sup> and 2<sup>nd</sup> stages of the gas turbine stator and rotating blades are cooled with steam taken from the HP steam turbine exhaust. The steam returning from this closed circuit cooling of the gas turbine is mixed with the IP steam before it enters the reheater coils in the HRSG.

### Deaerator

An integrated LP steam drum/deaerator is provided in the HRSG. This eliminates the need for an external deaerator. The deaerator removes any dissolved gases such as O<sub>2</sub> and CO<sub>2</sub> in the feed water by using LP steam in the steam drum as the stripping medium. The pressure in the LP Steam Drum is controlled by varying the amount of steam vented with the dissolved gases.

## Blowdown System

The steam drums of the HRSG are continuously purged to control the amount of built-up of dissolved solids. The continuous blowdown is routed to the Continuous Blowdown drum. Flash steam in the Continuous Blowdown drum is sent to the LP steam drum and the saturated water is letdown into the Intermittent Blowdown drum. Whenever required, blowdown from each steam drum in the HRSG system can be routed directly to the Intermittent Blowdown drum. Flash steam from the Intermittent Blowdown drum is vented to atmosphere and the liquid collected in Blowdown Sump.

## Steam Turbine

The inlet pressure of the HP section of the steam turbine is set at 166.5 bara. The exhaust from the LP section is set at a vacuum of 0.044 bara. The surface condenser uses circulating cooling water from the cooling towers as the cooling medium while the makeup water for the steam system is added to the well of the condenser.

## Demineralized Water System

Demineralized water system consists of mixed-bed exchangers, one in operation and one in stand-by, filled with cation/anion resins, with internal-type regeneration. The package includes facilities for resin bed regeneration, chemical storage and neutralization basin.

## **General Facilities**

Refer to the Baseline Case process descriptions in the section titled “Task 1.3: First Detailed Systems Study Analysis - Baseline Case” for the description and process flow diagram for this unit.

The stream data for this case are presented in Table A1.4.2 - 9.

## **RESULTS AND DISCUSSION**

Table A1.4.2 - 10 shows the overall system efficiency, coal (HHV) to power for this case along with those for the Baseline Case. Table A1.4.2 - 11 summarizes the auxiliary power consumption within the plant while Table A1.4.2 - 12 summarizes the main features of the power cycle for this case.

The following summarizes the results:

- The gas turbine firing temperatures (1<sup>st</sup> rotor inlet temperature of the HP and the LP turbines downstream of the HP and the reheat combustors, respectively) required to realize the target improvement goal in heat rate over the Baseline Case is 1592°C or 2898°F (which is 200°C or 360°F above the Baseline Case but is 142°C or 255°F lower than all of the previous increased firing temperature cases) while increasing the blade surface temperatures by about the same amount over the Baseline Case (200°C or 360°F).

This increase in the blade surface temperature is consistent with the projected values for advanced firing temperature and materials presented in Figure A1.4.2 - 1.

- The estimated NO<sub>x</sub> emissions for this reheat case is 42 ppmVd (15% O<sub>2</sub> basis) while that estimated for the Baseline Case is 18 ppmVd (15% O<sub>2</sub> basis) when utilizing combustors of the non-premixed type and maintaining a residence time of 30 ms in the dilution zone. These NO<sub>x</sub> emission is lower than the previous advanced cases due to the substantially lower flame temperature in the reheat combustor and consequently a significantly lower to the total NO<sub>x</sub> emission from the gas turbine. The estimated NO<sub>x</sub> emissions for the reheat case is 39 ppmVd (15% O<sub>2</sub> basis) when the residence time is reduced to 5 ms in the dilution zone.

## **CONCLUSIONS**

It may be concluded from the above results that much lower increases in both firing temperature and blade surface temperature (as compared to the previous non-reheat cases with advanced firing temperatures) are required over the Baseline Case to achieve the heat rate improvement goal set for this study. On the other hand, significant increase in gas turbine pressure ratio is required to limit the exhaust temperature.

Again, advanced low NO<sub>x</sub> combustor designs described under Task 1.4.1 may not suffice since the air to fuel ratio is too small. More diluent addition may be a challenge for the combustor design since the O<sub>2</sub> content of the combustor exhaust gas is already very low at 0.5%. SCRs would be required to limit the NO<sub>x</sub> emissions to the desired 2 ppmVd (15% O<sub>2</sub> basis) value. Higher SCR catalyst volume would be required for this advanced firing temperature case, however, since the amount of NO<sub>x</sub> generated within the combustor is substantially higher than that in the Baseline Case. A correspondingly higher pressure drop across the SCR would result making the heat rate penalty a little more significant than that seen in the sensitivity case developed for the Baseline Case in Task 1.3.

In addition, a major challenge associated with developing a gas turbine for this cycle is the need for a very high pressure ratio of 70. Even with this very high pressure ratio the gas turbine exhaust remained high at 704°C or 1299°F. The required steam superheat and reheat temperatures for this case had to be consequently increased to 661°C or 1222°F in order to minimize the irreversibility in heat transfer. A steam turbine capable of operating at significantly high temperatures is thus required. More expensive superheater and reheater coils in the HRSG and the piping between the HRSG and the steam turbine are also required due to the higher grade metallurgical requirements.

## **INTERCOOLED CLOSED CIRCUIT AIR COOLED GAS TURBINE**

### **APPROACH**

This case investigates the effect of utilizing closed loop air cooling (instead of closed loop steam cooling) in the HP sections of the gas turbine. An air compressor boosts the pressure of the

cooling air leaving the turbine blades (to compensate for the pressure drops in the closed circuit air flow path) and returns the air to the combustor of the gas turbine. The following summarizes the main features of this gas turbine:

- Pressure ratio of 50
- Spray intercooled gas turbine air compressor
- Closed circuit air cooled gas turbine
- Addition of an air compressor to boost pressure of the cooling air to compensate for the pressure drops in the closed circuit air flow path while returning the air to the combustor of the gas turbine
- No air extraction
- N<sub>2</sub> returned from an IP ASU.

The advantages / disadvantages of closed loop air intercooling are:

- An advantage of this method as compared to the closed circuit steam cooling method is that the cooling air recuperates heat removed from the working fluid in the gas turbine by recycling it back to the combustor of the gas turbine whereas in the case of steam cooling the heat removed from the fluid within the turbine enters the steam cycle, i.e. heat is removed from the topping cycle and introduced into the bottoming cycle.
- Reduced RIT as compared to the previous advanced cases while realizing the same heat rate advantage over the Baseline Case.
- On the other hand, the reliability of the cooling air compressor is a concern. A possible solution in the event that this compressor trips is to open a fast acting relief valve upstream of the compressor to allow the free flow of cooling air. Thus it may be important to locate this compressor downstream of the turbine blades. The resulting increase in the plant heat rate is quite small due to the increase in the power consumption of the compressor in this location where the air stream being compressed is hotter.

The direct contact intercooling utilizes steam condensate sprayed into the air stream. The gas turbine exhaust temperature for this case with a pressure ratio of 50 is limited to 620°C (1148°F) at the ISO operating point.

The overall block flow diagram depicting the overall plant configuration for this case is presented in Figure A1.4.2 - 26.

## **PROCESS DESCRIPTION**

Process description for the 50 pressure ratio intercooled closed loop air cooled gas turbine case with IP ASU and no extraction air is presented in the following.

### **Air Separation Unit and N<sub>2</sub> Preheat**

The primary purpose of the ASU is to supply high pressure, high purity O<sub>2</sub> (at a nominal 95 mole %) to the Gasification unit Figure A1.4.2 - 8 depicts the main features of this unit. For the purpose of computer simulation, the ASU has been modeled as two separate sections: An elevated pressure (EP) section which provides compressed air to the cold box operating at

elevated pressure, and a low pressure (LP) section which provides compressed air to the cold box operating at lower pressure. This ASU set up with an EP and LP section provides a valid approximation for the performance of an ASU providing oxygen and nitrogen to an IGCC facility in which only a fraction of the entire amount of  $N_2$  available from the ASU is required at pressure for gas turbine injection. The actual design of the ASU will be determined by the ASU vendor. The EP section produces the  $N_2$  which is sent to the gas turbine. The Sulfur Recovery unit also consumes a small quantity of  $O_2$ .  $O_2$  and  $N_2$  in air are separated by means of cryogenic distillation. Approximately 60% of the  $N_2$  separated from the air leaves the distillation unit at pressure and is compressed and injected into the gas turbines for  $NO_x$  emissions control as well as providing additional motive fluid.

For both the EP and LP section, ambient air is sent through a filter to remove dust and other particulate matter and then compressed before providing the air to the “cold box.” Interstage cooling and after-cooling of the compressor is accomplished with cooling water. For the EP section, a portion of the  $N_2$  stream produced in the cold box is compressed, preheated and provided to the gas turbine to provide the thermal diluent for  $NO_x$  control within the combustor of the gas turbine as well as provide extra motive fluid for expansion in the turbine.

The compressed air is treated to remove moisture,  $CO_2$  and any hydrocarbons present. This air pretreatment system consists of two molecular sieve vessels. The vessels are operated in a staggered cycle: while one vessel is being used to filter the compressed air, the other is regenerated with the waste  $N_2$  stream from the distillation columns. The waste  $N_2$  is heated to the required regeneration temperature with medium pressure (MP) steam. The clean, dry air is liquefied utilizing a combination of chilling, feed/effluent heat exchange, compression and turbo-expansion. The expander may be compressor loaded or generator loaded. A multi-column system separates the liquefied air into a high purity  $N_2$  stream and a high purity  $O_2$  stream. This cold box is modeled as a separator such that the inlet and outlet stream conditions are consistent with data provided by an air separation unit vendor in the past. Current designs for the cold box consist of pumped liquid  $O_2$  systems to avoid buildup of hydrocarbons within the cold box which could lead to a hazardous situation. The overall performance of the ASU consisting of a pumped liquid  $O_2$  system, however, is similar to that of the system modeled in Aspen for this study.

The  $O_2$  stream required by the gasifier and the  $N_2$  stream provided to the gas turbine are compressed in multistage intercooled compressors. The  $N_2$  serves the purpose of a thermal diluent in the gas turbine combustor for  $NO_x$  control and it also increases the motive fluid for expansion. It is preheated to a temperature of  $288^\circ C$  against HP and high temperature boiler feed water (BFW) extracted from the HRSG located in the power block before it is injected into the gas turbine combustor. The resulting cooler HP BFW is pumped back to the power block.

### **Coal Receiving and Handling Unit**

Refer to the Baseline Case process description in section titled “Task 1.3: First Detailed Systems Study Analysis - Baseline Case” for the description and block flow diagram for this unit.

### **Gasification Unit**

Refer to the Baseline Case process description in section titled “Task 1.3: First Detailed Systems Study Analysis - Baseline Case” for the description and process flow diagram for this unit.

### **CO Shift / Low Temperature Gas Cooling Unit**

Refer to the Baseline Case process description in section titled “Task 1.3: First Detailed Systems Study Analysis - Baseline Case” for the description for this unit. The process flow diagram for this case is depicted in Figure A1.4.2 - 9.

### **Acid Gas Removal Unit (Selexol®)**

Refer to the Baseline Case process description in section titled “Task 1.3: First Detailed Systems Study Analysis - Baseline Case” for the description and block flow diagram for this unit.

### **Syngas Humidification Unit**

Refer to the Baseline Case process description in section titled “Task 1.3: First Detailed Systems Study Analysis - Baseline Case” for the description for this unit. The process flow diagram for this case is depicted in Figure A1.4.2 - 10.

### **CO<sub>2</sub> Compression / Dehydration Unit**

Refer to the Baseline Case process description in section titled “Task 1.3: First Detailed Systems Study Analysis - Baseline Case” for the description and process flow diagram for this unit.

### **Sulfur Recovery / Tail Gas Treating Unit**

Refer to the Baseline Case process description in section titled “Task 1.3: First Detailed Systems Study Analysis - Baseline Case” for the description for this unit. The process flow diagram for this case is depicted in Figure A1.4.2 - 11.

### **Power Block**

The process scheme for the combined-cycle power block consists of the advanced firing temperature closed loop, air-cooled gas turbine with the pressure ratio of 50 supporting a reheat steam turbine. The process flow diagram for this unit is depicted in Figure A1.4.2 - 27. The overall integration of the steam system between the Power Block and the balance of the IGCC plant is shown on the Steam Balance Diagram Figure A1.4.2 - 28.

The power block consists of the following major systems:

- Intercooled Closed Loop Air Cooled Gas Turbine

- Heat Recovery Steam Generator (HRSG)
- Steam Turbine and the associated Vacuum Condensate System
- Integral Deaerator
- Blowdown System
- Miscellaneous Supporting Facilities:
  - boiler chemical injection
  - demineralized water package.

The performance of the advanced gas turbine operating on the decarbonized syngas was developed utilizing Thermoflex.

Ambient air is drawn into the gas turbine air compressor via a filter to remove air-borne particulates, especially those that are larger than 10 microns. A portion of the air is sent to the turbo-expander for cooling. The humidified fuel gas is mixed with the cooling air from the gas turbine and the remaining compressed air and combusted in the turbine. The preheated nitrogen is injected into the turbine through separate nozzles for NO<sub>x</sub> control. The combined LHV of the humid syngas and diluent nitrogen is 4,720 kJ/nm<sup>3</sup> or 120 Btu/scf.

The hot gas turbine exhaust flows through a customized Heat Recovery Steam Generator (HRSG). The HRSG consists basically of the following sub-systems:

- LP steam
- HP steam
- Reheat steam

In addition to these sub-systems, the HRSG is integrated with the rest of the IGCC plant. The HRSG has its own stack, which is equipped with a continuous emissions monitoring system (CEMS).

### LP Steam System

Low temperature heat is recovered from the syngas generation / processing units (Process) by heating the vacuum cold condensate from the surface condenser + makeup BFW. The makeup BFW is sprayed directly into the surface condenser and the combined stream of the cold vacuum condensate + makeup is drawn from the Surface Condenser by the Vacuum Condensate Pump and is sent to the vacuum condensate heaters in the Low Temperature Gas Cooling Unit and Black Water Flash section of the Gasification Unit to recover the low temperature heat. The hot vacuum condensate is further heated in the LP Economizer in the HRSG.

The hot vacuum condensate is combined with LP Condensate returning from the Gasification Unit and is supplied as BFW to the LP Steam Drum in the HRSG. The saturated steam from the LP Steam Drum is mixed with the saturated LP steam produced in the Process units. The combined flow is sent through the LP Superheater coils in the HRSG and then is fed to the LP section of the Steam Turbine.

The LP Feed Water Booster Pump sends heated BFW from the LP steam drum to the Process users in the Syngas plant.

### BFW Pump

The main BFW pump of the HRSG supplies both IP and HP BFW to the IP and HP steam systems as well as makeup to the CO Shift/LTGC unit. It is a multistage centrifugal pump, with intermediate bleeds to support the IP steam system and supply the makeup. The discharge pressure of the BFW pump is dictated by the design conditions set at the inlet of the steam turbine.

### IP Steam System

The IP BFW is taken from a bleed off of the main BFW Feed pump. The makeup water for the syngas humidifier is taken from the IP bleed before the economizer. The IP BFW is routed to the IP Steam Generators in the CO Shift/LTGC unit and the Sulfur Recovery Unit. The surplus IP steam from other process units merges with the reheat steam system.

### HP Steam System

The discharge from the main BFW Feed pump is mixed with the HP boiler feed water returning from the Fuel Gas and Nitrogen heaters before it flows through two HP Economizers in the HRSG. The HP BFW Circulating pump sends part of the preheated HP boiler feed water exiting the first HP Economizer to the Fuel Gas and Nitrogen heaters.

A portion of the preheated HP BFW is routed to the HP Steam Generator in the CO Shift/LTGC unit and the HP Waste Heat Boiler in the Sulfur Recovery Unit and the remainder is fed to the HP Steam drum. Saturated HP steam generated in the HP steam drum mixes with surplus HP steam from other process units and then is superheated in HP Superheater coils within the HRSG. The superheated HP steam from the HRSG is sent to the inlet of the steam turbine.

A small portion of the main BFW Feed pump discharge is used as attemperator water for the control of the temperature of the superheated steam.

### Reheat Steam System

To improve the efficiency of the combined-cycle, the exit steam from the HP section of the steam turbine is returned to the HRSG to raise its temperature by absorbing additional heat. This reheated steam is combined with the IP steam from the syngas production plant, superheated to approximately the same temperature as the HP steam, and then is fed to the inlet of the IP section of the steam turbine.

### Deaerator

An integrated LP steam drum/deaerator is provided in the HRSG. This eliminates the need for an external deaerator. The deaerator removes any dissolved gases such as O<sub>2</sub> and CO<sub>2</sub> in the feed water by using LP steam in the steam drum as the stripping medium. The pressure in the LP Steam Drum is controlled by varying the amount of steam vented with the dissolved gases.

### Blowdown System

The steam drums of the HRSG are continuously purged to control the amount of built-up of dissolved solids. The continuous blowdown is routed to the Continuous Blowdown drum. Flash steam in the Continuous Blowdown drum is sent to the LP steam drum and the saturated water is letdown into the Intermittent Blowdown drum. Whenever required, blowdown from each steam drum in the HRSG system can be routed directly to the Intermittent Blowdown drum. Flash steam from the Intermittent Blowdown drum is vented to atmosphere and the liquid collected in Blowdown Sump.

### Steam Turbine

The inlet pressure of the HP section of the steam turbine is set at 166.5 bara. The exhaust from the LP section is set at a vacuum of 0.044 bara. The surface condenser uses circulating cooling water from the cooling towers as the cooling medium while the makeup water for the steam system is added to the well of the condenser.

### Demineralized Water System

Demineralized water system consists of mixed-bed exchangers, one in operation and one in stand-by, filled with cation/anion resins, with internal-type regeneration. The package includes facilities for resin bed regeneration, chemical storage and neutralization basin.

### **General Facilities**

Refer to the Baseline Case process descriptions in the section titled “Task 1.3: First Detailed Systems Study Analysis - Baseline Case” for the description and process flow diagram for this unit.

The stream data for this case are presented in Table A1.4.2 - 13.

## **RESULTS AND DISCUSSION**

Table A1.4.2 - 14 shows the overall system efficiency, coal (HHV) to power for these above described cases along with those for the Baseline Case. Table A1.4.2 - 15 summarizes the auxiliary power consumption within the plant while Table A1.4.2 - 16 summarizes the main features of the power cycle for this case.

The following summarizes the results:

- The required gas turbine firing temperature for this closed circuit air cooled gas turbine case with intercooling is 1678°C or 3053°F to obtain an overall plant heat rate similar to those of the previous advanced steam cooled cases, i.e., similar improvement in overall plant heat rate over the Baseline Case. This firing temperature as well as the turbine blade temperatures are 56°C or 100°F lower than the previous advanced cases.

- The combustor inlet air which is a mixture of the returned cooling air (leaving the booster compressor) and the remainder of gas turbine compressor discharge air is only slightly hotter (7°C or 13°F) than that in the previous steam cooled intercooled case at the same overall pressure ratio of 50..
- The estimated NO<sub>x</sub> emissions for this case is 115 ppmVd (15% O<sub>2</sub> basis) while that estimated for the Baseline Case is 18 ppmVd (15% O<sub>2</sub> basis) when utilizing combustors of the non-premixed type and maintaining a residence time of 30 ms in the dilution zone. This NO<sub>x</sub> emission is lower than the previous advanced intercooled (non-reheat) case with steam cooling and an overall pressure ratio of 50 due to the lower firing temperature. The estimated NO<sub>x</sub> emissions for the 50 pressure ratio gas turbine closed circuit air cooled gas turbine case is 35 ppmVd (15% O<sub>2</sub> basis) when the residence time is reduced to 5 ms in the dilution zone.

## CONCLUSIONS

From the results of this analysis, it may be concluded that incorporation of closed circuit air cooling of the blades in the HP sections of the gas turbine allows a significant reduction in the firing temperature and the blade temperatures while achieving similar overall plant heat rate. Incorporation of aero-derivative compressor design would be required for this intercooled and high pressure ratio gas turbine.

Again, advanced low NO<sub>x</sub> combustor designs described under Task 1.4.1 may not suffice since the air to fuel ratio is too small to cause rapid quenching of the flame within the combustor to limit the formation of NO<sub>x</sub>. More diluent addition to the combustor may be a partial solution. The O<sub>2</sub> content of the combustor exhaust gas at 3.5% is higher than the previous advanced cases leaving room for some additional diluent addition. SCR may also be required to limit the NO<sub>x</sub> emission to the desired 2 ppmVd (15% O<sub>2</sub> basis) value. Higher SCR catalyst volume would be required for this advanced firing temperature case, however, since the amount of NO<sub>x</sub> generated within the combustor is substantially higher than that in the Baseline Case. A correspondingly higher pressure drop across the SCR would result making the heat rate penalty a little more significant than that seen in the sensitivity case developed for the Baseline Case in Task 1.3.

## AIR PARTIAL OXIDATION TOPPING CYCLE

### APPROACH

This advanced cycle investigates the addition of an air partial oxidation (PO<sub>x</sub>) topping cycle to an advanced steam cooled gas turbine. The partially oxidized syngas after partial expansion in a turbo-generator (PO<sub>x</sub> turbine) and heat exchange is supplied to the advanced gas turbine (O<sub>x</sub> turbine). The PO<sub>x</sub> unit is operated at a pressure of 70 atm while the O<sub>x</sub> turbine integrated with this PO<sub>x</sub> unit has a pressure ratio of about 37. A high operating pressure is chosen for the PO<sub>x</sub> unit and a moderate pressure ratio is chosen for the O<sub>x</sub> turbine in order to limit the PO<sub>x</sub> turbine exhaust temperature while obtaining a reasonable pressure ratio across the PO<sub>x</sub> turbine.

The advanced gas turbine (Ox turbine) includes a direct contact spray intercooler which is selected due to its advantages over a shell and tube intercooler as discussed in the previous section. Humidified, preheated, decarbonized syngas is combusted with less than the stoichiometric amount of air in the POx unit followed by complete combustion with excess air in the oxidizing combustor. IP nitrogen supplied by the ASU is added to the combustor as a thermal dilution for NOx control as well as to increase the amount of motive fluid for expansion. The following summarizes the main features of this gas turbine:

- POx topping cycle operating at a pressure of 70 atm
- Spray intercooled advanced steam cooled gas turbine (Ox turbine) with pressure ratio of 37
- Air extraction from the Ox turbine to provide air for the POx unit but none supplied to the ASU
- N<sub>2</sub> returned from an IP ASU.

The advantages of utilizing this air POx topping cycle are:

- Reduction in firing temperature of the Ox turbine while achieving the heat rate reduction goal for this study.
- Potential for lower NOx due to lower heating value of the syngas fired in the advanced gas turbine since the syngas is partially oxidized and due to the lower firing temperature in the advanced gas turbine.

There are certain challenges, however, with respect to implementation of this air POx topping cycle:

- Concerns with POx turbine seals.
- Control issues as discussed in a previous section.
- H<sub>2</sub> embrittlement and corrosion due to loss of oxide protective layer, especially in the POx turbine.
- Carbonyl formation and metal dusting when utilized in “un-decarbonized” syngas applications.

The overall block flow diagrams depicting the overall plant configuration for this case is presented in Figure A1.4.2 - 29.

## **PROCESS DESCRIPTION**

Process description for the case with the intercooled 70 pressure ratio gas turbine, IP ASU and no extraction air is presented in the following.

### **Air Separation Unit and N<sub>2</sub> Preheat**

The primary purpose of the ASU is to supply high pressure, high purity O<sub>2</sub> (at a nominal 95 mole %) to the Gasification unit. Figure A1.4.2 - 30 depicts the main features of this unit. For the purpose of computer simulation, the ASU has been modeled as two separate sections: An elevated pressure (EP) section which provides compressed air to the cold box operating at

elevated pressure, and a low pressure (LP) section which provides compressed air to the cold box operating at lower pressure. This ASU set up with an EP and LP section provides a valid approximation for the performance of an ASU providing oxygen and nitrogen to an IGCC facility in which only a fraction of the entire amount of  $N_2$  available from the ASU is required at pressure for gas turbine injection. The actual design of the ASU will be determined by the ASU vendor. The EP section produces the  $N_2$  which is sent to the gas turbine. The Sulfur Recovery unit also consumes a small quantity of  $O_2$ .  $O_2$  and  $N_2$  in air are separated by means of cryogenic distillation. Approximately 60% of the  $N_2$  separated from the air leaves the distillation unit at pressure and is compressed and injected into the gas turbines for  $NO_x$  emissions control as well as providing additional motive fluid.

For both the EP and LP section, ambient air is sent through a filter to remove dust and other particulate matter and then compressed before providing the air to the “cold box.” Interstage cooling and after-cooling of the compressor is accomplished with cooling water. For the EP section, a portion of the  $N_2$  stream produced in the cold box is compressed, preheated and provided to the gas turbine to provide the thermal diluent for  $NO_x$  control within the combustor of the gas turbine as well as provide extra motive fluid for expansion in the turbine.

The compressed air is treated to remove moisture,  $CO_2$  and any hydrocarbons present. This air pretreatment system consists of two molecular sieve vessels. The vessels are operated in a staggered cycle: while one vessel is being used to filter the compressed air, the other is regenerated with the waste  $N_2$  stream from the distillation columns. The waste  $N_2$  is heated to the required regeneration temperature with medium pressure (MP) steam. The clean, dry air is liquefied utilizing a combination of chilling, feed/effluent heat exchange, compression and turbo-expansion. The expander may be compressor loaded or generator loaded. A multi-column system separates the liquefied air into a high purity  $N_2$  stream and a high purity  $O_2$  stream. This cold box is modeled as a separator such that the inlet and outlet stream conditions are consistent with data provided by an air separation unit vendor in the past. Current designs for the cold box consist of pumped liquid  $O_2$  systems to avoid buildup of hydrocarbons within the cold box which could lead to a hazardous situation. The overall performance of the ASU consisting of a pumped liquid  $O_2$  system, however, is similar to that of the system modeled in Aspen for this study.

The  $O_2$  stream required by the gasifier and the  $N_2$  stream provided to the gas turbine are compressed in multistage intercooled compressors. The  $N_2$  serves the purpose of a thermal diluent in the gas turbine combustor for  $NO_x$  control and it also increases the motive fluid for expansion. It is preheated to a temperature of  $288^\circ C$  against HP and high temperature boiler feed water (BFW) extracted from the HRSG located in the power block before it is injected into the gas turbine combustor. The resulting cooler HP BFW is pumped back to the power block.

### **Coal Receiving and Handling Unit**

Refer to the Baseline Case process description in section titled “Task 1.3: First Detailed Systems Study Analysis - Baseline Case” for the description and block flow diagram for this unit.

### **Gasification Unit**

Refer to the Baseline Case process description in section titled “Task 1.3: First Detailed Systems Study Analysis - Baseline Case” for the description and process flow diagram for this unit.

### **CO Shift / Low Temperature Gas Cooling Unit**

Refer to the Baseline Case process description in section titled “Task 1.3: First Detailed Systems Study Analysis - Baseline Case” for the description for this unit. The process flow diagram for this case is depicted in Figure A1.4.2 - 31.

### **Acid Gas Removal Unit (Selexol®)**

Refer to the Baseline Case process description in section titled “Task 1.3: First Detailed Systems Study Analysis - Baseline Case” for the description and block flow diagram for this unit.

### **Syngas Humidification Unit**

One of the primary purposes of this humidification unit is to dilute the syngas to the gas turbines with moisture to meet the specification of no more than 65 mole% of H<sub>2</sub> as stipulated by GE for their 7FB gas turbines. This same specification is assumed for the 70 pressure ratio gas turbine. The moisture acts as a thermal diluent in the combustor of the gas turbine and thus reduces the NO<sub>x</sub> formation. In addition, it increases the motive fluid for expansion in the gas turbine and thus the humidification operation provides a means for efficient recovery of low temperature waste heat in the plant. As depicted in

Figure A1.4.2 - 32, fuel gas from the Acid Gas Removal unit is compressed in an intercooled multistage compressor. The syngas is then humidified in a packed column where it is contacted with circulating water in a counter-current manner. The circulating water is heated by shifted syngas in the low temperature gas cooling section. The makeup water to the humidifier is provided by IP BFW that is extracted from the deaerator in the power block. The required amount of moisture can be controlled by resetting the recirculating water flow controller, based on the measurements of the H<sub>2</sub> content, flow rate, temperature and pressure of the feed gas, as well as the temperature and pressure of the humidified syngas. Blowdown from the humidifier to avoid solids buildup within the column is equivalent to 0.5% of the water evaporated in the column. The blowdown is routed to the primary wastewater treating unit. The humidified fuel gas is heated to a temperature of 288°C using high temperature HP BFW extracted from the HRSG. The resulting cooler HP BFW is pumped back to the power block.

### **CO<sub>2</sub> Compression / Dehydration Unit**

Refer to the Baseline Case process description in section titled “Task 1.3: First Detailed Systems Study Analysis - Baseline Case” for the description and process flow diagram for this unit.

## **Sulfur Recovery / Tail Gas Treating Unit**

Refer to the Baseline Case process description in section titled “Task 1.3: First Detailed Systems Study Analysis - Baseline Case” for the description for this unit. The process flow diagram for this case is depicted in Figure A1.4.2 - 23.

## **Power Block**

The process scheme for the combined-cycle power block consists of the advanced firing temperature Air POX Topping Cycle gas turbine with the pressure ratio of 70 supporting a reheat steam turbine. The process flow diagram for this unit is depicted in Figure A1.4.2 - 33. The overall integration of the steam system between the Power Block and the balance of the IGCC plant is shown on the Steam Balance Diagram, Figure A1.4.2 - 34.

The power block consists of the following major systems:

- Air POX Gas Turbine
- Heat Recovery Steam Generator (HRSG)
- Steam Turbine and the associated Vacuum Condensate System
- Integral Deaerator
- Blowdown System
- Miscellaneous Supporting Facilities:
  - boiler chemical injection
  - demineralized water package.

The performance of the advanced gas turbine operating on the decarbonized syngas was developed utilizing Thermoflex.

Ambient air is drawn into the gas turbine air compressor via a filter to remove air-borne particulates, especially those that are larger than 10 microns. A portion of the air which is less than the stoichiometric amount needed to combust the humidified syngas is cooled against the air from the POX turbine air compressor. The air is further cooled in a direct contact spray cooler utilizing steam condensate. The air is compressed and further heated then mixed with the humidified syngas and combusted in the POX turbine.

After cooling in the humidified syngas preheater, POx turbine effluent is sent to the second gas turbine with an oxidizing combustor. The preheated nitrogen is injected into the turbine through separate nozzles for NOx control. The combined LHV of the humid syngas and diluent nitrogen is 4,720 kJ/nm<sup>3</sup> or 120 Btu/scf.

The hot gas turbine exhaust flows through a customized Heat Recovery Steam Generator (HRSG). The HRSG consists basically of the following sub-systems:

- LP steam
- HP steam
- Reheat steam

In addition to these sub-systems, the HRSG is integrated with the rest of the IGCC plant. The HRSG has its own stack, which is equipped with a continuous emissions monitoring system (CEMS).

### LP Steam System

Low temperature heat is recovered from the syngas generation / processing units (Process) by heating the vacuum cold condensate from the surface condenser + makeup BFW. The makeup BFW is sprayed directly into the surface condenser and the combined stream of the cold vacuum condensate + makeup is drawn from the Surface Condenser by the Vacuum Condensate Pump and is sent to the vacuum condensate heaters in the Low Temperature Gas Cooling Unit and Black Water Flash section of the Gasification Unit to recover the low temperature heat. The hot vacuum condensate is further heated in the LP Economizer in the HRSG.

The hot vacuum condensate is combined with LP Condensate returning from the Gasification Unit and is supplied as BFW to the LP Steam Drum in the HRSG. The saturated steam from the LP Steam Drum is mixed with the saturated LP steam produced in the Process units. The combined flow is sent through the LP Superheater coils in the HRSG and then is fed to the LP section of the Steam Turbine.

The LP Feed Water Booster Pump sends heated BFW from the LP steam drum to the Process users in the Syngas plant.

### BFW Pump

The main BFW pump of the HRSG supplies both IP and HP BFW to the IP and HP steam systems as well as makeup to the CO Shift/LTGC unit. It is a multistage centrifugal pump, with intermediate bleeds to support the IP steam system and supply the makeup. The discharge pressure of the BFW pump is dictated by the design conditions set at the inlet of the steam turbine.

### IP Steam System

The IP BFW is taken from a bleed off of the main BFW Feed pump. The makeup water for the syngas humidifier is taken from the IP bleed before the economizer. The IP BFW is routed to the IP Steam Generators in the CO Shift/LTGC unit and the Sulfur Recovery Unit. The surplus IP steam from other process units merges with the reheat steam system.

### HP Steam System

The discharge from the main BFW Feed pump is mixed with the HP boiler feed water returning from the Fuel Gas and Nitrogen heaters before it flows through two HP Economizers in the HRSG. The HP BFW Circulating pump sends part of the preheated HP boiler feed water exiting the first HP Economizer to the Fuel Gas and Nitrogen heaters.

A portion of the preheated HP BFW is routed to the HP Steam Generator in the CO Shift/LTGC unit and the HP Waste Heat Boiler in the Sulfur Recovery Unit and the remainder is fed to the HP Steam drum. Saturated HP steam generated in the HP steam drum mixes with surplus HP steam

from other process units and then is superheated in HP Superheater coils within the HRSG. The superheated HP steam from the HRSG is sent to the inlet of the steam turbine.

A small portion of the main BFW Feed pump discharge is used as attemperator water for the control of the temperature of the superheated steam.

### Reheat Steam System

To improve the efficiency of the combined-cycle, the exit steam from the HP section of the steam turbine is returned to the HRSG to raise its temperature by absorbing additional heat. This reheated steam is combined with the IP steam from the syngas production plant, superheated to approximately the same temperature as the HP steam, and then is fed to the inlet of the IP section of the steam turbine.

### Gas Turbine Cooling

The 1<sup>st</sup> and 2<sup>nd</sup> stages of the gas turbine stator and rotating blades are cooled with steam taken from the HP steam turbine exhaust. The steam returning from this closed circuit cooling of the gas turbine is mixed with the IP steam before it enters the reheater coils in the HRSG.

### Deaerator

An integrated LP steam drum/deaerator is provided in the HRSG. This eliminates the need for an external deaerator. The deaerator removes any dissolved gases such as O<sub>2</sub> and CO<sub>2</sub> in the feed water by using LP steam in the steam drum as the stripping medium. The pressure in the LP Steam Drum is controlled by varying the amount of steam vented with the dissolved gases.

### Blowdown System

The steam drums of the HRSG are continuously purged to control the amount of built-up of dissolved solids. The continuous blowdown is routed to the Continuous Blowdown drum. Flash steam in the Continuous Blowdown drum is sent to the LP steam drum and the saturated water is letdown into the Intermittent Blowdown drum. Whenever required, blowdown from each steam drum in the HRSG system can be routed directly to the Intermittent Blowdown drum. Flash steam from the Intermittent Blowdown drum is vented to atmosphere and the liquid collected in Blowdown Sump.

### Steam Turbine

The inlet pressure of the HP section of the steam turbine is set at 166.5 bara. The exhaust from the LP section is set at a vacuum of 0.044 bara. The surface condenser uses circulating cooling water from the cooling towers as the cooling medium while the makeup water for the steam system is added to the well of the condenser.

## Demineralized Water System

Demineralized water system consists of mixed-bed exchangers, one in operation and one in stand-by, filled with cation/anion resins, with internal-type regeneration. The package includes facilities for resin bed regeneration, chemical storage and neutralization basin.

## **General Facilities**

Refer to the Baseline Case process descriptions in the section titled “Task 1.3: First Detailed Systems Study Analysis - Baseline Case” for the description and process flow diagram for this unit.

The stream data for this case are presented in Table A1.4.2 - 17.

## **RESULTS AND DISCUSSION**

Table A1.4.2 - 18 shows the overall system efficiency, coal (HHV) to power for this case along with those for the Baseline Case. Table A1.4.2 - 19 summarizes the auxiliary power consumption within the plant while Table A1.4.2 - 20 summarizes the main features of the power cycle for this case.

The following summarizes the results:

- The gas turbine firing temperatures (1<sup>st</sup> rotor inlet temperature) of the advanced steam cooled gas turbine (Ox turbine) firing the partially oxidized syngas required to realize the target improvement goal in heat rate over the Baseline Case is 1699°C or 3090°F (which is 307°C or 553°F above the Baseline Case but is only 35°C or 63°F lower than the first two advanced cases investigated. The difference in the blade surface temperatures of the advanced gas turbine between this case and the previous cases is consistent with the firing temperature, i.e., higher or lower by the same amount as the firing temperature (see Figure A1.4.2 - 1).
- The estimated NO<sub>x</sub> emissions for this air PO<sub>x</sub> based case is 117 ppmVd (15% O<sub>2</sub> basis) while that estimated for the Baseline Case is 18 ppmVd (15% O<sub>2</sub> basis) when utilizing combustors of the non-premixed type and maintaining a residence time of 30 ms in the dilution zone. The estimated NO<sub>x</sub> emissions for the air PO<sub>x</sub> based case is 32 ppmVd (15% O<sub>2</sub> basis) when the residence time is reduced to 5 ms in the dilution zone.

## **CONCLUSIONS**

It may be concluded from the above results that only slight reductions in firing temperature and blade surface temperature may be realized for the advanced gas turbine (Ox turbine) when integrated with the PO<sub>x</sub> system as compared to the first two advanced cases investigated while achieving the required heat rate improvement goal set for this study. On the other hand, this firing temperature is higher than both the reheat and the closed circuit air cooled gas turbine

cases. The pressure ratio for the advanced gas turbine is modest at 37 but the exhaust temperature is much higher than the desired value of 649°C or 1200°F.

Again, advanced low NO<sub>x</sub> combustor designs described under Task 1.4.1 may not suffice since the air to fuel ratio is quite small. More diluent addition may be a challenge for the combustor design since the O<sub>2</sub> content of the combustor exhaust gas is already very low at 2.96%. SCRs would be required to limit the NO<sub>x</sub> emissions to the desired 2 ppmVd (15% O<sub>2</sub> basis) value. Higher SCR catalyst volume would be required for this advanced case, however, since the amount of NO<sub>x</sub> generated within the combustor is substantially higher than that in the Baseline Case. A correspondingly higher pressure drop across the SCR would result making the heat rate penalty a little more significant than that seen in the sensitivity case developed for the Baseline Case in Task 1.3.

In addition, major challenges are associated with the development of the PO<sub>x</sub> turbine such as concerns with its seals, H<sub>2</sub> embrittlement and corrosion due to loss of oxide protective layer as well as the overall fuel control issues. The advanced gas turbine (Ox turbine) exhaust temperature is high at 698°C or 1289°F<sup>13</sup>. The required steam superheat and reheat temperatures for this case had to be consequently increased to 655°C or 1211°F in order to minimize the irreversibility in heat transfer. A steam turbine capable of operating at significantly high temperatures is thus required. More expensive superheater and reheater coils in the HRSG and the piping between the HRSG and the steam turbine are also required due to the higher grade metallurgical requirements. The heat exchange equipment and piping within the PO<sub>x</sub> unit will also cause a significant increase in the plant cost.

## SELECTION OF ADVANCED BRAYTON CYCLE

It may be concluded from the results obtained by this detailed analysis of the above discussed advanced Brayton cycles that the more promising advanced Brayton cycles are the high pressure ratio intercooled gas turbines employing either closed circuit steam or air cooling. The following summarizes the attributes of these two advanced cycles:

- Required gas turbine pressure ratio of 50 is close to that of a commercially proven aero-engine while limiting the exhaust temperature to a reasonable value.
- Spray intercooling which has been proven in a commercial aero-engine derived gas turbine has the following advantages:
  - Lower compressor discharge temperature than that in a non-intercooled gas turbine with the same pressure ratio
    - Savings in materials of construction may be realized
    - Produces lower NO<sub>x</sub> emission not only due to lower compressor discharge temperature (or combustor inlet air temperature) but also due to the higher humidity of this air stream (caused by using the spray intercooler)
  - Higher specific power output

---

<sup>13</sup> Note that this exhaust temperature may be reduced by increasing the pressure ratio across the Ox turbine. However, this will then require a further increase in the operating pressure of the PO<sub>x</sub> unit, i.e., beyond the already high 70 atm in order to maintain a reasonable pressure ratio across the PO<sub>x</sub> turbine.

- Reduced compressor work (in a simple cycle gas turbine, approximately half of turbine power is used in compression)
- Spray water increases the motive fluid for expansion in the turbine.

Next, comparing these two advanced cycles:

- The required firing and blade surface temperatures for the closed circuit air cooled case are a bit lower (by about 56°C or 100°F) along with NO<sub>x</sub> emissions as compared to the corresponding closed circuit steam cooled case.
- However, closed circuit air cooling has not been demonstrated while the reliability of the cooling air compressor is a concern.
- On the other hand, start-up and shutdown procedures for the closed circuit air cooled case may be simpler than those for the closed circuit steam cooled case.
- The steam cooled case however, incorporates proven cooling technology and H class combined cycles (utilizing the steam cooled gas turbines) have been operated successfully in commercial applications which include startup and shutdown operations.

Based on these above attributes of these two advanced cycles, the most promising cycle for further analysis appears to be the steam cooled case, i.e., an advanced Brayton cycle employing a high pressure ratio gas turbine with spray intercooling, closed circuit steam cooling and an advanced firing temperature. Sensitivity analysis is conducted on this selected cycle of incorporating higher compressor and turbine efficiencies, high efficiency exhaust diffuser, assessing the impact of application of superconductivity technology to transformers and generators as well as assessing the impact of a low NO<sub>x</sub> strategy consisting of increasing the amount of diluent added to the combustor.

## **SENSITIVITY ANALYSIS OF SELECTED ADVANCED BRAYTON CYCLE**

### **APPROACH**

Since the most technological challenge in the development of the advanced Brayton cycle is its advanced firing temperature (requiring advanced materials), the approach taken in this sensitivity analysis is to quantify the reduction in the firing temperature made possible by incorporating improvements in the other areas (Items 1 through 4 listed in the following) while realizing the same improvement in overall plant efficiency over the Baseline Case.

The sensitivity analysis also prioritizes the development needs of the advanced Brayton cycle. Low NO<sub>x</sub> strategies are also investigated (Item 5 below) as well as use of air cooling as an alternate to closed circuit steam cooling of the turbine 1<sup>st</sup> stage (Item 6 below) which has very high operating temperature, the film of air forming on the outside surface of the blade providing an additional insulating layer (i.e., in addition to thermal barrier coatings to protect the metal).

1. Increasing the gas turbine air compressor efficiency
2. Increasing the gas turbine expander
3. High efficiency exhaust diffuser
4. Application of superconductivity technology to transformers and generators

5. Low NO<sub>x</sub> strategy
  - a. Increased diluent nitrogen addition
  - b. Reduction in firing temperature
6. Air (film) cooled 1<sup>st</sup> stage turbine.

The above sensitivity analysis is conducted on the selected advanced Brayton cycle case which consists of the high pressure ratio gas turbine (pressure ratio of 50), spray intercooling, closed circuit steam cooling, the advanced firing temperature and no air extraction for the ASU.

Since the most technological challenge in the development of this advanced Brayton cycle is its advanced firing temperature (requiring advanced materials), the approach taken in this sensitivity analysis is to quantify the reduction in the firing temperature made possible by incorporating improvements in the other areas (Items 1 through 4 listed in the preceding) while realizing the same improvement in overall plant efficiency over the Baseline Case.

## **RESULTS AND DISCUSSION**

### **Gas Turbine Compressor Efficiency**

The LP and HP compressor polytropic efficiencies for the baseline case are 92% and 91.3%, respectively. By increasing the polytropic efficiency of both the LP and HP compressors by 1 percentage point (i.e., to 93% for the LP Air compressor and to 92.3% for the HP compressor), only a 11°C or 19 °F reduction in the firing temperature may be realized (while maintaining the same overall plant efficiency).

Next, by increasing the polytropic efficiency of both the LP and HP compressors by 2 percentage points (i.e., to 94% for the LP Air compressor and to 93.3% for the HP compressor), a 20°C or 36°F reduction in the firing temperature may be realized (again while maintaining the same overall plant efficiency).

The results of this analysis thus indicate that very substantial aerodynamic design improvements are required to the gas turbine compressor to realize a significant reduction in the required firing temperature. The need for very high firing temperature is not diminished by a significant amount however, and shows that major emphasis should be placed on technology developments required to realize the very high firing temperature identified by this study.

### **Gas Turbine Expander Efficiency**

The uncooled isentropic stage efficiencies for the baseline case are:

Baseline Case	Uncooled Isentropic Efficiency
Stage 1	89.5
Stage 2	90.5
Stage 3	90.5
Stage 4	92
Stage 5	92

By increasing each of these stage efficiencies by 1 percentage point, only a 20°C or 36°F reduction in the firing temperature may be realized (while maintaining the same overall plant efficiency). The resulting stage efficiencies are listed below:

Stage Efficiency Increased by 1% Point	Uncooled Isentropic Efficiency
Stage 1	90.5
Stage 2	91.5
Stage 3	91.5
Stage 4	93
Stage 5	93

The results of this analysis are similar to the previous compressor efficiency analysis, i.e., indicate that very substantial aerodynamic design improvements are required to the gas turbine expander to realize a significant reduction in the required firing temperature. The need for very high firing temperature is not diminished by a significant amount however, and shows that major emphasis should be placed on technology developments required to realize the very high firing temperature identified by this study.

### **High Efficiency Exhaust Diffuser**

The coefficient of performance for a conventional diffuser is typically around 0.6. According to Meruit Inc. as mentioned previously in the Screening Analysis, the gas turbine exhaust diffuser can be designed to have a coefficient of performance as high as 0.9 utilizing their proprietary design consisting of an Annular Recirculating Diffuser. With an increase in the diffuser coefficient of performance to 0.9, about 30°C or 54°F reduction in the firing temperature may be realized (while maintaining the same overall plant efficiency).

Once again the need for very high firing temperature is not diminished by a significant amount however, and shows that major emphasis should be placed on technology developments required to realize the very high firing temperature identified by this study.

## **Application of Superconductivity Technology**

Superconductivity technology offers higher efficiency electrical equipment such as generators and transformers. The efficiencies of these equipment for the Baseline Case are listed below:

Baseline Case	Uncooled Isentropic Efficiency
Gas Turbine Generator	98.6
Transformer Efficiency (24/345 kV)	0.997
Transformer Efficiency (24/4.16 kV)	0.995
Transformer Efficiency (4,160/480 V)	0.995

As seen from the above data, the efficiencies are already quite high and the application of the more efficient electrical equipment is not expected to make a significant improvement in the overall plant performance or conversely a significant reduction in the required firing temperature of the gas turbine for a targeted overall plant performance.

## **Low NOx Strategies**

As discussed previously, a partial solution to reducing the NOx emission may be to limit the residence time in the dilution zone of the combustor by constructing a short combustor (reducing the residence time from 30 ms to 5 ms reduced the NOx by as much as ~ 70% for the very high rotor inlet cases while the burnout of H<sub>2</sub>, CO and CH<sub>4</sub> was not affected significantly, the fuel being decarbonized syngas contains only small concentrations of CO and CH<sub>4</sub>). As mentioned previously, a short residence time combustor, however, will pose a problem if natural gas firing is required either at startup or as a backup fuel and other means of NOx control would be preferred. Thus, other strategies are considered as follows.

## **Increased Diluent Nitrogen Addition**

Increasing the diluent addition to the syngas is a strategy investigated in this sensitivity analysis which may be done in addition to installing an SCR. In the Baseline Case, the combined LHV of the humidified syngas and diluent N<sub>2</sub> (provided by the ASU) is 4,720 kJ/nm<sup>3</sup> or 120 Btu/scf. The ASU can be designed to provide additional nitrogen for syngas dilution. With an ASU designed to provide the maximum amount of N<sub>2</sub>, the resulting (lowest) combined LHV of the humidified syngas and diluent N<sub>2</sub> is 3,980 kJ/nm<sup>3</sup> or 101 Btu/scf. The increased nitrogen dilution reduces the NOx significantly, from 42 ppmvd to 10 ppmvd (at 15% O<sub>2</sub> concentration) with the shorter combustors, i.e., corresponding to a residence time of 5 ms in the 2<sup>nd</sup> PSR. However, the firing temperature of gas turbine is also reduced, by about 22°C or 40°F resulting in an increase in the net plant heat rate by about 2.2%.

## **Reduced Firing Temperature**

The trade-off between heat rate and NOx emission by reducing the firing temperature is investigated in this sensitivity analysis. The results of this analysis are graphically presented in Figure A1.4.2 - 35 and show that a 56°C or 100°F reduction in firing temperature from the initial

1734°C or 3153°F results in approximately 1.5% increase in heat rate while the NOx reduces from 42 ppmvd to 28 ppmvd (at 15% O<sub>2</sub> concentration) with the shorter combustors, i.e., corresponding to a residence time of 5 ms in the 2<sup>nd</sup> PSR. A further 56°C or 100°F reduction in firing temperature (i.e. 93°C or 200°F reduction from the initial 1734°C or 3153°F) results in an additional 1.5% or total of 3% increase in heat rate while the NOx reduces from 42 ppmvd to 20 ppmvd (at 15% O<sub>2</sub> concentration).

### **Air (Film) Cooled 1<sup>st</sup> Stage Turbine**

Open-circuit film-cooling of the blades has the advantage of forming a protective layer on the outside surface of the blade, i.e., by creating an additional insulating layer in addition to thermal barrier coatings to protect the metal. The effect on plant performance of utilizing air (film) cooling of the 1<sup>st</sup> stage turbine stationary and rotating blades instead of closed circuit steam cooling is investigated in this sensitivity analysis performed on the selected advanced case. The 2<sup>nd</sup> and 3<sup>rd</sup> stages of the turbine employ closed circuit steam cooling while the 4<sup>th</sup> and 5<sup>th</sup> stages employ open circuit air cooling as in the selected advanced case. Note that the gas temperature entering the 2<sup>nd</sup> stage at about 1500°C or 2740°F is much lower. The results of this analysis show that the heat rate penalty of utilizing air (film) cooling for the 1<sup>st</sup> stage instead of closed circuit steam cooling is about 0.8%, quantifying the trade-off between plant performance and the need for developing the necessary more advanced materials required with closed circuit steam cooling of the 1<sup>st</sup> stage.

## **ECONOMIC ANALYSIS**

Rough order of magnitude (ROM) plant cost estimates, operating and maintenance cost estimates, and levelized cost of electricity are developed for the Baseline Case and the selected advanced Brayton cycle case consisting of the intercooled gas turbine in order to assess the economic incentive for funding the development of such an advanced engine. The ROM plant cost estimate for the Baseline Case is \$2,285/kW while that for the Advanced Brayton cycle is \$2,107/kW (on a 4<sup>th</sup> quarter 2007 basis) which is a 7.8% reduction in cost. This significant reduction in the total plant cost on a per kW basis is primarily due to:

1. the higher efficiency of the advanced Brayton cycle which increases the plant power output for a given coal throughput and consequently decreases the associated capital charges
2. and due to the higher specific power output of the advanced combined cycle which reduces the relative equipment sizes in the power block.

The plant section costs were factored primarily from the costs estimates presented in the DOE / NETL report titled, “Cost and Performance Baseline for Fossil Energy Plants,” Report No. DOE / NETL - 2007/1282, dated May 2007. The relative cost of the advanced intercooled gas turbine was developed using methodology presented for aero-derivative gas turbines in the Final Report prepared for Gas Research Institute by Fluor titled, “Evaluation of Advanced Gas Turbine Cycles,” Report No. GRI-93/0250, dated August 1993. The operating and maintenance costs as

well as the 20-year period levelized cost of electricity were estimated utilizing methodology consistent with that used in the above cited DOE / NETL report.

The levelized cost of electricity for the Baseline Case was estimated at \$85.72/MWhr while that for the Advanced Brayton cycle case was estimated at \$79.08/MWhr (at a capacity factor of 80% and with the Pittsburgh No. 8 coal priced at \$1.73/MM Btu, HHV) which is almost an 8% reduction over the Baseline Case. If a cost penalty of \$30/ST CO<sub>2</sub> emitted is assigned to the two cases, then the levelized cost of electricity of the Baseline Case is increased to \$89.08/MWhr while that for the Advanced Brayton cycle case is increased to \$82.19/MWhr.

Next, with respect to the impact of including an SCR to reduce NO<sub>x</sub> emissions to an ultra low value (2 ppmvd, 15% O<sub>2</sub> basis) on the cost of electricity, a previous study conducted for the DOE / NETL under contract DE-FC26-00NT40845 determined that it was insignificant.

### DEVELOPMENT NEEDS

The promising advanced Brayton cycle identified to meet the efficiency objectives of this project has the following characteristics:

Type Brayton cycle	Intercooled high pressure ratio
Overall Compression Ratio	50
LP Compressor Pressure Ratio	2.75
HP Compressor Pressure Ratio	18.8
Intercooler Type	Spray
Gas Turbine Specific Power	1,630 kW/(kg/s) or 740 kW/(lb/s)
Net Plant Specific Power	1,639 kW/(kg/s) or 743 kW/(lb/s) <sup>14</sup>
Gas Turbine Exhaust Mass Flow Rate to Inlet Mass Flow Rate Ratio	1.457 <sup>15</sup>
Firing Temperature (1 <sup>st</sup> Stage Rotor Inlet)	1734°C or 3153°F
Turbine Cooling	Closed circuit steam cooling of HP stages and open circuit air cooling of LP stages
Shaft Arrangement	HP compressor driven by HP turbine. LP compressor and generator driven by LP turbine, operating at 3600 RPM.
Bottoming Rankine Cycle, Superheat Pressure / Superheat Temperature / Reheat temperature	166.5 barA / 618°C / 618°C or 2415 psia / 1145°F / 1145°F

The greatest technological challenge for the development of this gas turbine is in the area of advanced materials required to withstand the very high firing temperature. Thus, the sensitivity

<sup>14</sup> Corresponds to about 340 MW net IGCC output with the inlet air flow of a GE LMS100PA gas turbine.

<sup>15</sup> This ratio is significantly higher than current engines operating on natural gas or distillate because of (1) spray intercooling, (2) syngas firing with diluent addition and (3) no air extraction for the ASU.

analysis performed and discussed in a previous section on this cycle measured the reduction in the firing temperature that may be made possible (and thus the required advanced turbine materials to meet the overall plant thermal efficiency goal) by making performance enhancements in other areas such as gas turbine component aerodynamic improvements and the electrical equipment. Their individual contributions are summarized in the following table. As discussed previously, the individual contributions are not highly significant but the data shows that the sum total contribution can be significant, as much as 70°C or 126°F reduction in the firing temperature. A reduction of 70°C or 126°F in the firing temperature has the additional benefit of reducing NO<sub>x</sub> emission. Based on data developed in the previous sensitivity analysis of the effect of firing temperature on NO<sub>x</sub>, a significant reduction in the NO<sub>x</sub> from 42 ppmvd to 26 ppmvd (at 15% O<sub>2</sub> concentration) may be realized (while utilizing the shorter combustors, i.e., corresponding to a residence time of 5 ms in the 2<sup>nd</sup> PSR) with the 70°C or 126°F decrease in firing temperature. The data presented in this table also helps prioritize these other areas of research.

	<b>Contribution to Reduction in Firing Temperature</b>
Increasing the gas turbine air compressor efficiency by 2% points	20°C or 36°F
Increasing the gas turbine expander by 1% point	20°C or 36°F
High efficiency exhaust diffuser (C <sub>p</sub> = 0.9)	30°C or 54°F
Application of superconductivity technology to transformers and generators	Insignificant
<b>Combined Contribution</b>	<b>70°C or 126°F</b>

## COMBUSTOR NEEDS

The table below summarizes the main features of the combustor required by this advanced Brayton cycle.

Combustor	
Inlet Air Temperature	523°C (973°F)
Discharge Temperature	1781°C (3237°F)
Inlet Air O <sub>2</sub> Concentration, Volume %	19.9
Discharge O <sub>2</sub> Concentration, Volume %	1.6
Decarbonized Syngas Adiabatic Flame Temperature	1875°C (3407°F)

As seen from this data, a combustor to withstand the very high temperatures is required while the relatively small amount of excess air used to increase the firing temperature further exacerbates the technological challenge for the development of such a combustor. As discussed in a previous section, the NO<sub>x</sub> continues to form in the dilution zone of the combustors because of the very high combustor discharge temperature. Thus, the current approaches to low NO<sub>x</sub> combustor designs described under Task 1.4.1 may not suffice since the air to fuel ratio is too small to cause rapid quenching of the flame within the combustor to limit the formation of NO<sub>x</sub>. If a short combustor is utilized to minimize the residence time and thus limit the NO<sub>x</sub> formation, then

natural gas as a backup fuel or startup cannot be considered. The gasification island will have to be started up first while flaring the syngas and then the gas turbine will have to be brought online.

As discussed in the sensitivity analysis presented in a previous section where the ASU is designed to provide the maximum amount of  $N_2$ , the resulting (lowest) combined LHV of the humidified syngas and diluent  $N_2$  is  $3,980 \text{ kJ/nm}^3$  or 101 Btu/scf. The increased nitrogen dilution does reduce the  $NO_x$  significantly, from 42 ppmvd to 10 ppmvd (at 15%  $O_2$  concentration) with the shorter combustors, i.e., corresponding to a residence time of 5 ms in the 2<sup>nd</sup> PSR. However, the firing temperature of gas turbine is also reduced, by about  $22^\circ\text{C}$  or  $40^\circ\text{F}$  resulting in an increase in the net plant heat rate by as much as 2.2%. Furthermore, increasing the diluent addition may increase the challenge for the combustor design since the  $O_2$  content of the combustor exhaust gas is already very low at 1.6%.

SCRs would be required to limit the  $NO_x$  emissions to the desired 2 ppmVd (15%  $O_2$  basis) value. Higher SCR catalyst volume would be required for these advanced firing temperature cases, however, since the amount of  $NO_x$  generated within the combustor is substantially higher than that in the Baseline Case.

## **Materials**

Materials that can withstand a combination of creep, pressure loading, high cycle and thermal fatigue at these temperatures are required. Materials presently used such as wrought, sheet-formed nickel-based super-alloys provide good thermo-mechanical fatigue; creep and oxidation resistance for static parts and can be formed into the required shapes (combustor barrels and transition pieces), weldability and suitability to repair and overhaul operations. The severe temperatures require that large portions of the combustor be protected using thermal barrier coatings. These coatings are applied over the surface of existing materials to provide protection against wear, erosion, oxidation / hot corrosion, as well as for improving and maintaining the surface finish.

Materials technology for the combustor should be aimed at replacement of conventional wrought nickel-based products with:

- More suitable Ni-based alloys
- Oxide dispersion strengthened metallic systems
- Ceramic matrix composites.

Thermal barrier coatings for combustor applications is currently based primarily on systems comprising of a bondcoat of MCrAlY (where M is the base metal such as Ni and / or Co) and a topcoat of ceramic material. Developments aimed at applying thicker coatings to enable the higher firing temperature as well as increasing the phase stability and resistance to sintering of the ceramic topcoat at higher temperatures are required. Furthermore, thermal barrier coatings that can withstand an environment containing water vapor at a high partial pressure are required.

## COMPRESSOR NEEDS

The overall pressure ratio of 50 for this advanced Brayton cycle is significantly higher than what has been currently demonstrated but such a high pressure ratio has been proposed for an advanced aero engine (Pratt & Whitney's baseline engine proposed for Boeing's 787 transport plane) and is close to that of the aero-derivative GE LMS100 intercooled gas turbine which has a pressure ratio of 41 at ISO conditions.

The advanced Brayton cycle design will thus have to be based on modifying an existing aero-derivative engine such as the GE LMS100; by adding stages at the front-end of the LP compressor<sup>16</sup> and / or at the back-end of the HP compressor depending on the existing Mach number limitations. An added advantage of utilizing the GE LMS100 engine is that it is configured with an intercooler. The suction air flow of this engine is 208 kg/s or 458 lb/s at ISO conditions. With a plant specific power output of 1,639 kW/(kg/s) or 743 kW/(lb/s) for the advanced Brayton cycle IGCC, the net plant output on a per gas turbine basis would be 1,639 kW/(kg/s) X 208 kg/s or 340 MW; or for a two gas turbine based plant, the net output would be 680 MW, a reasonable (i.e., economically viable) plant size.

If an aircraft engine is modified instead, the major mechanical changes from aircraft to this ground-based engine involves replacing the turbofan and installing a new LP compressor using lower cost materials, combustor changes, HP turbine changes to handle increased flow and to reduce cost, and a new, lower cost LP turbine to expand to atmospheric pressure. Additional shaft length to accommodate scrolls for the intercooler would also be needed. The key to keeping development costs to a minimum is keeping gas path the same, thereby allowing the compressors, especially the high pressure compressor to remain unchanged, except for materials.

In either case, the development of the advanced Brayton cycle which requires an aero-frame engine should be based on the use of existing compressor gas path designs. This would significantly reduce the cost of development.

Finally, it must be stated that in general, the challenge facing the compressor is to provide improved cycle efficiency, operability and reduced costs by optimizing the work done by each stage. The need to maintain compressor performance and integrity through life, while reducing parts costs and the use of more effective manufacturing processes is paramount, as is the need to achieve operational lifetimes in excess of 100,000 hours. Many of these targets are dependent upon improved design and aero-thermal analysis methods.

### **Intercooler**

Spray intercooling has been commercially practiced in the GE LM6000 SPRINT engine for a number of years. Presence of any water droplets in the intercooler discharge would lead to erosion of the HP compressor blading and erosion resistant coatings for existing materials or development of erosion resistant materials may be required. Proper design of the spray system is essential to minimize droplet carryover into the HP compressor. A demister pad installed at the discharge end of the intercooler with low pressure drop characteristics would be very desirable.

---

<sup>16</sup> Addition of front-end stages increases the suction air flow.

## **TURBINE NEEDS**

### **Cooling Technology**

The 1<sup>st</sup>, 2<sup>nd</sup> and 3<sup>rd</sup> stages of the turbine employ closed circuit steam cooling while the 4<sup>th</sup> and 5<sup>th</sup> stages employ open circuit air cooling. Steam with its very high specific heat is an excellent cooling medium while the advantage with closed circuit cooling is that the momentum and dilution losses which are incurred in open circuit cooling are avoided. On the other hand, open circuit film cooling of the blades (utilizing air) has the advantage of forming a protective layer on the outside surface of the blade, i.e., by creating an additional insulating layer (i.e., in addition to thermal barrier coatings to protect the metal).

The effect on plant performance of utilizing air (film) cooling of the 1<sup>st</sup> stage turbine stationary and rotating blades (where the temperatures are highest) instead of closed circuit steam cooling was discussed in sensitivity analysis of this cycle. The 2<sup>nd</sup> and 3<sup>rd</sup> stages of the turbine employed closed circuit steam cooling while the 4<sup>th</sup> and 5<sup>th</sup> stages employ open circuit air cooling as in the selected advanced case. Note that the gas temperature entering the 2<sup>nd</sup> stage at about 1500°C or 2740°F is much lower than that in the 1<sup>st</sup> stage. The results of this analysis as discussed previously showed that the heat rate penalty of utilizing air (film) cooling for the 1<sup>st</sup> stage instead of closed circuit steam cooling was about 0.8%, quantifying the trade-off between plant performance and the need for developing the necessary more advanced materials required with closed circuit steam cooling of the 1<sup>st</sup> stage.

### **Turbine Blade Materials**

A main consideration in the design of blades is to avoid creep failure due to the combined effect of high stresses and temperatures with target lifetime being in excess of 50,000 operating hours. Turbine blades are subjected to severe thermal stresses caused by the many start-up / shutdown operations and unexpected trips. Furthermore, the rotating blades are subjected to high frequency excitations as they pass through the wake of the upstream combustor and the stationary blades. These excitations can lead to fatigue failure.

To meet these requirements while the turbine firing temperatures are being increased, conventionally cast nickel-based super-alloys are being replaced by directional solidification blades as well as single crystal blades which provide even more significant benefits. However, alloys with greater defect tolerance need to be developed and demonstrated. Development of alloys having improved castability, higher corrosion resistance and reduced heat treatment times are required.

In order to achieve increased creep strength, higher levels of alloying with Al, Ti, Ta, Re, W have been used. Cr additions had to be reduced to offset the increased tendency to form topologically close-packed phases which limit ductility and reduced strength. Lower Cr concentrations reduce the corrosion resistance of the alloys which in turn has led to the development of protective coatings. Coatings are applied over the surface of existing materials

to provide protection against wear, erosion, oxidation / hot corrosion, as well as for improving and maintaining the surface finish. The coating process includes aluminizing, chromizing and application of the MCrAlY (M = Ni / Co). Ceramic coatings provide thermal barrier protection to reduce metal temperatures. These coatings need to be able to withstand an environment containing water vapor at a high partial pressure are required.

Development of ceramic matrix composites may also be required for the very hot components or sections of the turbine. Ceramic composites employing silicon carbide fibers in a ceramic matrix such as silicon carbide or alumina are commercially available while single crystal oxide fibers are under consideration.

## **DEVELOPMENT COSTS AND TIME**

Based on the development costs and timeline for advanced gas turbines as documented in a previous study conducted for the DOE / NETL under contract DE-FC26-00NT40845, the design and component test phase may take approximately 40 to 42 months. Initial build could commence with long lead items about half way through the first phase and last 24 to 27 months. At the end of the approximately 54 months, test of the initial unit could begin and could last approximately 15 months. Cost for such a program can be between \$250 and \$275 million, the program being predicated on a minimum commitment of 8 engines.

## **BIBLIOGRAPHY**

1. Robson, F.L., "Advanced Turbine Systems Study - System Scoping and Feasibility Study," Doe Contract De-Ac21-92mc29247, United Technologies Research Center, March 1993.
2. Hannis, J. (Siemens Industrial Turbomachinery), G. McColvin (Siemens Industrial Turbomachinery), C. J. Small (Rolls-Royce plc), J. Wells (RWE npower), "Mat UK Energy Materials Review Materials R&D Priorities For Gas Turbine Based Power Generation," July 10, 2007.
3. Primary author: Stewart Miller, abstracted from Materials World, vol. 4, 1996, "Advanced materials mean advanced engines," Robert Schafrik (GE Aircraft Engines Cincinnati, Ohio), Robert Spragu (GE Aircraft Engines, retired Cincinnati, Ohio), "Gas Turbine Materials," Advanced Materials & Processes, May 2004.

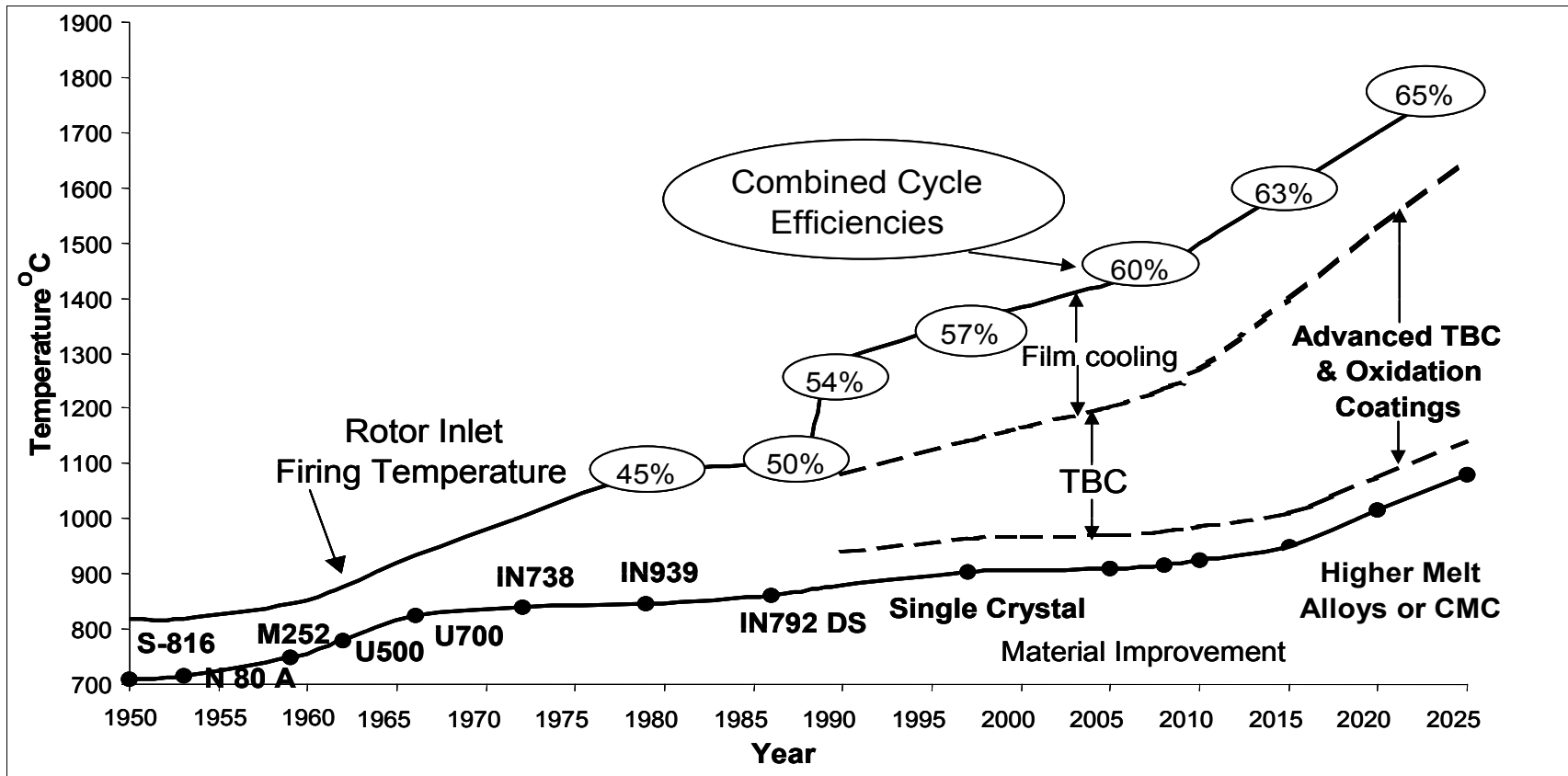


Figure A1.4.2 - 1: Effect of Increasing Firing and 1<sup>st</sup> Stage Stator Blade Temperatures

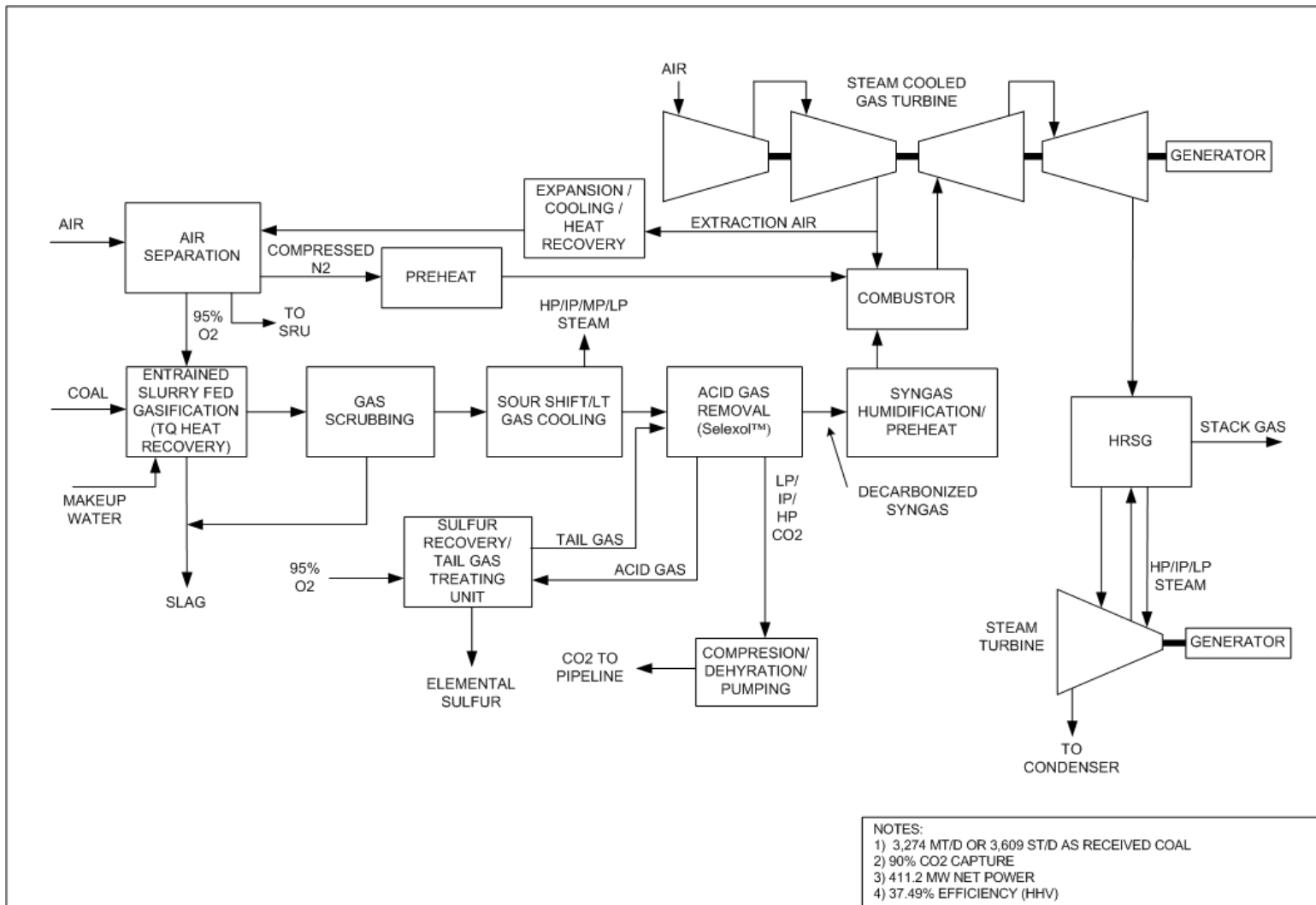


Figure A1.4.2 - 2: Overall Block Flow Diagram – IGCC with CO<sub>2</sub> Capture – Simple Cycle GT / PR=37 / IP ASU

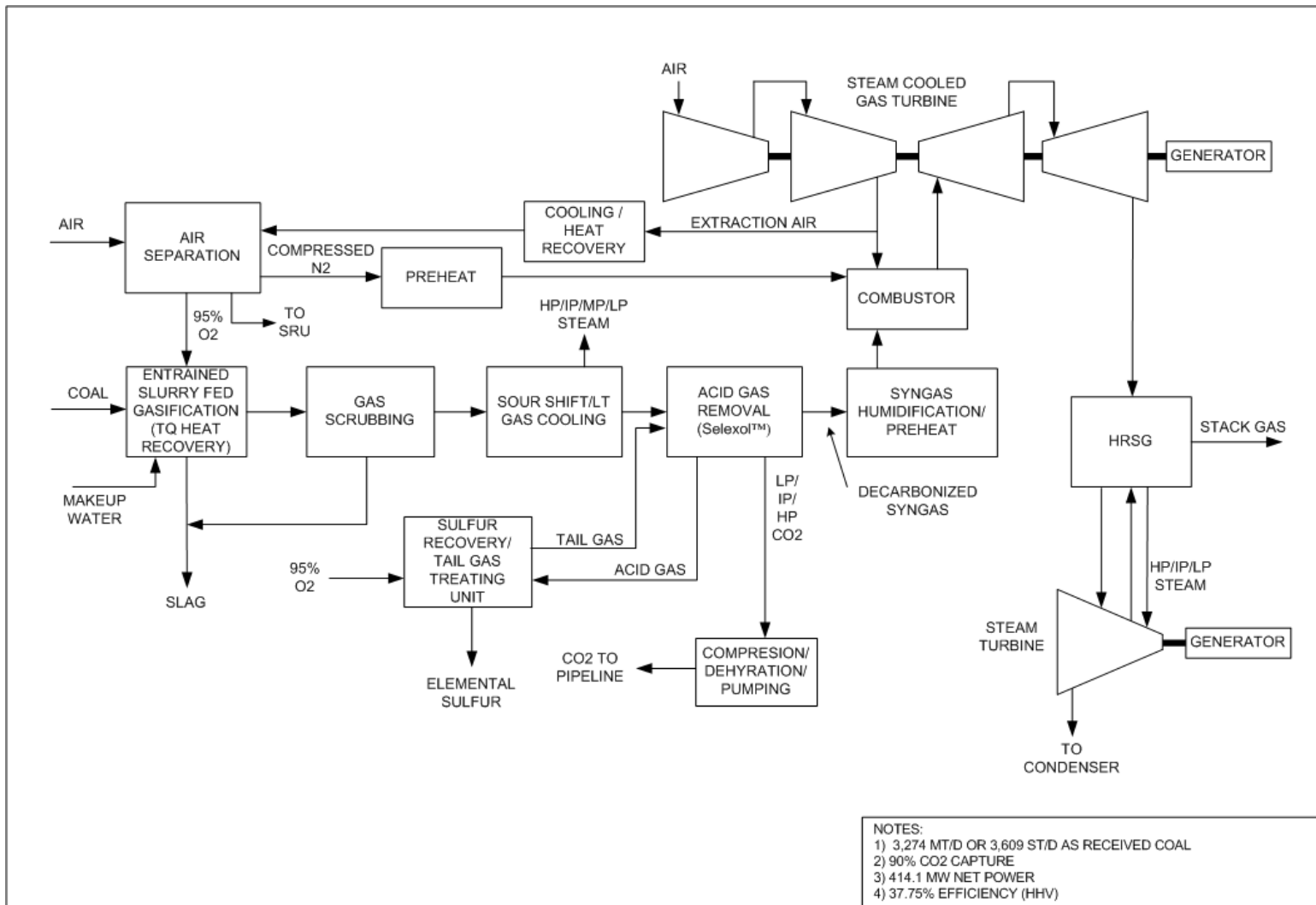


Figure A1.4.2 - 3: Overall Block Flow Diagram – IGCC with CO<sub>2</sub> Capture – Simple Cycle GT / PR=37 / HP ASU

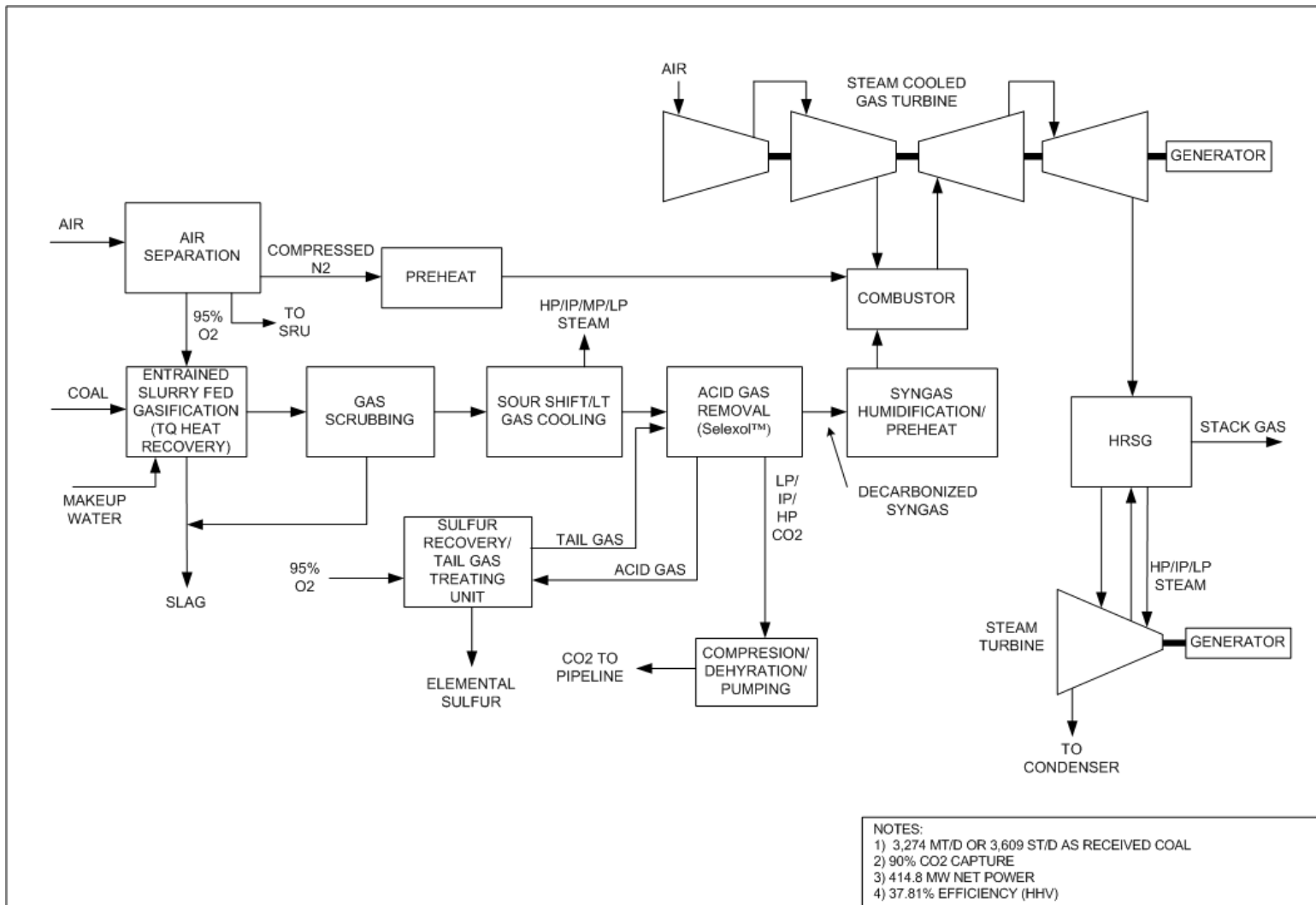


Figure A1.4.2 - 4: Overall Block Flow Diagram – IGCC with CO<sub>2</sub> Capture – Simple Cycle GT / PR=37 / No Air Extraction

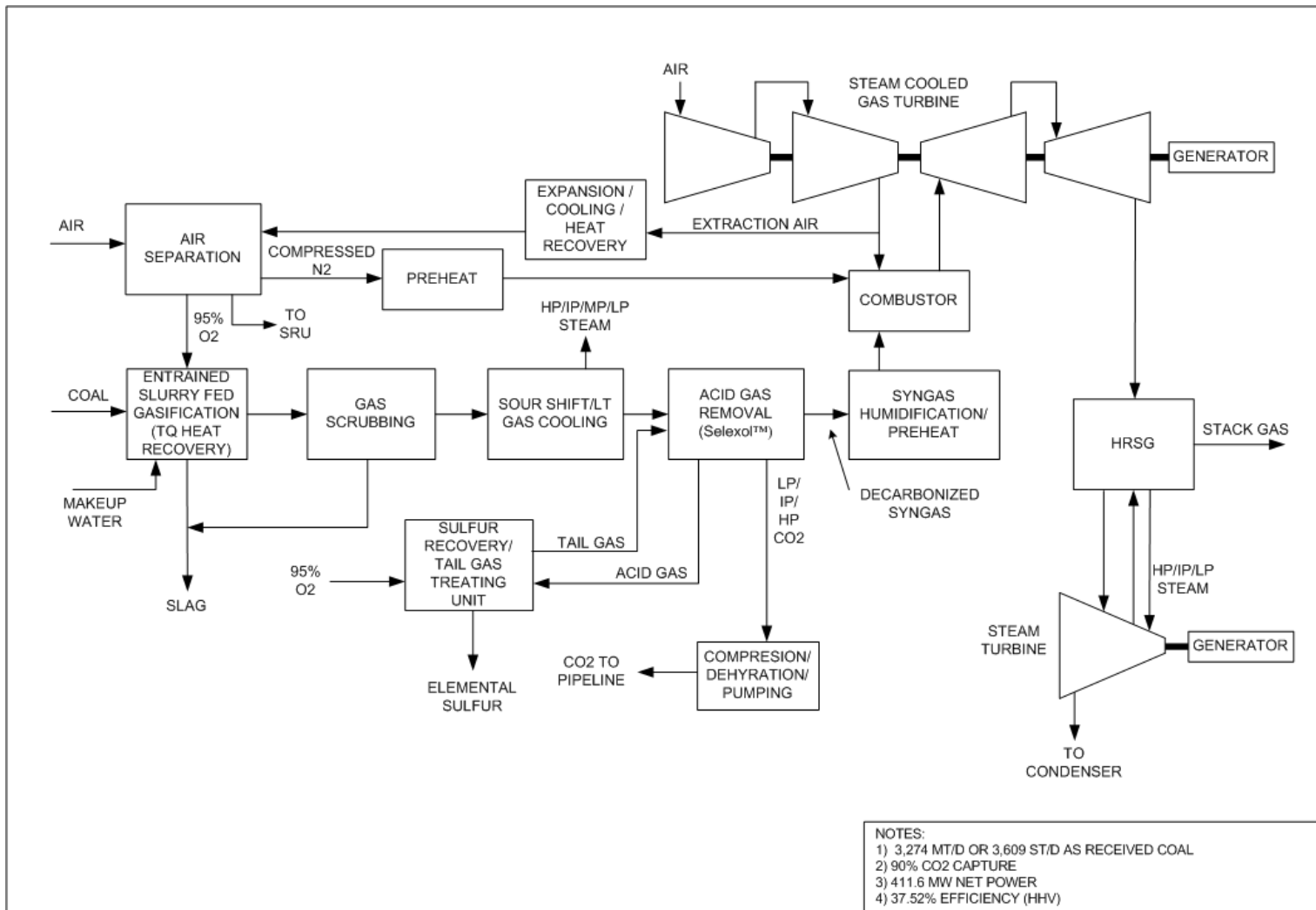


Figure A1.4.2 - 5: Overall Block Flow Diagram – IGCC with CO<sub>2</sub> Capture – Simple Cycle GT / PR=50 / IP ASU

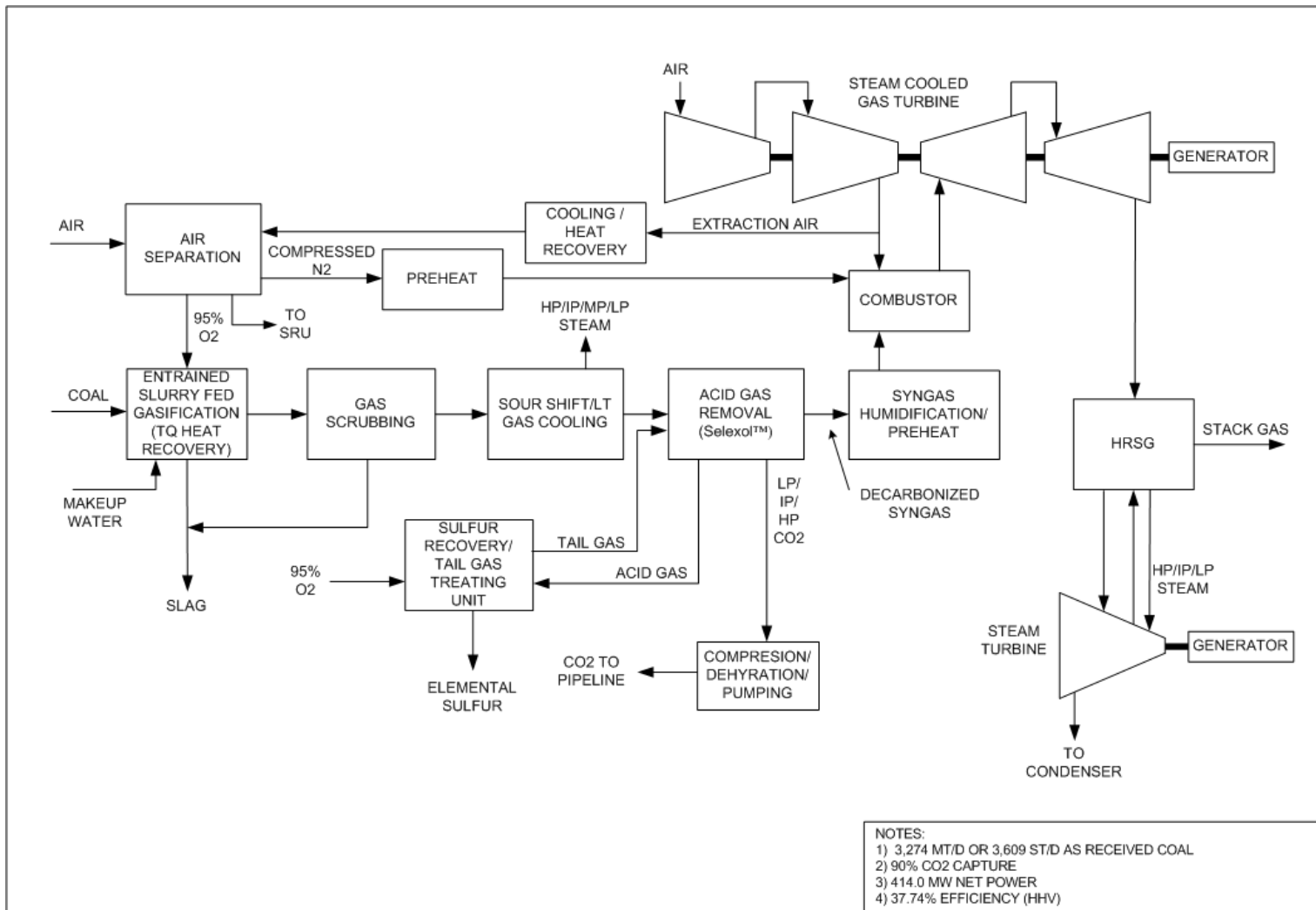


Figure A1.4.2 - 6: Overall Block Flow Diagram – IGCC with CO<sub>2</sub> Capture – Simple Cycle GT / PR=50 / HP ASU

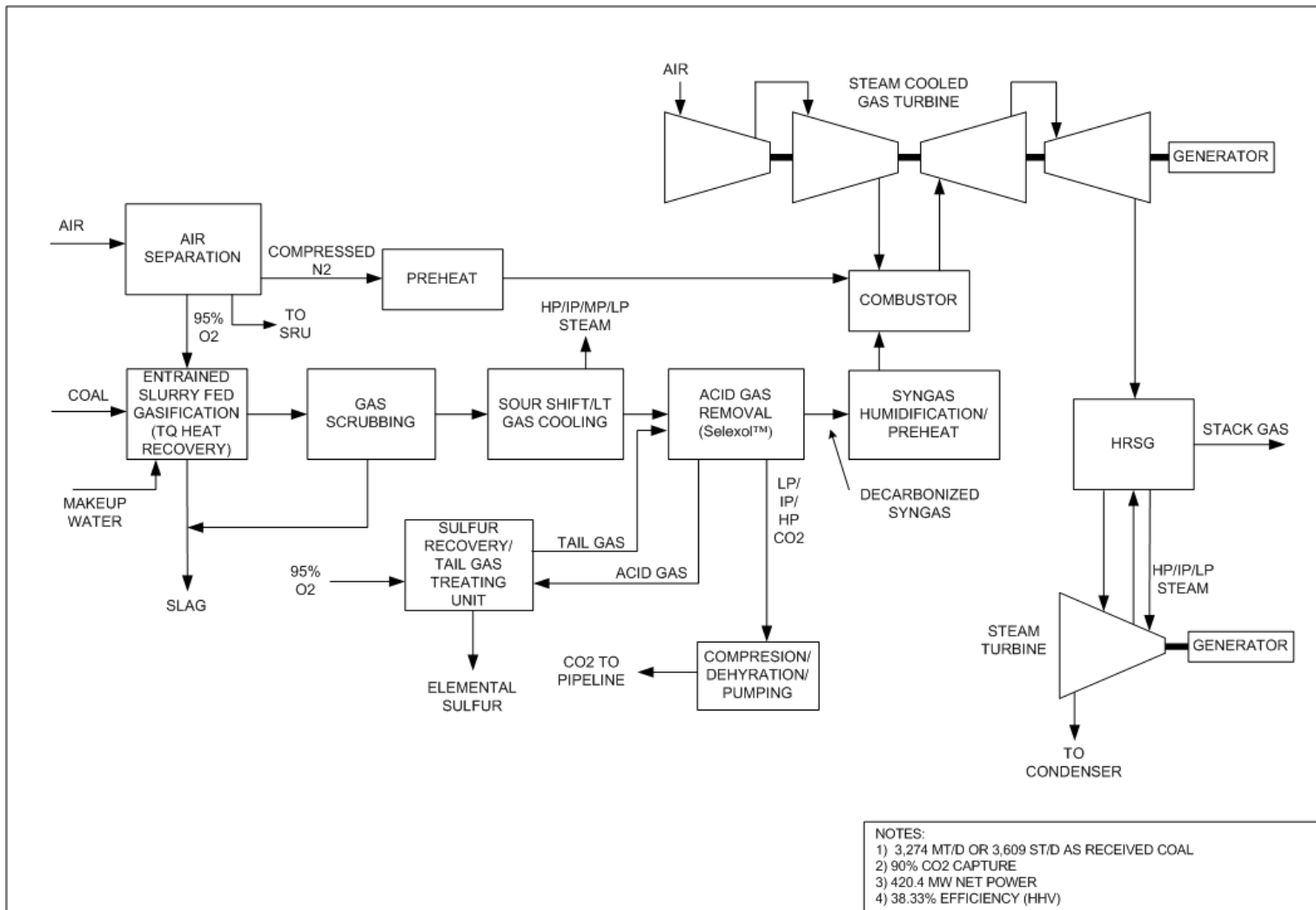
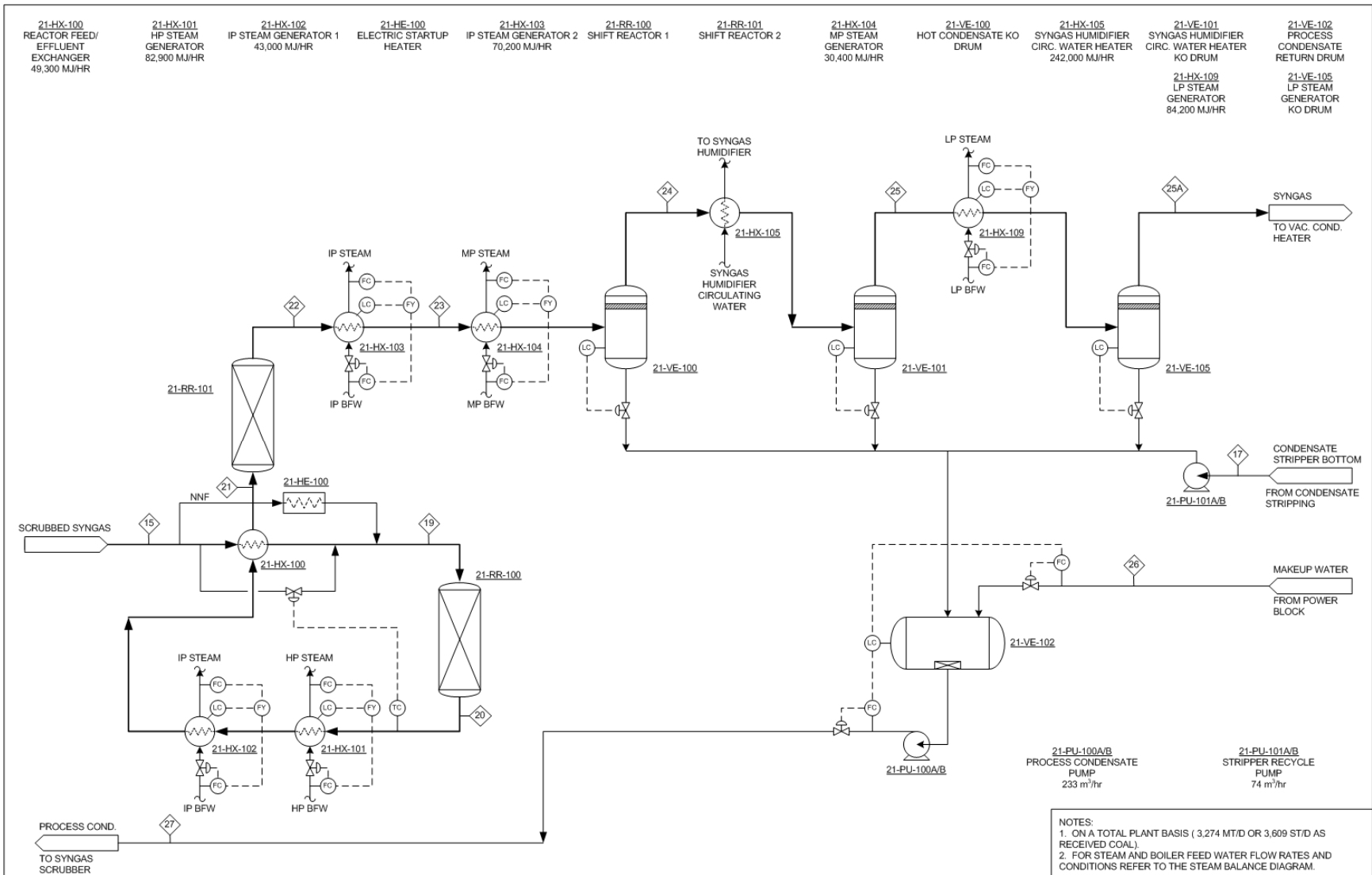
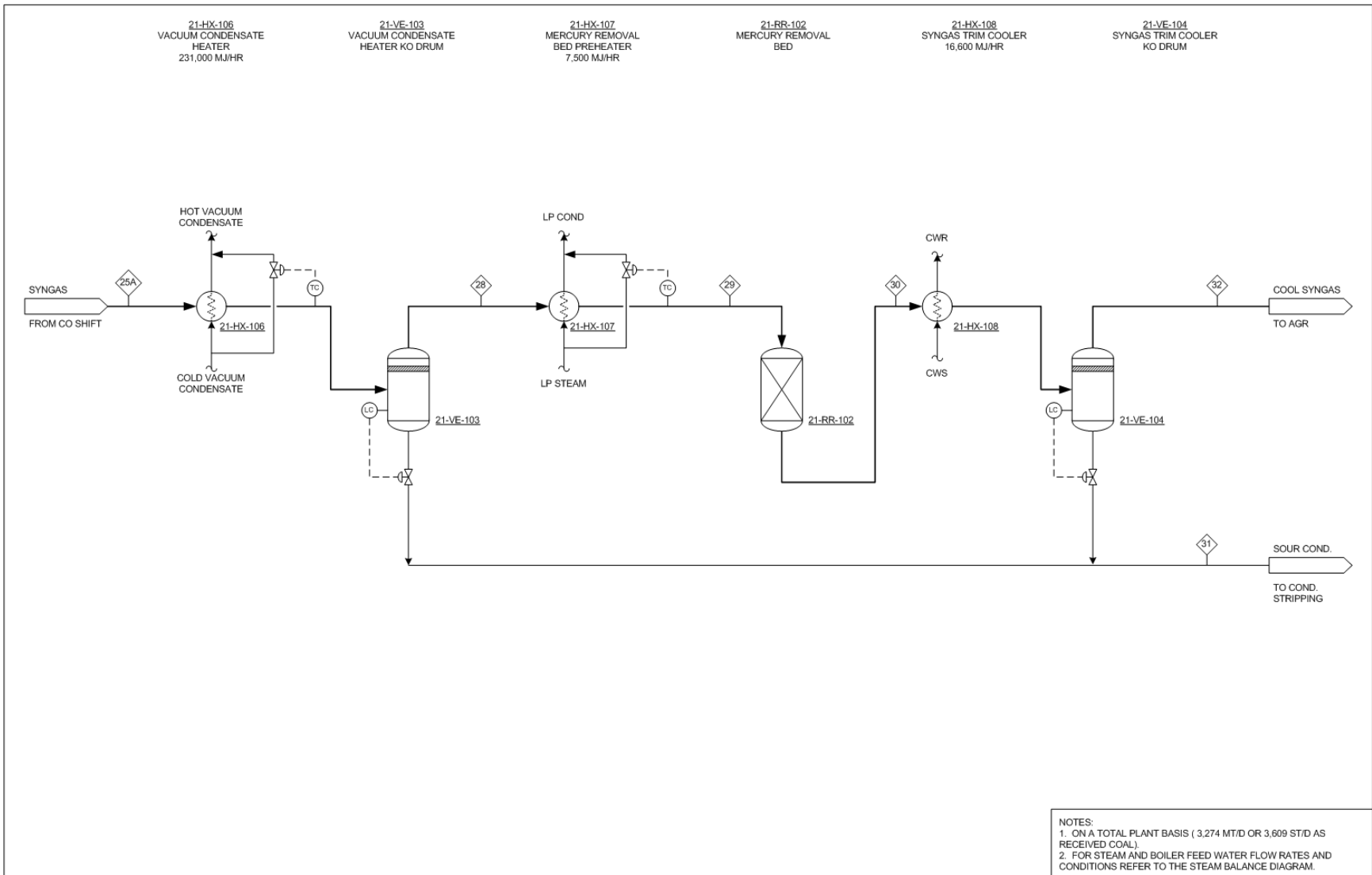


Figure A1.4.2 - 7: Overall Block Flow Diagram – IGCC with CO<sub>2</sub> Capture – Simple Cycle GT / PR=50 / No Air Extraction





**Figure A1.4.2 - 9: Process Flow Diagram – CO Shift / Low Temperature Gas Cooling Unit - Simple Cycle GT with PR=50, Intercooled Cycle GT with PR=50 & Intercooled Closed Circuit Air Cooled GT**



**Figure A1.4.2 - 9: Process Flow Diagram – CO Shift / Low Temperature Gas Cooling Unit - Simple Cycle GT with PR=50, Intercooled Cycle GT with PR=50 & Intercooled Closed Circuit Air Cooled GT - continued**

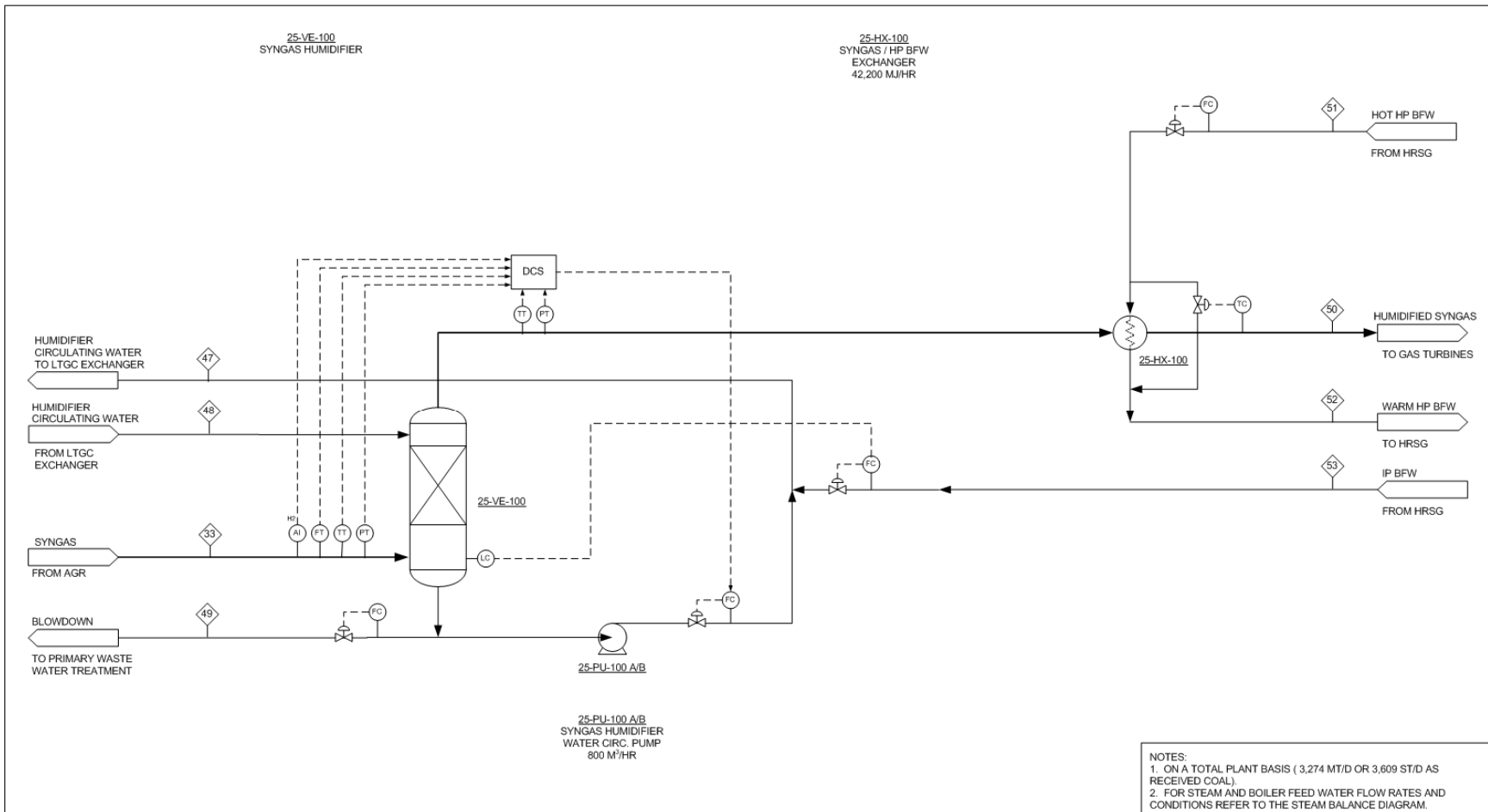


**Figure A1.4.2 - 10: Process Flow Diagram – Syngas Humidification Unit - Simple Cycle GT with PR=50, Intercooled Cycle GT with PR=50 & Intercooled Closed Circuit Air Cooled GT**

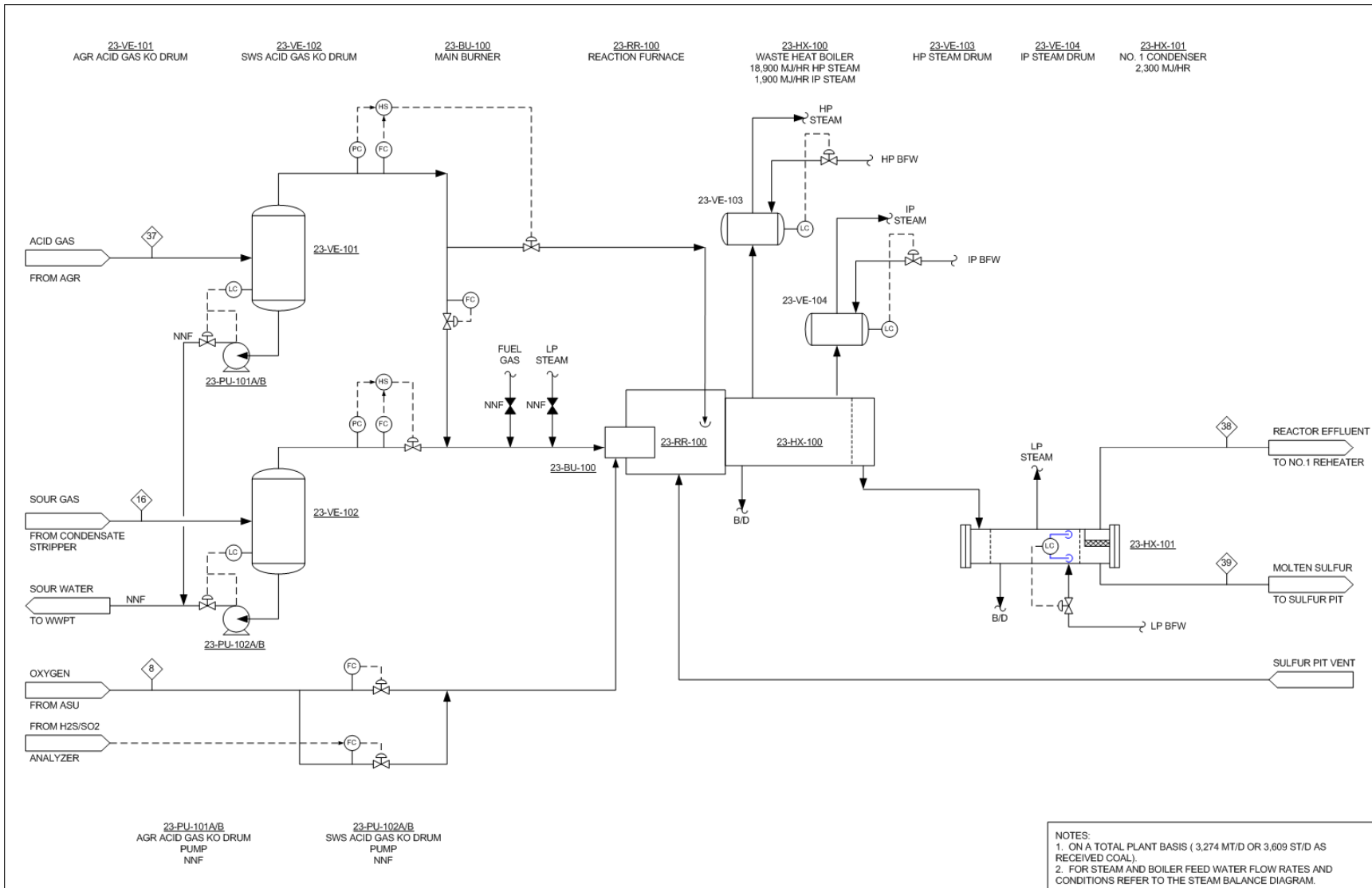


**Figure A1.4.2 - 11: Process Flow Diagram – Sulfur Recovery / Tail Gas Treating Unit - Simple Cycle GT with PR=50, Intercooled Cycle GT with PR=50 & Intercooled Closed Circuit Air Cooled GT**

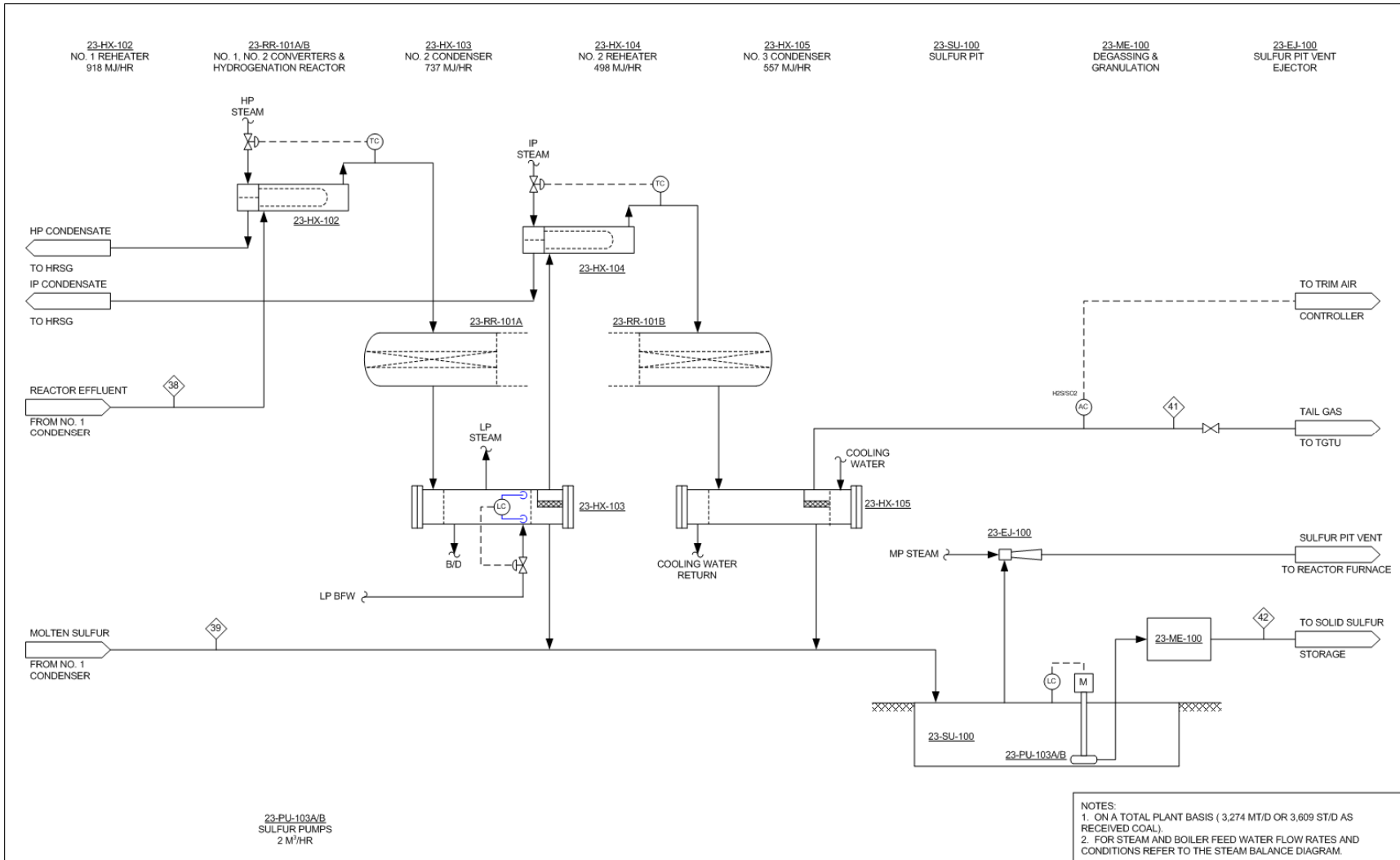


**Figure A1.4.2 -11: Process Flow Diagram – Sulfur Recovery / Tail Gas Treating Unit - Simple Cycle GT with PR=50,  
 Intercooled Cycle GT with PR=50 & Intercooled Closed Circuit Air Cooled GT - continued**

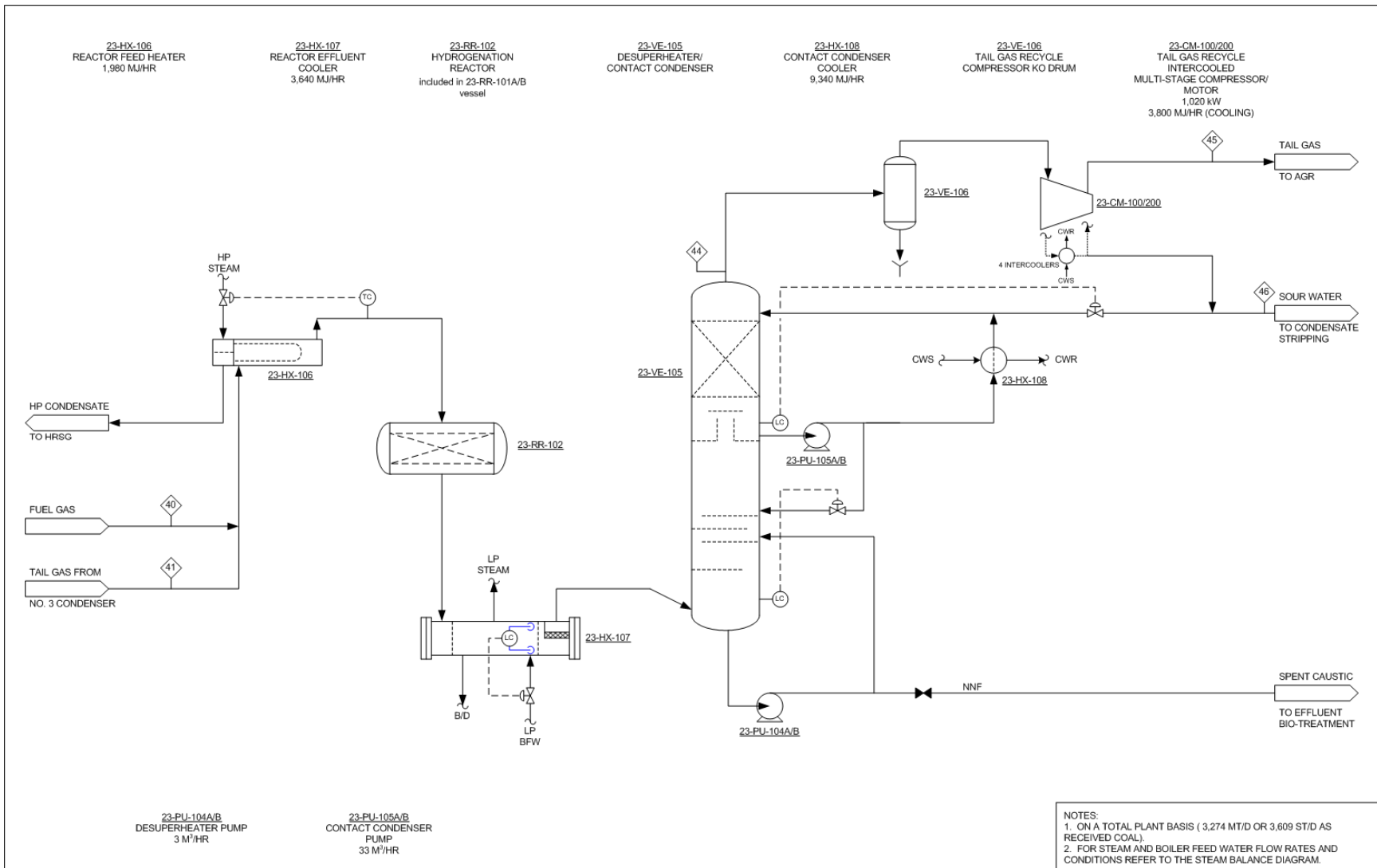


**Figure A1.4.2 - 11: Process Flow Diagram – Sulfur Recovery / Tail Gas Treating Unit - Simple Cycle GT with PR=50, Intercooled Cycle GT with PR=50 & Intercooled Closed Circuit Air Cooled GT - continued**

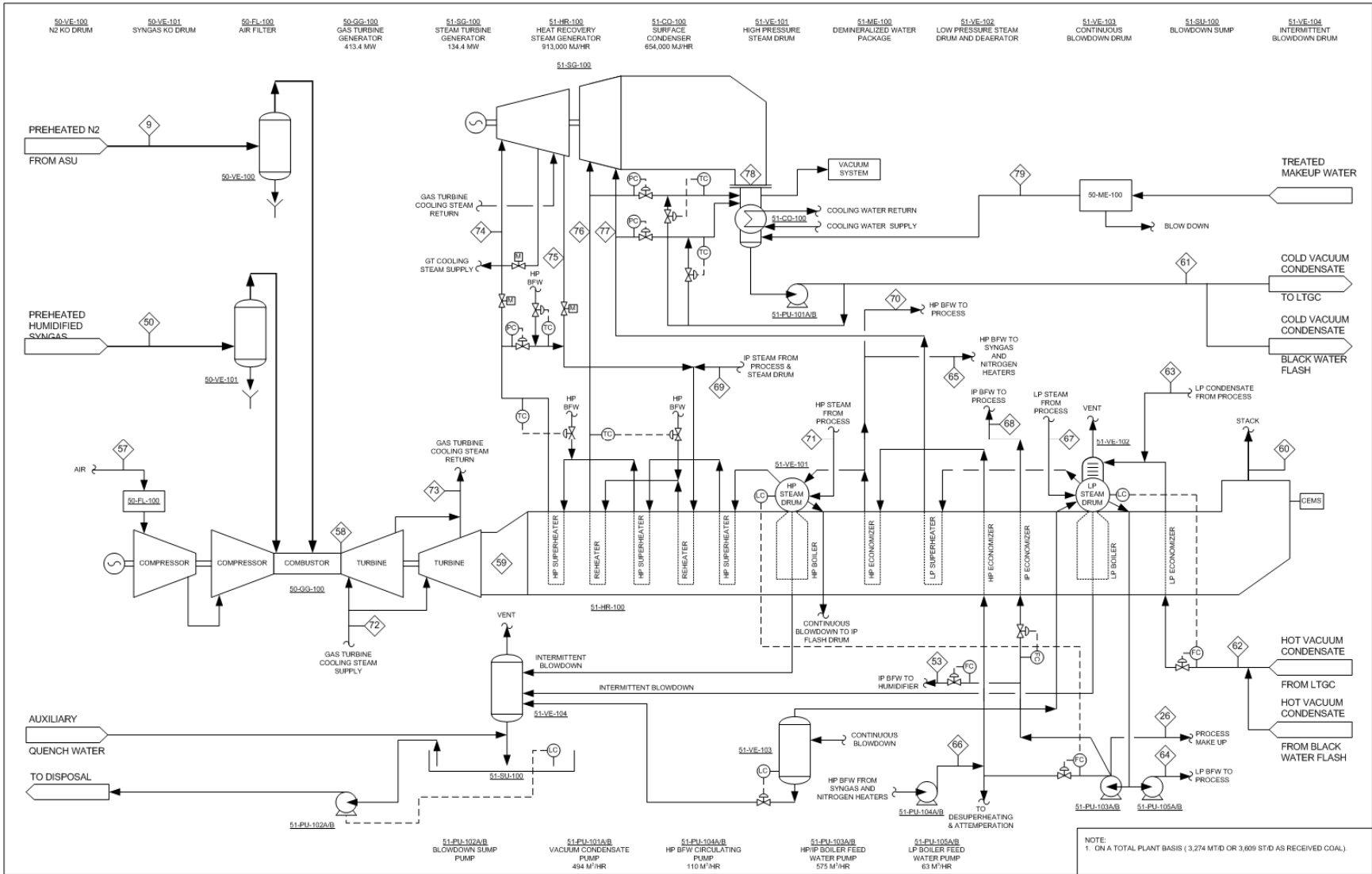


Figure A1.4.2 - 12: Process Flow Diagram – Power Block - Simple Cycle GT with PR=50



**Table A1.4.2 - 1: Stream Data – Simple Cycle Gas Turbine**

Basis: 3,274 Tonne/D (As Received) or 3,078 Tonne/D (Dry Basis) Pittsburgh No. 8 Coal

Mol Fraction	1	2	3	4	5	6	7	8	9	10 (not used)	11	12
O2		0.2077	0.2077	0.2077	0.9500	0.9500	0.9500	0.9500	0.0062			
N2		0.7722	0.7722	0.7722	0.0230	0.0176	0.0211	0.0176	0.9891			
Ar		0.0094	0.0094	0.0094	0.0270	0.0324	0.0289	0.0324	0.0047			
H2												
CO												
CO2		0.0003	0.0003	0.0003								
H2O		0.0104	0.0104	0.0104							1.0000	1.0000
CH4												
H2S												
SO2												
Cl2												
HCl												
NH3												
COS												
Total		1.0000	1.0000	1.0000	1.0000	1.0000	1.0000	1.0000	1.0000		1.0000	1.0000
Coal (As Received), kg/hr	136,416											
kgmol/hr (w/o Solids)	-	17,804	11,395	6,409	2,431	1,288	3,719	82	8,779		2,260	2,260
kg/hr (w/o Solids)	-	513,714	328,800	184,914	78,082	41,455	119,537	2,645	246,637		40,717	40,717
Temp., C	15.0	15.0	15.0	15.0	92.7	81.6	88.9	19.4	287.8		349.1	140.6
Press., bar	1.01	1.01	1.01	1.01	87.08	87.08	87.08	3.04	61.23		180.96	177.47
Enthalpy, MJ/hr	-123,514	-52,216	-33,420	-18,796	3,618	1,443	5,060	-16	67,788		67,203	24,584
See Note	1, 2	2	2	2	2	2	2	2	2		3	3

Note:

1. Enthalpy expressed as HHV = 3,949,275 MJ/hr.
2. The reference state for thermodynamic properties is the standard enthalpy of formation of ideal gas at 25°C and 1 atm.
3. Enthalpy corresponds to ASME Steam Tables Basis.

**Table A1.4.2 - 1: Stream Data – Simple Cycle Gas Turbine – continued**

Basis: 3,274 Tonne/D (As Received) or 3,078 Tonne/D (Dry Basis) Pittsburgh No. 8 Coal

Mol Fraction	13	14	15	16	17	18	19	20	21	22	23	24
O2												
N2	0.0000		0.0042	0.0015			0.0042	0.0042	0.0042	0.0042	0.0042	0.0042
Ar	0.0000		0.0036	0.0030			0.0036	0.0036	0.0036	0.0036	0.0036	0.0036
H2	0.0003		0.1661	0.1403			0.1661	0.3283	0.3283	0.3494	0.3494	0.3494
CO	0.0004		0.1935	0.0400			0.1935	0.0313	0.0313	0.0103	0.0103	0.0103
CO2	0.0008		0.0687	0.1456	0.0000		0.0687	0.2310	0.2310	0.2521	0.2521	0.2521
H2O	0.9977	1.0000	0.5563	0.0210	0.9999	1.0000	0.5563	0.3940	0.3940	0.3729	0.3729	0.3729
CH4	0.0000		0.0020	0.0014			0.0020	0.0020	0.0020	0.0020	0.0020	0.0020
H2S	0.0002		0.0040	0.0451	0.0000		0.0040	0.0042	0.0042	0.0042	0.0042	0.0042
SO2												
Cl2												
HCl												
NH3	0.0006		0.0013	0.6013	0.0001		0.0013	0.0013	0.0013	0.0013	0.0013	0.0013
COS	0.0000		0.0002	0.0009	0.0000		0.0002	0.0000	0.0000	0.0000	0.0000	0.0000
Total	1.0000	1.0000	1.0000	1.0000	1.0000	1.0000	1.0000	1.0000	1.0000	1.0000	1.0000	1.0000
kgmol/hr (w/o Solids)	291	447	29,185	40	3,871	1,160	29,185	29,185	29,185	29,185	29,185	29,185
kg/hr (w/o Solids)	5,256	8,062	562,306	811	69,747	20,896	562,307	562,304	562,304	562,304	562,304	562,304
kg/hr Solids	12,141	3,455										
kg/hr Total	17,397	11,516	562,306	811	69,747	20,896	562,307	562,304	562,304	562,304	562,304	562,304
Temp., C	<93.3	60.2	243.2	44.8	123.4	156.7	287.8	442.5	287.9	307.9	246.1	219.4
Press., bar	1.01	1.01	71.34	2.07	2.21	4.59	70.99	70.01	68.98	68.00	67.65	67.31
Enthalpy, MJ/hr	<-81,402	-140,031	-5,176,778	-3,812	-1,077,473	57,741	-5,127,453	-5,127,384	-5,302,621	-5,302,623	-5,372,787	-5,403,169
See Note	1	1	1	1	1	2	1	1	1	1	1	1

Note:

1. The reference state for thermodynamic properties is the standard enthalpy of formation of ideal gas at 25°C and 1 atm.
2. Enthalpy corresponds to ASME Steam Tables Basis.

**Table A1.4.2 - 1: Stream Data – Simple Cycle Gas Turbine – continued**

Basis: 3,274 Tonne/D (As Received) or 3,078 Tonne/D (Dry Basis) Pittsburgh No. 8 Coal

Mol Fraction	25	25A	26	27	28	29	30	31	32	33	34	35	36
O2													
N2	0.0053	0.0057		0.0000	0.0067	0.0067	0.0067		0.0067	0.0124		0.0000	0.0002
Ar	0.0046	0.0050		0.0000	0.0058	0.0058	0.0058	0.0000	0.0058	0.0096	0.0000	0.0000	0.0005
H2	0.4382	0.4773		0.0000	0.5576	0.5576	0.5576	0.0000	0.5576	0.9090	0.0000	0.0006	0.0200
CO	0.0129	0.0140		0.0000	0.0164	0.0164	0.0164		0.0164	0.0266	0.0000	0.0001	0.0016
CO2	0.3159	0.3440		0.0007	0.4018	0.4018	0.4018	0.0003	0.4018	0.0375	0.9973	0.9980	0.9763
H2O	0.2142	0.1443	1.0000	0.9986	0.0016	0.0016	0.0016	0.9920	0.0016	0.0001	0.0027	0.0012	0.0008
CH4	0.0025	0.0027		0.0000	0.0031	0.0031	0.0031	0.0000	0.0031	0.0049	0.0000	0.0000	0.0006
H2S	0.0052	0.0057		0.0001	0.0066	0.0066	0.0066	0.0001	0.0066	0.0000	0.0000	0.0000	0.0000
SO2													
Cl2													
HCl													
NH3	0.0014	0.0014		0.0005	0.0003	0.0003	0.0003	0.0075	0.0003				
COS	0.0000	0.0000		0.0000	0.0000	0.0000	0.0000		0.0000	0.0000	0.0000	0.0000	0.0000
Total	1.0000	1.0000	1.0000	1.0000	1.0000	1.0000	1.0000	1.0000	1.0000	1.0000	1.0000	1.0000	1.0000
kgmol/hr	23,262	21,354	5,819	17,516	18,278	18,278	18,278	3,076	18,278	11,164	1,097	2,798	3,118
kg/hr	455,392	420,954	104,829	315,908	365,525	365,525	365,525	55,429	365,525	56,252	48,185	122,960	134,413
Temp., C	187.9	170.0	150.0	156.5	40.6	51.7	51.7	40.6	26.7	16.7	0.1	3.6	11.7
Press., bar	66.96	66.62	78.78	75.84	66.28	65.95	65.45	66.28	65.10	62.44	1.08	3.24	10.00
Enthalpy, MJ/hr	-4,024,884	-3,584,365	-1,613,105	-4,843,274	-2,939,946	-2,932,427	-2,932,427	-875,292	-2,948,995	-205,309	-432,012	-1,101,938	-1,201,992
See Note	1	1	1	1	1	1	1	1	1	1	1	1	1

Note: 1. The reference state for thermodynamic properties is the standard enthalpy of formation of ideal gas at 25°C and 1 atm.

**Table A1.4.2 - 1: Stream Data – Simple Cycle Gas Turbine – continued**

Basis: 3,274 Tonne/D (As Received) or 3,078 Tonne/D (Dry Basis) Pittsburgh No. 8 Coal

Mol Fraction	37	38	39	40	41	42	43	44	45	46	47	48
O2												
N2	0.0014	0.0438		0.0124	0.0451		0.0001	0.0789	0.0811	0.0001	0.0000	0.0000
Ar	0.0024	0.0090		0.0096	0.0092		0.0003	0.0166	0.0170	0.0000	0.0000	0.0000
H2	0.1588	0.1010		0.9089	0.1041		0.0091	0.3589	0.3686	0.0000	0.0001	0.0001
CO	0.0071	0.1102		0.0266	0.1136		0.0008	0.0232	0.0239	0.0000	0.0000	0.0000
CO2	0.3092	0.1533		0.0375	0.1580		0.9895	0.4473	0.4594	0.0080	0.0001	0.0001
H2O	0.0563	0.4670		0.0001	0.5421			0.0280	0.0018	0.9891	0.9997	0.9997
CH4	0.0030			0.0049			0.0003	0.0003	0.0003		0.0000	0.0000
H2S	0.4412	0.0768			0.0182		0.0000	0.0462	0.0474	0.0026		
SO2		0.0384			0.0091							
Cl2												
HCl												
NH3	0.0202							0.0003	0.0003	0.0000		
COS	0.0006	0.0006			0.0006		0.0000	0.0002	0.0002	0.0000		
Total	1.0000	1.0000		1.0000	1.0000		1.0000	1.0000	1.0000	1.0000	1.0000	1.0000
Sulfur, kg/hr			2,824			3,927						
kgmol/hr	297	388	44	12	376	78	7,004	216	211	174	38,892	38,892
kg/hr	9,122	9,755	2,824	60	8,651	3,927	305,396	5,631	5,529	3,183	700,664	700,664
Temp., C	48.9	176.7	176.7	14.5	287.8	25.0	40.7	26.6	26.7	28.2	137.9	208.3
Press., bar	2.07	1.87	1.87	1.30	1.30	1.01	138.93	1.24	68.89	3.45	67.15	66.47
Enthalpy, MJ/hr	-43,299	-74,978	4,736	-218	-75,248	0	-2,790,513	-40,294	-39,127	-49,774	-10,820,556	-10,579,111
See Note	1	1	1	1	1	1	1	1	1	1	1	1

Note: 1. The reference state for thermodynamic properties is the standard enthalpy of formation of ideal gas at 25°C and 1 atm.

**Table A1.4.2 - 1: Stream Data – Simple Cycle Gas Turbine – continued**

Basis: 3,274 Tonne/D (As Received) or 3,078 Tonne/D (Dry Basis) Pittsburgh No. 8 Coal

Mol Fraction	49	50	51	52	53	54	55	56	57	58	59	60
O2									0.2074	0.0366	0.0429	0.0429
N2		0.0089							0.7724	0.6630	0.6606	0.6606
Ar		0.0069							0.0098	0.0080	0.0081	0.0081
H2	0.0002	0.6500										
CO		0.0190										
CO2	0.0001	0.0268							0.0003	0.0144	0.0137	0.0137
H2O	0.9997	0.2850	1.0000	1.0000	1.0000				0.0101	0.2779	0.2747	0.2747
CH4		0.0035										
H2S		0.0000										
SO2												
Cl2												
HCl												
NH3												
COS		0.0000										
Total	1.0000	1.0000	1.0000	1.0000	1.0000				1.0000	1.0000	1.0000	1.0000
kgmol/hr	22	15,612	3,212	3,212	4,471				37,298	54,266	57,062	57,062
kg/hr	401	136,391	57,870	57,870	80,540				1,076,465	1,395,013	1,469,565	1,469,565
Temp., C	136.2	287.8	349.2	213.9	150.0	659.9	472.8	177.8	15.0	1,766.1	655.2	160.9
Press., bar	61.75	61.41	180.96	177.47	82.74	50.31	15.75	15.55	1.01	48.66	1.07	1.01
Enthalpy, MJ/hr	-6,192	-1,154,344	95,548	53,338	51,096				-106,617	-540,226	-2,936,000	-3,860,583
See Note	1	1	2	2	2	1	1	1	1	1,3	1,3	1,3

- Note:
1. The reference state for thermodynamic properties is the standard enthalpy of formation of ideal gas at 25°C and 1 atm.
  2. Enthalpy corresponds to ASME Steam Tables Basis.
  3. For NOx see Performance Summary, Table 1.

**Table A1.4.2 - 1: Stream Data – Simple Cycle Gas Turbine – continued**

Basis: 3,274 Tonne/D (As Received) or 3,078 Tonne/D (Dry Basis) Pittsburgh No. 8 Coal

Mol Fraction	61	62	63	64	65	66	67	68	69	70	71	72
H2O	1.0000	1.0000	1.0000	1.0000	1.0000	1.0000	1.0000	1.0000	1.0000	1.0000	1.0000	1.0000
Total	1.0000	1.0000	1.0000	1.0000	1.0000	1.0000	1.0000	1.0000	1.0000	1.0000	1.0000	1.0000
kgmol/hr	27,345	27,345	5,414	3,190	5,362	5,362	0	3,520	1,025	6,258	6,012	11,654
kg/hr	492,636	492,636	97,528	57,465	96,600	96,600	0	63,417	18,473	112,736	108,305	209,945
Temp., C	23.2	147.5	134.9	148.6	349.2	260.8	156.7	225.6	229.2	349.2	356.0	371.1
Press., bar	16.82	11.44	4.57	11.75	180.96	177.47	4.57	32.00	27.51	178.88	174.07	50.50
Enthalpy, MJ/hr	48,853	306,597	55,355	36,027	159,495	80,944	0	61,499	51,787	186,297	277,859	655,737
See Note	1	1	1	1	1	1	1	1	1	1	1	1

Note: 1. Enthalpy corresponds to ASME Steam Tables Basis.

Mol Fraction	73	74	75	76	77	78	79
H2O	1.0000	1.0000	1.0000	1.0000	1.0000	1.0000	1.0000
Total	1.0000	1.0000	1.0000	1.0000	1.0000	1.0000	1.0000
kgmol/hr	11,085	14,049	14,557	15,583	247	15,830	11,516
kg/hr	199,704	253,093	262,254	280,725	4,451	285,175	207,461
Temp., C	551.7	611.9	439.2	611.5	214.0	30.5	15.6
Press., bar	49.64	166.51	27.51	24.82	3.17	0.04	3.40
Enthalpy, MJ/hr	675,830	911,238	871,771	1,042,346	12,880	671,573	13,659
See Note	1	1	1	1	1	1	1

Note: 1. Enthalpy corresponds to ASME Steam Tables Basis.

**Table A1.4.2 - 1: Stream Data – Simple Cycle Gas Turbine – continued**

Basis: 3,274 Tonne/D (As Received) or 3,078 Tonne/D (Dry Basis) Pittsburgh No. 8 Coal

Mol Fraction	80	81	82	83
O2				
N2				
Ar				
H2				
CO				
CO2				
H2O	1.0000	1.0000	0.9981	1.0000
CH4				
H2S				
SO2				
Cl2				
HCl			0.0016	
NH3			0.0003	
COS				
Total	1.0000	1.0000	1.0000	1.0000
kgmol/hr	51,374	3,283	2,280	738
kg/hr	925,515	59,148	41,151	13,298
Temp., C	15.6	15.6	26.7	15.6
Press., bar	1.014	1.014	1.4	1.0
Enthalpy, MJ/hr	60,725	3,881	-620	873
See Note	1	1	2	1

Note:

1. Enthalpy corresponds to ASME Steam Tables Basis.
2. The reference state for thermodynamic properties is the standard enthalpy of formation of ideal gas at 25°C and 1 atm.

**Table A1.4.2 - 2: Plant Performance Summary – Simple Cycle Gas Turbine  
(ISO Ambient Conditions)**

PERFORMANCE SUMMARY	Baseline Case		Simple Cycle High RIT GT					
	24		37			50		
<b>Pressure Ratio</b>	<b>24</b>		<b>37</b>			<b>50</b>		
Fuel Feed Rate, ST/D (MF)	3,392		3,392			3,392		
MMBtu/hr (HHV)	3,744		3,744			3,744		
Fuel Feed Rate, MT/D (MF)	3,078		3,078			3,078		
GJ/hr (HHV)	3,949		3,949			3,949		
ASU	IP	HP	IP	HP	IP	IP	HP	IP
Gas Turbine Air Extraction	Yes	Yes	Yes	Yes	No	Yes	Yes	No
<b>Power Generation, kWe</b>								
Gas Turbine	318,378	318,323	349,031	349,491	392,709	363,997	363,967	413,402
Steam Turbine	157,600	159,033	153,362	154,966	145,633	138,341	139,790	134,435
Clean Syngas Expander	2,320	2,320	856	856	856	0	0	0
Gas Turbine Extraction Air Expander	4,745	0	10,271	0	0	14,590	0	0
<b>Auxiliary Power Consumption, kWe</b>	99,795	93,924	102,266	91,176	124,391	105,350	89,728	127,386
<b>Net Plant Output, kWe</b>	383,247	385,753	411,254	414,136	414,807	411,579	414,028	420,451
<b>Generation Efficiency (HHV)</b>								
Net Heat Rate, Btu/kWh	9,769	9,706	9,104	9,041	9,026	9,097	9,043	8,905
Net Heat Rate, kJ/kWh	10,305	10,238	9,603	9,536	9,521	9,595	9,539	9,393
% Fuel to Power	34.94	35.16	37.49	37.75	37.81	37.52	37.74	38.33
<b>Estimated NOx, ppmVd (15% O2 Basis)</b>	18		183			251		
Raw Water Makeup, m3/kWh	0.0026	0.0026	0.0023	0.0023	0.0023	0.0023	0.0023	0.0022

Note: The NOx emission corresponds to a 30 ms residence time in the 2<sup>nd</sup> PSR.

**Table A1.4.2 - 3: Auxiliary (In-Plant) Power Consumption Summary – Simple Cycle Gas Turbine**

AUXILLARY POWER CONSUMPTION	Baseline Case		Simple Cycle High RIT GT					
	24		37			50		
Pressure Ratio	IP	HP	IP	HP	IP	IP	HP	IP
ASU	Yes	Yes	Yes	Yes	No	Yes	Yes	No
Gas Turbine Air Extraction	Yes	Yes	Yes	Yes	No	Yes	Yes	No
	kWe	kWe	kWe	kWe	kWe	kWe	kWe	kWe
Coal Handling	401	401	401	401	401	401	401	401
Coal Milling	802	802	802	802	802	802	802	802
Coal Slurry Pumps	274	274	274	274	274	288	288	288
Slag Handling and Dewatering	155	155	155	155	155	155	155	155
Miscellaneous Syngas Plant Equipment	380	380	478	478	478	519	519	519
Air Separation Unit Air Compressors	14,778	15,788	14,771	16,817	37,083	14,779	17,570	37,092
Air Separation Auxiliaries	1,290	1,290	1,290	1,290	1,291	1,290	1,290	1,291
Oxygen Compressor	12,522	11,122	12,521	9,915	12,520	12,703	9,284	12,701
Nitrogen Compressor	22,007	16,415	25,177	14,450	25,177	27,853	12,649	27,853
CO <sub>2</sub> Compressor	19,368	19,368	19,374	19,374	19,365	19,365	19,365	19,365
Tail Gas Recycle Compressor	998	998	1,004	1,004	1,003	1,024	1,023	1,024
Boiler Feedwater Pumps	4,047	4,054	3,782	3,768	3,826	3,799	3,764	3,811
Cooling Tower and Pumps	7,242	7,340	6,319	6,519	6,034	6,255	6,488	5,884
Steam Condensate Pump	42	44	31	36	19	31	40	19
Selexol Acid Gas Removal	11,788	11,788	12,152	12,152	12,152	12,357	12,357	12,357
Syngas Compression								
Syngas Humidification	214	214	201	201	201	198	198	198
Claus Plant Auxiliaries	100	100	100	100	100	100	100	100
Gas Turbine Auxiliaries	517	517	517	517	517	517	517	517
Steam Turbine Auxiliaries	517	517	517	517	517	517	517	517
General Makeup and Demineralized Water	322	322	311	312	310	309	310	306
Miscellaneous Balance-of-Plant and Lighting	1,000	1,000	1,000	1,000	1,000	1,000	1,000	1,000
Transformer Losses	1,031	1,034	1,088	1,093	1,166	1,088	1,091	1,187
Total Auxiliary Power Consumption	99,795	93,924	102,266	91,176	124,391	105,350	89,728	127,386
Raw Water Makeup, m <sup>3</sup> /kWh	0.0026	0.0026	0.0023	0.0023	0.0023	0.0023	0.0023	0.0022

**Table A1.4.2 - 4: Main Features of the Power Cycle –Simple Cycle Gas Turbine**

	Baseline Case		Simple Cycle High RIT GT					
<b>Gas Turbine</b>								
Pressure Ratio	24		37			50		
ASU	IP	HP	IP	HP	IP	IP	HP	IP
Air Extraction	Yes		Yes	Yes	No	Yes	Yes	No
Power Output, kW	318,378	318,323	349,031	349,491	392,709	363,997	363,967	413,402
Rotor Inlet Temperature	1392°C (2538°F)		1734°C (3153°F)			1734°C (3153°F)		
<b>Combustor</b>								
Inlet Air Temperature	487°C (908°F)		583°C (1081°F)			659°C (1219°F)		
Discharge Temperature	1433°C (2611°F)		1781°C (3237°F)			1780°C (3236°F)		
Inlet Air Flow, kg/s	421.8 kg/s (930 lb/s)		258.2 kg/s (569.3 lb/s)			274.2 kg/s (604.5 lb/s)		
Inlet Air O <sub>2</sub> Concentration, Vol %	20.74		20.74			20.74		
Discharge O <sub>2</sub> Concentration, Vol %	7.8		2.7			3.4		
Adiabatic Flame Temperature	1891°C (3435°F)		1931°C (3508°F)			1964°C (3567°F)		
<b>Estimated NO<sub>x</sub> (15% O<sub>2</sub> Dry Basis)</b>								
2nd PSR Residence Time = 30 ms <sup>1</sup>	18		183			251		
2nd PSR Residence Time = 5 ms <sup>2</sup>	17		50			67		
Exhaust Temperature	582°C (1079°F)		718°C (1325°F)			656°C (1213°F)		
Air Extracted, % of Inlet Air	14		20	20	0	20	20	0
<b>Steam Cycle</b>								
Power Output, kW	157,600	159,033	153,362	154,966	145,633	138,341	139,790	134,435
HP Steam Pressure	166.5 bara (2415 psia)		166.5 bara (2415 psia)			166.5 bara (2415 psia)		
Superheat & Reheat Temperatures	538°C (1000°F)		675°C (1247°F)			612°C (1134°F)		
<b>Overall Plant Performance</b>								
Fuel Feed Rate, MT/D (MF)	3,078		3,078			3,078		
GJ/hr (HHV)	3,949		3,949			3,949		
Net Plant Output, kW	383,247	385,753	411,254	414,136	414,807	411,579	414,028	420,451
Net Heat Rate, Btu/kWh	9,769	9,706	9,104	9,041	9,026	9,097	9,043	8,905
kJ/kWh	10,305	10,238	9,603	9,536	9,521	9,595	9,539	9,393
% Fuel to Power	34.94	35.16	37.49	37.75	37.81	37.52	37.74	38.33
Raw Water Makeup, m <sup>3</sup> /kWh	0.0026	0.0026	0.0023	0.0023	0.0023	0.0023	0.0023	0.0022

1) NO<sub>x</sub> values are predicted using a Chemkin 2 PSR model with a 0.44 millisecond residence time in the first reactor and a 30 millisecond residence time in the second reactor.

2) NO<sub>x</sub> values are predicted using a Chemkin 2 PSR model with a 0.44 millisecond residence time in the first reactor and a 5 millisecond residence time in the second reactor.

**LP Compressor Pressure Ratio Versus Efficiency**  
**Overall Pressure Ratio = 50**

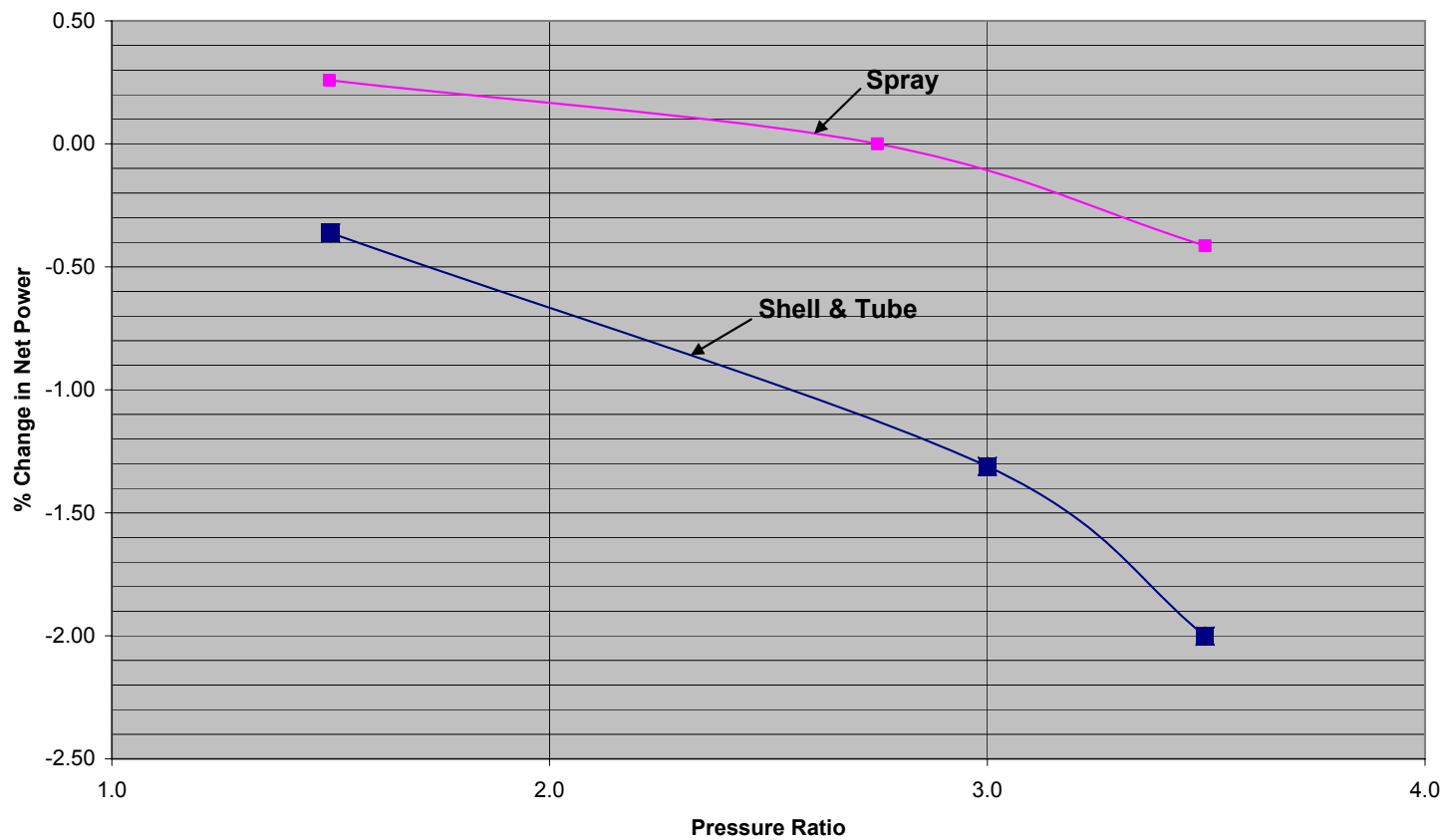


**Figure A1.4.2 - 14: Spray vs Shell and Tube Intercooler**

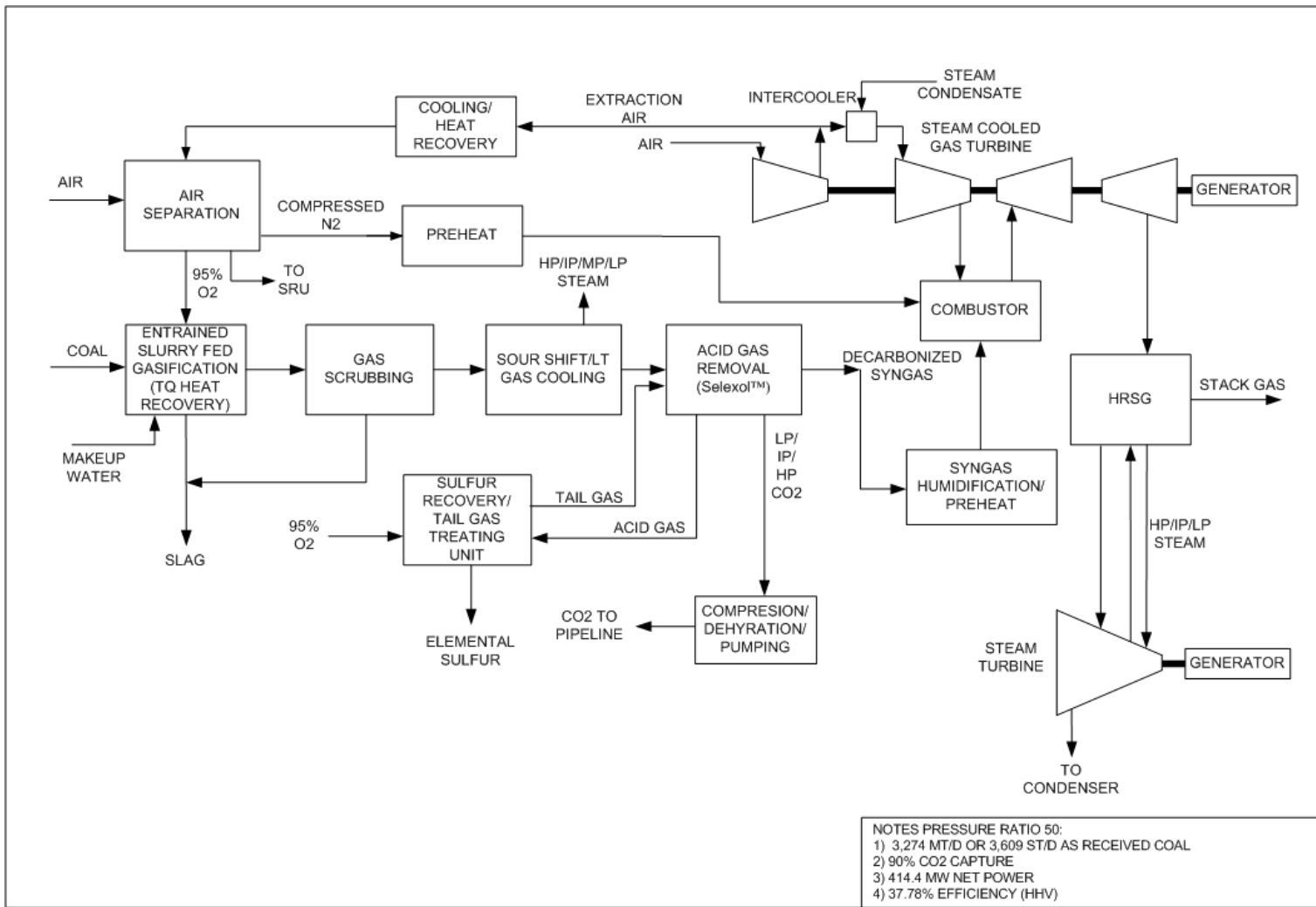


Figure A1.4.2 - 15: Overall Block Flow Diagram – IGCC with CO<sub>2</sub> Capture – Intercooled GT / PR=50 / HP ASU



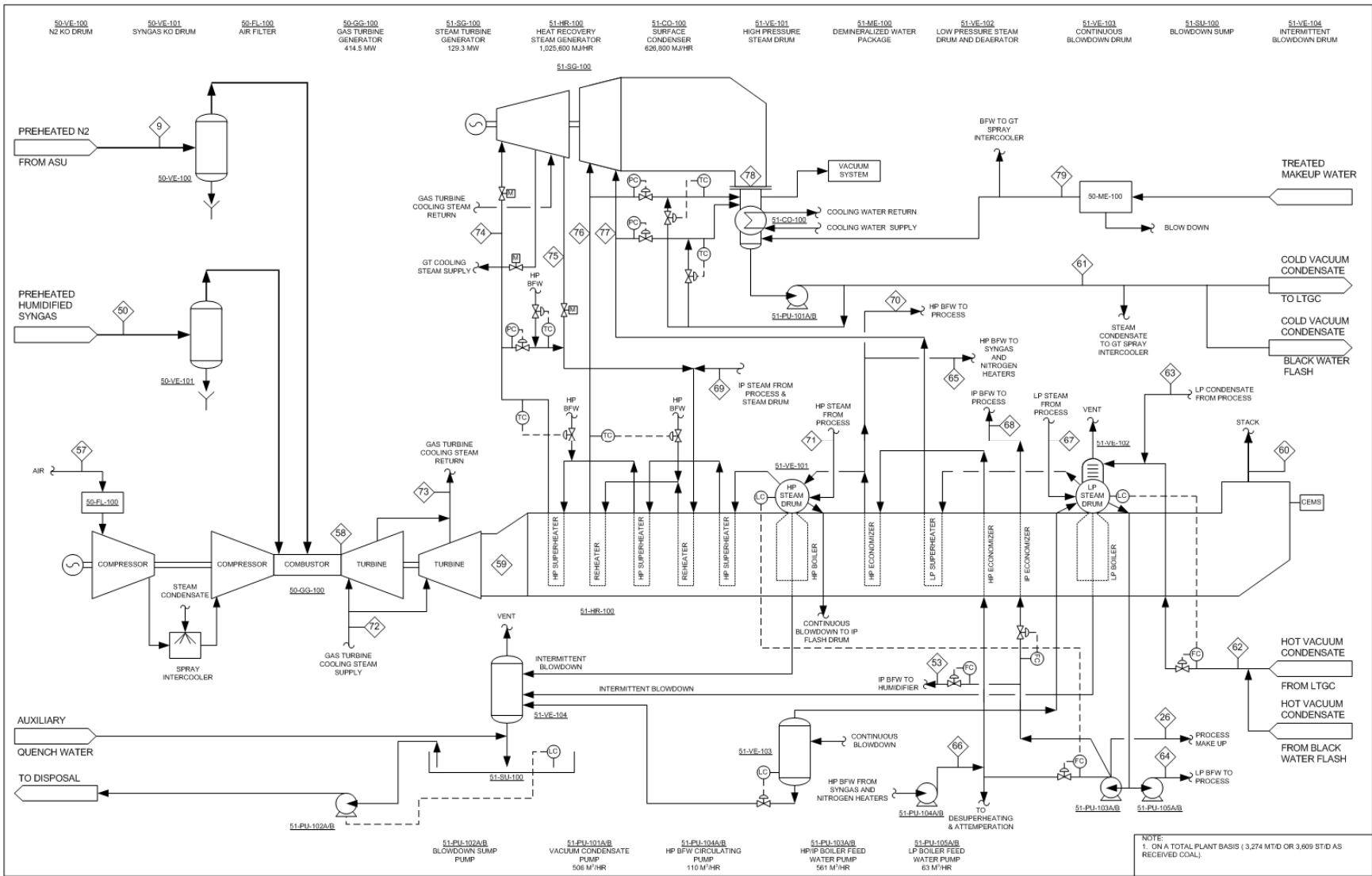


Figure A1.4.2 - 17: Process Flow Diagram – Power Block - Intercooled GT with PR=50



**Table A1.4.2 - 5: Stream Data – Intercooled Gas Turbine**

Basis: 3,274 Tonne/D (As Received) or 3,078 Tonne/D (Dry Basis) Pittsburgh No. 8 Coal

Mol Fraction	1	2	3	4	5	6	7	8	9	10 (not used)	11	12
O2		0.2077	0.2077	0.2077	0.9500	0.9500	0.9500	0.9500	0.0062			
N2		0.7722	0.7722	0.7722	0.0230	0.0176	0.0211	0.0176	0.9891			
Ar		0.0094	0.0094	0.0094	0.0270	0.0324	0.0289	0.0324	0.0047			
H2												
CO												
CO2		0.0003	0.0003	0.0003								
H2O		0.0104	0.0104	0.0104							1.0000	1.0000
CH4												
H2S												
SO2												
Cl2												
HCl												
NH3												
COS												
Total		1.0000	1.0000	1.0000	1.0000	1.0000	1.0000	1.0000	1.0000		1.0000	1.0000
Coal (As Received), kg/hr	136,416											
kgmol/hr (w/o Solids)	-	17,804	11,395	6,409	2,431	1,288	3,719	82	8,779		2,260	2,260
kg/hr (w/o Solids)	-	513,714	328,800	184,914	78,082	41,455	119,537	2,645	246,637		40,717	40,717
Temp., C	15.0	15.0	15.0	15.0	92.7	81.6	88.9	19.4	287.8		349.1	140.6
Press., bar	1.01	1.01	1.01	1.01	87.08	87.08	87.08	3.04	61.23		180.96	177.47
Enthalpy, MJ/hr	-123,514	-52,216	-33,420	-18,796	3,618	1,443	5,060	-16	67,788		67,203	24,584
See Note	1, 2	2	2	2	2	2	2	2	2		3	3

Note:

1. Enthalpy expressed as HHV = 3,949,275 MJ/hr.
2. The reference state for thermodynamic properties is the standard enthalpy of formation of ideal gas at 25°C and 1 atm.
3. Enthalpy corresponds to ASME Steam Tables Basis.

**Table A1.4.2 - 5: Stream Data – Intercooled Gas Turbine - continued**

Basis: 3,274 Tonne/D (As Received) or 3,078 Tonne/D (Dry Basis) Pittsburgh No. 8 Coal

Mol Fraction	13	14	15	16	17	18	19	20	21	22	23	24
O2												
N2	0.0000		0.0042	0.0015			0.0042	0.0042	0.0042	0.0042	0.0042	0.0042
Ar	0.0000		0.0036	0.0030			0.0036	0.0036	0.0036	0.0036	0.0036	0.0036
H2	0.0003		0.1661	0.1403			0.1661	0.3283	0.3283	0.3494	0.3494	0.3494
CO	0.0004		0.1935	0.0400			0.1935	0.0313	0.0313	0.0103	0.0103	0.0103
CO2	0.0008		0.0687	0.1456	0.0000		0.0687	0.2310	0.2310	0.2521	0.2521	0.2521
H2O	0.9977	1.0000	0.5563	0.0210	0.9999	1.0000	0.5563	0.3940	0.3940	0.3729	0.3729	0.3729
CH4	0.0000		0.0020	0.0014			0.0020	0.0020	0.0020	0.0020	0.0020	0.0020
H2S	0.0002		0.0040	0.0451	0.0000		0.0040	0.0042	0.0042	0.0042	0.0042	0.0042
SO2												
Cl2												
HCl												
NH3	0.0006		0.0013	0.6013	0.0001		0.0013	0.0013	0.0013	0.0013	0.0013	0.0013
COS	0.0000		0.0002	0.0009	0.0000		0.0002	0.0000	0.0000	0.0000	0.0000	0.0000
Total	1.0000	1.0000	1.0000	1.0000	1.0000	1.0000	1.0000	1.0000	1.0000	1.0000	1.0000	1.0000
kgmol/hr (w/o Solids)	291	447	29,185	40	3,871	1,160	29,185	29,185	29,185	29,185	29,185	29,185
kg/hr (w/o Solids)	5,256	8,062	562,306	811	69,747	20,896	562,307	562,304	562,304	562,304	562,304	562,304
kg/hr Solids	12,141	3,455										
kg/hr Total	17,397	11,516	562,306	811	69,747	20,896	562,307	562,304	562,304	562,304	562,304	562,304
Temp., C	<93.3	60.2	243.2	44.8	123.4	156.7	287.8	442.5	287.9	307.9	246.1	219.4
Press., bar	1.01	1.01	71.34	2.07	2.21	4.59	70.99	70.01	68.98	68.00	67.65	67.31
Enthalpy, MJ/hr	<-81,402	-140,031	-5,176,778	-3,812	-1,077,473	57,741	-5,127,453	-5,127,384	-5,302,621	-5,302,623	-5,372,787	-5,403,169
See Note	1	1	1	1	1	2	1	1	1	1	1	1

- Note:
1. The reference state for thermodynamic properties is the standard enthalpy of formation of ideal gas at 25°C and 1 atm.
  2. Enthalpy corresponds to ASME Steam Tables Basis.

**Table A1.4.2 - 5: Stream Data – Intercooled Gas Turbine - continued**

Basis: 3,274 Tonne/D (As Received) or 3,078 Tonne/D (Dry Basis) Pittsburgh No. 8 Coal

Mol Fraction	25	25A	26	27	28	29	30	31	32	33	34	35	36
O2													
N2	0.0053	0.0057		0.0000	0.0067	0.0067	0.0067		0.0067	0.0124		0.0000	0.0002
Ar	0.0046	0.0050		0.0000	0.0058	0.0058	0.0058	0.0000	0.0058	0.0096	0.0000	0.0000	0.0005
H2	0.4382	0.4773		0.0000	0.5576	0.5576	0.5576	0.0000	0.5576	0.9090	0.0000	0.0006	0.0200
CO	0.0129	0.0140		0.0000	0.0164	0.0164	0.0164		0.0164	0.0266	0.0000	0.0001	0.0016
CO2	0.3159	0.3440		0.0007	0.4018	0.4018	0.4018	0.0003	0.4018	0.0375	0.9973	0.9980	0.9763
H2O	0.2142	0.1443	1.0000	0.9986	0.0016	0.0016	0.0016	0.9920	0.0016	0.0001	0.0027	0.0012	0.0008
CH4	0.0025	0.0027		0.0000	0.0031	0.0031	0.0031	0.0000	0.0031	0.0049	0.0000	0.0000	0.0006
H2S	0.0052	0.0057		0.0001	0.0066	0.0066	0.0066	0.0001	0.0066	0.0000	0.0000	0.0000	0.0000
SO2													
Cl2													
HCl													
NH3	0.0014	0.0014		0.0005	0.0003	0.0003	0.0003	0.0075	0.0003				
COS	0.0000	0.0000		0.0000	0.0000	0.0000	0.0000		0.0000	0.0000	0.0000	0.0000	0.0000
Total	1.0000	1.0000	1.0000	1.0000	1.0000	1.0000	1.0000	1.0000	1.0000	1.0000	1.0000	1.0000	1.0000
kgmol/hr	23,262	21,354	5,819	17,516	18,278	18,278	18,278	3,076	18,278	11,164	1,097	2,798	3,118
kg/hr	455,392	420,954	104,829	315,908	365,525	365,525	365,525	55,429	365,525	56,252	48,185	122,960	134,413
Temp., C	187.9	170.0	150.0	156.5	40.6	51.7	51.7	40.6	26.7	16.7	0.1	3.6	11.7
Press., bar	66.96	66.62	78.78	75.84	66.28	65.95	65.45	66.28	65.10	62.44	1.08	3.24	10.00
Enthalpy, MJ/hr	-4,024,884	-3,584,365	-1,613,105	-4,843,274	-2,939,946	-2,932,427	-2,932,427	-875,292	-2,948,995	-205,309	-432,012	-1,101,938	-1,201,992
See Note	1	1	1	1	1	1	1	1	1	1	1	1	1

Note: 1. The reference state for thermodynamic properties is the standard enthalpy of formation of ideal gas at 25°C and 1 atm.

**Table A1.4.2 - 5: Stream Data – Intercooled Gas Turbine - continued**

Basis: 3,274 Tonne/D (As Received) or 3,078 Tonne/D (Dry Basis) Pittsburgh No. 8 Coal

Mol Fraction	37	38	39	40	41	42	43	44	45	46	47	48
O2												
N2	0.0014	0.0438		0.0124	0.0451		0.0001	0.0789	0.0811	0.0001	0.0000	0.0000
Ar	0.0024	0.0090		0.0096	0.0092		0.0003	0.0166	0.0170	0.0000	0.0000	0.0000
H2	0.1588	0.1010		0.9089	0.1041		0.0091	0.3589	0.3686	0.0000	0.0001	0.0001
CO	0.0071	0.1102		0.0266	0.1136		0.0008	0.0232	0.0239	0.0000	0.0000	0.0000
CO2	0.3092	0.1533		0.0375	0.1580		0.9895	0.4473	0.4594	0.0080	0.0001	0.0001
H2O	0.0563	0.4670		0.0001	0.5421			0.0280	0.0018	0.9891	0.9997	0.9997
CH4	0.0030			0.0049			0.0003	0.0003	0.0003		0.0000	0.0000
H2S	0.4412	0.0768			0.0182		0.0000	0.0462	0.0474	0.0026		
SO2		0.0384			0.0091							
Cl2												
HCl												
NH3	0.0202							0.0003	0.0003	0.0000		
COS	0.0006	0.0006			0.0006		0.0000	0.0002	0.0002	0.0000		
Total	1.0000	1.0000		1.0000	1.0000		1.0000	1.0000	1.0000	1.0000	1.0000	1.0000
Sulfur, kg/hr			2,824			3,927						
kgmol/hr	297	388	44	12	376	78	7,004	216	211	174	38,892	38,892
kg/hr	9,122	9,755	2,824	60	8,651	3,927	305,396	5,631	5,529	3,183	700,664	700,664
Temp., C	48.9	176.7	176.7	14.5	287.8	25.0	40.7	26.6	26.7	28.2	137.9	208.3
Press., bar	2.07	1.87	1.87	1.30	1.30	1.01	138.93	1.24	68.89	3.45	67.15	66.47
Enthalpy, MJ/hr	-43,299	-74,978	4,736	-218	-75,248	0	-2,790,513	-40,294	-39,127	-49,774	-10,820,556	-10,579,111
See Note	1	1	1	1	1	1	1	1	1	1	1	1

Note: 1. The reference state for thermodynamic properties is the standard enthalpy of formation of ideal gas at 25°C and 1 atm.

**Table A1.4.2 - 5: Stream Data – Intercooled Gas Turbine - continued**

Basis: 3,274 Tonne/D (As Received) or 3,078 Tonne/D (Dry Basis) Pittsburgh No. 8 Coal

Mol Fraction	49	50	51	52	53	54	55	56	57	58	59	60
O2									0.2074	0.0158	0.0246	0.0246
N2		0.0089							0.7728	0.6336	0.6310	0.6310
Ar		0.0069							0.0094	0.0077	0.0085	0.0085
H2	0.0002	0.6500										
CO		0.0190										
CO2	0.0001	0.0268							0.0003	0.0157	0.0148	0.0148
H2O	0.9997	0.2850	1.0000	1.0000	1.0000				0.0101	0.3272	0.3212	0.3212
CH4		0.0035										
H2S		0.0000										
SO2												
Cl2												
HCl												
NH3												
COS		0.0000										
Total	1.0000	1.0000	1.0000	1.0000	1.0000				1.0000	1.0000	1.0000	1.0000
kgmol/hr	22	15,612	3,212	3,212	4,471				31,720	49,689	52,831	52,831
kg/hr	401	136,391	57,870	57,870	80,540				915,306	1,249,537	1,333,317	1,333,317
Temp., C	136.2	287.8	349.2	213.9	150.0	659.9	472.8	177.8	15.0	1,780.6	661.1	161.0
Press., bar	61.75	61.41	180.96	177.47	82.74	50.31	15.75	15.55	1.01	48.67	1.07	1.01
Enthalpy, MJ/hr	-6,192	-1,154,344	95,548	53,338	51,096				-90,671	-1,040,938	-3,314,377	-4,188,915
See Note	1	1	2	2	2	1	1	1	1	1,3	1,3	1,3

Note:

1. The reference state for thermodynamic properties is the standard enthalpy of formation of ideal gas at 25°C and 1 atm.
2. Enthalpy corresponds to ASME Steam Tables Basis.
3. For NOx see Performance Summary, Table 1.

**Table A1.4.2 - 5: Stream Data – Intercooled Gas Turbine - continued**

Basis: 3,274 Tonne/D (As Received) or 3,078 Tonne/D (Dry Basis) Pittsburgh No. 8 Coal

Mol Fraction	61	62	63	64	65	66	67	68	69	70	71	72
H2O	1.0000	1.0000	1.0000	1.0000	1.0000	1.0000	1.0000	1.0000	1.0000	1.0000	1.0000	1.0000
Total	1.0000	1.0000	1.0000	1.0000	1.0000	1.0000	1.0000	1.0000	1.0000	1.0000	1.0000	1.0000
kgmol/hr	28,019	28,019	5,412	3,190	5,362	5,362	0	3,520	1,022	6,258	6,012	12,336
kg/hr	504,770	504,770	97,508	57,465	96,600	96,600	0	63,417	18,413	112,736	108,305	222,245
Temp., C	23.2	150.1	134.9	148.6	349.2	260.9	156.7	225.6	229.2	349.2	356.0	371.1
Press., bar	16.82	11.44	4.57	11.75	180.96	177.47	4.57	32.00	27.51	178.88	174.07	50.50
Enthalpy, MJ/hr	50,056	307,800	55,343	36,027	159,491	80,939	0	61,499	51,619	186,292	277,859	694,156
See Note	1	1	1	1	1	1	1	1	1	1	1	1

Note: 1. Enthalpy corresponds to ASME Steam Tables Basis.

Mol Fraction	73	74	75	76	77	78	79
H2O	1.0000	1.0000	1.0000	1.0000	1.0000	1.0000	1.0000
Total	1.0000	1.0000	1.0000	1.0000	1.0000	1.0000	1.0000
kgmol/hr	11,715	13,183	13,183	14,855	280	15,135	12,884
kg/hr	211,047	237,498	237,498	267,613	5,049	272,662	232,108
Temp., C	551.7	618.1	439.1	617.7	214.0	30.5	15.6
Press., bar	49.64	166.51	51.02	24.82	3.17	0.04	3.40
Enthalpy, MJ/hr	750,316	858,989	781,313	997,400	14,613	642,105	15,282
See Note	1	1	1	1	1	1	1

Note: 1. Enthalpy corresponds to ASME Steam Tables Basis.

**Table A1.4.2 - 5: Stream Data – Intercooled Gas Turbine - continued**

Basis: 3,274 Tonne/D (As Received) or 3,078 Tonne/D (Dry Basis) Pittsburgh No. 8 Coal

Mol Fraction	80	81	82	83
O2				
N2				
Ar				
H2				
CO				
CO2				
H2O	1.0000	1.0000	0.9981	1.0000
CH4				
H2S				
SO2				
Cl2				
HCl			0.0016	
NH3			0.0003	
COS				
Total	1.0000	1.0000	1.0000	1.0000
kgmol/hr	52,351	3,283	2,280	738
kg/hr	943,120	59,148	41,151	13,298
Temp., C	15.6	15.6	26.7	15.6
Press., bar	1.014	1.014	1.4	1.0
Enthalpy, MJ/hr	61,880	3,881	-620	873
See Note	1	1	2	1

Note:

1. Enthalpy corresponds to ASME Steam Tables Basis.
2. The reference state for thermodynamic properties is the standard enthalpy of formation of ideal gas at 25°C and 1 atm.

**Table A1.4.2 - 6: Plant Performance Summary – Intercooled Gas Turbine**

PERFORMANCE SUMMARY	Baseline Case		Intercooled High RIT GT		
			50	70	
<b>Pressure Ratio</b>	<b>24</b>		<b>50</b>	<b>70</b>	
Fuel Feed Rate, ST/D (MF)	3,392		3,392	3,392	
MMBtu/hr (HHV)	3,744		3,744	3,744	
Fuel Feed Rate, MT/D (MF)	3,078		3,078	3,078	
GJ/hr (HHV)	3,949		3,949	3,949	
ASU	IP	HP	HP	IP	IP
Gas Turbine Air Extraction	Yes	Yes	Yes	No	No
Power Generation, kWe					
Gas Turbine	318,378	318,323	374,664	414,531	436,825
Steam Turbine	157,600	159,033	132,820	129,254	112,891
Clean Syngas Expander	2,320	2,320	0	0	0
Gas Turbine Extraction Air Expander	4,745	0	0	0	0
Auxiliary Power Consumption, kWe	99,795	93,924	93,041	127,121	132,364
Net Plant Output, kWe	383,247	385,753	414,443	416,665	417,351
Generation Efficiency (HHV)					
Net Heat Rate, Btu/kWh	9,769	9,706	9,034	8,986	8,971
Net Heat Rate, kJ/kWh	10,305	10,238	9,529	9,478	9,463
% Fuel to Power	34.94	35.16	37.78	37.98	38.04
Estimated NOx, ppmVd (15% O2 Basis)	18		166		231
Raw Water Makeup, m3/kWh	0.0026	0.0026	0.0023	0.0023	0.0023

Note: The NOx emission corresponds to a 30 ms residence time in the 2<sup>nd</sup> PSR.

**Table A1.4.2 - 7: Auxiliary (In-Plant) Power Consumption Summary – Intercooled Gas Turbine**

AUXILLARY POWER CONSUMPTION	Baseline Case		Intercooled High RIT GT		
	24		50		70
Pressure Ratio	IP	HP	HP	IP	IP
ASU					
Gas Turbine Air Extraction	Yes	Yes	Yes	No	No
	kWe	kWe	kWe	kWe	kWe
Coal Handling	401	401	401	401	401
Coal Milling	802	802	802	802	802
Coal Slurry Pumps	274	274	288	288	314
Slag Handling and Dewatering	155	155	155	155	155
Miscellaneous Syngas Plant Equipment	380	380	519	519	595
Air Separation Unit Air Compressors	14,778	15,788	21,320	37,092	37,086
Air Separation Auxiliaries	1,290	1,290	1,290	1,291	1,290
Oxygen Compressor	12,522	11,122	9,281	12,701	12,991
Nitrogen Compressor	22,007	16,415	12,649	27,853	31,049
CO <sub>2</sub> Compressor	19,368	19,368	19,365	19,365	19,368
Tail Gas Recycle Compressor	998	998	1,023	1,024	1,057
Boiler Feedwater Pumps	4,047	4,054	3,661	3,700	3,516
Cooling Tower and Pumps	7,242	7,340	6,133	5,718	5,563
Steam Condensate Pump	42	44	33	19	20
Selexol Acid Gas Removal	11,788	11,788	12,357	12,357	12,357
Syngas Compression					1,963
Syngas Humidification	214	214	198	198	183
Claus Plant Auxiliaries	100	100	100	100	100
Gas Turbine Auxiliaries	517	517	517	517	517
Steam Turbine Auxiliaries	517	517	517	517	517
General Makeup and Demineralized Water	322	322	334	326	329
Miscellaneous Balance-of-Plant and Lighting	1,000	1,000	1,000	1,000	1,000
Transformer Losses	1,031	1,034	1,099	1,178	1,191
Total Auxiliary Power Consumption	99,795	93,924	93,042	127,121	132,364
Raw Water Makeup, m <sup>3</sup> /kWh	0.0026	0.0026	0.0023	0.0023	0.0023

**Table A1.4.2 - 8: Main Features of the Power Cycle – Intercooled Gas Turbine**

	Baseline Case		Intercooled High RIT GT		
<b>Gas Turbine</b>					
Pressure Ratio	24		50		70
ASU	IP	HP	HP	IP	IP
Air Extraction	Yes		Yes	No	No
Power Output, kW	318,378	318,323	374,664	414,531	436,825
Rotor Inlet Temperature	1392°C (2538°F)		1734°C (3153°F)		1734°C (3153°F)
<b>Combustor</b>					
Inlet Air Temperature	487°C (908°F)		523°C (973°F)		590°C (1094°F)
Discharge Temperature	1433°C (2611°F)		1781°C (3237°F)		1780°C (3236°F)
Inlet Air Flow, kg/s	421.8 kg/s (930 lb/s)		240.7 kg/s (530.6 lb/s)		252.2 kg/s (556.1 lb/s)
Inlet Air O2 Concentration, Vol %	20.74		19.90		19.81
Discharge O2 Concentration, Vol %	7.8		1.6		2.1
Adiabatic Flame Temperature	1891°C (3435°F)		1875°C (3407°F)		1901°C (3454°F)
Estimated NOx (15% O2 Dry Basis)					
2nd PSR Residence Time = 30 ms <sup>1</sup>	18		166		231
2nd PSR Residence Time = 5 ms <sup>2</sup>	17		42		56
Exhaust Temperature	582°C (1079°F)		661°C (1222°F)		597°C (1107°F)
Air Extracted, % of Inlet Air	14		20	0	0
<b>Steam Cycle</b>					
Power Output, kW	157,600	159,033	132,820	129,254	112,891
HP Steam Pressure	166.5 bara (2415 psia)		166.5 bara (2415 psia)		166.5 bara (2415 psia)
Superheat & Reheat Temperatures	538°C (1000°F)		618°C (1145°F)		554°C (1029°F)
<b>Overall Plant Performance</b>					
Fuel Feed Rate, MT/D (MF)	3,078		3,078		3,078
GJ/hr (HHV)	3,949		3,949		3,949
Net Plant Output, kW	383,247	385,753	414,443	416,665	417,351
Net Heat Rate, Btu/kWh	9,769	9,706	9,034	8,986	8,971
kJ/kWh	10,305	10,238	9,529	9,478	9,463
% Fuel to Power	34.94	35.16	37.78	37.98	38.04
Raw Water Makeup, m3/kWh	0.0026	0.0026	0.0023	0.0023	0.0023

1. NOx values are predicted using a Chemkin 2 PSR model with a 0.44 millisecond residence time in the first reactor and a 30 millisecond residence time in the second reactor.
2. NOx values are predicted using a Chemkin 2 PSR model with a 0.44 millisecond residence time in the first reactor and a 5 millisecond residence time in the second reactor.

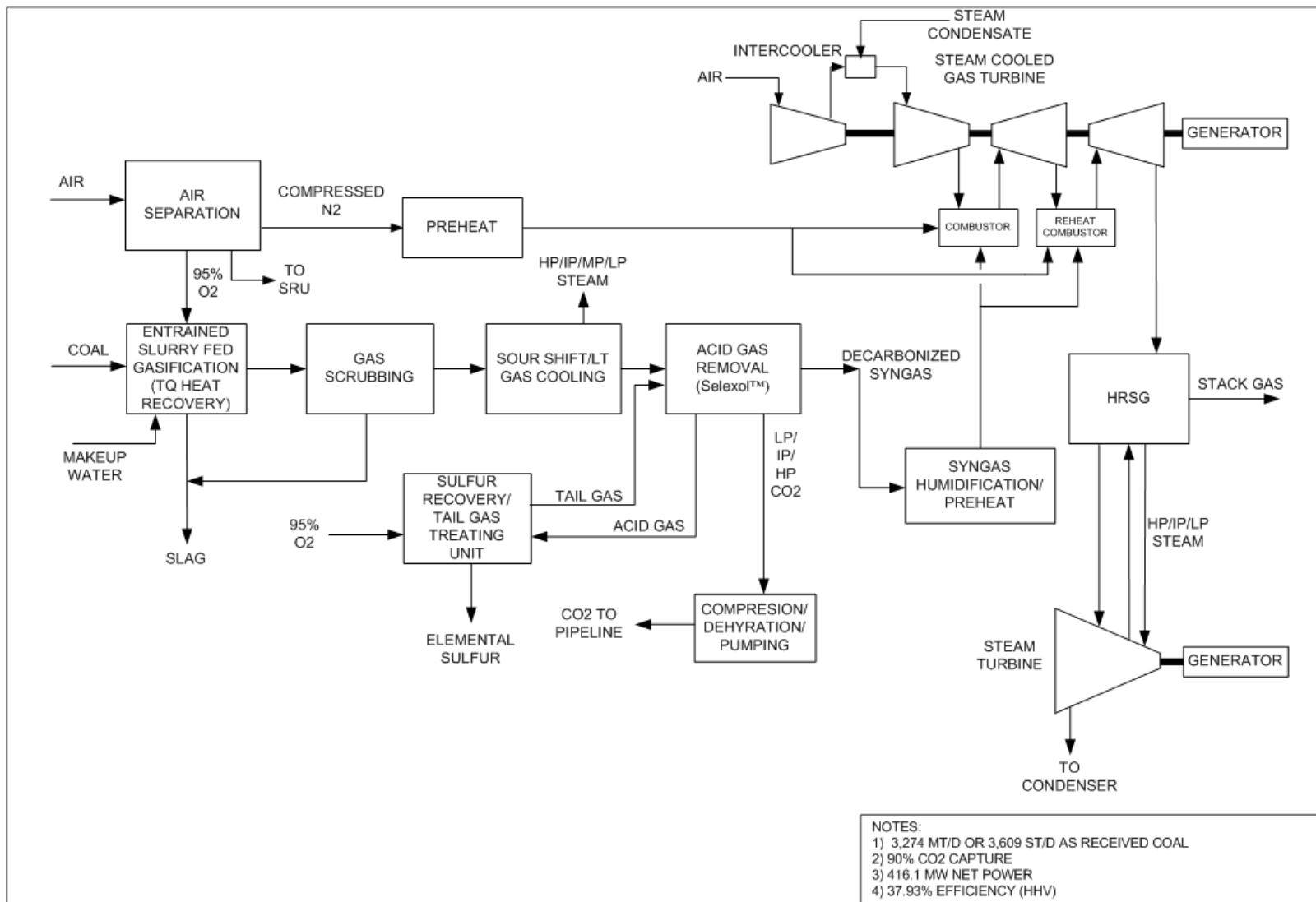


Figure A1.4.2 - 19: Overall Block Flow Diagram – IGCC with CO<sub>2</sub> Capture – Intercooled-Reheat GT

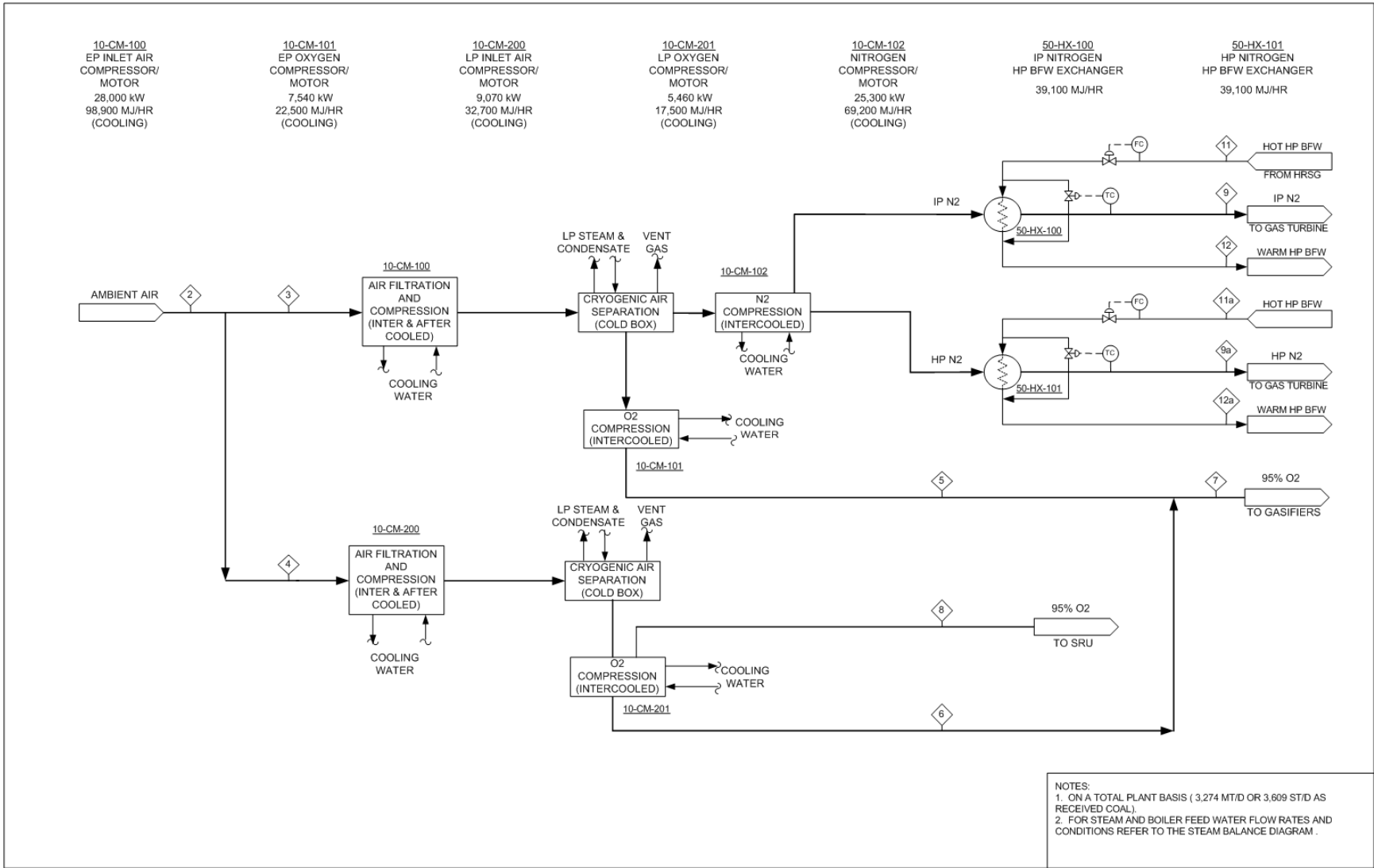
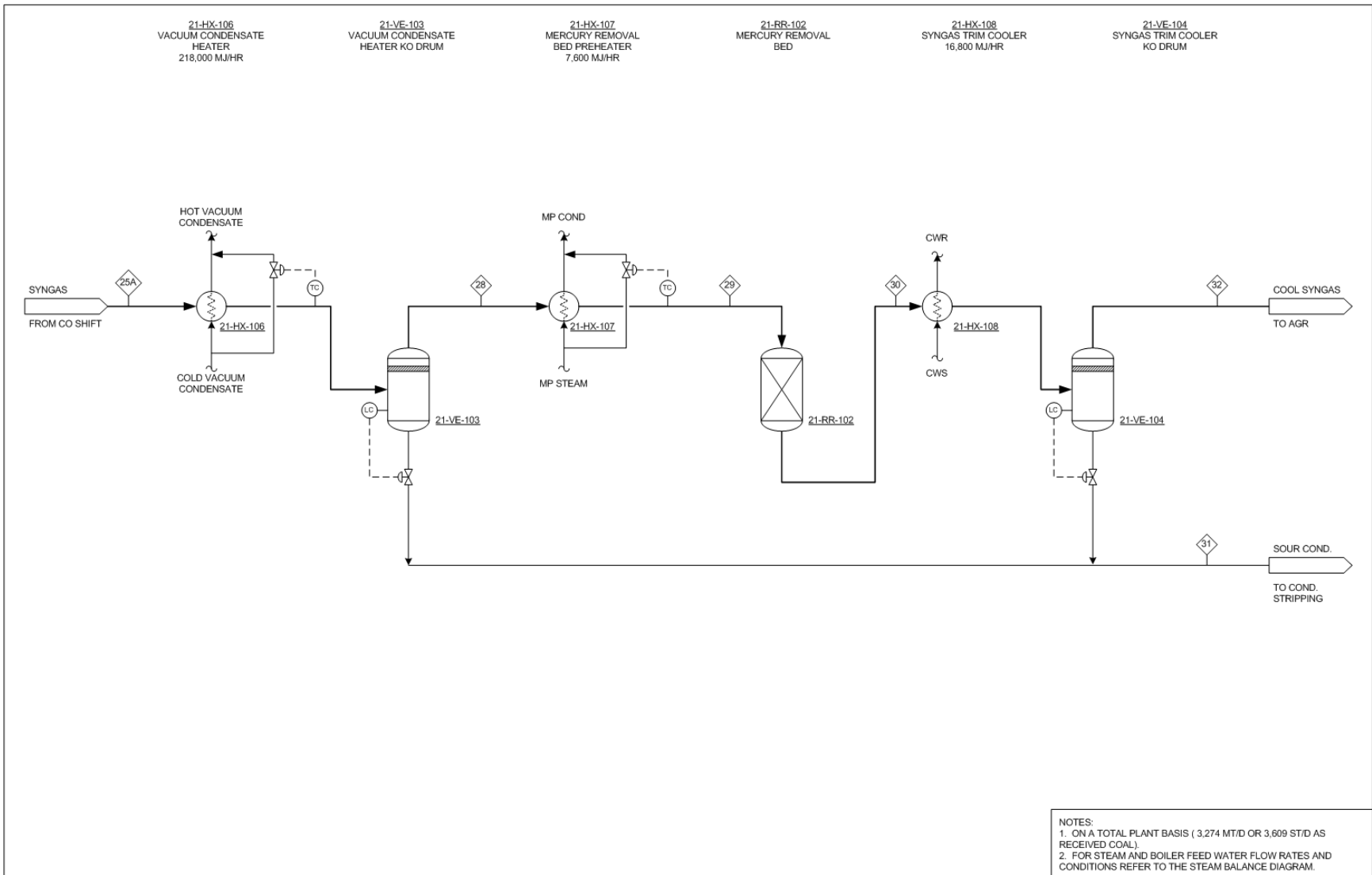
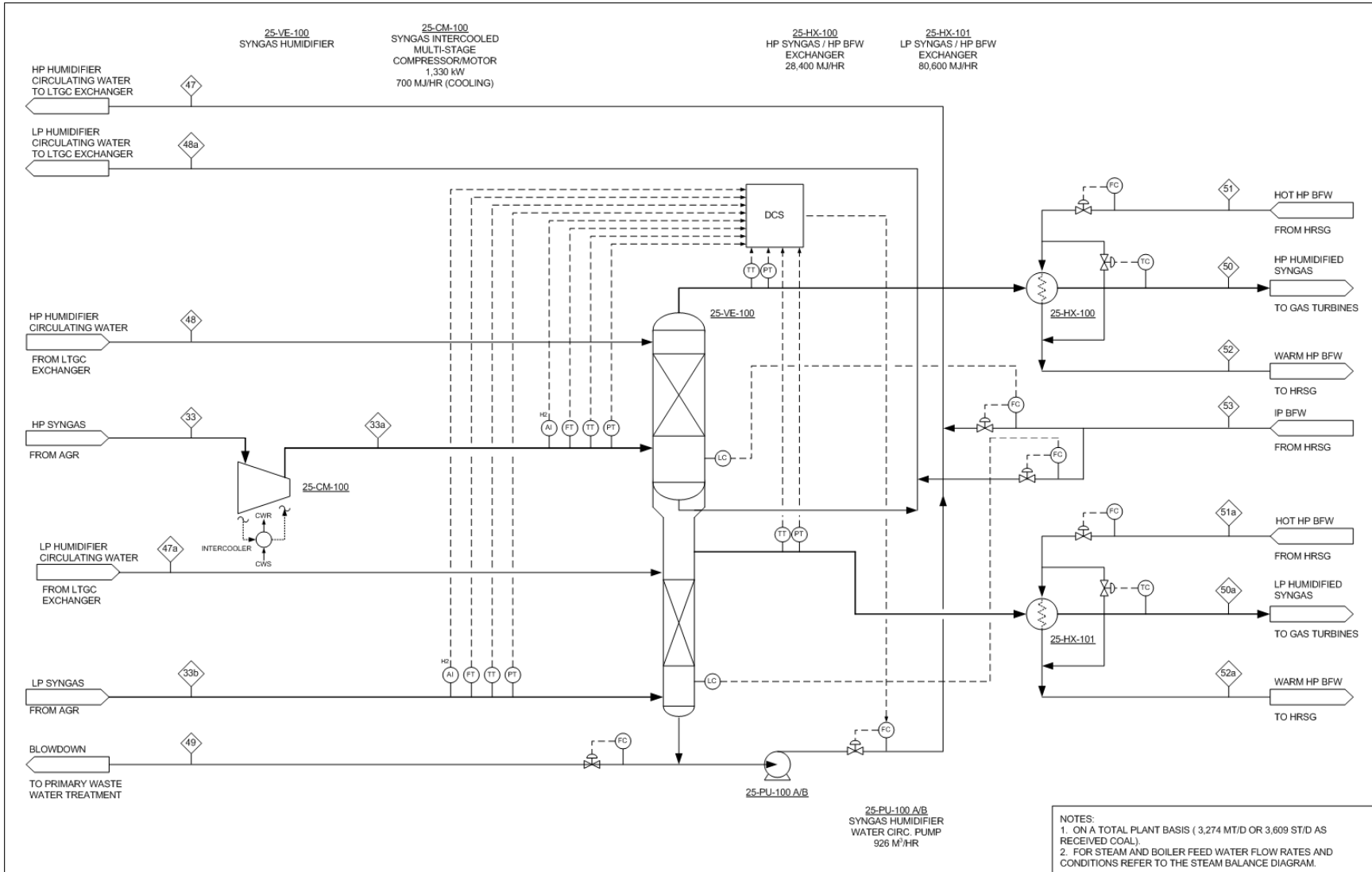


Figure A1.4.2 - 20: Process Flow Diagram – Air Separation Unit – Intercooled-Reheat GT





**Figure A1.4.2 -21: Process Flow Diagram – CO Shift / Low Temperature Gas Cooling Unit - Intercooled-Reheat GT - continued**



**Figure A1.4.2 - 22: Process Flow Diagram – Syngas Humidification Unit - Intercooled-Reheat GT**

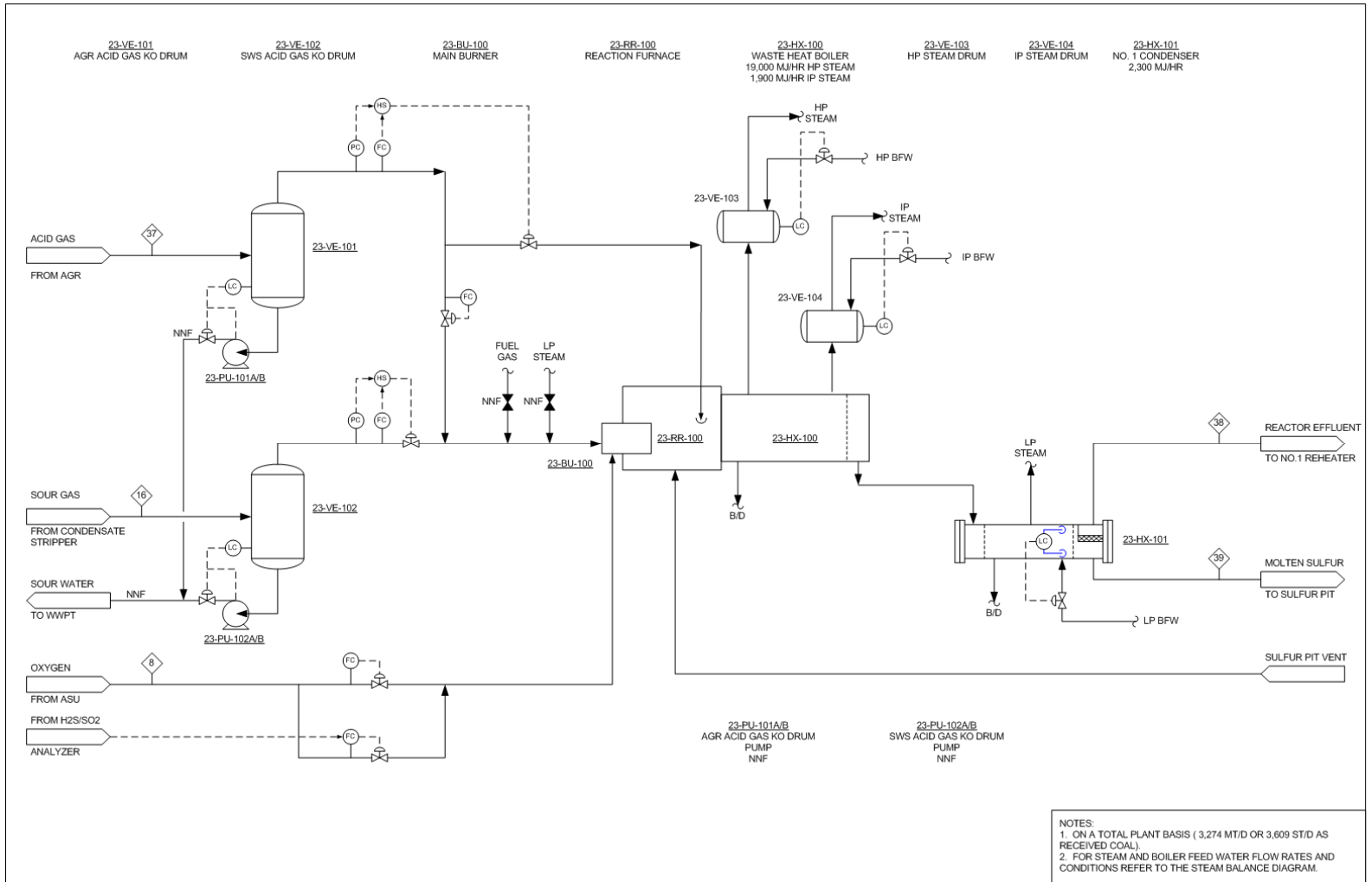


**Figure A1.4.2 - 23: Process Flow Diagram – Sulfur Recovery / Tail Gas Treating Unit - Intercooled Reheat GT & Air POX Topping Cycle GT**

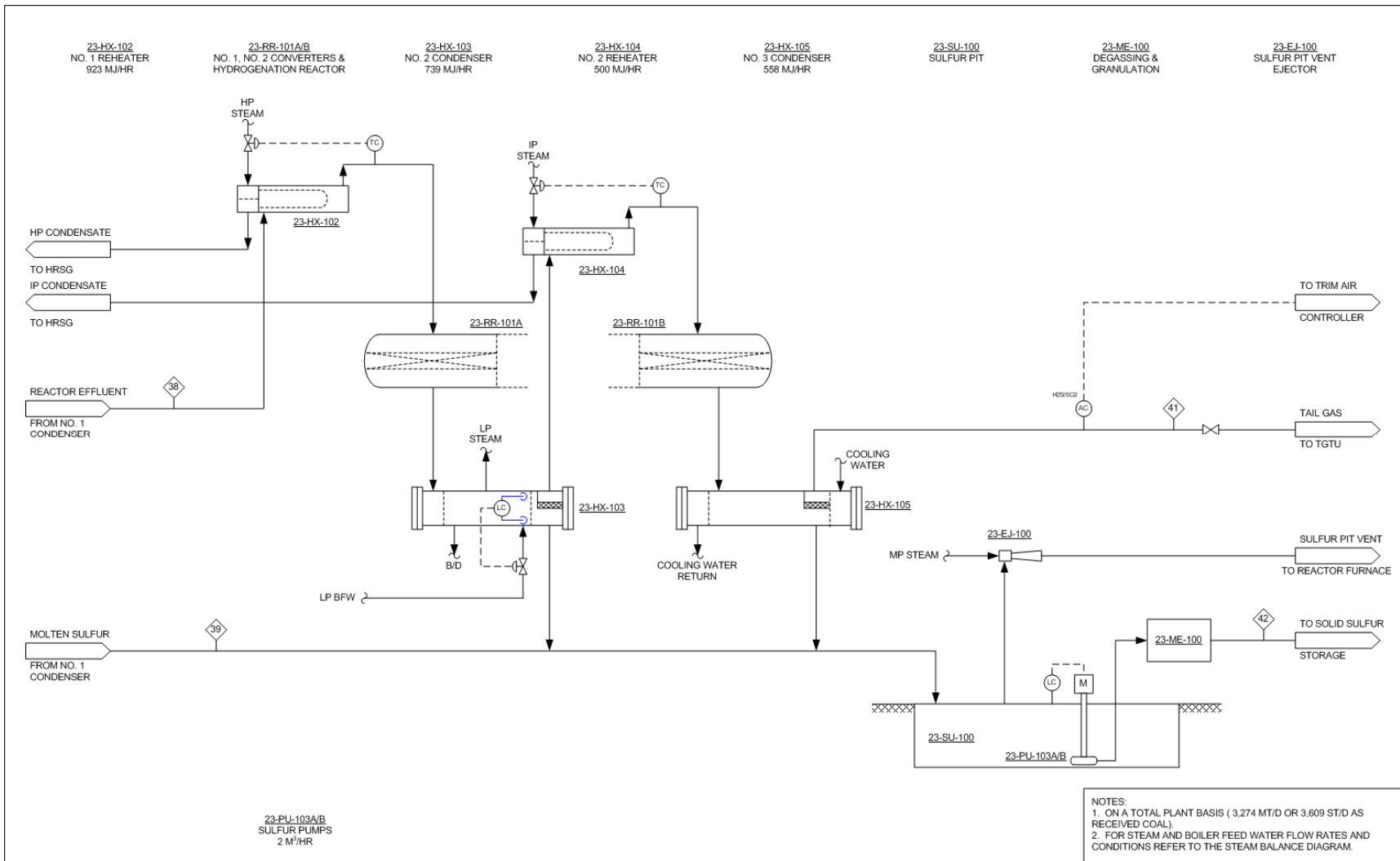


**Figure A1.4.2 -23: Process Flow Diagram – Sulfur Recovery / Tail Gas Treating Unit - Intercooled Reheat GT & Air POX Topping Cycle - continued**

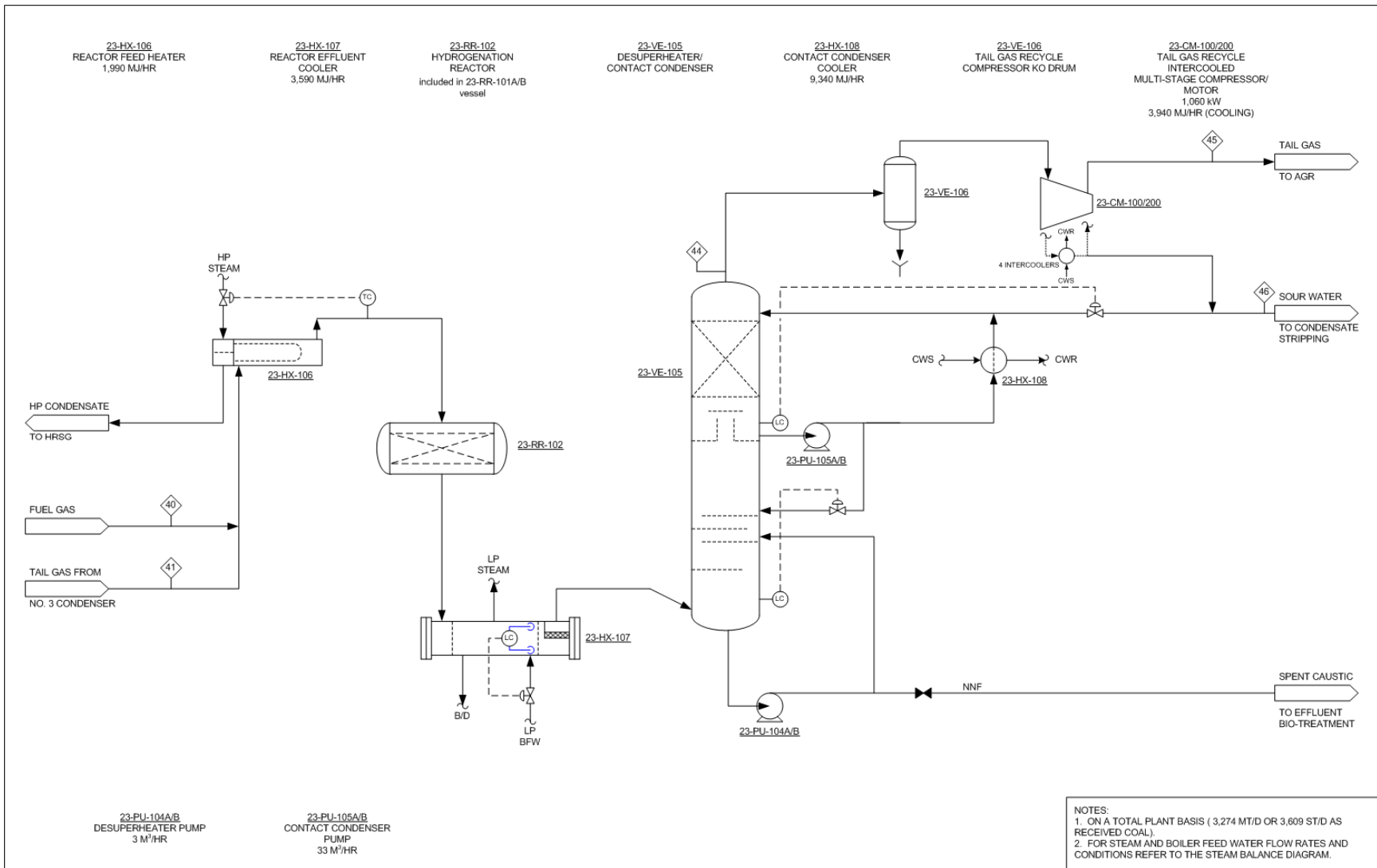


**Figure A1.4.2 -23: Process Flow Diagram – Sulfur Recovery / Tail Gas Treating Unit - Intercooled Reheat GT & Air POX Topping Cycle – continued**

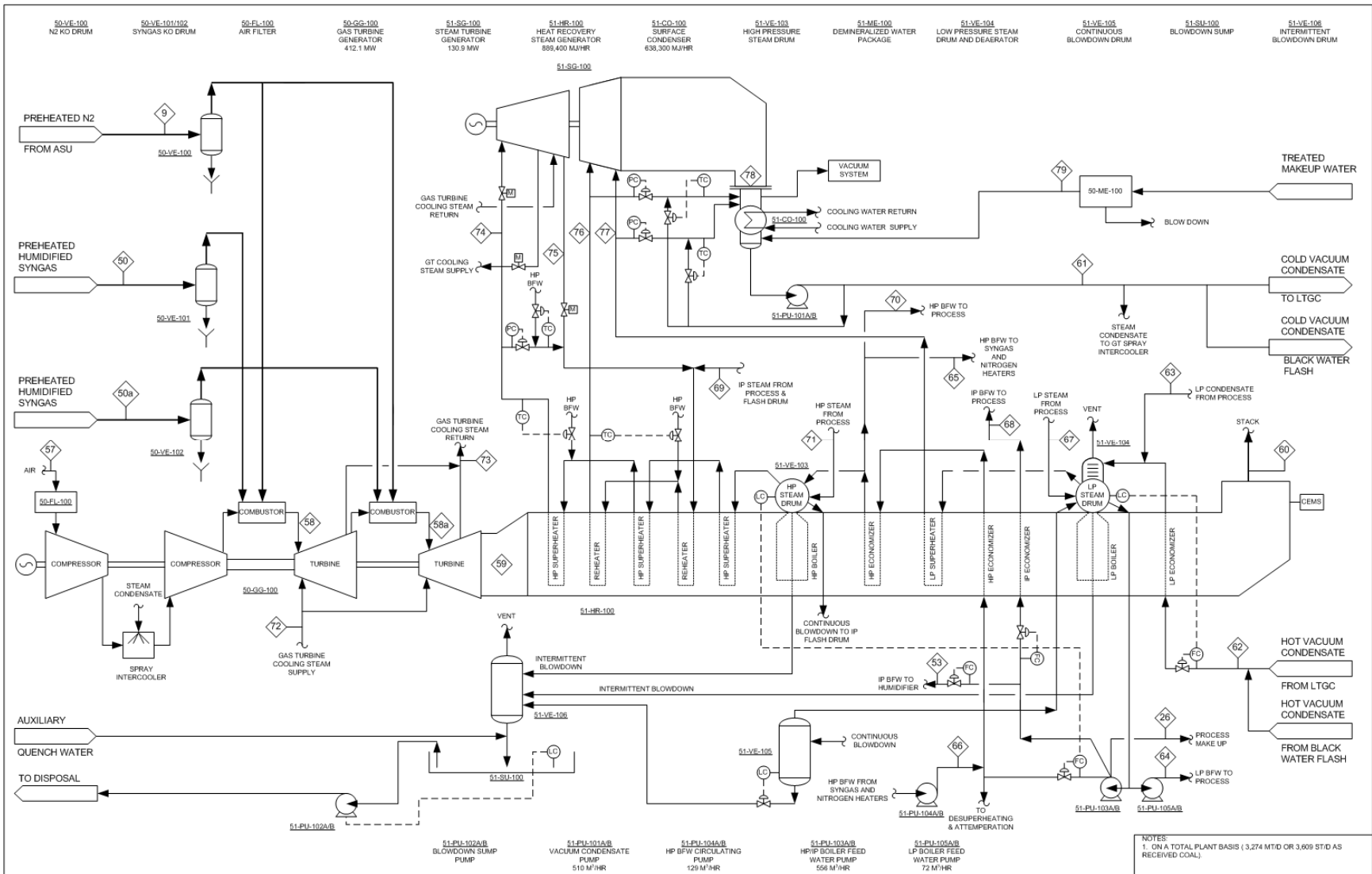


Figure A1.4.2 - 24: Process Flow Diagram – Power Block - Intercooled-Reheat GT

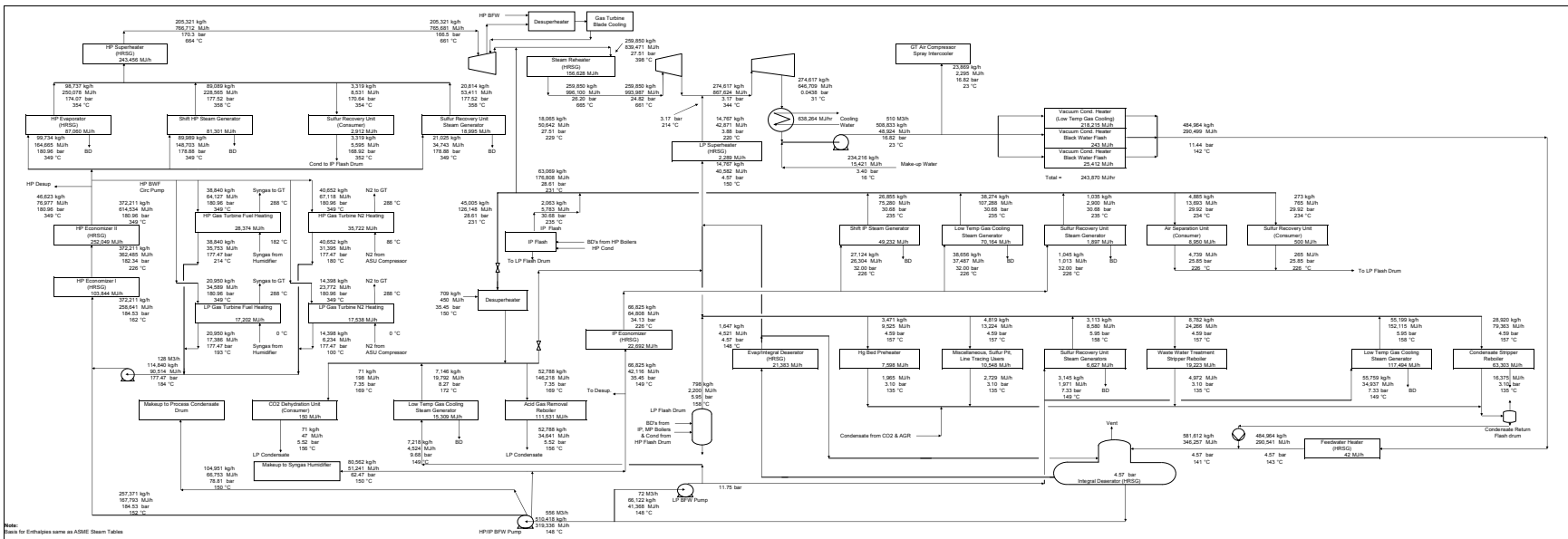


Figure A1.4.2 - 25: Steam Balance Diagram -- Intercooled-Reheat GT

**Table A1.4.2 - 9: Stream Data – Intercooled-Reheat Gas Turbine**

Basis: 3,274 Tonne/D (As Received) or 3,078 Tonne/D (Dry Basis) Pittsburgh No. 8 Coal

Mol Fraction	1	2	3	4	5	6	7	8	9	10 (not used)	11	12
O2		0.2077	0.2077	0.2077	0.9500	0.9500	0.9500	0.9500	0.0062			
N2		0.7722	0.7722	0.7722	0.0230	0.0176	0.0211	0.0176	0.9891			
Ar		0.0094	0.0094	0.0094	0.0270	0.0324	0.0289	0.0324	0.0047			
H2												
CO												
CO2		0.0003	0.0003	0.0003								
H2O		0.0104	0.0104	0.0104							1.0000	1.0000
CH4												
H2S												
SO2												
Cl2												
HCl												
NH3												
COS												
Total		1.0000	1.0000	1.0000	1.0000	1.0000	1.0000	1.0000	1.0000		1.0000	1.0000
Coal (As Received), kg/hr	136,416											
kgmol/hr (w/o Solids)	-	17,801	11,394	6,407	2,431	1,288	3,718	82	8,778		2,260	2,260
kg/hr (w/o Solids)	-	513,627	328,759	184,868	78,072	41,444	119,516	2,645	246,606		40,717	40,717
Temp., C	15.0	15.0	15.0	15.0	94.6	83.1	90.6	19.4	287.8		349.1	140.6
Press., bar	1.01	1.01	1.01	1.01	94.11	94.11	94.11	3.04	61.23		180.96	177.47
Enthalpy, MJ/hr	-123,514	-52,208	-33,416	-18,791	3,683	1,459	5,142	-16	67,762		67,203	24,584
See Note	1, 2	2	2	2	2	2	2	2	2		3	3

Note:

1. Enthalpy expressed as HHV = 3,949,275 MJ/hr.
2. The reference state for thermodynamic properties is the standard enthalpy of formation of ideal gas at 25°C and 1 atm.
3. Enthalpy corresponds to ASME Steam Tables Basis.

**Table A1.4.2 - 9: Stream Data – Intercooled-Reheat Gas Turbine**

Basis: 3,274 Tonne/D (As Received) or 3,078 Tonne/D (Dry Basis) Pittsburgh No. 8 Coal

Mol Fraction	13	14	15	16	17	18	19	20	21	22	23	24
O2												
N2	0.0000		0.0042	0.0016			0.0042	0.0042	0.0042	0.0042	0.0042	0.0042
Ar	0.0000		0.0036	0.0033			0.0036	0.0036	0.0036	0.0036	0.0036	0.0036
H2	0.0004		0.1657	0.1629			0.1657	0.3278	0.3278	0.3485	0.3485	0.3485
CO	0.0004		0.1930	0.0459			0.1930	0.0309	0.0309	0.0102	0.0102	0.0102
CO2	0.0009		0.0686	0.1498	0.0000		0.0686	0.2309	0.2309	0.2516	0.2516	0.2516
H2O	0.9973	1.0000	0.5574	0.0245	0.9999	1.0000	0.5574	0.3951	0.3951	0.3744	0.3744	0.3744
CH4	0.0000		0.0020	0.0016			0.0020	0.0020	0.0020	0.0020	0.0020	0.0020
H2S	0.0002		0.0040	0.0447	0.0000		0.0040	0.0042	0.0042	0.0042	0.0042	0.0042
SO2												
Cl2												
HCl												
NH3	0.0006		0.0013	0.5648	0.0001		0.0013	0.0013	0.0013	0.0013	0.0013	0.0013
COS	0.0000		0.0002	0.0009	0.0000		0.0002	0.0000	0.0000	0.0000	0.0000	0.0000
Total	1.0000	1.0000	1.0000	1.0000	1.0000	1.0000	1.0000	1.0000	1.0000	1.0000	1.0000	1.0000
kgmol/hr (w/o Solids)	290	447	29,261	42	3,640	1,160	29,261	29,261	29,261	29,261	29,261	29,261
kg/hr (w/o Solids)	5,230	8,062	563,709	852	65,573	20,896	563,709	563,706	563,706	563,706	563,706	563,706
kg/hr Solids	12,141	3,455										
kg/hr Total	17,371	11,516	563,709	852	65,573	20,896	563,709	563,706	563,706	563,706	563,706	563,706
Temp., C	<93.3	60.2	248.2	47.6	123.4	156.7	287.8	440.5	287.8	307.2	246.1	232.8
Press., bar	1.01	1.01	78.39	2.07	2.21	4.59	78.05	77.07	76.04	75.06	74.71	74.37
Enthalpy, MJ/hr	<-81,402	-140,031	-5,192,926	-4,092	-1,012,997	57,741	-5,148,793	-5,148,742	-5,323,379	-5,323,381	-5,393,528	-5,408,834
See Note	1	1	1	1	1	2	1	1	1	1	1	1

Note:

1. The reference state for thermodynamic properties is the standard enthalpy of formation of ideal gas at 25°C and 1 atm.
2. Enthalpy corresponds to ASME Steam Tables Basis.

**Table A1.4.2 - 9: Stream Data – Intercooled-Reheat Gas Turbine**

Basis: 3,274 Tonne/D (As Received) or 3,078 Tonne/D (Dry Basis) Pittsburgh No. 8 Coal

Mol Fraction	25	25A	26	27	28	29	30	31	32	33	33A	33B	34
O2													
N2	0.0051	0.0058		0.0000	0.0067	0.0067	0.0067		0.0067	0.0124	0.0124	0.0124	
Ar	0.0045	0.0050		0.0000	0.0058	0.0058	0.0058	0.0000	0.0058	0.0096	0.0096	0.0096	0.0000
H2	0.4294	0.4834		0.0000	0.5577	0.5577	0.5577	0.0000	0.5577	0.9091	0.9091	0.9091	0.0000
CO	0.0126	0.0142		0.0000	0.0163	0.0163	0.0163		0.0163	0.0265	0.0265	0.0265	0.0000
CO2	0.3096	0.3484		0.0008	0.4019	0.4019	0.4019	0.0004	0.4019	0.0375	0.0375	0.0375	0.9973
H2O	0.2299	0.1333	1.0000	0.9985	0.0015	0.0015	0.0015	0.9913	0.0015	0.0001	0.0001	0.0001	0.0027
CH4	0.0024	0.0027		0.0000	0.0031	0.0031	0.0031	0.0000	0.0031	0.0049	0.0049	0.0049	0.0000
H2S	0.0051	0.0058		0.0001	0.0066	0.0066	0.0066	0.0002	0.0066	0.0000	0.0000	0.0000	0.0000
SO2													
Cl2													
HCl													
NH3	0.0014	0.0014		0.0006	0.0003	0.0003	0.0003	0.0082	0.0003				
COS	0.0000	0.0000		0.0000	0.0000	0.0000	0.0000		0.0000	0.0000	0.0000	0.0000	0.0000
Total	1.0000	1.0000	1.0000	1.0000	1.0000	1.0000	1.0000	1.0000	1.0000	1.0000	1.0000	1.0000	1.0000
kgmol/hr	23,740	21,082	5,826	17,639	18,276	18,276	18,276	2,806	18,276	7,511	7,511	3,653	1,097
kg/hr	464,014	416,030	104,951	318,177	365,469	365,469	365,469	50,561	365,469	37,830	37,830	18,401	48,191
Temp., C	195.1	170.0	150.0	159.3	40.6	51.7	51.7	40.6	26.7	1.9	26.7	16.7	0.1
Press., bar	74.02	73.68	85.84	75.84	73.33	73.01	72.51	72.16	72.16	69.84	83.22	39.01	1.08
Enthalpy, MJ/hr	-4,134,011	-3,520,581	-1,614,931	-4,872,614	-2,940,743	-2,933,146	-2,933,146	-798,000	-2,949,910	-141,406	-135,942	-432,065	-432,065
See Note	1	1	1	1	1	1	1	1	1	1	1	1	1

Note: 1. The reference state for thermodynamic properties is the standard enthalpy of formation of ideal gas at 25°C and 1 atm.

**Table A1.4.2 - 9: Stream Data – Intercooled-Reheat Gas Turbine**

Basis: 3,274 Tonne/D (As Received) or 3,078 Tonne/D (Dry Basis) Pittsburgh No. 8 Coal

Mol Fraction	35	36	37	38	39	40	41	42	43	44	45	46
O2												
N2	0.0000	0.0002	0.0014	0.0436		0.0124	0.0449		0.0001	0.0784	0.0806	0.0001
Ar	0.0000	0.0005	0.0024	0.0090		0.0096	0.0092		0.0003	0.0165	0.0170	0.0000
H2	0.0006	0.0200	0.1589	0.1012		0.9089	0.1043		0.0091	0.3599	0.3699	0.0000
CO	0.0001	0.0016	0.0070	0.1107		0.0266	0.1141		0.0008	0.0229	0.0235	0.0000
CO2	0.9980	0.9763	0.3094	0.1538		0.0375	0.1585		0.9895	0.4486	0.4611	0.0080
H2O	0.0012	0.0008	0.0563	0.4664		0.0001	0.5418			0.0280	0.0010	0.9892
CH4	0.0000	0.0006	0.0030			0.0049			0.0003	0.0002	0.0003	
H2S	0.0000	0.0000	0.4403	0.0770			0.0183		0.0000	0.0449	0.0461	0.0026
SO2				0.0377			0.0083					
Cl2												
HCl												
NH3			0.0207							0.0004	0.0004	0.0000
COS	0.0000	0.0000	0.0006	0.0006			0.0006		0.0000	0.0002	0.0002	0.0000
Total	1.0000	1.0000	1.0000	1.0000		1.0000	1.0000		1.0000	1.0000	1.0000	1.0000
					2,815			3,927				
kgmol/hr	2,798	3,119	297	390	44	11	378	79	7,005	218	212	174
kg/hr	122,975	134,429	9,113	9,795	2,815	55	8,682	3,927	305,433	5,662	5,555	3,182
Temp., C	3.6	11.7	48.9	176.7	176.7	15.2	287.8	25.0	40.7	26.6	26.7	28.2
Press., bar	3.24	10.00	2.07	1.87	1.87	1.30	1.30	1.01	138.93	1.24	75.95	3.45
Enthalpy, MJ/hr	-1,102,072	-1,202,137	-43,299	-75,293	4,720	-199	-75,570	0	-2,790,851	-40,628	-39,432	-49,765
See Note	1	1	1	1	1	1	1	1	1	1	1	1

Note: 1. The reference state for thermodynamic properties is the standard enthalpy of formation of ideal gas at 25°C and 1 atm.

**Table A1.4.2 - 9: Stream Data – Intercooled-Reheat Gas Turbine**

Basis: 3,274 Tonne/D (As Received) or 3,078 Tonne/D (Dry Basis) Pittsburgh No. 8 Coal

Mol Fraction	47	47A	48	48A	49	50	50A	51	51A	52	52A	53
O2												
N2	0.0000	0.0000	0.0000	0.0000		0.0089	0.0089					
Ar	0.0000	0.0000	0.0000	0.0000		0.0069	0.0069					
H2	0.0001	0.0002	0.0001	0.0002	0.0001	0.6500	0.6500					
CO	0.0000	0.0000	0.0000	0.0000		0.0189	0.0189					
CO2	0.0001	0.0001	0.0001	0.0001	0.0001	0.0267	0.0272					
H2O	0.9998	0.9996	0.9998	0.9996	0.9998	0.2852	0.2847	1.0000	1.0000	1.0000	1.0000	1.0000
CH4	0.0000	0.0000	0.0000	0.0000		0.0035	0.0035					
H2S						0.0000	0.0000					
SO2												
Cl2												
HCl												
NH3												
COS						0.0000	0.0000					
Total	1.0000	1.0000	1.0000	1.0000	1.0000	1.0000	1.0000	1.0000	1.0000	1.0000	1.0000	1.0000
Sulfur, kg/hr												
kgmol/hr	36,152	33,163	36,152	33,163	22	10,500	5,114	2,156	2,257	2,156	2,257	4,472
kg/hr	651,286	597,445	651,286	597,445	401	91,671	44,720	38,840	40,652	38,840	40,652	80,562
Temp., C	156.2	179.9	203.3	153.6	155.6	287.8	287.8	349.2	349.2	213.6	180.0	150.0
Press., bar	87.92	61.06	87.23	61.75	38.32	61.41	37.98	180.96	180.96	177.47	177.47	87.91
Enthalpy, MJ/hr	-10,001,182	-9,101,226	-9,850,376	-9,181,766	-6,157	-776,179	-377,821	64,127	67,118	35,753	31,395	51,110
See Note	1	1	1	1	1	1	1	2	2	2	2	2

- Note:
1. The reference state for thermodynamic properties is the standard enthalpy of formation of ideal gas at 25°C and 1 atm.
  2. Enthalpy corresponds to ASME Steam Tables Basis.

**Table A1.4.2 - 9: Stream Data – Intercooled-Reheat Gas Turbine**  
 Basis: 3,274 Tonne/D (As Received) or 3,078 Tonne/D (Dry Basis) Pittsburgh No. 8 Coal

Mol Fraction	54 (Not Used)	55(Not Used)	56(Not Used)	57	58	58A	59	60
O2				0.2074	0.0465	0.0047	0.0122	0.0122
N2				0.7728	0.6499	0.6210	0.6228	0.6228
Ar				0.0094	0.0079	0.0076	0.0076	0.0076
H2								
CO								
CO2				0.0003	0.0131	0.0164	0.0157	0.0157
H2O				0.0101	0.2826	0.3504	0.3416	0.3416
CH4								
H2S								
SO2								
Cl2								
HCl								
NH3								
COS								
Total				1.0000	1.0000	1.0000	1.0000	1.0000
kgmol/hr				28,394	40,282	47,329	49,478	49,478
kg/hr				819,326	1,034,279	1,177,654	1,236,410	1,236,410
Temp., C				15.0	1,636.1	1,606.7	704.1	161
Press., bar				1.01	68.64	26.40	1.07	1.01
Enthalpy, MJ/hr				-81,163	-633,041	-1,595,364	-3,288,540	-4,186,622
See Note				1	1,3	1,3	1,3	1,3

- Note:
1. The reference state for thermodynamic properties is the standard enthalpy of formation of ideal gas at 25°C and 1 atm.
  2. Enthalpy corresponds to ASME Steam Tables Basis.
  3. For NOx see Performance Summary, Table 1.

**Table A1.4.2 - 9: Stream Data – Intercooled-Reheat Gas Turbine**  
 Basis: 3,274 Tonne/D (As Received) or 3,078 Tonne/D (Dry Basis) Pittsburgh No. 8 Coal

Mol Fraction	61	62	63	64	65	66	67	68	69	70	71	72
H2O	1.0000	1.0000	1.0000	1.0000	1.0000	1.0000	1.0000	1.0000	1.0000	1.0000	1.0000	1.0000
Total	1.0000	1.0000	1.0000	1.0000	1.0000	1.0000	1.0000	1.0000	1.0000	1.0000	1.0000	1.0000
kgmol/hr	28,245	28,245	28,245	3,670	4,412	4,412	728	3,709	1,003	6,162	5,916	11,569
kg/hr	508,833	508,833	96,577	66,122	79,492	79,492	13,119	66,825	18,065	111,014	106,584	208,412
Temp., C	22.5	142.3	134.9	148.6	349.2	196.4	153.5	225.6	229.2	349.2	356.0	371.1
Press., bar	16.82	11.44	4.57	11.75	180.96	177.47	4.57	32.00	27.51	178.88	174.07	72.62
Enthalpy, MJ/hr	48,924	290,499	54,815	41,455	131,244	67,148	36,156	64,805	50,642	183,446	273,445	640,513
See Note	1	1	1	1	1	1	1	1	1	1	1	1

Note: 1. Enthalpy corresponds to ASME Steam Tables Basis.

Mol Fraction	73	74	75	76	77	78	79
H2O	1.0000	1.0000	1.0000	1.0000	1.0000	1.0000	1.0000
Total	1.0000	1.0000	1.0000	1.0000	1.0000	1.0000	1.0000
kgmol/hr	11,004	11,397	11,397	14,424	820	15,244	13,001
kg/hr	198,246	205,321	205,321	259,850	14,767	274,617	234,216
Temp., C	551.7	661.2	531.5	660.8	214.0	30.6	15.6
Press., bar	71.39	166.51	74.15	24.82	3.17	0.04	3.40
Enthalpy, MJ/hr	700,674	765,681	715,183	993,987	42,734	646,709	15,367
See Note	1	1	1	1	1	1	1

Note: 1. Enthalpy corresponds to ASME Steam Tables Basis.

**Table A1.4.2 - 9: Stream Data – Intercooled-Reheat Gas Turbine**  
 Basis: 3,274 Tonne/D (As Received) or 3,078 Tonne/D (Dry Basis) Pittsburgh No. 8 Coal

Mol Fraction	80	81	82	83
O2				
N2				
Ar				
H2				
CO				
CO2				
H2O	1.0000	1.0000	0.9981	1.0000
CH4				
H2S				
SO2				
Cl2				
HCl			0.0016	
NH3			0.0003	
COS				
Total	1.0000	1.0000	1.0000	1.0000
kgmol/hr	53,078	3,283	2,278	735
kg/hr	956,211	59,148	41,099	13,246
Temp., C	15.6	15.6	26.7	15.6
Press., bar	1.014	1.014	1.4	1.0
Enthalpy, MJ/hr	62,739	3,881	-620	869
See Note	1	1	2	1

- Note:
1. Enthalpy corresponds to ASME Steam Tables Basis.
  2. The reference state for thermodynamic properties is the standard enthalpy of formation of ideal gas at 25°C and 1 atm.

**Table A1.4.2 - 10: Plant Performance Summary – Intercooled-Reheat Gas Turbine**

<b>PERFORMANCE SUMMARY</b>	<b>Baseline Case</b>		<b>Intercooled - Reheat High RIT GT</b>
<b>Pressure Ratio</b>	<b>24</b>		<b>70</b>
Fuel Feed Rate, ST/D (MF)	3,392		3,392
MMBtu/hr (HHV)	3,744		3,744
Fuel Feed Rate, MT/D (MF)	3,078		3,078
GJ/hr (HHV)	3,949		3,949
ASU	IP	HP	IP
Gas Turbine Air Extraction	Yes	Yes	No
Power Generation, kWe			
Gas Turbine	318,378	318,323	412,147
Steam Turbine	157,600	159,033	130,891
Clean Syngas Expander	2,320	2,320	0
Gas Turbine Extraction Air Expander	4,745	0	0
Auxiliary Power Consumption, kWe	99,795	93,924	126,936
Net Plant Output, kWe	383,247	385,753	416,102
Generation Efficiency (HHV)			
Net Heat Rate, Btu/kWh	9,769	9,706	8,998
Net Heat Rate, kJ/kWh	10,305	10,238	9,491
% Fuel to Power	34.94	35.16	37.93
Estimated NOx, ppmVd (15% O2 Basis)	18		42
Raw Water Makeup, m3/kWh	0.0026	0.0026	0.0023

Note: The NOx emission corresponds to a 30 ms residence time in the 2<sup>nd</sup> PSR.

**Table A1.4.2 - 11: Auxiliary (In-Plant) Power Consumption Summary – Intercooled-Reheat Gas Turbine**

AUXILLARY POWER CONSUMPTION	Baseline Case		Intercooled - Reheat High RIT GT
	24		70
Pressure Ratio			
ASU	IP	HP	IP
Gas Turbine Air Extraction	Yes	Yes	No
	kWe	kWe	kWe
Coal Handling	401	401	401
Coal Milling	802	802	802
Coal Slurry Pumps	274	274	314
Slag Handling and Dewatering	155	155	155
Miscellaneous Syngas Plant Equipment	380	380	596
Air Separation Unit Air Compressors	14,778	15,788	37,086
Air Separation Auxiliaries	1,290	1,290	1,290
Oxygen Compressor	12,522	11,122	12,991
Nitrogen Compressor	22,007	16,415	25,286
CO <sub>2</sub> Compressor	19,368	19,368	19,367
Tail Gas Recycle Compressor	998	998	1,057
Boiler Feedwater Pumps	4,047	4,054	3,659
Cooling Tower and Pumps	7,242	7,340	5,794
Steam Condensate Pump	42	44	22
Selexol Acid Gas Removal	11,788	11,788	11,419
Syngas Compression			1,326
Syngas Humidification	214	214	1,732
Claus Plant Auxiliaries	100	100	100
Gas Turbine Auxiliaries	517	517	517
Steam Turbine Auxiliaries	517	517	517
General Makeup and Demineralized Water	322	322	329
Miscellaneous Balance-of-Plant and Lighting	1,000	1,000	1,000
Transformer Losses	1,031	1,034	1,176
Total Auxiliary Power Consumption	99,795	93,924	126,936
Raw Water Makeup, m <sup>3</sup> /kWh	0.0026	0.0026	0.0023

**Table A1.4.2 - 12: Main Features of the Power Cycle – Intercooled-Reheat Gas Turbine**

	Baseline Case		Intercooled-Reheat High RIT GT	
<b>Gas Turbine</b>				
Pressure Ratio	24		70 (Overall)	27 (After Reheat)
ASU	IP	HP	IP	
Air Extraction	Yes		No	
Power Output, kW	318,378	318,323	412,147	
Rotor Inlet Temperature	1392°C (2538°F)		1592°C (2898°F)	
Combustor			HP	Reheat
Inlet Air Temperature	487°C (908°F)		590°C (1094°F)	1302°C (2375°F)
Discharge Temperature	1433°C (2611°F)		1636°C (2977°F)	1607°C (2924°F)
Inlet Air Flow, kg/s	421.8 kg/s (930 lb/s)		215.8 kg/s (475.8 lb/s)	292.2 kg/s (644.3 lb/s)
Inlet Air O2 Concentration, Vol %	20.74		19.81	4.76
Discharge O2 Concentration, Vol %	7.8		4.6	0.5
Adiabatic Flame Temperature	1891°C (3435°F)		1901°C (3454°F)	1639°C (2982°F)
Estimated NOx (15% O2 Dry Basis)				
2nd PSR Residence Time = 30 ms <sup>1</sup>	18		42	
2nd PSR Residence Time = 5 ms <sup>2</sup>	17		39	
Exhaust Temperature	582°C (1079°F)		704°C (1299°F)	
Air Extracted, % of Inlet Air	14		0	
<b>Steam Cycle</b>				
Power Output, kW	157,600	159,033	130,891	
HP Steam Pressure	166.5 bara (2415 psia)		166.5 bara (2415 psia)	
Superheat & Reheat Temperatures	538°C (1000°F)		661°C (1222°F)	
<b>Overall Plant Performance</b>				
Fuel Feed Rate, MT/D (MF)	3,078		3,078	
GJ/hr (HHV)	3,949		3,949	
Net Plant Output, kW	383,247	385,753	416,102	
Net Heat Rate, Btu/kWh	9,769	9,706	8,998	
kJ/kWh	10,305	10,238	9,491	
% Fuel to Power	34.94	35.16	37.93	
Raw Water Makeup, m3/kWh	0.0026	0.0026	0.0023	

1. NOx values are predicted using a Chemkin 2 PSR model with a 0.44 millisecond residence time in the first reactor and a 30 millisecond residence time in the second reactor.
2. NOx values are predicted using a Chemkin 2 PSR model with a 0.44 millisecond residence time in the first reactor and a 5 millisecond residence time in the second reactor.

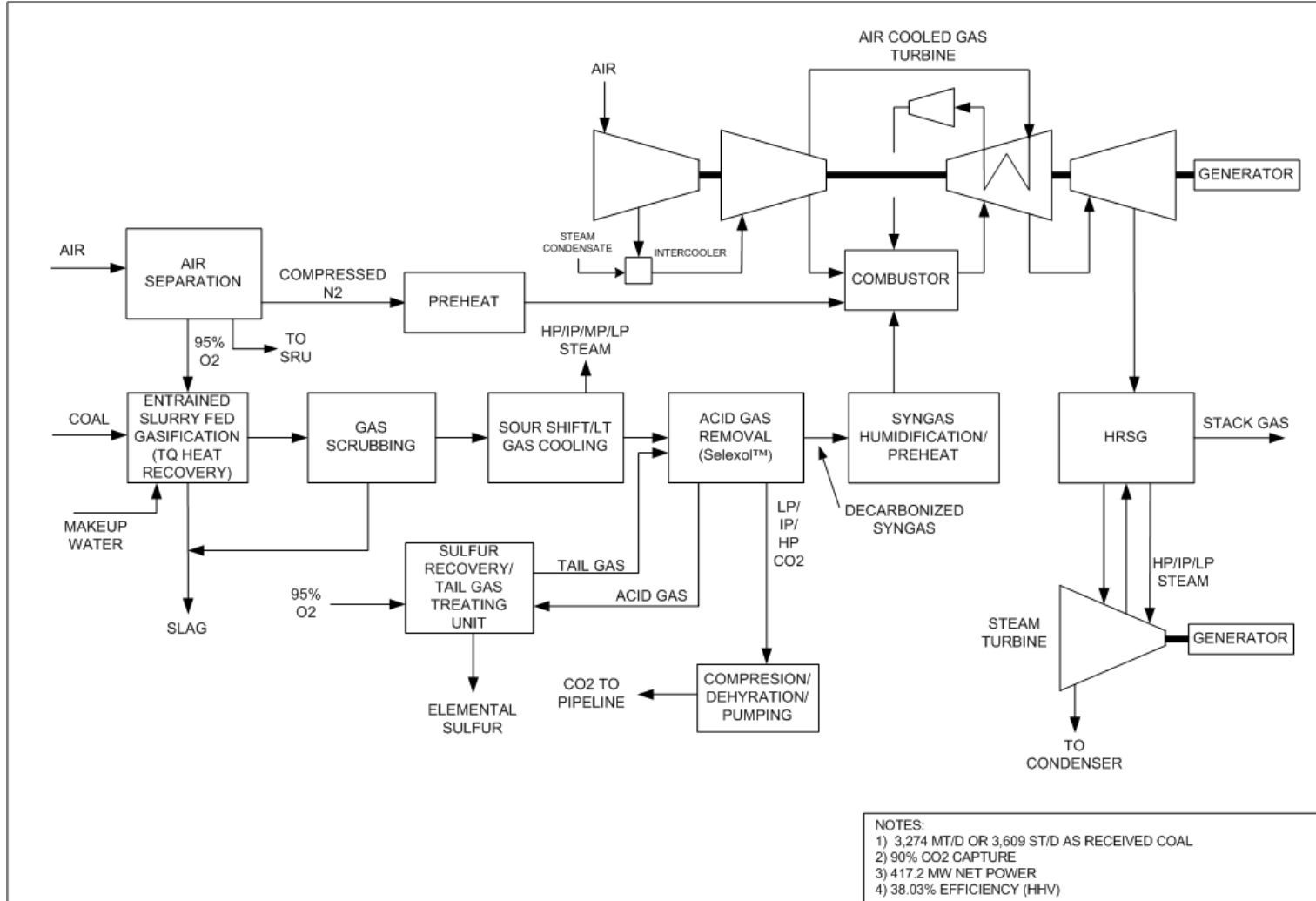
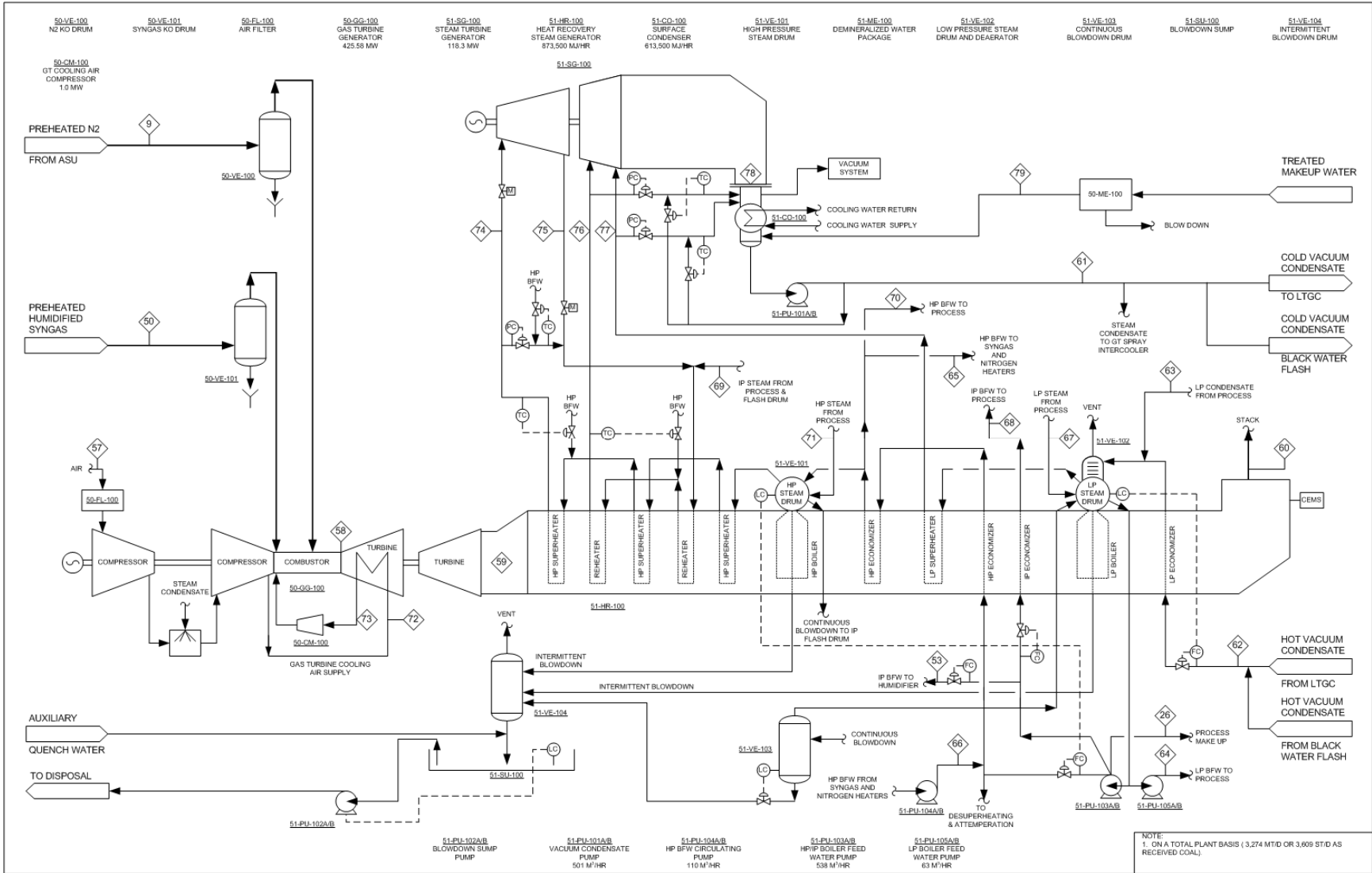


Figure A1.4.2 - 26: Overall Block Flow Diagram – IGCC with CO<sub>2</sub> Capture – Intercooled Closed Circuit Air Cooled GT



**Figure A1.4.2 - 27: Process Flow Diagram – Power Block – Intercooled Closed Circuit Air Cooled GT**

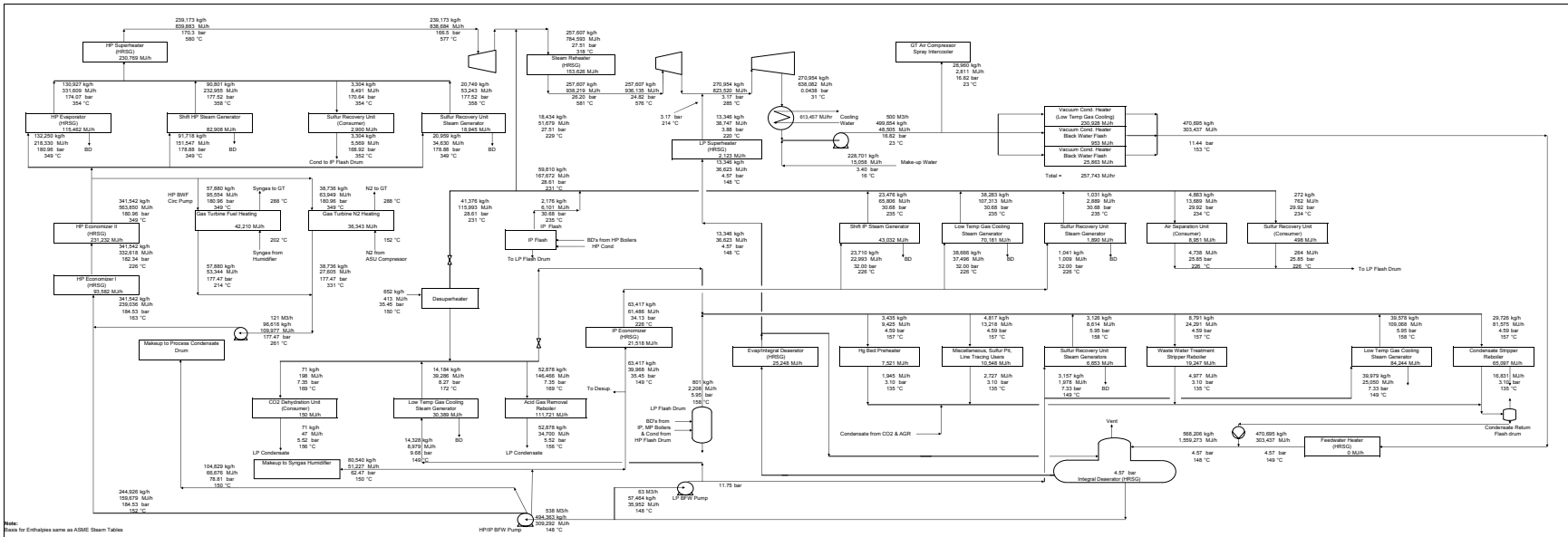


Figure A1.4.2 - 28: Steam Balance Diagram -- Intercooled Closed Circuit Air Cooled GT

**Table A1.4.2 - 13: Stream Data – Intercooled Closed Circuit Air Cooled Gas Turbine**

Basis: 3,274 Tonne/D (As Received) or 3,078 Tonne/D (Dry Basis) Pittsburgh No. 8 Coal

Mol Fraction	1	2	3	4	5	6	7	8	9	10 (not used)	11	12
O2		0.2077	0.2077	0.2077	0.9500	0.9500	0.9500	0.9500	0.0062			
N2		0.7722	0.7722	0.7722	0.0230	0.0176	0.0211	0.0176	0.9891			
Ar		0.0094	0.0094	0.0094	0.0270	0.0324	0.0289	0.0324	0.0047			
H2												
CO												
CO2		0.0003	0.0003	0.0003								
H2O		0.0104	0.0104	0.0104							1.0000	1.0000
CH4												
H2S												
SO2												
Cl2												
HCl												
NH3												
COS												
Total		1.0000	1.0000	1.0000	1.0000	1.0000	1.0000	1.0000	1.0000		1.0000	1.0000
Coal (As Received), kg/hr	136,416											
kgmol/hr (w/o Solids)	-	17,804	11,395	6,409	2,431	1,288	3,719	82	8,779		2,260	2,260
kg/hr (w/o Solids)	-	513,714	328,800	184,914	78,082	41,455	119,537	2,645	246,637		40,717	40,717
Temp., C	15.0	15.0	15.0	15.0	92.7	81.6	88.9	19.4	287.8		349.1	140.6
Press., bar	1.01	1.01	1.01	1.01	87.08	87.08	87.08	3.04	61.23		180.96	177.47
Enthalpy, MJ/hr	-123,514	-52,216	-33,420	-18,796	3,618	1,443	5,060	-16	67,788		67,203	24,584
See Note	1, 2	2	2	2	2	2	2	2	2		3	3

Note:

1. Enthalpy expressed as HHV = 3,949,275 MJ/hr.
2. The reference state for thermodynamic properties is the standard enthalpy of formation of ideal gas at 25°C and 1 atm.
3. Enthalpy corresponds to ASME Steam Tables Basis.

**Table A1.4.2 - 13: Stream Data – Intercooled Closed Circuit Air Cooled Gas Turbine - continued**

Basis: 3,274 Tonne/D (As Received) or 3,078 Tonne/D (Dry Basis) Pittsburgh No. 8 Coal

Mol Fraction	13	14	15	16	17	18	19	20	21	22	23	24
O2												
N2	0.0000		0.0042	0.0015			0.0042	0.0042	0.0042	0.0042	0.0042	0.0042
Ar	0.0000		0.0036	0.0030			0.0036	0.0036	0.0036	0.0036	0.0036	0.0036
H2	0.0003		0.1661	0.1404			0.1661	0.3283	0.3283	0.3494	0.3494	0.3494
CO	0.0004		0.1935	0.0400			0.1935	0.0313	0.0313	0.0103	0.0103	0.0103
CO2	0.0008		0.0687	0.1458	0.0000		0.0687	0.2310	0.2310	0.2521	0.2521	0.2521
H2O	0.9977	1.0000	0.5563	0.0210	0.9999	1.0000	0.5563	0.3940	0.3940	0.3729	0.3729	0.3729
CH4	0.0000		0.0020	0.0014			0.0020	0.0020	0.0020	0.0020	0.0020	0.0020
H2S	0.0002		0.0040	0.0452	0.0000		0.0040	0.0042	0.0042	0.0042	0.0042	0.0042
SO2												
Cl2												
HCl												
NH3	0.0006		0.0013	0.6008	0.0001		0.0013	0.0013	0.0013	0.0013	0.0013	0.0013
COS	0.0000		0.0002	0.0009	0.0000		0.0002	0.0000	0.0000	0.0000	0.0000	0.0000
Total	1.0000	1.0000	1.0000	1.0000	1.0000	1.0000	1.0000	1.0000	1.0000	1.0000	1.0000	1.0000
kgmol/hr (w/o Solids)	291	447	29,185	40	3,871	1,160	29,185	29,185	29,185	29,185	29,185	29,185
kg/hr (w/o Solids)	5,256	8,062	562,308	811	69,746	20,896	562,308	562,306	562,306	562,306	562,306	562,306
kg/hr Solids	12,141	3,455										
kg/hr Total	17,397	11,516	562,308	811	69,746	20,896	562,308	562,306	562,306	562,306	562,306	562,306
Temp., C	<93.3	60.2	243.2	44.8	123.4	156.7	287.8	442.5	287.9	307.9	246.1	219.4
Press., bar	1.01	1.01	71.34	2.07	2.21	4.59	70.99	70.01	68.98	68.00	67.65	67.31
Enthalpy, MJ/hr	<-81,402	-140,031	-5,176,801	-3,811	-1,077,456	57,741	-5,127,476	-5,127,408	-5,302,643	-5,302,646	-5,372,810	-5,403,193
See Note	1	1	1	1	1	2	1	1	1	1	1	1

Note:

1. The reference state for thermodynamic properties is the standard enthalpy of formation of ideal gas at 25°C and 1 atm.
2. Enthalpy corresponds to ASME Steam Tables Basis.

**Table A1.4.2 - 13: Stream Data – Intercooled Closed Circuit Air Cooled Gas Turbine - continued**

Basis: 3,274 Tonne/D (As Received) or 3,078 Tonne/D (Dry Basis) Pittsburgh No. 8 Coal

Mol Fraction	25	26	26	27	28	29	30	31	32	33	34	35	36
O2													
N2	0.0053	0.0057		0.0000	0.0067	0.0067	0.0067		0.0067	0.0124		0.0000	0.0002
Ar	0.0046	0.0050		0.0000	0.0058	0.0058	0.0058	0.0000	0.0058	0.0096	0.0000	0.0000	0.0005
H2	0.4382	0.4773		0.0000	0.5576	0.5576	0.5576	0.0000	0.5576	0.9090	0.0000	0.0006	0.0200
CO	0.0129	0.0140		0.0000	0.0164	0.0164	0.0164		0.0164	0.0266	0.0000	0.0001	0.0016
CO2	0.3159	0.3440		0.0007	0.4018	0.4018	0.4018	0.0003	0.4018	0.0375	0.9973	0.9980	0.9763
H2O	0.2142	0.1443	1.0000	0.9986	0.0016	0.0016	0.0016	0.9920	0.0016	0.0001	0.0027	0.0012	0.0008
CH4	0.0025	0.0027		0.0000	0.0031	0.0031	0.0031	0.0000	0.0031	0.0049	0.0000	0.0000	0.0006
H2S	0.0052	0.0057		0.0001	0.0066	0.0066	0.0066	0.0001	0.0066	0.0000	0.0000	0.0000	0.0000
SO2													
Cl2													
HCl													
NH3	0.0014	0.0014		0.0005	0.0003	0.0003	0.0003	0.0075	0.0003				
COS	0.0000	0.0000		0.0000	0.0000	0.0000	0.0000		0.0000	0.0000	0.0000	0.0000	0.0000
Total	1.0000	1.0000	1.0000	1.0000	1.0000	1.0000	1.0000	1.0000	1.0000	1.0000	1.0000	1.0000	1.0000
kgmol/hr	23,262	21,354	5,819	17,516	18,278	18,278	18,278	3,076	18,278	11,164	1,097	2,798	3,118
kg/hr	455,393	420,954	104,829	315,909	365,525	365,525	365,525	55,429	365,525	56,252	48,185	122,960	134,413
Temp., C	187.9	170.0	150.0	156.5	40.6	51.7	51.7	40.6	26.7	16.7	0.1	3.6	11.7
Press., bar	66.96	66.62	78.78	75.84	66.28	65.95	65.45	66.28	65.10	62.44	1.08	3.24	10.00
Enthalpy, MJ/hr	-4,024,902	-3,584,366	-1,613,105	-4,843,282	-2,939,947	-2,932,427	-2,932,427	-875,292	-2,948,996	-205,308	-432,011	-1,101,936	-1,201,990
See Note	1	1	1	1	1	1	1	1	1	1	1	1	1

Note: 1. The reference state for thermodynamic properties is the standard enthalpy of formation of ideal gas at 25°C and 1 atm.

**Table A1.4.2 - 13: Stream Data – Intercooled Closed Circuit Air Cooled Gas Turbine - continued**

Basis: 3,274 Tonne/D (As Received) or 3,078 Tonne/D (Dry Basis) Pittsburgh No. 8 Coal

Mol Fraction	37	38	39	40	41	42	43	44	45	46	47	48
O2												
N2	0.0014	0.0438		0.0124	0.0451		0.0001	0.0789	0.0811	0.0001	0.0000	0.0000
Ar	0.0024	0.0090		0.0096	0.0092		0.0003	0.0166	0.0170	0.0000	0.0000	0.0000
H2	0.1588	0.1010		0.9090	0.1041		0.0091	0.3590	0.3687	0.0000	0.0001	0.0001
CO	0.0069	0.1101		0.0265	0.1135		0.0008	0.0232	0.0238	0.0000	0.0000	0.0000
CO2	0.3091	0.1533		0.0376	0.1580		0.9895	0.4473	0.4594	0.0080	0.0001	0.0001
H2O	0.0563	0.4670		0.0001	0.5423			0.0280	0.0018	0.9891	0.9997	0.9997
CH4	0.0030			0.0048			0.0003	0.0003	0.0003		0.0000	0.0000
H2S	0.4413	0.0769			0.0182		0.0000	0.0461	0.0474	0.0026		
SO2		0.0383			0.0090							
Cl2												
HCl												
NH3	0.0202							0.0003	0.0003	0.0000		
COS	0.0006	0.0006			0.0006		0.0000	0.0002	0.0002	0.0000		
Total	1.0000	1.0000		1.0000	1.0000		1.0000	1.0000	1.0000	1.0000	1.0000	1.0000
Sulfur, kg/hr			2,825			3,929						
kgmol/hr	297	388	44	12	376	78	7,004	216	211	174	38,891	38,891
kg/hr	9,123	9,755	2,825	59	8,650	3,929	305,395	5,629	5,526	3,183	700,661	700,661
Temp., C	48.9	176.7	176.7	14.5	287.8	25.0	40.7	26.6	26.7	28.2	137.9	208.3
Press., bar	2.07	1.87	1.87	1.30	1.30	1.01	138.93	1.24	68.89	3.45	67.15	66.47
Enthalpy, MJ/hr	-43,297	-74,977	4,738	-217	-75,249	0	-2,790,506	-40,282	-39,116	-49,779	-10,820,511	-10,579,064
See Note	1	1	1	1	1	1	1	1	1	1	1	1

Note:

1. The reference state for thermodynamic properties is the standard enthalpy of formation of ideal gas at 25°C and 1 atm.

**Table A1.4.2 - 13: Stream Data – Intercooled Closed Circuit Air Cooled Gas Turbine - continued**

Basis: 3,274 Tonne/D (As Received) or 3,078 Tonne/D (Dry Basis) Pittsburgh No. 8 Coal

Mol Fraction	49	50	51	52	53	54 (Not Used)	55 (Not Used)	56 (Not Used)	57	58	59	60
O2									0.2074	0.0353	0.0444	0.0444
N2		0.0089							0.7728	0.6451	0.6498	0.6498
Ar		0.0069							0.0094	0.0079	0.0086	0.0086
H2	0.0002	0.6500										
CO		0.0190										
CO2	0.0001	0.0268							0.0003	0.0140	0.0133	0.0133
H2O	0.9997	0.2850	1.0000	1.0000	1.0000				0.0101	0.2977	0.2840	0.2840
CH4		0.0035										
H2S		0.0000										
SO2												
Cl2												
HCl												
NH3												
COS		0.0000										
Total	1.0000	1.0000	1.0000	1.0000	1.0000				1.0000	1.0000	1.0000	1.0000
kgmol/hr	22	15,612	3,213	3,213	4,471				38,018	55,630	58,795	58,795
kg/hr	401	136,391	57,880	57,880	80,540				1,097,061	1,418,412	1,509,047	1,509,047
Temp., C	136.2	287.8	349.1	213.9	150.0				15.0	1,712.2	620.0	161.0
Press., bar	61.75	61.41	180.96	177.47	82.74				1.01	48.67	1.07	1.01
Enthalpy, MJ/hr	-6,192	-1,154,345	95,554	53,344	51,096				-108,676	-915,626	-3,218,338	-4,100,621
See Note	1	1	2	2	2				1	1,3	1,3	1,3

Note:

1. The reference state for thermodynamic properties is the standard enthalpy of formation of ideal gas at 25°C and 1 atm.
2. Enthalpy corresponds to ASME Steam Tables Basis.
3. For NOx see Performance Summary, Table 1.

**Table A1.4.2 - 13: Stream Data – Intercooled Closed Circuit Air Cooled Gas Turbine - continued**

Basis: 3,274 Tonne/D (As Received) or 3,078 Tonne/D (Dry Basis) Pittsburgh No. 8 Coal

Mol Fraction	61	62	63	64	65	66	67	68	69	70	71	72
O2												0.1990
N2												0.7414
Ar												0.0091
CO2												0.0003
H2O	1.0000	1.0000	1.0000	1.0000	1.0000	1.0000	1.0000	1.0000	1.0000	1.0000	1.0000	0.0502
Total	1.0000	1.0000	1.0000	1.0000	1.0000	1.0000	1.0000	1.0000	1.0000	1.0000	1.0000	1.0000
kgmol/hr	27,735	27,735	27,735	3,190	5,363	5,363	0	3,520	1,023	6,254	6,009	6,685
kg/hr	499,654	499,654	109,569	57,464	96,616	96,616	0	63,417	18,434	112,676	108,246	189,979
Temp., C	22.7	152.7	134.7	148.6	349.1	260.9	156.7	225.6	229.2	349.1	356.0	522.8
Press., bar	16.82	11.44	4.57	11.75	180.96	177.47	4.57	32.00	27.51	178.88	174.07	50.62
Enthalpy, MJ/hr	48,505	303,437	102,578	36,027	159,503	80,949	0	61,499	51,679	186,177	277,707	19,619
See Note	1	1	1	1	1	1	1	1	1	1	1	2

- Note:
1. Enthalpy corresponds to ASME Steam Tables Basis.
  2. The reference state for thermodynamic properties is the standard enthalpy of formation of ideal gas at 25°C and 1 atm.

Mol Fraction	73	74	75	76	77	78	79
O2	0.1990						
N2	0.7414						
Ar	0.0091						
CO2	0.0003						
H2O	0.0502	1.0000	1.0000	1.0000	1.0000	1.0000	1.0000
Total	1.0000	1.0000	1.0000	1.0000	1.0000	1.0000	1.0000
kgmol/hr	6,351	13,276	13,276	14,299	741	15,040	12,695
kg/hr	180,480	239,173	239,173	257,607	13,346	270,954	228,701
Temp., C	160.9	576.8	401.1	576.4	214.0	30.5	15.6
Press., bar	1.0	166.51	51.02	24.82	3.17	0.04	3.40
Enthalpy, MJ/hr	-52,460	838,684	764,781	936,135	38,622	638,082	15,058
See Note	1	2	2	2	2	2	2

- Note:
1. The reference state for thermodynamic properties is the standard enthalpy of formation of ideal gas at 25°C and 1 atm.
  2. Enthalpy corresponds to ASME Steam Tables Basis.

**Table A1.4.2 - 13: Stream Data – Intercooled Closed Circuit Air Cooled Gas Turbine - continued**

Basis: 3,274 Tonne/D (As Received) or 3,078 Tonne/D (Dry Basis) Pittsburgh No. 8 Coal

Mol Fraction	80	81	82	83
O2				
N2				
Ar				
H2				
CO				
CO2				
H2O	1.0000	1.0000	0.9981	1.0000
CH4				
H2S				
SO2				
Cl2				
HCl			0.0016	
NH3			0.0003	
COS				
Total			1.0000	
kgmol/hr	51,772	3,283	2,281	738
kg/hr	932,689	59,148	41,161	13,298
Temp., C	15.6	15.6	26.7	15.6
Press., bar	1.014	1.014	1.4	1.0
Enthalpy, MJ/hr	61,196	3,881	-621	873
See Note	1	1	2	1

- Note:
1. Enthalpy corresponds to ASME Steam Tables Basis.
  2. The reference state for thermodynamic properties is the standard enthalpy of formation of ideal gas at 25°C and 1 atm.

**Table A1.4.2 - 14: Plant Performance Summary – Intercooled Closed Circuit Air Cooled Gas Turbine**

<b>PERFORMANCE SUMMARY</b>	<b>Baseline Case</b>	<b>Intercooled - Closed Circuit Air-Cooled Gas Turbine</b>
<b>Pressure Ratio</b>	<b>24</b>	<b>50</b>
Fuel Feed Rate, ST/D (MF)	3,392	3,392
MMBtu/hr (HHV)	3,744	3,744
Fuel Feed Rate, MT/D (MF)	3,078	3,078
GJ/hr (HHV)	3,949	3,949
ASU	IP	IP
Gas Turbine Air Extraction	Yes	No
Power Generation, kWe		
Gas Turbine	318,378	425,808
Steam Turbine	157,600	118,289
Clean Syngas Expander	2,320	0
Gas Turbine Extraction Air Expander	4,745	0
Auxiliary Power Consumption, kWe	99,795	126,848
Net Plant Output, kWe	383,247	417,249
Generation Efficiency (HHV)		
Net Heat Rate, Btu/kWh	9,769	8,973
Net Heat Rate, kJ/kWh	10,305	9,465
% Fuel to Power	34.94	38.03
Estimated NOx, ppmVd (15% O2 Basis)	18	115
Raw Water Makeup, m3/kWh	0.0026	0.0022

Note: The NOx emission corresponds to a 30 ms residence time in the 2<sup>nd</sup> PSR.

**Table A1.4.2 - 15: Auxiliary (In-Plant) Power Consumption Summary – Intercooled Closed Circuit Air Cooled Gas Turbine**

<b>AUXILLARY POWER CONSUMPTION</b>	<b>Baseline Case</b>	<b>Closed Circuit Air-Cooled Gas Turbine</b>
<b>Pressure Ratio</b>	<b>24</b>	<b>50</b>
ASU	IP	IP
Gas Turbine Air Extraction	Yes	No
	kWe	kWe
Coal Handling	401	401
Coal Milling	802	802
Coal Slurry Pumps	274	288
Slag Handling and Dewatering	155	155
Miscellaneous Syngas Plant Equipment	380	519
Air Separation Unit Air Compressors	14,778	37,092
Air Separation Auxiliaries	1,290	1,291
Oxygen Compressor	12,522	12,701
Nitrogen Compressor	22,007	27,853
CO <sub>2</sub> Compressor	19,368	19,365
Tail Gas Recycle Compressor	998	1,024
Boiler Feedwater Pumps	4,047	3,512
Cooling Tower and Pumps	7,242	5,638
Steam Condensate Pump	42	19
Selexol Acid Gas Removal	11,788	12,357
Syngas Compression		
Syngas Humidification	214	198
Claus Plant Auxilliaries	100	100
Gas Turbine Auxiliaries	517	517
Steam Turbine Auxiliaries	517	517
General Makeup and Demineralized Water	322	321
Miscellaneous Balance-of-Plant and Lighting	1,000	1,000
Transformer Losses	1,031	1,179
<b>Total Auxiliary Power Consumption</b>	<b>99,795</b>	<b>126,848</b>
Raw Water Makeup, m <sup>3</sup> /kWh	0.0026	0.0022

**Table A1.4.2 - 16: Main Features of the Power Cycle – Intercooled Closed Circuit Air Cooled Gas Turbine**

	<b>Baseline Case</b>	<b>Intercooled - Closed-Circuit Air Cooled Gas Turbine</b>
<b>Gas Turbine</b>		
Pressure Ratio	24	50
ASU	IP	IP
Air Extraction	Yes	No
Power Output, kW	318,378	425,808
Rotor Inlet Temperature	1392°C (2538°F)	1678°C (3053°F)
<b>Combustor</b>		
Inlet Air Temperature	487°C (908°F)	530°C (986°F)
Discharge Temperature	1433°C (2611°F)	1712°C (3114°F)
Inlet Air Flow, kg/s	421.8 kg/s (930	288 kg/s (634 lb/s)
Inlet Air O <sub>2</sub> Concentration, Vol %	20.74	19.90
Discharge O <sub>2</sub> Concentration, Vol %	7.8	3.5
Adiabatic Flame Temperature	1891°C (3435°F)	1919°C (3486°F)
<b>Estimated NO<sub>x</sub> (15% O<sub>2</sub> Dry Basis)</b>		
2nd PSR Residence Time = 30 ms <sup>1</sup>	18	115
2nd PSR Residence Time = 5 ms <sup>2</sup>	17	35
Exhaust Temperature	582°C (1079°F)	620°C (1148°F)
Air Extracted, % of Inlet Air	14	0
<b>Steam Cycle</b>		
Power Output, kW	157,600	118,289
HP Steam Pressure	166.5 bara (2415	166.5 bara (2415 psia)
Superheat & Reheat Temperatures	538°C (1000°F)	577°C (1070°F)
<b>Overall Plant Performance</b>		
Fuel Feed Rate, MT/D (MF)	3,078	3,078
GJ/hr (HHV)	3,949	3,949
Net Plant Output, kW	383,247	417,249
Net Heat Rate, Btu/kWh	9,769	8,973
kJ/kWh	10,305	9,465
% Fuel to Power	34.94	38.03
Raw Water Makeup, m <sup>3</sup> /kWh	0.0026	0.0022

1. NO<sub>x</sub> values are predicted using a Chemkin 2 PSR model with a 0.44 millisecond residence time in the first reactor and a 30 millisecond residence time in the second reactor.

2. NO<sub>x</sub> values are predicted using a Chemkin 2 PSR model with a 0.44 millisecond residence time in the first reactor and a 5 millisecond residence time in the second reactor.

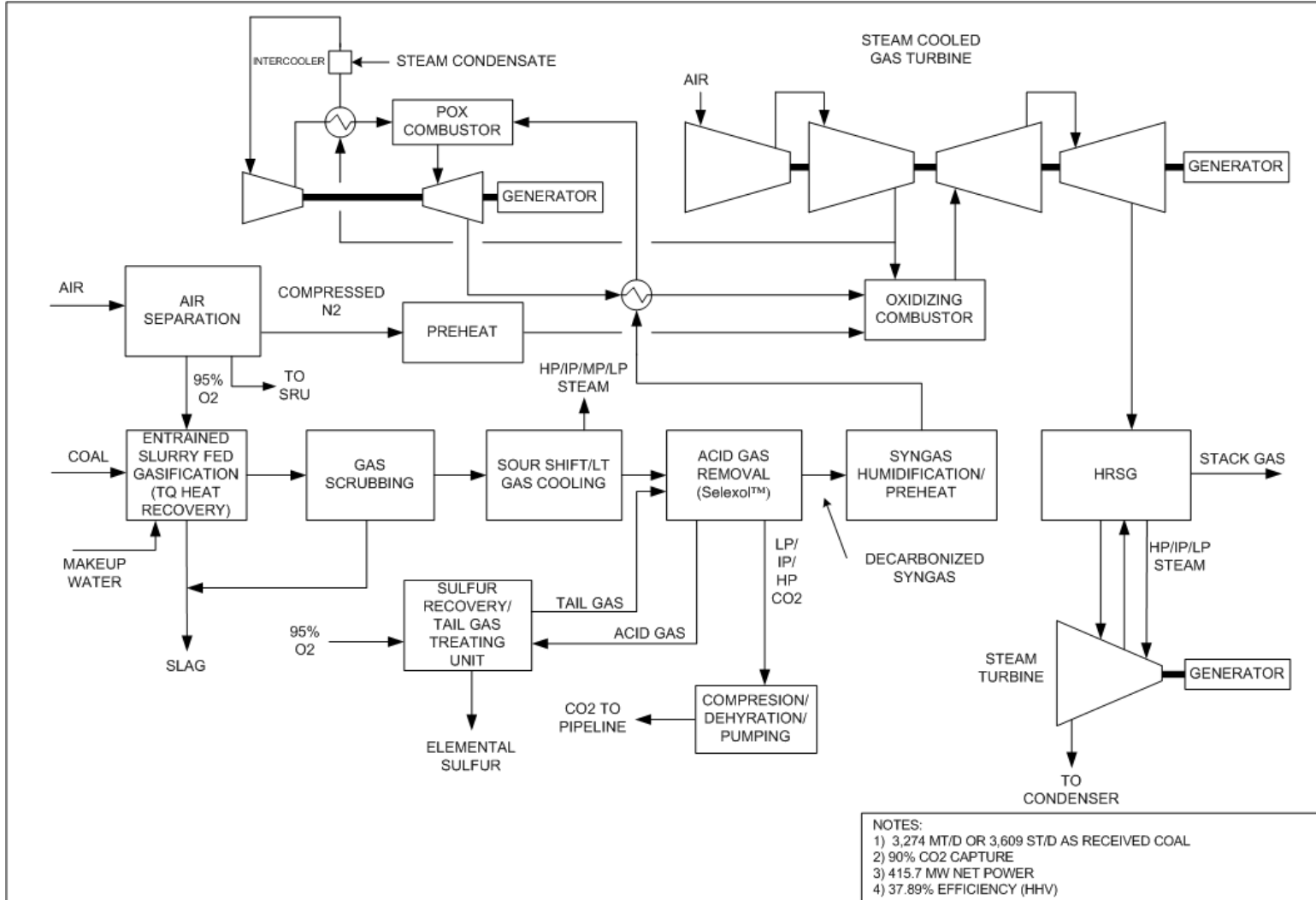


Figure A1.4.2 - 29: Overall Block Flow Diagram – IGCC with CO<sub>2</sub> Capture – Air PO<sub>x</sub> Topping Cycle

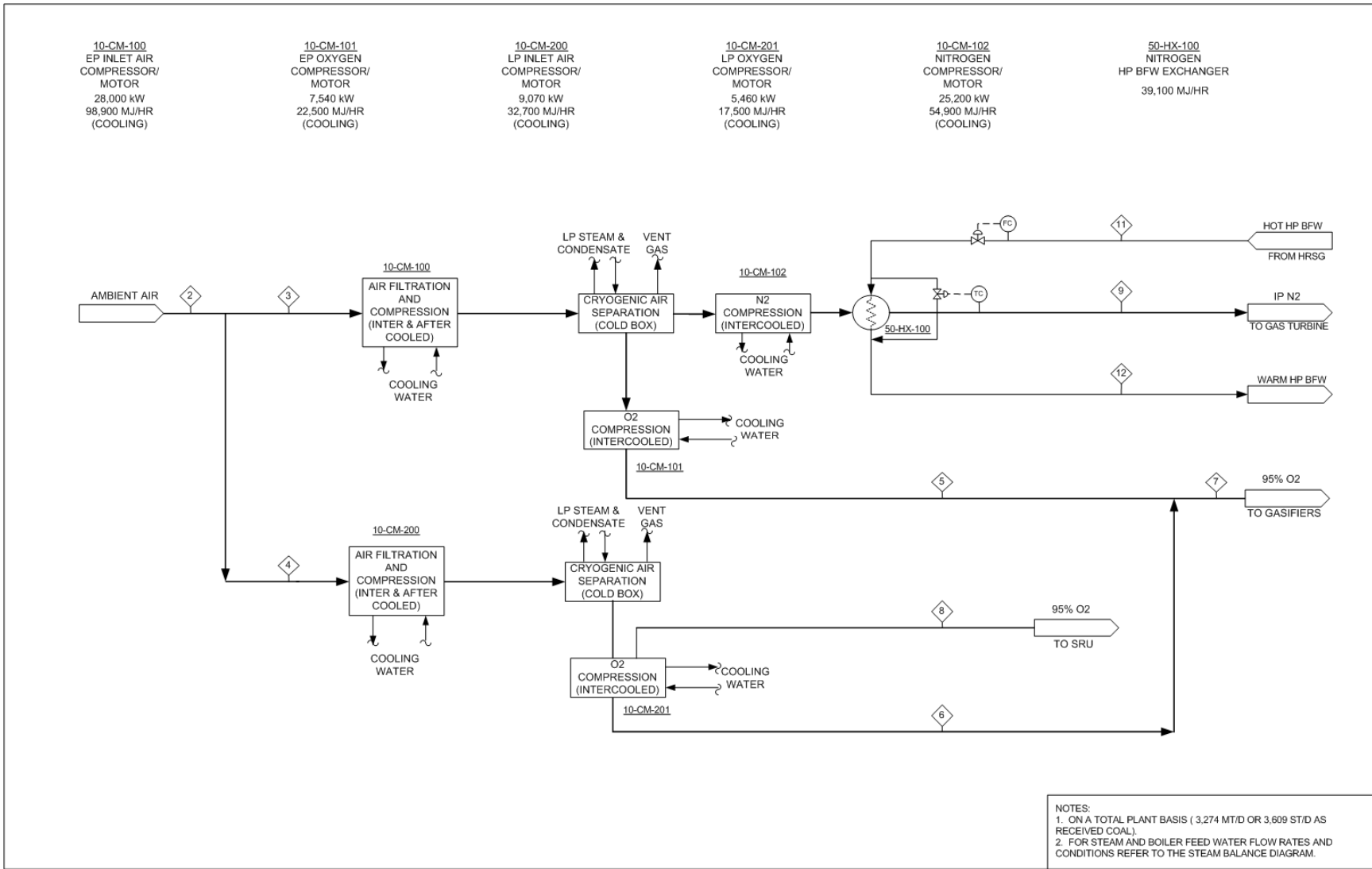
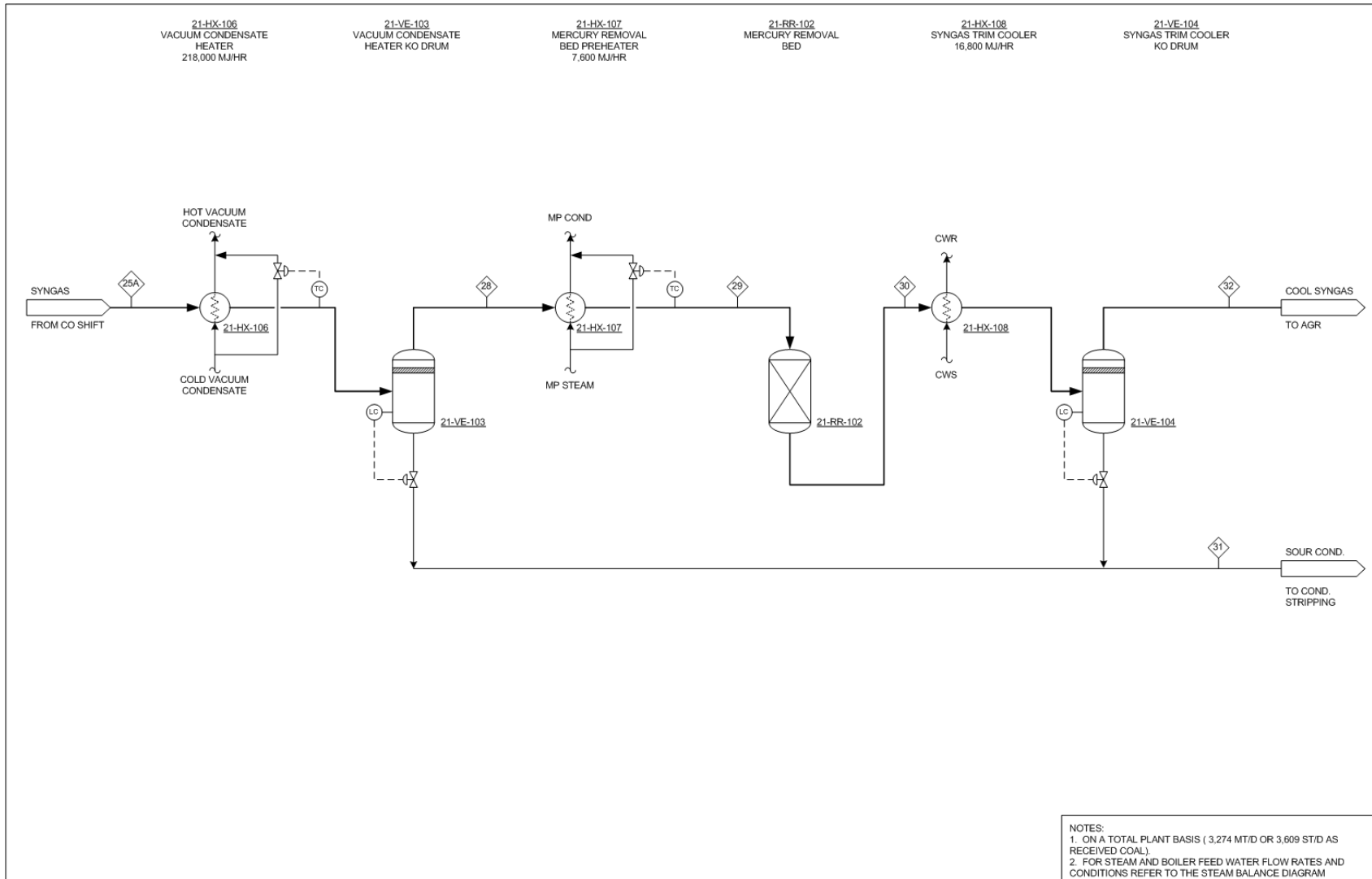
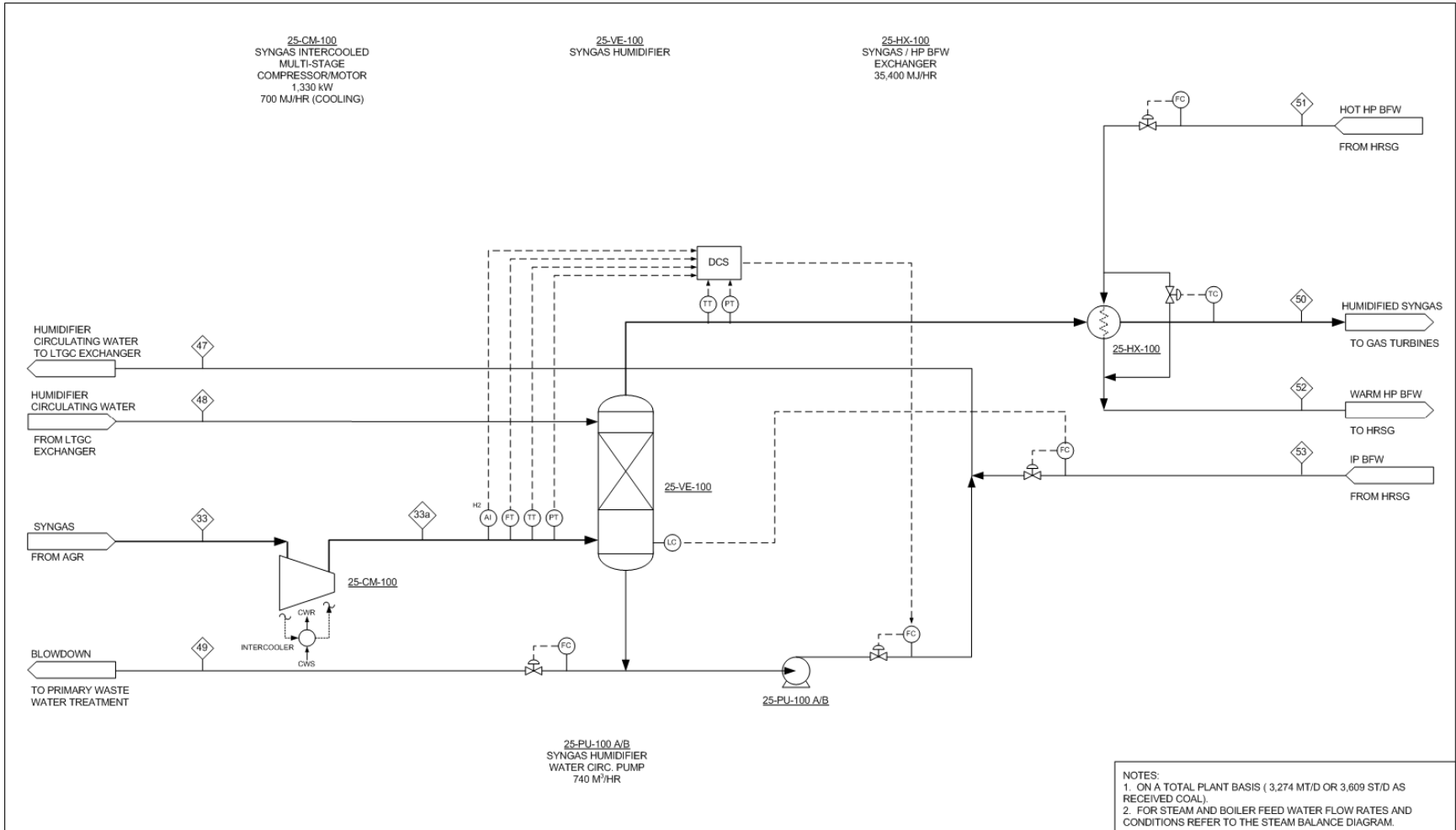


Figure A1.4.2 - 30: Process Flow Diagram – Air Separation Unit – Air POx Topping Cycle





**Figure A1.4.2 -31: Process Flow Diagram – CO Shift / Low Temperature Gas Cooling Unit - Air POx Topping Cycle - continued**



**Figure A1.4.2 - 32: Process Flow Diagram – Syngas Humidification Unit - Air POx Topping Cycle**

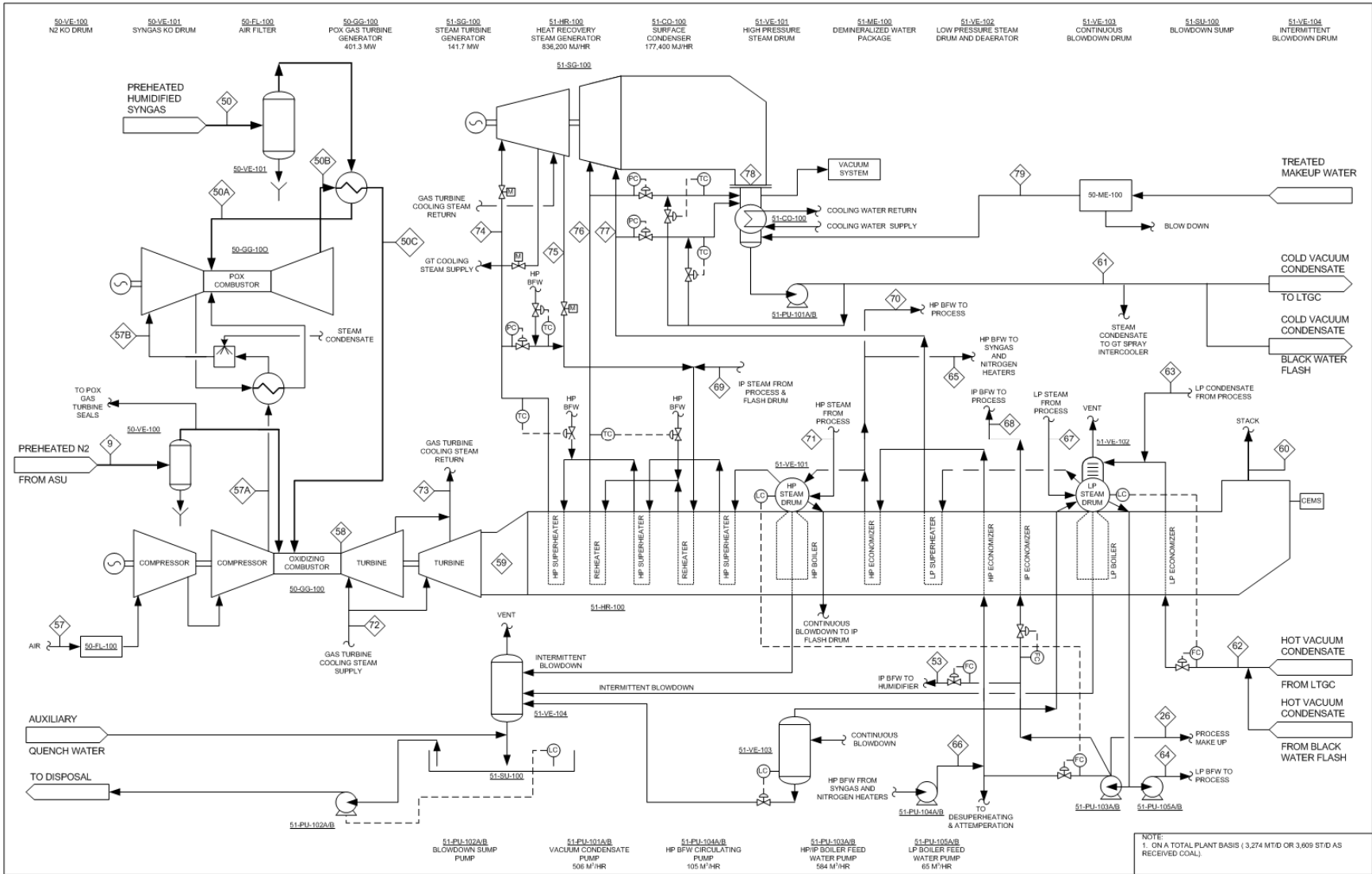


**Figure A1.4.2 - 33: Process Flow Diagram – Power Block - Air POx Topping Cycle**

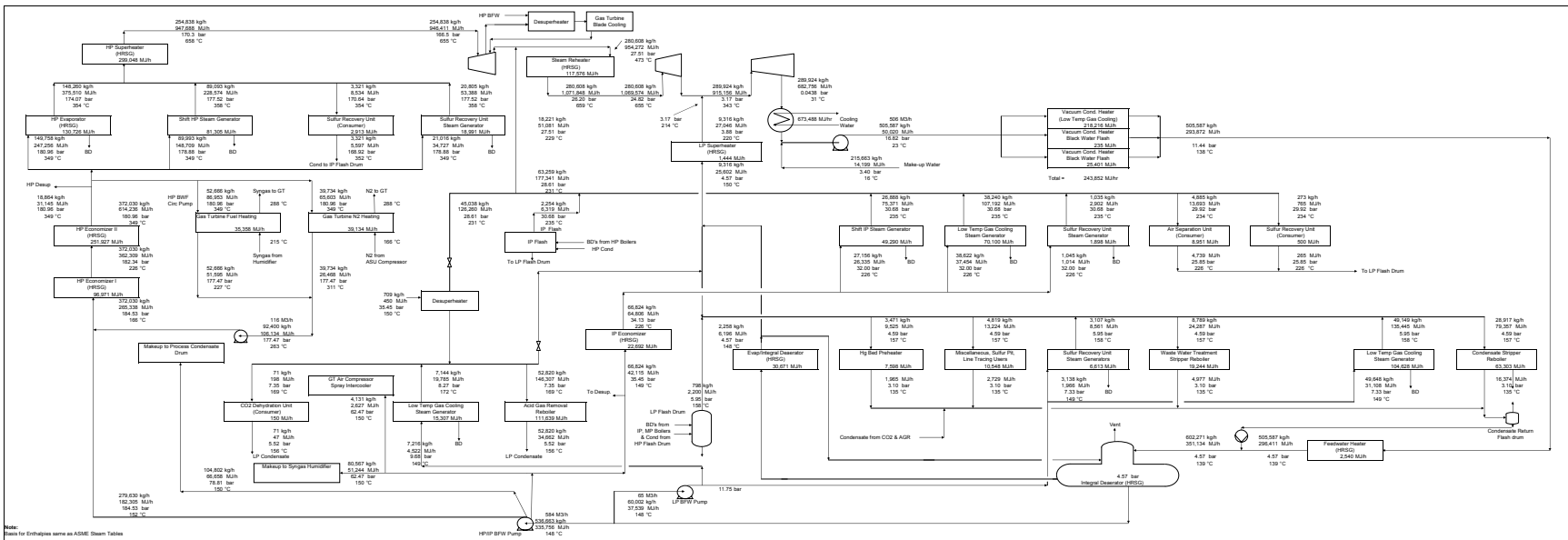


Figure A1.4.2 - 34: Steam Balance Diagram – Air POx Topping Cycle

**Table A1.4.2 - 17: Stream Data – Air Partial Oxidation Topping Cycle**

Basis: 3,274 Tonne/D (As Received) or 3,078 Tonne/D (Dry Basis) Pittsburgh No. 8 Coal

Mol Fraction	1	2	3	4	5	6	7	8	9	10 (not used)	11	12
O2		0.2077	0.2077	0.2077	0.9500	0.9500	0.9500	0.9500	0.0062			
N2		0.7722	0.7722	0.7722	0.0230	0.0176	0.0211	0.0176	0.9891			
Ar		0.0094	0.0094	0.0094	0.0270	0.0324	0.0289	0.0324	0.0047			
H2												
CO												
CO2		0.0003	0.0003	0.0003								
H2O		0.0104	0.0104	0.0104							1.0000	1.0000
CH4												
H2S												
SO2												
Cl2												
HCl												
NH3												
COS												
Total		1.0000	1.0000	1.0000	1.0000	1.0000	1.0000	1.0000	1.0000		1.0000	1.0000
Coal (As Received), kg/hr	136,416											
kgmol/hr (w/o Solids)	-	17,801	11,393	6,407	2,430	1,288	3,718	82	8,777		2,260	2,260
kg/hr (w/o Solids)	-	513,627	328,746	184,880	78,069	41,447	119,516	2,645	246,596		40,717	40,717
Temp., C	15.0	15.0	15.0	15.0	94.6	83.1	90.6	19.4	287.8		349.1	140.6
Press., bar	1.01	1.01	1.01	1.01	94.11	94.11	94.11	3.04	61.23		180.96	177.47
Enthalpy, MJ/hr	-123,514	-52,208	-33,415	-18,792	3,683	1,459	5,142	-16	67,776		67,203	24,584
See Note	1, 2	2	2	2	2	2	2	2	2		3	3

Note:

1. Enthalpy expressed as HHV = 3,949,275 MJ/hr.
2. The reference state for thermodynamic properties is the standard enthalpy of formation of ideal gas at 25°C and 1 atm.
3. Enthalpy corresponds to ASME Steam Tables Basis.

**Table A1.4.2 - 17: Stream Data – Air Partial Oxidation Topping Cycle - continued**

Basis: 3,274 Tonne/D (As Received) or 3,078 Tonne/D (Dry Basis) Pittsburgh No. 8 Coal

Mol Fraction	13	14	15	16	17	18	19	20	21	22	23	24
O2												
N2	0.0000		0.0042	0.0016			0.0042	0.0042	0.0042	0.0042	0.0042	0.0042
Ar	0.0000		0.0036	0.0033			0.0036	0.0036	0.0036	0.0036	0.0036	0.0036
H2	0.0004		0.1657	0.1621			0.1657	0.3278	0.3278	0.3485	0.3485	0.3485
CO	0.0004		0.1930	0.0459			0.1930	0.0309	0.0309	0.0102	0.0102	0.0102
CO2	0.0009		0.0686	0.1501	0.0000		0.0686	0.2309	0.2309	0.2516	0.2516	0.2516
H2O	0.9973	1.0000	0.5574	0.0242	0.9999	1.0000	0.5574	0.3951	0.3951	0.3744	0.3744	0.3744
CH4	0.0000		0.0020	0.0016			0.0020	0.0020	0.0020	0.0020	0.0020	0.0020
H2S	0.0002		0.0040	0.0447	0.0000		0.0040	0.0042	0.0042	0.0042	0.0042	0.0042
SO2												
Cl2												
HCl												
NH3	0.0006		0.0013	0.5655	0.0001		0.0013	0.0013	0.0013	0.0013	0.0013	0.0013
COS	0.0000		0.0002	0.0009	0.0000		0.0002	0.0000	0.0000	0.0000	0.0000	0.0000
Total	1.0000	1.0000	1.0000	1.0000	1.0000	1.0000	1.0000	1.0000	1.0000	1.0000	1.0000	1.0000
kgmol/hr (w/o Solids)	290	447	29,257	42	3,640	1,160	29,257	29,257	29,257	29,257	29,257	29,257
kg/hr (w/o Solids)	5,230	8,062	563,644	851	65,568	20,896	563,645	563,642	563,642	563,642	563,642	563,642
kg/hr Solids	12,141	3,455										
kg/hr Total	17,371	11,516	563,644	851	65,568	20,896	563,645	563,642	563,642	563,642	563,642	563,642
Temp., C	<93.3	60.2	248.2	47.4	123.4	156.7	287.8	440.5	287.7	307.1	246.1	232.8
Press., bar	1.01	1.01	78.39	2.07	2.21	4.59	78.05	77.07	76.04	75.06	74.71	74.37
Enthalpy, MJ/hr	<-81,402	-140,031	-5,192,088	-4,086	-1,012,922	57,741	-5,147,955	-5,147,905	-5,322,602	-5,322,605	-5,392,689	-5,407,992
See Note	1	1	1	1	1	2	1	1	1	1	1	1

Note:

1. The reference state for thermodynamic properties is the standard enthalpy of formation of ideal gas at 25°C and 1 atm.
2. Enthalpy corresponds to ASME Steam Tables Basis.

**Table A1.4.2 - 17: Stream Data – Air Partial Oxidation Topping Cycle - continued**

Basis: 3,274 Tonne/D (As Received) or 3,078 Tonne/D (Dry Basis) Pittsburgh No. 8 Coal

Mol Fraction	25	25A	26	27	28	29	30	31	32	33	34	35	36
O2													
N2	0.0052	0.0058		0.0000	0.0067	0.0067	0.0067		0.0067	0.0124		0.0000	0.0002
Ar	0.0045	0.0050		0.0000	0.0058	0.0058	0.0058	0.0000	0.0058	0.0096	0.0000	0.0000	0.0005
H2	0.4349	0.4834		0.0000	0.5577	0.5577	0.5577	0.0000	0.5577	0.9091	0.0000	0.0006	0.0200
CO	0.0127	0.0142		0.0000	0.0163	0.0163	0.0163		0.0163	0.0265	0.0000	0.0001	0.0016
CO2	0.3136	0.3484		0.0008	0.4019	0.4019	0.4019	0.0004	0.4019	0.0375	0.9973	0.9980	0.9763
H2O	0.2201	0.1333	1.0000	0.9985	0.0015	0.0015	0.0015	0.9913	0.0015	0.0001	0.0027	0.0012	0.0008
CH4	0.0024	0.0027		0.0000	0.0031	0.0031	0.0031	0.0000	0.0031	0.0049	0.0000	0.0000	0.0006
H2S	0.0052	0.0058		0.0001	0.0066	0.0066	0.0066	0.0002	0.0066	0.0000	0.0000	0.0000	0.0000
SO2													
Cl2													
HCl													
NH3	0.0014	0.0014		0.0006	0.0003	0.0003	0.0003	0.0082	0.0003				
COS	0.0000	0.0000		0.0000	0.0000	0.0000	0.0000		0.0000	0.0000	0.0000	0.0000	0.0000
Total	1.0000	1.0000	1.0000	1.0000	1.0000	1.0000	1.0000	1.0000	1.0000	1.0000	1.0000	1.0000	1.0000
kgmol/hr	23,440	21,082	5,817	17,626	18,276	18,276	18,276	2,806	18,276	11,165	1,097	2,798	3,119
kg/hr	458,604	416,033	104,802	317,957	365,472	365,472	365,472	50,561	365,472	56,229	48,192	122,977	134,431
Temp., C	193.0	170.0	150.0	159.0	40.6	51.7	51.7	40.6	26.7	26.7	0.1	3.6	11.7
Press., bar	74.02	73.68	78.78	75.84	73.33	73.01	72.51	73.33	72.16	83.22	1.08	3.24	10.00
Enthalpy, MJ/hr	-4,064,454	-3,520,614	-1,612,638	-4,869,742	-2,940,773	-2,933,176	-2,933,176	-798,006	-2,949,939	-202,060	-432,072	-1,102,090	-1,202,157
See Note	1	1	1	1	1	1	1	1	1	1	1	1	1

Note: 1. The reference state for thermodynamic properties is the standard enthalpy of formation of ideal gas at 25°C and 1 atm.

**Table A1.4.2 - 17: Stream Data – Air Partial Oxidation Topping Cycle - continued**

Basis: 3,274 Tonne/D (As Received) or 3,078 Tonne/D (Dry Basis) Pittsburgh No. 8 Coal

Mol Fraction	37	38	39	40	41	42	43	44	45	46	47	48
O2												
N2	0.0014	0.0435		0.0124	0.0449		0.0001	0.0784	0.0806	0.0001	0.0000	0.0000
Ar	0.0024	0.0090		0.0096	0.0092		0.0003	0.0165	0.0170	0.0000	0.0000	0.0000
H2	0.1587	0.1012		0.9090	0.1043		0.0091	0.3601	0.3701	0.0000	0.0002	0.0002
CO	0.0070	0.1106		0.0266	0.1140		0.0008	0.0227	0.0233	0.0000	0.0000	0.0000
CO2	0.3092	0.1538		0.0375	0.1585		0.9895	0.4489	0.4614	0.0080	0.0001	0.0001
H2O	0.0563	0.4664		0.0001	0.5421			0.0280	0.0010	0.9892	0.9996	0.9996
CH4	0.0030			0.0048			0.0003	0.0002	0.0002		0.0000	0.0000
H2S	0.4407	0.0773			0.0183		0.0000	0.0446	0.0459	0.0026		
SO2		0.0375			0.0080							
Cl2												
HCl												
NH3	0.0206							0.0004	0.0004	0.0000		
COS	0.0006	0.0006			0.0006		0.0000	0.0002	0.0002	0.0000		
Total	1.0000	1.0000		1.0000	1.0000		1.0000	1.0000	1.0000	1.0000	1.0000	1.0000
Sulfur, kg/hr			2,819			3,936						
kgmol/hr	297	390	44	11	378	79	7,005	218	212	174	35,663	35,663
kg/hr	9,121	9,797	2,819	53	8,681	3,936	305,438	5,659	5,553	3,181	642,494	642,494
Temp., C	48.9	176.7	176.7	14.3	287.8	25.0	40.7	26.6	26.7	28.2	144.8	221.7
Press., bar	2.07	1.87	1.87	1.30	1.30	1.01	138.93	1.24	75.95	3.45	87.92	87.23
Enthalpy, MJ/hr	-43,306	-75,309	4,728	-194	-75,593	0	-2,790,899	-40,632	-39,437	-49,756	-9,899,635	-9,655,116
See Note	1	1	1	1	1	1	1	1	1	1	1	1

Note: 1. The reference state for thermodynamic properties is the standard enthalpy of formation of ideal gas at 25°C and 1 atm.

**Table A1.4.2 - 17: Stream Data – Air Partial Oxidation Topping Cycle - continued**

Basis: 3,274 Tonne/D (As Received) or 3,078 Tonne/D (Dry Basis) Pittsburgh No. 8 Coal

Mol Fraction	49	50	50A	50B	50C	51	52	53	57	57A	57A	58	59	60
O2									0.2074	0.2074	0.1867	0.0257	0.0342	0.0342
N2		0.0089	0.0089	0.1020	0.1020				0.7728	0.7728	0.6958	0.6514	0.6498	0.6498
Ar		0.0069	0.0069	0.0048	0.0048				0.0094	0.0094	0.0085	0.0079	0.0079	0.0079
H2	0.0003	0.6500	0.6500	0.5208	0.5208									
CO		0.0189	0.0189	0.0286	0.0286									
CO2	0.0001	0.0268	0.0268	0.0128	0.0128				0.0003	0.0003	0.0003	0.0153	0.0144	0.0144
H2O	0.9996	0.2850	0.2850	0.3284	0.3284	1.0000	1.0000	1.0000	0.0101	0.0101	0.1087	0.2997	0.2937	0.2937
CH4		0.0035	0.0035	0.0026	0.0026									
H2S		0.0000	0.0000	0.0000	0.0000									
SO2														
Cl2														
HCl														
NH3														
COS		0.0000	0.0000	0.0000	0.0000									
Total	1.0000	1.0000	1.0000	1.0000	1.0000	1.0000	1.0000	1.0000	1.0000	1.0000	1.0000	1.0000	1.0000	1.0000
kgmol/hr	22	15,615	15,615	17,541	17,541	4,945	4,945	4,472	34,566	2,072	2,301	51,194	54,469	54,469
kg/hr	401	136,395	136,395	200,340	200,340	89,093	89,093	80,567	997,452	59,783	63,914	1,303,352	1,391,026	1,391,026
Temp., C	144.0	287.8	615.6	787.2	503.8	349.2	226.8	150.0	15.0	582.7	154.4	1,744.9	698.1	159.4
Press., bar	82.53	82.19	75.84	37.99	37.99	180.96	177.47	87.91	1.01	37.23	36.05	35.80	1.07	1.01
Enthalpy, MJ/hr	-6,178	-1,156,045	-984,167	-1,104,900	-1,275,000	86,953	51,595	95,548	-98,809	29,975	-52,403	-824,293	-2,982,484	-3,953,052
See Note	1	1	1	1	1	2	2	2	1	1	1	1,3	1,3	1,3

- Note:
1. The reference state for thermodynamic properties is the standard enthalpy of formation of ideal gas at 25°C and 1 atm.
  2. Enthalpy corresponds to ASME Steam Tables Basis.
  3. For NOx see Performance Summary, Table 1.

**Table A1.4.2 - 17: Stream Data – Air Partial Oxidation Topping Cycle - continued**

Basis: 3,274 Tonne/D (As Received) or 3,078 Tonne/D (Dry Basis) Pittsburgh No. 8 Coal

Mol Fraction	61	62	63	64	65	66	67	68	69	70	71	72
H2O	1.0000	1.0000	1.0000	1.0000	1.0000	1.0000	1.0000	1.0000	1.0000	1.0000	1.0000	1.0000
Total	1.0000	1.0000	1.0000	1.0000	1.0000	1.0000	1.0000	1.0000	1.0000	1.0000	1.0000	1.0000
kgmol/hr	28,064	28,064	28,064	3,331	5,129	5,129	392	3,709	1,011	6,162	5,916	12,892
kg/hr	505,587	505,587	96,685	60,002	92,400	92,400	7,062	66,824	18,221	111,008	106,577	232,257
Temp., C	23.2	137.9	134.9	148.6	349.2	263.0	153.5	225.6	229.2	349.2	356.0	371.1
Press., bar	16.82	11.44	4.57	11.75	180.96	177.47	4.57	32.00	27.51	178.88	174.07	36.89
Enthalpy, MJ/hr	50,020	293,872	54,876	37,618	152,556	78,063	19,461	64,803	51,081	183,437	273,427	732,010
See Note	1	1	1	1	1	1	1	1	1	1	1	1

Note: 1. Enthalpy corresponds to ASME Steam Tables Basis.

Mol Fraction	73	74	75	76	77	78	79
H2O	1.0000	1.0000	1.0000	1.0000	1.0000	1.0000	1.0000
Total	1.0000	1.0000	1.0000	1.0000	1.0000	1.0000	1.0000
kgmol/hr	12,263	14,146	14,146	15,576	517	16,093	11,971
kg/hr	220,927	254,838	254,838	280,608	9,316	289,924	215,663
Temp., C	526.1	655.2	428.3	654.8	214.0	30.6	15.6
Press., bar	27.51	166.51	37.64	24.82	3.17	0.04	3.40
Enthalpy, MJ/hr	741,822	946,411	837,020	1,069,574	26,959	682,756	14,199
See Note	1	1	1	1	1	1	1

Note: 1. Enthalpy corresponds to ASME Steam Tables Basis.

**Table A1.4.2 - 17: Stream Data – Air Partial Oxidation Topping Cycle - continued**

Basis: 3,274 Tonne/D (As Received) or 3,078 Tonne/D (Dry Basis) Pittsburgh No. 8 Coal

Mol Fraction	80	81	82	83
O2				
N2				
Ar				
H2				
CO				
CO2				
H2O	1.0000	1.0000	0.9981	1.0000
CH4				
H2S				
SO2				
Cl2				
HCl			0.0016	
NH3			0.0003	
COS				
Total			1.0000	
kgmol/hr	52,464	3,283	2,278	736
kg/hr	945,148	59,148	41,114	13,261
Temp., C	15.6	15.6	26.7	15.6
Press., bar	1.014	1.014	1.4	1.0
Enthalpy, MJ/hr	62,013	3,881	-620	870
See Note	1	1	2	1

Note:

1. Enthalpy corresponds to ASME Steam Tables Basis.
2. The reference state for thermodynamic properties is the standard enthalpy of formation of ideal gas at 25°C and 1 atm.

**Table A1.4.2 - 18: Plant Performance Summary – Air Partial Oxidation Topping Cycle**

<b>PERFORMANCE SUMMARY</b>	<b>Baseline Case</b>	<b>Intercooled - Air POX Gas Turbine</b>
<b>Pressure Ratio</b>	<b>24</b>	<b>70</b>
Fuel Feed Rate, ST/D (MF)	3,392	3,392
MMBtu/hr (HHV)	3,744	3,744
Fuel Feed Rate, MT/D (MF)	3,078	3,078
GJ/hr (HHV)	3,949	3,949
ASU	IP	IP
Gas Turbine Air Extraction	Yes	No
Power Generation, kWe		
Gas Turbine	318,378	401,277
Steam Turbine	157,600	141,692
Clean Syngas Expander	2,320	0
Gas Turbine Extraction Air Expander	4,745	0
Auxiliary Power Consumption, kWe	99,795	127,309
Net Plant Output, kWe	383,247	415,660
Generation Efficiency (HHV)		
Net Heat Rate, Btu/kWh	9,769	9,008
Net Heat Rate, kJ/kWh	10,305	9,501
% Fuel to Power	34.94	37.89
Estimated NO <sub>x</sub> , ppmVd (15% O <sub>2</sub> Basis)	18	117
Raw Water Makeup, m <sup>3</sup> /kWh	0.0026	0.0023

Note: The NO<sub>x</sub> emission corresponds to a 30 ms residence time in the 2<sup>nd</sup> PSR.

**Table A1.4.2 - 19: Auxiliary (In-Plant) Power Consumption Summary – Air Partial Oxidation Topping Cycle**

<b>AUXILLARY POWER CONSUMPTION</b>	<b>Baseline Case</b>	<b>Intercooled - Air POX Gas</b>
<b>Pressure Ratio</b>	<b>24</b>	<b>70</b>
ASU	IP	IP
Gas Turbine Air Extraction	Yes	No
	kWe	kWe
Coal Handling	401	401
Coal Milling	802	802
Coal Slurry Pumps	274	314
Slag Handling and Dewatering	155	155
Miscellaneous Syngas Plant Equipment	380	595
Air Separation Unit Air Compressors	14,778	37,086
Air Separation Auxiliaries	1,290	1,290
Oxygen Compressor	12,522	12,991
Nitrogen Compressor	22,007	25,236
CO <sub>2</sub> Compressor	19,368	19,367
Tail Gas Recycle Compressor	998	1,057
Boiler Feedwater Pumps	4,047	3,864
Cooling Tower and Pumps	7,242	6,002
Steam Condensate Pump	42	20
Selexol Acid Gas Removal	11,788	12,357
Syngas Compression		1,963
Syngas Humidification	214	183
Claus Plant Auxilliaries	100	100
Gas Turbine Auxiliaries	517	517
Steam Turbine Auxiliaries	517	517
General Makeup and Demineralized Water	322	315
Miscellaneous Balance-of-Plant and Lighting	1,000	1,000
Transformer Losses	1,031	1,176
<b>Total Auxiliary Power Consumption</b>	<b>99,795</b>	<b>127,309</b>
Raw Water Makeup, m <sup>3</sup> /kWh	0.0026	0.0023

**Table A1.4.2 - 20: Main Features of the Power Cycle – Air Partial Oxidation Topping Cycle**

	Baseline Case		Air POX Gas Turbine	
<b>Gas Turbine</b>				
Pressure Ratio	24		70 (Overall)	37 (After Oxidizing Combustor)
ASU	IP	HP	IP	
Air Extraction	Yes		No	
Power Output, kW	318,378	318,323	21,237	380,040
Rotor Inlet Temperature	1392°C (2538°F)		927°C (1700°F) / 1699°C (3090°F)	
Combustor			POx	Ox
Inlet Air Temperature	487°C (908°F)		514°C (958°F)	583°C (1081°F)
Discharge Temperature	1433°C (2611°F)		927°C (1700°F)	1954°C (3550°F)
Inlet Air Flow, kg/s	421.8 kg/s (930 lb/s)		17.8 kg/s (39.2 lb/s)	239.3 kg/s (527.5 lb/s)
Inlet Air O2 Concentration, Vol %	20.74		18.70	20.74
Discharge O2 Concentration, Vol %	7.8		0	2.96
Adiabatic Flame Temperature	1891°C (3435°F)			1880°C (3416°F)
Estimated NOx (15% O2 Dry Basis)				
2nd PSR Residence Time = 30 ms <sup>1</sup>	18		117	
2nd PSR Residence Time = 5 ms <sup>2</sup>	17		32	
Exhaust Temperature	582°C (1079°F)		698°C (1289°F)	
Air Extracted, % of Inlet Air	14		0	
<b>Steam Cycle</b>				
Power Output, kW	157,600	159,033	141,692	
HP Steam Pressure	166.5 bara (2415 psia)		166.5 bara (2415 psia)	
Superheat & Reheat Temperatures	538°C (1000°F)		655°C (1211°F)	
<b>Overall Plant Performance</b>				
Fuel Feed Rate, MT/D (MF)	3,078		3,078	
GJ/hr (HHV)	3,949		3,949	
Net Plant Output, kW	383,247	385,753	415,660	
Net Heat Rate, Btu/kWh	9,769	9,706	9,008	
kJ/kWh	10,305	10,238	9,501	
% Fuel to Power	34.94	35.16	37.89	
Raw Water Makeup, m3/kWh	0.0026	0.0026	0.0023	

1. NOx values are predicted using a Chemkin 2 PSR model with a 0.44 millisecond residence time in the first reactor and a 30 millisecond residence time in the second reactor.
2. NOx values are predicted using a Chemkin 2 PSR model with a 0.44 millisecond residence time in the first reactor and a 5 millisecond residence time in the second reactor.

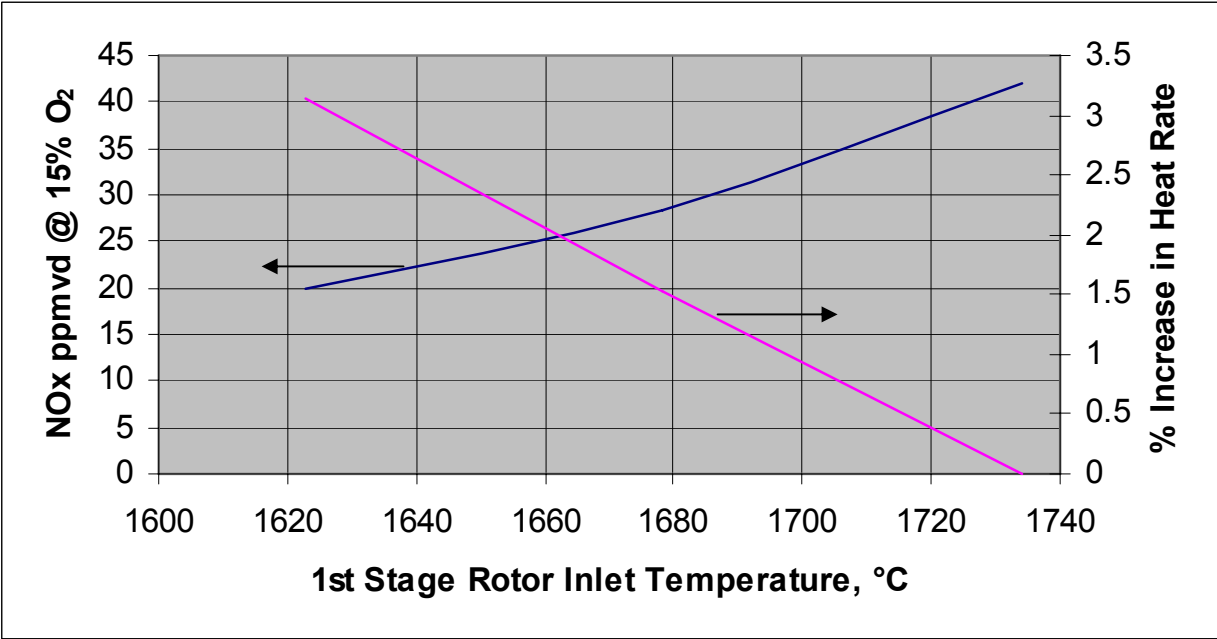


**Figure A1.4.2 - 35: Effect of Firing Temperature on Net Plant Heat rate and NOx Emission (using Short Combustor)**

## TASK 2.1 - EVALUATION OF IMPACT OF RAMGEN COMPRESSION TECHNOLOGY ON IGCC PLANT PERFORMANCE

### SUMMARY

The DOE has established high efficiency objectives for IGCC plants to be introduced in the future carbon constrained world as part of its portfolio of technologies aimed at energy independence.

Ramgen Power Systems is developing novel shock compression and combustion technologies that may favorably impact plant efficiency and cost, but has been limited in its ability to develop a comprehensive assessment of their impact on overall plant design. Their technologies that have a potential for application in an IGCC are:

- Shock compression which has the potential to achieve very high compression ratio and very high efficiency, simultaneously.
- Advanced vortex combustion which is a unique lean pre-mix, dry low-NO<sub>x</sub> design capable of handling high velocities and therefore, the fast burning hydrogen-rich fuels produced and used within the IGCC processes (not part of the current study).

A thermodynamic assessment of the Ramgen turbomachinery technology has been completed. Based on the results of this study, the following conclusions may be drawn (subject to verification of the turbomachinery efficiencies as quoted by Ramgen by test work):

- The Ramgen LP and IP CO<sub>2</sub> compressors with their higher efficiencies can save about 0.5 MW in in-plant electric power consumption for a 380 MW IGCC near zero emission power plant with 90% CO<sub>2</sub> capture.
- Among the various practical heat recovery options evaluated for the Ramgen HP CO<sub>2</sub> non-intercooled compressor, use of a LiBr absorption refrigeration system provides the most efficient route for conversion of this low temperature heat. The chilled water produced by the absorption refrigeration unit is utilized for chilling the Selexol solvent in the AGR unit, thereby reducing the mechanical refrigeration load. The net IGCC plant output is reduced, however, even with the reduction in the mechanical refrigeration load and with a higher HP compressor efficiency.
- The Ramgen HP CO<sub>2</sub> compressor with intercooling provides greater advantage. The net result of utilizing this Ramgen compressor which has a significantly higher efficiency than that of the Baseline Case compressor is that the plant output is increased by 1.1 MW over the Baseline Case. This increment is only slightly lower (0.3 MW) than that obtained by utilizing the Ramgen high efficiency non-intercooled HP compressor with the conversion of the exhaust heat by a hypothetical working fluid (with variable evaporation and condensing temperatures) which represents an upper limit for this heat conversion process. Thus, from an overall plant thermal efficiency standpoint, the Ramgen high efficiency intercooled compressor technology is more promising. The net

increase in power output over the Baseline Case of utilizing the Ramgen LP, IP and intercooled HP compressors is 1.61 MW for this 380 MW IGCC plant.

- Next, by applying the Ramgen technology to other major turbomachinery in the IGCC plant in addition to the CO<sub>2</sub> compressors (i.e., to the gas turbine extraction air expander, the ASU air and nitrogen compressors), the net power output over the Baseline Case is increased significantly, by as much as 6 MW for this 380 MW IGCC plant.

## APPROACH

This section presents a thermodynamic assessment of the Ramgen technology for pressurizing the captured CO<sub>2</sub> to sequestration pressure in a coal based near zero emission IGCC power plant. The study also includes an assessment of the application of this technology to the other major turbomachinery within the plant. The main features of this IGCC plant are:

- Air Separation Unit (ASU) consisting of an Low Pressure (LP) and an Elevated Pressure (EP) train and High Pressure (HP) nitrogen return to the gas turbine
- General Electric (GE) type high pressure oxygen blown entrained bed gasifier
- Sour Shifting of the scrubbed syngas
- Selexol Acid Gas Removal (AGR) process for desulfurization and CO<sub>2</sub> capture
- CO<sub>2</sub> compression, dehydration and pumping to sequestration pressure
- Syngas humidification
- “H class” steam cooled gas turbine based combined cycle with air extraction which provides a portion of the air required by the ASU.

A Baseline Case utilizing the current state-of-the-art compression technology has been defined under Tasks 1.2 and 1.3 of this contract. The cases incorporating the advanced turbomachinery technology are compared to this Baseline Case. The plant consumes 3,078 Tonne/D or 3,392 ST/D of Pittsburgh No. 8 coal and generates about 380 MW of electric power on a net basis while capturing 90% of the carbon in the raw syngas as CO<sub>2</sub>.

Figure A2.1-1 depicts the configuration of the CO<sub>2</sub> compression / dehydration system for the Baseline Case while the corresponding stream data are presented in Table A2.1-1. As shown, this unit receives CO<sub>2</sub> product streams from the Acid Gas Removal unit at three different pressures:

1. LP CO<sub>2</sub> at 1.08 bar
2. Intermediate Pressure (IP) CO<sub>2</sub> at 3.24 bar
3. HP CO<sub>2</sub> at 10 bar.

The LP CO<sub>2</sub> stream after compression to the IP pressure in the “1<sup>st</sup> Stage or LP Compressor” (and aftercooling) is combined with the IP CO<sub>2</sub> stream. Next the IP CO<sub>2</sub> stream after compression to the HP pressure in the “2<sup>nd</sup> Stage or IP Compressor” (and aftercooling) is combined with the HP CO<sub>2</sub> stream. The HP CO<sub>2</sub> is further compressed in the “3<sup>rd</sup> Stage or HP Compressor” to a pressure of 83 bar which is above the mixture critical pressure, aftercooled,

dehydrated utilizing glycerol as the drying agent and then pumped as a supercritical fluid to the final pressure of 139 bar. Inter-stage cooling is effected with cooling water. Any condensate collected in the compression process is routed to the solvent flash drum in the AGR Unit.

Options evaluated in this advanced compression study include compression with intercooling, and without intercooling with various options for recovery of the low temperature heat contained in the compressed stream.

Figure A2.1 – 2 depicts the ASU along with the gas turbine extraction air expander system for the Baseline Case. The corresponding stream data are presented in Table A2.1 - 2.

## **RESULTS AND DISCUSSION**

### **Ramgen Turbomachinery**

Tables A2.1- 3 and 4 summarize the CO<sub>2</sub> compressor characteristics for the LP, IP and HP compression along with the heat recovery options from the HP compressor discharge while utilizing the Ramgen technology. The characteristics of the current state-of-the-art technology Baseline Case are also included in these tables for comparison purposes.

### **LP and IP CO<sub>2</sub> Compressors**

Both the Baseline and the Ramgen cases utilize adiabatic LP and IP compression without intercooling since the pressure ratios are low, the pressure ratios being set by the pressure of the IP and HP CO<sub>2</sub> streams being added from the AGR. The exhaust temperature from these compressors is thus too low to justify heat recovery and the heat is rejected to cooling water. The Ramgen LP and IP compressors with their higher efficiencies as compared to the Baseline compressors can save about 0.5 MW in in-plant electric power consumption for this 380 MW IGCC plant.

### **Non-Intercooled HP CO<sub>2</sub> Compressor**

Figure A2.1 – 3 depicts the CO<sub>2</sub> compression / dehydration unit for the cases with the non-intercooled HP CO<sub>2</sub> compressor with various heat recovery options downstream of this compressor. The stream data are the same as those presented previously for the Baseline Case in Table A2.1 - 1.

The following summarizes the description of each of the heat recovery options studied for this non-intercooled HP compressor. The temperature of the stream leaving the HP compressor is 211°C or 412°F. Table A2.1- 5 summarizes the resulting thermal performance of the IGCC plant for these various cases. As can be observed from this data, among the various practical heat recovery options evaluated for the Ramgen HP CO<sub>2</sub> non-intercooled compressor, use of a LiBr absorption refrigeration system provides the most efficient route for conversion of this low temperature heat. The chilled water produced by the absorption refrigeration unit is utilized for chilling the Selexol solvent in the AGR unit, thereby reducing the mechanical refrigeration load.

The net IGCC plant output is reduced as compared to the Baseline Case, however, despite the reduction in the mechanical refrigeration load and higher HP compressor efficiency.

1. *Aftercooler Heat Recovered to Generate LP Steam*

LP saturated steam at a pressure of 5.95 bar or 86 psia is generated against the hot CO<sub>2</sub> stream leaving the HP compressor and is supplied to the steam turbine after superheating in the HRSG. The net result on plant performance as compared to the Baseline Case is presented in the following:

- a. Net Increase in Steam Cycle Power Output = 1.16 MW
- b. Increase in gasification Island Aux Power (primarily due to increased cooling water duty) = 0.1 MW
- c. Increase in HP CO<sub>2</sub> Compressor Power = 1.9 MW
- d. Net Power =  $1.9 - 1.16 + 0.1 = 0.84$  MW decrease over Baseline Case.

2. *Aftercooler Heat Recovered to provide a portion of the Syngas Humidifier Heat Requirement*

MP steam generation in Low Temperature Gas Cooling (LTGC) unit is increased by reducing humidifier circulating water heater duty in LTGC. The additional duty required for the humidifier is obtained from the compressor discharge. This is accomplished by dividing the humidifier circulating water into two circuits. The first recovers heat in the LTGC section of the plant as in the Baseline Case while the second circuit recovers heat from the CO<sub>2</sub> leaving the HP CO<sub>2</sub> compressor. The circulating water in this second circuit is heated to a higher temperature (hot end approach temperature of 11°C or 20°F in the aftercooler) than the water in the first circuit such that the temperature of the water in the first circuit is lowered and MP steam generation in LTGC is maximized. The temperature of the water after the two water circuits are combined before entering the humidifier is held the same as the temperature of the heated circulating water in the Baseline Case. The water temperature of the circulating water in the first circuit is lowered from 185°C or 365°F to 183°C or 362°F which allows the steam production in the upstream LTGC MP Boiler to be increased by lowering the temperature of the syngas leaving the MP Boiler by 1.7°C or 3°F while maintaining a 11°C or 20°F hot end pinch in the LTGC Humidifier Circulating Water Heater (a 1.7°C decrease in gas temperature has a significant effect on the amount of heat duty since the syngas being cooled is saturated with water vapor). The net result on plant performance as compared to the Baseline Case is presented in the following:

- a. Net increase in Steam Cycle Output = 0.87 MW
- b. Increase in Gasification Island Aux Power (primarily due to increased cooling water duty) = 0.1 MW
- c. Increase in HP CO<sub>2</sub> Compressor Power = 1.9 MW
- d. Net Power =  $1.9 - 0.87 + 0.1 = 1.13$  MW decrease over Baseline Case.

3. *Aftercooler Heat for Syngas Humidifier and LiBr Refrigeration Unit*

After recovering the higher temperature heat from the CO<sub>2</sub> stream leaving the HP compressor (similar to the previous case), additional heat is recovered for operating a LiBr absorption refrigeration unit to produce chilled water at 7°C or 44.6°F. The chilled water is used for pre-chilling the Selexol solvent in the AGR unit to reduce its

mechanical refrigeration load. The net result on plant performance as compared to the Baseline Case is presented in the following:

- a. Net Increase in Steam Cycle Output = 0.87 MW
- b. Heat available (by cooling the gas down to 85°C or 185°F after recovering heat for the humidifier) = 22.10 GJ/hr or 20.954 MMBtu/hr
- c. Corresponding LiBr Refrigeration Duty (with an Efficiency of 67.02%<sup>q</sup>) = (22.10 GJ/hr or 20.954 MMBtu/hr) \* 0.6702 = 14.81 GJ/hr or 14.04 MM Btu/hr
  - i. Maximum Chilled Water Refrigeration that may be utilized in the Selexol Unit = 29.00 GJ/hr or 27.49 MMBtu/hr
  - ii. Thus, the entire Chilled Water may be utilized in the Selexol Unit
  - iii. Total Selexol Solvent Chilling Duty required = 72.79 GJ/hr or 69.01MMBtu/hr
  - iv. Corresponding Power required by Mechanical Refrigeration (for all the Selexol Solvent Chilling Duty) = 4.613 MW
- d. Decrease in Selexol Refrigeration Unit Power by supplementing with Chilled Water = (14.81 GJ/hr or 14.04 MMBtu/hr) / (72.79 GJ/hr or 69.01MMBtu/hr) \* 4.613 MW = 0.94 MW
- e. Increase in Balance of Plant Aux Power (primarily due to increased cooling water duty) = 0.1 MW
- f. Increase in HP CO<sub>2</sub> Compressor Power = 1.9 MW
- g. Net Power = (1.9 - 0.87 - 0.94 + 0.10) MW = 0.19 MW decrease over Baseline Case.

#### 4. *Aftercooler Heat for LiBr Refrigeration Unit Only*

Heat is recovered from the hot CO<sub>2</sub> stream leaving the compressor and is utilized for operating a LiBr absorption refrigeration unit to produce chilled water. The chilled water in addition to being used for pre-chilling the solvent in the Selexol unit to reduce refrigeration load is utilized in the ASU compressor intercoolers to reduce compression power. The net result on plant performance as compared to the Baseline Case is presented in the following:

- a. Heat Available for the Absorption Refrigeration Unit (by cooling the gas down to 85°C or 185°F) = 46.90 GJ/hr or 44.46 MMBtu/hr
- b. Corresponding LiBr Refrigeration Duty (with an Efficiency of 67.02%) = (46.90 GJ/hr or 44.46 MMBtu/hr) \* 0.6702 = 31.43 GJ/hr or 29.80 MMBtu/hr
  - i. Maximum Chilled Water Refrigeration that may be utilized in the Selexol Unit = 29.00 GJ/hr or 27.49 MMBtu/hr
  - ii. Since all of the Chilled Water cannot be utilized in the AGR unit, the excess Chilled Water is utilized in the ASU compressor intercoolers
- c. Decrease in Selexol Refrigeration Unit Power = (29.00 GJ/hr or 27.49 MMBtu/hr) / (72.79 GJ/hr or 69.01 MMBtu/hr) \* 4.613 MW = 1.84 MW
- d. Remaining LiBr Refrigeration Duty that may be utilized in the ASU = (31.43 GJ/hr or 29.8 MMBtu/hr) – (29.00 GJ/hr or 27.49 MMBtu/hr) = 2.43 GJ/hr or 2.31 MMBtu/hr
- e. Decrease in ASU Compressor Power = 0.01 MW

---

<sup>q</sup> Efficiency defined by the ratio of the chilling duty produced by the refrigeration unit and the heat duty supplied to or required by the refrigeration unit.

- f. Increase in HP CO<sub>2</sub> Compressor Power = 1.9 MW
- g. Increase in Balance of Plant Aux Power (primarily due to increased cooling water duty) = 0.1 MW
- h. Net Power = (1.9 - 1.84 - 0.01 + 0.10) MW = 0.15 MW decrease over Baseline Case.

5. *Aftercooler Heat for Ammonia Absorption Refrigeration Unit*

Heat is recovered from the hot CO<sub>2</sub> stream leaving the compressor and is utilized for operating an NH<sub>3</sub> absorption refrigeration unit to replace a portion of the AGR unit refrigeration load. The net result on plant performance as compared to the Baseline Case is presented in the following:

- a. Heat Available for the Absorption Refrigeration Unit (by cooling the gas down to 118°C or 244°F) = 34.62 GJ/hr or 32.82 MMBtu/hr
- b. Corresponding Refrigeration Duty (with an Efficiency of 48.46%) = (34.62 GJ/hr or 32.82 MMBtu/hr) \* 0.4846 = 16.78 GJ/hr or 15.9 MM Btu/hr
  - i. Maximum Refrigeration that may be utilized in the Selexol Unit = 72.79 GJ/hr or 69.01 MMBtu/hr
  - ii. Thus, the entire Absorption Refrigeration Duty may be utilized in the AGR unit
- c. Decrease in Selexol Refrigeration Unit Power = (16.78 GJ/hr or 15.9 MMBtu/hr) / (72.79 GJ/hr or 69.01MMBtu/hr)\* 4.613 MW = 1.06 MW
- d. Increase in Balance of Plant Aux Power (primarily due to increased cooling water duty) = 0.1 MW
- e. Increase in HP CO<sub>2</sub> Compressor Power = 1.9 MW
- f. Net Power = (1.9 – 1.06 + 0.1) MW = 0.94 MW decrease over Baseline Case.

6. *Aftercooler Heat for a Low Temperature Rankine Cycle*

Heat is recovered from the hot CO<sub>2</sub> stream leaving the compressor to preheat and evaporate a low boiling point fluid such as an organic fluid at pressure and then expanded in a turbine. Exhaust from the turbine is condensed against cooling water and the liquid is provided to the preheater (economizer) followed by the evaporator located downstream of CO<sub>2</sub> compressor to complete the cycle. The analysis is performed assuming an ideal Rankine cycle (to determine if there is any merit in this approach) and then an efficiency of 90% is applied to the cycle to obtain the cycle power output. The evaporation temperature of the working fluid is varied while maintaining a constant 11°C or 20°F temperature difference between the heat source (CO<sub>2</sub> stream) and the working fluid evaporation temperature. The quantity of heat thus recovered increases as the evaporation temperature is decreased. On the other hand, the thermodynamic efficiency of converting the recovered heat to power is reduced in accordance with the Carnot Cycle efficiency. A 5.6°C or 10°F difference is maintained between the cooling water return temperature and the condensing temperature of the working fluid. It is assumed that the entire heat duty is utilized for evaporation, i.e., superheat duty is insignificant, and that sufficient low temperature heat is available downstream for preheating of the condensate. The net result on plant performance as compared to the Baseline Case is described in the following:

- a. Figure A2.1- 4 shows the Power Generated as a function of Temperature of the CO<sub>2</sub> stream leaving the Evaporator, T<sub>g</sub>
  - b. Maximum amount of Power Generated (at T<sub>g</sub> = 116°C or 240°F) = 1.7 MW
  - c. Increase in HP CO<sub>2</sub> Compressor Power = 1.9 MW
  - d. Increase in Balance of Plant Aux Power (primarily due to increased cooling water duty) = 0.1 MW
  - e. Net Power = 1.9 - 1.7 + 0.1 = 0.3 MW decrease over Baseline Case.
7. *Aftercooler Heat to Evaporate Hypothetical Working Fluid with Variable Evaporation and Condensing Temperatures*
- This case is developed to establish the upper limit for conversion of the heat contained in the CO<sub>2</sub> stream leaving the compressor. The hypothetical fluid is assumed to have a variable boiling point such that the temperature difference between the CO<sub>2</sub> stream and the evaporating fluid remains constant. This fluid is also assumed to condense at a variable temperature such that the temperature difference between the cooling water and the condensing fluid remains constant. In this manner, the irreversibility in heat transfer is kept to a minimum. Again an efficiency of 90% is applied to the cycle to obtain the cycle power output. The temperature of the working fluid is maintained a constant 11°C or 20°F below the heat source (CO<sub>2</sub> stream) during the entire evaporation process and 5.6°C or 10°F above the cooling water temperature during the entire condensing process. The amount of heat recovered from the CO<sub>2</sub> stream is varied. The quantity of heat thus recovered increases as this temperature is decreased. On the other hand, the thermodynamic efficiency of converting the recovered heat to power is reduced in accordance with the Carnot Cycle efficiency. The net result on plant performance as compared to the Baseline Case is presented in the following:
- a. Figure A2.1- 5 shows that the Power Generated increases as the Temperature of the CO<sub>2</sub> stream leaving the Evaporator decreases, T<sub>g</sub>
  - b. At T<sub>g</sub> of 71°C or 160°F which is similar to the Baseline Case Compressor Exit Temperature (cannot go lower; otherwise heat recovery for a similar cycle can be implemented in the Baseline Case), Power Generated = 3.42 MW
  - c. Increase in HP CO<sub>2</sub> Compressor Power = 1.9 MW
  - d. Increase in Balance of Plant Aux Power (primarily due to increased cooling water duty) = 0.1 MW
  - e. Net Power = (3.42 – 1.9 - 0.1) MW = 1.42 MW increase over Baseline Case.

### **Intercooled HP CO<sub>2</sub> Compressor**

The following summarizes the description of the intercooled HP compressor. The resulting thermal performance of this IGCC plant is also summarized in Table A2.1- 5.

8. *Intercooled HP CO<sub>2</sub> Compressor*
- This configuration is similar to the Baseline Case with two intercoolers but the CO<sub>2</sub> compressor efficiencies as provided by Ramgen are significantly higher than those for the Baseline Case. The heat of compression being of low quality is all rejected to cooling water as is done in the Baseline Case. The net result on plant performance as compared to the Baseline Case is presented in the following:
- a. Decrease in HP CO<sub>2</sub> Compressor Power = 1.1 MW

- b. Decrease in Balance of Plant Aux Power (due to reduced cooling water duty) = 0.01 MW
- c. Net Power Generated =  $1.1 + 0.01 = 1.11$  MW increase over Baseline Case.

### **Application of Ramgen Technology to Other Turbomachinery**

The Ramgen technology is applied to the gas turbine extraction air expander and then also to the EP and LP air compressors and the nitrogen compressor in the ASU. Figure A2.1 - 6 depicts the ASU along with the gas turbine extraction air expander system for case utilizing the Ramgen high efficiency gas turbine extraction air expander and the air compressors. The stream data are presented previously for the Baseline Case in Table A2.1 - 8.

Tables A2.1- 6 and 7 summarize the characteristics for these turbomachinery with the Ramgen technology. These plants also include the Ramgen high efficiency LP, IP and HP (intercooled) compressors.

#### *1. High Efficiency Gas Turbine Extraction Air Expander (and Intercooled HP CO<sub>2</sub> Compressor)*

This case is similar to the Baseline Case in configuration. The CO<sub>2</sub> compressor efficiency is significantly higher than that in the Baseline Case. The heat of compression from CO<sub>2</sub> compressor being of low quality is all rejected to cooling water as is done in the Baseline Case. The Ramgen design ASU air expander with an isentropic efficiency of 95% based on data provided by Ramgen is significantly higher than that in the Baseline Case and consequently its power output as seen in Table A2.1-6, is significantly higher than that in the Baseline Case. The LP steam generation downstream of this expander is reduced since the temperature of the air leaving the expander is reduced due to the higher expander efficiency. Consequently, the steam turbine output is decreased but only slightly. The net result on plant performance as compared to the Baseline Case is presented in the following:

- a. Increase in Power recovered in Air Expander = 1.1 MW
- b. Decrease in steam turbine output due to lower LP steam produced in ASU WHB = 0.3 MW
- c. Net Decrease in CO<sub>2</sub> Compressor Power (LP + IP + HP) = 1.6 MW
- d. Decrease in Balance of Plant Aux Power (due to reduced cooling water duty) = 0.03 MW
- e. Net Power Generated =  $1.1 - 0.3 + 1.6 + 0.03 = 2.43$  MW increase over Baseline Case.

#### *2. High Efficiency ASU Compressors (and High Efficiency Gas Turbine Extraction Air Expander and Intercooled HP CO<sub>2</sub> Compressor)*

This case is similar to the above case, i.e., the configuration is again similar to the Baseline Case. The CO<sub>2</sub> compressor and gas turbine extraction air expander efficiencies are significantly higher than those in the Baseline Case. The heat of compression from CO<sub>2</sub> compressor being of low quality is all rejected to cooling water as is done in the Baseline Case. The Ramgen design ASU air expander efficiency with an isentropic efficiency of 95% based on data provided by Ramgen is significantly higher than that in

the Baseline Case, and consequently its power output is higher than that in the Baseline Case. The LP steam generation downstream of this expander is reduced since the temperature of the air leaving the expander is reduced due to the higher expander efficiency. The configuration and efficiencies as proposed by Ramgen are used for the EP Air Compressor, LP Air Compressor, and Nitrogen Compressor in the ASU. Waste heat is recovered from the air leaving the EP Air and LP Air compressors. As shown in Table A2.1- 7, lower number of intercoolers are used in the Ramgen design for the EP and LP Air Compressors and the Nitrogen Compressor in the ASU than those used in the Baseline Case. The recovered waste heat from the air compressors is used in LiBr absorption refrigeration units to produced chilling of the Selexol solvent in the AGR unit which replaces a portion of the mechanical refrigeration required. The higher exhaust temperature of the nitrogen stream leaving the nitrogen compressor is taken advantage of by returning the Boiler Feed Water (BFW) used in preheating the nitrogen to the Heat Recovery Steam generator (HRSG) in the power block at a higher temperature. In this manner the LP steam generation in the HRSG is increased. The net result on plant performance as compared to the Baseline Case is presented in the following:

- a. Increase in Power recovered in Air Expander = 1.1 MW
- b. Heat Available (by cooling the EP and LP ASU compressor discharge air streams down to 85°C or 185°F) = 26.07 GJ/hr or 24.72 MMBtu/hr
- c. Corresponding Chilled Water Refrigeration Duty (with an Efficiency of 67.02%) = 26.15 GJ/hr or 24.79 MMBtu/hr \* 0.6702 = 17.47 GJ/hr or 16.57 MMBtu/hr
  - i. Maximum Chilled Water Refrigeration that may be utilized in the Selexol Unit = 29.00 GJ/hr or 27.49 MMBtu/hr
  - ii. Thus, the entire Chilled Water may be utilized in the Selexol Unit
- d. Decrease in AGR Refrigeration unit Power = [(17.47 GJ/hr/ 72.79 GJ/hr) or (16.57 MMBtu/hr/69.01 MMBtu/hr)] \* 4.613 MW = 1.1 MW
- e. Increase in EP ASU Compressor Power = 0.2 MW
- f. Increase in LP ASU Compressor Power = 0.4 MW
- g. Decrease in Nitrogen Compressor Power = 2.2 MW
- h. Net Decrease in CO<sub>2</sub> Compressor Power (LP + IP + HP) = 1.6 MW
- i. Decrease in Balance of Plant Aux Power (primarily due to reduced cooling water duty) = 0.02 MW
- j. Increase in Steam Turbine Output = 0.5 MW
- k. Net Power = (1.1 + 1.1 - 0.2 - 0.4 + 2.2 + 1.6 + 0.02 + 0.5) MW = 5.92 MW increase over Baseline Case.

## CONCLUSIONS

Based on the results of this study, the following conclusions may be drawn (subject to verification of the turbomachinery efficiencies as quoted by Ramgen by test work):

- The Ramgen LP and IP CO<sub>2</sub> compressors with their higher efficiencies can save about 0.5 MW in in-plant electric power consumption for this 380 MW IGCC near zero emission power plant.

- Among the various practical heat recovery options evaluated (i.e., not considering the hypothetical working fluid with variable evaporation and condensing temperatures) for the Ramgen HP non-intercooled compressor case, use of a LiBr absorption refrigeration system provides the most efficient route for conversion of this low temperature heat. The chilled water produced by the absorption refrigeration unit is utilized for chilling the Selexol solvent in the AGR unit, thereby reducing the mechanical refrigeration load. The net impact on the IGCC plant output, however, even with the reduction in the mechanical refrigeration load and a higher HP compressor efficiency is that the output is reduced.
- The Ramgen HP compressor with intercooling provides the greatest advantage. The net result of utilizing this higher efficiency compressor is that the plant output is increased by 1.1 MW over the Baseline Case. This increment is only slightly lower (0.3 MW) than that obtained by utilizing the Ramgen high efficiency non-intercooled HP compressor with the conversion of the exhaust heat by a hypothetical working fluid (with variable evaporation and condensing temperatures) which represents an upper limit for this heat conversion process. Thus, from an overall plant thermal efficiency standpoint, the Ramgen high efficiency intercooled compressor technology is more promising. The net increase in power output over the Baseline Case of utilizing the Ramgen LP, IP and intercooled HP compressors is 1.61 MW for this 380 MW IGCC plant.
- Next, by applying the Ramgen technology to the gas turbine extraction air expander, the ASU air and nitrogen compressors in addition to the CO<sub>2</sub> compressors, the net power output over the Baseline Case is increased significantly, by as much as 5.92 MW for this 380 MW IGCC plant. Note that it was possible to utilize the entire amount of chilled water produced (via the LiBr refrigeration unit) by recovering the heat of compression of the LP and EP ASU compressors in the Selexol unit whereas in the case of the non-intercooled CO<sub>2</sub> compressor, the amount of chilled water produced utilizing its heat of compression was in excess of what could be utilized in the Selexol unit. This resulted in utilizing the excess chilled water less efficiently in the ASU air compressor intercoolers.



**Table A2.1 - 1: Stream Data – Baseline Case CO<sub>2</sub> Compression**

Basis: 3,274 Tonne/D (As Received) or 3,078 Tonne/D (Dry Basis) Pittsburgh No. 8 Coal

Mol Fraction	34	35	36	43
N2	0.000000	0.000003	0.000165	0.000075
Ar	0.000001	0.000028	0.000542	0.000253
H2	0.000011	0.000585	0.019960	0.009123
CO	0.000006	0.000139	0.001588	0.000763
CO2	0.997256	0.997967	0.976307	0.989497
H2O	0.002665	0.001241	0.000843	
CH4	0.000001	0.000008	0.000580	0.000262
H2S	0.000045	0.000019	0.000009	0.000019
COS	0.000016	0.000009	0.000005	0.000008
Total	1.000000	1.000000	1.000000	1.000000
kg mol/hr	1096.77	2798.08	3118.81	7004.64
kg/hr	48191.52	122975.82	134429.65	305434.42
Temp., C	0.08	3.59	11.73	31.76
Press., bar	1.08	3.24	10.00	138.93
Enthalpy, MJ/hr	-432069.57	-1102082.67	-1202147.07	-2798852.46
See Note	1	1	1	1

Note:

1. The reference state for thermodynamic properties is the standard enthalpy of formation of ideal gas at 25°C and 1 atm.

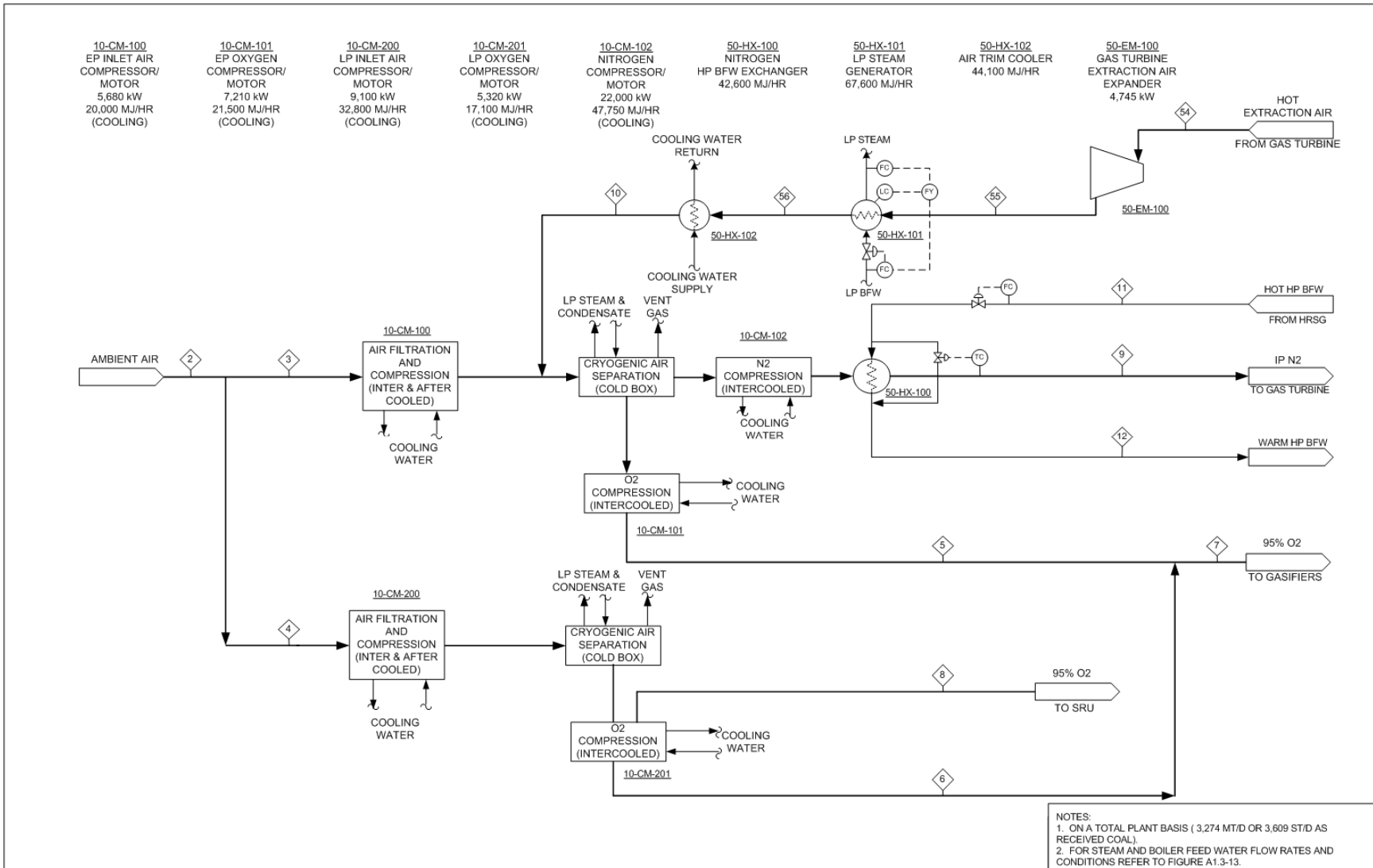


**Figure A2.1 - 2: Process Flow Diagram – Baseline Case ASU and Gas Turbine Air Extraction**



**Table A2.1 - 2: Stream Data – Baseline Case ASU and Gas Turbine Air Extraction**

Basis: 3,274 Tonne/D (As Received) or 3,078 Tonne/D (Dry Basis) Pittsburgh No. 8 Coal

Mol Fraction	2	3	4	5	6	7	8	9	10	11	12
O2	0.2077	0.2077	0.2077	0.9504	0.9500	0.9502	0.9500	0.0062	0.2090		
N2	0.7722	0.7722	0.7722	0.0230	0.0176	0.0212	0.0176	0.9891	0.7788		
Ar	0.0094	0.0094	0.0094	0.0266	0.0324	0.0286	0.0324	0.0047	0.0093		
H2											
CO											
CO2	0.0003	0.0003	0.0003						0.0003		
H2O	0.0104	0.0104	0.0104						0.0026	1.0000	1.0000
Total	1.0000	1.0000	1.0000	1.0000	1.0000	1.0000	1.0000	1.0000	1.0000	1.0000	1.0000
kgmol/hr (w/o Solids)	8,734	2,311	6,423	2,426	1,291	3,717	82	8,780	9,009	1,754	1,754
kg/hr (w/o Solids)	252,016	66,689	185,327	77,921	41,563	119,484	2,635	246,663	260,681	31,608	31,608
Temp., C	15.0	15.0	15.0	91.5	80.6	87.7	19.4	287.8	26.7	349.1	140.6
Press., bar	1.01	1.01	1.01	82.94	82.94	82.94	3.04	35.09	15.34	180.96	177.47
Enthalpy, MJ/hr	-25,616	-6,778	-18,838	3,567	1,435	5,003	-16	67,738	-7,311	52,169	19,084
See Note	1	1	1	1	1	1	1	1	1	2	2

Notes:

1. The reference state for thermodynamic properties is the standard enthalpy of formation of ideal gas at 25°C and 1 atm.
2. Enthalpy corresponds to ASME Steam Tables Basis.

**Table A2.1 – 2 : Stream Data – Baseline Case ASU and Gas Turbine Air Extraction (Continued)**

Basis: 3,274 Tonne/D (As Received) or 3,078 Tonne/D (Dry Basis) Pittsburgh No. 8 Coal

Mol Fraction	54	55	56
O2	0.2074	0.2074	0.2074
N2	0.7728	0.7728	0.7728
Ar	0.0092	0.0092	0.0092
CO2	0.0003	0.0003	0.0003
H2O	0.0103	0.0103	0.0103
Total	1.0000	1.0000	1.0000
kgmol/hr	9,079	9,079	9,079
kg/hr	261,950	261,950	261,950
Temp., C	483.9	407.0	177.8
Press., bar	24.13	15.75	15.55
Enthalpy, MJ/hr	102,174	80,160	16,660
See Note	1	1	1

Note:

1. The reference state for thermodynamic properties is the standard enthalpy of formation of ideal gas at 25°C and 1 atm.

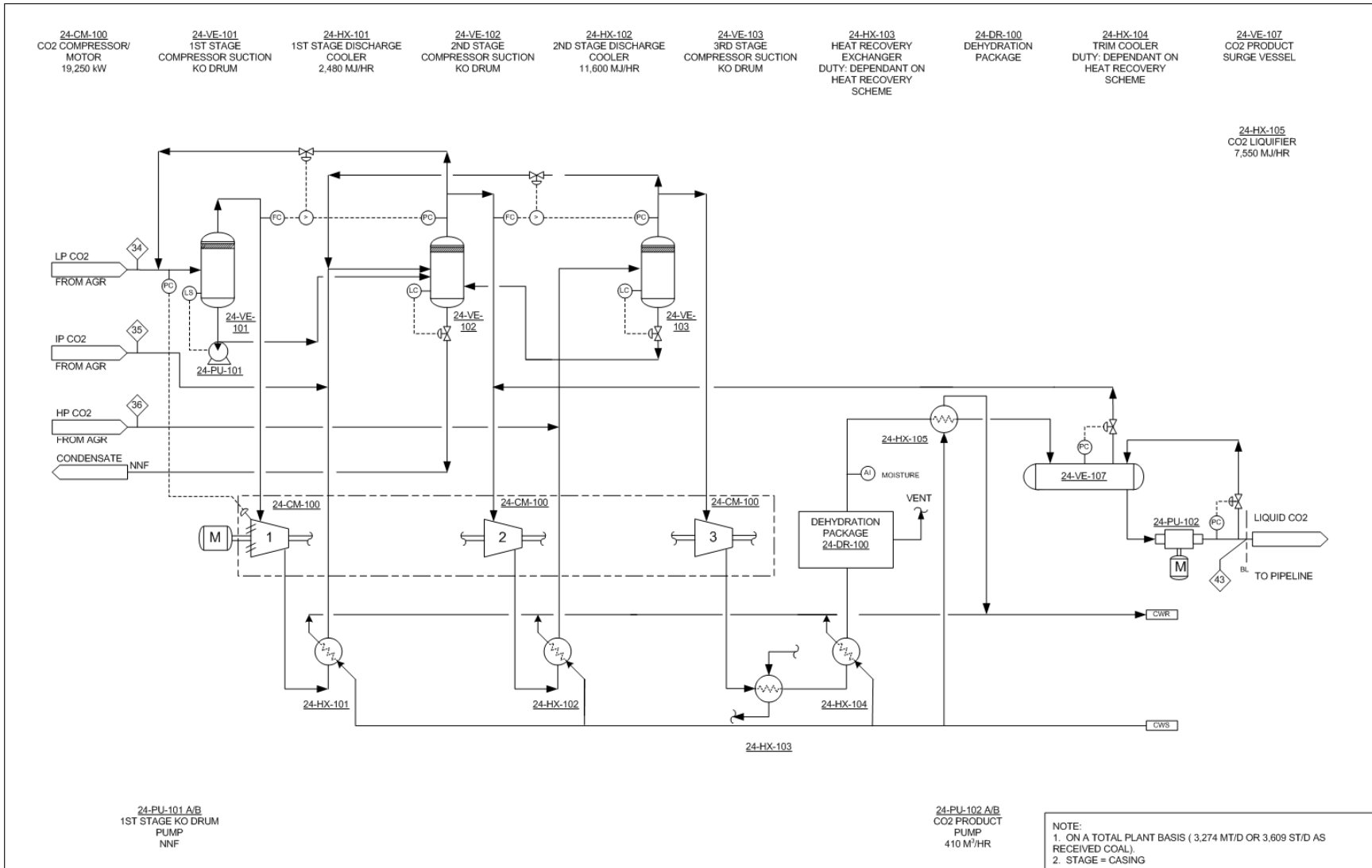


**Figure A2.1 - 3: Process Flow Diagram – CO<sub>2</sub> Compression / Dehydration Unit with Ramgen Non-intercooled HP Compressor**

**Table A2.1 - 3: Ramgen LP and IP CO<sub>2</sub> Compression Technology Characteristics**

Case	Baseline	Ramgen Technology
Number of Intercoolers	None	None
LP Compressor Isentropic Efficiency, %	83.19	91.6
IP Compressor Isentropic Efficiency, %	83.13	91.3
Compressor Power Consumption (LP + IP), MW	5.4	4.9

**Table A2.1 - 4: Ramgen HP CO<sub>2</sub> Compression Technology Characteristics**

Case	Baseline	Ramgen Technology - Non-intercooled Compression							Ramgen Technology - Intercooled Compression
		Low Pressure Steam Generation	Syngas Humidification	Syngas Humidification and LiBr Absorption Refrigeration	LiBr Absorption Refrigeration	NH <sub>3</sub> Absorption Refrigeration	Low Temperature Rankine Cycle	Hypothetical Cycle (Working Fluid with Variable Evaporation Temperature but Constant Condensing Temperature)	
Compressor Discharge Heat Utilization	None								None
Number of Intercoolers	2	None							2
Isentropic Efficiencies, %	83.76 83.76 81.89	90.4							92.0 92.0 92.0
Compressor Power Consumption (HP), MW	12.5	14.4							11.4

**Table A2.1 - 5: Impact on Plant Performance with Ramgen CO<sub>2</sub> Compression (LP + IP + HP) Technology**

Case	Baseline	Ramgen Technology - Non-intercooled Compression							Ramgen Technology - Intercooled Compression
		Low Pressure Steam Generation	Syngas Humidification	Syngas Humidification and LiBr Absorption Refrigeration	LiBr Absorption Refrigeration	NH <sub>3</sub> Absorption Refrigeration	Low Temperature Rankine Cycle	Hypothetical Cycle (Working Fluid with Variable Evaporation Temperature but Constant Condensing Temperature)	None
HP Compressor Discharge Heat Utilization	None								
Number of Intercoolers	2	0	0	0	0	0	0	0	2
Net Change in IGCC Plant Output over Baseline Case, MW	-	0.35 Decrease	0.64 Decrease	0.30 Increase	0.34 Increase	0.45 Decrease	0.19 Increase	1.91 Increase	1.61 Increase

**Table A2.1 - 6: Ramgen Air Expander Technology Characteristics**

Case	Baseline	Ramgen Technology
Isentropic Efficiencies, %	77.5	95.0
Power Generation, MW	4.7	5.8

**Table A2.1 - 7: Ramgen ASU Compressor Technology Characteristics**

Case	EP ASU Air Compressor		LP ASU Air Compressor		Nitrogen Compressor	
	Baseline	Ramgen Technology	Baseline	Ramgen Technology	Baseline	Ramgen Technology
Heat Recovery	None	LiBr Absorption Refrigeration	None	LiBr Absorption Refrigeration	None	None
Number of Intercoolers	4	1	2	None	2	1
Polytropic Efficiencies, %	80.8 89.6 85.4 85.1 85.1	91.7 91.7	80.9 86.8 85.3	91.5	86.55 83.01 79.41	91.5 91.5
Compressor Power Consumption, MW	5.7	5.9	9.1	9.5	22.0	19.8

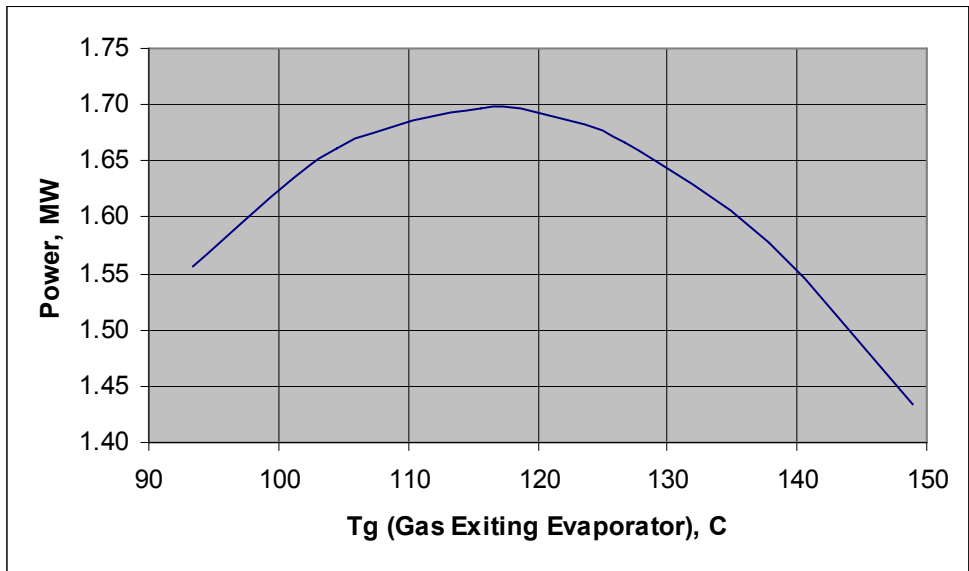


**Figure A2.1 - 4: Power from a Rankine Cycle**

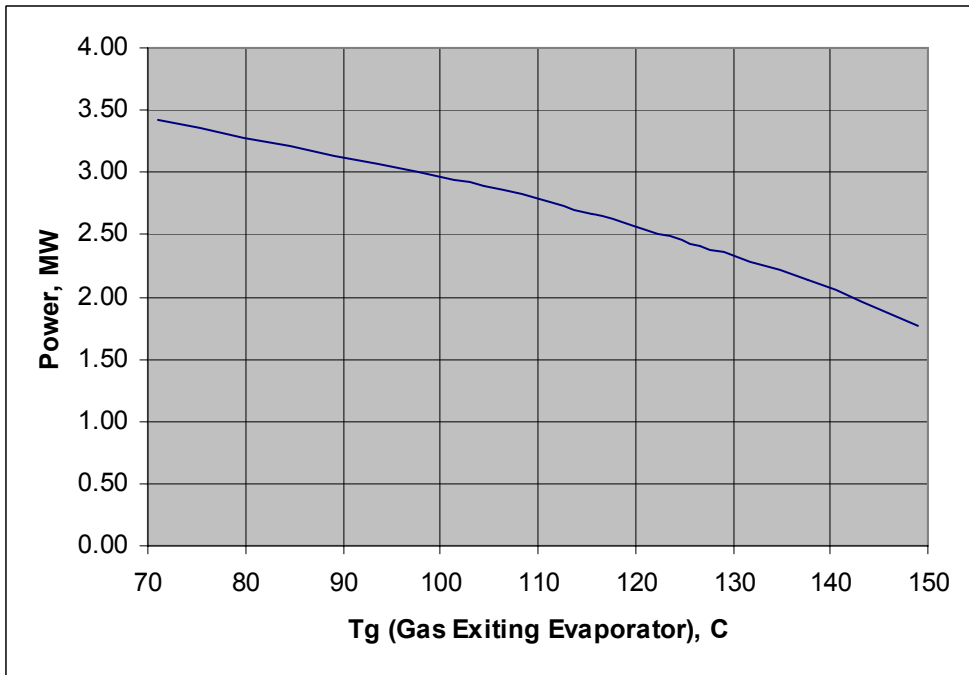


**Figure A2.1 - 5: Power from a Hypothetical Working Fluid with Variable Evaporation and Condensing Temperatures**



**Table A2.1 - 8: Stream Data – Baseline Case ASU and Gas Turbine Air Extraction**

Basis: 3,274 Tonne/D (As Received) or 3,078 Tonne/D (Dry Basis) Pittsburgh No. 8 Coal

Mol Fraction	2	3	4	5	6	7	8	9	10	11	12
O2	0.2077	0.2077	0.2077	0.9504	0.9500	0.9502	0.9500	0.0062	0.2090		
N2	0.7722	0.7722	0.7722	0.0230	0.0176	0.0212	0.0176	0.9891	0.7788		
Ar	0.0094	0.0094	0.0094	0.0266	0.0324	0.0286	0.0324	0.0047	0.0093		
H2											
CO											
CO2	0.0003	0.0003	0.0003						0.0003		
H2O	0.0104	0.0104	0.0104						0.0026	1.0000	1.0000
Total	1.0000	1.0000	1.0000	1.0000	1.0000	1.0000	1.0000	1.0000	1.0000	1.0000	1.0000
kgmol/hr (w/o Solids)	8,734	2,311	6,423	2,426	1,291	3,717	82	8,780	9,009	2,260	2,260
kg/hr (w/o Solids)	252,016	66,689	185,327	77,921	41,563	119,484	2,635	246,663	260,681	40,717	40,717
Temp., C	15.0	15.0	15.0	91.5	80.6	87.7	19.4	287.8	26.7	349.1	140.6
Press., bar	1.01	1.01	1.01	82.94	82.94	82.94	3.04	35.09	15.34	180.96	177.47
Enthalpy, MJ/hr	-25,616	-6,778	-18,838	3,567	1,435	5,003	-16	67,738	-7,311	67,203	24,584
See Note	1	1	1	1	1	1	1	1	1	2	2

Notes:

1. The reference state for thermodynamic properties is the standard enthalpy of formation of ideal gas at 25°C and 1 atm.
2. Enthalpy corresponds to ASME Steam Tables Basis.

**Table A2.1 – 8 : Stream Data – Baseline Case ASU and Gas Turbine Air Extraction (Continued)**

Basis: 3,274 Tonne/D (As Received) or 3,078 Tonne/D (Dry Basis) Pittsburgh No. 8 Coal

Mol Fraction	54	55	56
O2	0.2074	0.2074	0.2074
N2	0.7728	0.7728	0.7728
Ar	0.0092	0.0092	0.0092
CO2	0.0003	0.0003	0.0003
H2O	0.0103	0.0103	0.0103
Total	1.0000	1.0000	1.0000
kgmol/hr	9,079	9,079	9,079
kg/hr	261,950	261,950	261,950
Temp., C	483.9	421.3	177.8
Press., bar	24.13	15.75	15.55
Enthalpy, MJ/hr	102,174	84,198	16,660
See Note	1	1	1

Note:

1. The reference state for thermodynamic properties is the standard enthalpy of formation of ideal gas at 25°C and 1 atm.

## **TASK 2.2: GAS TURBINE OPERATING REQUIREMENTS FOR GASIFICATION BASED FUEL CELL / GAS TURBINE SYSTEM**

### **EXECUTIVE SUMMARY**

This study was conducted in support of the DOE goal to advance IGCC based power generation utilizing SOFC-GT hybrid systems. The current task is to identify the desired performance characteristics and design basis for a gas turbine that will be integrated with an SOFC in IGCC applications. The main objective was met by developing a steady-state simulation of the entire plant and then using dynamic simulations of the hybrid SOFC/GT subsystem to investigate the turbo-machinery performance. From these investigations the desired performance characteristics and a basis for design of turbo-machinery for use in a fuel cell gas turbine power block were developed.

Two SOFC-GT hybrid cycles that meet DOE criteria were numerically modeled and their dynamic performance simulated as part of a perturbation and response analyses. The main difference between the two cycles is the means by which cathode recycle is accomplished; initially via an ejector and ultimately via a blower during the evolution of the study. Models of these two subsystems were built specifically to assist in these studies. The dynamic models of the entire system stem from the 220 kW Siemens Westinghouse hybrid system model that was developed at the National Fuel Cell Research Center and validated with experimental data. These correlations between the model and experiment have been described in numerous journal publications. The main changes to the 220 kW model were to scale up the power block to 100 MW, replace tubular fuel cell geometry with planar geometry, replace centrifugal turbo-machinery with axial design and adjust overpotential parameters in the SOFC to match SECA target performance goals of  $500 \text{ mW/cm}^2$  at 80% fuel utilization. Since experimental data at the 100 MW system level is unavailable, model performance was compared and validated against ASPEN, industry standard software used in plant design. Very good correlation was found between the models described in this work and that of ASPEN.

These studies primary focused on the impact of perturbations to the steady state design operating point that led to gas turbine failure in the form of compressor surge and design and operational strategies to avoid this phenomenon. The pressure fluctuations associated with compressor surge will likely damage if not destroy the fuel cell before the turbo-machinery if pressure regulators are not placed between the fuel cell stack and the turbo-machinery. The main perturbations investigated that lead to surge were load shed and dilution of syngas hydrogen content with nitrogen or steam. Fuel cell shutdowns also led to surge. The design strategies that were found to help in avoiding surge include designing the turbine and compressor to allow greater surge margin under steady state operation, minimizing the plenum volume between the fuel cell outlet and turbine inlet, minimizing gas turbine rotational moment of inertia and designing for compressor speed lines that are more vertical in nature. Modification of the turbo-machinery design pressure ratio and mass flow to achieve more stable dynamic response to load shed and fuel dilution perturbations usually comes with an efficiency penalty. But, the efficiency penalty associated with these design modifications may be worth the increase in stability. This argument is further supported if the gas turbine is mainly seen as a means of feeding air to the fuel cell.

The dynamic response of the fuel cell was studied for the above mentioned perturbations. These responses include anode-cathode inlet pressure difference, anode and cathode inlet-outlet temperature differences, average fuel cell cathode temperature, tri-layer (electrolyte) temperature and gas turbine shaft speed. In many cases the perturbation investigated did not lead to compressor surge but these other failure mechanisms were observed.

Two separate control strategies were employed in this study; the first controls gas turbine shaft speed at 3,600 RPM, assuming a synchronous generator and the second (cascade controller) primarily controls fuel cell temperature and secondarily controls gas turbine shaft speed, assuming an asynchronous generator. Careful tuning of the controls is necessary in order to avoid dynamic operational paths taken between initial and final steady state operating points that tend towards surge. The main difference between the two control strategies is that when RPM is the only control parameter, surge is more easily avoided but fuel cell temperature can vary dramatically. The cascade controller is very effective at controlling fuel cell temperature but because this parameter is controlled by varying gas turbine shaft speed, surge becomes a factor. The fuel cell temperature strategy should be designed to accept some delays in mass flow response (which the fuel cell should be able to handle due to its large thermal mass) so that the hybrid system will have better surge avoidance. When fuel cell temperature *is not* a control parameter, cathode recycle blowers were found to lead to less compressor operating point fluctuation than when an ejector is used for the same purpose. Thus, a blower is preferred for surge avoidance and superior dynamic response to perturbations with this control strategy. When fuel cell temperature *is* a control parameter, there was very little difference in surge avoidance between systems that used a cathode blower or an ejector. In general, it was found that machines driving synchronous generators were less likely to experience surge but were unable to effectively control fuel cell temperature for all the perturbations studied. The converse of this is true for asynchronous machines. Using the cathode blower in place of the ejector was found to increase steady state cycle efficiency by approximately three percentage points for the three different cycle pressure scenarios investigated. It is unknown whether currently available blowers can operate at the temperatures required or whether blowers could maintain the pressure ratios required in the current cycles.

Many studies that merit further investigation are suggested.

## **OBJECTIVE**

The objective of the current task is to identify the desired performance characteristics and design basis for a gas turbine that will be integrated with an SOFC in IGCC applications.

## **SCOPE OF WORK**

The main objective will be met by developing a steady-state simulation of the entire plant and then using dynamic simulations of the hybrid SOFC/GT sub-system to investigate the turbo-machinery performance. From these investigations the desired performance characteristics and a basis for design of turbo-machinery for use in a fuel cell gas turbine power block will be developed.

## APPROACH

In this task steady-state analyses of a fully integrated gasification combined cycle plant that contains a solid oxide fuel cell gas turbine power block are being accomplished. The steady-state analyses are being conducted for the complete plant for three different operating pressure ratios in the power block. Dynamic modeling is being employed to determine the desired power block configuration and the desired gas turbine characteristics considering only operation around one steady-state solution of the entire IGCC plant (i.e., only one pressure ratio). Knowledge gained from the dynamic modeling is being used to produce a final optimized IGCC plant flow sheet. Two hybrid sub-systems were considered and investigated for optimizing the gas turbine performance characteristics in this work. One of these hybrid sub-systems utilizes an ejector for cathode recirculation and is presented in Figure A2.2 - 1.

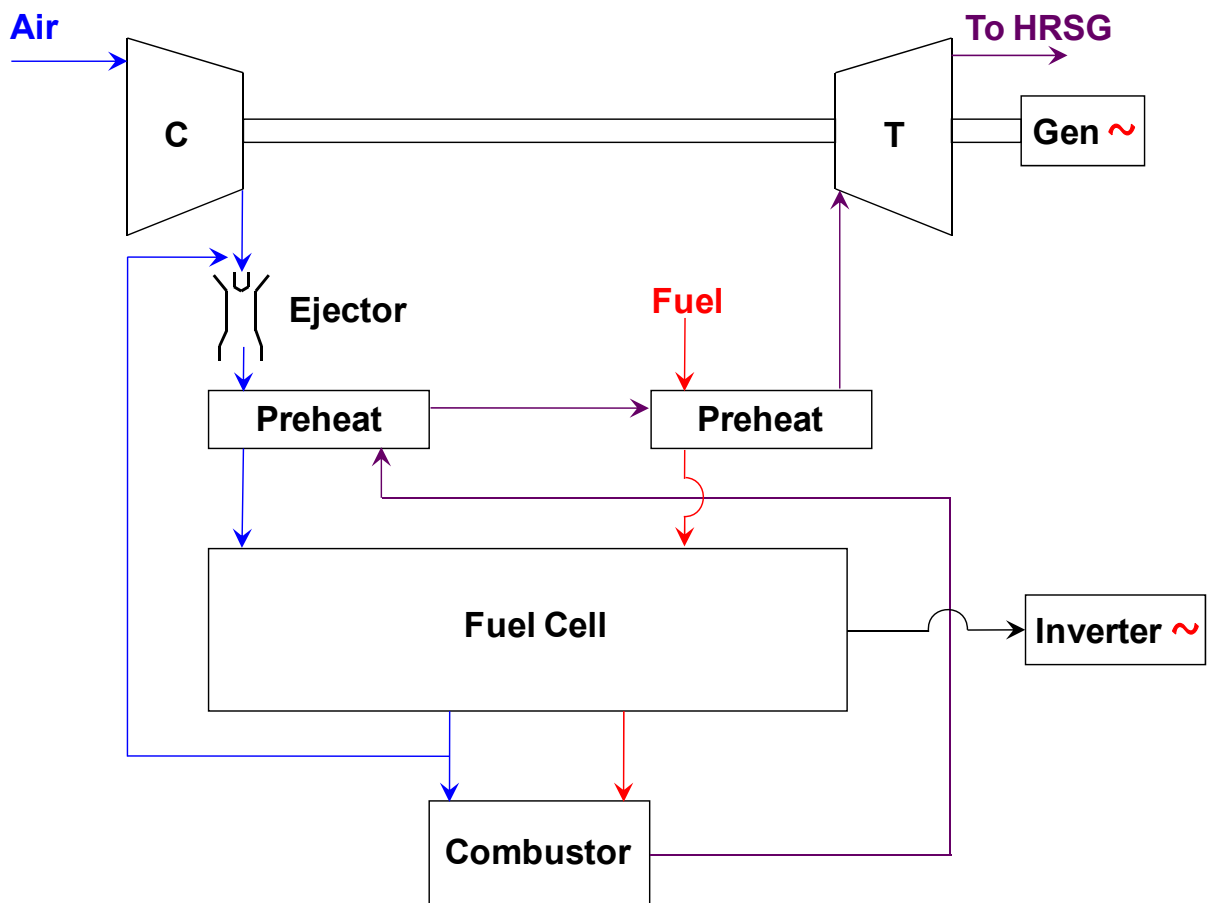


**Figure A2.2 - 1. Diagram of the pressurized 100 MW SOFC/GT hybrid power block utilizing an ejector for cathode recirculation.**

The other hybrid sub-system utilizes a blower for cathode recirculation and is presented in Figure A2.2 - 2.

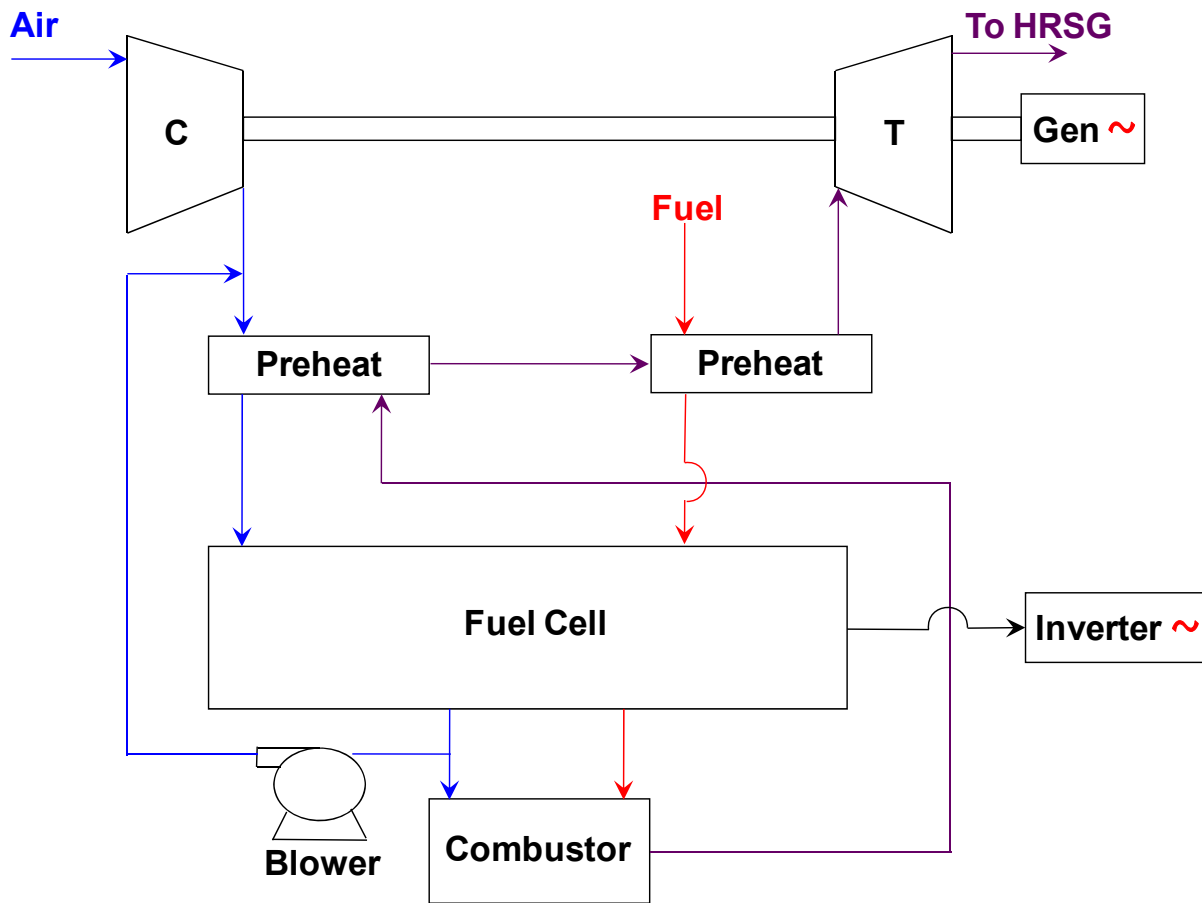


**Figure A2.2 - 2. Diagram of the pressurized 100 MW SOFC/GT hybrid power block utilizing a blower for cathode recirculation.**

The performance maps for the compressor and turbine are manipulated over a reasonably large range to settle upon the performance characteristics and design basis that are desired for this type of SOFC/GT power block.

The work in this task will be accomplished in a step-by-step fashion according to the following process as established with the U.S. Department of Energy:

1. Establish design basis for DOE's approval
2. Establish syngas pressure at SOFC system inlet for steady state design point operation
3. Develop syngas composition and temperature at inlet of SOFC system based on steady state analysis of gasification plant
4. Define ambient air composition, temperature and pressure at inlet of GT
5. Define pressure at inlet of HRSG for steady state design point operation
6. Develop SOFC/GT steady state performance including SOFC inlet syngas and GT inlet air flow rates, and HRSG inlet gas flow rate, composition and temperature for a 100 MW (SOFC + GT Gross AC Output) module\*

7. Establish/modify the axial compressor and turbine design bases (acquire, develop, and/or modify maps)
8. Apply dynamic SOFC/GT model to assess dynamic performance, identify control challenges, and characterize the GT
9. Assess whether SOFC/GT integration needs to be revised. Iterate to Steps 6-8 and stop when sufficient information on desired turbo-machinery performance characteristics for the FC/GT power block are determined
10. Complete integration of IGFC plant and develop overall plant performance.

\*A first approximation of complete IGFC plant performance will be developed for three different SOFC operating pressures. After step 6 is completed for the three different SOFC operating pressures only one operating pressure will be considered for the SOFC/GT dynamic simulations. This SOFC operating pressure will be 5 atm (or other single operating pressure to be determined in consultation with DOE).

## RESULTS AND DISCUSSION

### SOFC-GT Hybrid System Model Development

The dynamic model developed for this work was based upon a model previously developed and evaluated to well simulate the performance of an experimental SOFC/GT hybrid system. The previous model was developed for the Siemens Westinghouse Power Corporation 220 kW pressurized SOFC/GT hybrid system presented in Figure A2.2 - 3. The model has been shown to accurately predict the dynamic performance of the system as tested at the University of California, Irvine in peer-reviewed publications [see e.g., Roberts and Brouwer, 2006, Roberts et al., 2006].

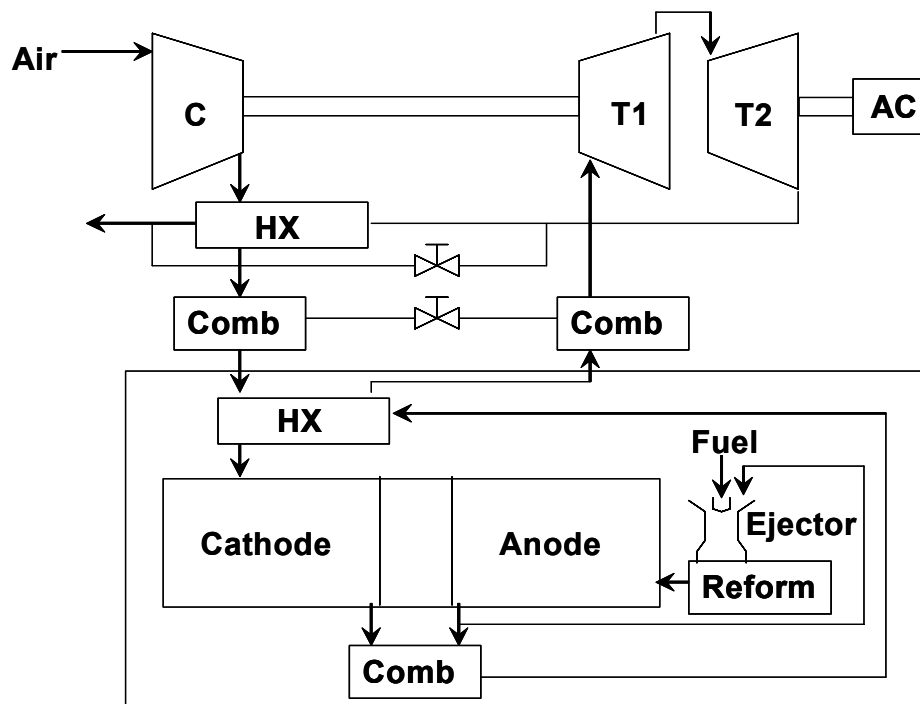


Figure A2.2 - 3. Diagram of the pressurized 220 kW SOFC/GT hybrid system.

The original 220 kW dynamic FC/GT model was modified for the current work by removing turbine 2, both external combustors, both bypass valves, the external recuperator, the external reformer and the anode ejector from the cycle shown in Figure A2.2 - 3. The resulting cycle configurations used in the current work are presented in Figure A2.2 - 1 and Figure A2.2 - 2. The notable differences in addition to those mentioned above are the inclusion of anode preheater, a single shaft power turbine and the scale up in power output to 100 MW. Of the two cycle configurations one uses a cathode ejector (Figure A2.2 - 1) and the other a cathode blower (Figure A2.2 - 2). Within the SOFC block there is a combustion zone at the outlet of the anode and cathode. This combustion process acts to preheat both the incoming cathode air stream and anode fuel stream, represented as “preheat” in Figure A2.2 - 1 and Figure A2.2 - 2.

The specifications of the fuel stream fed to the 100 MW SOFC/GT from the output of the IGFC’s gasifier are given in Table A2.2 - 1. These specifications were determined by a steady state simulation of the entire IGFC system as presented in the Attachment. The accomplishment of this steady state simulation and the specification of the SOFC/GT fuel stream presented in Table A2.2 - 1 represent the successful completion of the first step in the work process as outlined above.

**Table A2.2 - 1: SOFC/GT fuel stream specifications.**

Temperature (K)	505
Pressure (bar)	15.51
Flow Rate (kmol/hr)	11,136.74
Flow Rate (kg/hr)	56,000.59
<u>Mole Fraction (%)</u>	
N <sub>2</sub>	1.02
Ar	1.08
H <sub>2</sub>	91
CO	2.62
CO <sub>2</sub>	3.78
H <sub>2</sub> O	0.01
CH <sub>4</sub>	0.49
Total (%)	100

In order to achieve the desired 100 MW power output from the SOFC/GT the number of cells within the SOFC was increased and the design mass flow rates for the GT were scaled up. The volume of the combustion zone within the SOFC and the volume associated with the plenum of the GT were also scaled up.

Conservation of energy calculations were performed for the fuel cell component blocks within the model and found to be satisfactory. Equation 1 shows the calculation used to determine the percent error:

$$\text{Percent Error} = \left( \frac{\sum(\dot{N} * X_i * h_i)_{in} - \sum(\dot{N} * X_i * h_i)_{out}}{\sum(\dot{N} * X_i * h_i)_{in}} \right) * 100\% \quad (1)$$

where  $\dot{N}$  is the molar flow rate into the component in kmol/s,  $X_i$  is the mole fraction of the species within the molar flow in %, and  $h_i$  is the total enthalpy of the stream in kJ/kmol.

Table A2.2 - 2 shows that all major fuel cell model components conserve energy to within very low percent errors.

**Table A2.2 - 2: Percent error in energy conservation for fuel cell components.**

<u>Component</u>	<u>Percent Error (%)</u>
Fuel Cell Combustor	5.10E-14
Fuel Cell Preheater	-9.00E-07
Fuel Cell	-9.7E-02

The design inputs of the SOFC/GT were modified to allow for pressure ratios of 5, 8, or 10; the three cycle pressures tested. An investigation of the reverse Joule Thompson heating effect (exhibited by hydrogen) on the gasifier fuel stream was found to cause no significant temperature change when throttling down from the gasifier outlet pressure of 15.51 bar to 5 bar at the anode.

The incoming fuel gas stream temperature was changed to 505 K. The fuel utilization has been set to 80% and a current controller was implemented to change fuel flow rate in order to maintain this set utilization value.

Currently no anode off-gas recirculation is being used in the cycle because the fuel stream is predominantly hydrogen with a sufficient steam-to-carbon ratio to avoid coking during reformation. The O/C ratio of the fuel stream was determined to be 1.48 and therefore coking was found to not be a problem based on calculations from Sasaki and Teraoka [2003]. Although the external reformer was removed from the original 220 kW dynamic model, internal reformation is still modeled within the fuel cell.

Calculations were conducted to consider whether anode recirculation should be included in the cycle. Figure A2.2 - 4 shows that both fuel cell and system efficiency are maximized when anode recirculation is minimized. This phenomenon occurs due to the fact that at 80% fuel utilization the recirculated stream consists predominantly of water which dilutes out the syngas fuel stream, absorbing sensible enthalpy from the fuel's heat release during reaction. In the case when the fuel stream is comprised primarily of methane, no variation in fuel cell or hybrid system efficiency was found to occur with variation of percent anode recirculation. These findings, coupled with sufficient steam-to-carbon ratio in the gasified stream to avoid coking suggests that it is desirable to operate the cycle without anode recirculation.

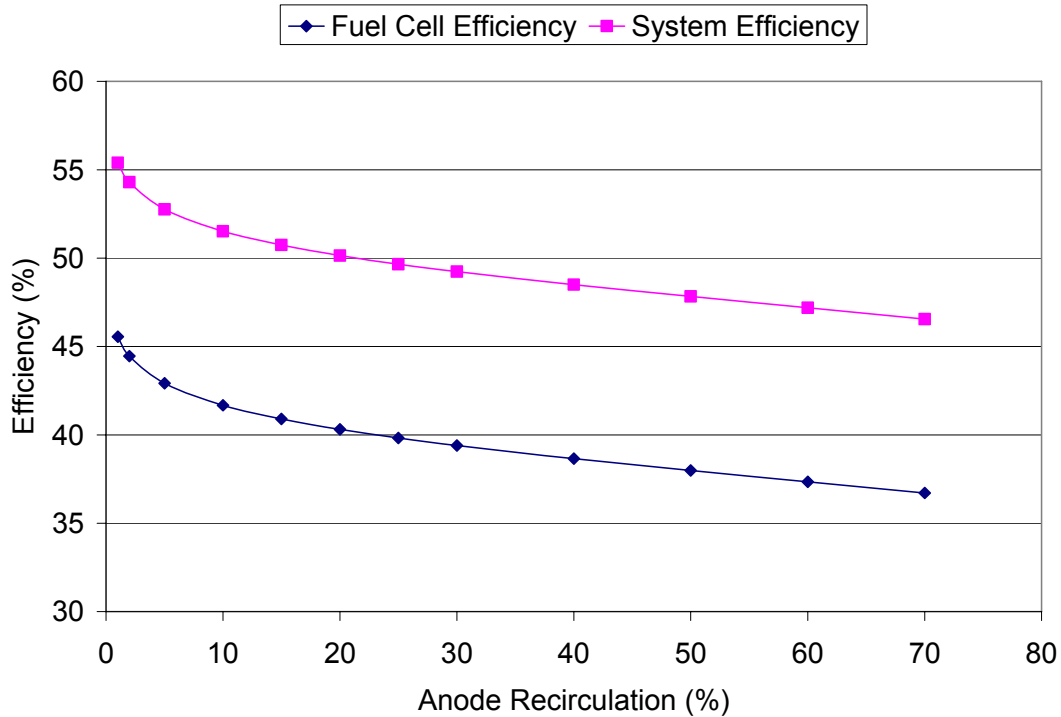


**Figure A2.2 - 4: SOFC/GT hybrid efficiencies vs. percent fuel recirculation of coal syngas (Fuel utilization set to 80%).**

Figure A2.2 - 5 shows that fuel cell inlet and outlet temperatures decrease with decreasing fuel recirculation suggesting that some amount of heating of the fuel will need to be accomplished before it enters the stack. This can be accomplished through a recuperator or special routing of the incoming fuel stream through the vessel that contains the stack to bring the fuel up to the minimum required temperature of 973 K. This anode recuperation strategy is not currently incorporated into the model. In Figure A2.2 - 5 the outlet temperatures of the cathode and the anode are indistinguishable. For the results shown in Figure A2.2 - 5 note that the temperature conditions required for the fuel cell in this study (i.e., those specified in the attachment) have not been imposed on the model, rather, these computations are conducted to determine feasibility and system design requirements to meet the specifications.

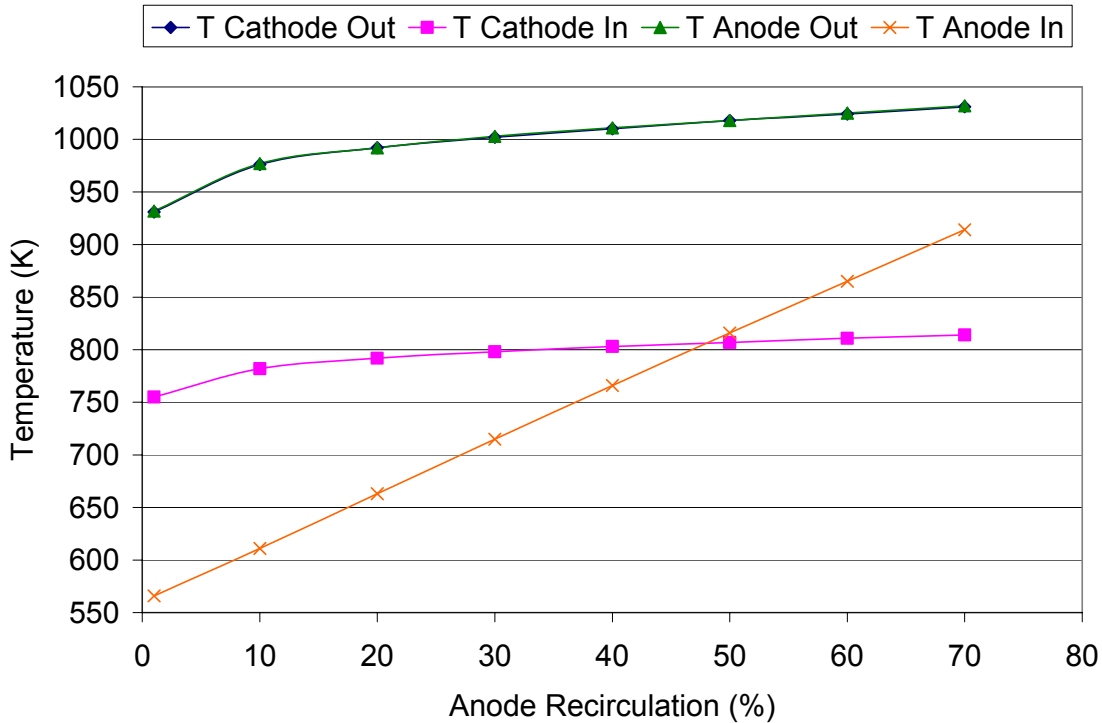


**Figure A2.2 - 5: SOFC/GT hybrid anode and cathode temperatures vs. percent fuel recirculation.**

The power turbine outlet pressure was changed to 104.439 kPa to accommodate the input requirements of the HRSG.

It was difficult to locate any literature that described the appropriate method for determining how to size the polar moment of inertia for a specific power class of a gas turbine-generator set. Limited access to industry data led to an estimate of 1,127 kg\*m<sup>2</sup> for the present work.

### **Solid Oxide Fuel Cell Model**

The design guidelines for the integrated hybrid gasification fuel cell power plant require a power density of 500 mW/cm<sup>2</sup> at a fuel utilization of 80%. These performance characteristics correspond to the ultimate SECA target goals. A voltage vs. current density curve for the 220 kW Siemens Westinghouse SOFC-GT hybrid model developed at the NFCRC (Roberts and Brouwer, 2006) and (Roberts et al., 2006) can be found in Figure A2.2 - 6. The activation, ohmic and concentration overpotential loss terms and other equations are provided in the plot. Performance for the fuel cell at 800°C, a fuel utilization of 80% and operating pressures of 1 and 5 atmospheres are shown.

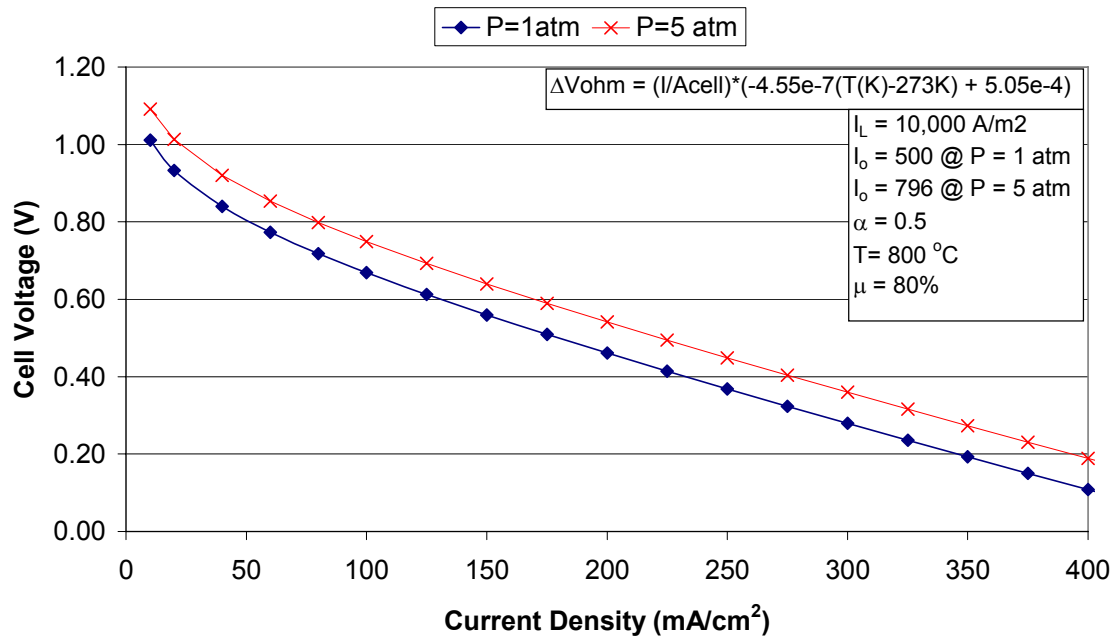


**Figure A2.2 - 6: Voltage vs. current density for Siemens Westinghouse 220 kW SOFC-GT hybrid system.**

A survey of the 2004 literature detailing planar SOFC stack performance for various SECA participants is shown in Figure A2.2 - 7, which clearly shows the advances in performance compared to the tubular SOFC shown in Figure A2.2 - 6.



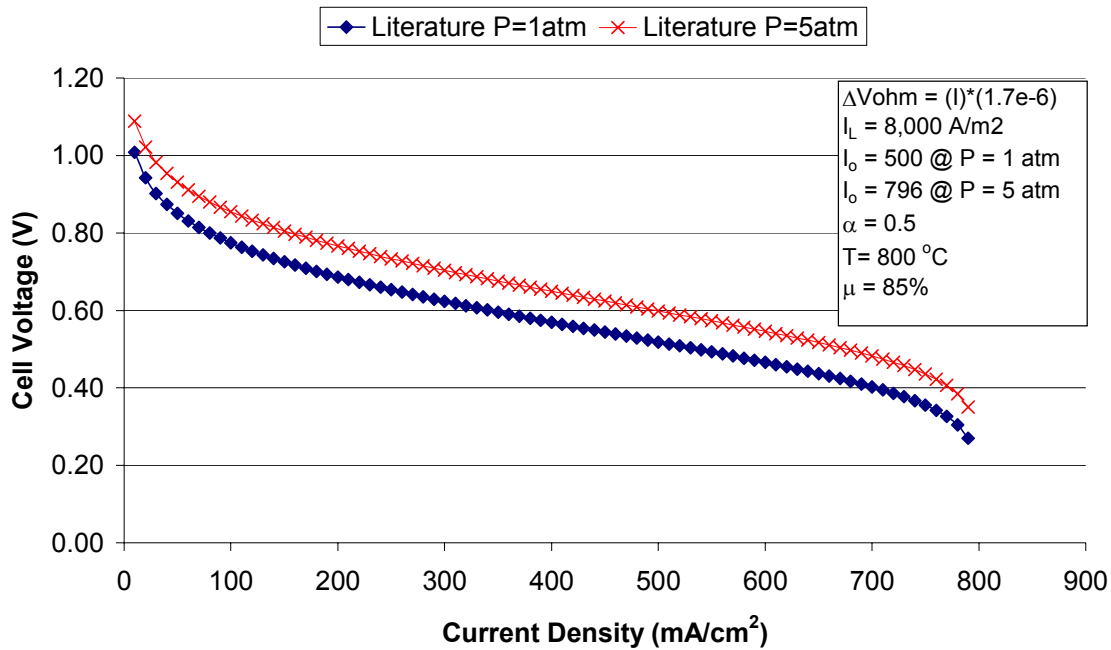


**Figure A2.2 - 8: Extrapolated voltage vs. current density based on 2004 SECA participant data.**

In order to meet the SECA goals of 500 mW/cm<sup>2</sup> and fuel utilization of 80%, overpotential loss terms were manipulated to give voltage vs. current density (Figure A2.2 - 9) and power density vs. performance current density (Figure A2.2 - 10). These analyses were conducted independent of the model for sake of time, but similar changes have been made within the model to achieve similar performance characteristics.

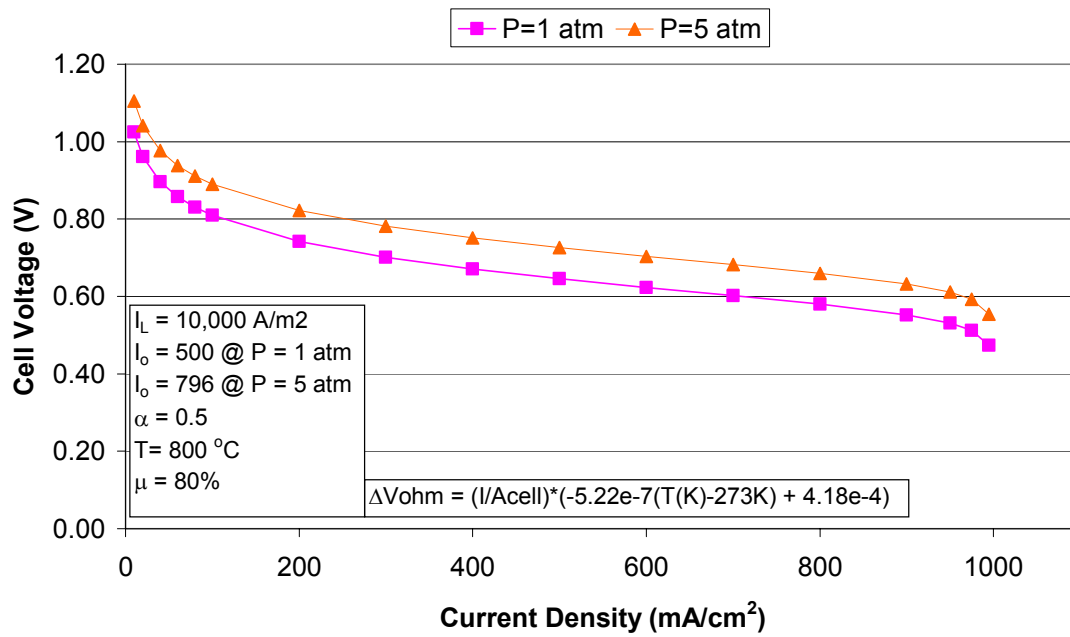
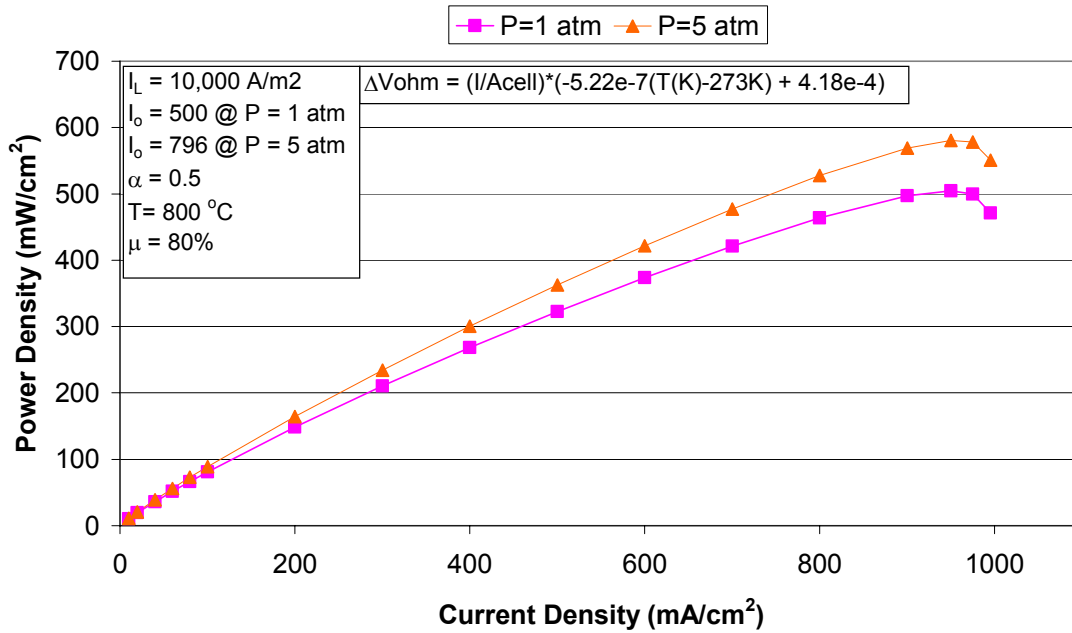
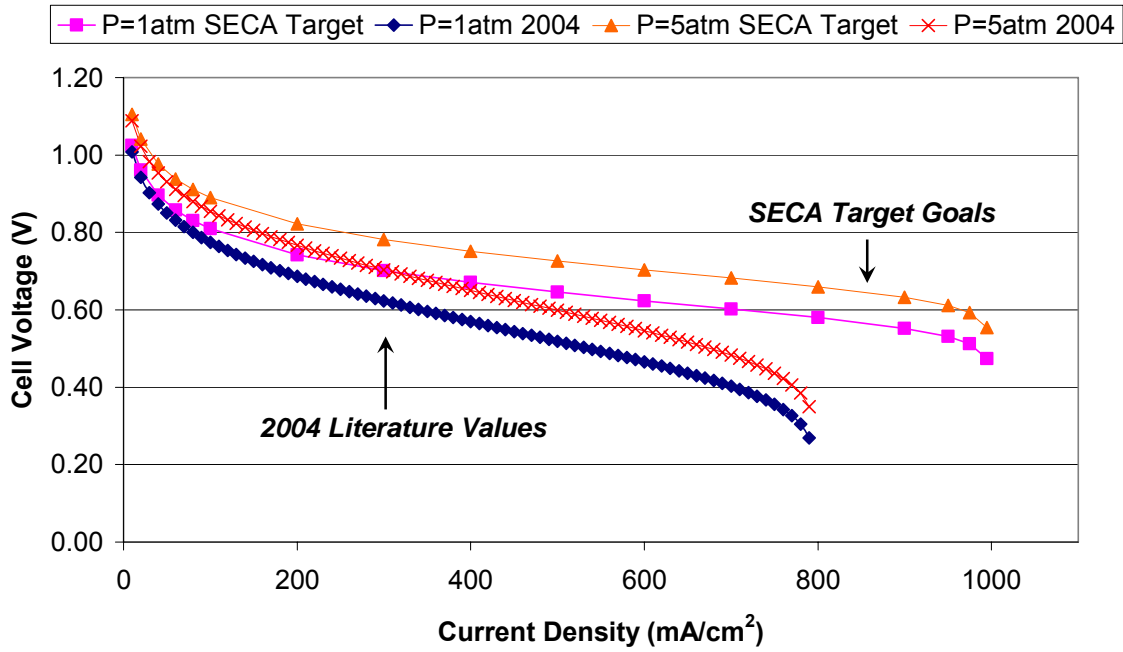


Figure A2.2 - 9: Voltage vs. current density based on ultimate SECA targets.



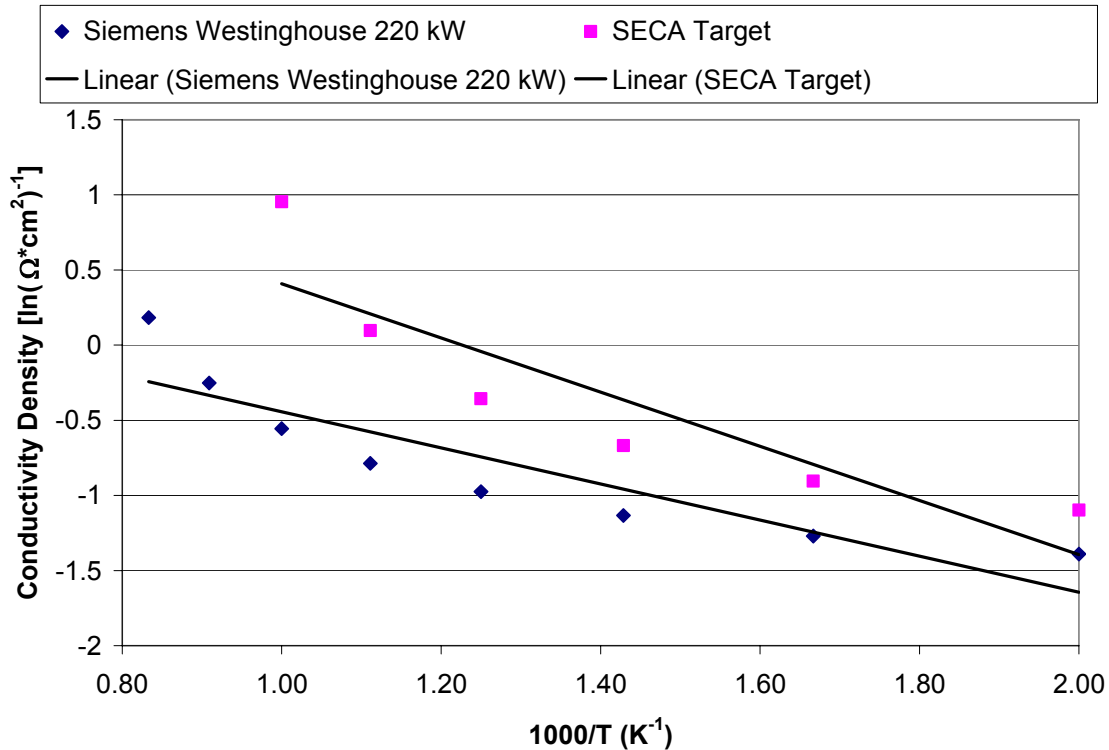
**Figure A2.2 - 10: Power density vs. current density based on ultimate SECA targets.**

Figure A2.2 - 11 combines the data of Figure A2.2 - 8 and Figure A2.2 - 9 to allow a comparison between the 2004 SECA literature data and the ultimate SECA targets.



**Figure A2.2 - 11: Voltage vs. current density based on 2004 literature and ultimate SECA targets.**

Figure A2.2 - 12 compares the difference in conductivities between the Siemens Westinghouse 220 kW and the SECA target SOFC.



**Figure A2.2 - 12: Total cell conductivity density vs. reciprocal temperature for Siemens Westinghouse 220 kW and SECA target SOFC.**

### **Gas Turbine Model**

The gas turbine in the original SOFC/GT hybrid system model developed at the NCFRC was based on an Ingersoll-Rand dual shaft centrifugal (compressor and turbine) unit sized at 75kW as described by (Roberts and Brouwer, 2006). The original GT model was modified for the present work to utilize a single shaft axial (compressor and turbine) GT to reflect what is typical of a larger size class on the order of 10-20 MW. The axial GT model uses equations to describe compressor pressure ratio vs. corrected mass flow and turbine corrected mass flow vs. pressure ratio for various corrected speeds. These equations were derived using methods outlined in (Pukrushpan et al., 2005) and are based on empirical data obtained from Gas Turbine Simulation Program (GSP, 2007), a tool developed at Delft Technical University which improved upon the NASA DYNGEN code. The empirical data obtained from GSP for the compressor can be found in Figure A2.2 - 13 and that for the turbine in Figure A2.2 - 14.

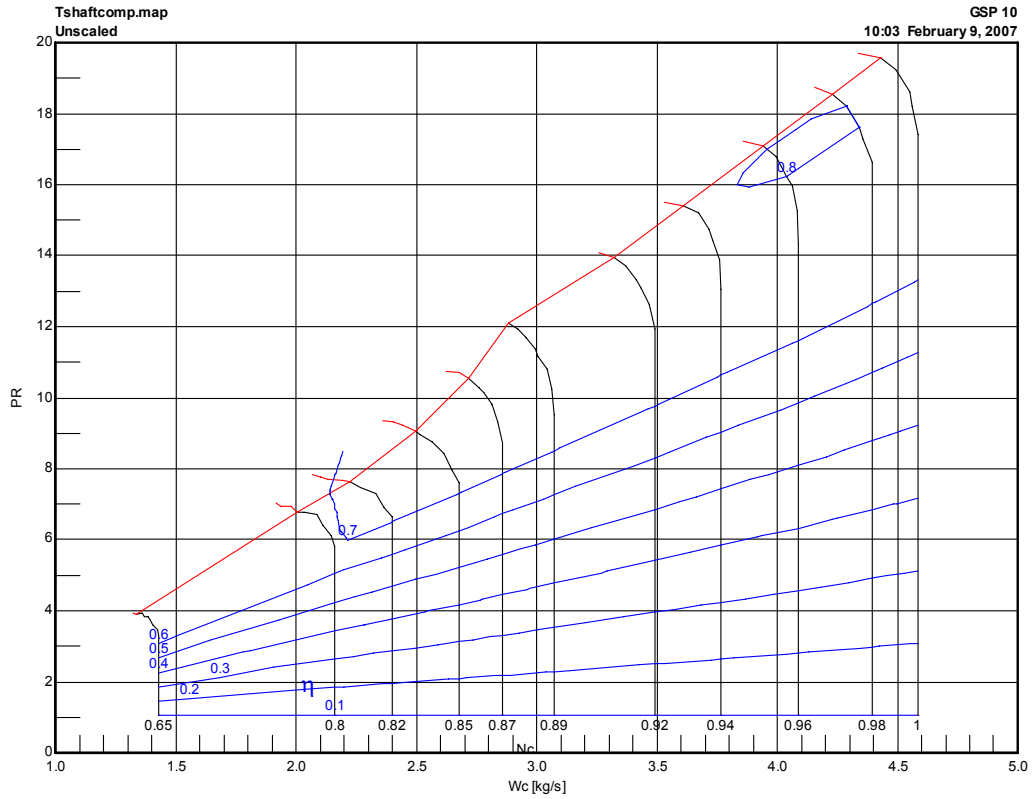


**Figure A2.2 - 13: Empirical axial compressor pressure ratio vs. corrected mass flow for various corrected speeds (in black). Red line is surge line and blue lines represent efficiency islands (Source: GSP).**

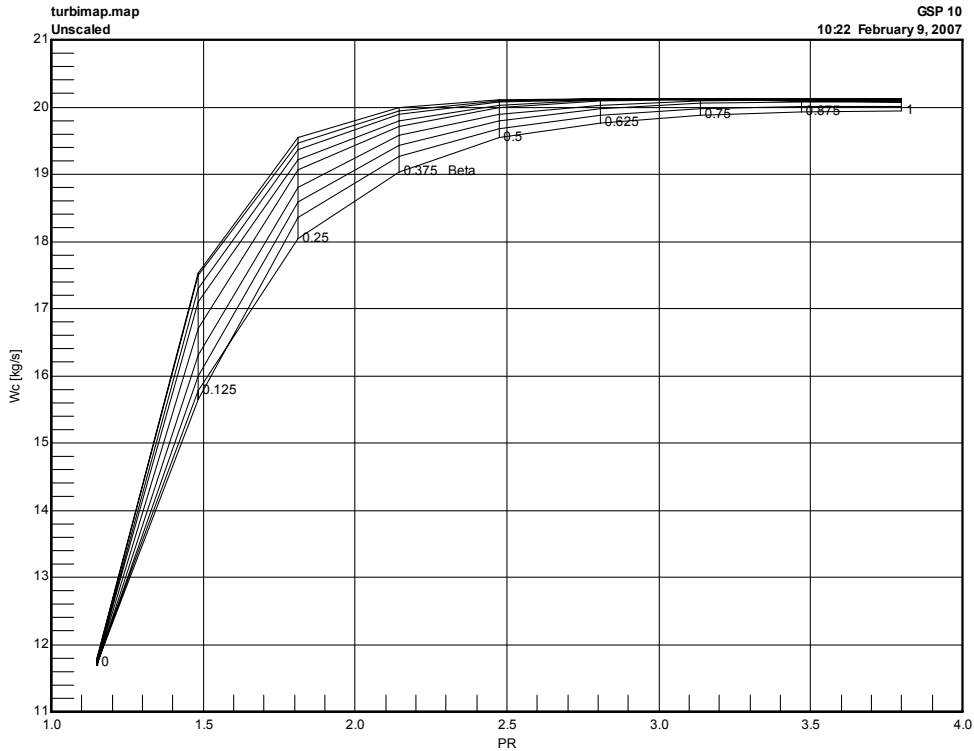


**Figure A2.2 - 14: Empirical axial turbine corrected mass flow vs. pressure ratio for various corrected speeds (Source: GSP).**

Multiple equations were derived to fit the compressor map data (Figure A2.2 - 13) to various degrees of accuracy and Equation 2 was chosen for use in the model due to its combination of accurate data fitting and model stability. Equation 2 is used to describe compressor pressure ratio vs. mass flow for various speed lines as follows

$$\left(1.63914 - 4.7649 * NRPM + 4.14787 * NRPM^2\right) * \left(1 - e^{(NPr*(79.8268 - 47.4069*NRPM) + 65.3714 - 103.65*NRPM)}\right) \quad (2)$$

where  $NPr$  is the normalized pressure ratio and  $NRPM$  is the normalized corrected speed. The results of this curve fit to the compressor map data are presented in Figure A2.2 - 15. The steady state design point and the surge line used in the model are also presented in Figure A2.2 - 15.

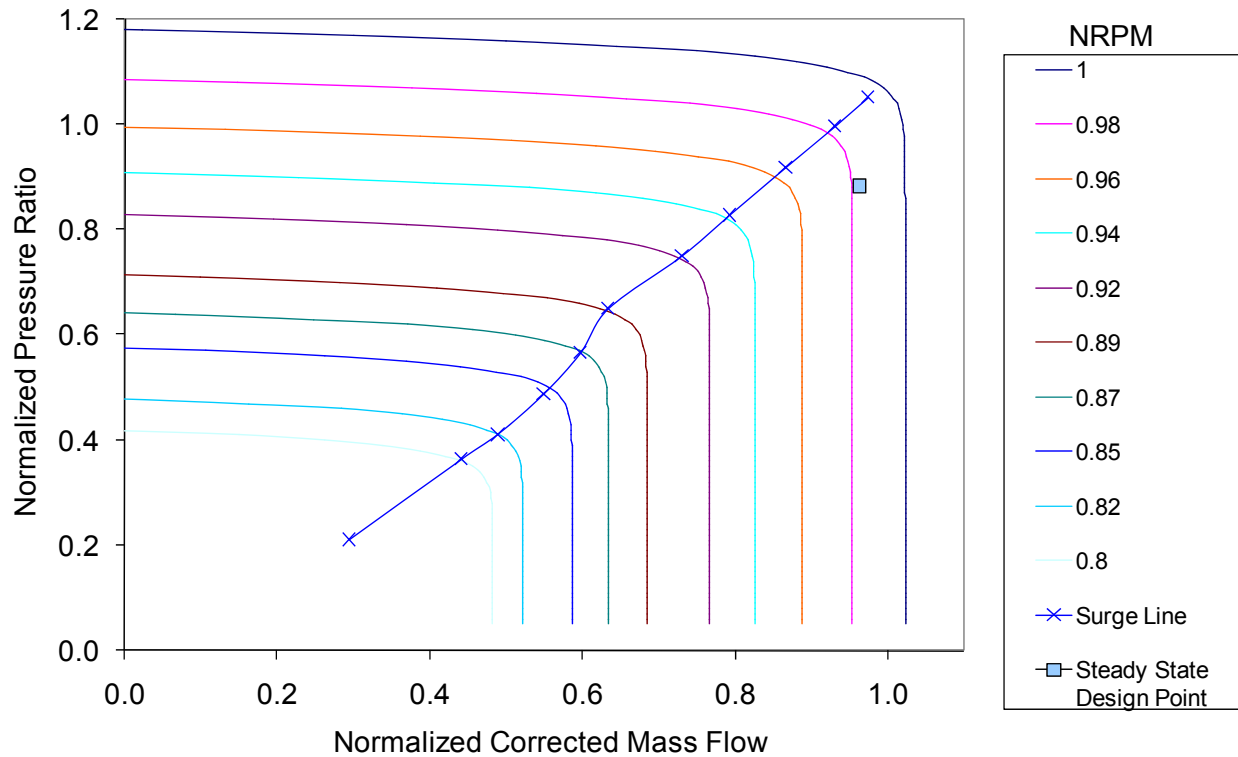


**Figure A2.2 - 15: Axial compressor pressure ratio vs. mass flow for various speeds using equation 2.**

Direct empirical performance maps using GSP data were used to describe compressor isentropic efficiency vs. mass flow as shown in Figure A2.2 - 16. In the model, a maximum design efficiency of 88% was used (Rao et al., 2006). These data points from Figure A2.2 - 16 were manipulated in MATLAB using a function called “Griddata” that interpolates them to a high resolution within the model, such that for a given pressure ratio and speed an accurate efficiency value is obtained. Note that the data presented in Figure A2.2 - 16 are normalized efficiency such that the maximum efficiency value shown (1.0) corresponds to the design value of 88%.

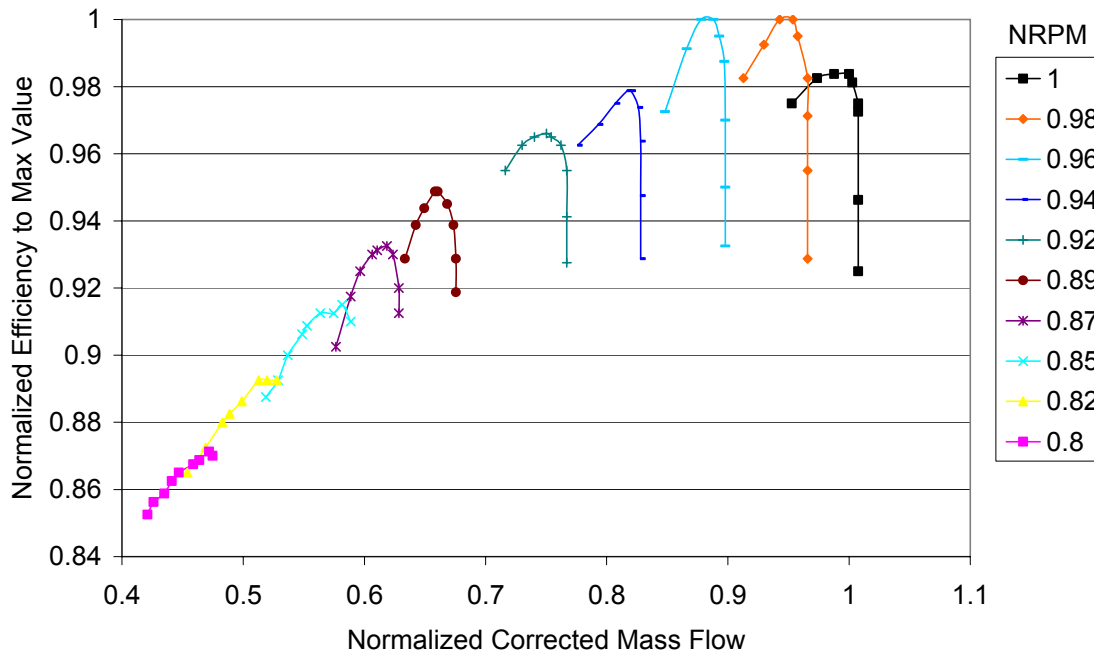


**Figure A2.2 - 16: Compressor isentropic efficiency (normalized to maximum design value) vs. mass flow.**

Multiple equations were derived to fit the turbine map data of Figure A2.2 - 14 to various degrees of accuracy. These curves were more difficult to accurately fit so that the more complex Equation 3 was chosen for use in the model. Equation 3 produced a combination of accurate data fitting and model stability in describing turbine pressure ratio vs. mass flow for the various speed lines as follows

$$\begin{aligned}
 & (3.53483 - 42.4802 * NRPM + 62.569 * NRPM^2 - 25.1289 * NRPM^3) + \\
 & NPR * (-29.6439 + 332.154 * NRPM - 488.381 * NRPM^2 + 196.34 * NRPM^3) + \\
 & NPR^2 * (105.781 - 978.61 * NRPM + 1435.25 * NRPM^2 - 577.368 * NRPM^3) + \\
 & NPR^3 * (-167.314 + 1380.84 * NRPM - 2019.72 * NRPM^2 + 812.741 * NRPM^3) + \\
 & NPR^4 * (123.012 - 941.015 * NRPM + 1372.94 * NRPM^2 - 552.554 * NRPM^3) + \\
 & NPR^5 * (-34.3682 + 249.094 * NRPM - 362.609 * NRPM^2 + 145.945 * NRPM^3)
 \end{aligned} \tag{3}$$

where  $NPr$  is the normalized pressure ratio and  $NRPM$  is the normalized corrected speed. The results from the curve fits of Equation 3 are presented in Figure A2.2 - 17. The steady state design point used in the model is also shown in Figure A2.2 - 17.

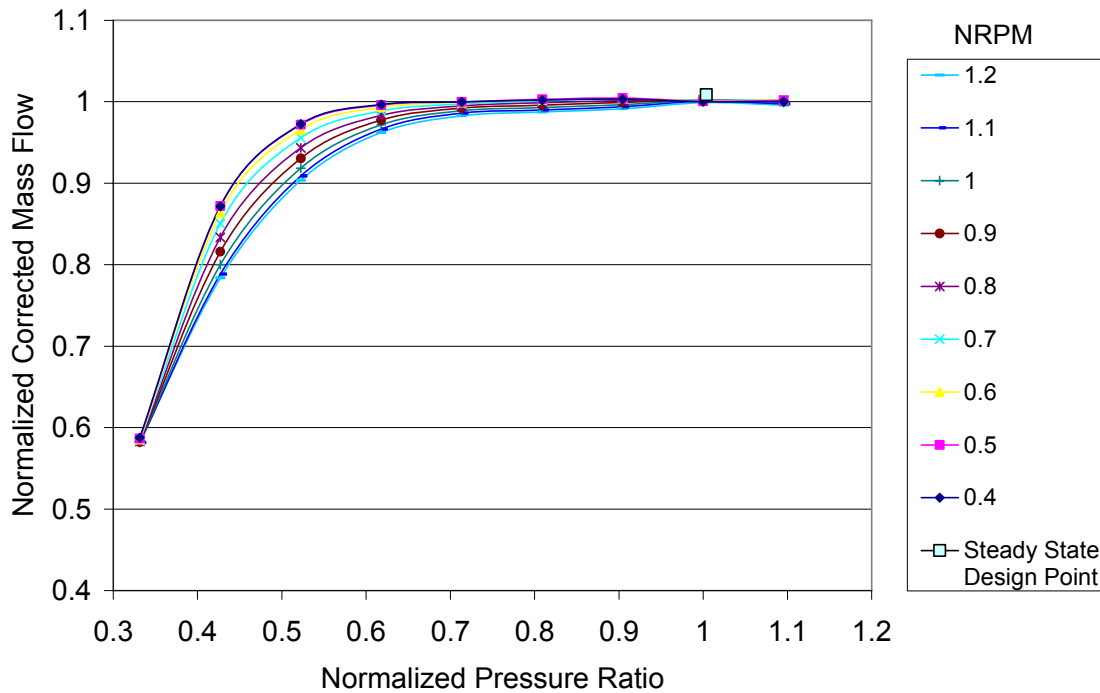


**Figure A2.2 - 17: Axial turbine mass flow vs. pressure ratio for various speeds using equation 3.**

Direct empirical performance maps using GSP data were used to describe turbine isentropic efficiency vs. pressure ratio (Figure A2.2 - 18). A maximum design efficiency of 92% was used (Rao et al., 2006). These data points from Figure A2.2 - 18 were manipulated in MATLAB using a function called “Griddata” that interpolates them to a high resolution within the model, such that for a given pressure ratio and speed an accurate efficiency value is obtained. Note that Figure A2.2 - 18 shows a maximum normalized efficiency value of 100%, which corresponds to the design value of 92%.

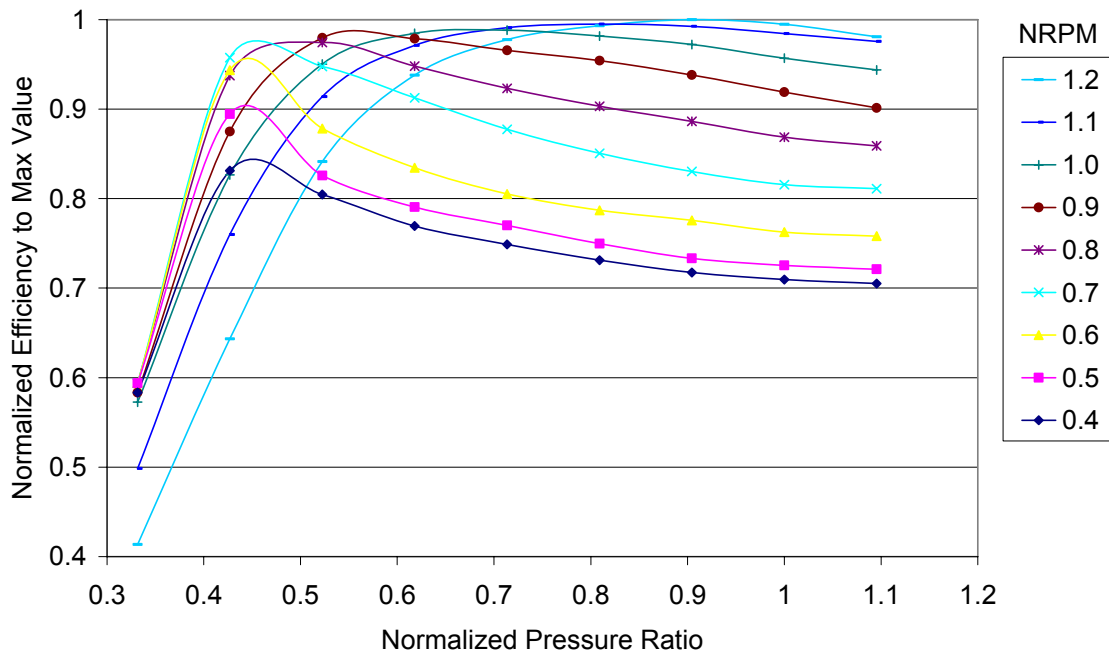


**Figure A2.2 - 18: Turbine isentropic efficiency (normalized to maximum design value) vs. pressure ratio.**

### **Cathode Ejector Model**

An ejector model that builds on previous work (Sun et al., 1996), (Keenan et al., 1950), (Cengel and Boles, 2002), (Ferrari et al., 2005), (Marsano et al., 2004) and (Wachter et al., 2006) was developed.

The ejector model solves for pressure, temperature and Mach number at each section of the ejector geometry. The ejector geometry is fixed but can be defined by the user to achieve different ejector performance characteristics. A diagram of the ejector can be found in Figure

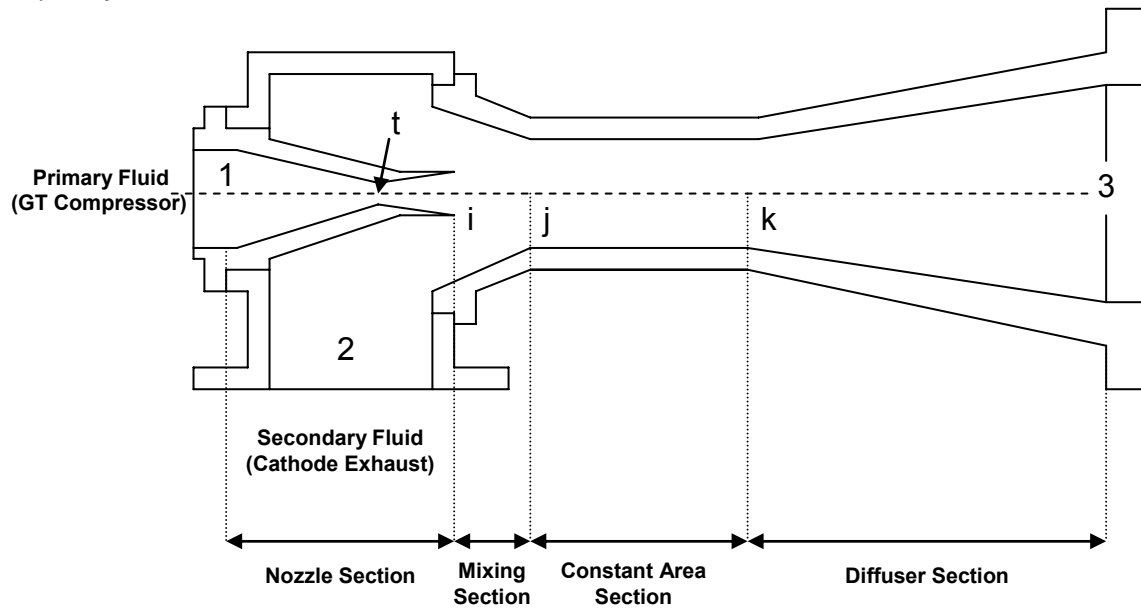


**Figure A2.2 - 19: Fuel cell cathode ejector.**

The solution steps are calculated under the following assumptions (Sun et al., 1996):

The assumptions consist of:

1. One-dimensional, steady state flow of an isentropic ideal gas.
2. Primary and secondary fluids have the same molecular weight and ratio of specific heats.
3. Primary and secondary fluids are supplied at zero velocities (i.e. stagnation conditions in states (1) and (2).
4. At (i) the two streams meet and mixing occurs at constant pressure between (i) and (j).
5. Transverse shock occurs at a plane between (j) and (k).
6. Velocity at (3) is zero, i.e. stagnation conditions.

A table of ejector geometries  $A_t$ ,  $A_{i1}$ ,  $A_{2i}$  and  $A_j = A_k$  are calculated for varying values of  $P_i/P_2$  using specified values of  $P_1$ ,  $P_2$ ,  $T_1$ ,  $T_2$  and  $\omega$ . Geometry is best characterized outside of the Simulink model using methods defined by (Keenan et al., 1950). The geometry necessary to create the appropriate pressure rise across the ejector  $P_3/P_2$ , accounting for pressure loss in the fuel cell and meeting the fuel cell inlet pressure design point is chosen. This is accomplished by guessing  $P_1$  (again this is outside of the Simulink model).  $P_1$  is the stagnation pressure value at the gas turbine compressor outlet. In the model  $P_1$  and gas turbine RPM will specify a mass flow rate from the compressor map that defines  $\dot{m}_1$  and also the stagnation temperature  $T_1$ .

For analysis of the primary nozzle (Figure A2.2 - 20) Table A2.2 - 3 is used with knowledge of ejector geometry ( $A/A^*$  from Table A2.2 - 3) to solve for  $M_{1is}$ .

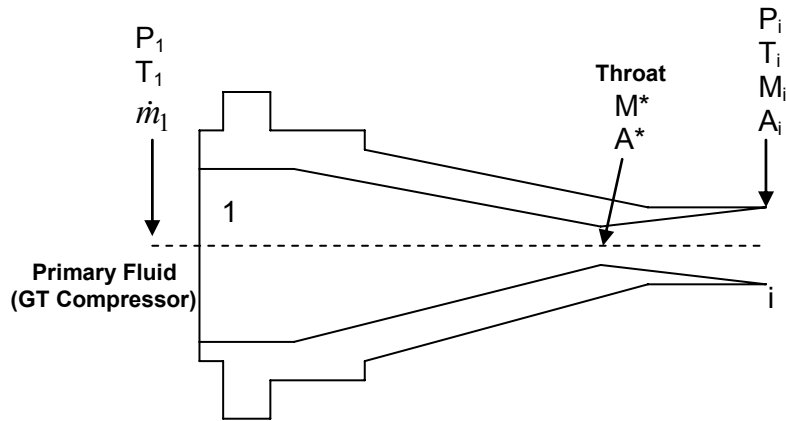
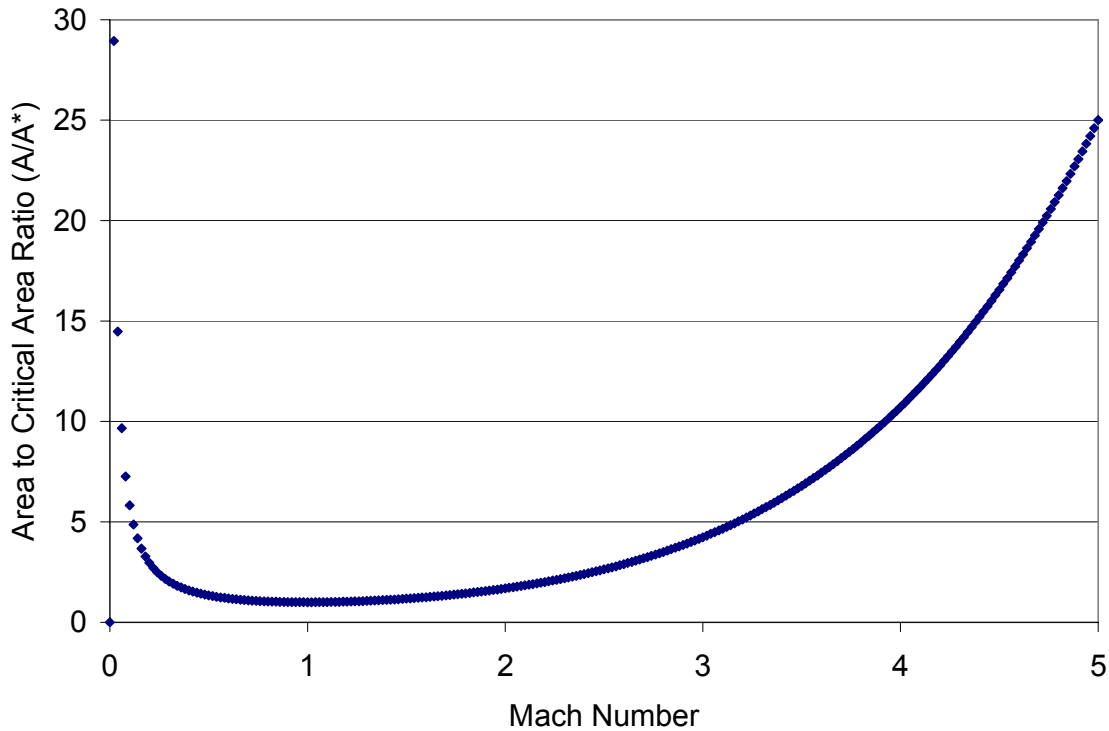


Figure A2.2 - 20: Cathode ejector primary nozzle.

Table A2.2 - 3: One-dimensional isentropic compressible-flow functions for an ideal gas with constant specific heats and molar mass,  $\gamma = 1.4$  (Truncated version, adapted from Fluid Mechanics, Frank M White Table B-1)

Ma	$P/P_1$	$\rho/\rho_1$	$T/T_1$	$A/A^*$
0	1	1	1	NA
0.02	0.99972	0.9998	0.99992	28.94213
0.04	0.998881	0.9992	0.99968	14.48149
0.06	0.997484	0.998202	0.999281	9.66591
0.08	0.995533	0.996807	0.998722	7.26161
0.1	0.993031	0.995017	0.998004	5.821829
0.12	0.989985	0.992836	0.997128	4.864318
0.14	0.9864	0.990267	0.996095	4.1824
0.16	0.982285	0.987314	0.994906	3.672739
0.18	0.977647	0.983982	0.993562	3.277926
0.2	0.972497	0.980277	0.992063	2.96352
0.22	0.966845	0.976204	0.990413	2.707602
0.24	0.960703	0.971771	0.988611	2.495562
0.26	0.954085	0.966984	0.98666	2.317287
0.28	0.947002	0.961851	0.984562	2.165554
0.3	0.93947	0.95638	0.982318	2.035065



**Figure A2.2 - 21: Area ratio vs. Mach number for isentropic flow of an ideal gas with  $k = 1.4$  (Air)**

From Figure A2.2 - 21 it is apparent that there are two solutions for  $M_{1is}$  for a specified area ratio  $A/A^*$ . In the case that  $A/A^* = 1.099$ ,  $M_{1is}$  is either 1.37 or 0.69. If we assume a supersonic nozzle (which is used in this model) then we chose  $M_{1is} = 1.37$ .

Again, the isentropic value of  $M_{1is}$  comes from a look up table of supersonic Mach numbers for a given area ratio.

The actual temperature  $T_{1ia}$  out of the primary nozzle will be greater than the isentropic value  $T_{1is}$  due to inefficiencies accounted for by a nozzle efficiency term  $\eta_n$  in the model, a value of 90% is used; 85% is claimed to be typical of supersonic converging-diverging nozzles (Sun et al., 1996)

$$T_{1ia} = T_1 \left( 1 + \frac{\eta_n (\gamma - 1)}{2} M_{1is}^2 \right)^{-1} \quad (4)$$

$T_{2i}$  is known from the cathode exit conditions.

The actual Mach number  $M_{1ia}$ , accounting for efficiency loss, is calculated using equation 5

$$M_{1ia} = \sqrt{\frac{2}{\gamma-1} \left[ \left( \frac{T_1}{T_{1ia}} \right) - 1 \right]} \quad (5)$$

Where  $M_{1ia} < M_{1is}$

By definition nozzle efficiency (equation 6) does not affect  $P_i$ , which is calculated using equation 7.

$$\eta_n = \frac{\text{Actual Kinetic Energy at Nozzle Exit}}{\text{Kinetic Energy at Nozzle Exit for Isentropic Flow from the Same Inlet State to the Same Exit Pressure}} = \frac{V_a^2 / 2}{V_s^2 / 2} = \frac{M_a^2 * T_a}{M_s^2 * T_s} \quad (6)$$

$$P_i = P_1 \left( 1 + \frac{\gamma-1}{2} M_{1is}^2 \right)^{\frac{-\gamma}{\gamma-1}} \quad (7)$$

Mixing occurs from i to j at constant pressure  $P_{1i} = P_{2i} = P_j$

With knowledge of  $P_2$  from the cathode exit conditions, equation 8 can be used to solve for  $M_{2i}$

$$M_{2i} = \sqrt{\frac{2}{\gamma-1} \left[ \left( \frac{P_2}{P_i} \right)^{\frac{\gamma-1}{\gamma}} - 1 \right]} \quad (8)$$

The entrainment ratio  $\omega$  can be solved for using equation 9

$$\frac{A_{2i}}{A_{1i}} = \frac{P_1}{P_2} \frac{\left[ \left( \frac{P_i}{P_1} \right)^{\frac{1}{\gamma}} \sqrt{1 - \left( \frac{P_i}{P_1} \right)^{\frac{\gamma-1}{\gamma}}} \right]}{\left[ \left( \frac{P_i}{P_2} \right)^{\frac{1}{\gamma}} \sqrt{1 - \left( \frac{P_i}{P_2} \right)^{\frac{\gamma-1}{\gamma}}} \right]} \omega \sqrt{\frac{T_2}{T_1}} \quad (9)$$

Rearranging equation 9 we get equation 10

$$\omega = \frac{A_{2i}P_2}{A_{1i}P_1} \frac{\left[ \left( \frac{P_i}{P_2} \right)^{\frac{1}{\gamma}} \sqrt{1 - \left( \frac{P_i}{P_2} \right)^{\frac{\gamma-1}{\gamma}}} \right]}{\left[ \left( \frac{P_i}{P_1} \right)^{\frac{1}{\gamma}} \sqrt{1 - \left( \frac{P_i}{P_1} \right)^{\frac{\gamma-1}{\gamma}}} \right]} \sqrt{\frac{T_1}{T_2}} \quad (10)$$

The temperature at j,  $T_j$ , accounts for the mixing of streams 1 and 2 at the outlet of the constant pressure mixing section and is solved for using equation 11

$$T_j = \int \left( \frac{\left[ \left( \sum \dot{N} \int C_p dT \right) + \frac{\dot{m}V^2}{2} \right]_{IN} - \left[ \left( \sum \dot{N} \int C_p dT \right) + \frac{\dot{m}V^2}{2} \right]_{OUT}}{\dot{V} * C_p * Conc.} \right) dT \quad (11)$$

Equation 12 is used to correct for the local speed of sound  $C^*$  which varies with temperature

$$M^* = \frac{V}{C^*} = \frac{MC}{C^*} = \frac{M\sqrt{\gamma RT}}{\sqrt{\gamma RT^*}} = M\sqrt{\frac{T}{T^*}} \quad (12)$$

Where  $T^*$  is the local temperature

$$T^* = \frac{2T_o}{\gamma + 1} \quad (13)$$

and  $T_o$  is the stagnation condition. Substitution gives equation 14

$$M^* = M \sqrt{\frac{T(\gamma + 1)}{2T_o}} \quad (14)$$

Equation 14 is substituted into equation 15 to solve for  $M_j^*$

$$M_j^* = \frac{M_{1ia}^* + \omega M_{2ia}^* \sqrt{\frac{T_2}{T_1}}}{\sqrt{\left(1 + \omega \frac{T_2}{T_1}\right)(1 + \omega)}} = \frac{M_{1ia} \sqrt{\frac{T_{1ia}(\gamma + 1)}{2T_1}} + \omega M_{2i} \sqrt{\frac{T_{2i}(\gamma + 1)}{2T_2}} \sqrt{\frac{T_2}{T_1}}}{\sqrt{\left(1 + \omega \frac{T_2}{T_1}\right)(1 + \omega)}} \quad (15)$$

$$M_j = \sqrt{\frac{2M_j^{*2}}{\gamma + 1 - M_j^{*2}(\gamma - 1)}} \quad (16)$$

Shock is assumed to occur in the constant area section of the ejector from j to k. Equation 17 describes a one-dimensional normal shock for an ideal gas with constant specific heats and molar mass and is used to solve for  $M_k$

$$M_k = \sqrt{\frac{\left(\frac{2}{\gamma - 1}\right) + M_j^2}{\left(\frac{2}{\gamma - 1}\right)\gamma M_j^2 - 1}} \quad (17)$$

The pressure rise across the shock is used to find  $P_k$

$$P_k = P_j \left(\frac{M_j}{M_k}\right) \sqrt{\frac{1 + \left(\frac{M_j^2(\gamma - 1)}{2}\right)}{1 + \left(\frac{M_k^2(\gamma - 1)}{2}\right)}} \quad (18)$$

Where  $P_j = P_i$

Equation 19 is used to account for the temperature change across the shock in the constant area section

$$T_k = T_j \left( \frac{1 + \left(\frac{M_j^2(\gamma - 1)}{2}\right)}{1 + \left(\frac{M_k^2(\gamma - 1)}{2}\right)} \right) \quad (19)$$

Finally  $P_3$  is determined using equation 20

$$P_3 = P_k \left[ 1 + \left(\frac{\eta_d(\gamma - 1)}{2}\right) M_k^2 \right]^{\frac{\gamma}{\gamma - 1}} \quad (20)$$

Where  $\eta_d$  is the diffuser efficiency; a value of 90% was used. 85% is claimed to be typical (Sun et al., 1996).

$P_{3a} < P_{3s}$  due to the definition of diffuser efficiency (equation 21)

$$\eta_d = \frac{\text{Kinetic Energy that can be Converted to Pressure Rise if the Fluid is Discharged at the Actual Exit Stagnation Pressure}}{\text{Maximum Kinetic Energy Available for Converting to Pressure Rise}} = \frac{\Delta h_s}{V_1^2 / 2} \quad (21)$$

Using the isentropic relation  $\frac{T_o}{T} = \left(\frac{P_o}{P}\right)^{\frac{\gamma-1}{\gamma}}$  which is equivalent to  $\frac{T_3}{T_k} = \left(\frac{P_3}{P_k}\right)^{\frac{\gamma-1}{\gamma}}$  and substitution into equation 20 we get equation 22 which is used to solve for the exit temperature of the ejector; an important value that will determine the effectiveness of the ejector to replace recuperation.

$$T_3 = T_k \left( 1 + \frac{\eta_d (\gamma - 1)}{2} M_k^2 \right) \quad (22)$$

$$T_{3a} < T_{3s}$$

In the model  $P_3$  will be checked to determine if it meets the necessary pressure conditions for the fuel cell and iterate on the geometry (external to the model) and compressor outlet pressure  $P_1$  in the model until convergence occurs. These methods are also employed by (Marsano et al., 2004) and (Wachter et al., 2006).

Figure A2.2 - 22, Figure A2.2 - 23 and Figure A2.2 - 24 show the ejector model performance for Mach number, pressure and temperature respectively at various locations in the ejector (see Figure A2.2 - 19). These results agree well with the literature (Chunnanond and Aphornratana, 2004) and (Cengel and Boles, 2002).

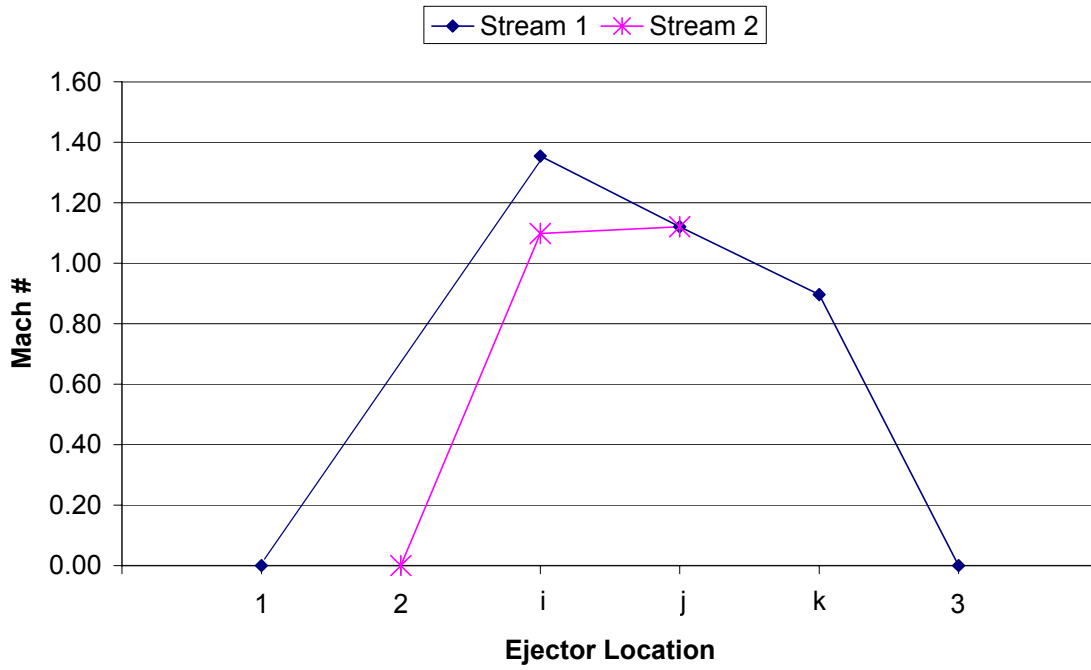


Figure A2.2 - 22: Mach number vs. ejector location for primary and secondary streams.

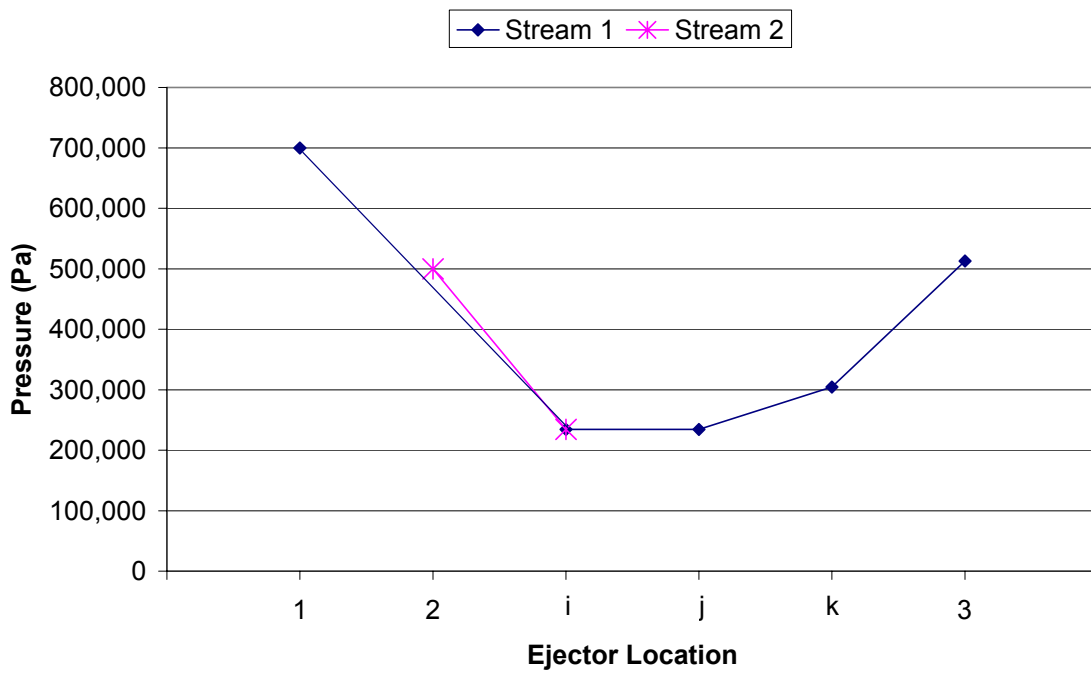
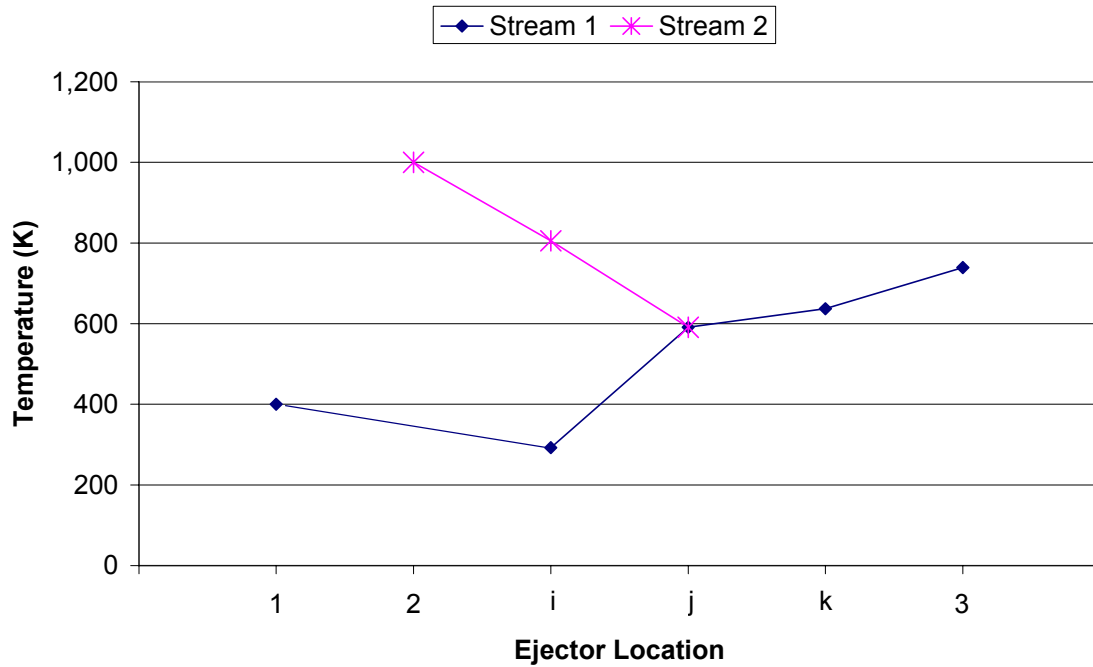
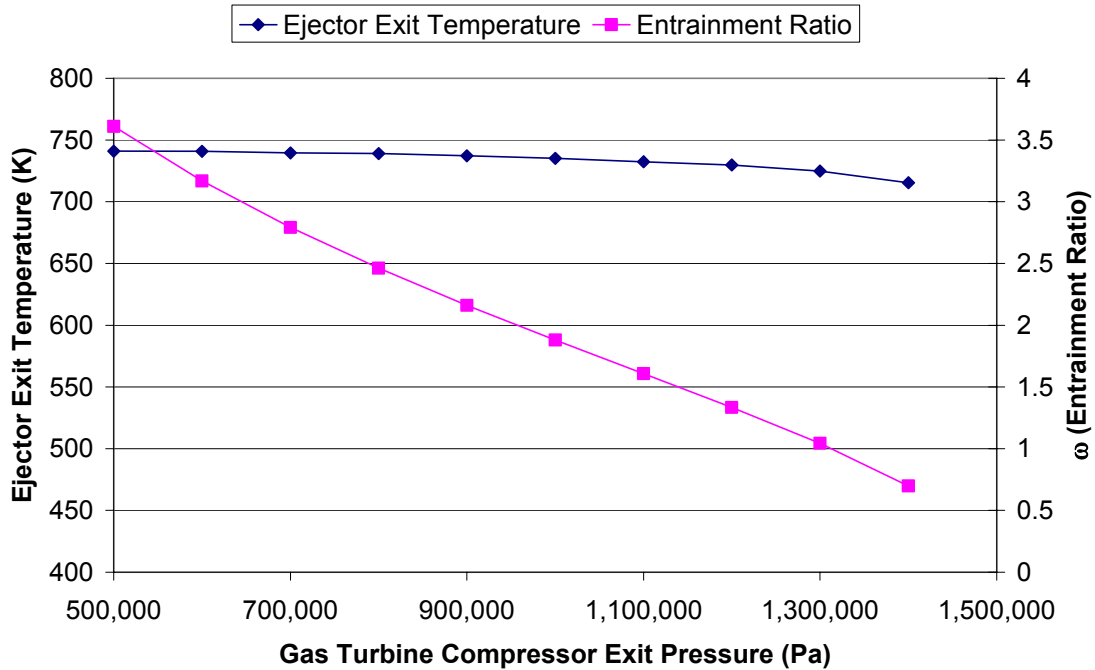


Figure A2.2 - 23: Pressure vs. ejector location for primary and secondary streams.



**Figure A2.2 - 24: Temperature vs. ejector location for primary and secondary streams.**

Figure A2.2 - 25 indicates that for a fixed primary stream temperature of 400 K (from the gas turbine compressor) and a fixed secondary stream temperature of 1000 K and pressure of 500 kPa (from the cathode exit) that the entrainment ratio and ejector exit temperature decrease with increasing primary stream inlet pressure; in agreement with the literature (Keenan and Neumann, 1942).



**Figure A2.2 - 25: Ejector exit temperature and entrainment ratio vs. primary stream pressure.**

### **Cathode BLOWER MODEL**

A cathode recycle blower model was developed and used in place of the ejector model. The purpose of the blower is to recirculate cathode exhaust for mixing with and preheating the air stream fed to the cathode inlet by the gas turbine compressor. A variable speed blower was modeled to allow the temperature of the mixture comprised of fresh air from the compressor and cathode exhaust to be controlled before entering the cathode. This variable speed blower would likely be driven by a motor utilizing a variable speed drive.

The inputs to the blower model are the molar flow rate, mole fractions and temperature of the cathode exhaust, as well as the blower motor power and cathode outlet pressure. Equation 23 governs a dynamic shaft torque balance for the blower from which the shaft velocity can be obtained:

$$J\omega \frac{d\omega}{dt} = P_{motor} + P_{blower} \quad (23)$$

where  $J$  is moment of inertia of the blower in  $\text{kg}\cdot\text{m}^2$ ,  $\omega$  is the rotational velocity of the blower shaft in  $\text{rad/s}$ ,  $P_{motor}$  is the motor power supplied to the blower in  $\text{W}$ ,  $P_{blower}$  is the blower power determined by thermodynamics in  $\text{W}$ .

Blower outlet pressure and flow rate are modeled to be linearly proportional to the blower shaft speed. Assuming a linear relationship between the shaft velocity, flow rate, and pressure ratio in the blower is a good simple first approximation. The blower power is then evaluated by

assuming an overall blower isentropic efficiency of 85%, which includes the blower, motor and variable speed drive efficiencies.

$$P_{blower} = -\frac{1}{\eta_{blower}} \frac{\gamma R T_1}{\gamma - 1} \left[ \left( \frac{P_2}{P_1} \right)^{\frac{\gamma-1}{\gamma}} - 1 \right] \quad (24)$$

Where  $P_{blower}$  is the isentropic blower power in W,  $\eta_{blower}$  is the isentropic blower efficiency,  $\gamma$  is the ratio of specific heats for air,  $R$  is the universal gas constant in J/mol\*K,  $T_1$  is the inlet temperature of the blower in K,  $P_1$  is the inlet pressure of the blower in Pa,  $P_2$  is the outlet pressure of the blower in Pa.

By assuming no reaction within the blower, and knowing the inlet species and temperature, the blower exit temperature can be calculated from conservation of energy. A mixing block that uses conservation of energy and species is used to solve for the outlet temperature and composition of the mixture of blower and compressor outlet streams. The outlet pressure of the blower must be equal to the outlet pressure of the compressor since these streams are mixed at the same pressure.

### **Hybrid System Steady State Analyses**

A number of user defined design parameters for the gas turbine and fuel cell are given in Table A2.2 - 4. These values represent the current steady state design parameters used in the hybrid model and are the result of numerous parametric studies that were carried out to optimize performance requirements.

Parametric analyses were conducted to determine the design factors from Table A2.2 - 4 that have a significant impact on average fuel cell cathode temperature Figure A2.2 - 26, fuel cell power density Figure A2.2 - 27 and ejector pressure drop Figure A2.2 - 28 since these steady state operational performance conditions were the most difficult to simultaneously achieve. This is due to the fact that as fuel cell power density increases, the heat generated in the fuel cell becomes greater, leading to increased temperature rise across the cathode for a given mass flow rate of air. The mass flow rate of air can be increased to cool the cathode but at a significant cost to cycle efficiency due to the increased compressor work required. Insights from Figure A2.2 - 26, Figure A2.2 - 27 and Figure A2.2 - 28 were used to optimize the hybrid system design parameters.

The legend in these plots shows the parameter and range of variation for each analysis. The legend is defined as follows:

E: denotes ejector, where  $P_i$  is pressure at the primary nozzle outlet,  $w$  is the mass flow entrainment ratio (cathode stream to compressor stream),  $P_1$  is the compressor inlet pressure  $P_2$  is the cathode outlet pressure,  $T_1$  is the compressor inlet temperature and  $T_2$  the cathode outlet temperature.

C: denotes compressor, where  $T_o$  is outlet temperature,  $\dot{m}$  is mass flow rate and  $Pr$  is pressure ratio.

T: denotes turbine where  $T_i$  is inlet temperature,  $P_i$  is inlet pressure,  $\dot{m}$  is mass flow rate,  $T_o$  is outlet temperature and Vol is plenum volume.

FC: denotes fuel cell where FF is friction factor, Cell# is the number of cells and Amps is current demand.

**Table A2.2 - 4: Gas turbine and fuel cell design parameters used for steady state operation.**

Compressor Design Parameters		Basis	
Speed	3,600	RPM	
Inlet Temperature	288	K	
Outlet Temperature	550	K	
Inlet Pressure	101.325	kPa	
Pressure Ratio	10		
Mass Flow	135	kg/s	
Max Isentropic Efficiency	88	%	Rao et al. (2006)
Filter Loss	1	%	

Turbine Design Parameters			
Speed	3,600	RPM	
Inlet Temperature	1,065	K	
Outlet Temperature	800	K	
Inlet Pressure	505	kPa	
Outlet Pressure	104.439	kPa	
Mass Flow	128	kg/s	
Max Isentropic Efficiency	92	%	Rao et al. (2006)
Plenum Volume	160	m <sup>3</sup>	

Shaft Design Parameters			
Polar Moment of Inertia	1,127	kg*m <sup>2</sup>	

Gas Turbine Generator Design Parameter			
Efficiency	98.6	%	Rao et al. (2006)

Fuel Cell Design Parameters			
Cell Number	1,939,700	#	
Cell Length	0.1	m	
Cell Width	0.1	m	
Cell Friction Factor	0.048		

Fuel Cell Inverter Design Parameter			
Efficiency	97	%	Rao et al. (2006)

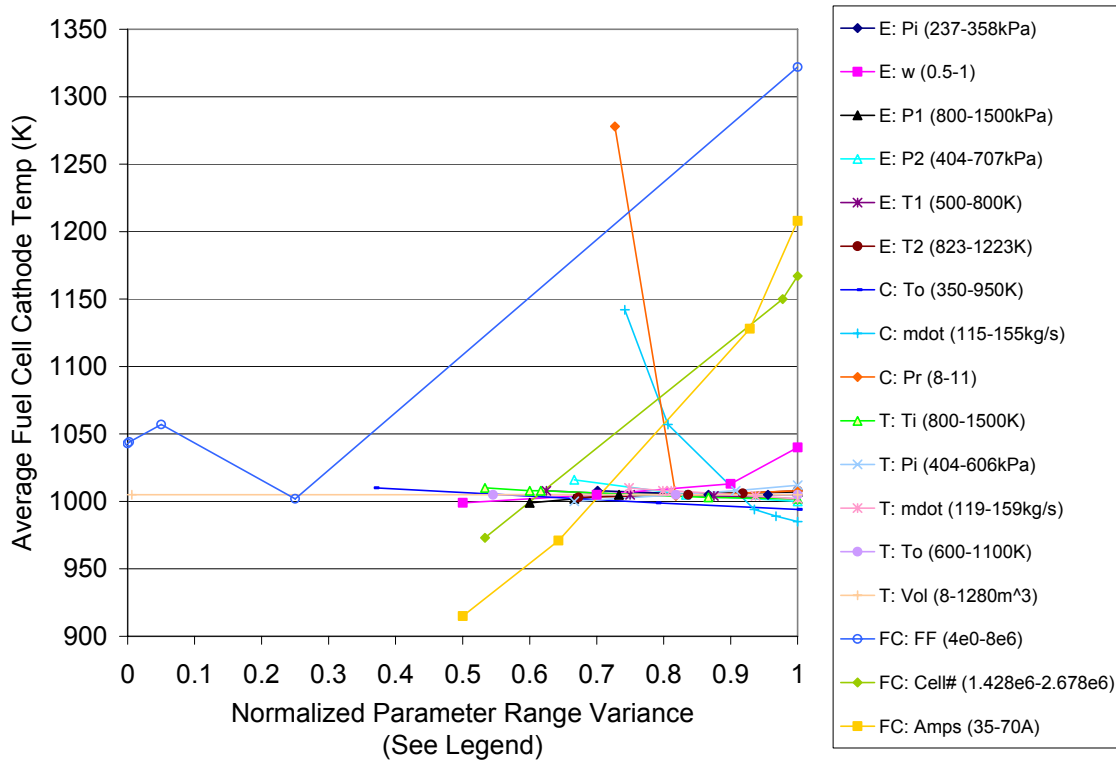


**Figure A2.2 - 26: Average fuel cell cathode operating temperature vs. multiple parameters.**

Each design parameter was varied independently over what was deemed a reasonable range while all the other parameters remained fixed. From Figure A2.2 - 26 it can be seen that fuel cell current demand, friction factor and cell number all have a significant impact on average cathode temperature. Compressor pressure ratio and mass flow rate also have a significant impact. Ejector entrainment ratio has a slight impact. All other parameters show negligible impact.

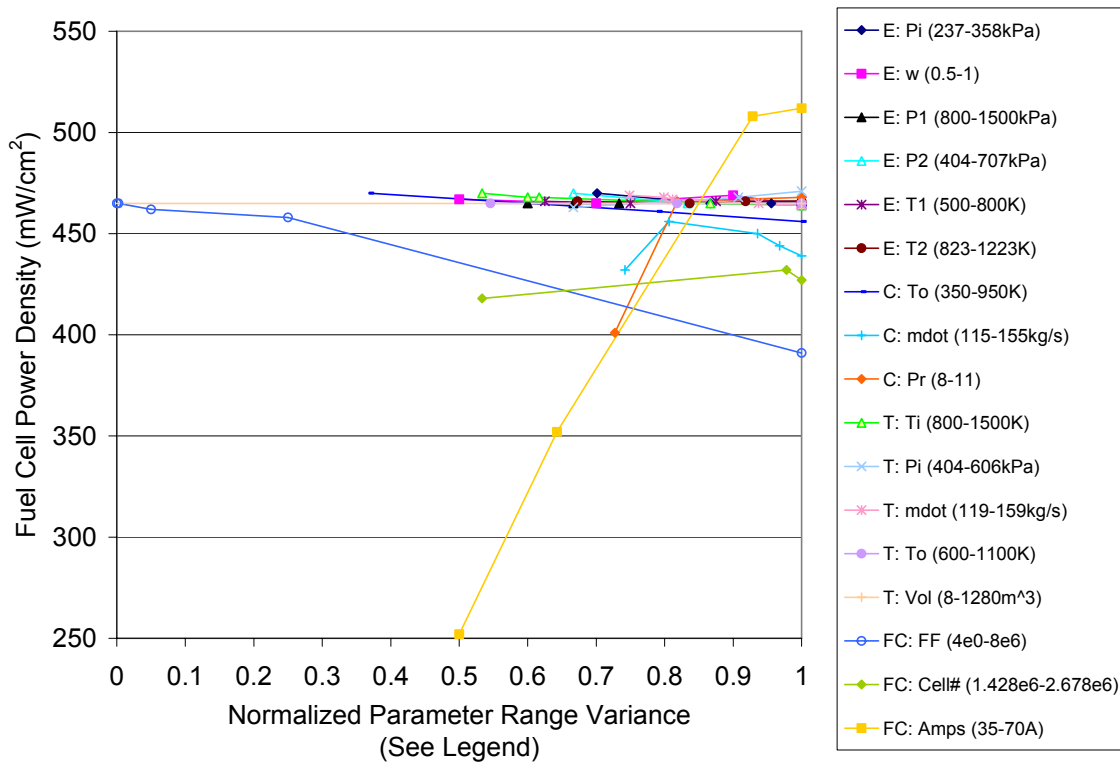


**Figure A2.2 - 27: Fuel cell power density vs. multiple parameters.**

From Figure A2.2 - 27 it can be seen that fuel cell current demand, friction factor and cell number all have a significant impact on fuel cell power density. Compressor pressure ratio, mass flow rate and outlet temperature also have a significant impact and compressor outlet pressure a slight impact. All other parameters show negligible impact.

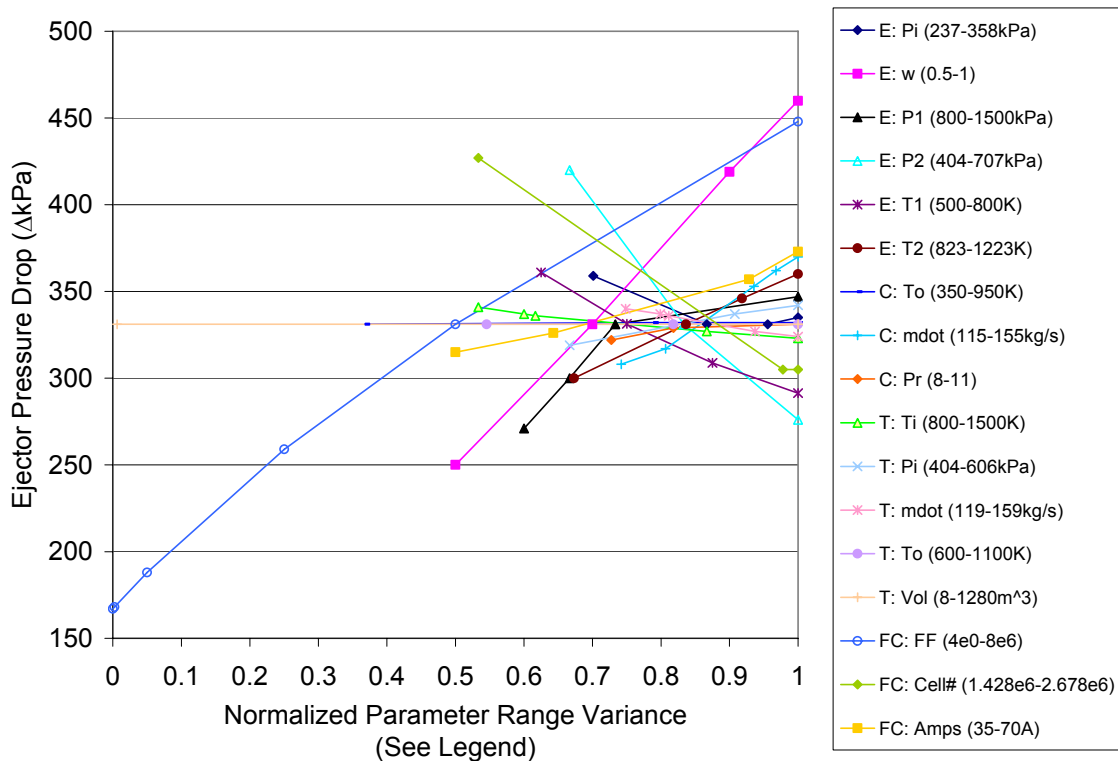


**Figure A2.2 - 28: Ejector pressure drop vs. multiple parameters.**

From Figure A2.2 - 28 it can be seen that just about every parameter has some impact on ejector pressure drop with fuel cell friction factor and ejector entrainment ratio having the greatest impacts.

The design parameters given in Table A2.2 - 4 were used to establish steady state performance of the hybrid system Table A2.2 - 5. The two DOE steady state operational goals that were the most difficult to meet while simultaneously meeting all other operational targets and satisfying energy and mass conservation within the context of the integrated systems were the minimum power density of 500 mW/cm<sup>2</sup> and a temperature rise across the cathode of less than 100 K. These two performance goals compete with each other since the temperature rise across the cathode increases with power density. A balance was struck leading to the steady state conditions in Table A2.2 - 5.

**Table A2.2 - 5: Gas turbine and fuel cell steady state performance values (cathode ejector).**

Fuel Cell Power	86.04	MW
Gas Turbine Power	14.28	MW
Total Power	100.32	MW
Fuel Cell Efficiency	51	%
Gas Turbine Efficiency	9	%
Total Cycle Efficiency	60	%
Average Fuel Cell Operating Temperature	1001	(K)
Temperature Rise Across Anode	101	$\Delta T$ (K)
Temperature Rise Across Cathode	158	$\Delta T$ (K)
Fuel Cell Current	55	A
Fuel Cell Voltage	0.83	Volts
Fuel Cell Power Density	457	$mW/cm^2$
Cathode Outlet Pressure	507	kPa
Air Preheat in Fuel Cell Stack	111	$\Delta T$ (K)
Pressure Drop Across Fuel Cell	63	$\Delta P$ (kPa)
Air Preheat in Ejector	222	$\Delta T$ (K)
Ejector Pressure Drop	316	$\Delta P$ (kPa)
Ejector Mass Flow Entrainment Ratio (Cathode:Compressor)	0.87	
Oxygen Utilization	18	%

Again, it is most likely possible to meet the combined goals of less than 100 K temperature rise across the cathode at  $500 mW/cm^2$  but this would only be achieved at significantly higher air mass flow rates, leading to lower system efficiency. Figure A2.2 - 29 presents results from the dynamic model that investigates the requirements for meeting these goals.

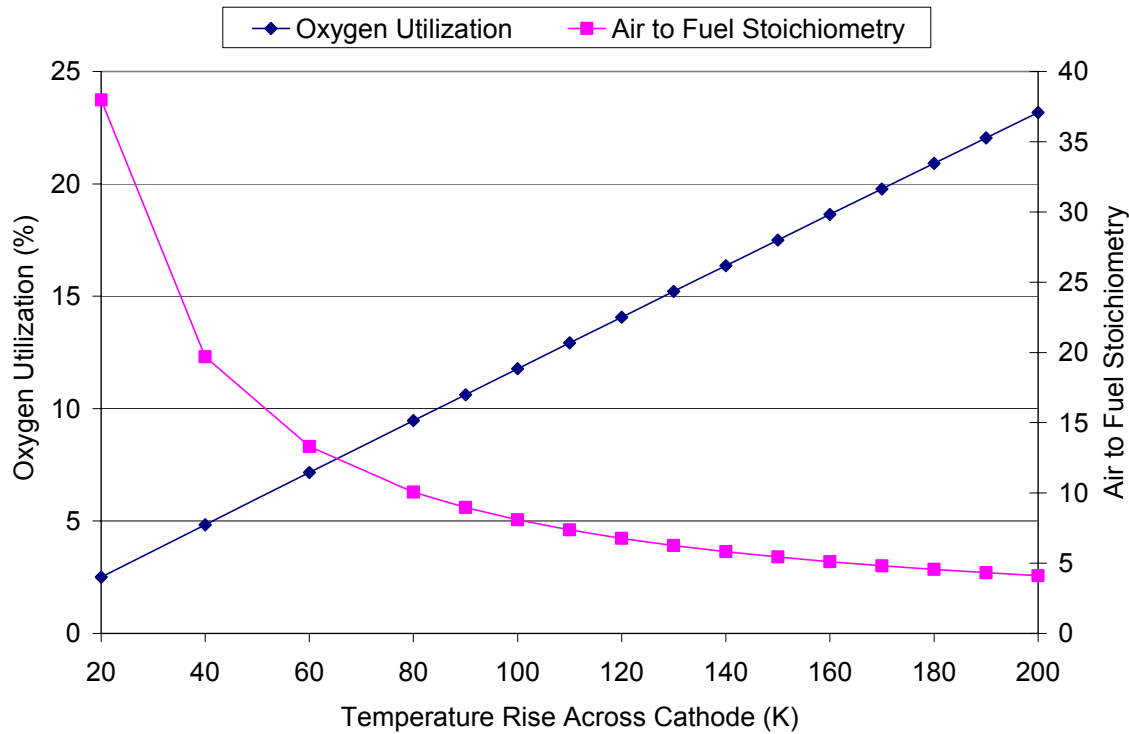


**Figure A2.2 - 29: Fuel cell oxygen utilization and air-to-fuel stoichiometry vs. cathode temperature rise.**

Currently the temperature rise across the cathode is 158 K, this corresponds to an oxygen utilization of 18% and air-to-fuel stoichiometry of 5. In order to meet the 100 K DOE target for temperature rise across the cathode an oxygen utilization of 12% and air-to-fuel stoichiometry of 8 would be required (Figure A2.2 - 29). This corresponds to a 60% increase in air-to-fuel stoichiometry, which will diminish cycle efficiency. Again, these tradeoffs led to the choice of steady state operational conditions shown in Table A2.2 - 5. Note that one of the main reasons the air flow requirement for low temperature rise is so severe in the current system configuration is due to the fact that no internal endothermic fuel reforming occurs in the fuel cell.

A comparison was made between steady state performance values for the hybrid system utilizing a cathode blower (

Table A2.2 - 6) and a cathode ejector (

Table A2.2 - 7). All of the DOE steady state operational goals are met in each case.

**Table A2.2 - 6: Hybrid system steady state values for various cycle pressures using a cathode blower.**

<b>Nominal Cycle Pressure</b>	<b>5atm</b>	<b>8atm</b>	<b>10atm</b>	
Fuel Cell Power	90,890	86,367	85,096	MW
Gas Turbine Power	19,864	22,301	22,795	MW
Blower Power	5,665	2,045	1,075	MW
Total Power	105,090	106,620	106,820	MW
Fuel Cell Efficiency	52.5	52.9	53.3	%
Gas Turbine Efficiency	11.5	13.7	14.3	%
Total Efficiency	60.7	65.3	66.9	%
Average Fuel Cell Operating Temperature	1016	1016	1015	(K)
Temperature Rise Across Anode	95	97	97	$\Delta T$ (K)
Temperature Rise Across Cathode	144	141	143	$\Delta T$ (K)
Fuel Cell Current	58	57.5	57	A
Fuel Cell Voltage	0.85	0.86	0.86	Volts
Fuel Cell Power Density	492	492	491	mW/cm <sup>2</sup>
Turbine Inlet Pressure	504	804	1011	kPa
Air Preheat in Fuel Cell Stack	144	145	143	$\Delta T$ (K)
Pressure Drop Across Fuel Cell Air Side	86	55	42	$\Delta P$ (kPa)
Air Preheat of Blower/Compressor Mixture	304	245	211	$\Delta T$ (K)
Blower Pressure Rise	69	44	32	$\Delta P$ (kPa)
Blower Molar Recycle Ratio (Blower:Cathode Outlet)	0.48	0.45	0.42	
Oxygen Utilization	0.17	0.17	0.17	%
Fuel Utilization	0.8	0.8	0.8	%
Compressor Outlet Pressure	590	859	1053	kPa

It is unknown whether currently available blowers can operate at the temperatures or maintain the pressure rises found necessary in these studies.

**Table A2.2 - 7: Hybrid system steady state values for various cycle pressures using a cathode ejector.**

<b>Nominal Cycle Pressure</b>	<b>5atm</b>	<b>8atm</b>	<b>10atm</b>	
Fuel Cell Power	91,220	86,764	84,505	MW
Gas Turbine Power	9,988	15,229	16,401	MW
Total Power	101,210	101,990	100,910	MW
Fuel Cell Efficiency	52.7	53.4	53.8	%
Gas Turbine Efficiency	5.8	9.4	10.4	%
Total Cycle Efficiency	58.4	62.8	64.3	%
Average Fuel Cell Operating Temperature	1024	1025	1023	(K)
Temperature Rise Across Anode	98	87	74	$\Delta T$ (K)
Temperature Rise Across Cathode	146	139	139	$\Delta T$ (K)
Fuel Cell Current	58	58	58	A
Fuel Cell Voltage	0.85	0.86	0.87	Volts
Fuel Cell Power Density	494	501	505	mW/cm <sup>2</sup>
Turbine Inlet Pressure	504	806	1008	kPa
Air Preheat in Fuel Cell Stack	148	145	141	$\Delta T$ (K)
Pressure Drop Across Fuel Cell Air Side	83	55	43	$\Delta P$ (kPa)
Air Preheat in Ejector	236	205	179	$\Delta T$ (K)
Ejector Pressure Drop	337	302	298	$\Delta P$ (kPa)
Ejector Mass Flow Entrainment Ratio (Cathode:Compressor)	0.83	0.76	0.68	
Oxygen Utilization	0.18	0.17	0.17	%
Fuel Utilization	0.8	0.8	0.8	%
Compressor Outlet Pressure	924	1163	1348	kPa

The steady-state analyses show that the hybrid fuel cell gas turbine cycle using a cathode recycle blower is more efficient than that using the ejector in each case by about 3 percentage points. This efficiency gain is predominantly realized by increased power output from the gas turbine, since the fuel cell operates very similarly in both cases. Much of the gas turbine power is consumed to overcome the pressure drop across the ejector in the case when it is used for cathode recirculation. The blower, in contrast, is electrically driven and doesn't require pressure from the compressor to produce cathode recirculation to preheat the cycle air flow. The blower work ends up being considerably less than the compressor work required by the ejector. Compressor efficiency is higher at lower pressure ratios and since the cathode blower allows for lower pressure ratio operation than the cathode ejector, this also augments cycle efficiency.

The results from the MATLAB Simulink model were compared to those of ASPEN, which is industry standard software for chemical plant design, as a means of validating the Simulink model. These results can be found in

Table A2.2 - 8 and Table A2.2 - 9.

**Table A2.2 - 8: Percent error between Simulink and ASPEN results for steady state power (using cathode blower).**

<b>Blower:</b>	<b>Fuel Cell Power</b>	<b>Gas Turbine Power</b>	<b>System Power</b>	<b>Blower Power</b>
<b>5 atm</b>	0.21%	-0.91%	-0.02%	0.50%
<b>8 atm</b>	0.03%	-1.20%	-0.17%	-2.95%
<b>10 atm</b>	0.02%	-1.21%	-0.22%	-1.76%

**Table A2.2 - 9: Percent error between Simulink and ASPEN results for steady state power (using cathode ejector).**

<b>Ejector:</b>	<b>Fuel Cell Power</b>	<b>Gas Turbine Power</b>	<b>System Power</b>
<b>5 atm</b>	-0.18%	-1.98%	-0.36%
<b>8 atm</b>	-0.25%	-1.64%	-0.45%
<b>10 atm</b>	-0.17%	-1.62%	-0.41%

The Simulink model predicts a slightly lower system power than ASPEN in all cases, where the percent error between the Simulink and ASPEN models ranges from -0.02% to -0.45%

## **HYBRID SYSTEM DYNAMIC ANALYSES**

### **Model Utilizing A Cathode Ejector**

A critical need in maintaining gas turbine operational stability and lifetime is the avoidance of compressor rotating stall and surge (Greitzer, 1980). In order to test the impact of various power demand and fuel composition changes on compressor performance, the hybrid power block model was subjected to a step change in these conditions from an initial steady state operating point and then allowed to reach a new final steady state operating point. For this section where a cathode ejector is used, the blue point in these figures always represents the steady state condition outlined in Table A2.2 - 5 and the red point the off design condition outcome of the dynamic test.

The bulk of this study focused on various hybrid system perturbations that result in compressor surge as well as other failure mechanisms such as excessive, anode-cathode inlet pressure difference, anode and cathode inlet-outlet temperature differences, average fuel cell cathode temperature, tri-layer (electrolyte) temperature and gas turbine shaft speed. Methods to mitigate these problems are investigated.

Two separate control strategies were implemented during the dynamic testing. “Control strategy #1” uses a proportional integral differential (PID) feedback loop to control gas turbine shaft speed at 3600 RPM. This strategy assumes use of a synchronous generator.

“Control strategy #2” uses a cascade PID loop that primarily controls fuel cell tri-layer temperature and secondarily controls gas turbine shaft speed, assuming an asynchronous generator. The hybrid system was subjected to the same set of dynamic perturbations for both control strategies to assess the impact that each has on compressor surge. The first set of dynamic analyses presented in this report will focus on control strategy #1.

## Control Strategy #1:

### Fuel Cell Current Demand Perturbations

A PID controller is employed within the model to keep the GT at an operational speed of 3600 RPM. It was found that RPM must be controlled during some dynamics to keep the model from diverging. In all dynamic tests the GT will start and end at this speed unless the model cannot converge upon a solution.

When a PID controller is used to maintain shaft RPM, very large load shed dynamics can be tolerated in the model. Figure A2.2 - 30 demonstrates that the compressor can recover from a 50% load shed when shaft RPM is controlled while avoiding the surge line. When the shaft speed is uncontrolled load ramps and sheds of 10% are not tolerated by the model due to divergence of shaft RPM.

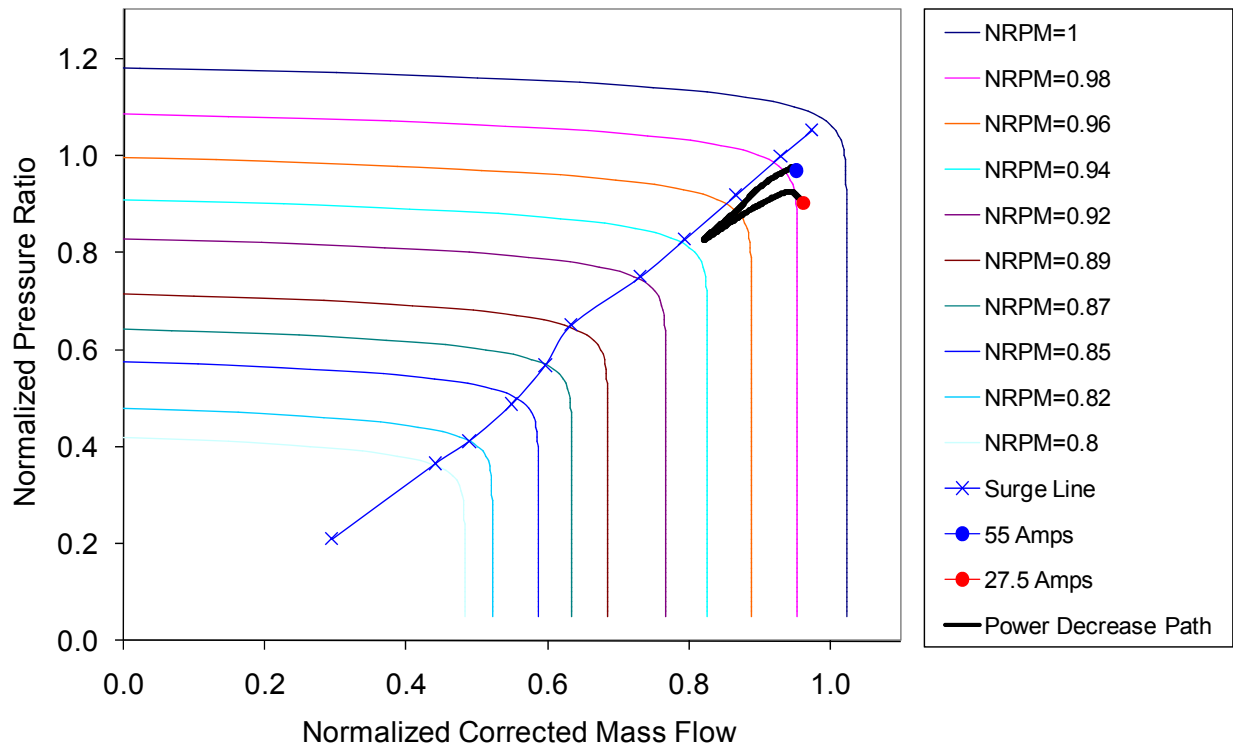
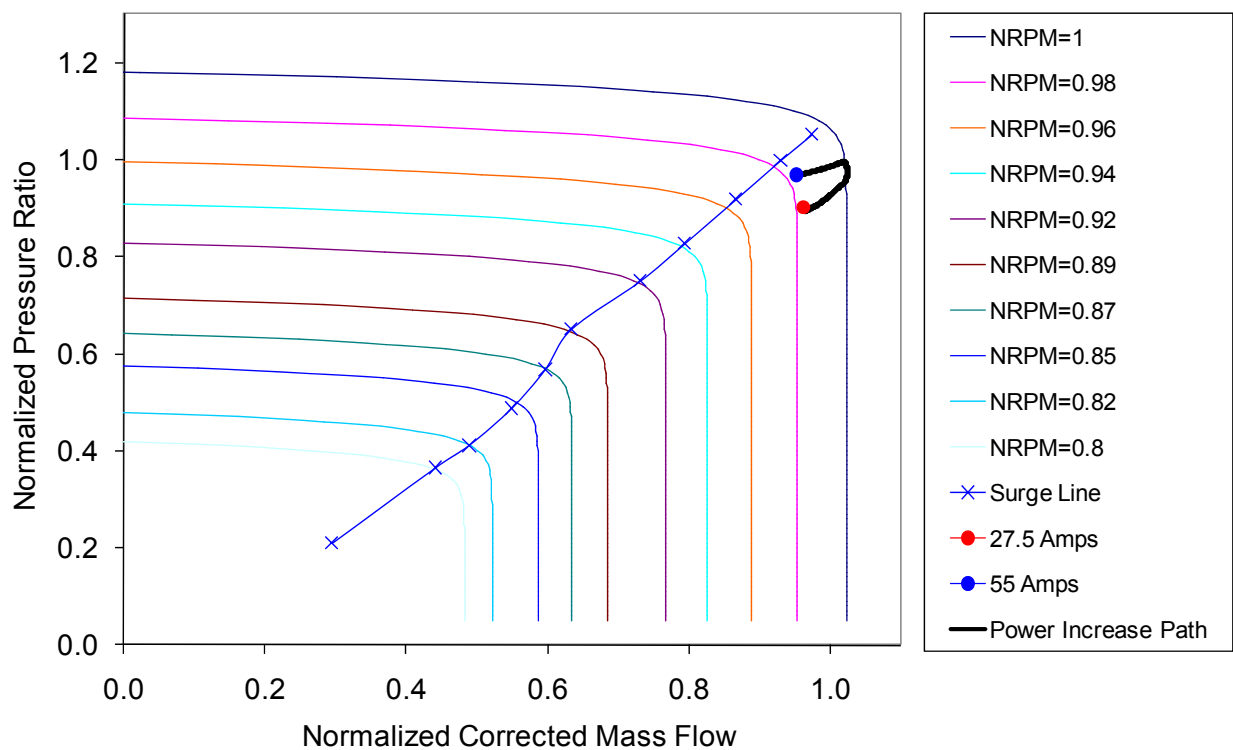


**Figure A2.2 - 30: Compressor dynamic response to a fuel cell load decrease from 100% (blue) to 50% (red) design state using weak controller parameters. PID control is applied to shaft RPM.**

The gas turbine model takes into account the polar moment of inertia when simulating rotational dynamics. The polar moment of inertia for a single shaft GT coupled to a generator

should take into account the entire rotating mass of all relevant components, i.e., compressor, shaft, turbine and generator. For this work the moment of inertia has been set to  $1,127 \text{ kg}\cdot\text{m}^2$ . In order to test the impact of varying the polar moment of inertia on system dynamics, the case in Figure A2.2 - 30 was run again at  $563.5 \text{ kg}\cdot\text{m}^2$  and  $2,254 \text{ kg}\cdot\text{m}^2$ . Both cases showed that the polar moment of inertia had a very limited impact of on the path taken by the system through the dynamic.

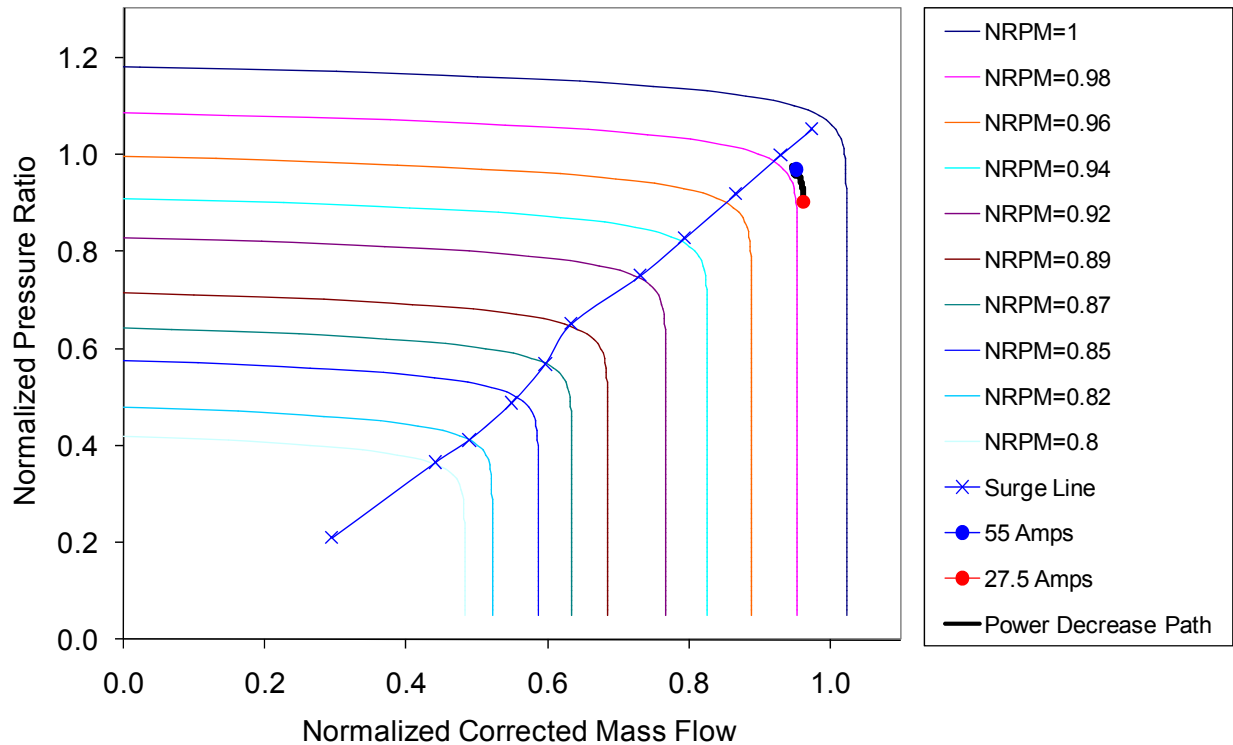
Figure A2.2 - 31 shows that when the fuel cell is subjected to a 50% increase in power demand (red point) the compressor must increase in speed, mass flow and pressure ratio along the path shown in black to eventually settle at a new steady state condition (blue point). Under this step change in power demand the compressor remains in a stable operational range, avoiding the surge line.



**Figure A2.2 - 31: Compressor dynamic response to a fuel cell load increase from 50% (red) to 100% (blue) design state using weak controller parameters. PID control is applied to shaft RPM.**

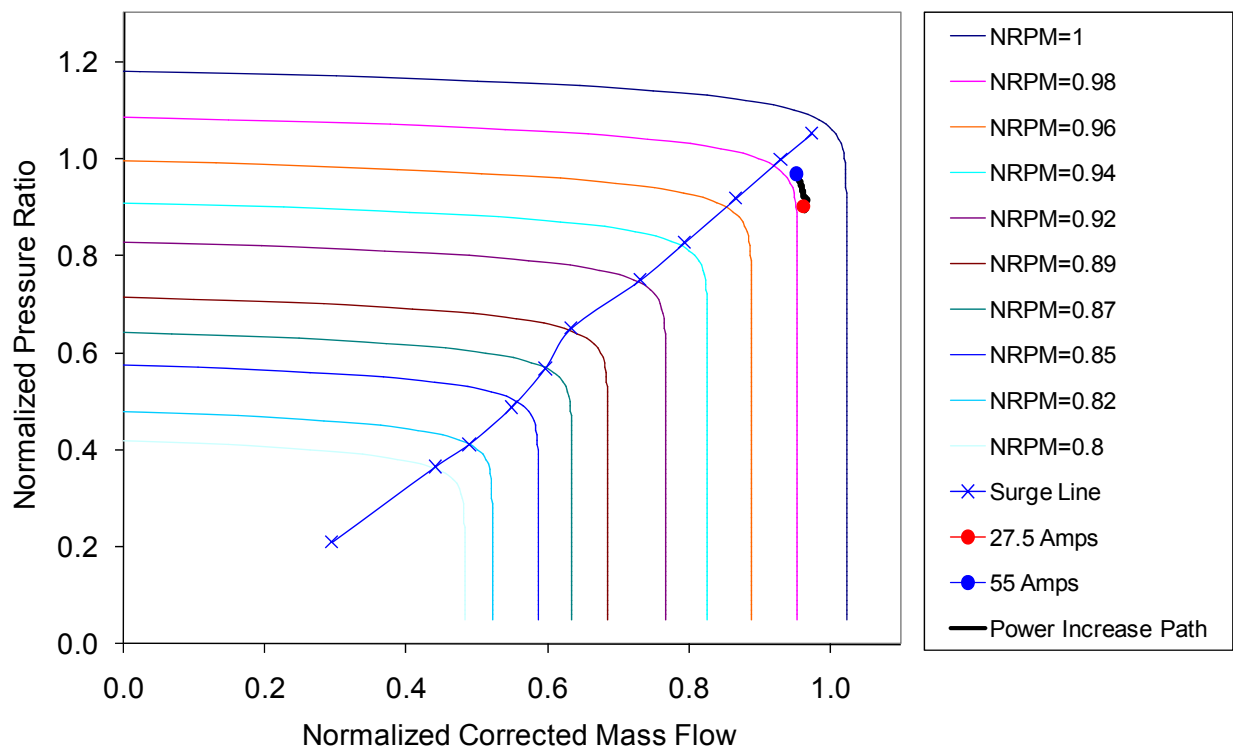
The compressor response to the load shed shown in Figure A2.2 - 30 is a decrease in speed, mass flow and pressure ratio from the initial steady state condition (blue point) along the path shown in black to eventually settle at a new steady state condition (red point). In order to investigate the impact that the PID controller parameters have on dynamic compressor response the cases shown in Figure A2.2 - 30 and Figure A2.2 - 31 were run again. In these new cases (Figure A2.2 - 32 and Figure A2.2 - 33) the PID parameters were altered in an effort to maintain constant shaft speed throughout the dynamic response.

Figure A2.2 - 32 shows the same load shed perturbation as shown in Figure A2.2 - 30 and demonstrates that changing PID parameters can alter the path travelled between the two steady state end points but not the steady state points themselves. The parameters used in the PID controller for Figure A2.2 - 30 are  $P = 50$ ,  $I = 0.1$  and  $D = 0$  and for Figure A2.2 - 32 are  $P = 1000$ ,  $I = 10$  and  $D = 0$ . The results of the new PID parameters used in Figure A2.2 - 32 are that constant shaft speed is maintained throughout the dynamic response and there is much less danger of surge as compared to Figure A2.2 - 30.



**Figure A2.2 - 32: Compressor dynamic response to a fuel cell load decrease from 100% (blue) to 50% (red) design state using robust controller parameters. PID control is applied to shaft RPM.**

The same trends outlined in comparing Figure A2.2 - 30 to Figure A2.2 - 32 are observed in comparing Figure A2.2 - 31 (50% load ramp with weak PID controller parameters) to Figure A2.2 - 33 (50% load ramp with robust PID controller parameters).



**Figure A2.2 - 33: Compressor dynamic response to a fuel cell load increase from 50% (red) to 100% (blue) design state using robust controller parameters. PID control is applied to shaft RPM.**

### Syngas Hydrogen Composition Perturbation (Balanced with Nitrogen)

For the fuel composition perturbations the “robust” PID controller parameters of  $P = 1000$ ,  $I = 10$  and  $D = 0$  were used. Figure A2.2 - 34 shows the dynamic response to a 50% decrease in fuel hydrogen replaced with nitrogen. The compressor follows a constant speed path that crosses the surge line as mass flow decreases and pressure ratio increases. Although it is unlikely that the syngas composition would be changed this drastically in the short step-wise fashion modeled here, it shows that if the power block was subjected to this type of dynamic input the compressor could be thrown into surge.

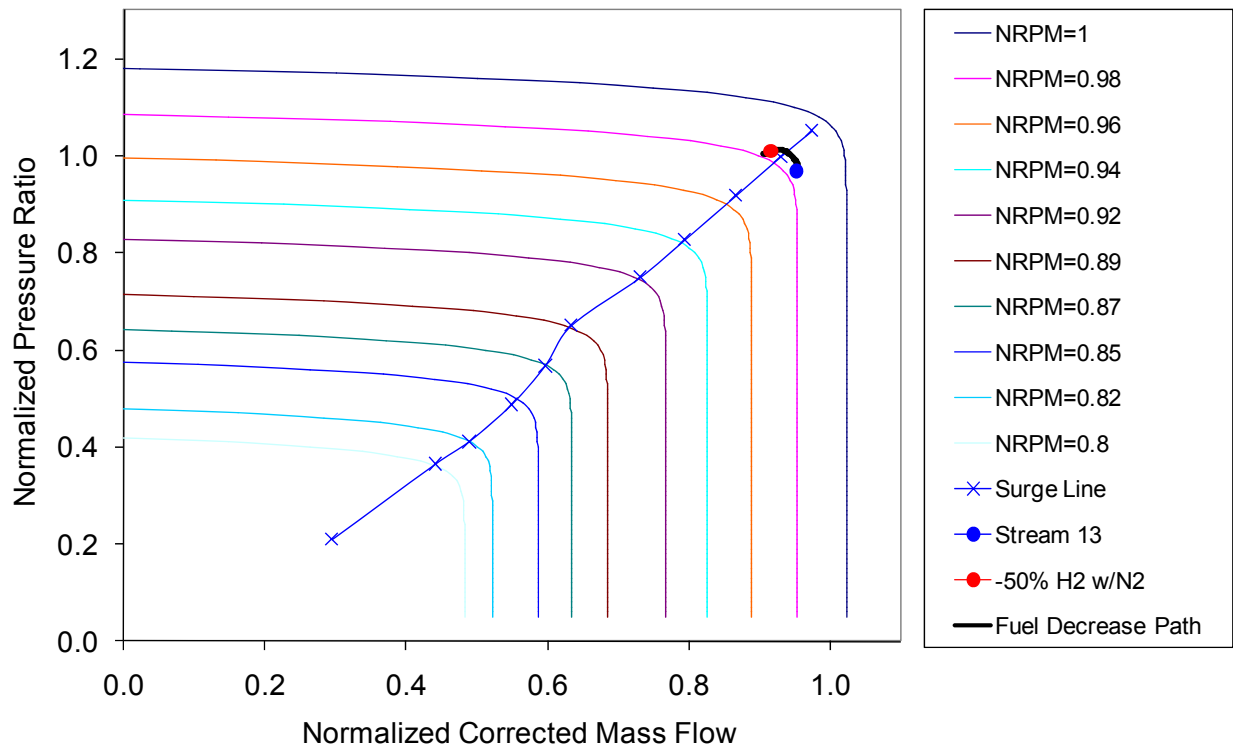


**Figure A2.2 - 34: Compressor dynamic response to a 50% decrease in fuel hydrogen balanced with nitrogen. Initial state A (blue) to final state B (red). PID control is applied to shaft RPM.**

### Syngas Hydrogen Composition Perturbation (Balanced with Steam)

Figure A2.2 - 35 shows the dynamic response to a 50% decrease in fuel hydrogen replaced with steam. In this case the compressor diverges from the ideal constant speed path and meets the surge line as mass flow decreases and pressure ratio increases.

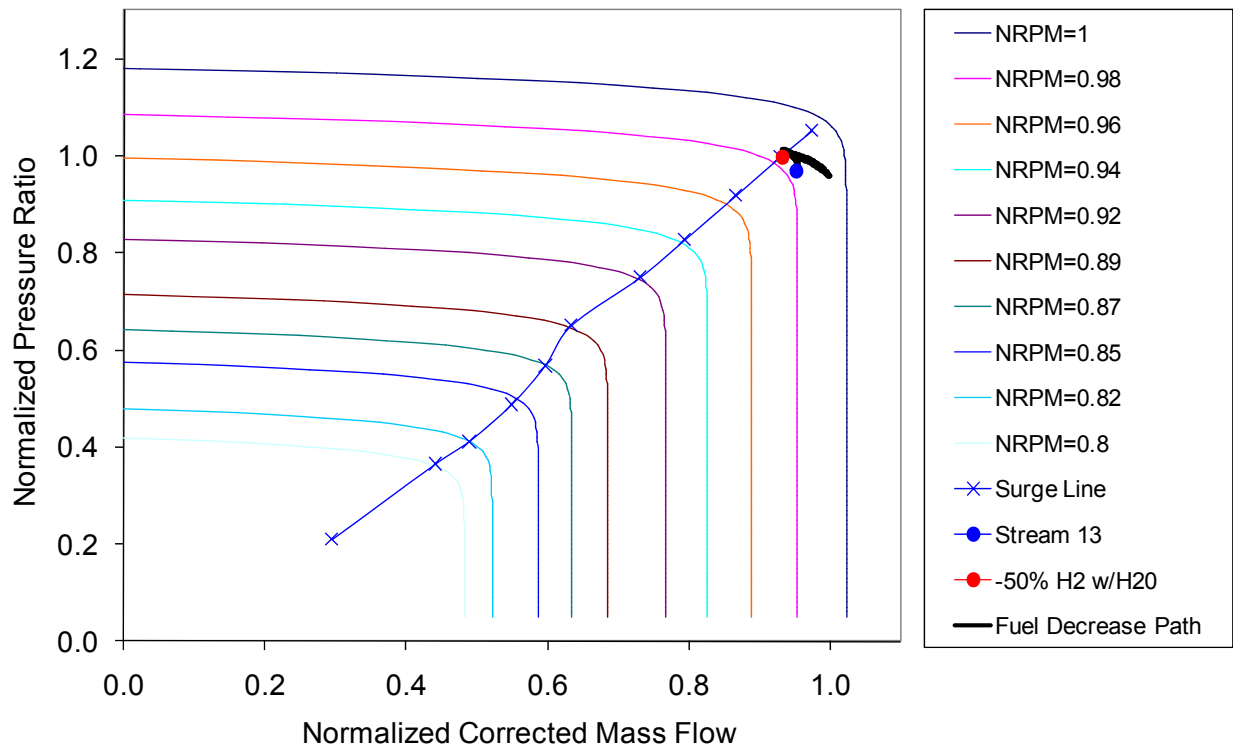


**Figure A2.2 - 35: Compressor dynamic response to a 50% decrease in fuel hydrogen balanced with steam. Initial state A (blue) to final state B (red). PID control is applied to shaft RPM.**

**Control Strategy #2:**

The only difference between control strategy #1 and #2 is that the latter controls fuel cell tri-layer temperature at 1100 K in all cases throughout the dynamic system response to perturbations. This is primarily accomplished by varying the air mass flow rate through the compressor. Unlike the previous analyses presented for control strategy #1 (Figure A2.2 - 30 - Figure A2.2 - 35) the compressor shaft speed is not controlled at 3,600 RPM, but rather can vary to accommodate/produce the necessary variations in air flow rates in order to maintain fuel cell temperature. This new controller is often referred to as a “cascade controller” throughout this report.

In the case of Figure A2.2 - 32 where fuel cell temperature is uncontrolled, surge is not encountered, but during this transient the fuel cell electrolyte temperature drops from 1,083 K at state A to 906 K at state B, and the average fuel cell temperature as measured across the cathode drops from 1009 K at state A to 854 K at state B. The new controller strives to reduce the magnitude of dynamic fuel cell temperature fluctuations and thus ensure stack life is not severely degraded during transients.

## Fuel Cell Current Demand Perturbations

Dynamic results corresponding to load sheds of 10%, 25% and 50% can be found in Figure A2.2 - 36, Figure A2.2 - 37 and Figure A2.2 - 38, respectively. It is apparent that for larger load sheds surge becomes more of a risk. Load sheds can lead to surge since for a lower fuel cell power set-point less fuel and air are needed in the fuel cell which in turn reduces mass flow through the compressor. If compressor mass flow decreases faster than the pressure ratio surge can occur (Kurz & White, 2004). The benefit of the cascade controller is that it holds the electrolyte temperature very close to 1,100 K throughout all cases except the 50% load shed where surge occurs. For the 10%, 25% and 50% load sheds the end state RPM is 3,515, 3,377, and divergent (surge) for the three cases, respectively.

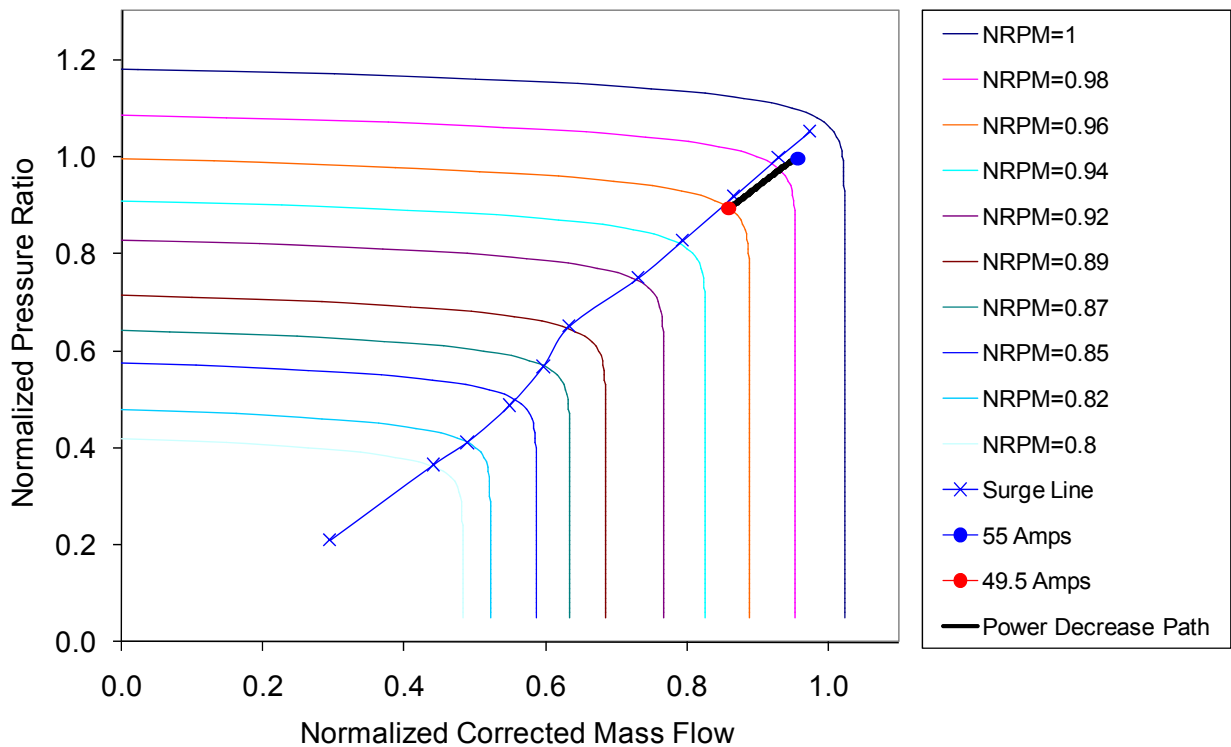


**Figure A2.2 - 36: Compressor dynamic response to a fuel cell load decrease from 100% (blue) to 90% (red) design state when cascade PID control is applied to fuel cell temperature and shaft RPM.**

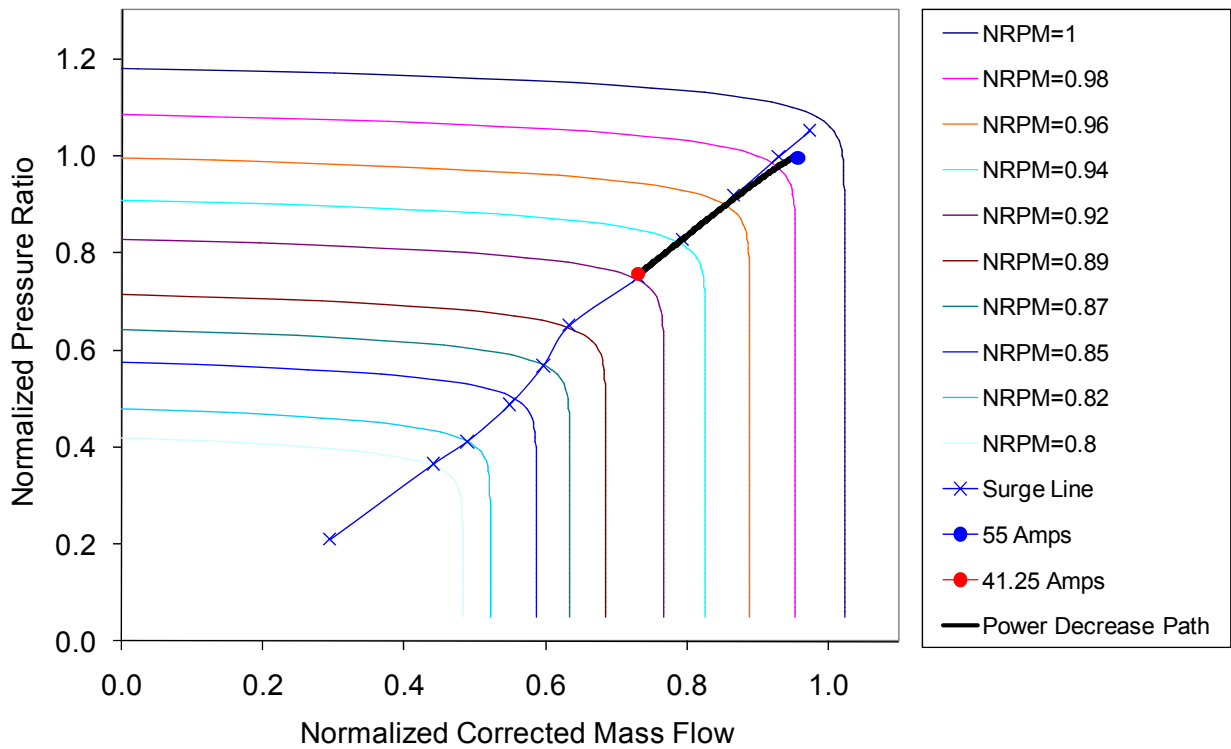


**Figure A2.2 - 37: Compressor dynamic response to a fuel cell load decrease from 100% (blue) to 75% (red) design state when cascade PID control is applied to fuel cell temperature and shaft RPM.**

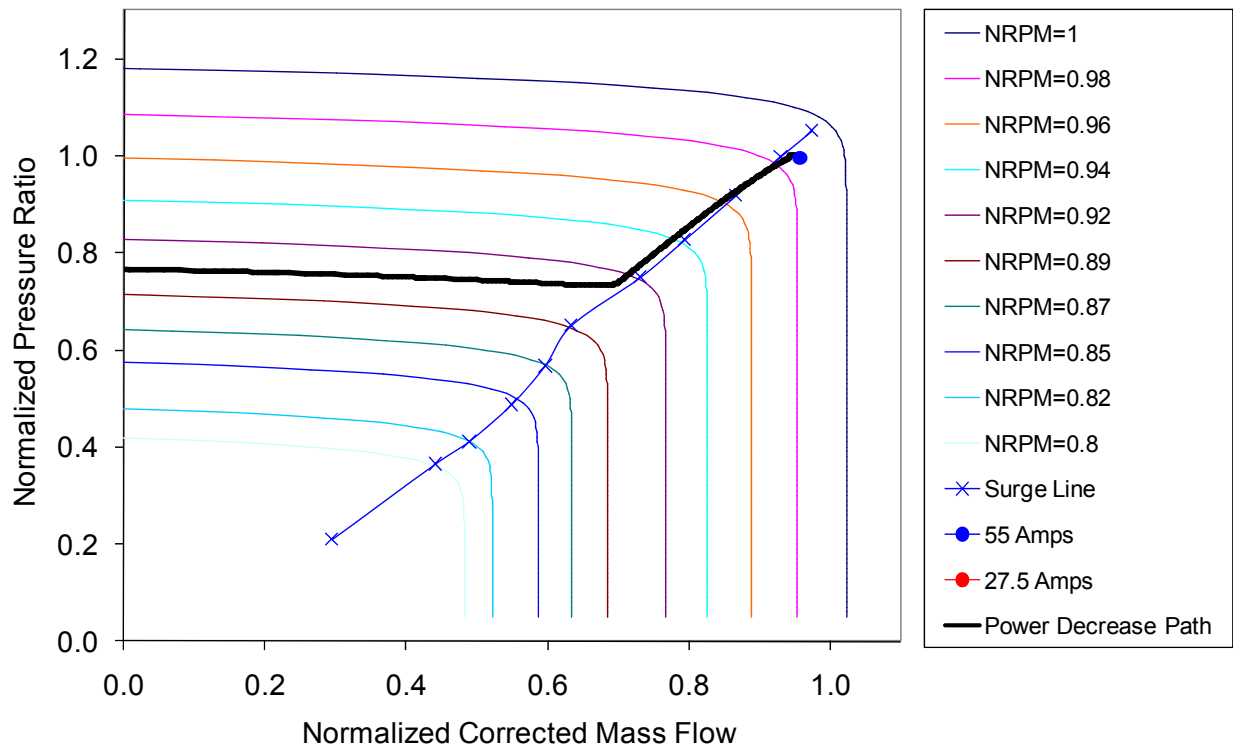


**Figure A2.2 - 38: Compressor dynamic response to a fuel cell load decrease from 100% (blue) to 50% (red) design state when cascade PID control is applied to fuel cell temperature and shaft RPM.**

### Syngas Hydrogen Composition Perturbation (Balanced with Nitrogen)

Another dynamic that the hybrid model was subjected to was a decrease in syngas hydrogen composition balanced with nitrogen. The results from 10%, 25% and 50% decreases in syngas hydrogen concentration can be found in Figure A2.2 - 39, Figure A2.2 - 40 and Figure A2.2 - 41, respectively. As syngas hydrogen content is decreased there is less heat generation in the fuel cell stack as the inert nitrogen absorbs sensible enthalpy, this in turn reduces the required compressor air mass flow for a given fuel cell stack temperature and surge is approached.

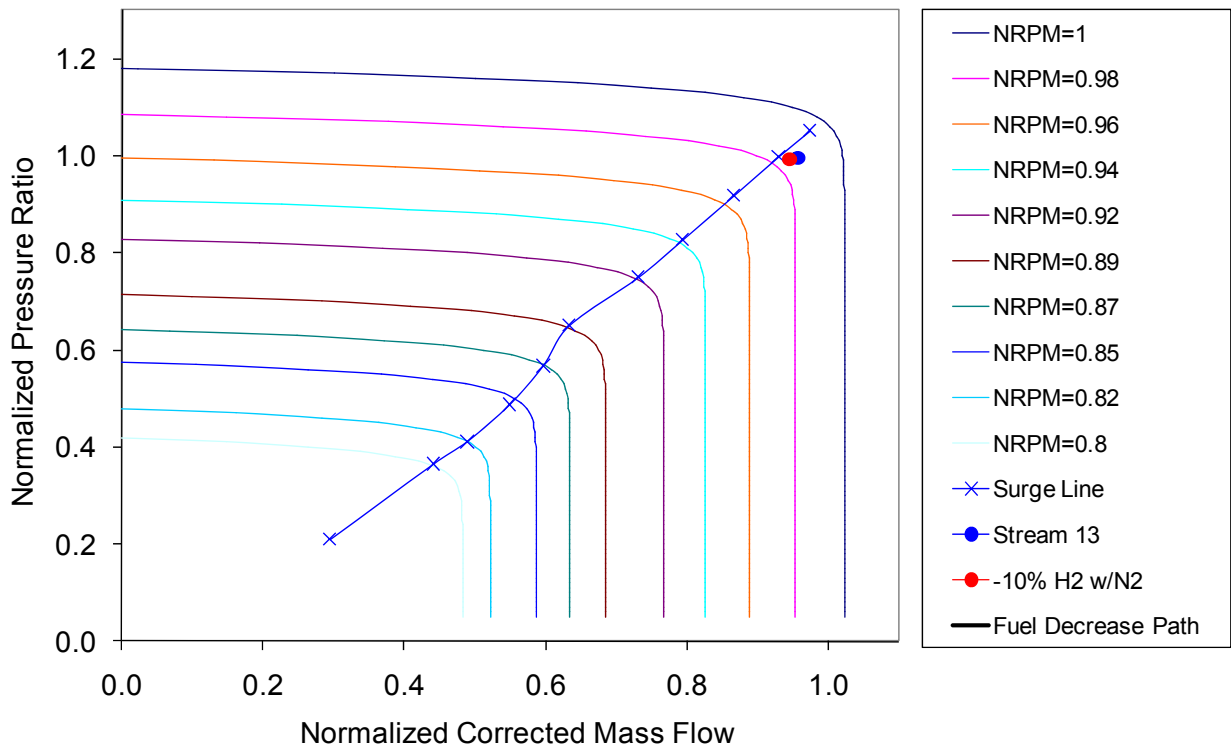


**Figure A2.2 - 39: Compressor dynamic response to a 10% decrease in fuel hydrogen balanced with nitrogen. Initial state A (blue) to final state B (red) when cascade PID control is applied to fuel cell temperature and shaft RPM.**

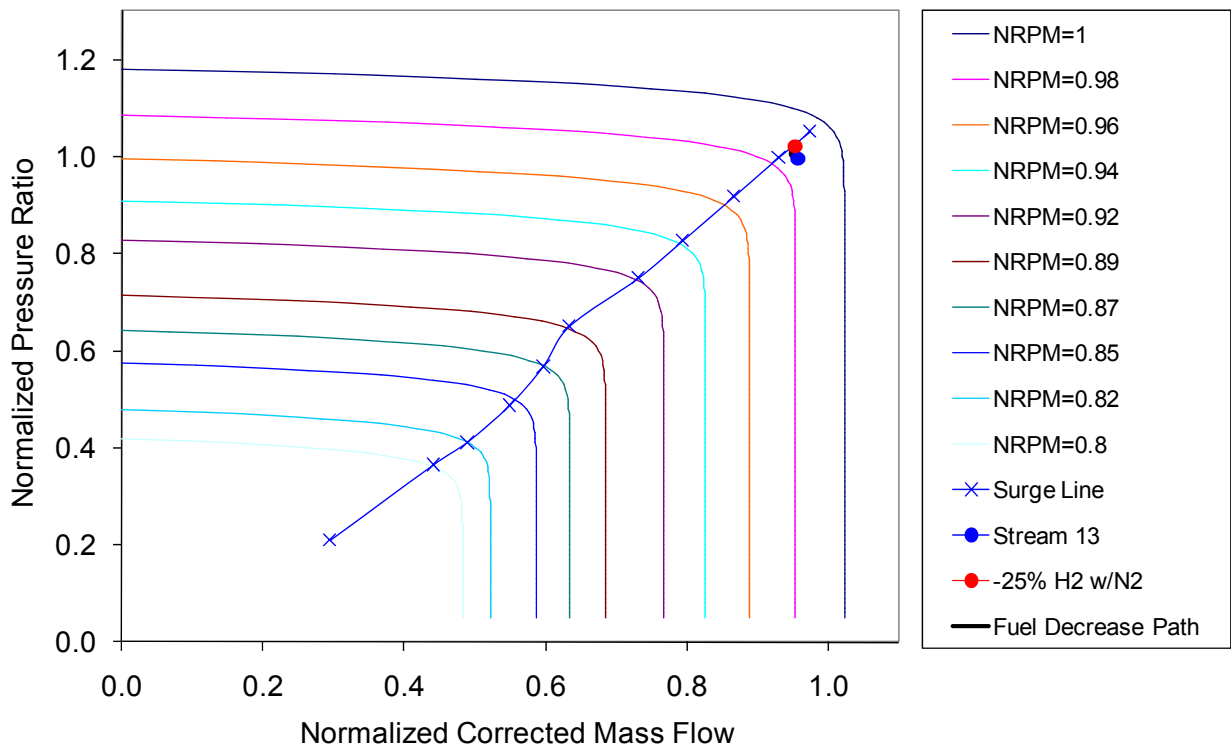


**Figure A2.2 - 40: Compressor dynamic response to a 25% decrease in fuel hydrogen balanced with nitrogen. Initial state A (blue) to final state B (red) when cascade PID control is applied to fuel cell temperature and shaft RPM.**

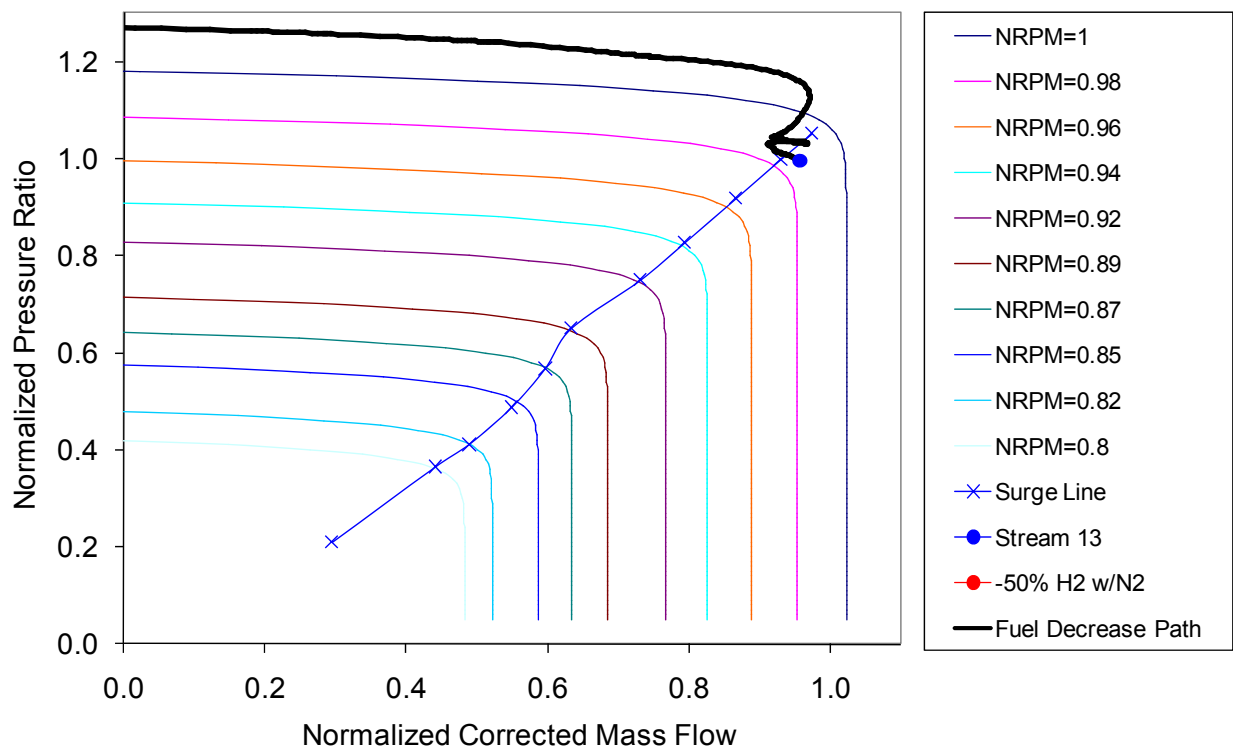


**Figure A2.2 - 41: Compressor dynamic response to a 50% decrease in fuel hydrogen balanced with nitrogen. Initial state A (blue) to final state B (red) when cascade PID control is applied to fuel cell temperature and shaft RPM.**

### Syngas Hydrogen Composition Perturbation (Balanced with Steam)

The effect of altering syngas composition by decreasing hydrogen content with the balance made up with steam was also investigated. The results from 10%, 25% and 50% decreases in syngas hydrogen concentration can be found in Figure A2.2 - 42, Figure A2.2 - 43 and Figure A2.2 - 44, respectively. As syngas hydrogen content is decreased there is less heat generation in the fuel cell stack as the steam absorbs sensible enthalpy, this in turn reduces the required compressor air mass flow for a given fuel cell stack temperature and surge is approached or actually occurs (as in the 50% concentration decrease case).

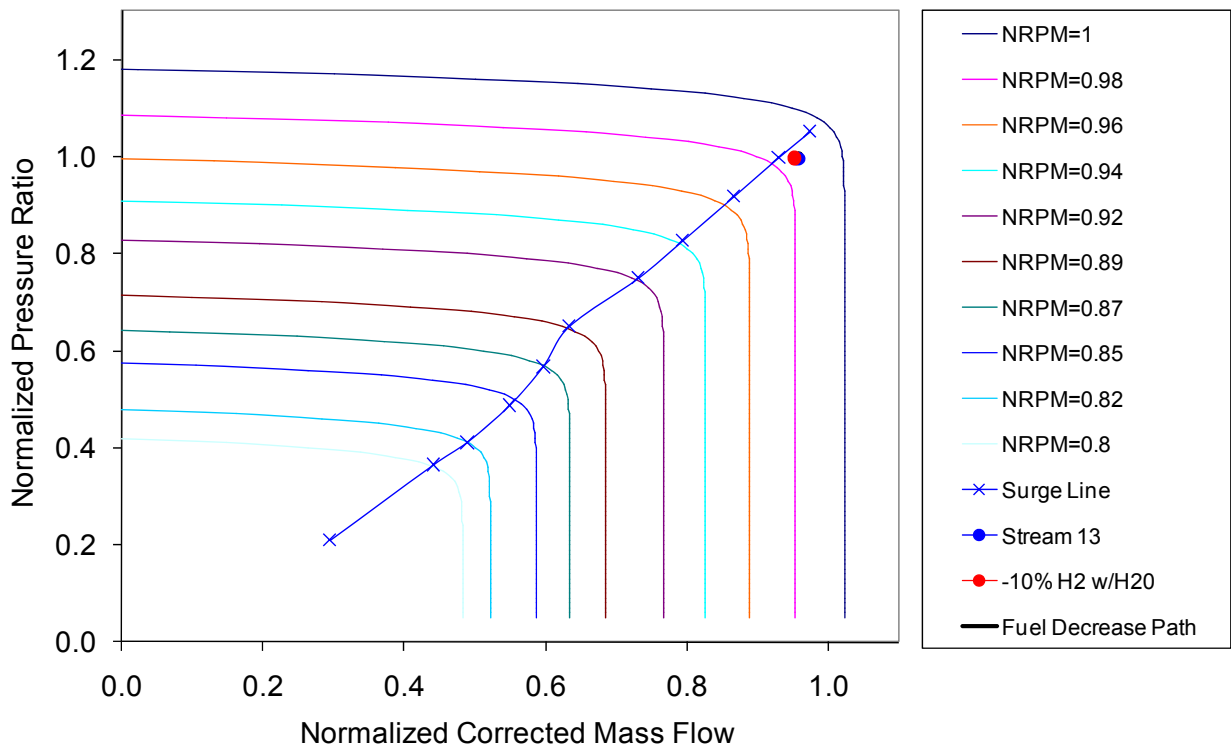


**Figure A2.2 - 42: Compressor dynamic response to a 10% decrease in fuel hydrogen balanced with steam. Initial state A (blue) to final state B (red) when cascade PID control is applied to fuel cell temperature and shaft RPM.**

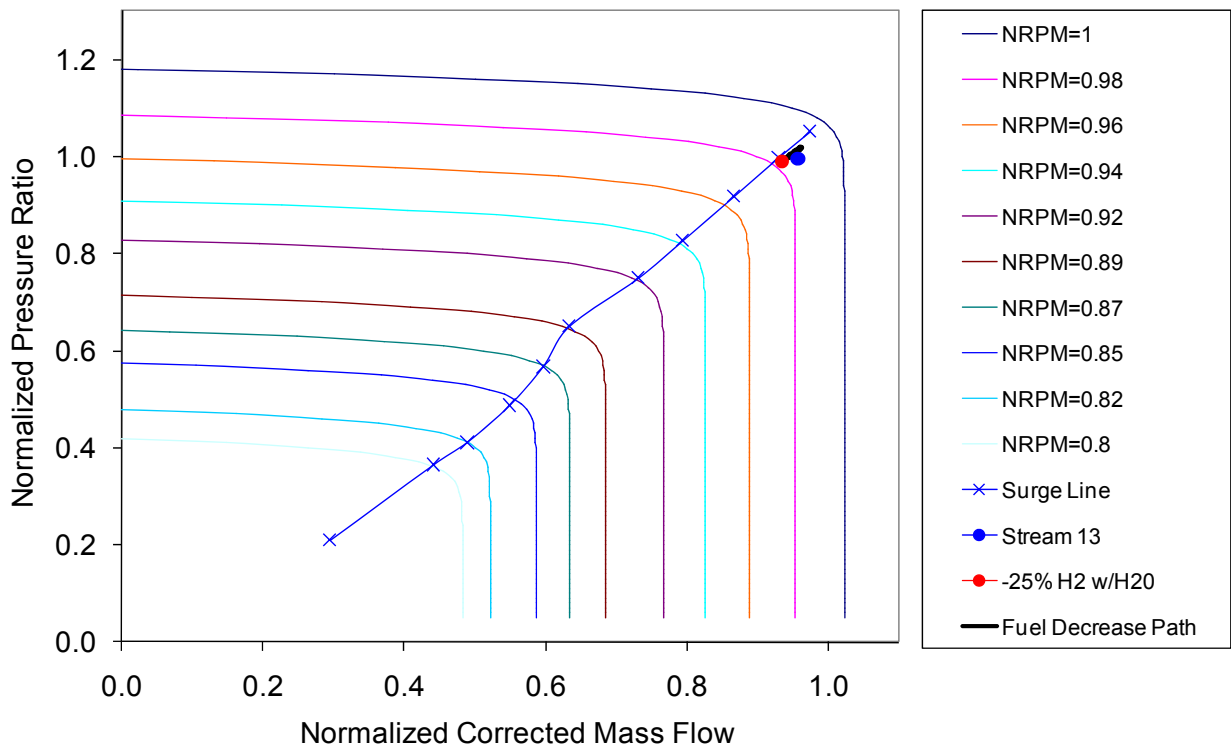


**Figure A2.2 - 43: Compressor dynamic response to a 25% decrease in fuel hydrogen balanced with steam. Initial state A (blue) to final state B (red) when cascade PID control is applied to fuel cell temperature and shaft RPM.**

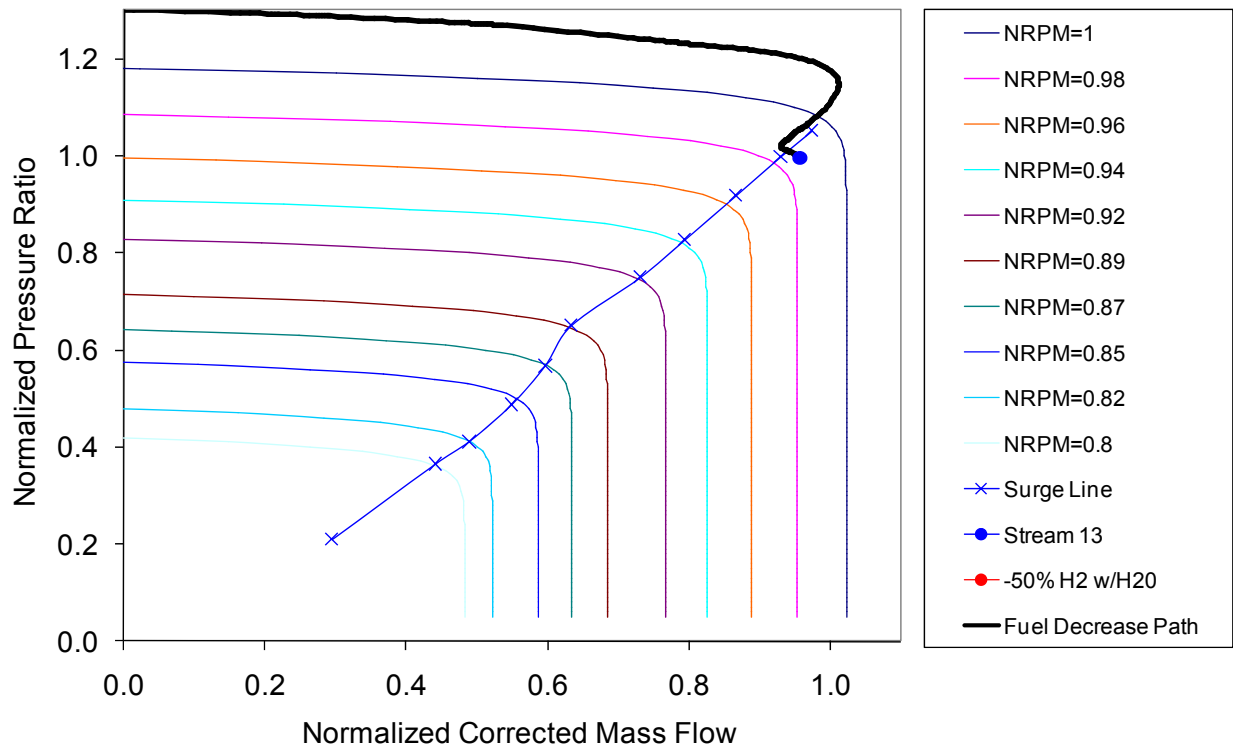


**Figure A2.2 - 44: Compressor dynamic response to a 50% decrease in fuel hydrogen balanced with steam. Initial state A (blue) to final state B (red) when cascade PID control is applied to fuel cell temperature and shaft RPM.**

**Fuel Cell Current Demand Perturbations (Affect of Various Design Parameters and Equations Used in Map Fits)**

Once the specific hybrid system dynamics that led to surge were established methods to avert this phenomenon were investigated. The current dynamic hybrid system model takes into account a plenum volume, which defines the volume between the compressor and turbine. This volume accounts for the volume of manifolds and flow channels within the fuel cell stack as well as any containment vessels, combustors, and plumbing used to integrate the fuel cell modules into the hybrid cycle. Ideally this volume should be minimized to avoid surge (Hill & Peterson, 1992). This is an inherent difficulty for a hybrid fuel cell gas turbine system in which the relatively compact combustor of the stand-alone gas turbine design is replaced with the large volume of a fuel cell and its associated plumbing.

The turbine inlet pressure is solved using equation 25:

$$\frac{dP}{dt} = \frac{RT}{V} (\dot{m}_{in} - \dot{m}_{out}) \quad (25)$$

Where  $V$  is the plenum volume,  $T$  is the turbine inlet temperature,  $\dot{m}_{in}$  is the mass flow rate out of the compressor and into the plenum volume and  $\dot{m}_{out}$  is the mass flow rate out of the plenum volume and into the turbine. Pressure is solved throughout the model in a backward-differencing fashion starting with the back pressure of the turbine. For large plenum volumes a change in compressor pressure ratio will be slow relative to changes in mass flow and movement on the compressor map will tend to be more horizontal. For small plenum volumes a change in compressor pressure ratio will be fast relative to changes in mass flow and movement on the compressor map will tend to be more vertical. Horizontal movements on the compressor map during load shed or through the addition of inerts into the syngas stream are characteristic of decreases in normalized mass flow that are greater in magnitude than decreases in normalized pressure ratio. These sorts of movements on the compressor map tend to result in surge.

Focusing on the 25% load shed case shown in Figure A2.2 - 37, which provides a base case for comparison throughout the remaining part of this section, the plenum volume in the model was modified and the effects on the compressor dynamics were found to be significant. Figure A2.2 - 45 shows the impact of increasing the plenum volume by an order of magnitude (from  $160\text{m}^3$  to  $1,600\text{m}^3$ ). Compared to Figure A2.2 - 37 it is apparent that mass flow decreases much faster than pressure ratio for the case of a larger plenum volume, which leads the compressor into the region associated with surge.

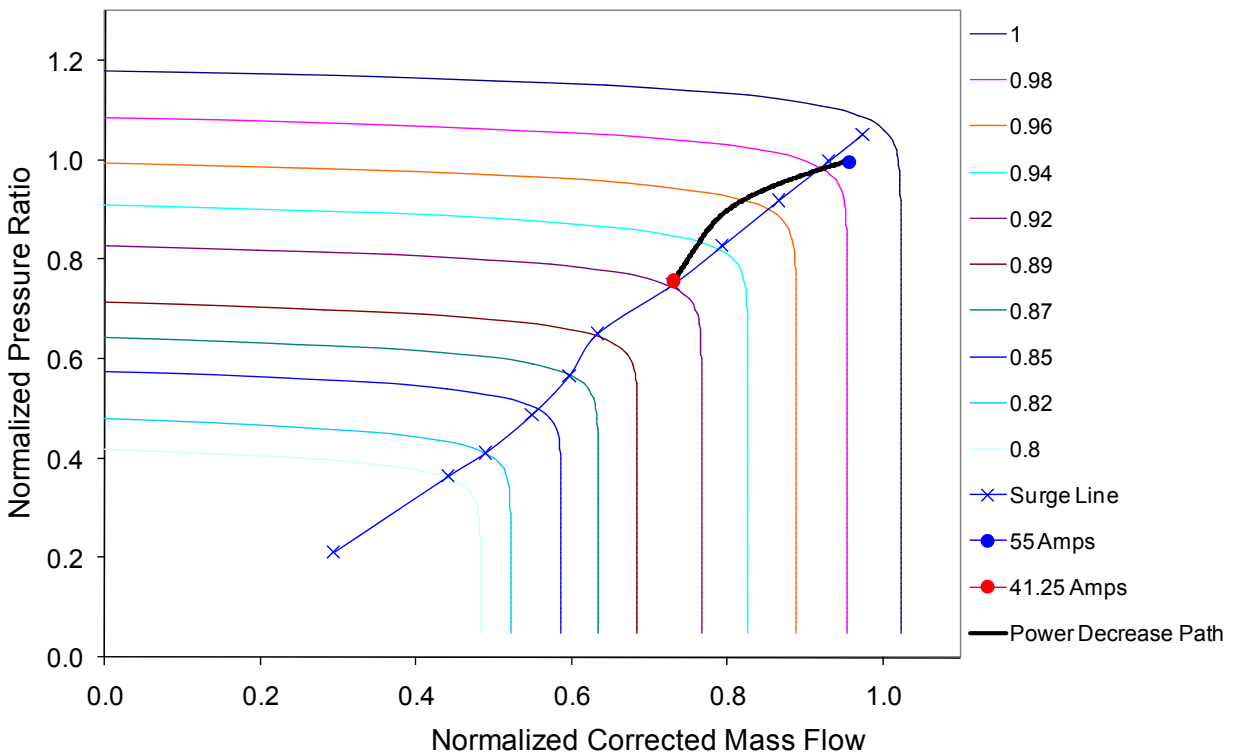


**Figure A2.2 - 45: Compressor dynamic response to a fuel cell load decrease from 100% (blue) to 75% (red) design state when plenum volume is increased by a factor of 10 compared to Figure A2.2 - 37.**

Figure A2.2 - 46 shows the effect that decreasing the plenum volume from 160m<sup>3</sup> to 10m<sup>3</sup> has on the 25% load shed dynamic. Here there is less of a tendency to approach the surge line compared to Figure A2.2 - 37. The two operating points that all cases have in common (Figure A2.2 - 37, Figure A2.2 - 45 and Figure A2.2 - 46) are the initial and final operating states. The initial state is the base case steady state operating point and the final state is a function of the fuel cell temperature controller set-point and the associated compressor mass flow and RPM needed to achieve this condition. If RPM was the only operating point controlled, it would determine the final operating state, but recall that RPM control produces conditions that would leave the fuel cell vulnerable to damaging temperature dynamics). So regardless of the path taken all cases lead to a final steady state operating point within the surge region. The key points associated with the change in plenum volume are (1) that plenum volume size affects the path between initial and final states, and (2) smaller plenum volume size reduces the tendency toward compressor surge during a load-shed dynamic.

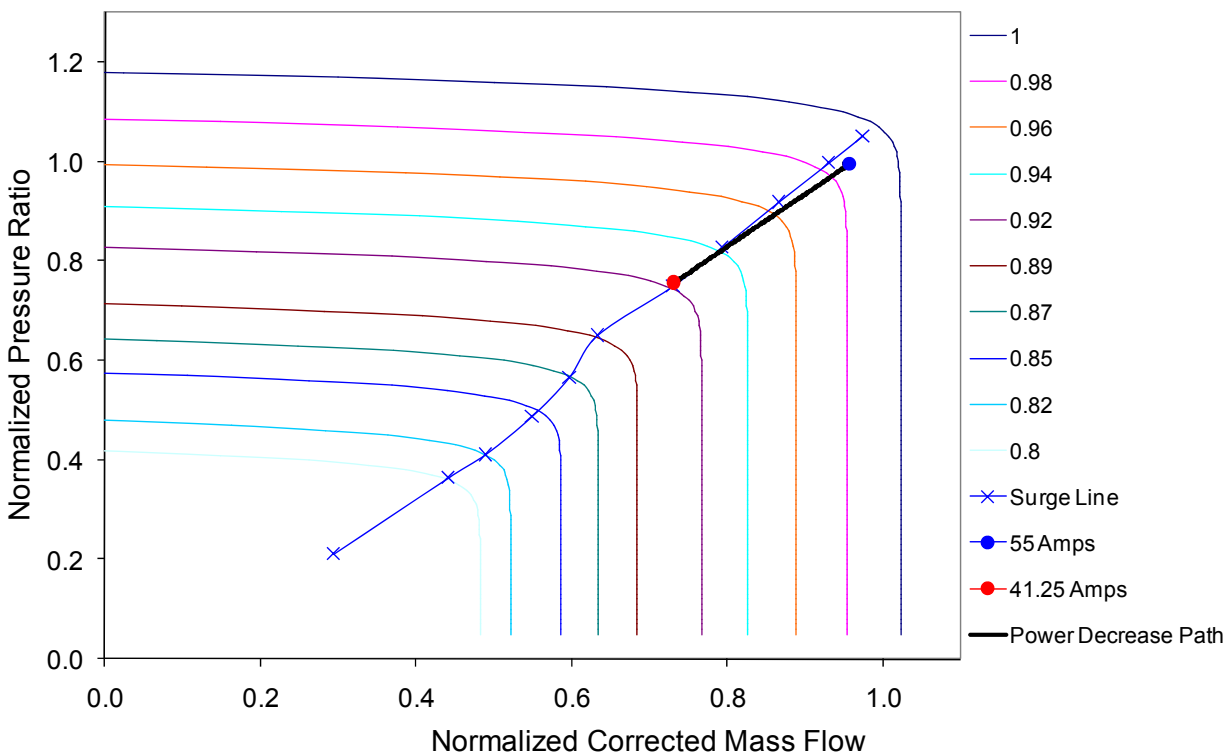


**Figure A2.2 - 46: Compressor dynamic response to a fuel cell load decrease from 100% (blue) to 75% (red) design state when plenum volume is decreased by a factor of 16 compared to Figure A2.2 - 37.**

Another design factor that will affect dynamic gas turbine response is the rotating moment of inertia of the gas turbine. This rotating mass is comprised of the compressor, shaft, turbine and generator. As the magnitude of the moment of inertia increases it becomes more difficult for the rotating mass to slow down or speed up in response to any sudden changes in mass flow, pressure ratio, etc. This impact can be seen in Figure A2.2 - 47 where the moment of

inertia was increased from 1,127 kg\*m<sup>2</sup> (as in the base case of Figure A2.2 - 37) to 1,127,000 kg\*m<sup>2</sup> and then subjected to the 25% load shed perturbation. Initially, as mass flow decreases the compressor follows a constant speed line and this leads to surge. These results suggest that the gas turbine system should be designed to possess as low a moment of inertia as possible to enable a more stable response to load shed perturbations.

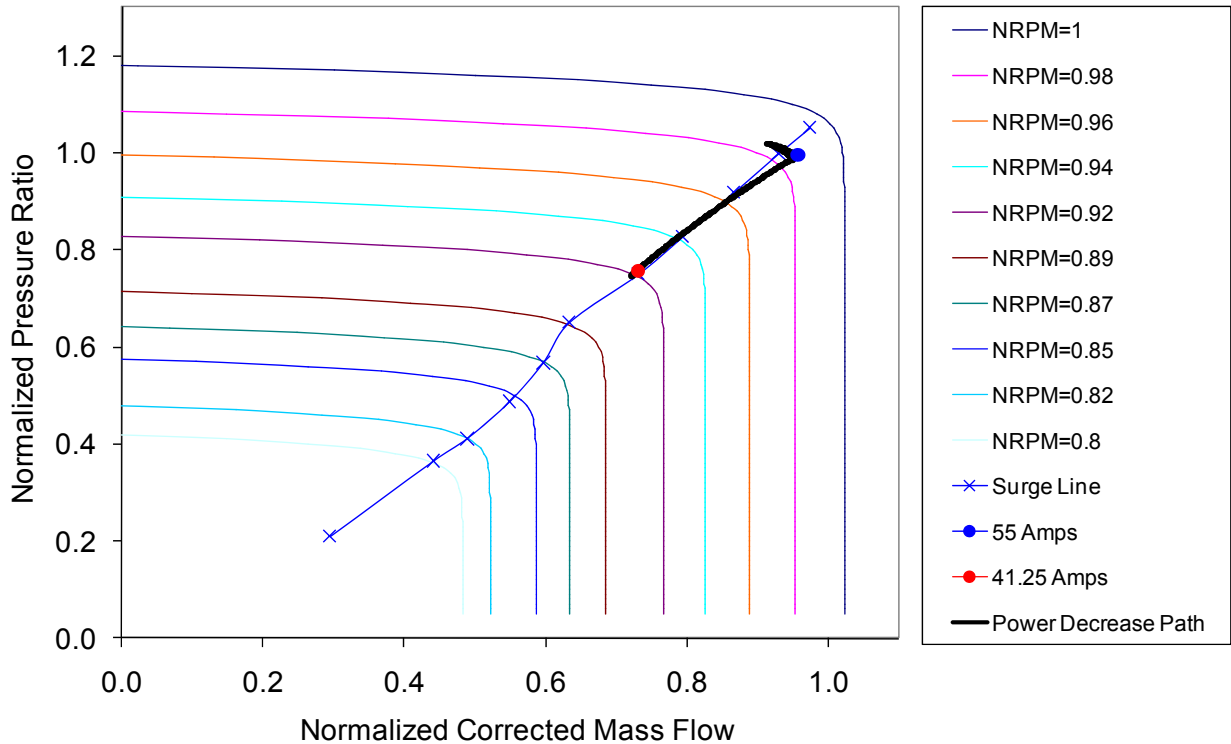


**Figure A2.2 - 47: Compressor dynamic response to a fuel cell load decrease from 100% (blue) to 75% (red) design state when rotating moment of inertia is increased by a factor of 1000 compared to Figure A2.2 - 37.**

Very little change in the dynamic response path relative to the base case of Figure A2.2 - 37 was observed when the moment of inertia was decreased from 1,127 kg\*m<sup>2</sup> to 1.127 kg\*m<sup>2</sup> and then subjected to the 25% load shed perturbation (Figure A2.2 - 48). Although these changes in moment of inertia are unrealistic they demonstrate the trends associated with this design parameter alteration.

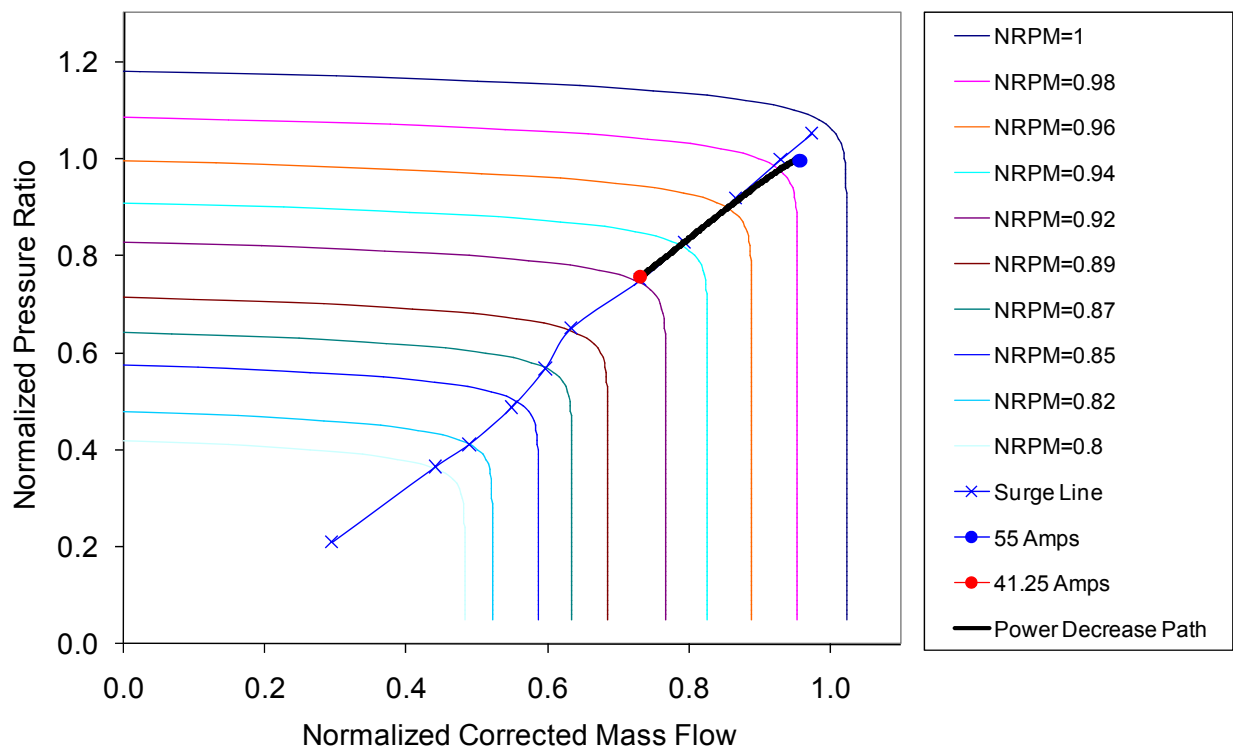


**Figure A2.2 - 48: Compressor dynamic response to a fuel cell load decrease from 100% (blue) to 75% (red) design state when rotating moment of inertia is decreased by a factor of 1,000 compared to Figure A2.2 - 37.**

Figure A2.2 - 49 investigates the impact of fuel cell electrolyte temperature controller set-point on compressor dynamics. It shows that when set-point temperature is increased from 1,100 K to 1,125 K less mass flow through the compressor is required. This leads the compressor deeper into the region of surge for both the initial and final steady state operating points compared to Figure A2.2 - 37. Again, the fuel cell temperature requirements determine compressor steady state operating points. Therefore, lower fuel cell electrolyte operating temperatures will help in avoiding surge.

Examining the influence of changing the RPM set-point from 3,600 in the base case to 4,000 showed no impact on either the steady state operating points or the dynamic path. This is to be expected since RPM is given secondary priority to fuel cell temperature in the cascade controller.

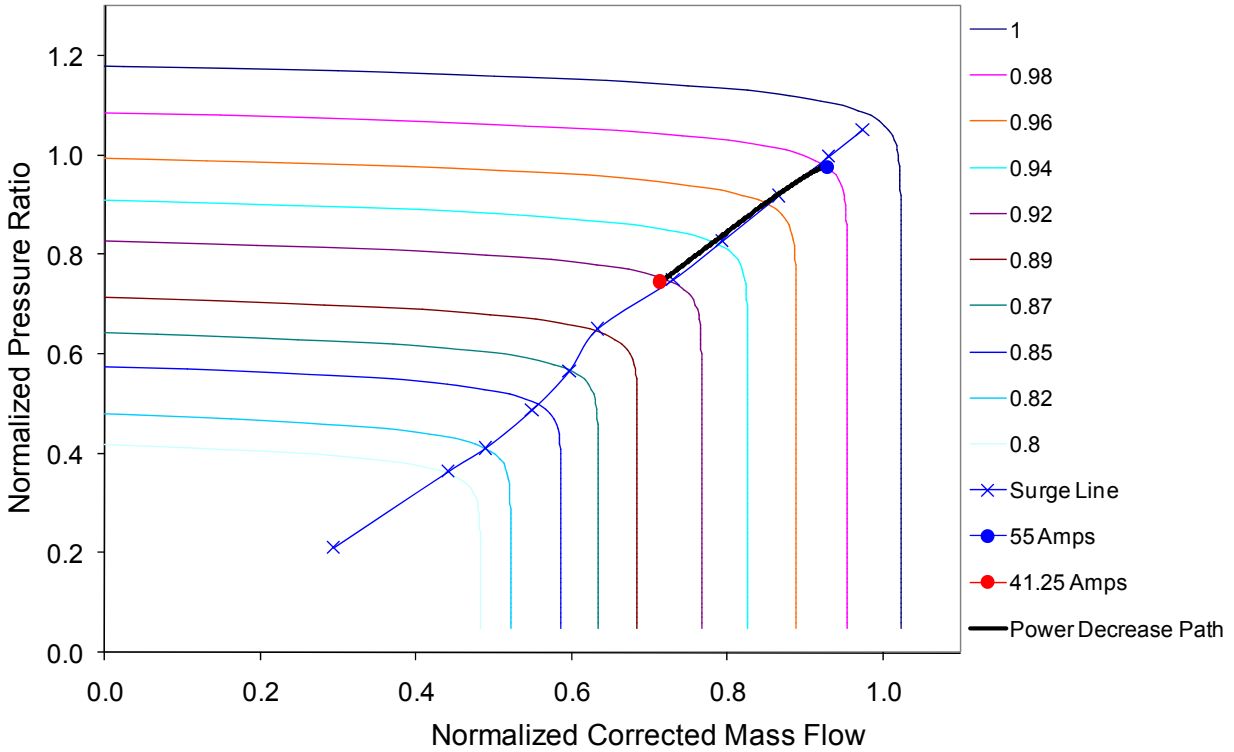


**Figure A2.2 - 49: Compressor dynamic response to a fuel cell load decrease from 100% (blue) to 75% (red) design state when fuel cell electrolyte set-point temperature is increased from 1,100 K in Figure A2.2 - 37 to 1,125 K.**

As mentioned previously, the compressor speed lines shown in the plots of normalized pressure ratio vs. normalized corrected mass flow are calculated using equation 26:

$$\left(1.63914 - 4.7649 * NRPM + 4.14787 * NRPM^2\right) * \left(1 - e^{(NRPM * (79.8268 - 47.4069 * NRPM) + 65.3714 - 103.65 * NRPM)}\right) \quad (26)$$

Each of the coefficients in equation 26 can be changed slightly in order to perturb the map in one direction or another which is equivalent to changing the operating point on the map. Examples of perturbing various coefficients can be seen in Figure A2.2 - 50.

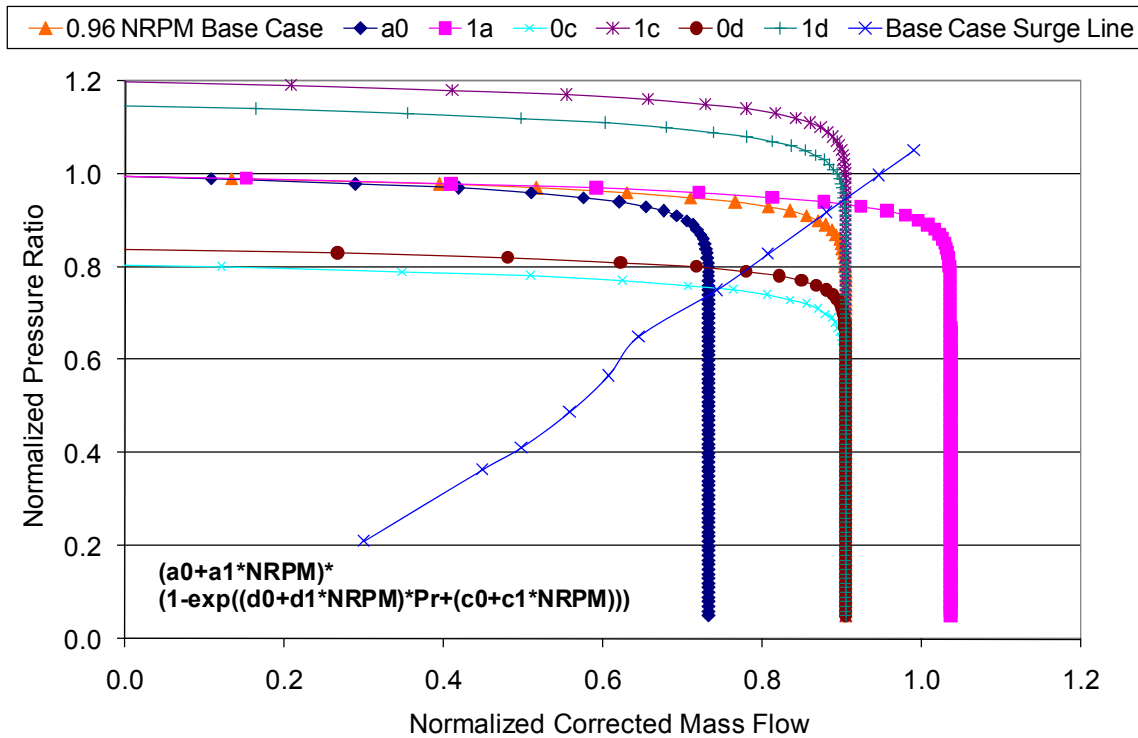


**Figure A2.2 - 50: Perturbation of 0.96 NRPM speed line by changing the individual coefficients in equation 26.**

The speed lines are moved up, down, left and right by changes to the coefficients. The surge line will also move relative to these perturbations but only the base case surge line is shown in Figure A2.2 - 50. The maps were perturbed from the base case steady state operating point by varying the value of one coefficient at a time to see how sensitive the model was to these changes. As can be seen in Table A2.2 - 10 there was very little tolerance when the speed lines were shifted right or left which mostly affects the relative value of compressor air mass flow. Two different cases were seen when the speed lines were shifted up and down. In the case that the steady state operating point falls on the vertical portion of the constant speed line there was no limit to the perturbation because there is no mass flow rate dependence on pressure, so although pressure ratio changes with each perturbation mass flow does not. This is consistent with literature stating that steep speed lines are desired in general compressor design philosophy to enhance compressor flow distortion tolerance (Greitzer, 1980). In the case that the perturbation affects vertical movement in the curved and horizontal portions of the speed line, tolerance is limited. Simultaneous perturbation of multiple coefficients was also tested with similar results.

**Table A2.2 - 10: Results of map perturbation on steady state operation point stability.**

Coefficient	Tolerated Perturbation (% Change)	Direction of Map Speed Line Relative Movement
a0 Max	7%	→
a0 Min	-4%	←
a1 Max	2%	←
a1 Min	-2.5%	→
a2 Max	1.5%	→
a2 Min	-2%	←
c0 Max	5%	↓
c0 Min	No limit	↑
c1 Max	No limit	↑
c1 Min	-4%	↓
d0 Max	4%	↓
d0 Min	No limit	↑
d1 Max	No limit	↑
d1 Min	-7%	↓

The effect of the equation defining the map fit on compressor dynamics was also tested. To do this equation 26 was replaced by equation 27 to model the speed lines of the compressor.

$$\frac{(-1.69305 + 2.69028 * NRPM)^*}{(1 - e^{(N Pr*(37.0184)+94.6897-136.894*NRPM)})} \quad (27)$$

Figure A2.2 - 51 shows that changing the equation that models the compressor speed lines does not impact steady state operating points or the path taken during a load shed dynamic compared to the base case of Figure A2.2 - 37.

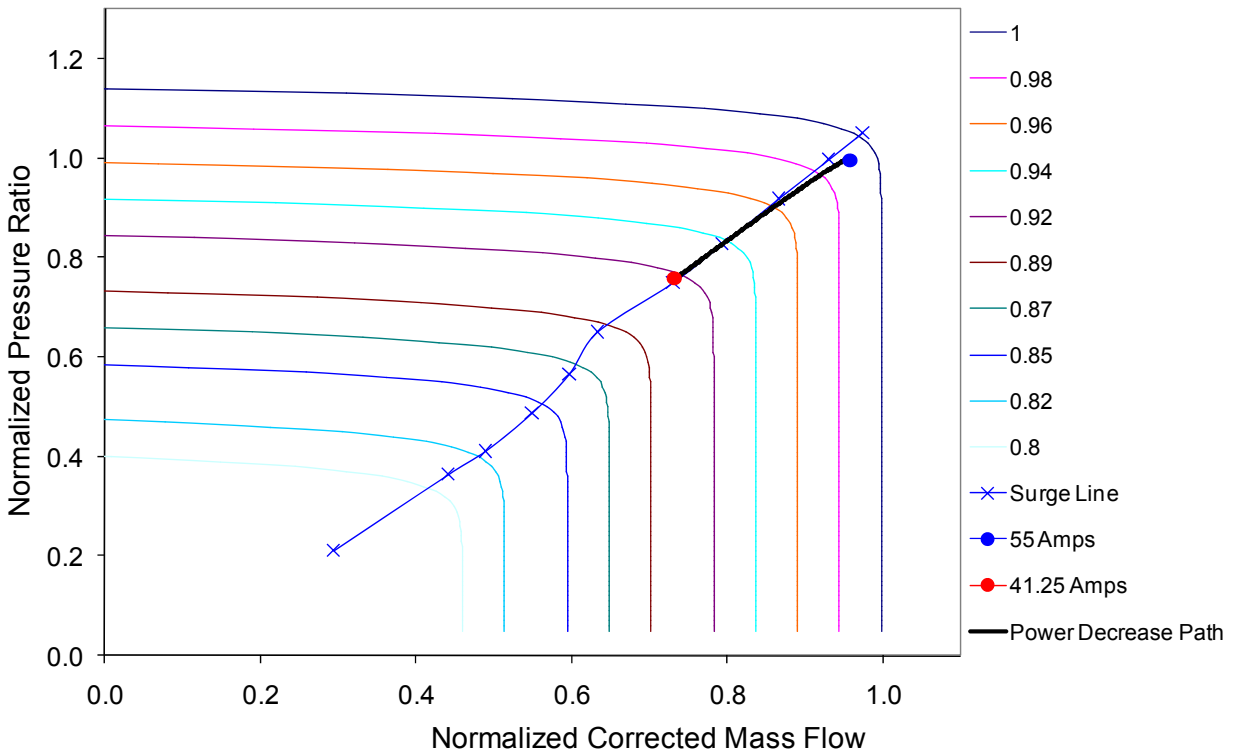


**Figure A2.2 - 51: Compressor dynamic response to a fuel cell load decrease from 100% (blue) to 75% (red) design state when equation 27 is used to calculate compressor speed lines vs. equation 26 in the base case of Figure A2.2 - 37.**

A more straight-forward approach to perturbing the maps involves simply changing the compressor design mass flow and pressure ratio in a way that will allow operation in a region of the compressor map that better avoids the surge line. The trade-off in this case is operation tending towards a region of choked flow resulting in a loss of compressor efficiency. It is typical to operate the compressor close to the surge line as this is normally where the highest efficiency operating points lie for various speeds (Saravanamuttoo et al., 2001).

The effect of decreasing the compressor's design mass flow by a factor of 3.6% (Figure A2.2 - 52) pushes normalized mass flow out away from the surge line for both the initial and final steady state operating points compared to the base case of Figure A2.2 - 37. Comparing the design operating points, overall gas turbine efficiency (net gas turbine power out divided by total fuel in) goes from 7.61% in the base case to 7.43% in this new case and hybrid system efficiency goes from 60.41% in the base case to 60.25% in this new case. So the efficiency penalty associated with decreasing compressor design mass flow is not severe (perhaps worth the increase in surge margin).

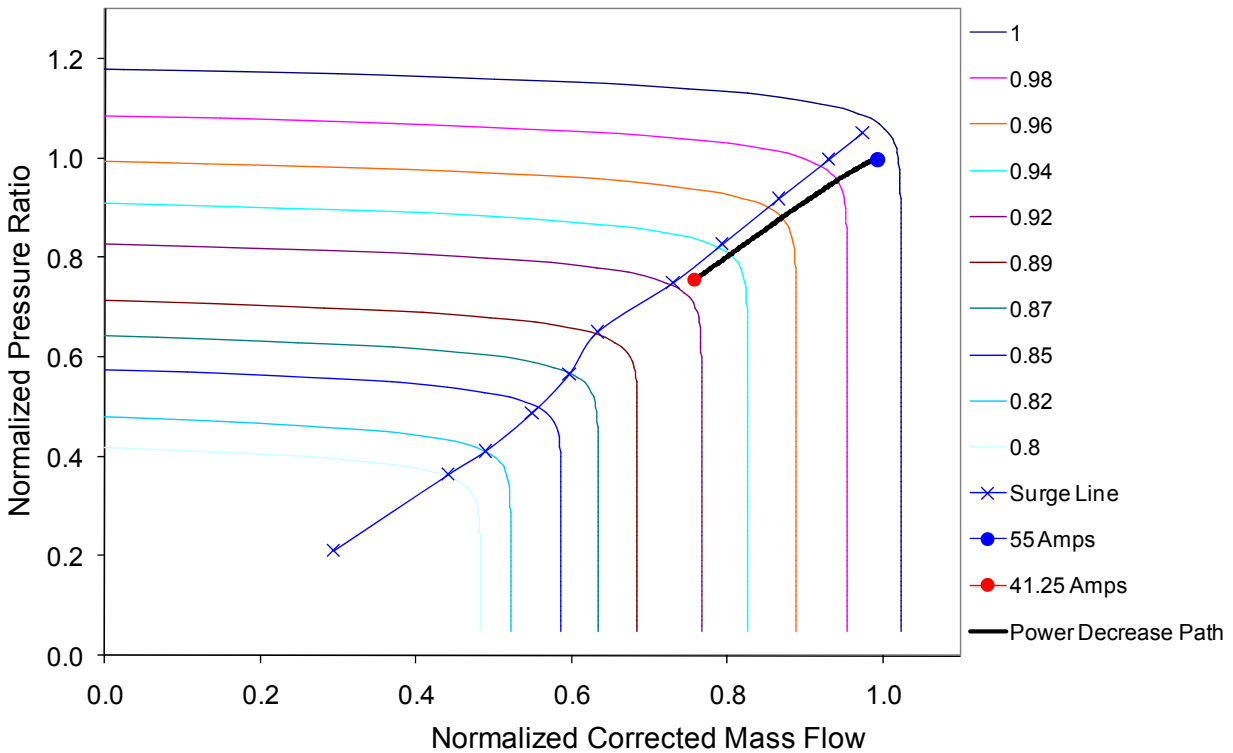


**Figure A2.2 - 52: Compressor dynamic response to a fuel cell load decrease from 100% (blue) to 75% (red) design operating conditions when design mass flow rate is decreased relative to the base case of Figure A2.2 - 37.**

A similar means of moving operation away from the surge line is to increase the design pressure ratio. The effect of increasing the compressor’s design pressure ratio (Figure A2.2 - 53) pushes normalized mass flow down away from the surge line for both the initial and final steady state operating points compared to the base case of Figure A2.2 - 37. In the current case the design pressure ratio was increased by a factor of 11.1%. Comparing the design operating points, overall gas turbine efficiency goes from 7.61% in the base case to 7.46% in this new case and hybrid system efficiency goes from 60.41% in the base case to 60.27% for the case with higher compressor design pressure ratio. Again the efficiency penalty is not dramatic and compared to decreasing design mass flow (Figure A2.2 - 52) increasing design pressure ratio allows further movement away from the surge line with less efficiency penalty (see Figure A2.2 - 53).

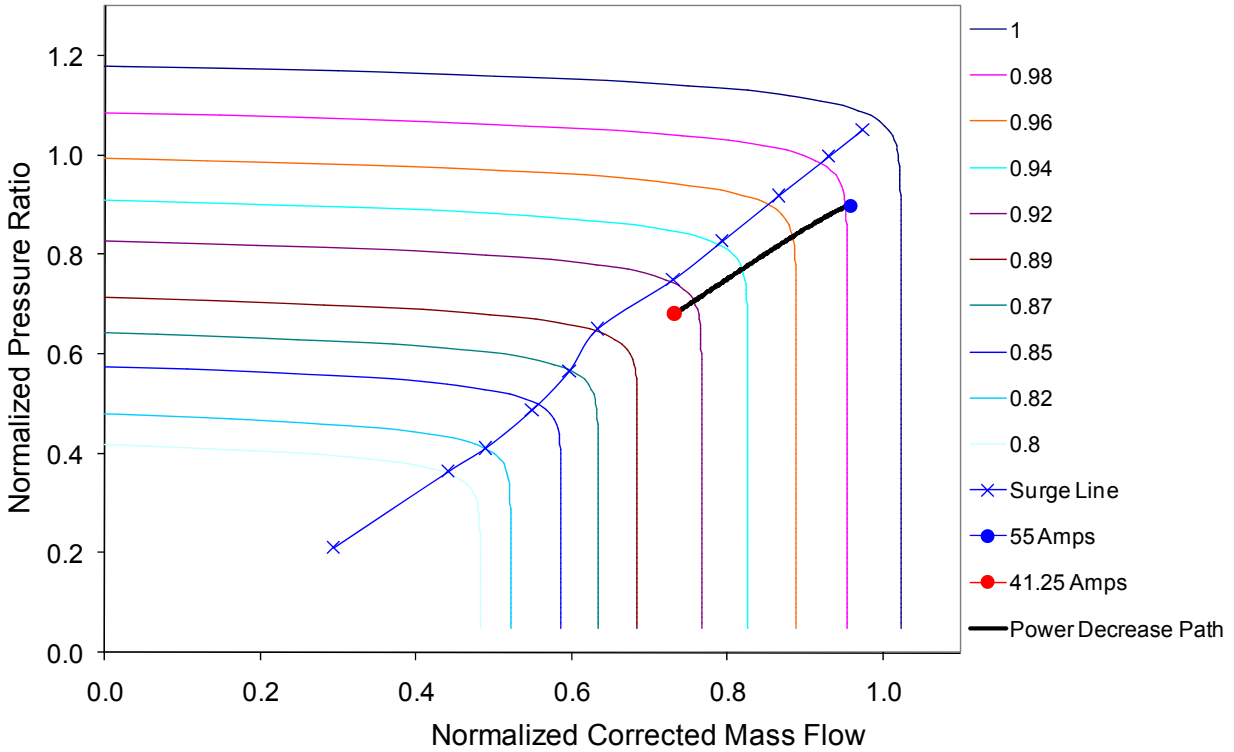


**Figure A2.2 - 53: Compressor dynamic response to a fuel cell load decrease from 100% (blue) to 75% (red) design state when design pressure ratio is increased relative to the base case of Figure A2.2 - 37.**

The combined effect of the reducing design mass flow by a factor of 3.6% and increasing design pressure ratio by a factor of 11.1% is presented in Figure A2.2 - 54. The dynamic response of the hybrid system, which remains far from the surge line throughout the transient response, demonstrates the additive beneficial effect of these compressor design changes.

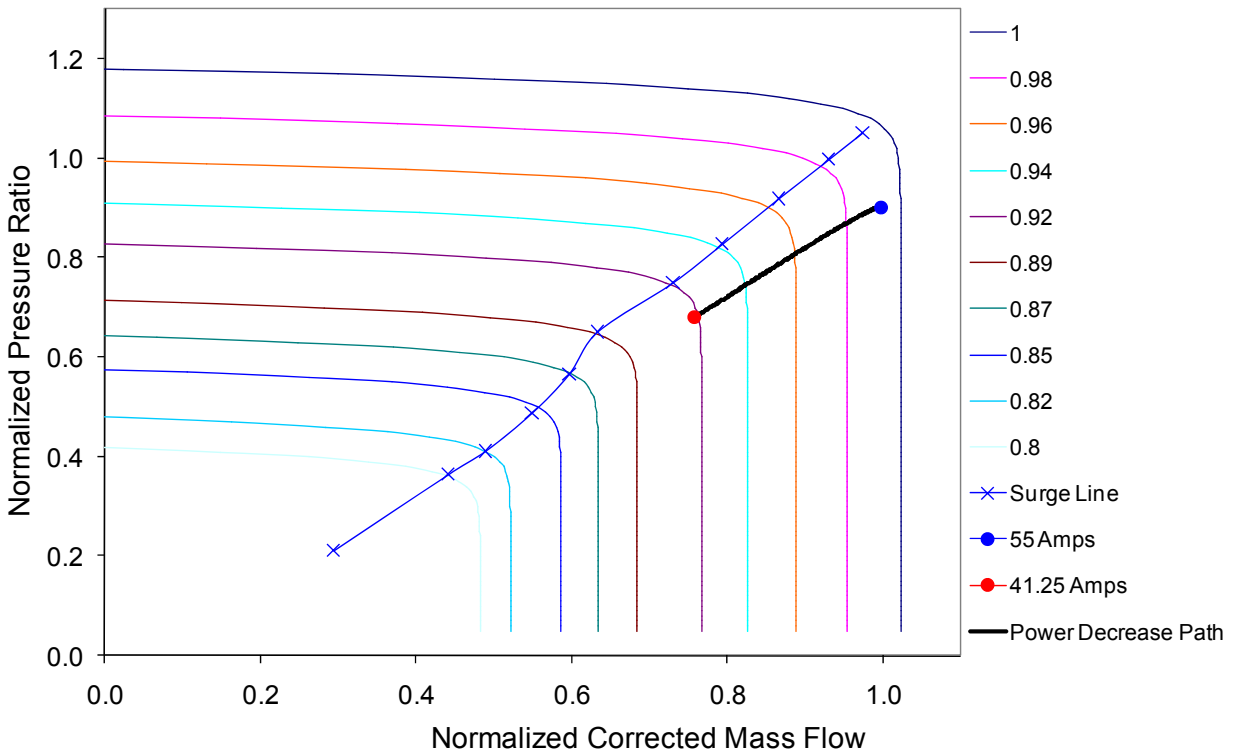


**Figure A2.2 - 54: Compressor dynamic response to a fuel cell load decrease from 100% (blue) to 75% (red) design state when both design mass flow rate is decreased and design pressure ratio is increased relative to the base case of Figure A2.2 - 37.**

### **Model Utilizing a Cathode Blower**

This section of the report is focused on the hybrid sub-system shown in Figure A2.2 - 2 where a cathode blower is used in place of the cathode ejector described in previous sections. Perturbations and dynamic responses similar to those shown in previous sections will be described. The initial steady state operating condition for the sub-system using the cathode blower differs from that of the sub-system with the cathode ejector (Figure A2.2 - 30 through Figure A2.2 - 51).

This section also includes a focus on dynamic failure mechanisms other than compressor surge and methods to mitigate these failures. These new dynamic responses that were checked for failures included anode-cathode inlet pressure difference, anode and cathode inlet-outlet temperature differences, average fuel cell cathode temperature, tri-layer (electrolyte) temperature and gas turbine shaft speed.

Two separate control strategies were implemented during the dynamic testing. “Control strategy #1” uses a proportional integral differential (PID) feedback loop to control gas turbine shaft speed at 3600 RPM. This strategy assumes use of a synchronous generator. Control strategy #1 also uses a cascade PID loop that primarily controls the mixture temperature of the blower

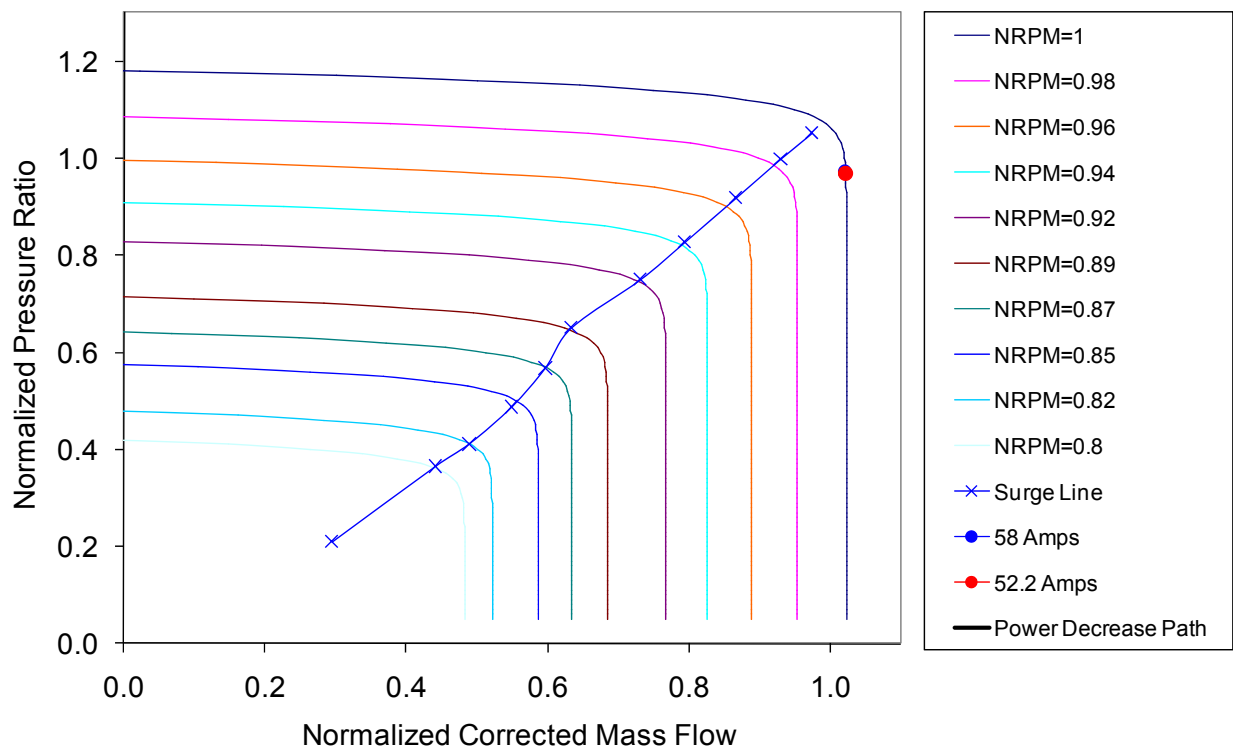
and compressor outlet streams by varying the blower mass flow recycle ratio and then secondarily controls the blower rotational speed.

“Control strategy #2” uses a cascade PID loop that primarily controls fuel cell tri-layer temperature and secondarily controls gas turbine shaft speed, assuming an asynchronous generator, and the same cascade PID controller on the blower as described in control strategy #1. The hybrid system was subjected to the same set of dynamic perturbations for both control strategies to assess the impact that each has on compressor surge. The first set of dynamic analyses presented in this report will focus on control strategy #1.

## Control Strategy #1

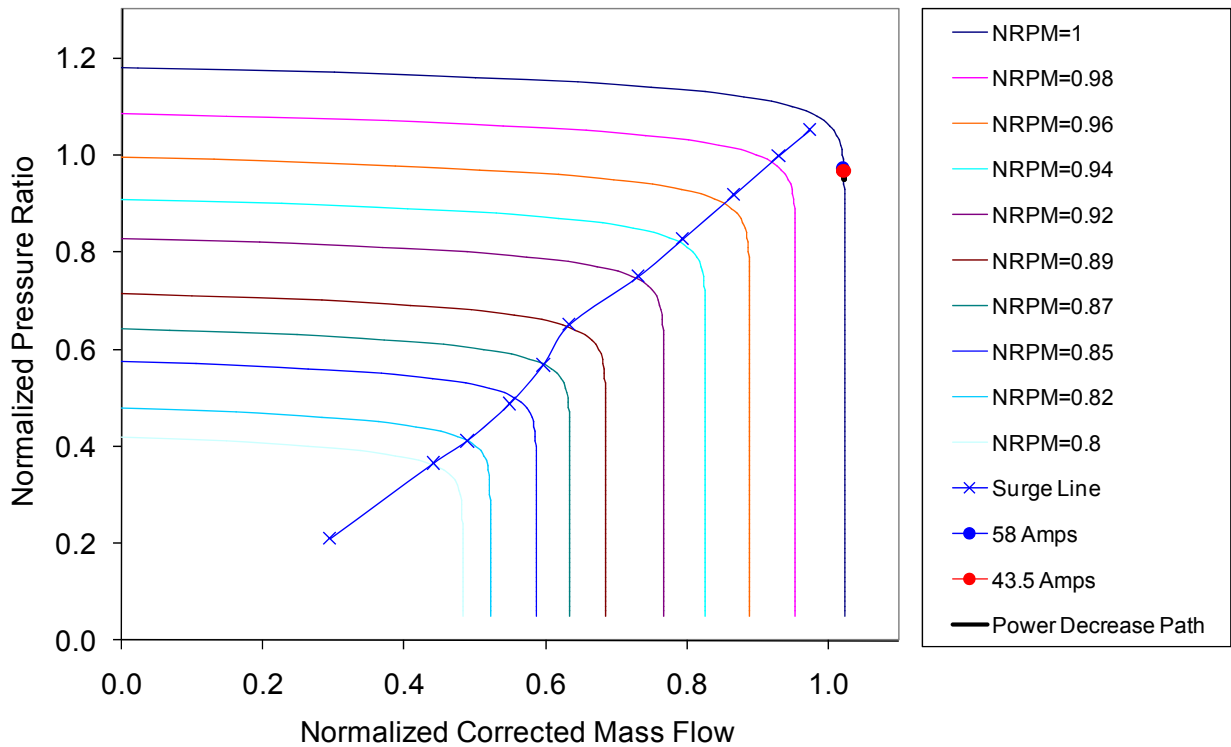
### Fuel Cell Current Demand Perturbations

When control strategy #1 is used and the fuel cell is subjected to a 10% drop in current demand perturbation there is virtually no change in compressor operating point (Figure A2.2 - 55). There is no control of the fuel cell temperature in this control strategy and the tri-layer temperature goes from an initial temperature of 1088 K to 1069 K at the final state of the transient.



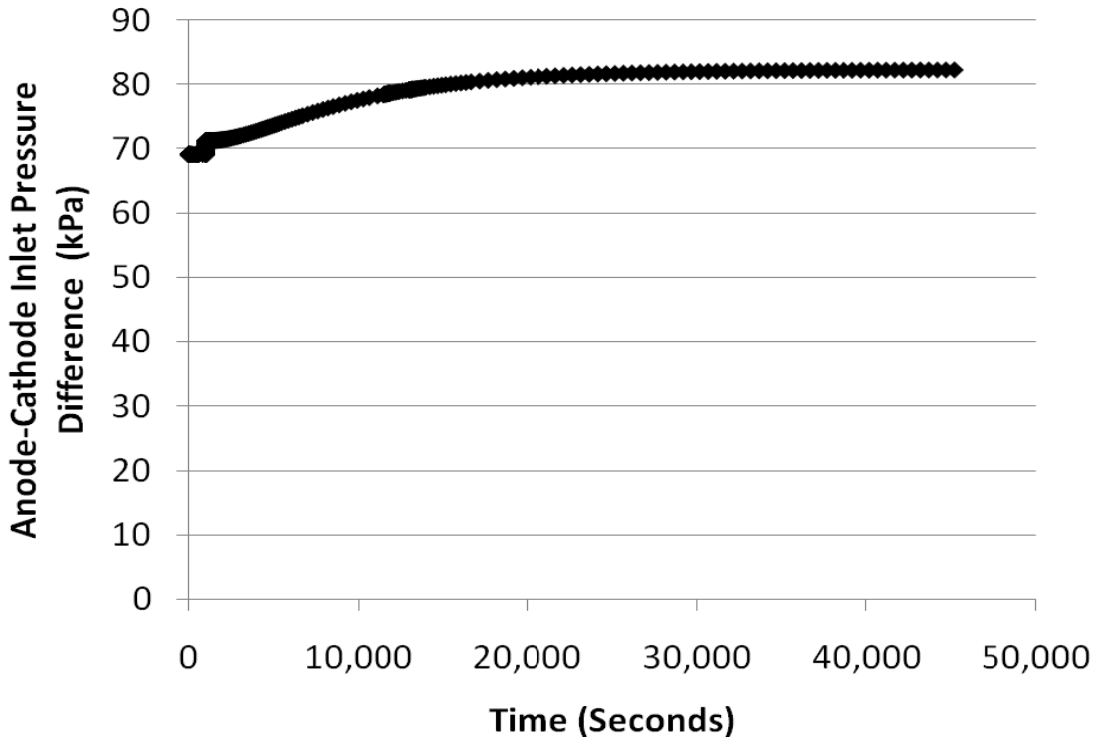
**Figure A2.2 - 55: Compressor dynamic response to a fuel cell load decrease from 100% (blue) to 90% (red) of design state. Gas turbine shaft speed controlled at 3,600 RPM and primary control of blower/compressor mixture temperature at 800 K and secondary control of blower speed.**

Figure A2.2 - 56 shows the case when the fuel cell is subjected to a 25% drop in current demand perturbation. Again there is virtually no change in compressor operating point. There is no control of the fuel cell temperature in this control strategy and the cathode outlet temperature goes from an initial temperature of 1088 K to 1029 K at the final state of the operating transient.



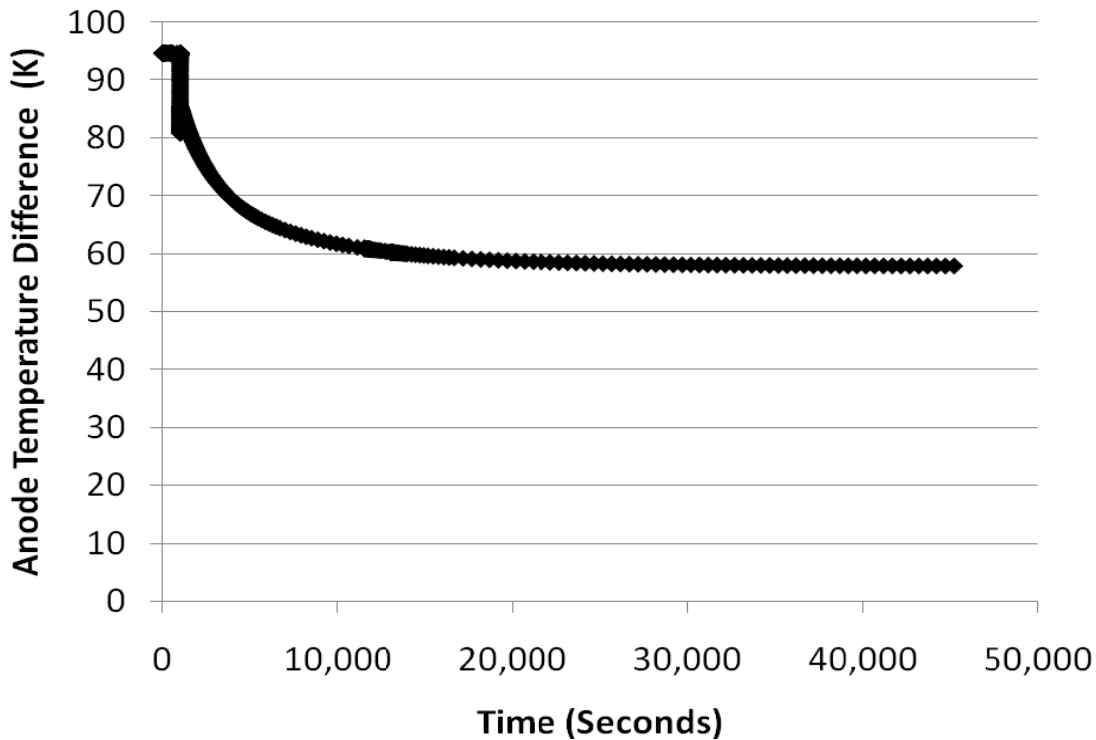
**Figure A2.2 - 56: Compressor dynamic response to a fuel cell load decrease from 100% (blue) to 75% (red) of design state. Gas turbine shaft speed controlled at 3,600 RPM and primary control of blower/compressor mixture temperature at 800 K and secondary control of blower speed.**

For this 25% drop in current demand perturbation many other potential failure mechanisms are also shown, particularly those that may occur in the fuel cell stack. Figure A2.2 - 57 shows the anode-cathode inlet pressure difference rises from a starting value of 69 kPa to 82 kPa at the new steady state condition. This initial 69 kPa difference is due to the much larger mass flow and therefore larger pressure drop in the cathode vs. the anode. The anode-cathode outlet pressures must be equal as the streams mix in the combustor. This initial pressure difference may be too high and may require larger cathode air flow channels than those used in the current design. The pressure difference rise resulting from this load shed perturbation is predominantly due to the decrease in syngas mass flow required and concomitant drop in anode inlet pressure. Note that the system is controlled to maintain a steady state fuel utilization of 80%.



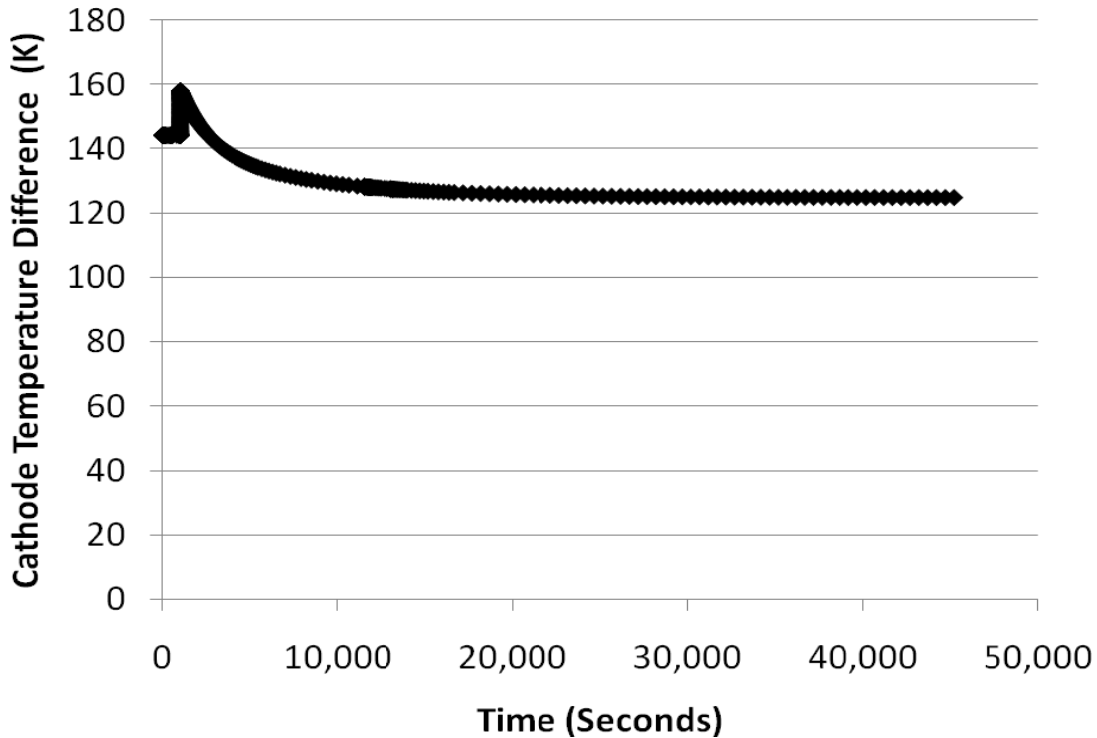
**Figure A2.2 - 57: Dynamic anode-cathode inlet pressure difference response to a fuel cell load decrease from 100% to 75% of design point. Gas turbine speed controlled at 3,600 RPM and primary control of blower/compressor mixture temperature at 800 K with secondary control of recycle blower speed.**

Figure A2.2 - 58 shows that the temperature difference across the anode drops due to the load shed perturbation. There is a 22 K drop in anode inlet temperature due to a lower combustion outlet temperature and therefore less preheating of the inlet stream and a 59 K drop in anode outlet temperature due to a relatively constant air flow rate as the heat of reaction is reduced. The overall anode temperature drop is dominated by the relatively constant air flow rate as the heat of reaction is reduced at lower fuel cell load. The DOE requirement for steady state operation is that the anode temperature rise be less than 100 K. This perturbation results in a temperature difference inside of the prescribed limits.



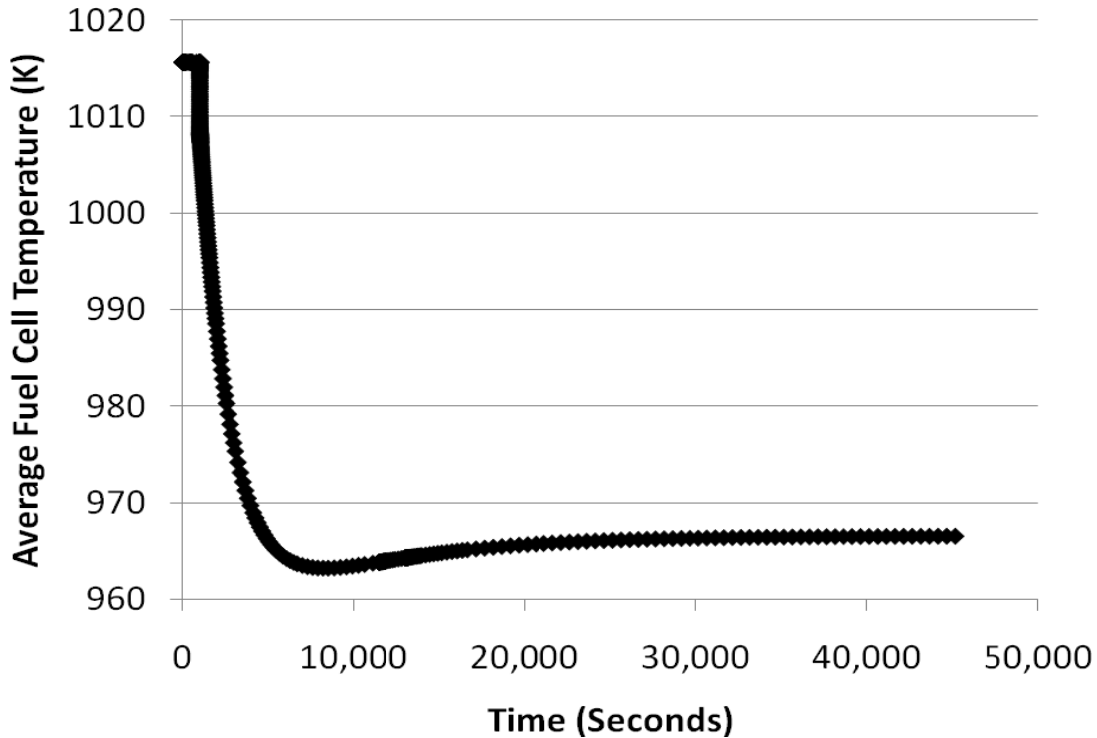
**Figure A2.2 - 58: Dynamic anode inlet-outlet temperature difference response to a fuel cell load decrease from 100% to 75% of design point. Gas turbine speed controlled at 3,600 RPM and primary control of blower/compressor mixture temperature at 800 K with secondary control of recycle blower speed.**

Figure A2.2 - 59 shows that the temperature difference across the cathode drops due to the load shed perturbation. There is a 40 K drop in cathode inlet temperature due to a lower combustor outlet temperature and less preheating of the stream and a 59 K drop in cathode outlet temperature due to a relatively constant air flow rate as the heat of reaction is reduced. The overall cathode temperature drop is dominated by the relatively constant air flow rate as the heat of reaction is reduced at lower fuel cell load. The DOE requirement for steady state operation is that the cathode temperature rise be less than 150 K. This perturbation results in a temperature difference inside of the prescribed limits.



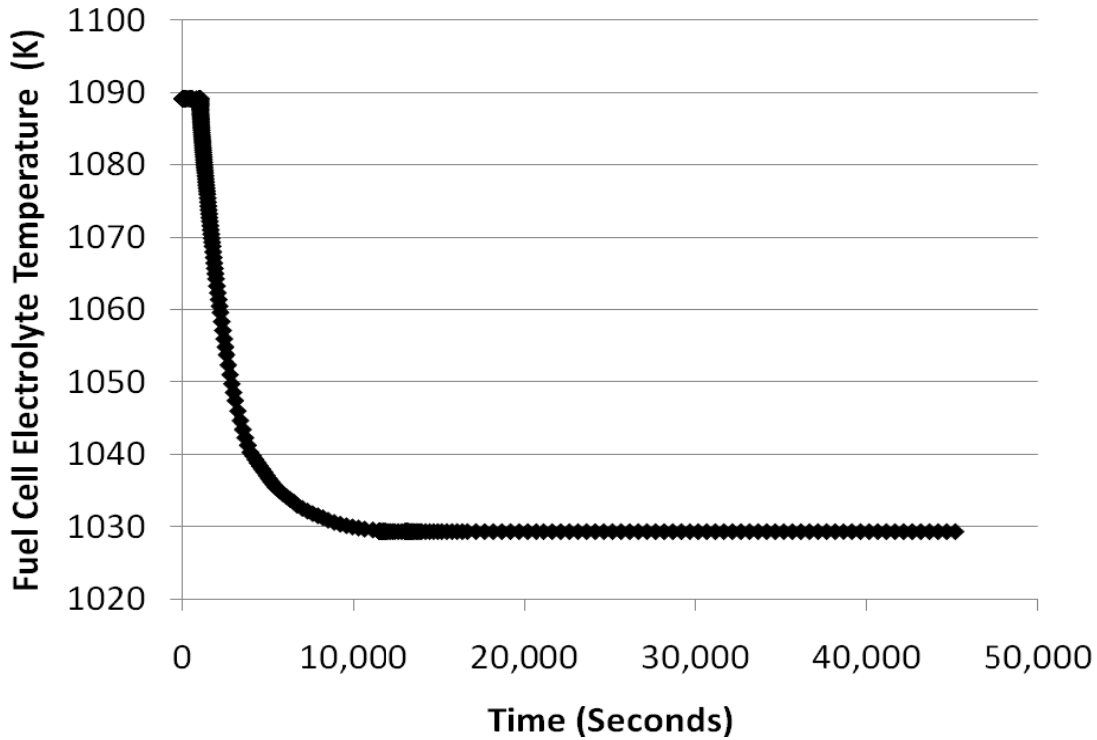
**Figure A2.2 - 59: Dynamic cathode inlet-outlet temperature difference response to a fuel cell load decrease from 100% to 75% of design point. Gas turbine speed controlled at 3,600 RPM and primary control of blower/compressor mixture temperature at 800 K with secondary control of recycle blower speed.**

Figure A2.2 - 60 shows that the average fuel cell temperature across the cathode drops from 1016 K to 967 K. The DOE requirement for steady state operation is that this average temperature be between 998 – 1048 K. This perturbation results in an average temperature outside of the prescribed limits.



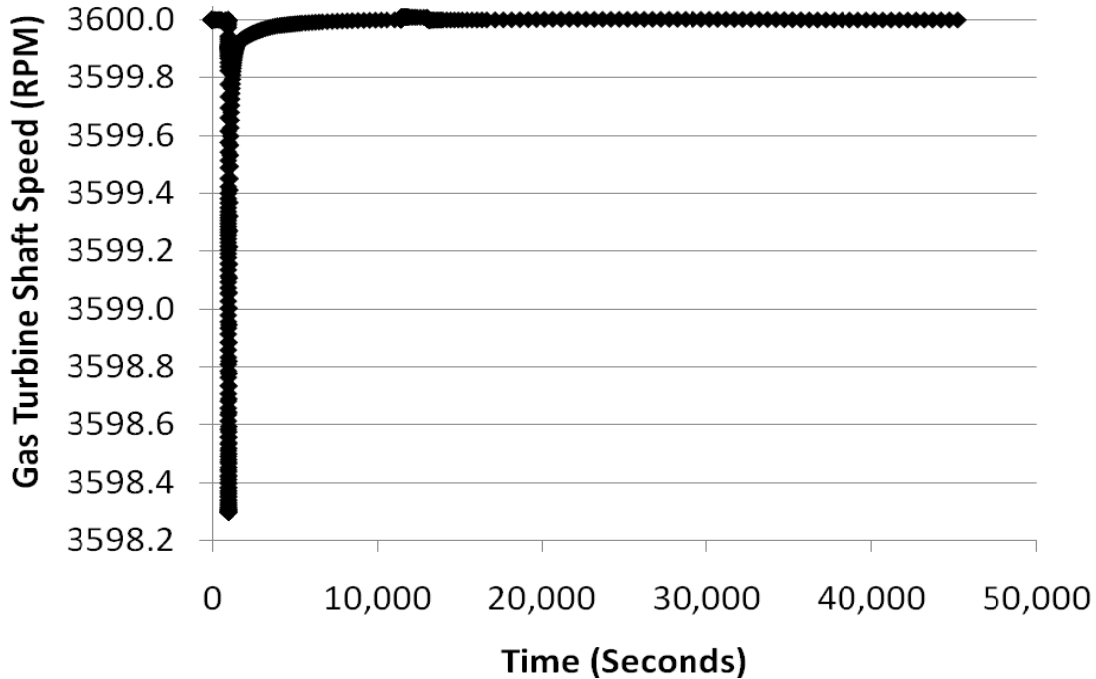
**Figure A2.2 - 60: Dynamic average fuel cell temperature response to a fuel cell load decrease from 100% to 75% of design point. Gas turbine speed controlled at 3,600 RPM and primary control of blower/compressor mixture temperature at 800 K with secondary control of recycle blower speed.**

Figure A2.2 - 61 shows that the tri-layer temperature drops from 1089 K to 1030 K. There is no specified DOE requirement for this parameter but like the average fuel cell temperature it is undesirable that it change significantly since thermal cycling can lead to material stress and failure. Maintaining a steady tri-layer temperature is the focus of the controller used in “control strategy #2”.



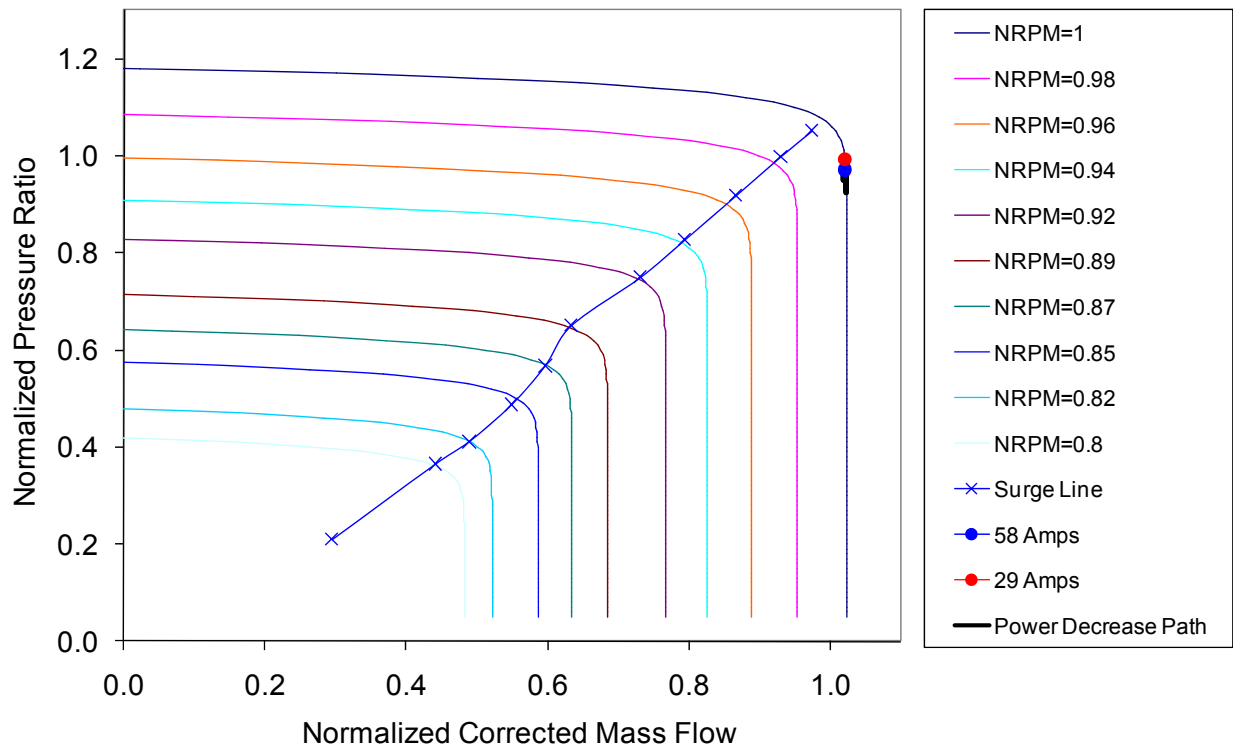
**Figure A2.2 - 61: Dynamic tri-layer temperature response to a fuel cell load decrease from 100% to 75% of design point. Gas turbine speed controlled at 3,600 RPM and primary control of blower/compressor mixture temperature at 800 K with secondary control of recycle blower speed.**

Figure A2.2 - 62 shows that after a minor decrease in gas turbine shaft speed, the controller regains the 3600 RPM set point. This control strategy assumes the use of a synchronous generator.



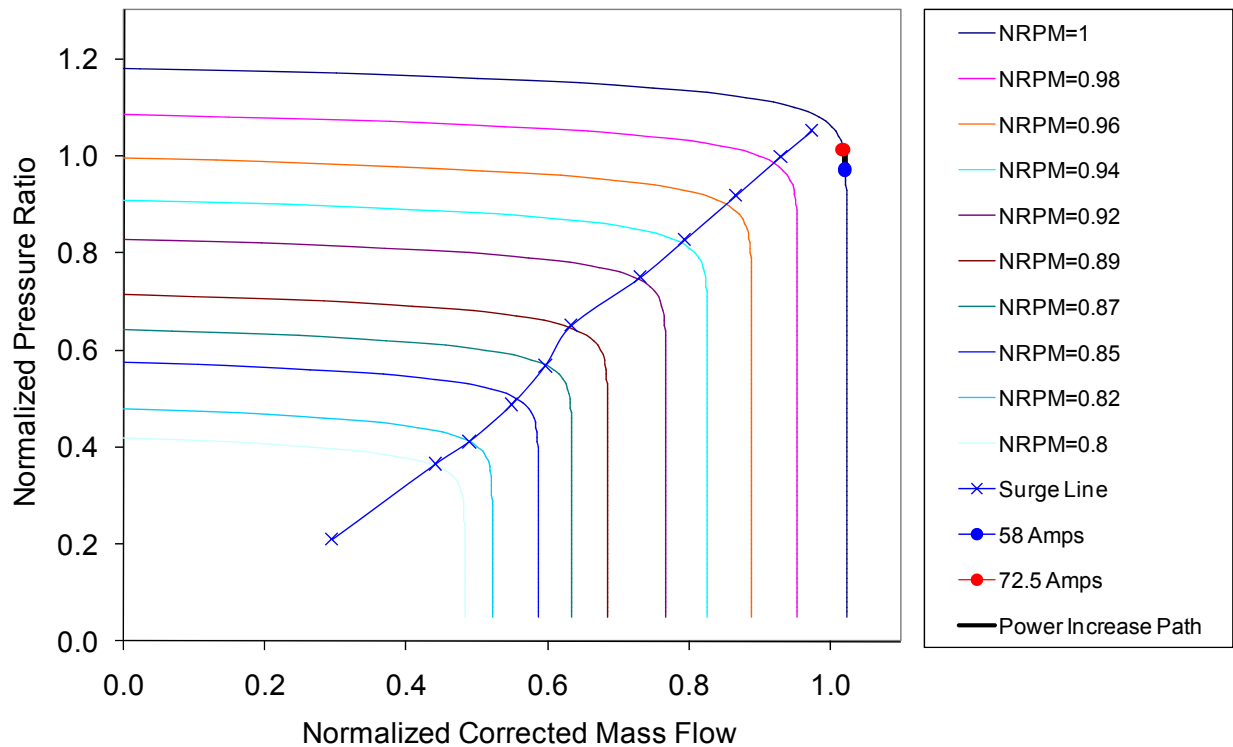
**Figure A2.2 - 62: Dynamic gas turbine shaft speed response to a fuel cell load decrease from 100% to 75% of design point. Gas turbine speed controlled at 3,600 RPM and primary control of blower/compressor mixture temperature at 800 K with secondary control of recycle blower speed.**

Figure A2.2 - 63 shows the case when the fuel cell is subjected to a 50% drop in current demand perturbation. In this case a dip in compressor pressure ratio is observed before the compressor reaches its final operating point. There is no control of the fuel cell temperature in this control strategy and the tri-layer temperature goes from an initial temperature of 1088 K to 931 K at the final state of the transient.



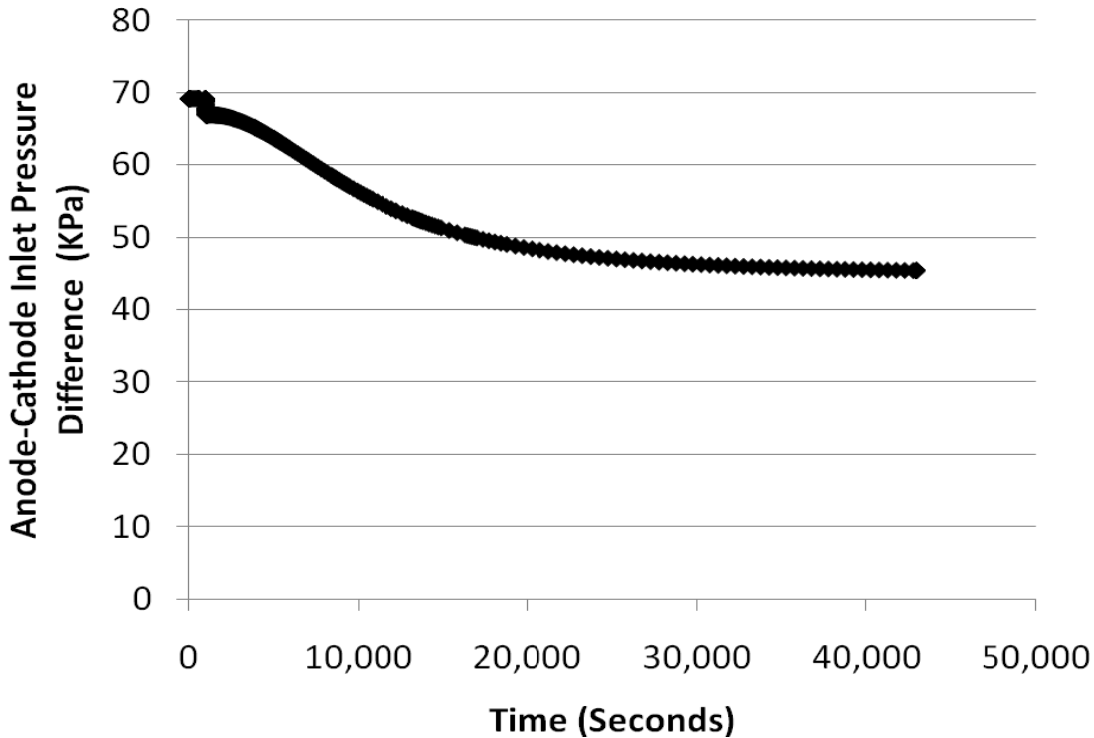
**Figure A2.2 - 63: Compressor dynamic response to a fuel cell load decrease from 100% (blue) to 50% (red) of design state. Gas turbine shaft speed controlled at 3,600 RPM and primary control of blower/compressor mixture temperature at 800 K and secondary control of blower speed.**

Figure A2.2 - 64 shows the case when the fuel cell is subjected to a 25% rise in current demand perturbation. Surge is avoided in this instance.



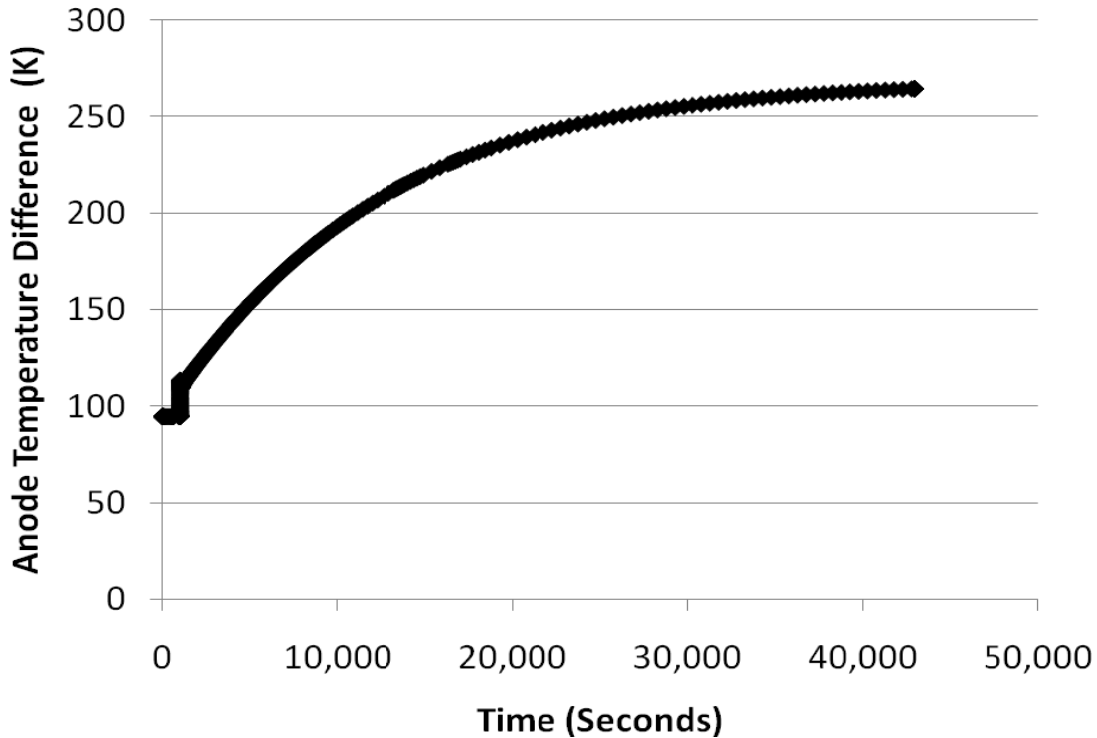
**Figure A2.2 - 64: Compressor dynamic response to a fuel cell load increase from 100% (blue) to 125% (red) of design state. Gas turbine shaft speed controlled at 3,600 RPM and primary control of blower/compressor mixture temperature at 800 K and secondary control of blower speed.**

When the fuel cell is subjected to a 25% increase in current demand the anode-cathode inlet pressure difference decreases (Figure A2.2 - 65) from a starting value of 69 kPa to 45 kPa at the new steady state condition. The pressure difference drop resulting from this perturbation is predominantly due to the increase in syngas mass flow required and concomitant increase in anode inlet pressure required after adding 25% load to the fuel cell while maintaining a steady state fuel utilization of 80%.



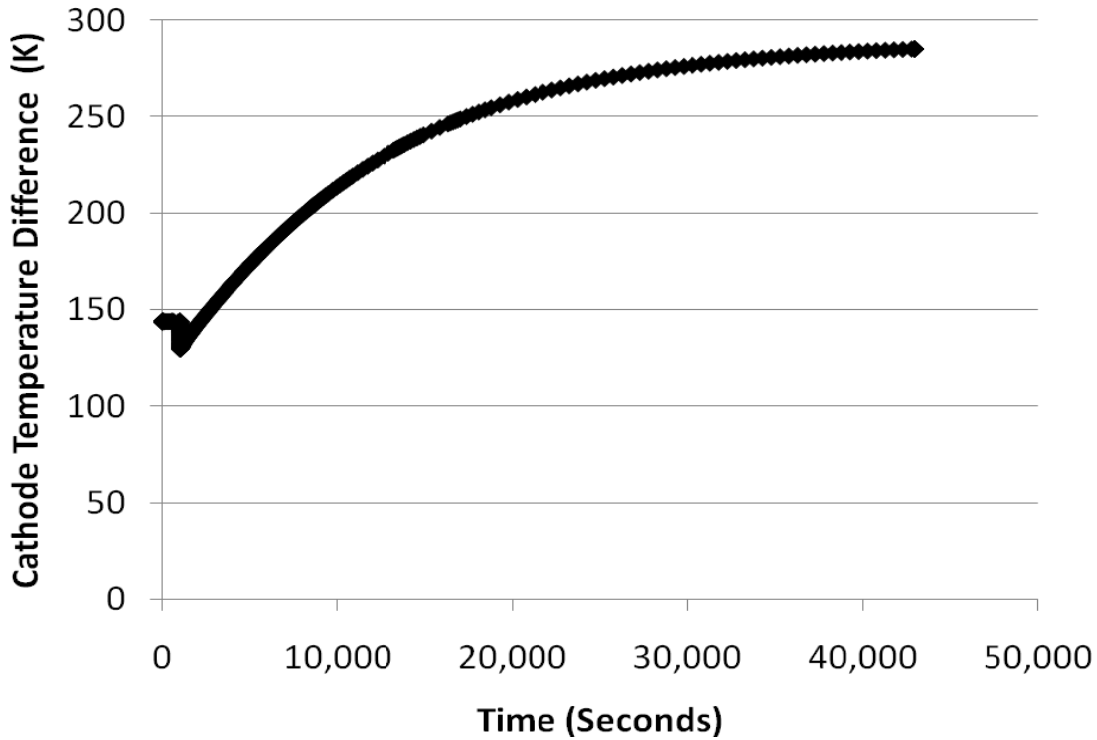
**Figure A2.2 - 65: Dynamic anode-cathode inlet pressure difference response to a fuel cell load increase from 100% to 125% of design point. Gas turbine speed controlled at 3,600 RPM and primary control of blower/compressor mixture temperature at 800 K with secondary control of recycle blower speed.**

Figure A2.2 - 66 shows that the temperature difference across the anode rises due to the load increase perturbation. There is a 137 K rise in anode inlet temperature due to more preheating of the stream and a 311 K rise in anode outlet temperature due to greater heat of reaction. The overall anode temperature rise is dominated by the fact that more heat is generated in the fuel cell at higher load while the air flow rate remains relatively constant. The DOE requirement for steady state operation is that the anode temperature rise be less than 100 K. Therefore, this 269 K anode temperature difference is problematic.



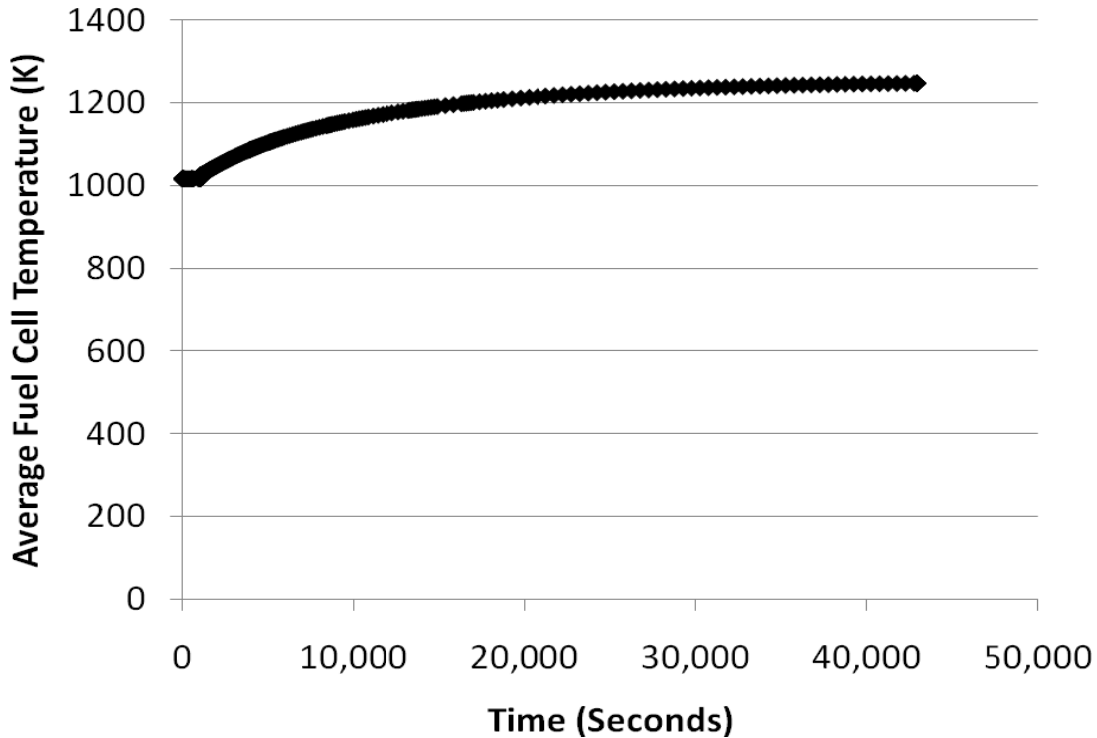
**Figure A2.2 - 66: Dynamic anode inlet-outlet temperature difference response to a fuel cell load increase from 100% to 125% of design point. Gas turbine speed controlled at 3,600 RPM and primary control of blower/compressor mixture temperature at 800 K with secondary control of recycle blower speed.**

Figure A2.2 - 67 shows that the temperature difference across the cathode rises due to the load increase perturbation. There is a 164 K rise in cathode inlet temperature due to more preheating of the stream and a 310 K rise in cathode outlet temperature due to greater heat of reaction. The overall cathode temperature rise is dominated by the fact that more heat is generated in the fuel cell at higher load while the air flow rate remains relatively constant. The DOE requirement for steady state operation is that the cathode temperature rise be less than 150 K. Therefore, this 290 K cathode temperature difference is problematic.



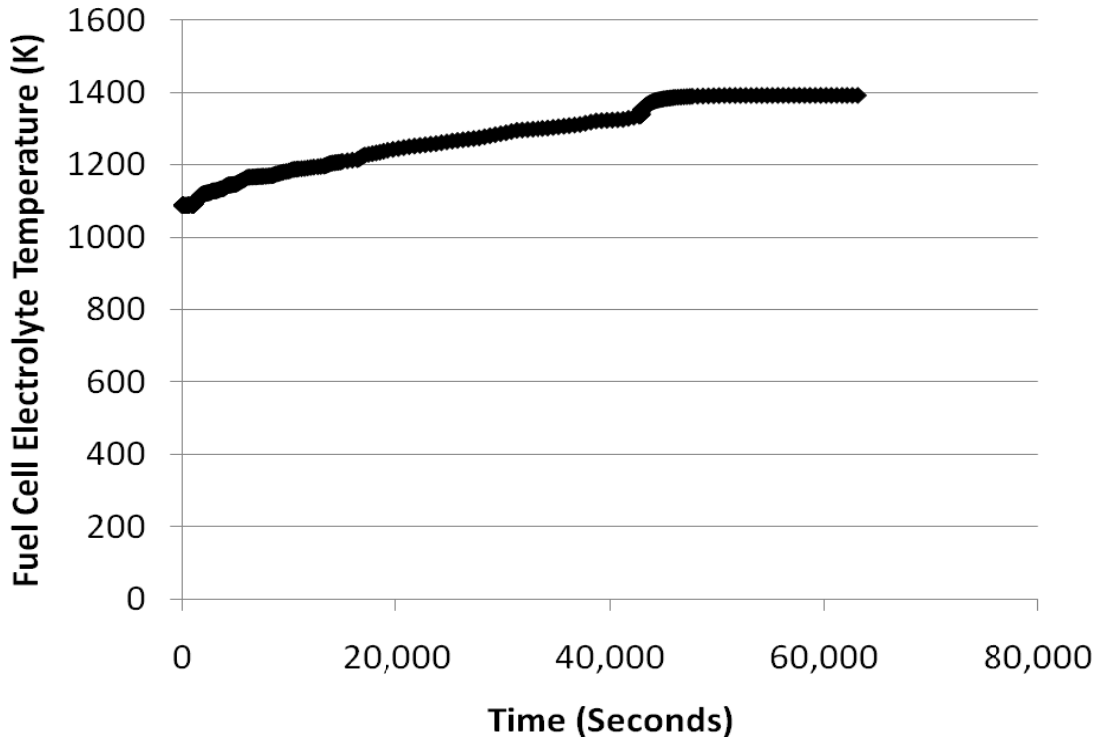
**Figure A2.2 - 67: Dynamic cathode inlet-outlet temperature difference response to a fuel cell load increase from 100% to 125% of design point. Gas turbine speed controlled at 3,600 RPM and primary control of blower/compressor mixture temperature at 800 K with secondary control of recycle blower speed.**

Figure A2.2 - 68 shows that the average fuel cell temperature across the cathode rises from 1016 K to 1253 K. The DOE requirement for steady state operation is that this average temperature be between 998 – 1048 K. This perturbation results in an average temperature much higher than the prescribed range.



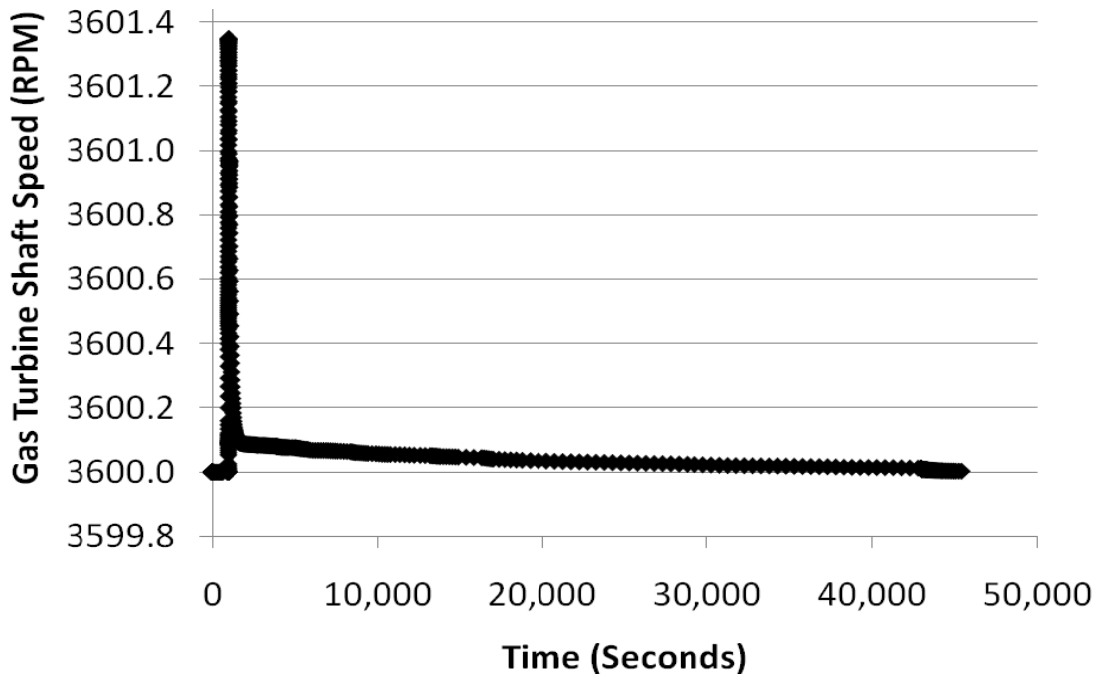
**Figure A2.2 - 68: Dynamic average fuel cell temperature response to a fuel cell load increase from 100% to 125% of design point. Gas turbine speed controlled at 3,600 RPM and primary control of blower/compressor mixture temperature at 800 K with secondary control of recycle blower speed.**

Figure A2.2 - 69 shows that the tri-layer temperature rises from 1089 K to 1400 K. There is no specified DOE requirement for this parameter but like the average fuel cell temperature it is undesirable that it change significantly since thermal cycling can lead to material stress and failure. Maintaining a steady tri-layer temperature is the focus of the controller used in “control strategy #2”.



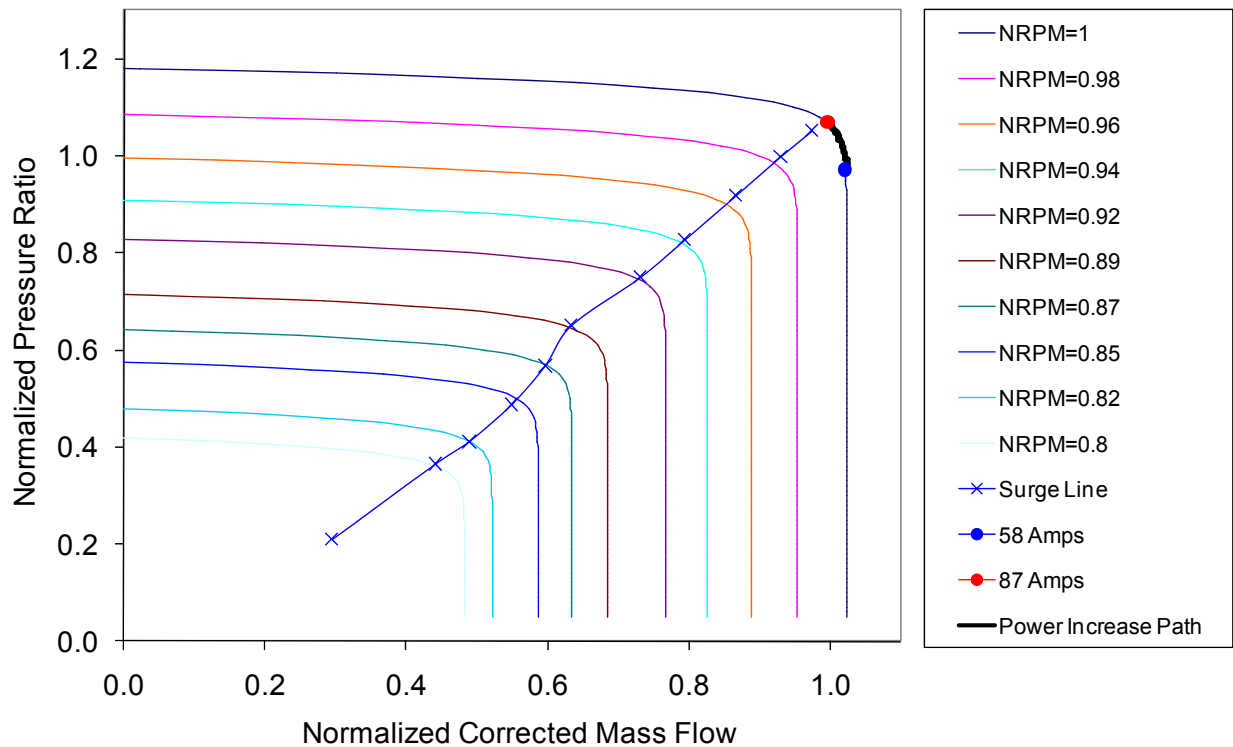
**Figure A2.2 - 69: Dynamic tri-layer temperature response to a fuel cell load increase from 100% to 125% of design point. Gas turbine speed controlled at 3,600 RPM and primary control of blower/compressor mixture temperature at 800 K with secondary control of recycle blower speed.**

Figure A2.2 - 70 shows that after a minor increase in gas turbine shaft speed, the controller regains the 3600 RPM set point. This control strategy assumes the use of a synchronous generator.



**Figure A2.2 - 70: Dynamic gas turbine shaft speed response to a fuel cell load increase from 100% to 125% of design point. Gas turbine speed controlled at 3,600 RPM and primary control of blower/compressor mixture temperature at 800 K with secondary control of recycle blower speed.**

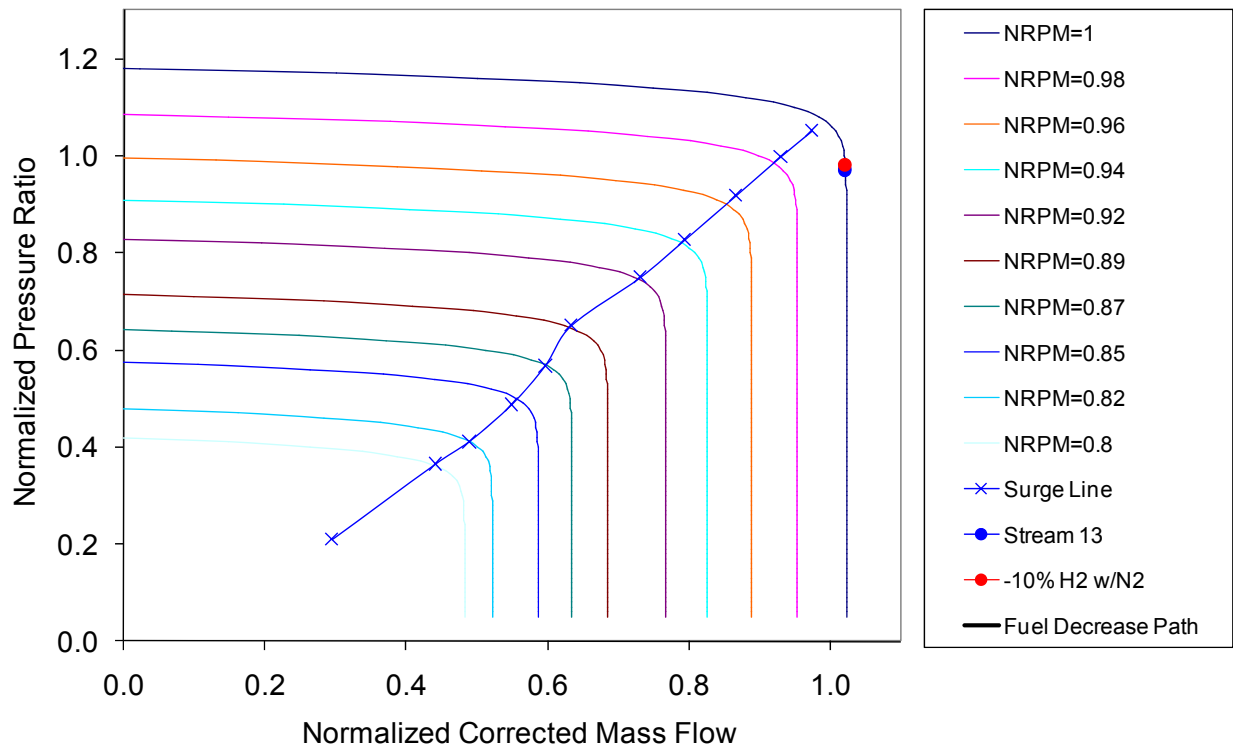
Figure A2.2 - 71 shows the case when the fuel cell is subjected to a 50% rise in current demand perturbation. There is a rise in compressor pressure ratio along a constant speed line that approaches the surge line at the final operating state. Gas turbine power reaches a negative value at the final state of this case, which makes this case either physically impossible or requires motoring of the gas turbine (running the electric generator backwards as a motor). There is no control of the fuel cell temperature in this control strategy and the tri-layer temperature goes from an initial temperature of 1088 K to 1910 K at the final state of the transient. Therefore, this control strategy fails to protect the fuel cell from a damaging temperature rise.



**Figure A2.2 - 71: Compressor dynamic response to a fuel cell load increase from 100% (blue) to 150% (red) of design state. Gas turbine shaft speed controlled at 3,600 RPM and primary control of blower/compressor mixture temperature at 800 K and secondary control of blower speed.**

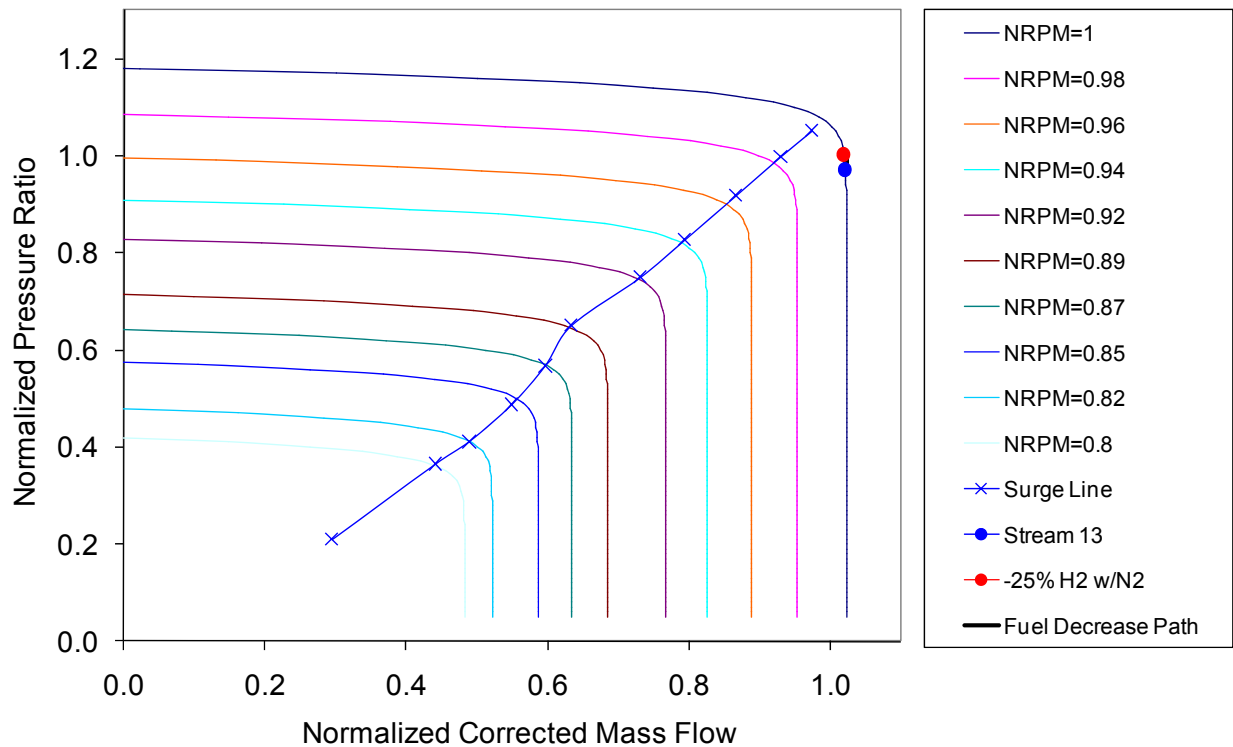
### **Syngas Hydrogen Composition Perturbations (Balanced with Nitrogen)**

Figure A2.2 - 72 shows the case when the fuel cell is subjected to a 10% decrease in syngas hydrogen content (balanced with nitrogen). There is virtually no change in compressor operating point during this dynamic perturbation. There is no control of the fuel cell temperature in this control strategy and the tri-layer temperature goes from an initial temperature of 1088 K to 1086 K at the final state of the operating transient.



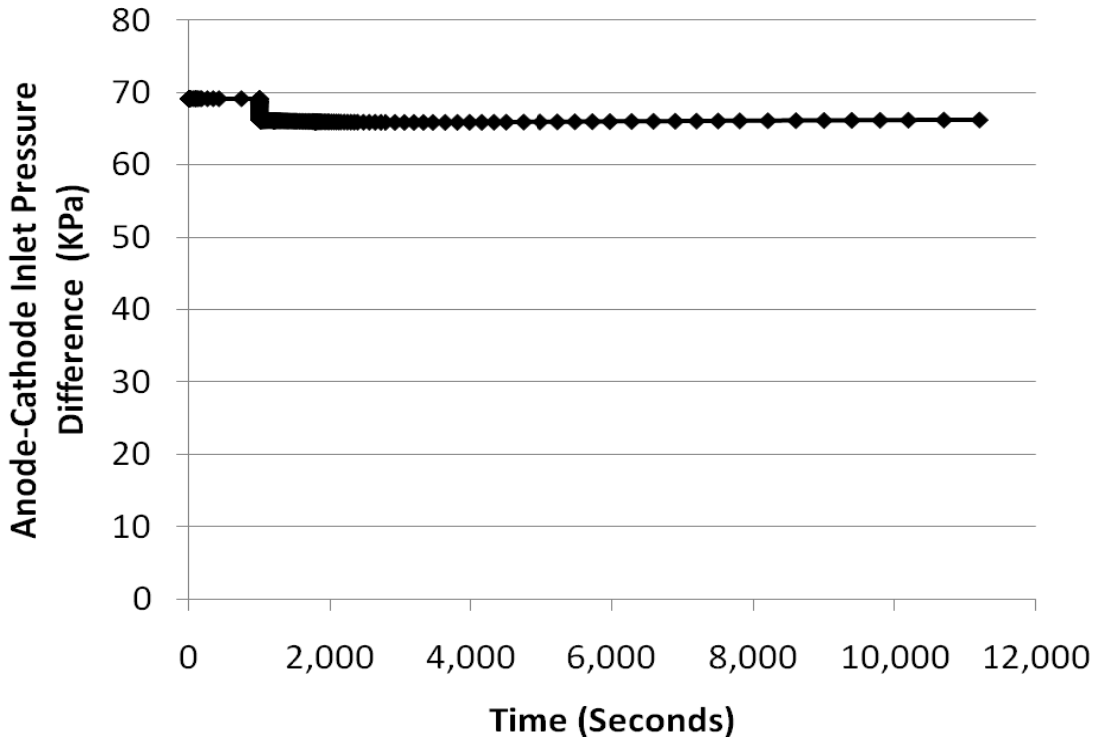
**Figure A2.2 - 72: Compressor dynamic response to a decrease in fuel hydrogen balanced with nitrogen from 100% (blue) to 90% (red) of design state. Gas turbine shaft speed controlled at 3,600 RPM and primary control of blower/compressor mixture temperature at 800 K and secondary control of blower speed.**

Figure A2.2 - 73 shows the case when the fuel cell is subjected to a 25% decrease in syngas hydrogen content. There is a slight increase in compressor pressure ratio from the initial to final state. There is no control of the fuel cell temperature in this control strategy and the tri-layer temperature goes from an initial temperature of 1088 K to 1083 K at the final state of the transient.



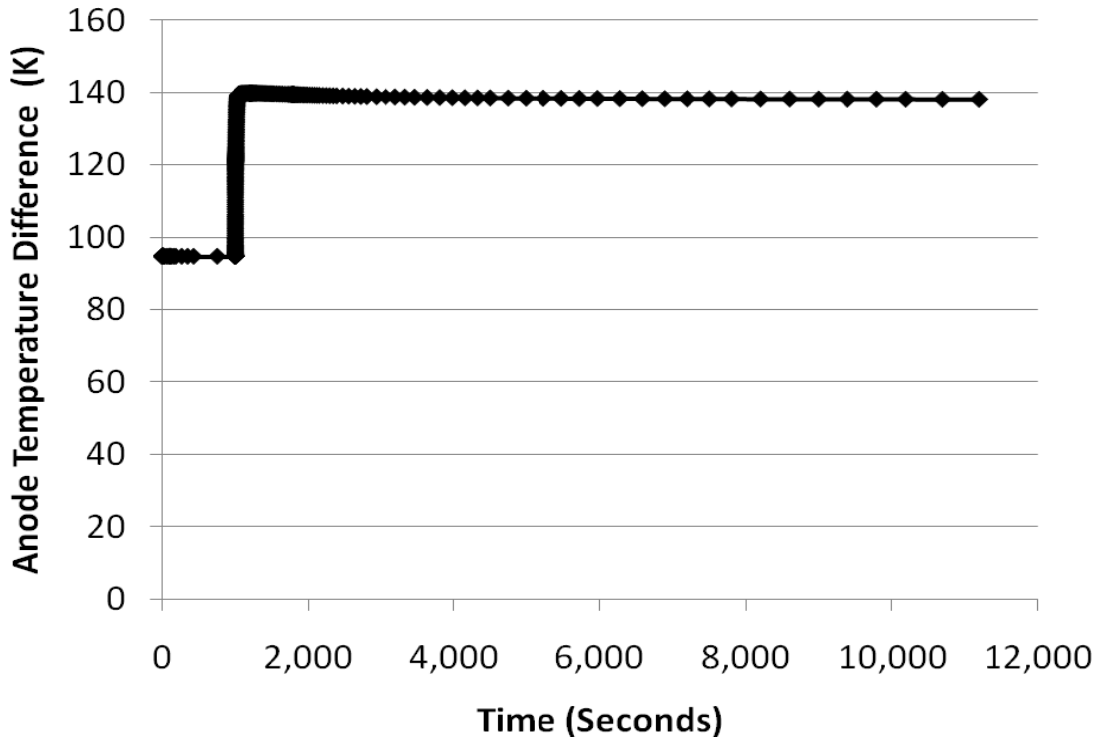
**Figure A2.2 - 73: Compressor dynamic response to a decrease in fuel hydrogen balanced with nitrogen from 100% (blue) to 75% (red) of design state. Gas turbine shaft speed controlled at 3,600 RPM and primary control of blower/compressor mixture temperature at 800 K and secondary control of blower speed.**

The anode-cathode inlet pressure difference decreases (Figure A2.2 - 74) from a starting value of 69 kPa to 66 kPa at the new steady state condition. This perturbation results in an increase in syngas mass flow since nitrogen dilutes syngas hydrogen content and the new steady state fuel utilization is required to be 80%. This increase in syngas mass flow raises not only the anode inlet pressure but also the cathode inlet pressure. The overall drop in pressure difference occurs due to a greater pressure rise across the anode than across the cathode.



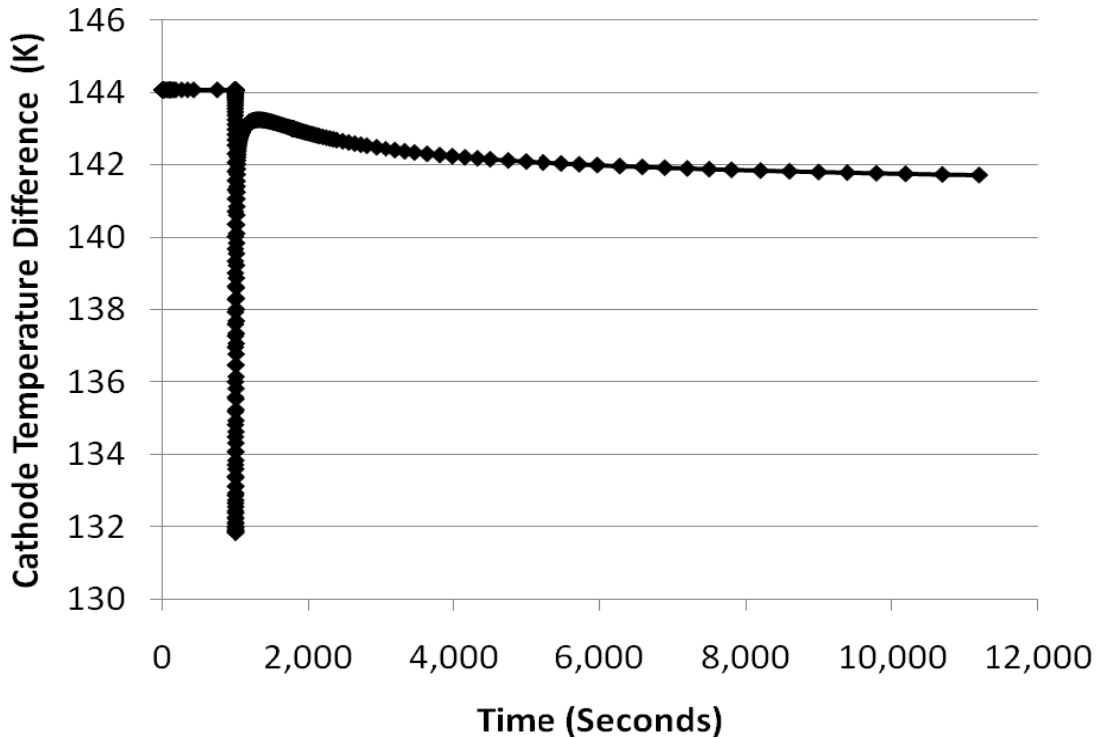
**Figure A2.2 - 74: Dynamic anode-cathode inlet pressure difference response to a decrease in fuel hydrogen balanced with nitrogen from 100% to 75% of design point. Gas turbine speed controlled at 3,600 RPM and primary control of blower/compressor mixture temperature at 800 K with secondary control of recycle blower speed.**

Figure A2.2 - 75 shows that the temperature difference across the anode rises due to the decrease in syngas hydrogen content balanced with nitrogen. There is a 48 K drop in anode inlet temperature due to more mass flow requiring preheating and a 5 K drop in anode outlet temperature due to greater nitrogen content to heat. The overall anode temperature rise is dominated by the fact that the increase in mass flow is difficult to preheat. The DOE requirement for steady state operation is that the anode temperature rise be less than 100 K. Therefore, this 138 K anode temperature difference is problematic.



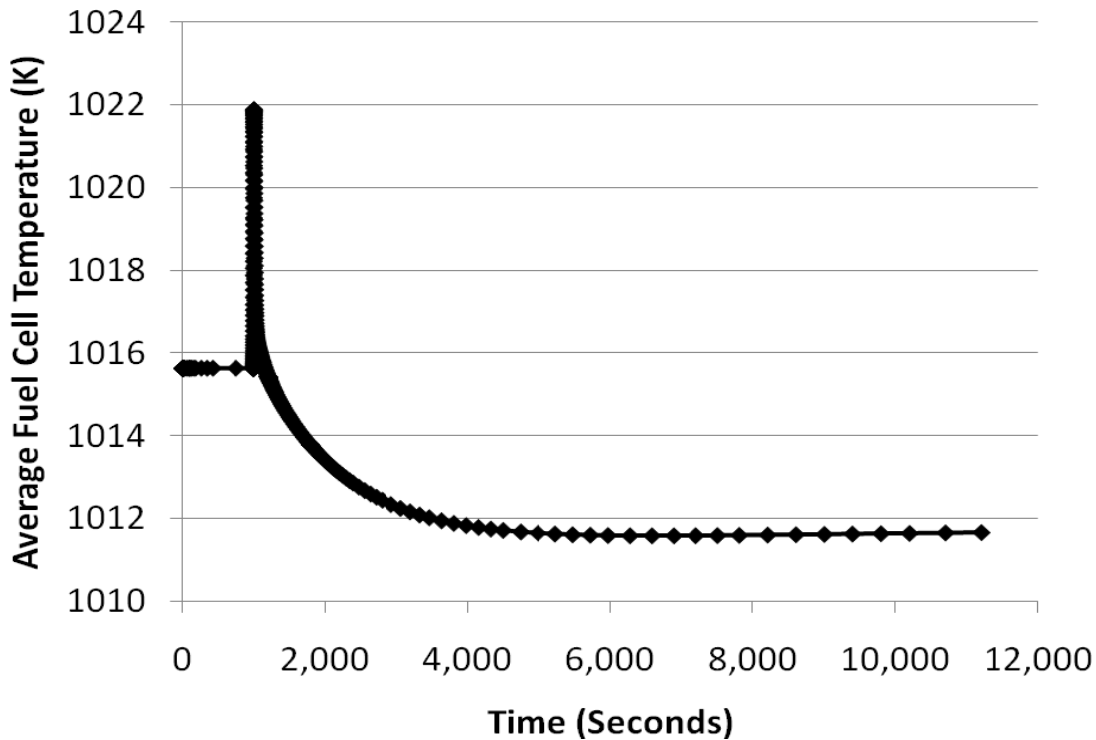
**Figure A2.2 - 75: Dynamic anode inlet-outlet temperature difference response to a decrease in fuel hydrogen balanced with nitrogen from 100% to 75% of design point. Gas turbine speed controlled at 3,600 RPM and primary control of blower/compressor mixture temperature at 800 K with secondary control of recycle blower speed.**

Figure A2.2 - 76 shows that the temperature difference across the cathode decreases due to the decrease in syngas hydrogen content balanced with nitrogen. There is a 3 K drop in cathode inlet temperature and a 5 K drop in cathode outlet temperature due to a lower combustor outlet temperature. The DOE requirement for steady state operation is that the cathode temperature rise be less than 150 K. Therefore, this 142 K cathode temperature difference is not problematic.



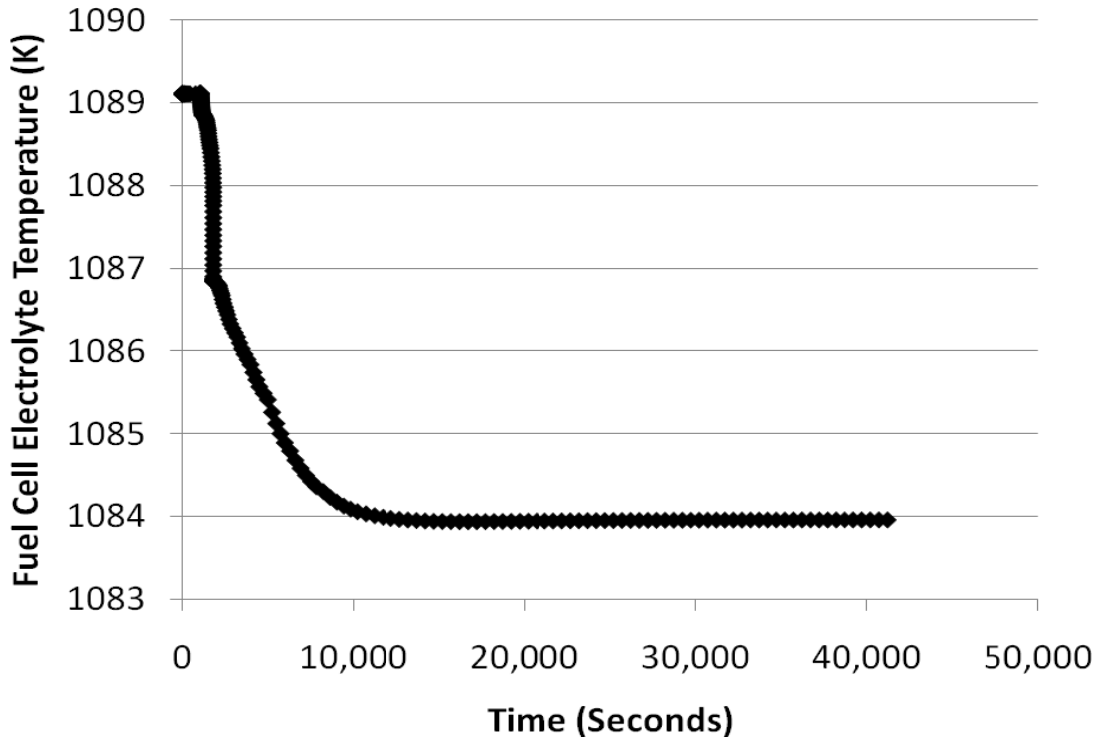
**Figure A2.2 - 76: Dynamic cathode inlet-outlet temperature difference response to a decrease in fuel hydrogen balanced with nitrogen from 100% to 75% of design point. Gas turbine speed controlled at 3,600 RPM and primary control of blower/compressor mixture temperature at 800 K with secondary control of recycle blower speed.**

Figure A2.2 - 77 shows that the average fuel cell temperature across the cathode decreases from 1016 K to 1012 K. The DOE requirement for steady state operation is that this average temperature be between 998 – 1048 K. This perturbation results in an average temperature within the prescribed range.



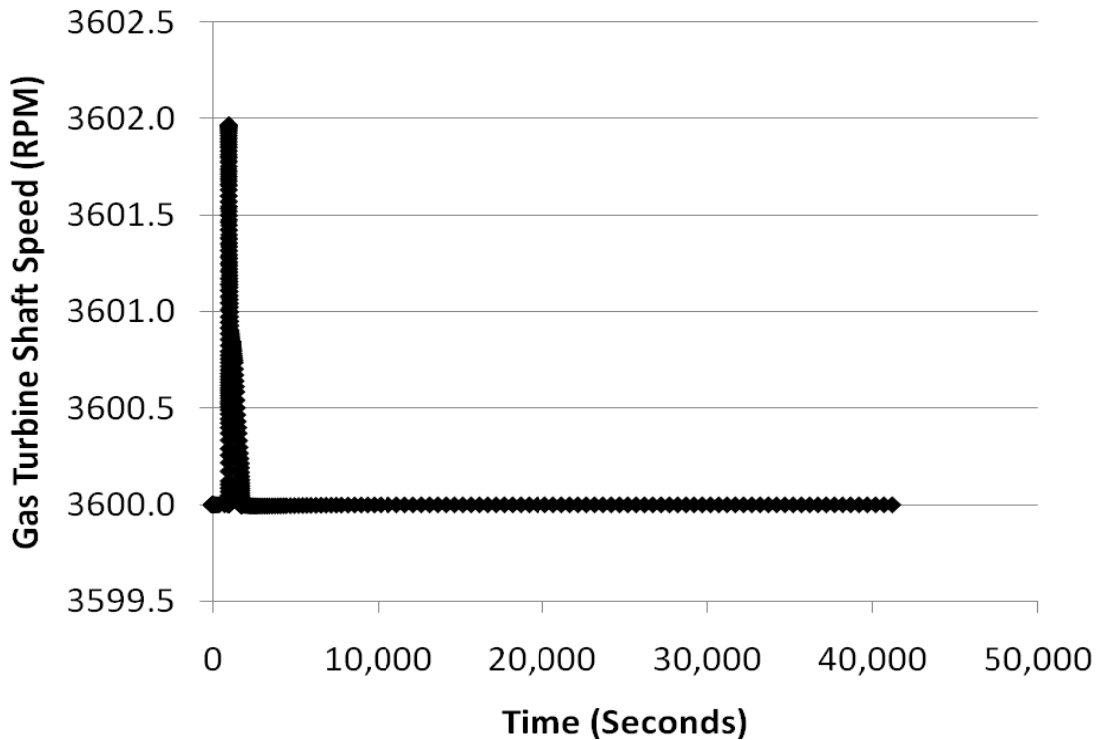
**Figure A2.2 - 77: Dynamic average fuel cell temperature response to a decrease in fuel hydrogen balanced with nitrogen from 100% to 75% of design point. Gas turbine speed controlled at 3,600 RPM and primary control of blower/compressor mixture temperature at 800 K with secondary control of recycle blower speed.**

Figure A2.2 - 78 shows that the tri-layer temperature drops from 1089 K to 1084 K, a minimal change. There is no specified DOE requirement for this parameter but like the average fuel cell temperature it is undesirable that it change significantly since thermal cycling can lead to material stress and failure. Maintaining a steady tri-layer temperature is the focus of the controller used in “control strategy #2”



**Figure A2.2 - 78: Dynamic tri-layer temperature response to a decrease in fuel hydrogen balanced with nitrogen from 100% to 75% of design state. Gas turbine speed controlled at 3,600 RPM and primary control of blower/compressor mixture temperature at 800 K with secondary control of recycle blower speed.**

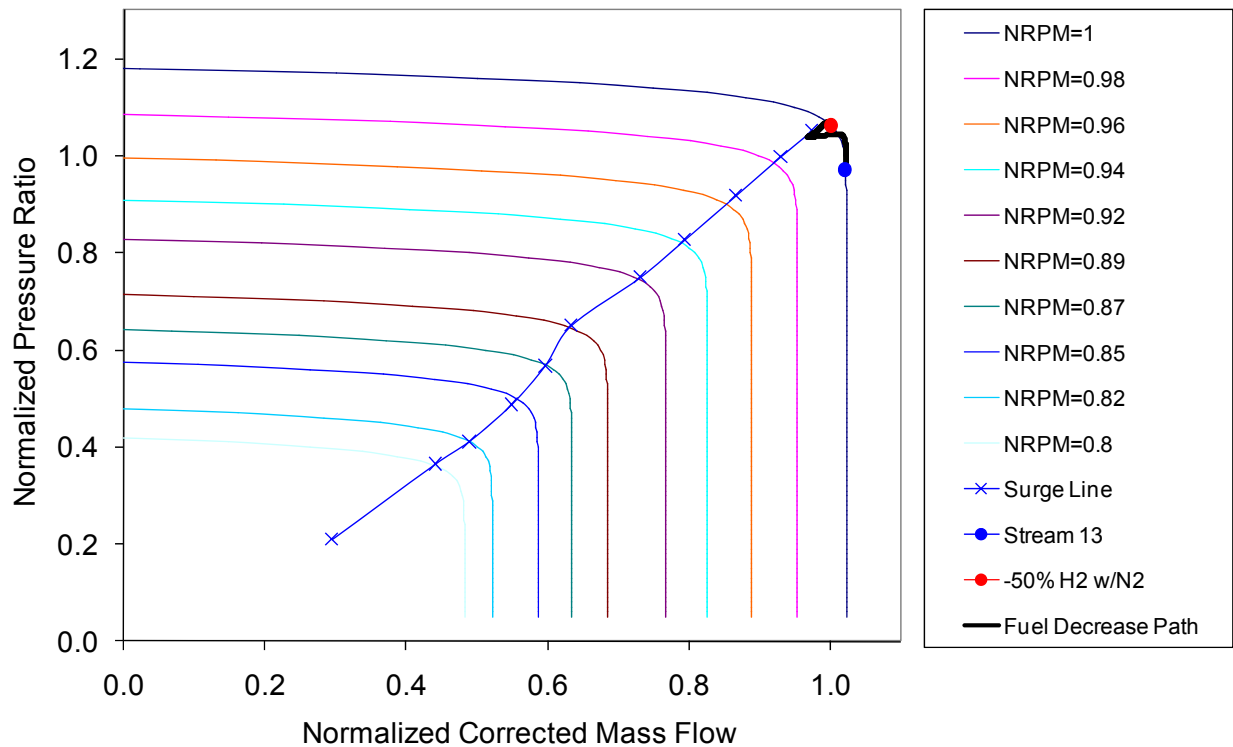
Figure A2.2 - 79 shows that after a minor increase in gas turbine shaft speed, the controller regains the 3600 RPM set point. This control strategy assumes the use of a synchronous generator.



**Figure A2.2 - 79: Dynamic gas turbine shaft speed response to a decrease in fuel hydrogen balanced with nitrogen from 100% to 75% of design point. Gas turbine speed controlled at 3,600 RPM and primary control of blower/compressor mixture temperature at 800 K with secondary control of recycle blower speed.**

Figure A2.2 - 80 shows the case when the fuel cell is subjected to a 50% decrease in syngas hydrogen content. In this case the path of the dynamic is erratic and the gas turbine power drops below zero in the model. This perturbation could have caused a compressor surge (as the approach to the surge line indicates). In addition, the final state produces zero gas turbine power, which is not desirable. There is no control of the fuel cell temperature in this control strategy and the tri-layer temperature goes from an initial temperature of 1088 K to 1144 K at the final state of the dynamic.

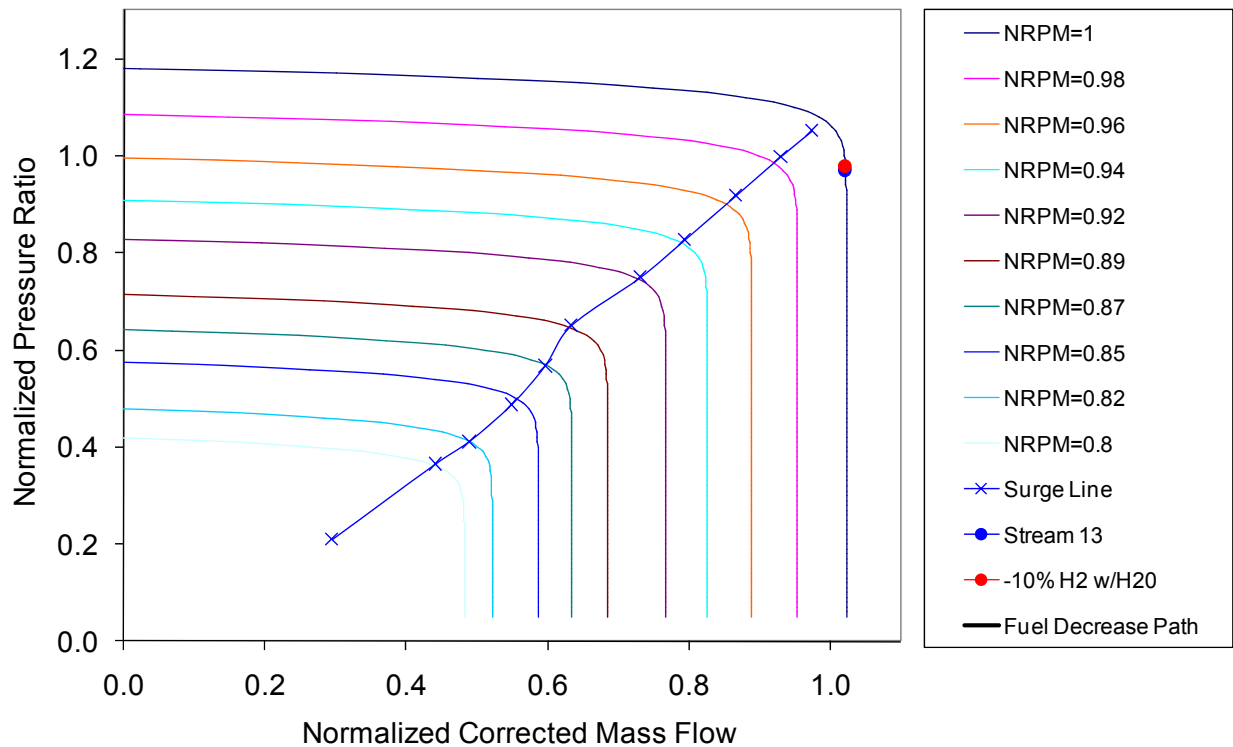
The overall trend observed in the dynamic system responses to fuel hydrogen content perturbations is that the compressor mass flow decreases and pressure ratio increases slightly as fuel hydrogen content decreases for a fixed compressor speed. This is because as inert content increasingly displaces fuel content in the syngas, it absorbs more heat of reaction which effectively cools the fuel cell (including the temperature of the cathode outlet stream). This leads to larger blower recycle ratios which are needed to maintain the required mixture temperature of 800 K for the blower and compressor outlet streams. This in turn requires higher blower speeds and outlet pressures to flow more mass through the cathode compartment requiring a corresponding increase in the compressor outlet pressure.



**Figure A2.2 - 80: Compressor dynamic response to a decrease in fuel hydrogen balanced with nitrogen from 100% (blue) to 50% (red) of design state. Gas turbine shaft speed controlled at 3,600 RPM and primary control of blower/compressor mixture temperature at 800 K and secondary control of blower speed.**

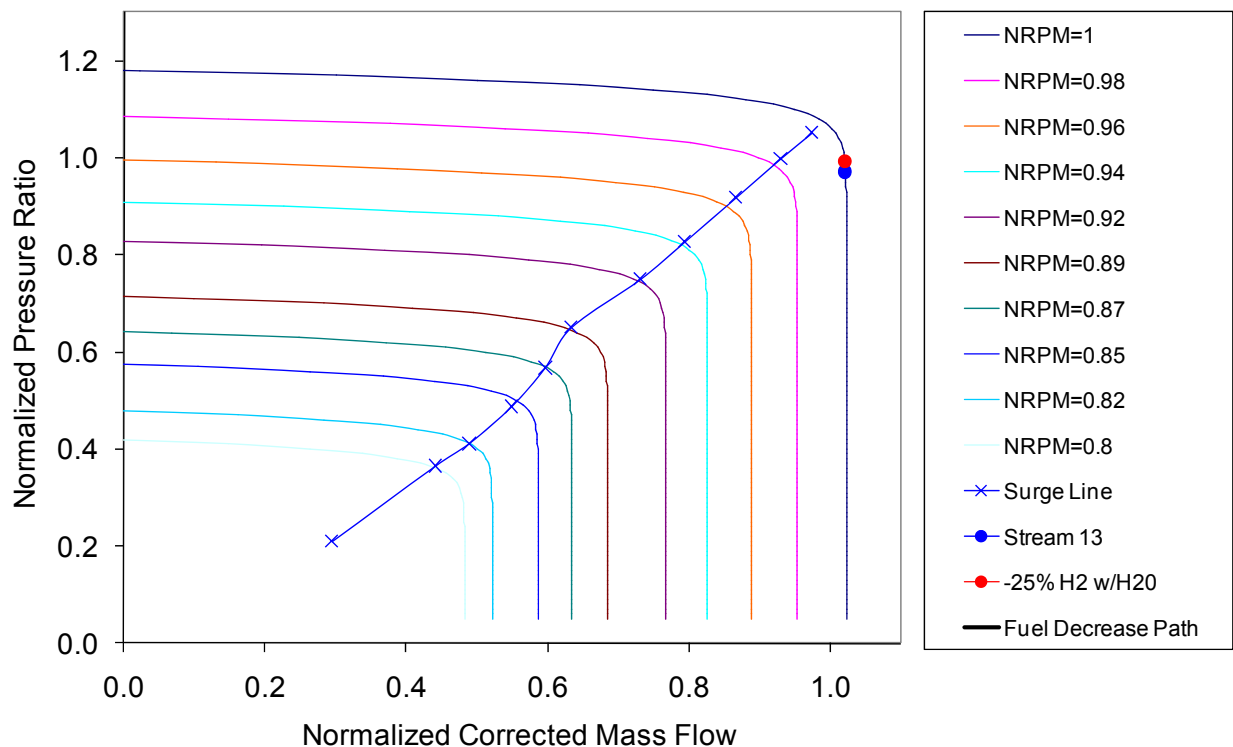
### Syngas Hydrogen Composition Perturbations (Balanced with Steam)

Figure A2.2 - 81 shows the case when the fuel cell is subjected to an instantaneous 10% decrease in syngas hydrogen content (balanced with steam). There is virtually no change in compressor operating point during this dynamic perturbation. There is no control of the fuel cell temperature in this control strategy and the tri-layer temperature goes from an initial temperature of 1088 K to 1087 K at the final state of the dynamic.



**Figure A2.2 - 81: Compressor dynamic response to a decrease in fuel hydrogen balanced with steam from 100% (blue) to 90% (red) of design state. Gas turbine shaft speed controlled at 3,600 RPM and primary control of blower/compressor mixture temperature at 800 K and secondary control of blower speed.**

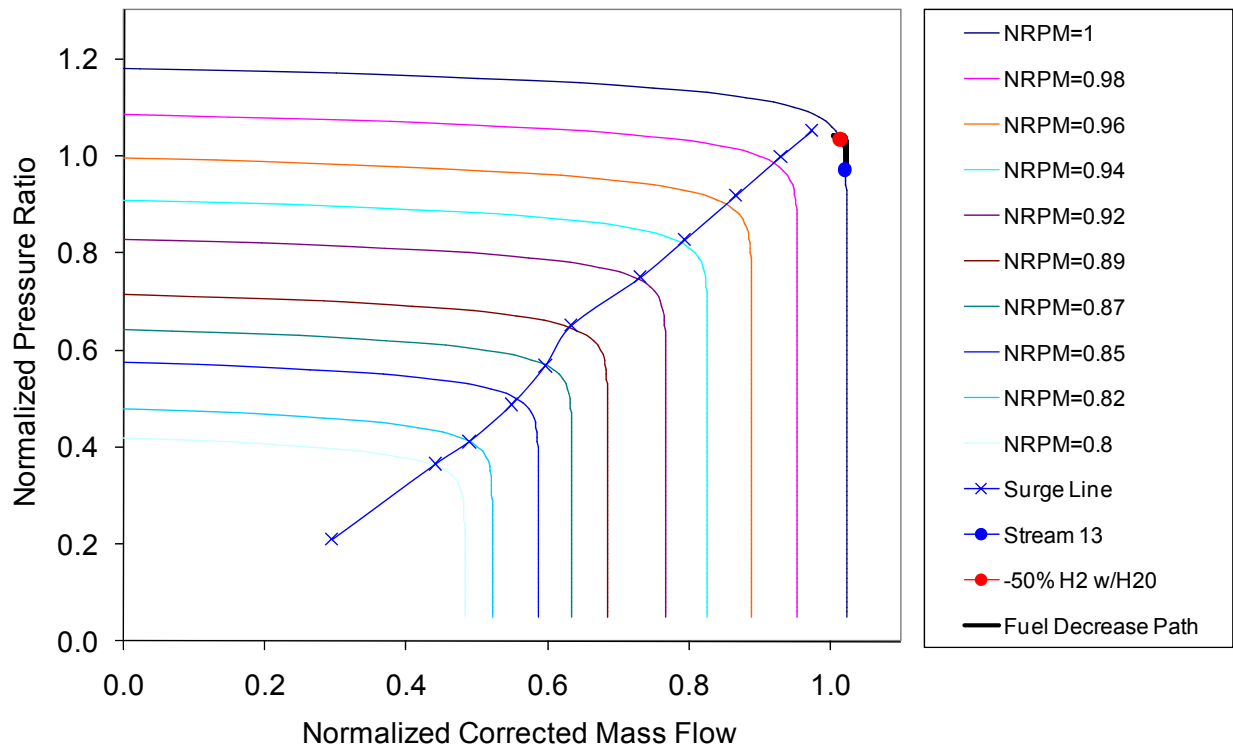
Figure A2.2 - 82 shows the case when the fuel cell is subjected to a 25% decrease in syngas hydrogen content balanced with steam. There is a slight increase in compressor pressure ratio from the initial to final state. There is no control of the fuel cell temperature in this control strategy and the tri-layer temperature goes from an initial temperature of 1088 K to 1085 K at the final state of the transient.



**Figure A2.2 - 82: Compressor dynamic response to a decrease in fuel hydrogen balanced with steam from 100% (blue) to 75% (red) of design state. Gas turbine shaft speed controlled at 3,600 RPM and primary control of blower/compressor mixture temperature at 800 K and secondary control of blower speed.**

Figure A2.2 - 83 shows the case when the fuel cell is subjected to a 50% decrease in syngas hydrogen content balanced with steam. There is an increase in compressor pressure ratio from the initial to final state. Unlike the case when nitrogen balances the decrease in hydrogen content (Figure A2.2 - 80), the system maintains operational stability but approaches the surge line. There is no control of the fuel cell temperature in this control strategy and the tri-layer temperature goes from an initial temperature of 1088 K to 1075 K at the final state of the dynamic.

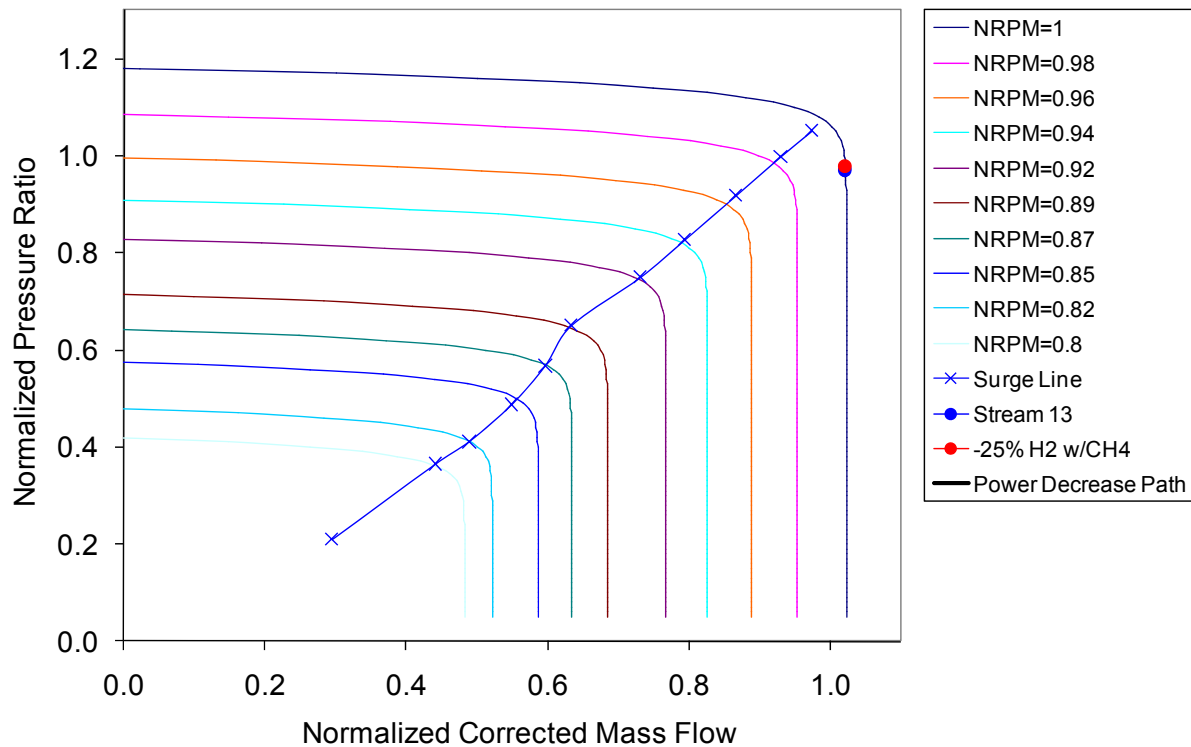
The overall trend during these fuel decrease dynamics is that the compressor mass flow decreases and pressure ratio increases slightly as fuel content decreases for a fixed compressor speed. This is because as steam content increasingly displaces fuel content in the syngas, it absorbs more heat of reaction which effectively cools the fuel cell (including the temperature of the cathode outlet stream). This leads to larger blower recycle ratios which are needed to maintain the required mixture temperature of 800 K for the blower and compressor outlet streams. This in turn requires higher blower speeds and outlet pressures and a correspondingly higher compressor outlet pressure.



**Figure A2.2 - 83: Compressor dynamic response to a decrease in fuel hydrogen balanced with steam from 100% (blue) to 50% (red) of design state. Gas turbine shaft speed controlled at 3,600 RPM and primary control of blower/compressor mixture temperature at 800 K and secondary control of blower speed.**

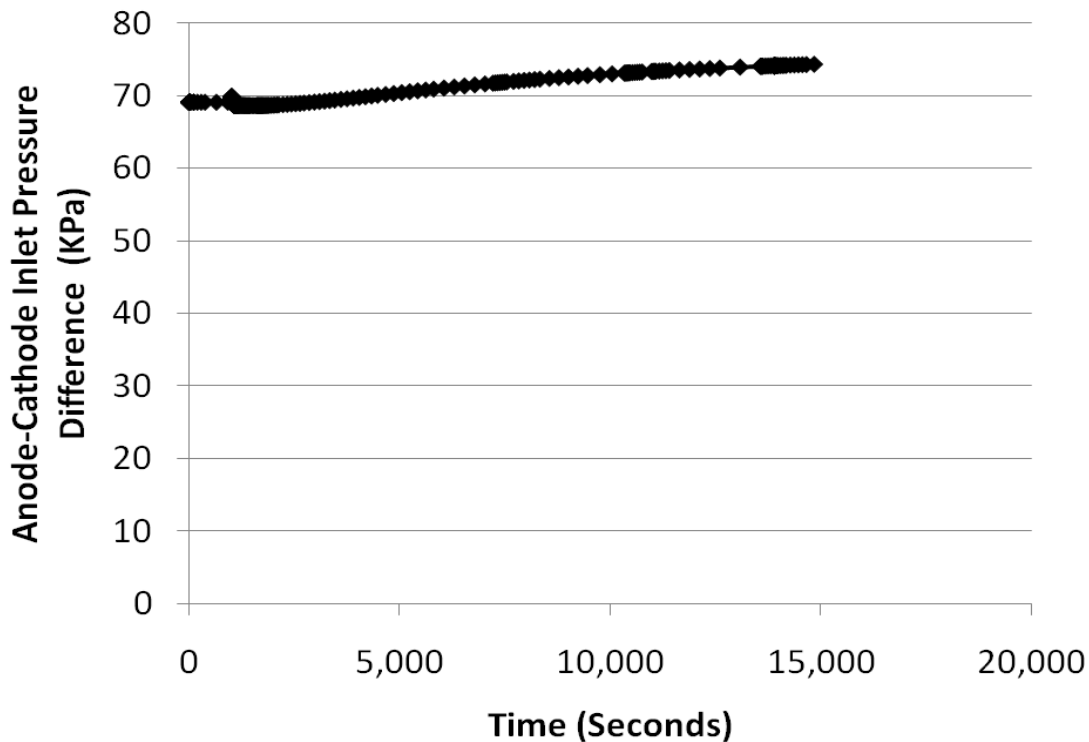
### **Syngas Hydrogen Composition Perturbations (Balanced with Methane)**

Figure A2.2 - 84 shows that when the fuel cell is subjected to a 25% decrease in syngas hydrogen content balanced with methane, this perturbation has very slight impact on compressor operation and does not threaten compressor surge.



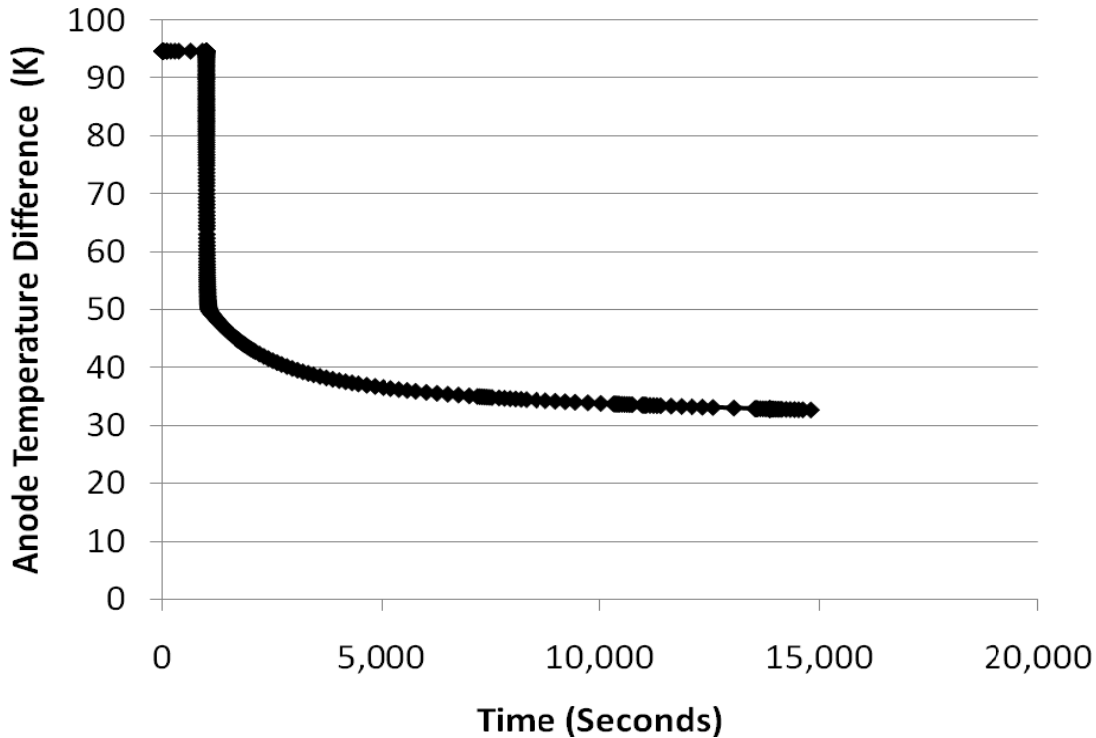
**Figure A2.2 - 84: Compressor dynamic response to a decrease in fuel hydrogen balanced with methane from 100% to 75% of design point. Gas turbine speed controlled at 3,600 RPM and primary control of blower/compressor mixture temperature at 800 K with secondary control of recycle blower speed.**

The anode-cathode inlet pressure difference increases (Figure A2.2 - 85) from a starting value of 69 kPa to 76 kPa at the new steady state condition. This perturbation results in a slight decrease in syngas mass flow since methane is considered a fuel source that ultimately contributes four hydrogen molecules for every molecule of methane and the new steady state fuel utilization is required to be 80%. The overall rise in pressure difference is dominated by a higher cathode inlet pressure.



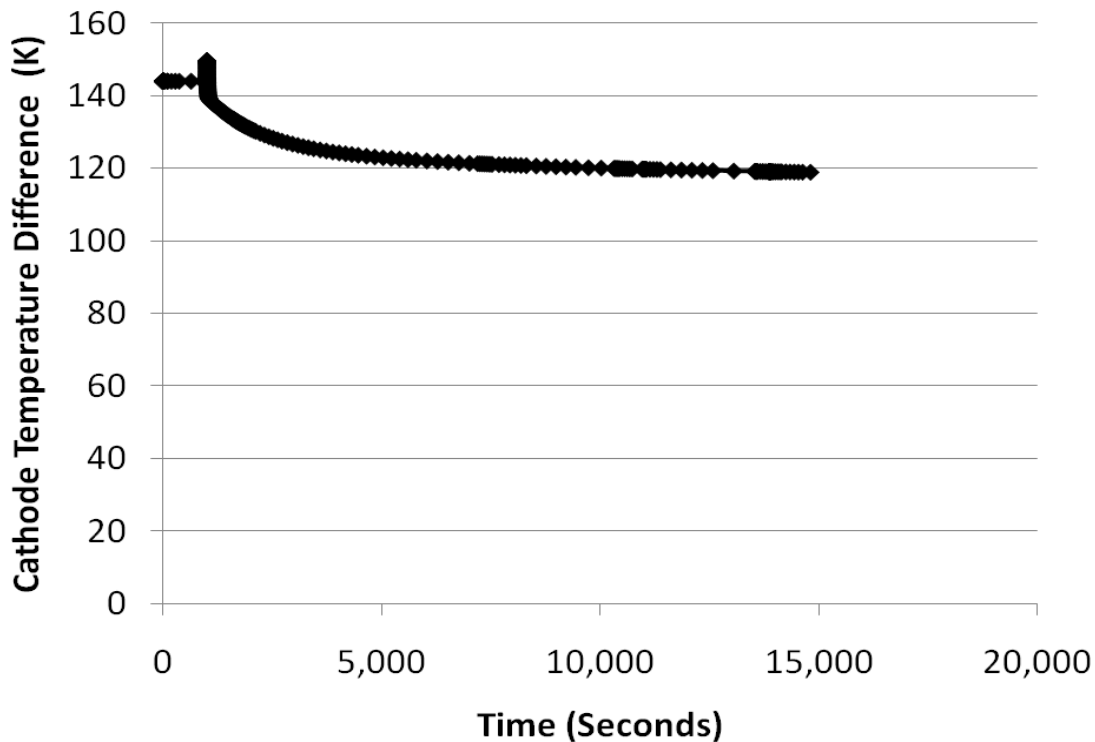
**Figure A2.2 - 85: Dynamic anode-cathode inlet pressure difference response to a decrease in fuel hydrogen balanced with methane from 100% to 75% of design point. Gas turbine speed controlled at 3,600 RPM and primary control of blower/compressor mixture temperature at 800 K with secondary control of recycle blower speed.**

Figure A2.2 - 86 shows that the temperature difference across the anode drops due to the decrease in syngas hydrogen content balanced with methane. Internal reformation of methane is an endothermic process and causes this temperature drop. There is a 22 K rise in anode inlet temperature due to less fuel requiring preheating and a 41 K drop in anode outlet temperature due to endothermic internal reformation of methane. The overall anode temperature drop is a combination of these two factors. The DOE requirement for steady state operation is that the anode temperature rise be less than 100 K. Therefore, this 32 K anode temperature difference is not problematic.



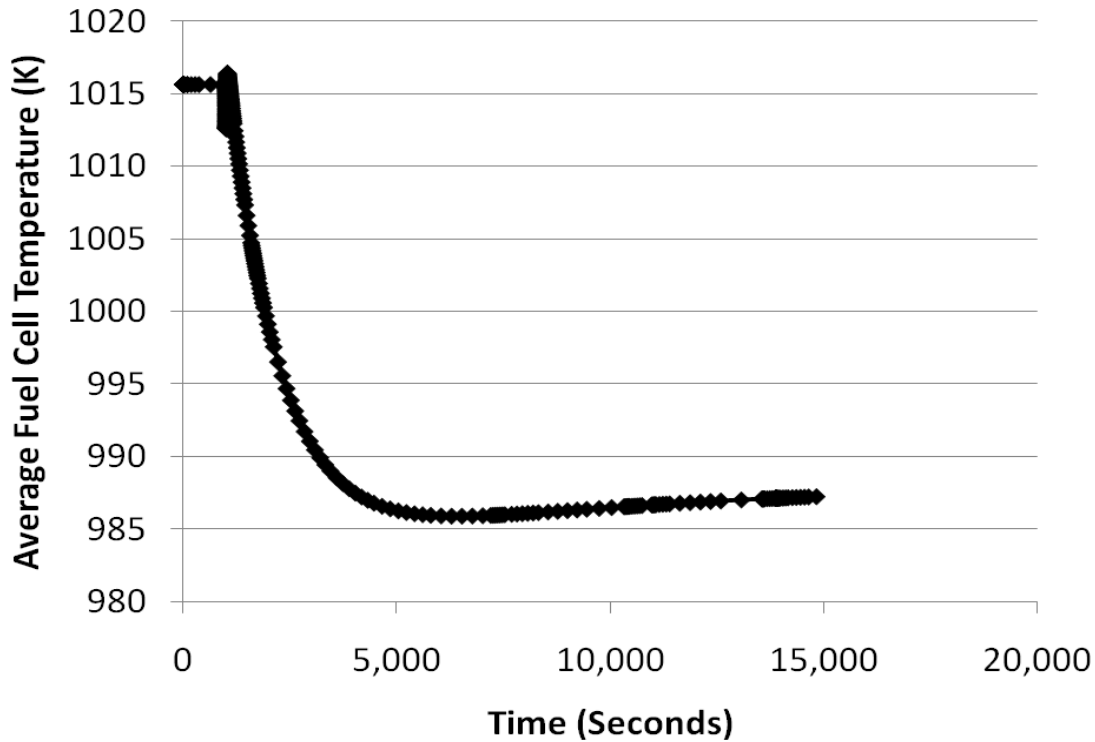
**Figure A2.2 - 86: Dynamic anode inlet-outlet temperature difference response to a decrease in fuel hydrogen balanced with methane from 100% to 75% of design point. Gas turbine speed controlled at 3,600 RPM and primary control of blower/compressor mixture temperature at 800 K with secondary control of recycle blower speed.**

Figure A2.2 - 87 shows that the temperature difference across the cathode drops due to the decrease in syngas hydrogen content balanced with methane. There is a 22 K drop in cathode inlet temperature due to a lower combustor outlet temperature and therefore less effective preheating and a 41 K drop in cathode outlet temperature due to endothermic internal reformation of methane. The DOE requirement for steady state operation is that the cathode temperature rise be less than 150 K. Therefore, this 118 K cathode temperature difference is not problematic.



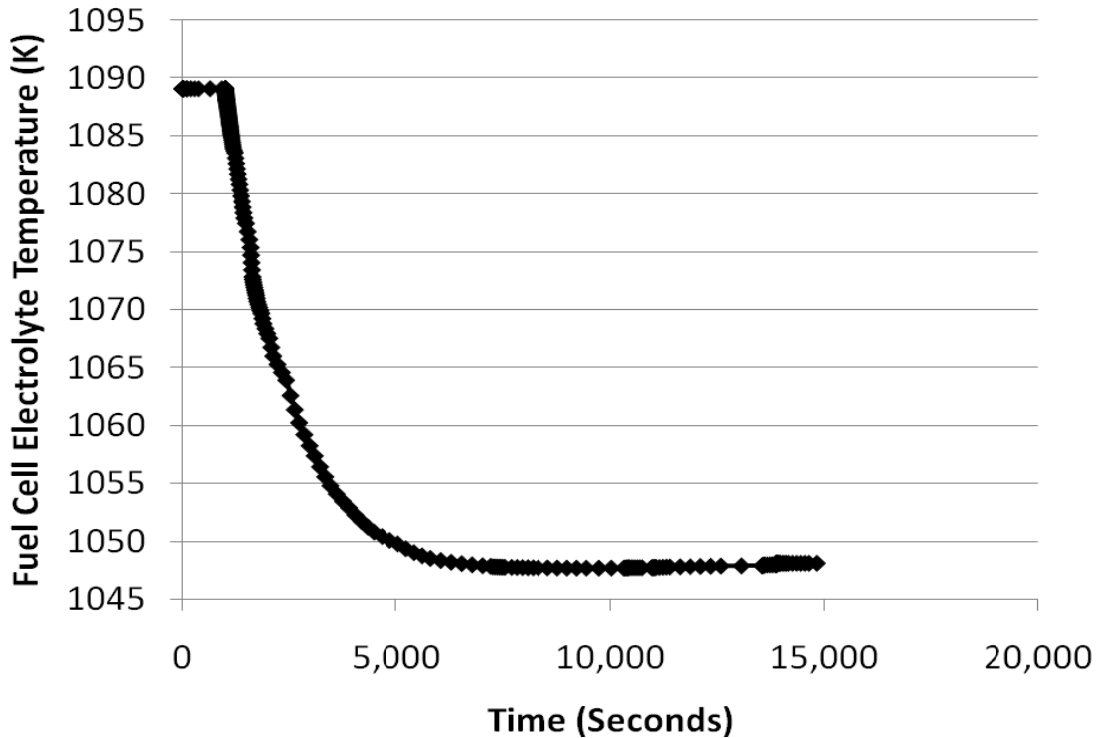
**Figure A2.2 - 87: Dynamic cathode inlet-outlet temperature difference response to a decrease in fuel hydrogen balanced with methane from 100% to 75% of design point. Gas turbine speed controlled at 3,600 RPM and primary control of blower/compressor mixture temperature at 800 K with secondary control of recycle blower speed.**

Figure A2.2 - 88 shows that the average fuel cell temperature across the cathode decreases from 1016 K to 988 K. The DOE requirement for steady state operation is that this average temperature be between 998 – 1048 K. This perturbation results in an average temperature outside of the prescribed range.



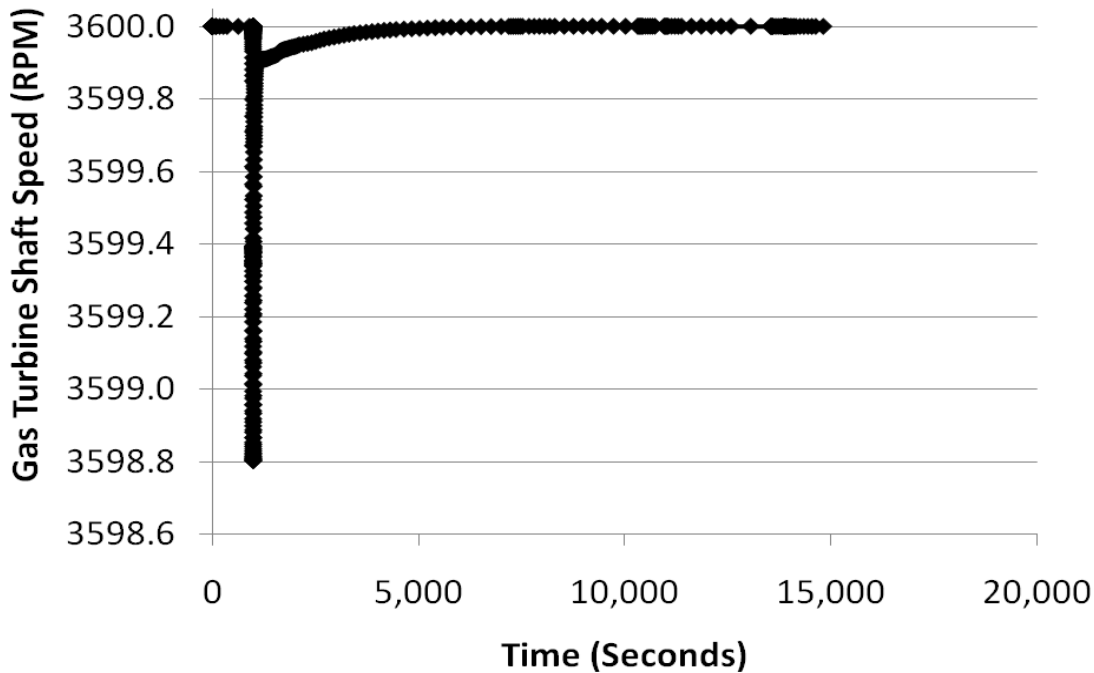
**Figure A2.2 - 88: Dynamic average fuel cell temperature response to a decrease in fuel hydrogen balanced with methane from 100% to 75% of design point. Gas turbine speed controlled at 3,600 RPM and primary control of blower/compressor mixture temperature at 800 K with secondary control of recycle blower speed.**

Figure A2.2 - 89 shows that the tri-layer temperature drops from 1089 K to 1048 K. There is no specified DOE requirement for this parameter but like the average fuel cell temperature it is undesirable that it change significantly since thermal cycling can lead to material stress and failure. Maintaining a steady tri-layer temperature is the focus of the controller used in “control strategy #2”



**Figure A2.2 - 89: Dynamic tri-layer temperature response to a decrease in fuel hydrogen balanced with methane from 100% to 75% of design point. Gas turbine speed controlled at 3,600 RPM and primary control of blower/compressor mixture temperature at 800 K with secondary control of recycle blower speed.**

Figure A2.2 - 90 shows that after a minor decrease in gas turbine shaft speed, the controller regains the 3600 RPM set point. This control strategy assumes the use of a synchronous generator.



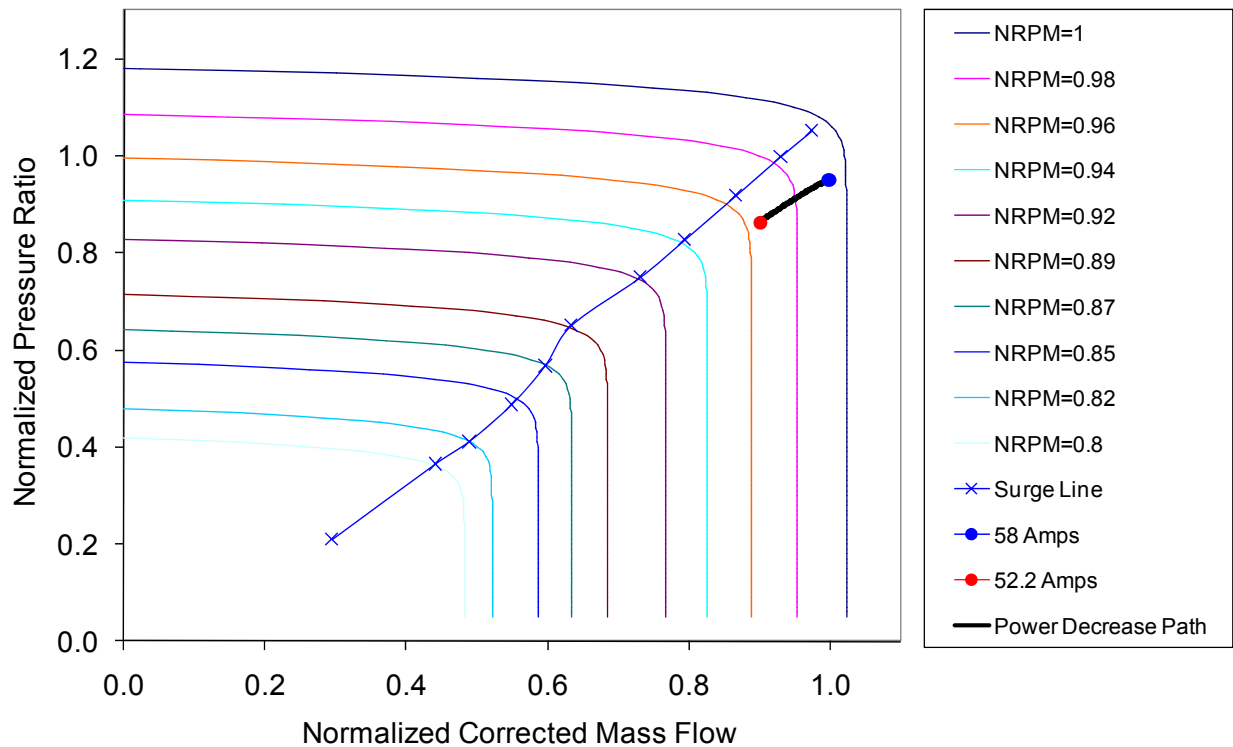
**Figure A2.2 - 90: Dynamic gas turbine shaft speed response to a decrease in fuel hydrogen balanced with methane from 100% to 75% of design point. Gas turbine speed controlled at 3,600 RPM and primary control of blower/compressor mixture temperature at 800 K with secondary control of recycle blower speed.**

## Control Strategy #2

### Fuel Cell Current Demand Perturbations

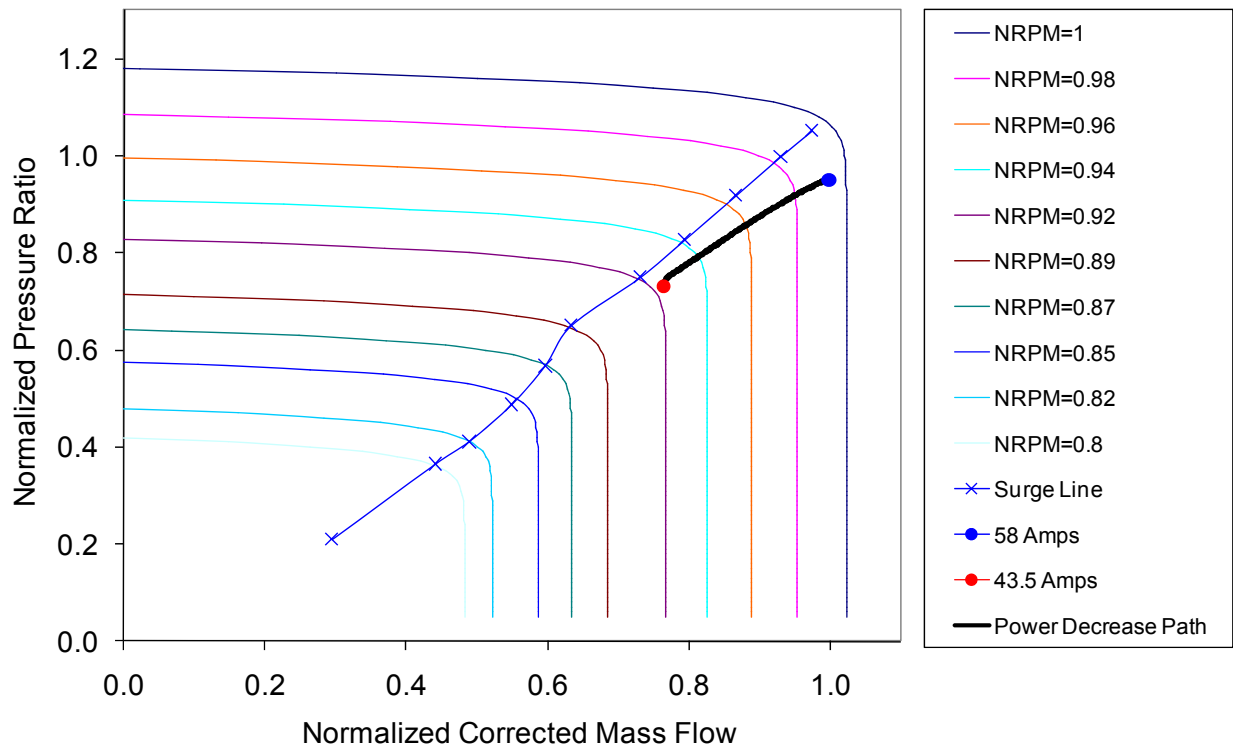
The only difference between control strategy #1 and #2 is that the latter controls fuel cell tri-layer temperature at 1100 K in all cases throughout the dynamic system response to perturbations. This is primarily accomplished by varying the air mass flow rate through the compressor. Unlike the previous analyses presented for control strategy #1 (Figure A2.2 - 55 - Figure A2.2 - 83) the compressor shaft speed is not controlled at 3,600 RPM, but rather can vary to accommodate/produce the necessary variations in air flow rates.

Figure A2.2 - 91 shows the case when the fuel cell is subjected to a 10% drop in current demand perturbation. Less air flow is needed at the final state to meet the steady-state fuel cell temperature requirement since there is less heat generation in the fuel cell at lower current demand. The path of the system dynamic response is very similar to that presented in previous reports when the system used an ejector instead of a blower for cathode recycle.



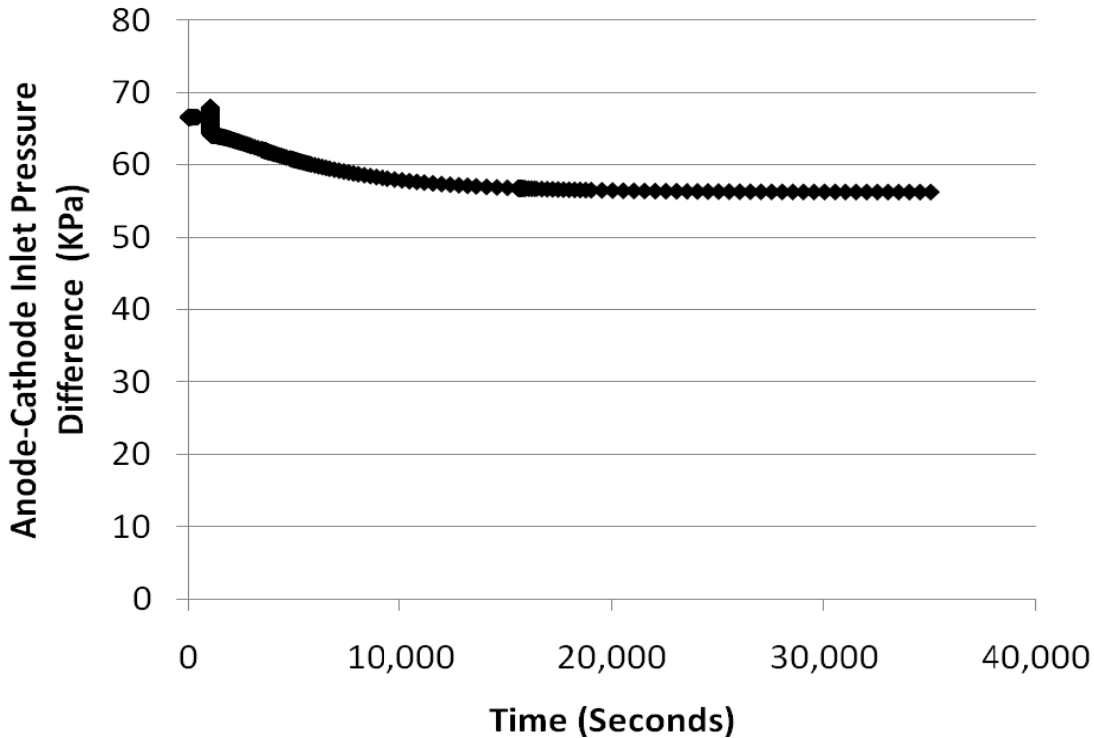
**Figure A2.2 - 91: Compressor dynamic response to a fuel cell load decrease from 100% (blue) to 90% (red) of design state. Primary control of fuel cell temperature at 1,100 K and secondary control of gas turbine shaft speed and primary control of blower/compressor mixture temperature at 800 K and secondary control of blower speed.**

Figure A2.2 - 92 shows the case when the fuel cell is subjected to a 25% drop in current demand perturbation. The mass flow and pressure ratio continue to drop relative to Figure A2.2 - 91 as expected. Note, however, that the surge margin (distance between the surge line and operating condition) is substantially reduced during the dynamic system response to the 25% reduction in current demand perturbation.



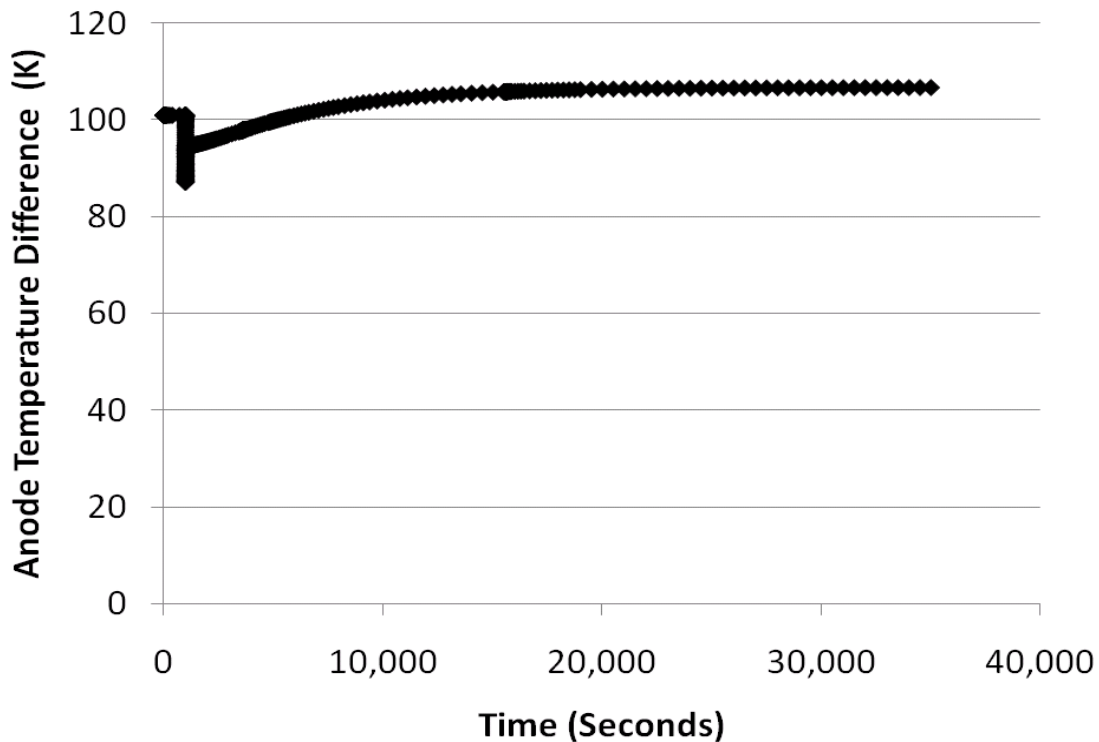
**Figure A2.2 - 92: Compressor dynamic response to a fuel cell load decrease from 100% (blue) to 75% (red) of design state. Primary control of fuel cell temperature at 1,100 K and secondary control of gas turbine shaft speed and primary control of blower/compressor mixture temperature at 800 K and secondary control of blower speed.**

When the fuel cell is subjected to a 25% drop in current demand the anode-cathode inlet pressure difference drops (Figure A2.2 - 93) from a starting value of 69 kPa to 56 kPa at the new steady state condition. This initial 69 kPa difference is due to the much larger mass flow and therefore larger pressure drop in the cathode vs. the anode. The anode-cathode outlet pressures must be equal as the streams converge in the combustor. This initial pressure difference may be too high and require larger cathode air flow channels than used in the current design. The pressure difference drop resulting from this perturbation shows an opposite trend from that seen using control strategy #1 (Figure A2.2 - 57). This is because compressor mass flow is significantly reduced in control strategy #2 in order to maintain the tri-layer temperature set point as load is shed. There is only a minor change to compressor mass flow when control strategy #1 is used. The trade off is that decreases in compressor mass flow can result in compressor surge. The decrease in pressure difference in Figure A2.2 - 93 is due to decreases in both syngas and air mass flow rates, with the reduced air flow rate having the larger of the two impacts. The steady state fuel utilization is maintained at 80%.



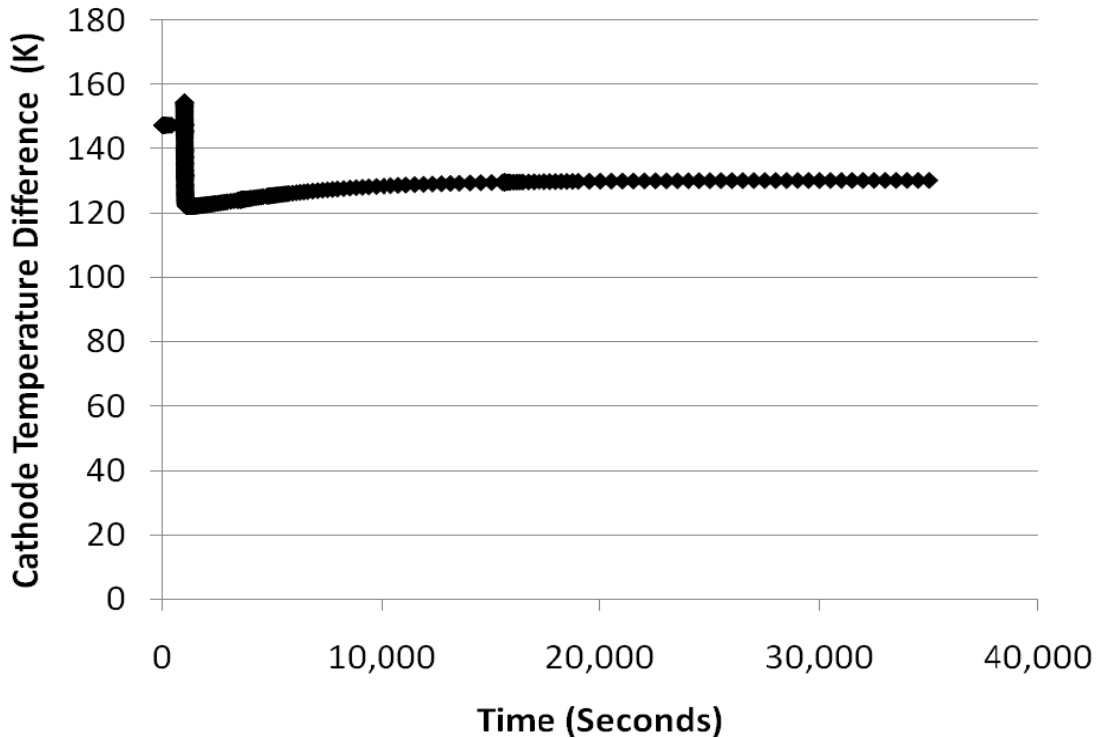
**Figure A2.2 - 93: Dynamic anode-cathode inlet pressure difference response to a fuel cell load decrease from 100% to 75% of design point. Primary control of fuel cell temperature at 1,100 K and secondary control of gas turbine speed and primary control of blower/compressor mixture temperature at 800 K with secondary control of recycle blower speed.**

Figure A2.2 - 94 shows that the temperature difference across the anode rises due to the load shed perturbation. This is the opposite trend of that observed using “control strategy #1” (Figure A2.2 - 58). There is a 6 K drop in anode inlet temperature due to a lower combustor outlet temperature and no change in anode outlet temperature since tri-layer temperature is controlled. The DOE requirement for steady state operation is that the anode temperature rise be less than 100 K. Therefore, this 107 K anode temperature difference is problematic.



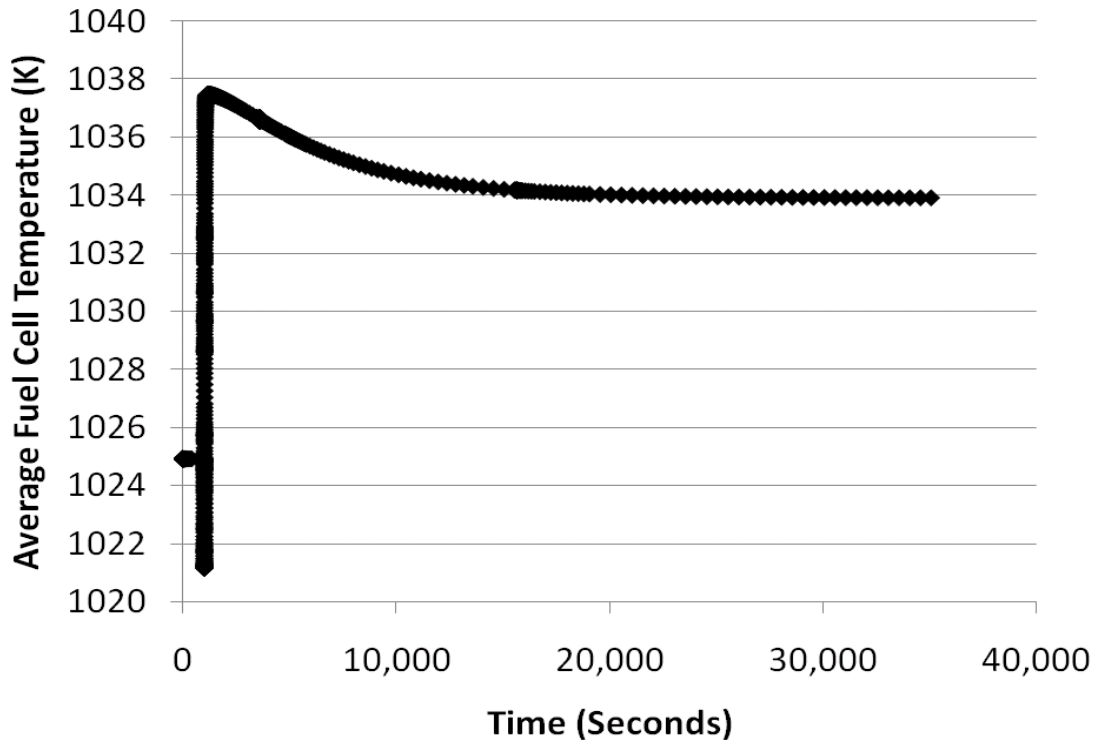
**Figure A2.2 - 94: Dynamic anode inlet-outlet temperature difference response to a fuel cell load decrease from 100% to 75% of design point. Primary control of fuel cell temperature at 1,100 K and secondary control of gas turbine speed and primary control of blower/compressor mixture temperature at 800 K with secondary control of recycle blower speed.**

Figure A2.2 - 95 shows that the temperature difference across the cathode drops due to the load shed perturbation. This is the same trend that was observed using “control strategy #1” (Figure A2.2 - 59). There is an 18 K rise in cathode inlet temperature due to easier preheating of the reduced air mass moving through the system and no change in cathode outlet temperature since tri-layer temperature is controlled. The DOE requirement for steady state operation is that the cathode temperature rise be less than 150 K. Therefore, this 130 K anode temperature difference is not problematic.



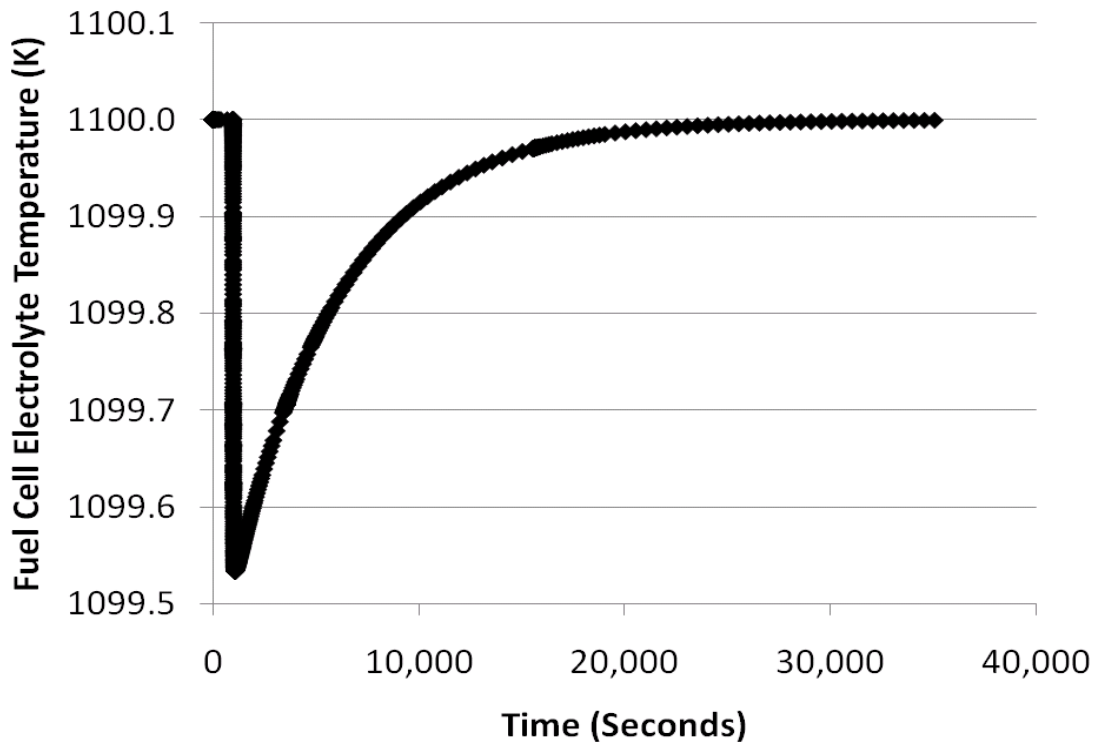
**Figure A2.2 - 95: Dynamic cathode inlet-outlet temperature difference response to a fuel cell load decrease from 100% to 75% of design point. Primary control of fuel cell temperature at 1,100 K and secondary control of gas turbine speed and primary control of blower/compressor mixture temperature at 800 K with secondary control of recycle blower speed.**

Figure A2.2 - 96 shows that the average fuel cell temperature across the cathode rises from 1016 K to 1034 K. The DOE requirement for steady state operation is that this average temperature be between 998 – 1048 K. This perturbation results in an average temperature within the prescribed limits. This is a key difference in comparison to control strategy #1 (Figure A2.2 - 60) in which the end state was outside of the prescribed temperature limits.



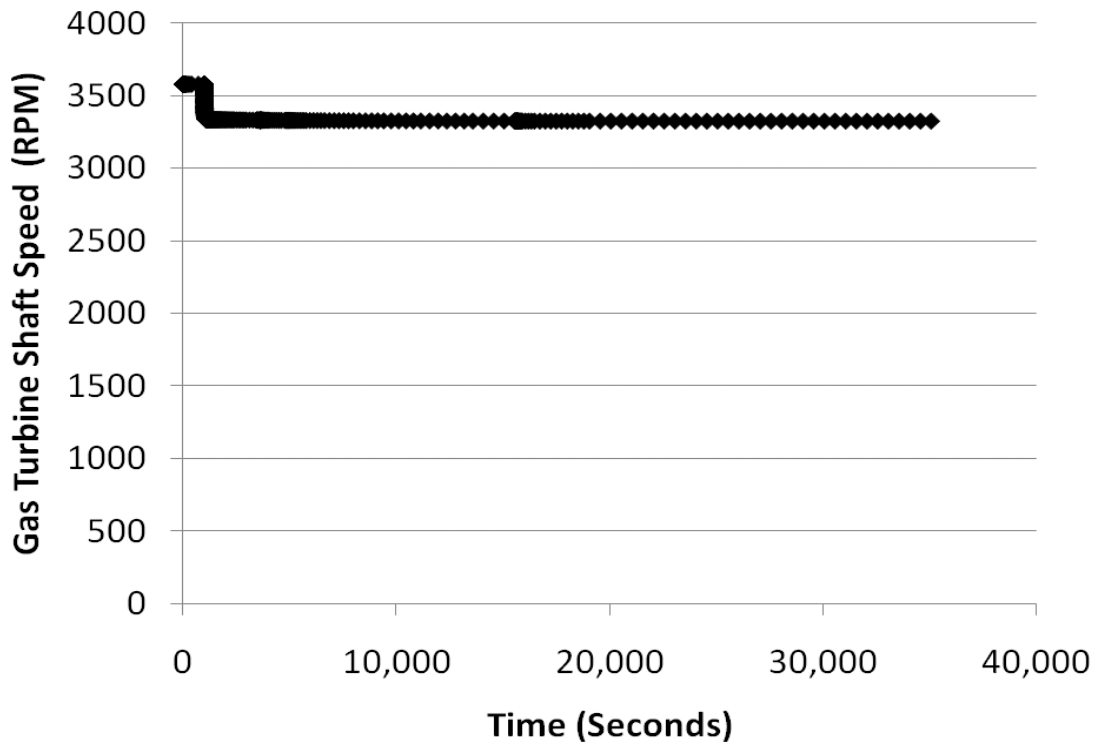
**Figure A2.2 - 96: Dynamic average fuel cell temperature response to a fuel cell load decrease from 100% to 75% of design point. Primary control of fuel cell temperature at 1,100 K and secondary control of gas turbine speed and primary control of blower/compressor mixture temperature at 800 K with secondary control of recycle blower speed.**

Figure A2.2 - 97 shows that after a minor decrease in tri-layer temperature, the control regains the 1100 K set point. This in contrast to the result of control strategy #1 (Figure A2.2 - 61), where there was a 59 K drop in temperature. There is no specified DOE requirement for this parameter but like the average fuel cell temperature it is undesirable that it change significantly since thermal cycling can lead to material stress and failure.



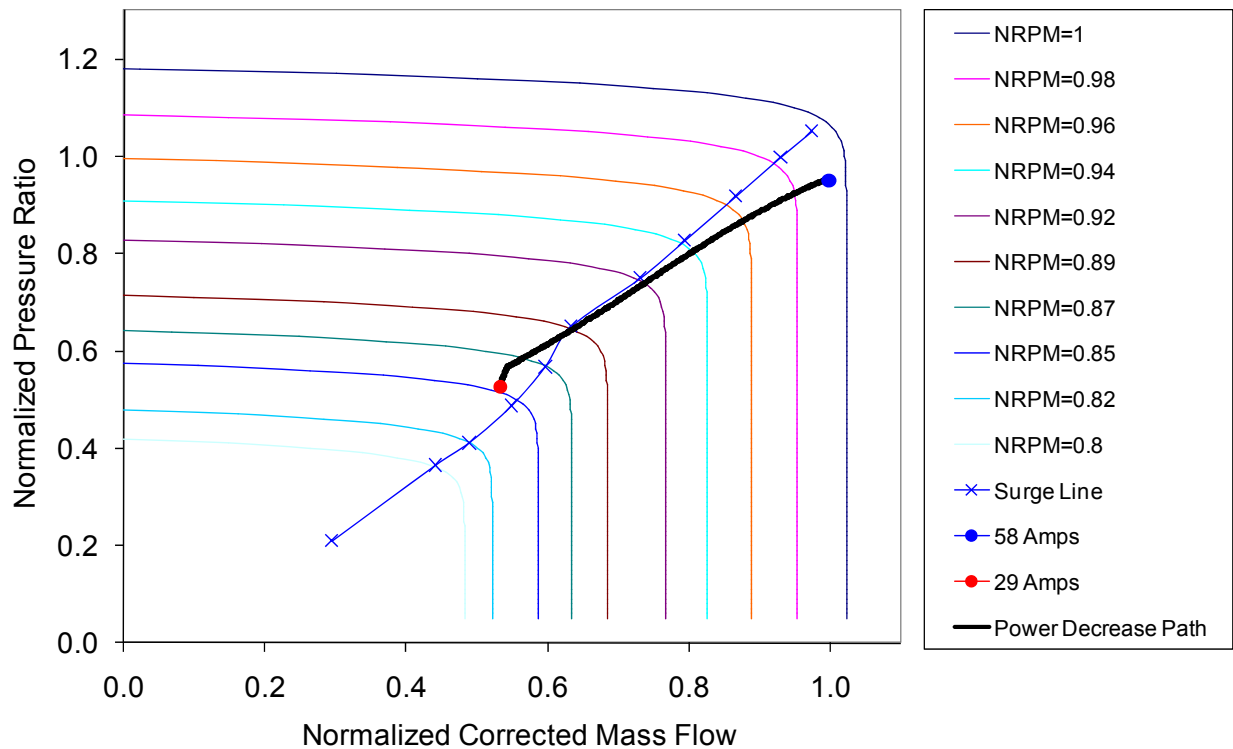
**Figure A2.2 - 97: Dynamic tri-layer temperature response to a fuel cell load decrease from 100% to 75% of design point. Primary control of fuel cell temperature at 1,100 K and secondary control of gas turbine speed and primary control of blower/compressor mixture temperature at 800 K with secondary control of recycle blower speed.**

Figure A2.2 - 98 shows that one strategy of controlling the tri-layer temperature is by varying compressor air flow rate using a variable speed gas turbine. In this case, gas turbine shaft speed decreases from 3577 to 3325 RPM. This control strategy assumes the use of an asynchronous generator.



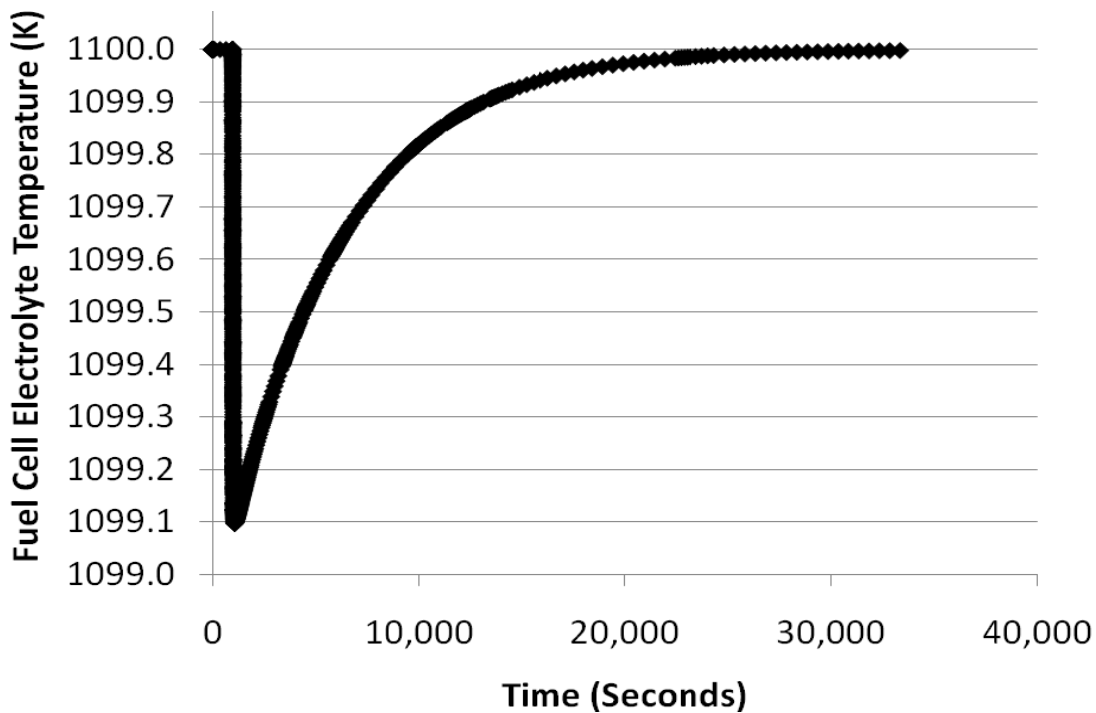
**Figure A2.2 - 98: Dynamic gas turbine shaft speed response to a fuel cell load decrease from 100% to 75% of design point. Primary control of fuel cell temperature at 1,100 K and secondary control of gas turbine speed and primary control of blower/compressor mixture temperature at 800 K with secondary control of recycle blower speed.**

Figure A2.2 - 99 shows the case when the fuel cell is subjected to an instantaneous 50% drop in current demand perturbation. The mass flow and pressure ratio drop to a region beyond the surge line. This was also found to occur for the same perturbation in the case when an ejector is used in place of the blower (see Figure A2.2 - 38). The final operating point shown in this case is therefore not stable and indicates a vulnerability of the system to induce compressor surge for this type of load-shed (current demand drop) perturbation.



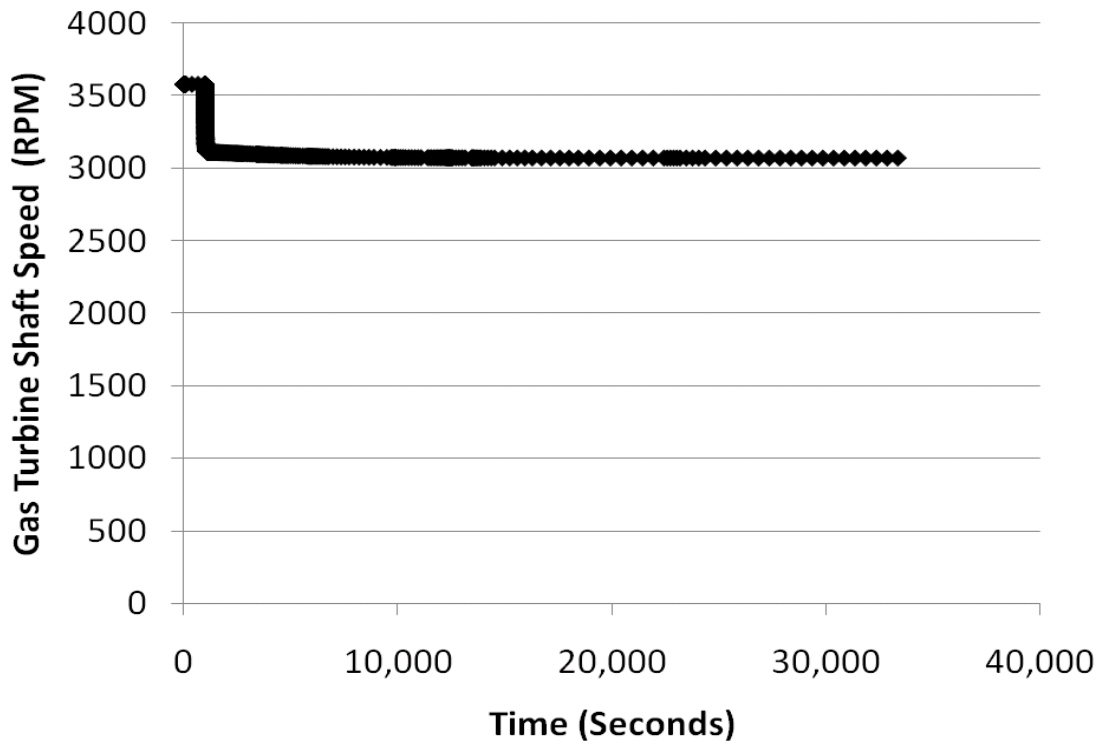
**Figure A2.2 - 99: Compressor dynamic response to a fuel cell load decrease from 100% (blue) to 50% (red) of design state. Primary control of fuel cell temperature at 1,100 K and secondary control of gas turbine shaft speed and primary control of blower/compressor mixture temperature at 800 K and secondary control of blower speed.**

Figure A2.2 - 100 shows that even in the case of a 50% reduction in fuel cell load, the controller can maintain tri-layer temperature at the 1100 K set point after a slight decrease. This in contrast to the result of control strategy #1 (results not shown), where there was a 157 K drop in tri-layer temperature.



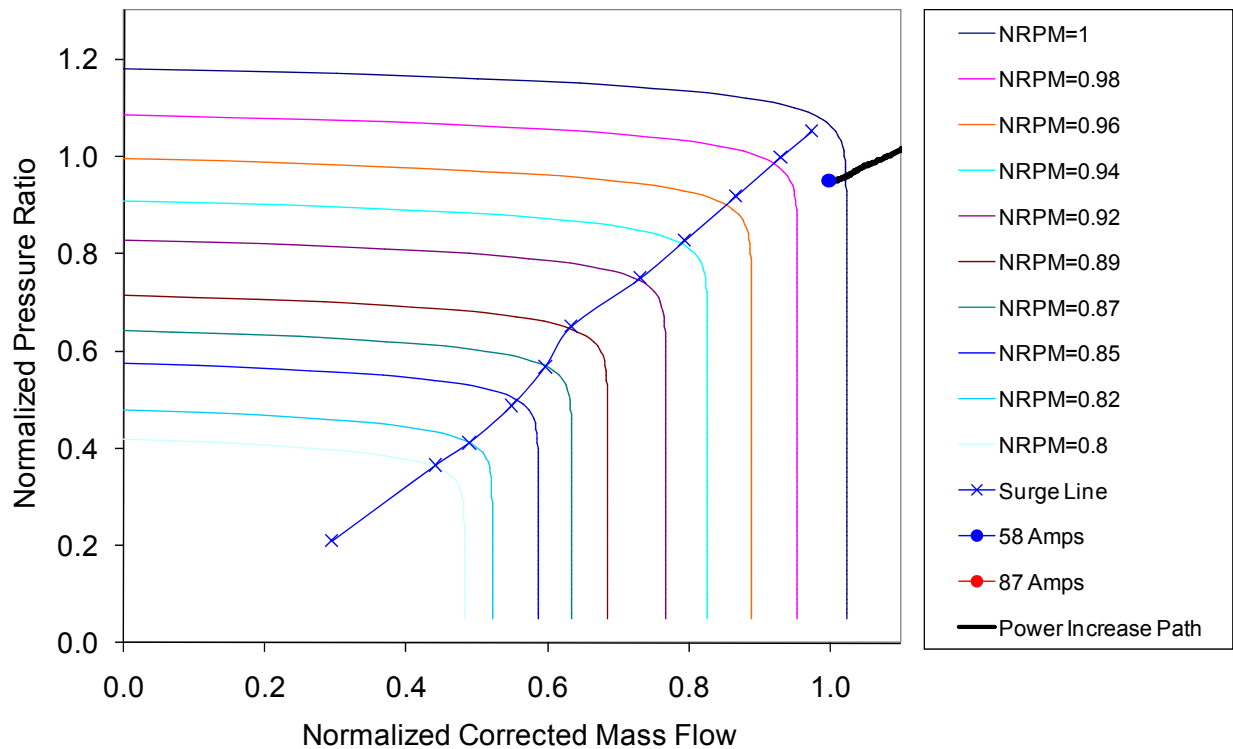
**Figure A2.2 - 100: Dynamic tri-layer temperature response to a fuel cell load decrease from 100% to 50% of design point. Primary control of fuel cell temperature at 1,100 K and secondary control of gas turbine speed and primary control of blower/compressor mixture temperature at 800 K with secondary control of recycle blower speed.**

Figure A2.2 - 101 shows that controlling the tri-layer temperature requires a gas turbine shaft speed decrease from 3577 to 3070 RPM.



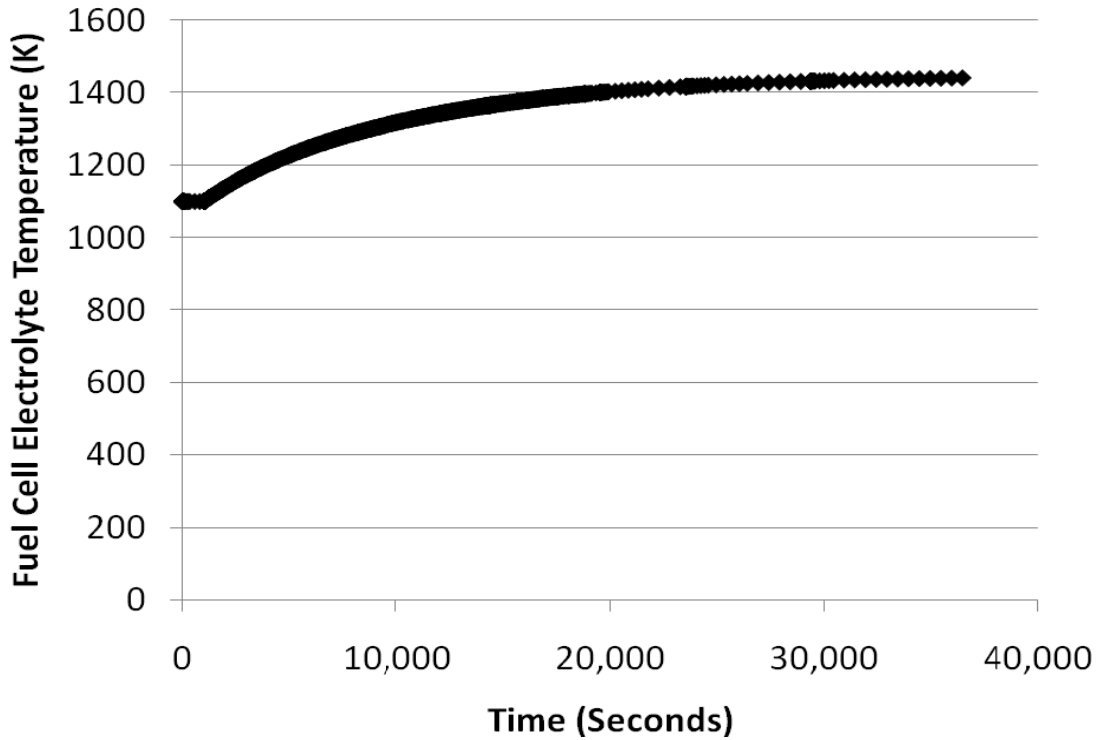
**Figure A2.2 - 101: Dynamic gas turbine shaft speed response to a fuel cell load decrease from 100% to 50% of design point. Primary control of fuel cell temperature at 1,100 K and secondary control of gas turbine speed and primary control of blower/compressor mixture temperature at 800 K with secondary control of recycle blower speed.**

Figure A2.2 - 102 shows the case when the fuel cell is subjected to an instantaneous 50% increase in current demand perturbation. The mass flow and shaft speed increase in an attempt to bring down the fuel cell temperature but ultimately fail to control the tri-layer temperature. Note, however, that the dynamic response of the compressor increases the surge margin indicating that the current system and control strategy is not vulnerable to compressor surge when perturbed by a current demand increase.



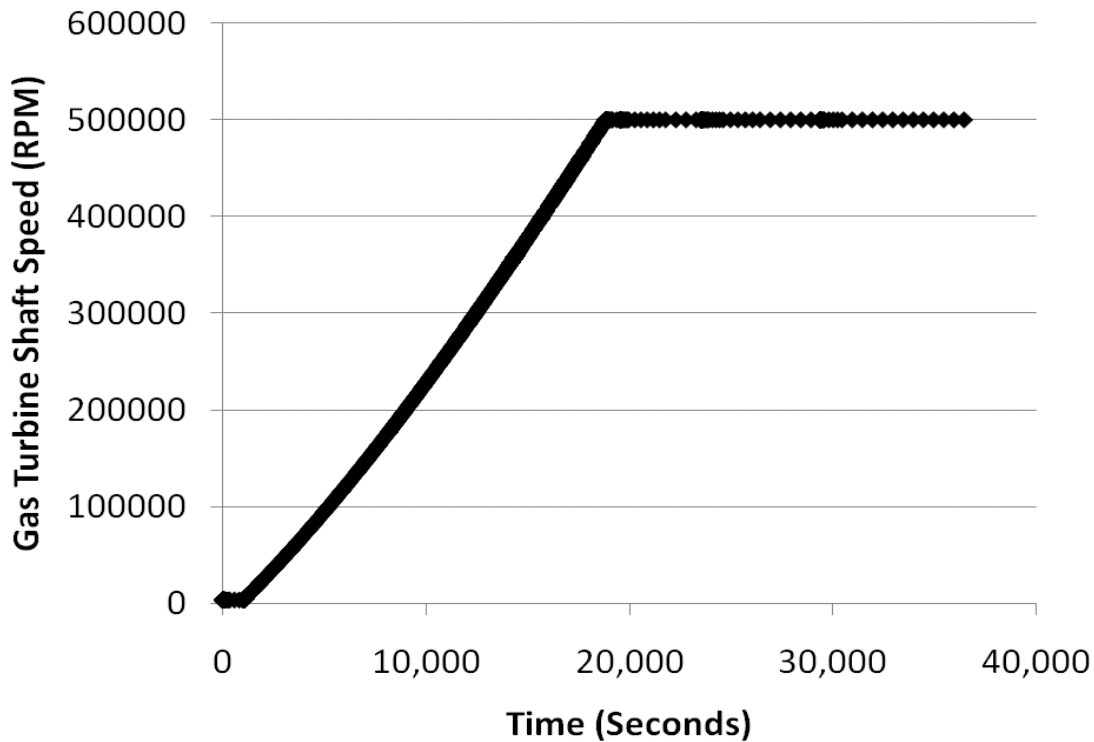
**Figure A2.2 - 102: Compressor dynamic response to a fuel cell load increase from 100% (blue) to 150% (red) of design state. Primary control of fuel cell temperature at 1,100 K and secondary control of gas turbine shaft speed and primary control of blower/compressor mixture temperature at 800 K and secondary control of blower speed.**

Figure A2.2 - 103 shows that when fuel cell load is increased to 125% of its design value the model is unable to converge on a steady state solution. This means that the controller cannot maintain tri-layer temperature at the 1100 K set point. This result is in contrast to that of control strategy #1 (Figure A2.2 - 69), where the model converged but only after reaching an unacceptable tri-layer temperature of 1400 K.



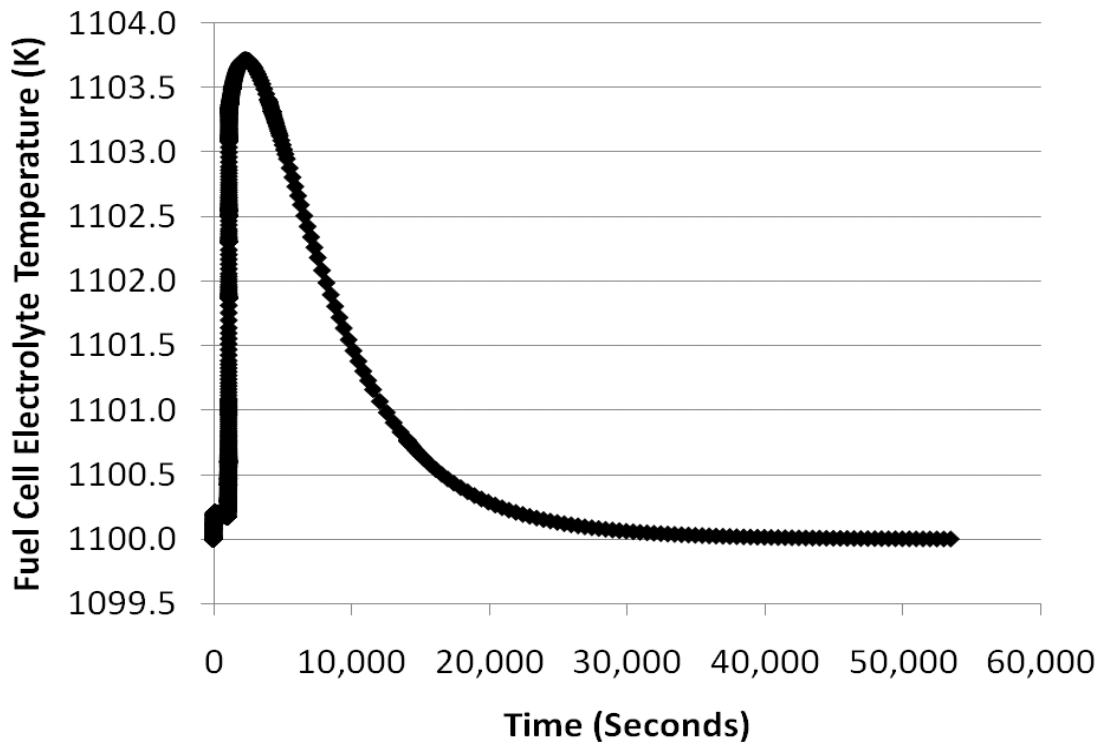
**Figure A2.2 - 103: Dynamic tri-layer temperature response to a fuel cell load increase from 100% to 125% of design point. Primary control of fuel cell temperature at 1,100 K and secondary control of gas turbine speed and primary control of blower/compressor mixture temperature at 800 K with secondary control of recycle blower speed.**

Figure A2.2 - 104 shows that gas turbine shaft speed increases from 3577 to a maximum threshold value of 500,000 RPM in a vain attempt to control tri-layer temperature.



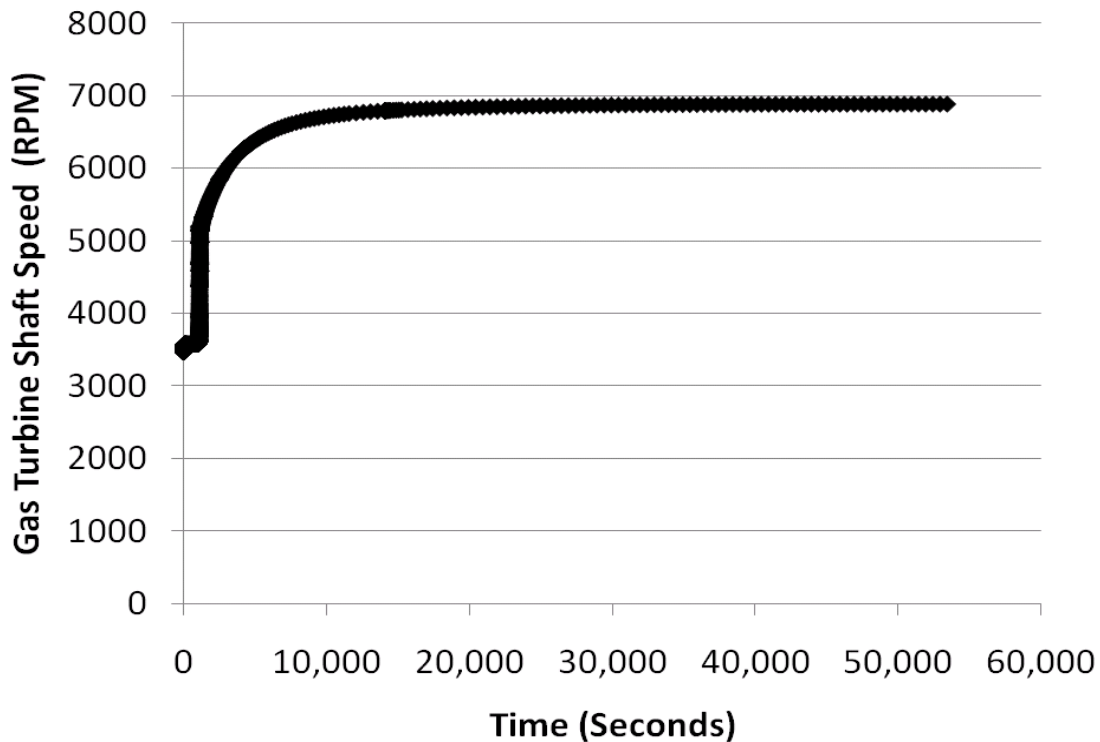
**Figure A2.2 - 104: Dynamic gas turbine shaft speed response to a fuel cell load increase from 100% to 125% of design point. Primary control of fuel cell temperature at 1,100 K and secondary control of gas turbine speed and primary control of blower/compressor mixture temperature at 800 K with secondary control of recycle blower speed.**

Figure A2.2 - 105 shows that when fuel cell load is increased to 102.5% of its design value the model is able to converge on a steady state solution. The controller is able to regain the 1100 K tri-layer temperature set point after a slight temperature increase.



**Figure A2.2 - 105: Dynamic tri-layer temperature response to a fuel cell load increase from 100% to 97.5% of design point. Primary control of fuel cell temperature at 1,100 K and secondary control of gas turbine speed and primary control of blower/compressor mixture temperature at 800 K with secondary control of recycle blower speed.**

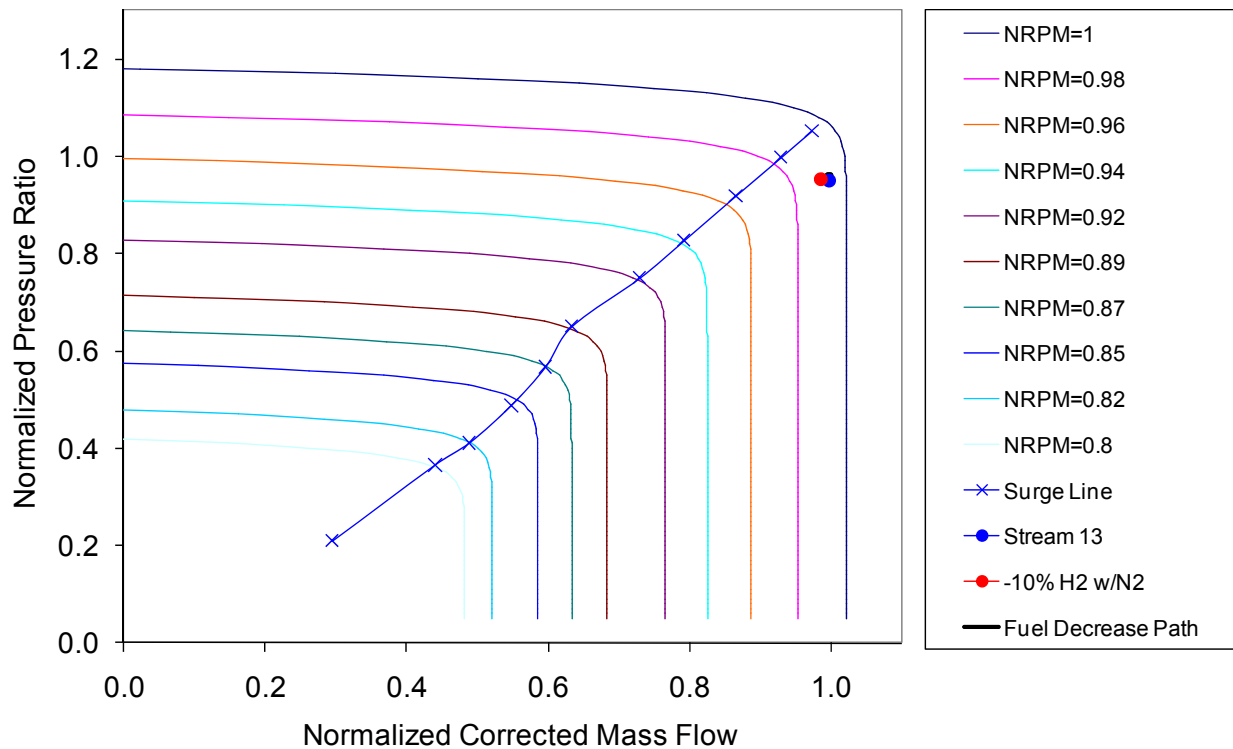
Figure A2.2 - 106 shows that gas turbine shaft speed must increase from 3577 to 6890 RPM in order to control tri-layer temperature. This high turbine speed may be unacceptable.



**Figure A2.2 - 106: Dynamic gas turbine shaft speed response to a fuel cell load increase from 100% to 97.5% of design point. Primary control of fuel cell temperature at 1,100 K and secondary control of gas turbine speed and primary control of blower/compressor mixture temperature at 800 K with secondary control of recycle blower speed.**

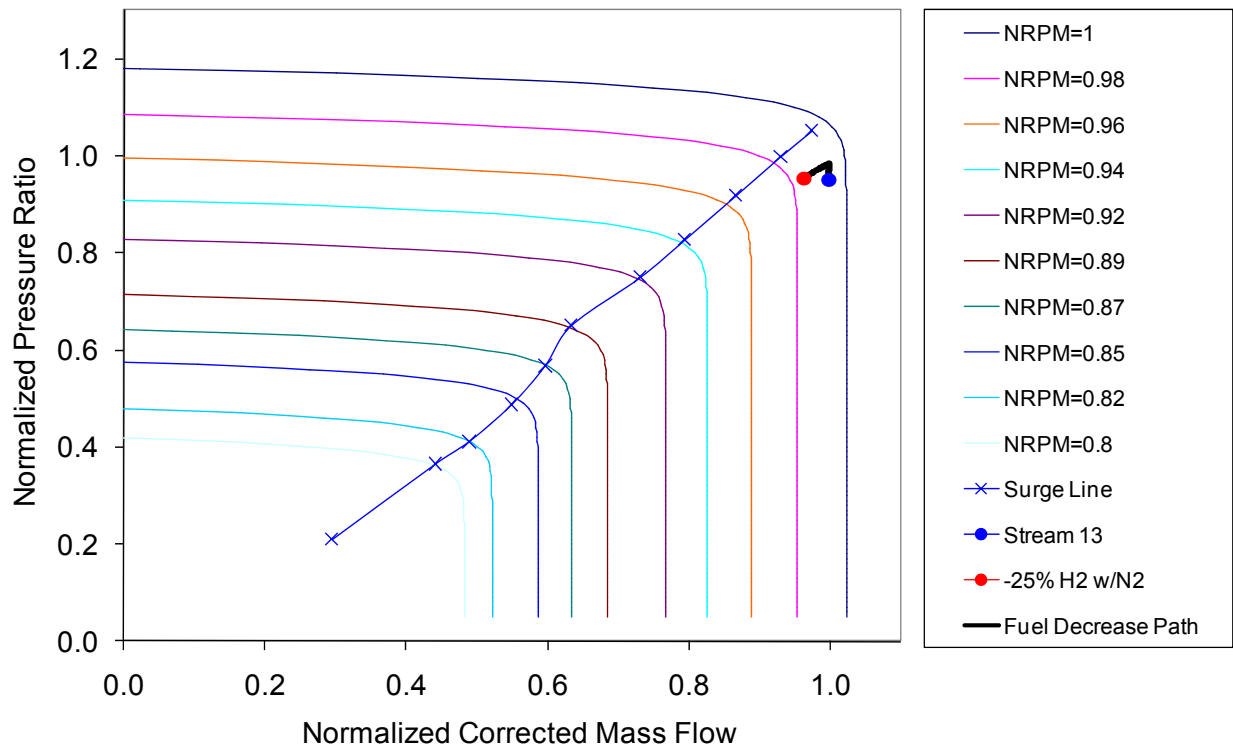
#### **Syngas Hydrogen Composition Perturbation (Balanced with Nitrogen)**

Figure A2.2 - 107 shows the case when the fuel cell is subjected to a perturbation of 10% decrease in syngas hydrogen content balanced with nitrogen. There is a slight decrease in air flow rate in response to this perturbation.



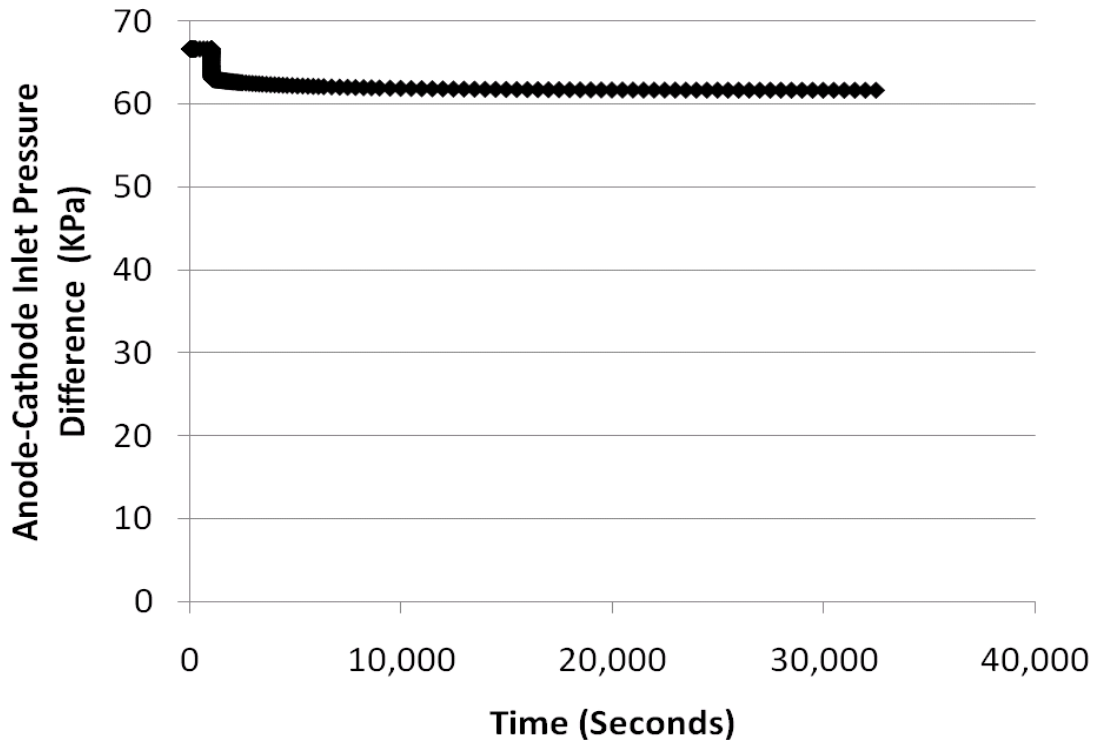
**Figure A2.2 - 107: Compressor dynamic response to a decrease in fuel hydrogen balanced with nitrogen from 100% (blue) to 90% (red) of design state. Primary control of fuel cell temperature at 1,100 K and secondary control of gas turbine shaft speed and primary control of blower/compressor mixture temperature at 800 K and secondary control of blower speed.**

Figure A2.2 - 108 shows the case when the fuel cell is subjected to a 25% decrease in syngas hydrogen content balanced with nitrogen. There is an initial rise in pressure ratio which eventually drops off and leads to a final state with lower air flow rate. Note also a tendency to narrow the surge margin in response to this fuel composition perturbation.



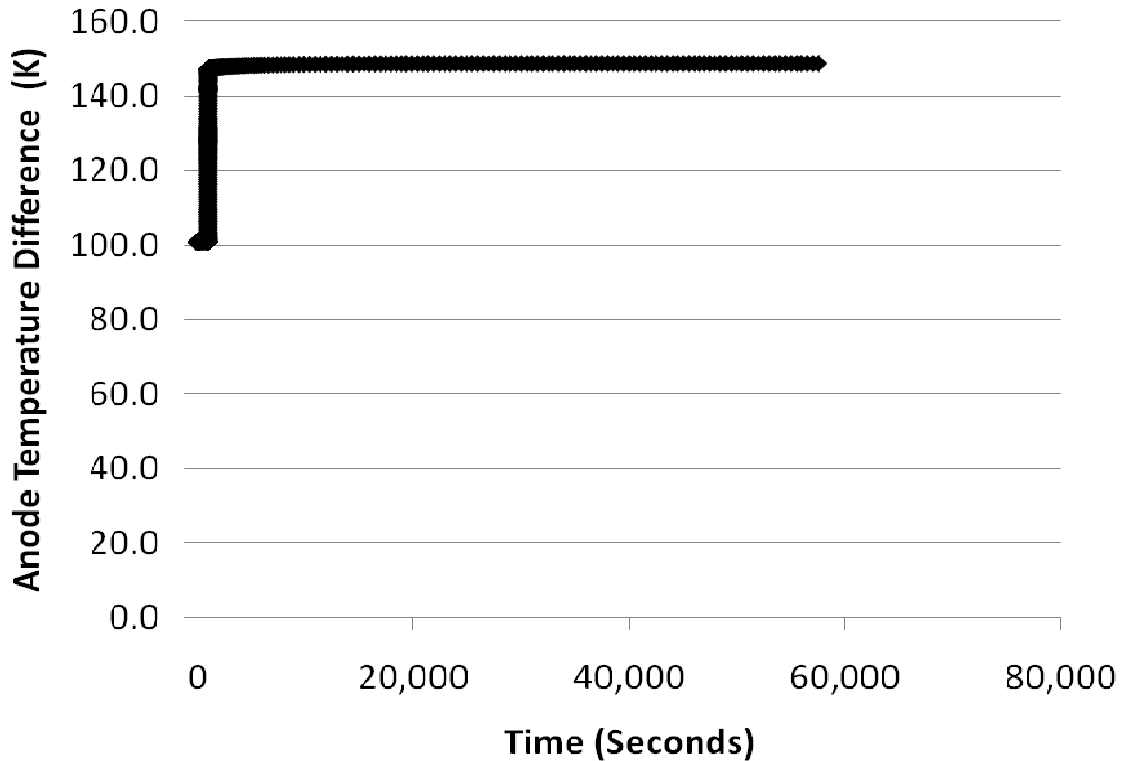
**Figure A2.2 - 108: Compressor dynamic response to a decrease in fuel hydrogen balanced with nitrogen from 100% (blue) to 75% (red) of design state. Primary control of fuel cell temperature at 1,100 K and secondary control of gas turbine shaft speed and primary control of blower/compressor mixture temperature at 800 K and secondary control of blower speed.**

When the fuel cell is subjected to a 25% decrease in syngas hydrogen content balanced with nitrogen, the anode-cathode inlet pressure difference decreases (Figure A2.2 - 109) from a starting value of 67 kPa to 62 kPa at the new steady state condition. This is the same trend that was observed using “control strategy #1” (Figure A2.2 - 74). This perturbation results in an increase in syngas mass flow since nitrogen dilutes syngas hydrogen content and the new steady state fuel utilization is required to be 80%. This increase in syngas mass flow raises not only the anode inlet pressure but also the cathode inlet pressure. The overall drop in pressure difference occurs due to a greater pressure rise across the anode than across the cathode.



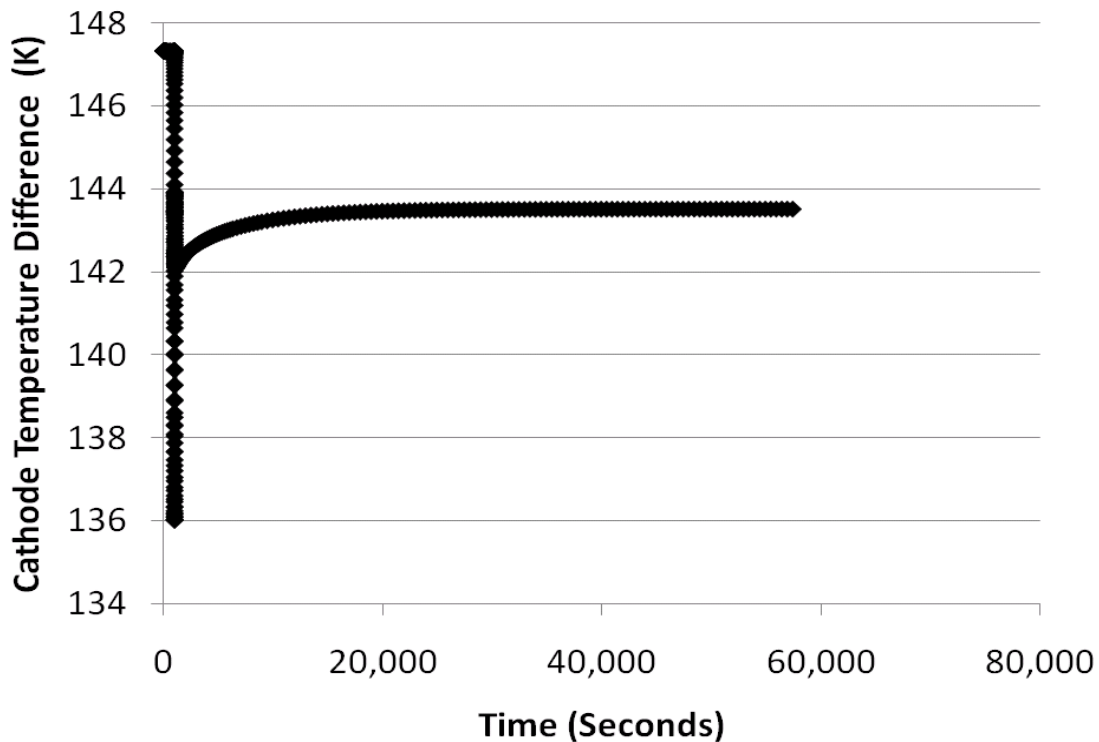
**Figure A2.2 - 109: Dynamic anode-cathode inlet pressure difference response to a decrease in fuel hydrogen balanced with nitrogen from 100% to 75% of design point. Primary control of fuel cell temperature at 1,100 K and secondary control of gas turbine speed and primary control of blower/compressor mixture temperature at 800 K with secondary control of recycle blower speed.**

Figure A2.2 - 110 shows that the temperature difference across the anode rises due to the decrease in syngas hydrogen content balanced with nitrogen. This is the same trend that was observed using “control strategy #1” (Figure A2.2 - 75). There is a 48 K drop in anode inlet temperature due to more mass flow requiring preheating and no change in anode outlet temperature due to control of this parameter. The overall anode temperature rise is dominated by the fact that the increase in mass flow is difficult to preheat. The DOE requirement for steady state operation is that the anode temperature rise be less than 100 K. Therefore, this 149 K anode temperature difference is problematic.



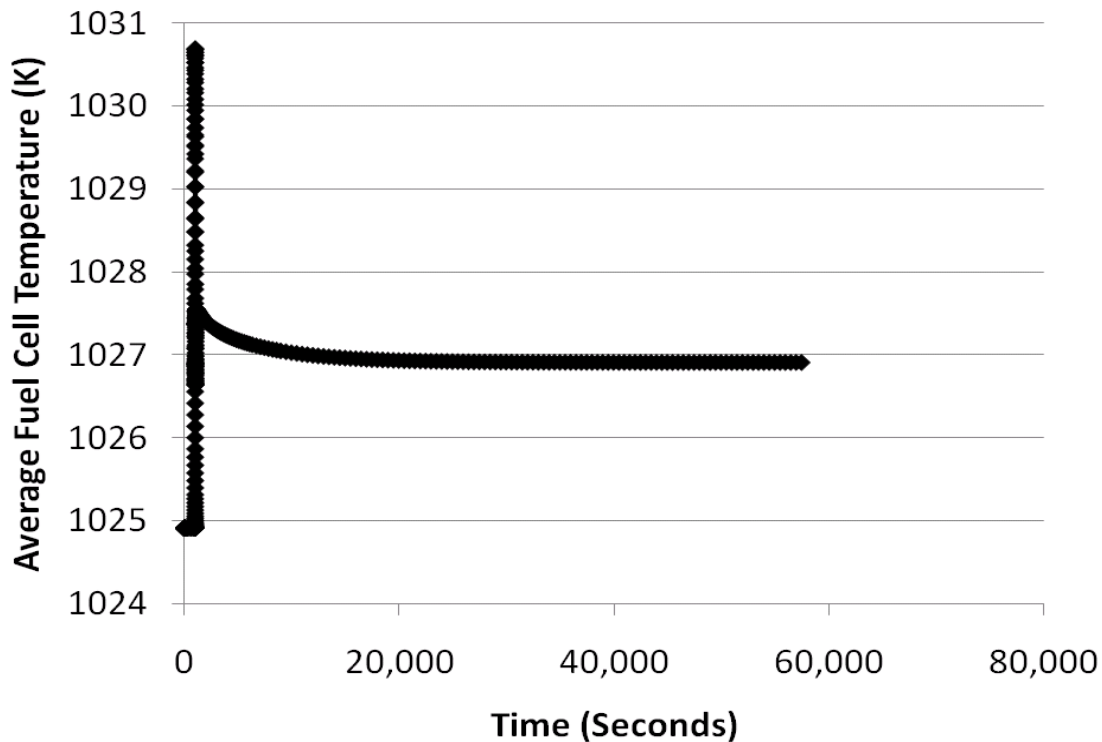
**Figure A2.2 - 110: Dynamic anode inlet-outlet temperature difference response to a decrease in fuel hydrogen balanced with nitrogen from 100% to 75% of design point. Primary control of fuel cell temperature at 1,100 K and secondary control of gas turbine speed and primary control of blower/compressor mixture temperature at 800 K with secondary control of recycle blower speed**

Figure A2.2 - 111 shows that the temperature difference across the cathode decreases due to the decrease in syngas hydrogen content balanced with nitrogen. This is the same trend that was observed using “control strategy #1” (Figure A2.2 - 76). There is a 4 K increase in cathode inlet temperature due to less air mass flow requiring preheating and no change in cathode outlet temperature due to control of this parameter. The DOE requirement for steady state operation is that the cathode temperature rise be less than 150 K. Therefore, this 144 K cathode temperature difference is not problematic.



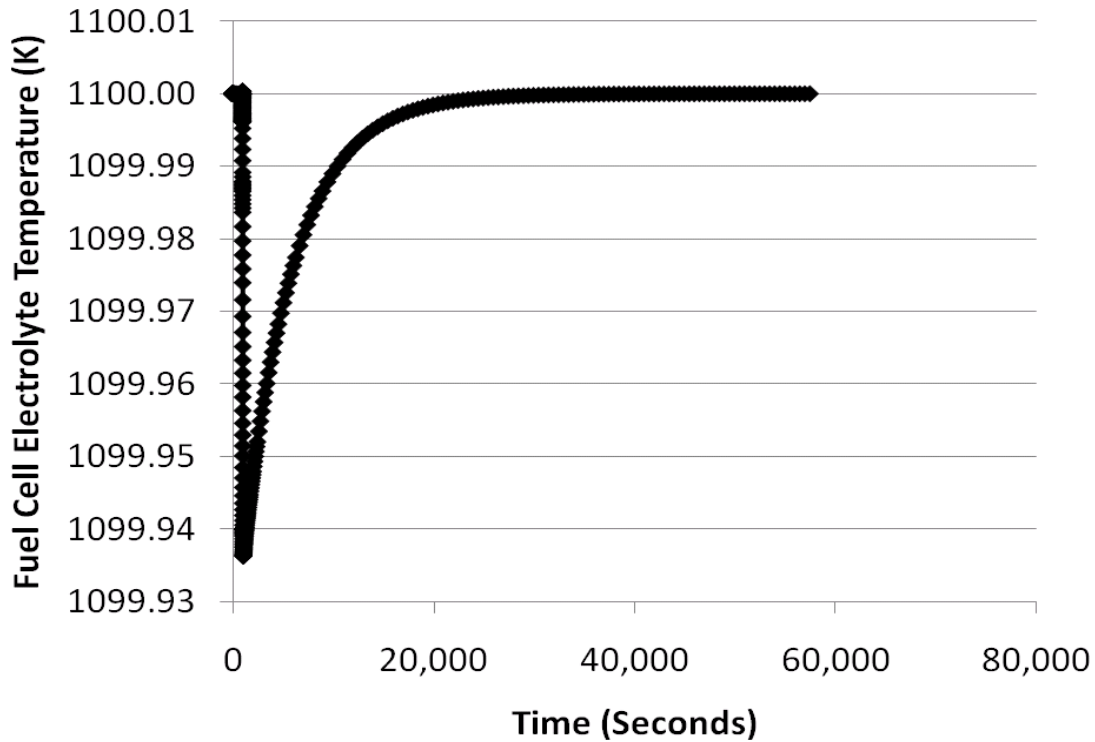
**Figure A2.2 - 111: Dynamic cathode inlet-outlet temperature difference response to a decrease in fuel hydrogen balanced with nitrogen from 100% to 75% of design point. Primary control of fuel cell temperature at 1,100 K and secondary control of gas turbine speed and primary control of blower/compressor mixture temperature at 800 K with secondary control of recycle blower speed.**

Figure A2.2 - 112 shows that the average fuel cell temperature across the cathode increases from 1025 K to 1027 K. This is opposite to the trend that was observed using “control strategy #1” (Figure A2.2 - 77). The DOE requirement for steady state operation is that this average temperature be between 998 – 1048 K. This perturbation results in an average temperature within the prescribed range.



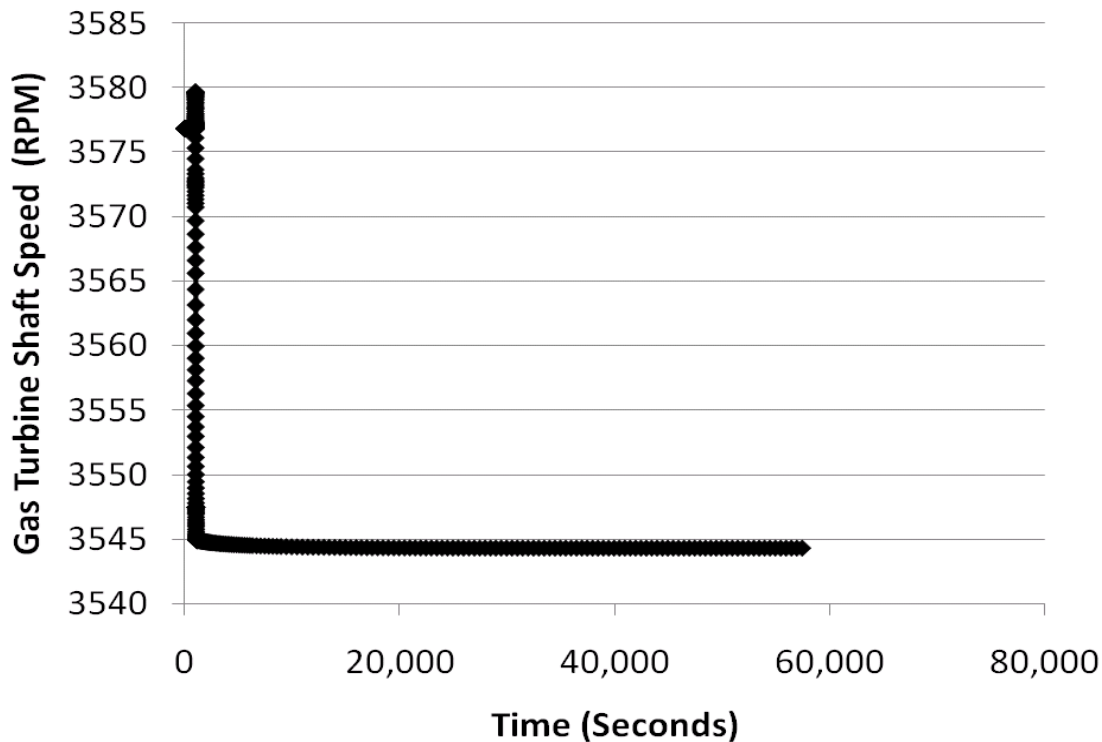
**Figure A2.2 - 112: Dynamic average fuel cell temperature response to a decrease in fuel hydrogen balanced with nitrogen from 100% to 75% of design point. Primary control of fuel cell temperature at 1,100 K and secondary control of gas turbine speed and primary control of blower/compressor mixture temperature at 800 K with secondary control of recycle blower speed.**

Figure A2.2 - 113 shows that after a minor decrease in tri-layer temperature, the control regains the 1100 K set point. This in contrast to the result of control strategy #1 (Figure A2.2 - 78), where there was a 5 K drop in temperature. There is no specified DOE requirement for this parameter but like the average fuel cell temperature it is undesirable that it change significantly since thermal cycling can lead to material stress and failure.



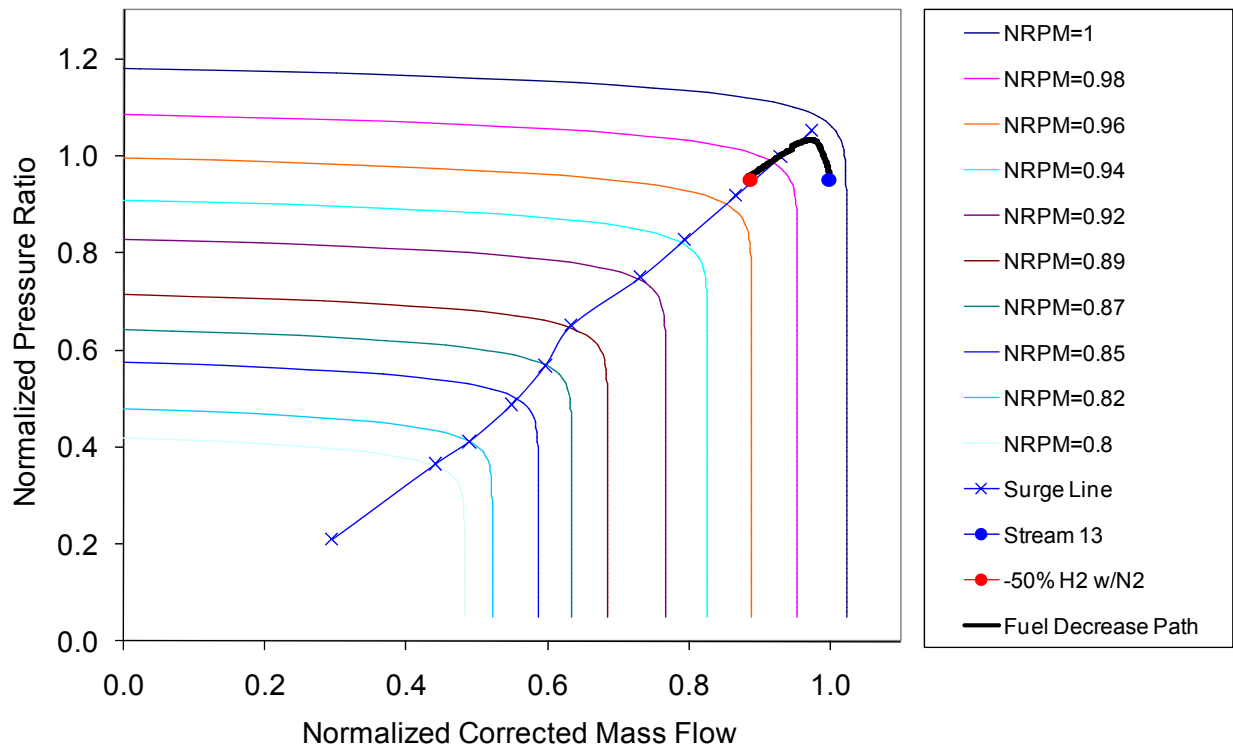
**Figure A2.2 - 113: Dynamic tri-layer temperature response to a decrease in fuel hydrogen balanced with nitrogen from 100% to 75% of design point. Primary control of fuel cell temperature at 1,100 K and secondary control of gas turbine speed and primary control of blower/compressor mixture temperature at 800 K with secondary control of recycle blower speed.**

Figure A2.2 - 114 shows that controlling the tri-layer temperature requires a gas turbine shaft speed decrease from 3577 to 3544 RPM.



**Figure A2.2 - 114: Dynamic gas turbine shaft speed response to a decrease in fuel hydrogen balanced with nitrogen from 100% to 75% of design point. Primary control of fuel cell temperature at 1,100 K and secondary control of gas turbine speed and primary control of blower/compressor mixture temperature at 800 K with secondary control of recycle blower speed.**

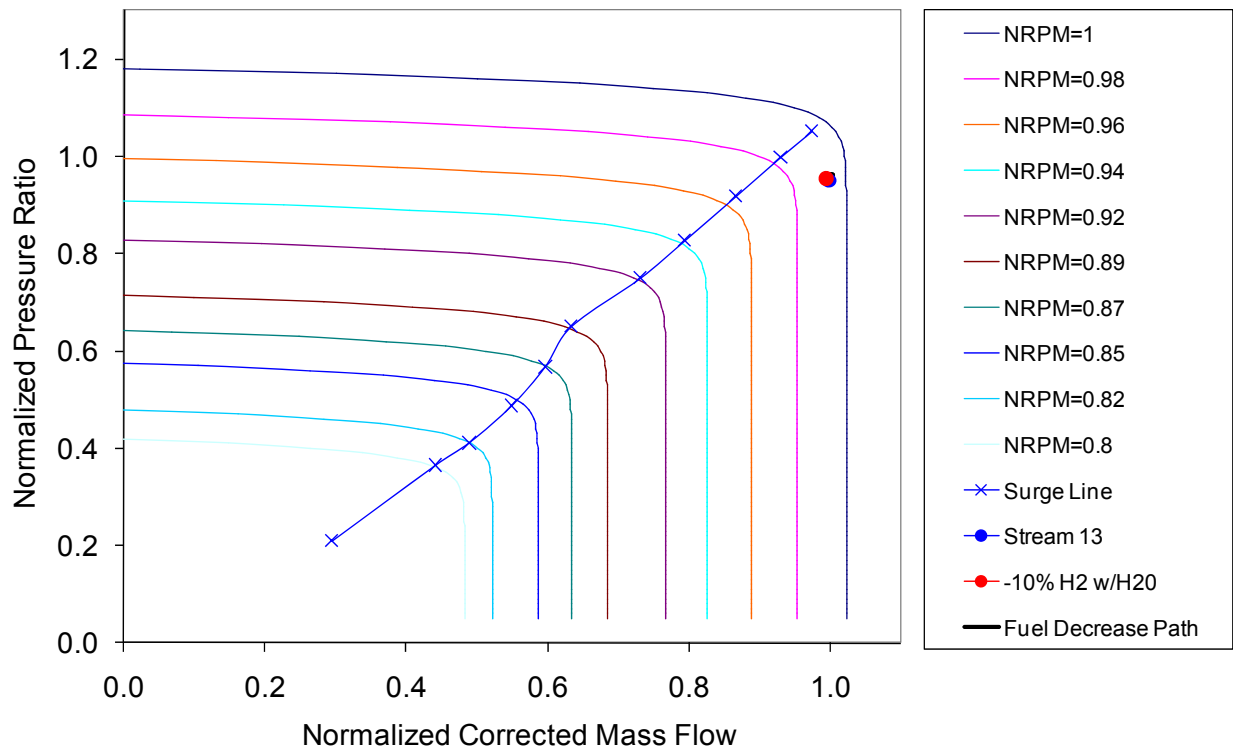
Figure A2.2 - 115 shows the case when the fuel cell is subjected to a 50% decrease in syngas hydrogen content balanced with nitrogen. There is an initial rise in pressure ratio which approaches surge followed by a decrease in air flow rate that crosses the surge line. The trends found in Figure A2.2 - 107 - Figure A2.2 - 115 are very similar to those found in Figure A2.2 - 39 - Figure A2.2 - 41 where an ejector was used in place of the blower with a similar control strategy. Of course, operation of the system beyond the surge line is not possible indicating the vulnerability of the current system and control strategy to surge when subjected to a substantial decrease in syngas hydrogen content perturbation.



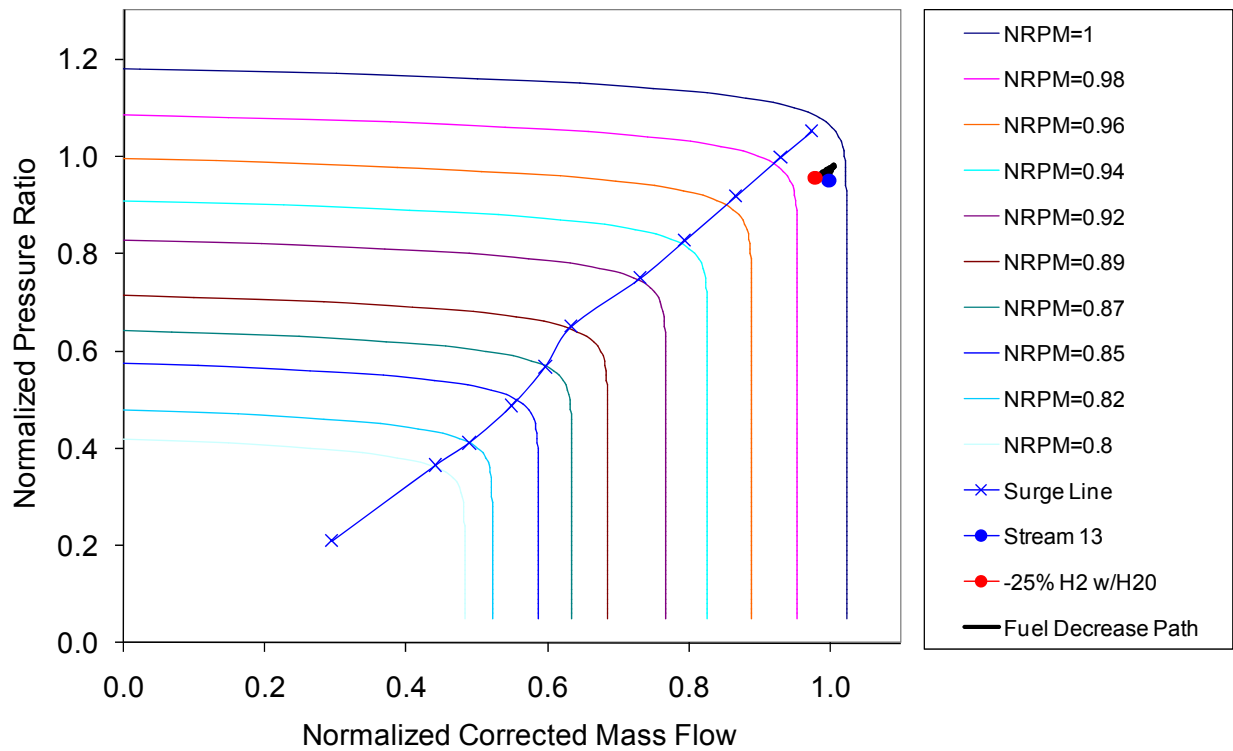
**Figure A2.2 - 115: Compressor dynamic response to a decrease in fuel hydrogen balanced with nitrogen from 100% (blue) to 50% (red) of design state. Primary control of fuel cell temperature at 1,100 K and secondary control of gas turbine shaft speed and primary control of blower/compressor mixture temperature at 800 K and secondary control of blower speed.**

### Syngas Hydrogen Composition Perturbation (Balanced with Steam)

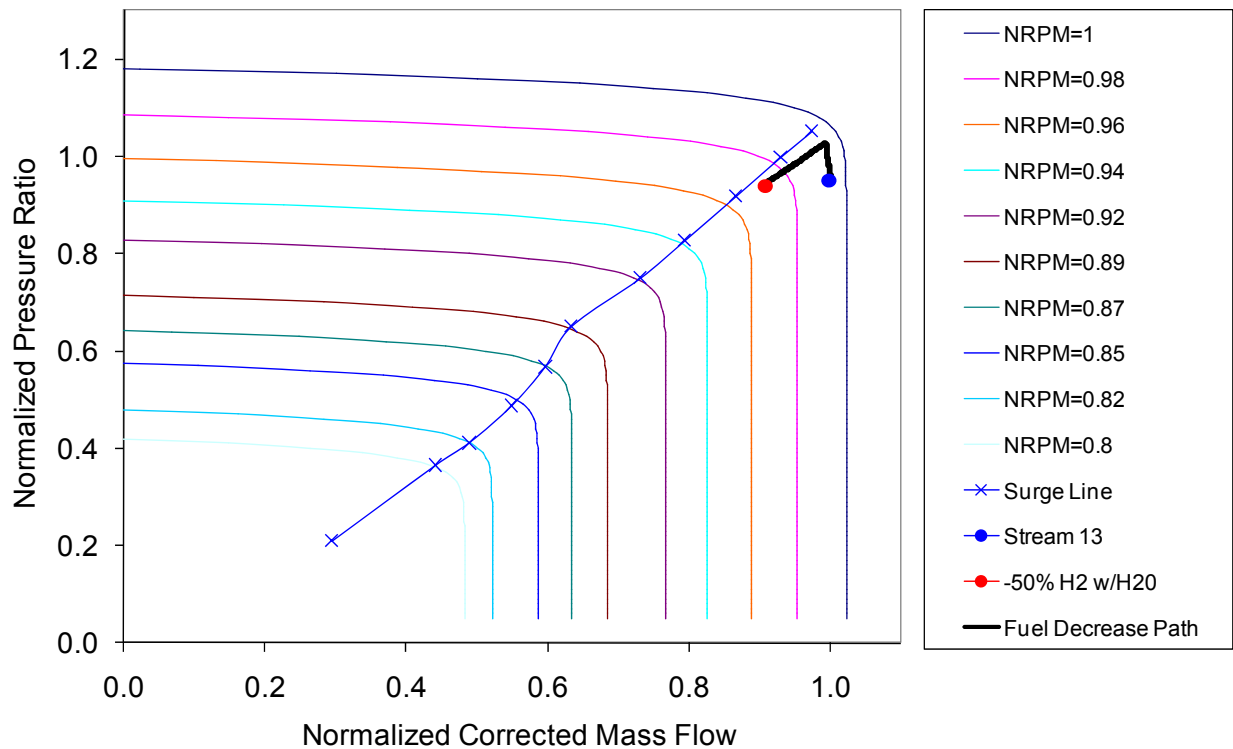
Figure A2.2 - 116, Figure A2.2 - 117 and Figure A2.2 - 118 show cases when the fuel cell is subjected to perturbations of 10%, 25% and 50% decrease in syngas hydrogen content balanced with steam, respectively. The trends mimic those found when nitrogen is used to balance decreases in syngas hydrogen content (Figure A2.2 - 107 - Figure A2.2 - 115) but have a slightly lower impact on the required decrease in air flow rate.



**Figure A2.2 - 116: Compressor dynamic response to a decrease in fuel hydrogen balanced with steam from 100% (blue) to 90% (red) of design state. Primary control of fuel cell temperature at 1,100 K and secondary control of gas turbine shaft speed and primary control of blower/compressor mixture temperature at 800 K and secondary control of blower speed.**



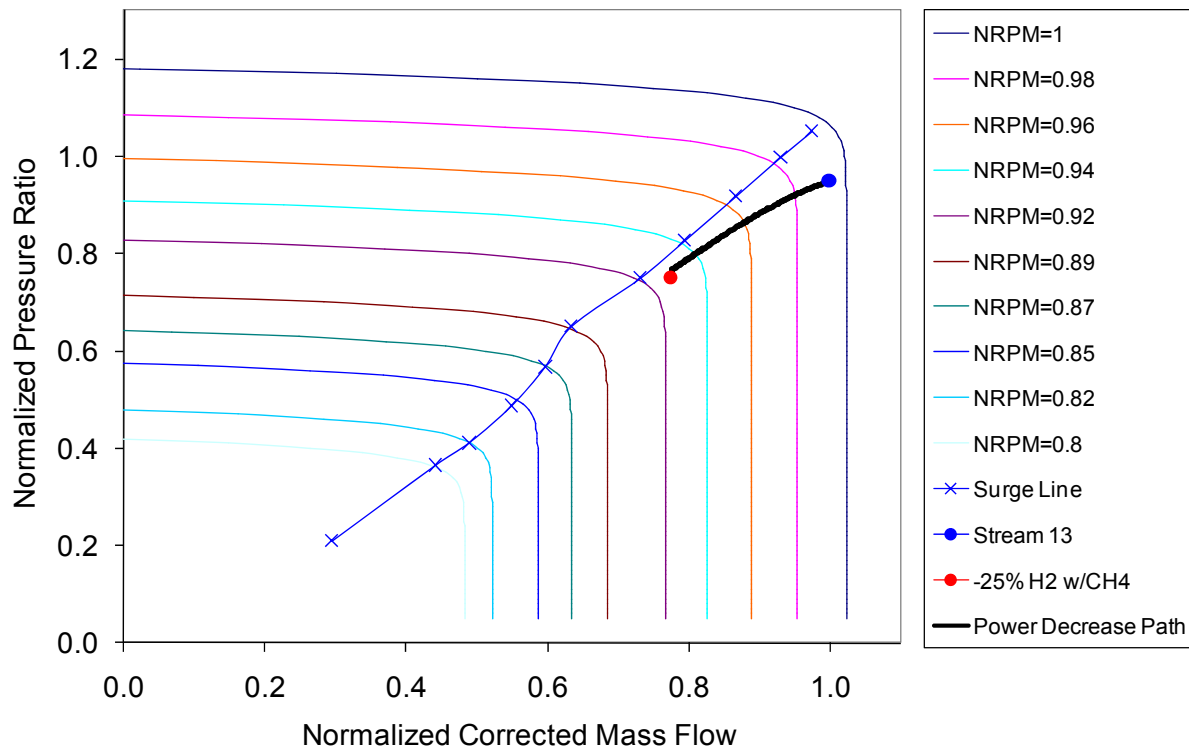
**Figure A2.2 - 117: Compressor dynamic response to a decrease in fuel hydrogen balanced with steam from 100% (blue) to 75% (red) of design state. Primary control of fuel cell temperature at 1,100 K and secondary control of gas turbine shaft speed and primary control of blower/compressor mixture temperature at 800 K and secondary control of blower speed.**



**Figure A2.2 - 118: Compressor dynamic response to a decrease in fuel hydrogen balanced with steam from 100% (blue) to 50% (red) of design state. Primary control of fuel cell temperature at 1,100 K and secondary control of gas turbine shaft speed and primary control of blower/compressor mixture temperature at 800 K and secondary control of blower speed.**

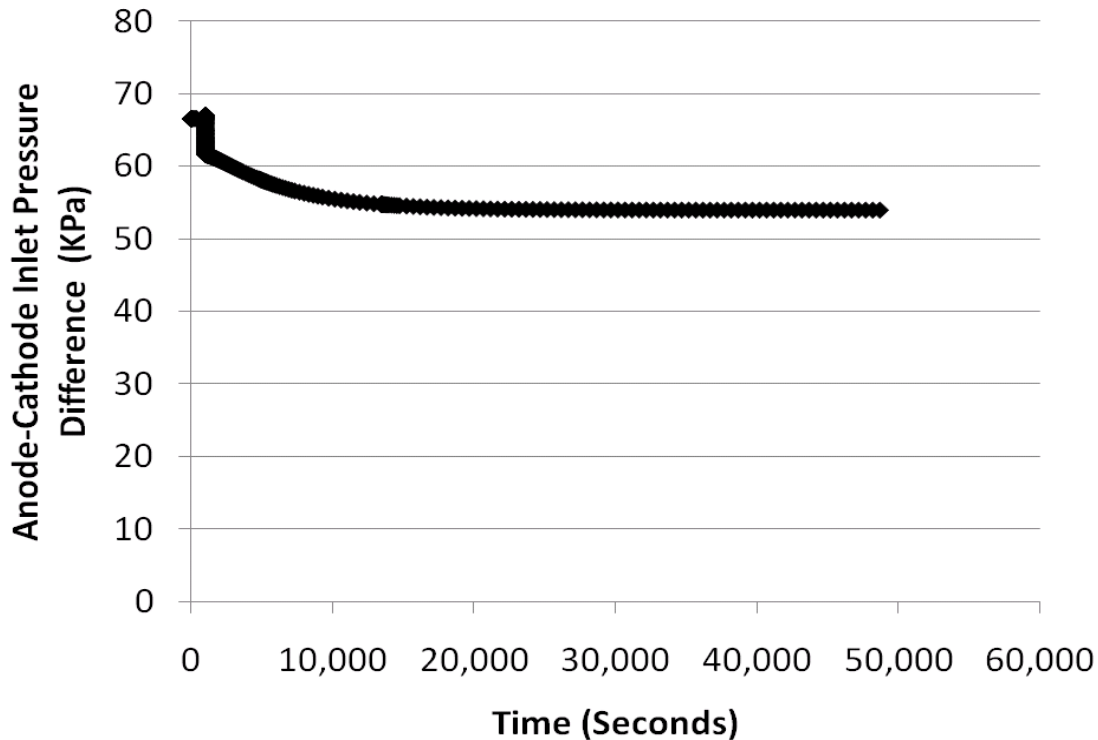
### **Syngas Hydrogen Composition Perturbation (Balanced with Methane)**

When the fuel cell is subjected to a 25% decrease in syngas hydrogen content balanced with methane (Figure A2.2 - 119) there is a large impact on compressor operation, with the surge line being approached. This is in contrast to “control strategy #1” (Figure A2.2 - 84) where there was almost no change in compressor operation resulting from this perturbation.



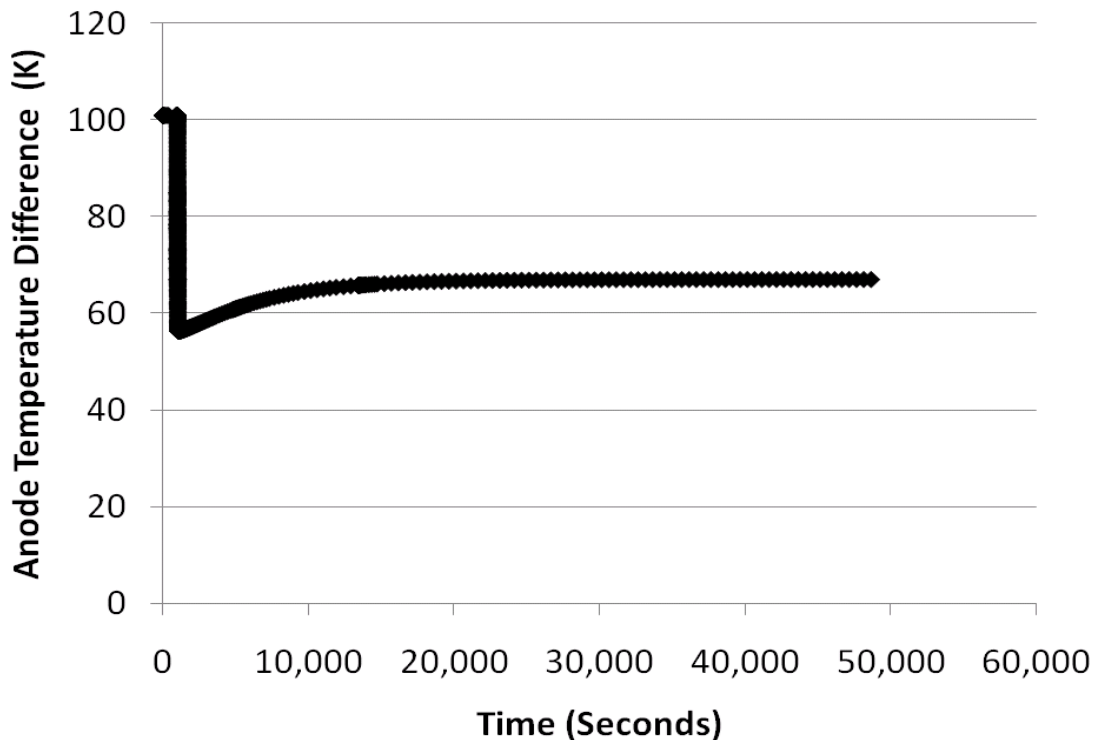
**Figure A2.2 - 119: Compressor dynamic response to a decrease in fuel hydrogen balanced with methane from 100% to 75% of design point. Primary control of fuel cell temperature at 1,100 K and secondary control of gas turbine speed and primary control of blower/compressor mixture temperature at 800 K with secondary control of recycle blower speed.**

The anode-cathode inlet pressure difference decreases (Figure A2.2 - 120) from a starting value of 67 kPa to 54 kPa at the new steady state condition. This in contrast to the result of control strategy #1 (Figure A2.2 - 85), where there was a rise in pressure difference. This perturbation results in a large decrease in air mass flow and a slight decrease in syngas mass flow since methane is considered a fuel source that ultimately contributes four hydrogen molecules for every molecule of methane and the new steady state fuel utilization is required to be 80%. The overall drop in pressure difference is dominated by the lower air mass flow rate.



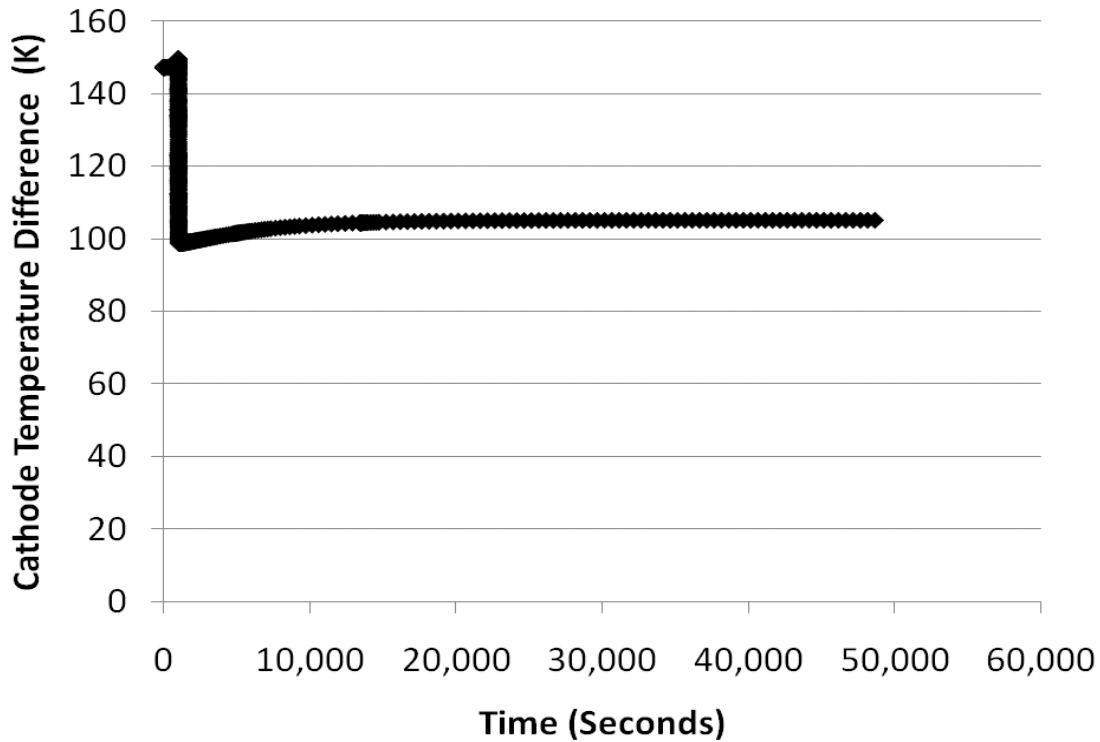
**Figure A2.2 - 120: Dynamic anode-cathode inlet pressure difference response to a decrease in fuel hydrogen balanced with methane from 100% to 75% of design point. Primary control of fuel cell temperature at 1,100 K and secondary control of gas turbine speed and primary control of blower/compressor mixture temperature at 800 K with secondary control of recycle blower speed.**

Figure A2.2 - 121 shows that the temperature difference across the anode drops due to the decrease in syngas hydrogen content balanced with methane. This same trend was observed when control strategy #1 was used (Figure A2.2 - 86). Internal reformation of methane is an endothermic process and causes this temperature drop. There is a 34 K rise in anode inlet temperature due to a higher combustor outlet temperature resulting from the higher syngas hydrocarbon content and no change in anode outlet temperature since this parameter is controlled. The overall anode temperature drop is dominated by the higher combustor temperature. The DOE requirement for steady state operation is that the anode temperature rise be less than 100 K. Therefore, this 67 K anode temperature difference is not problematic.



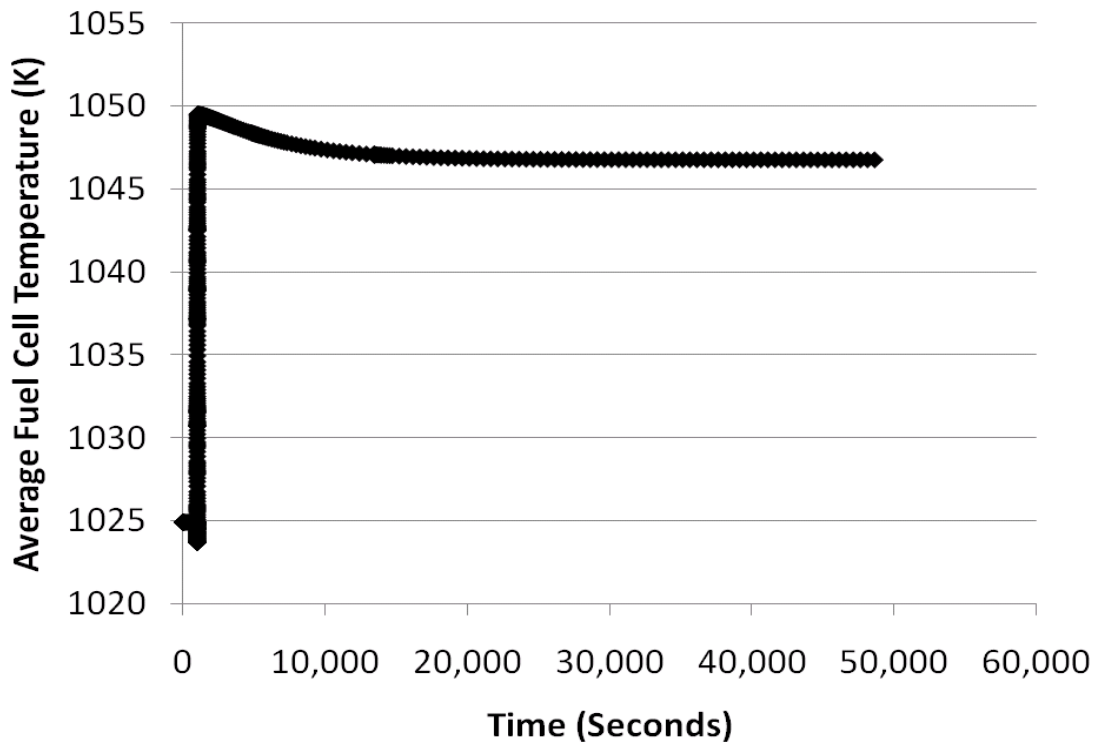
**Figure A2.2 - 121: Dynamic anode inlet-outlet temperature difference response to a decrease in fuel hydrogen balanced with methane from 100% to 75% of design point. Primary control of fuel cell temperature at 1,100 K and secondary control of gas turbine speed and primary control of blower/compressor mixture temperature at 800 K with secondary control of recycle blower speed.**

Figure A2.2 - 122 shows that the temperature difference across the cathode drops due to the decrease in syngas hydrogen content balanced with methane. This same trend was observed when control strategy #1 was used (Figure A2.2 - 87). There is a 43 K rise in cathode inlet temperature due to a higher combustor outlet temperature and no change in cathode outlet temperature due to control of this parameter. The DOE requirement for steady state operation is that the cathode temperature rise be less than 150 K. Therefore, this 105 K cathode temperature difference is not problematic.



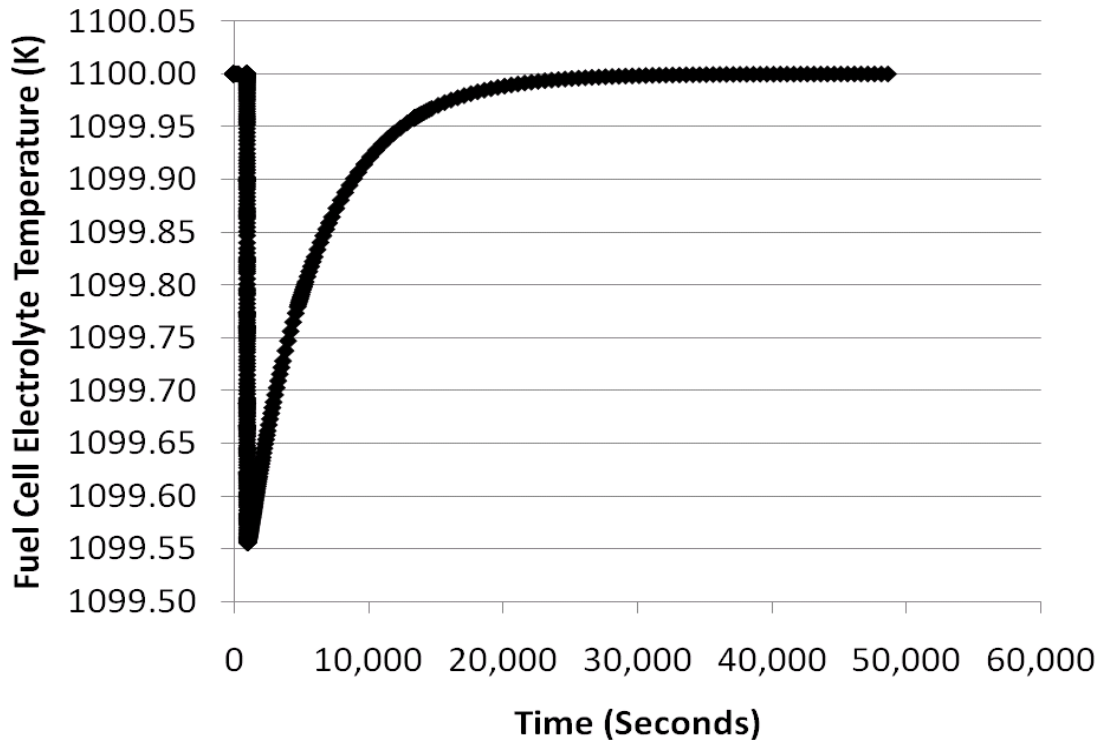
**Figure A2.2 - 122: Dynamic cathode inlet-outlet temperature difference response to a decrease in fuel hydrogen balanced with methane from 100% to 75% of design point. Primary control of fuel cell temperature at 1,100 K and secondary control of gas turbine speed and primary control of blower/compressor mixture temperature at 800 K with secondary control of recycle blower speed.**

Figure A2.2 - 123 shows that the average fuel cell temperature across the cathode increases from 1025 K to 1047 K. This is opposite to the trend that was observed using “control strategy #1” (Figure A2.2 - 88). The DOE requirement for steady state operation is that this average temperature be between 998 – 1048 K. This perturbation results in an average temperature within the prescribed range.



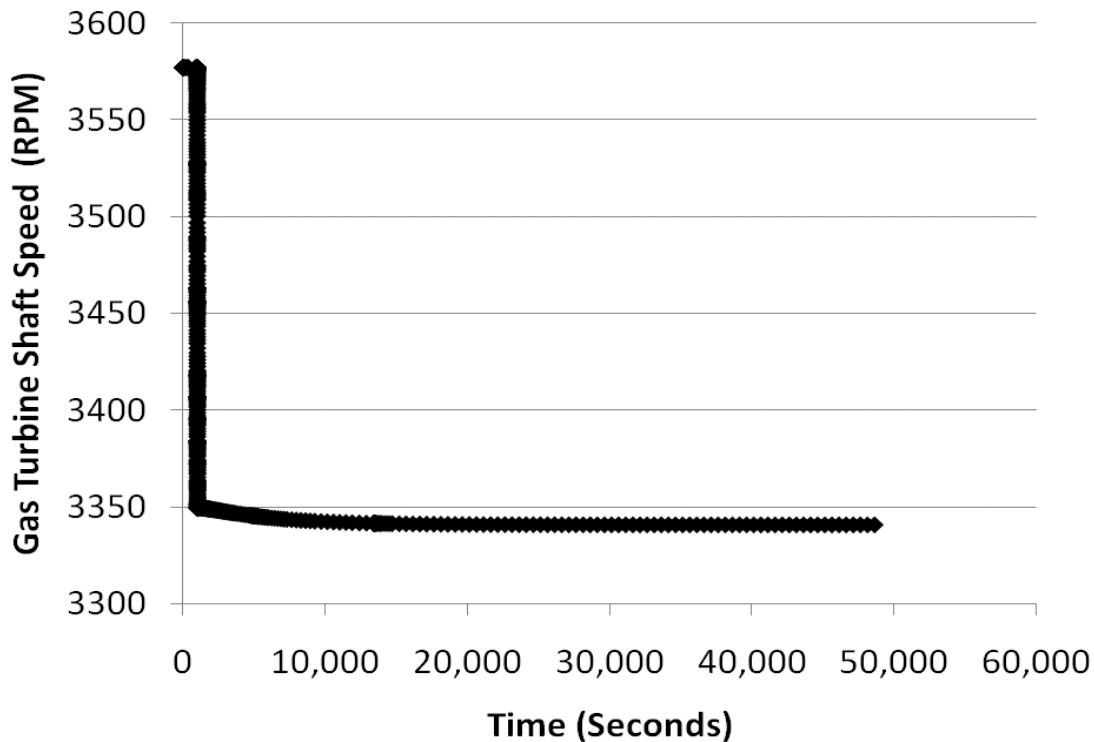
**Figure A2.2 - 123: Dynamic average fuel cell temperature response to a decrease in fuel hydrogen balanced with methane from 100% to 75% of design point. Primary control of fuel cell temperature at 1,100 K and secondary control of gas turbine speed and primary control of blower/compressor mixture temperature at 800 K with secondary control of recycle blower speed.**

Figure A2.2 - 124 shows that after a minor decrease in tri-layer temperature, the control regains the 1100 K set point. This in contrast to the result of control strategy #1 (Figure A2.2 - 89), where there was a 41 K drop in temperature. There is no specified DOE requirement for this parameter but like the average fuel cell temperature it is undesirable that it change significantly since thermal cycling can lead to material stress and failure.



**Figure A2.2 - 124: Dynamic tri-layer temperature response to a decrease in fuel hydrogen balanced with methane from 100% to 75% of design point. Primary control of fuel cell temperature at 1,100 K and secondary control of gas turbine speed and primary control of blower/compressor mixture temperature at 800 K with secondary control of recycle blower speed.**

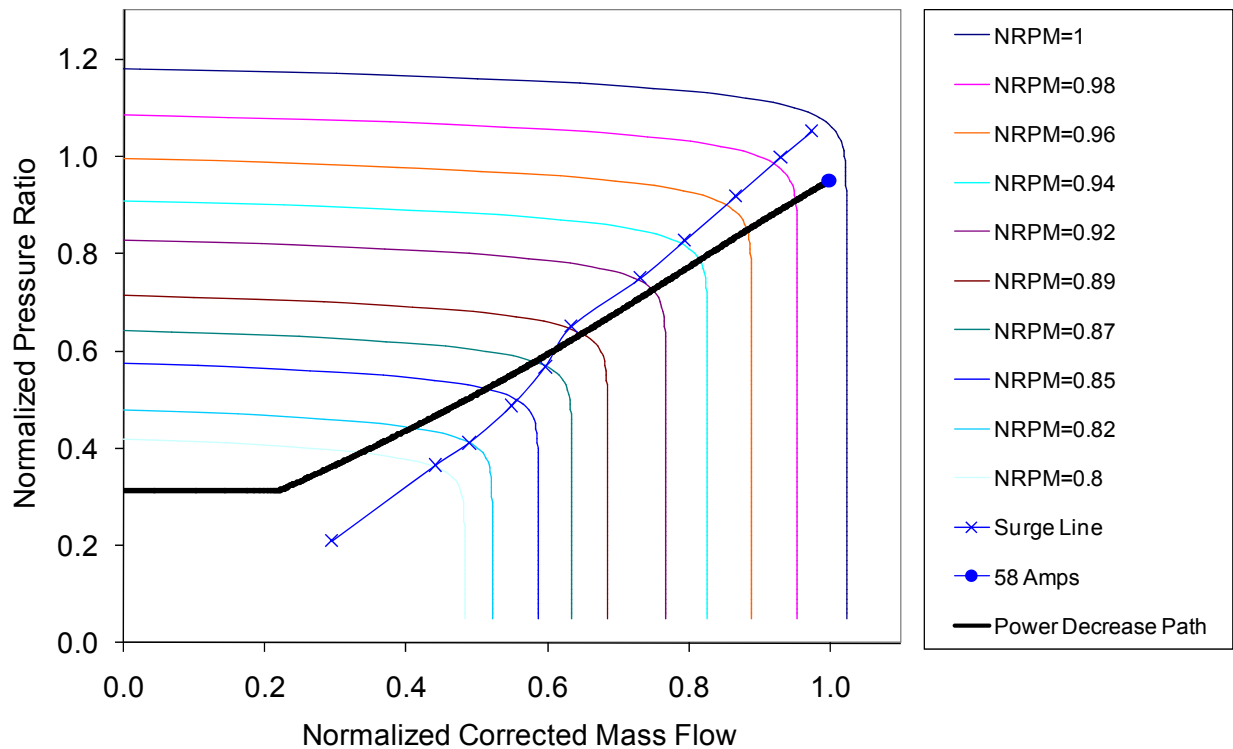
Figure A2.2 - 125 shows that controlling the tri-layer temperature requires a gas turbine shaft speed decrease from 3577 to 3340 RPM.



**Figure A2.2 - 125: Dynamic gas turbine shaft speed response to a decrease in fuel hydrogen balanced with methane from 100% to 75% of design point. Primary control of fuel cell temperature at 1,100 K and secondary control of gas turbine speed and primary control of blower/compressor mixture temperature at 800 K with secondary control of recycle blower speed.**

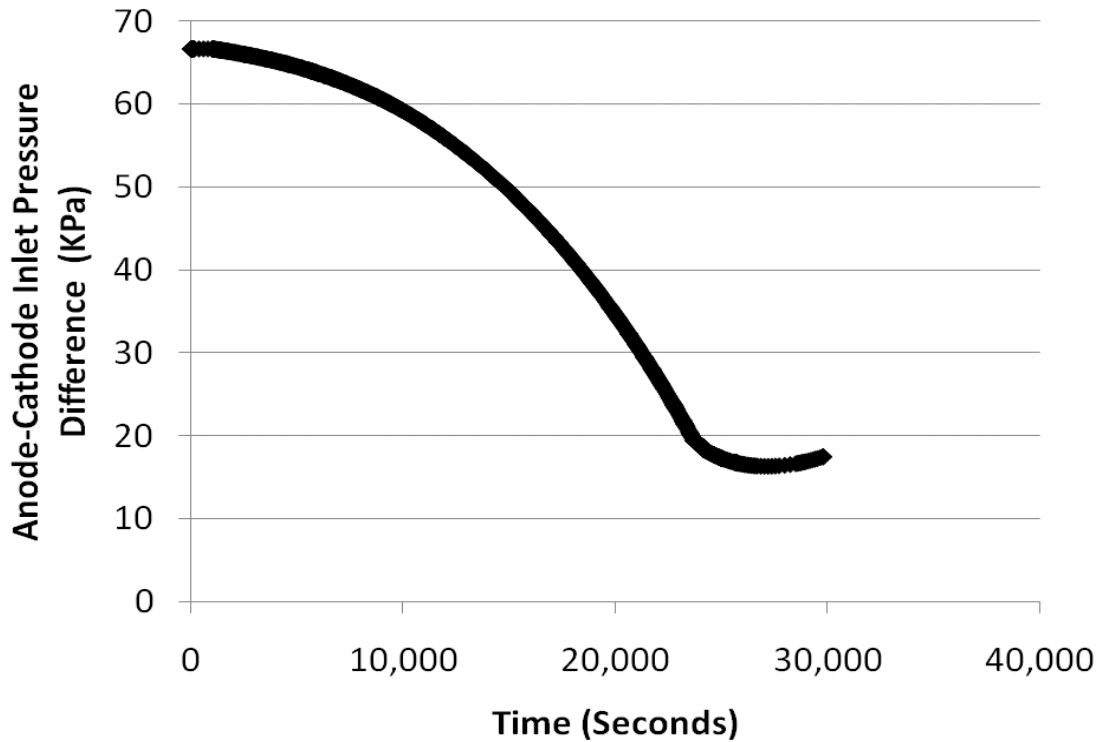
**Fuel Cell Shutdown (Continuous Linear Decrease in Current Demand Over Eight Hours)**

When the fuel cell is subjected to an 8 hour linear decrease in current demand perturbation (Figure A2.2 - 126 simulating a fuel cell shutdown event) the compressor ultimately crosses the surge line at approximately 45% of nominal load.



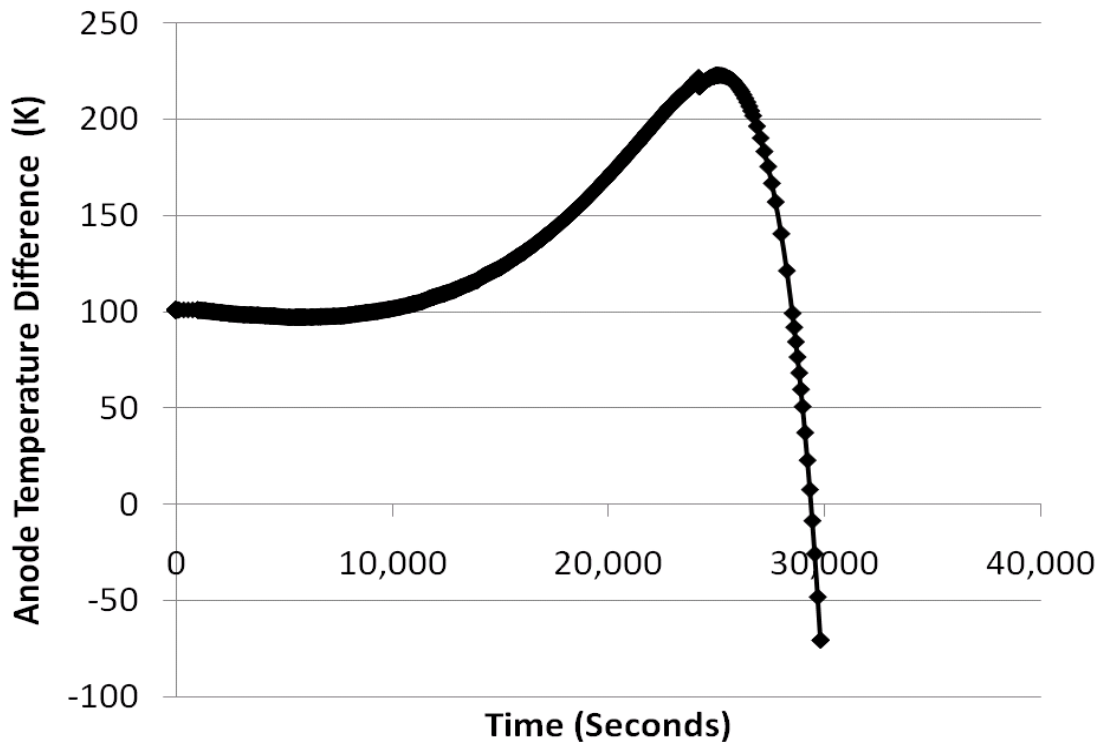
**Figure A2.2 - 126: Compressor dynamic response to a fuel cell shutdown over 8 hours. Primary control of fuel cell temperature at 1,100 K and secondary control of gas turbine speed and primary control of blower/compressor mixture temperature at 800 K with secondary control of recycle blower speed.**

The anode-cathode inlet pressure difference drops (Figure A2.2 - 127) as air mass flow continually drops. All the same trends observed when the system was perturbed by a 25% drop in current demand (Figure A2.2 - 93 - Figure A2.2 - 98) are seen here. The difference is that, in this case, after the compressor crosses the surge line about 3.6 hours into the 8 hour shutdown the model fails to converge.



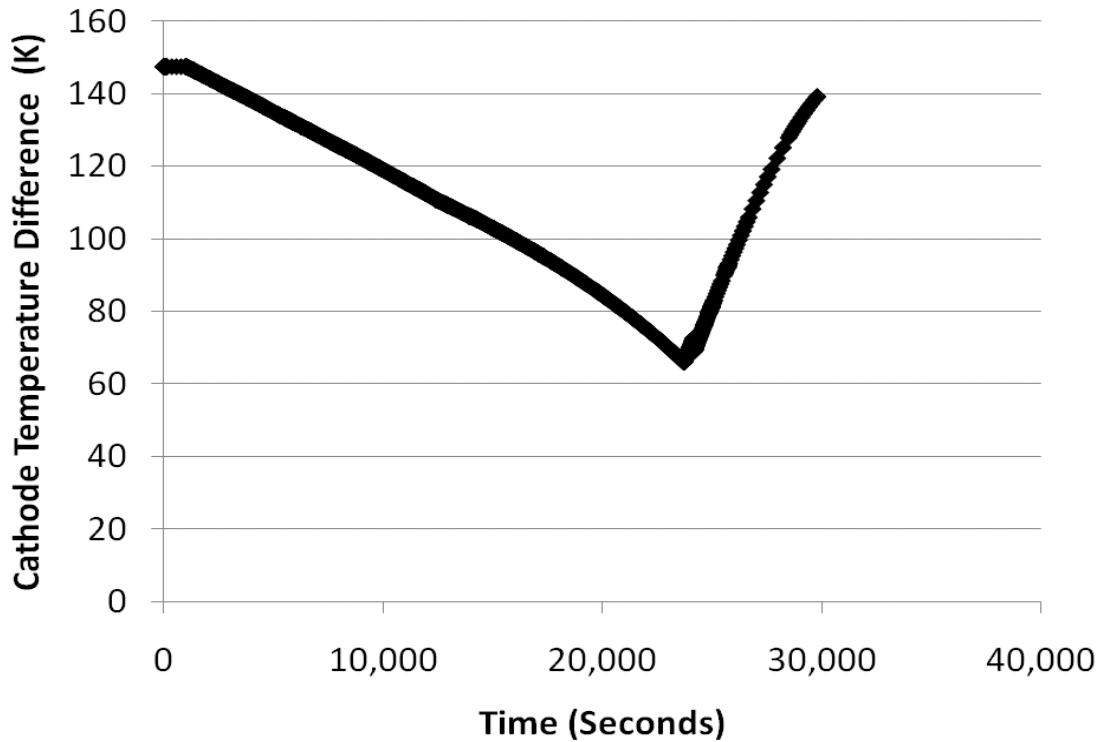
**Figure A2.2 - 127: Dynamic anode-cathode inlet pressure difference response to a fuel cell shutdown over 8 hours. Primary control of fuel cell temperature at 1,100 K and secondary control of gas turbine speed and primary control of blower/compressor mixture temperature at 800 K with secondary control of recycle blower speed.**

Figure A2.2 - 128 shows that the temperature difference across the anode initially rises. This results from a decreasing combustor outlet temperature, leading to drop in the anode inlet temperature. The anode outlet temperature is maintained by the controller during this period. Ultimately, the controller can no longer maintain the anode outlet temperature and the trend reverses, leading to a decrease in anode temperature difference.



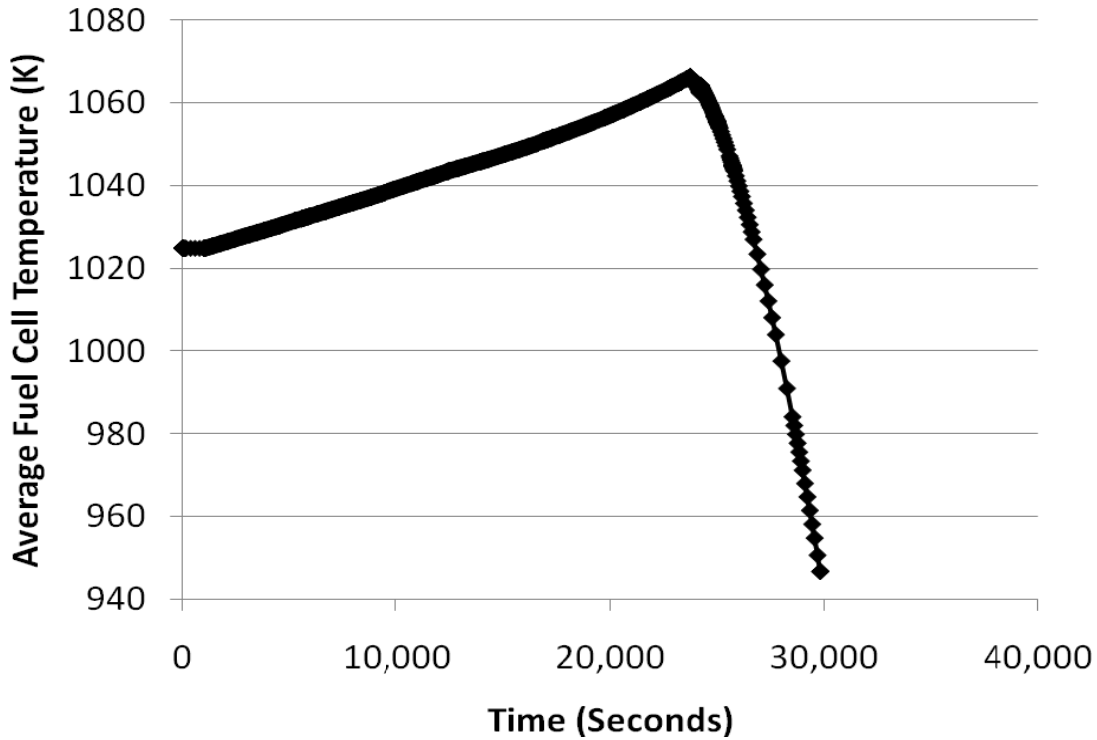
**Figure A2.2 - 128: Dynamic anode inlet-outlet temperature difference response to a fuel cell shutdown over 8 hours. Primary control of fuel cell temperature at 1,100 K and secondary control of gas turbine speed and primary control of blower/compressor mixture temperature at 800 K with secondary control of recycle blower speed.**

Figure A2.2 - 129 shows that the temperature difference across the cathode initially drops. This results from a decreasing air mass flow rate and easier preheating of this stream, leading to rise in the cathode inlet temperature. The cathode outlet temperature is maintained by the controller during this period. Ultimately, the controller can no longer maintain the cathode outlet temperature and the trend reverses, leading to an increase in cathode temperature difference.



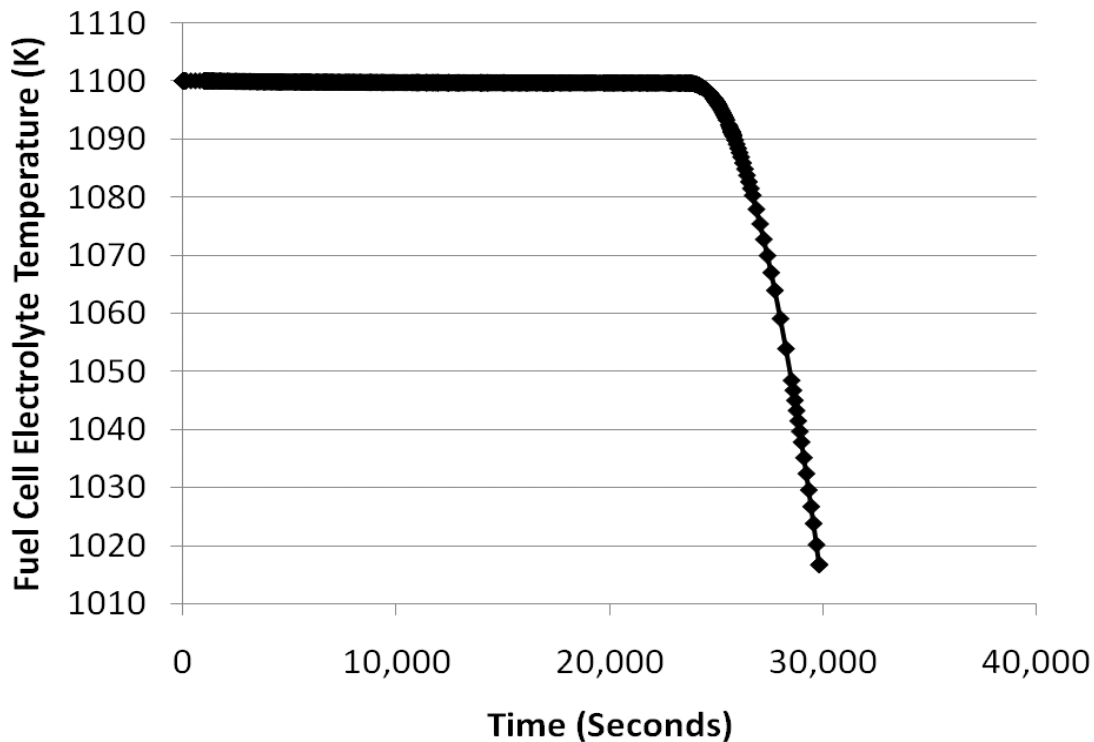
**Figure A2.2 - 129: Dynamic cathode inlet-outlet temperature difference response to a fuel cell shutdown over 8 hours. Primary control of fuel cell temperature at 1,100 K and secondary control of gas turbine speed and primary control of blower/compressor mixture temperature at 800 K with secondary control of recycle blower speed.**

Figure A2.2 - 130 shows that the average fuel cell temperature across the cathode initially rises. This results from an increase in both cathode inlet and outlet temperatures. Ultimately, the controller can no longer maintain the cathode outlet temperature and the trend reverses, leading to a decrease in average fuel cell temperature.



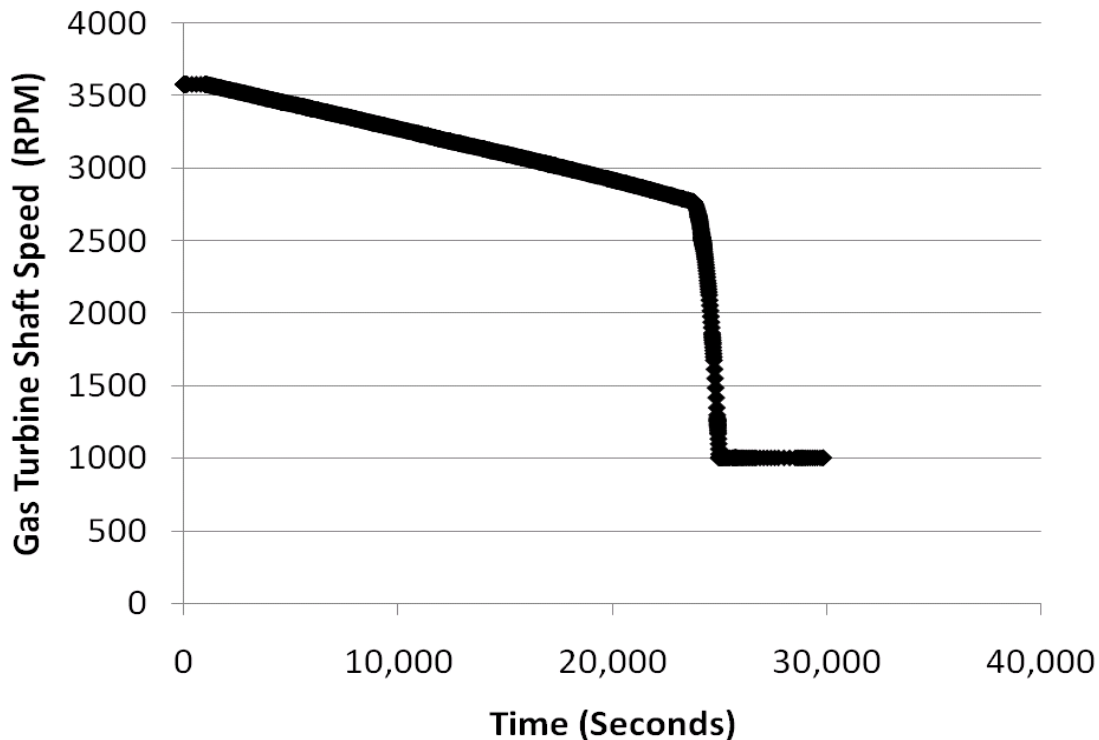
**Figure A2.2 - 130: Dynamic average fuel cell temperature response to a fuel cell shutdown over 8 hours. Primary control of fuel cell temperature at 1,100 K and secondary control of gas turbine speed and primary control of blower/compressor mixture temperature at 800 K with secondary control of recycle blower speed.**

Figure A2.2 - 131 shows that the tri-layer temperature is well controlled initially but ultimately drops when insufficient fuel is available.



**Figure A2.2 - 131: Dynamic tri-layer temperature response to a fuel cell shutdown over 8 hours. Primary control of fuel cell temperature at 1,100 K and secondary control of gas turbine speed and primary control of blower/compressor mixture temperature at 800 K with secondary control of recycle blower speed.**

Figure A2.2 - 132 shows that gas turbine shaft speed initially drops along a relatively constant linear slope. This drop occurs as the air flow rate is decreased in an effort to control the tri-layer temperature. Ultimately, gas turbine shaft speed settles on a threshold minimum value of 1000 RPM specified in the model.



**Figure A2.2 - 132: Dynamic gas turbine shaft speed response to a fuel cell shutdown over 8 hours. Primary control of fuel cell temperature at 1,100 K and secondary control of gas turbine speed and primary control of blower/compressor mixture temperature at 800 K with secondary control of recycle blower speed.**

**Fuel Cell Shutdown (Continuous Linear Decrease in Current Demand Over Eight Days)**

An 8 day shutdown was modeled in order to determine how close the hybrid system was able to reach steady state operating conditions during the 8 hour shutdown. Figure A2.2 - 133 shows that the compressor follows roughly the same path as seen in Figure A2.2 - 126 indicating close to steady state operation during the 8 hour shutdown. The 8 hour shutdown crosses the surge line at roughly the same fuel cell current load value as observed during the 8 day shutdown case, further strengthening the argument that steady state operation is reached in both cases.

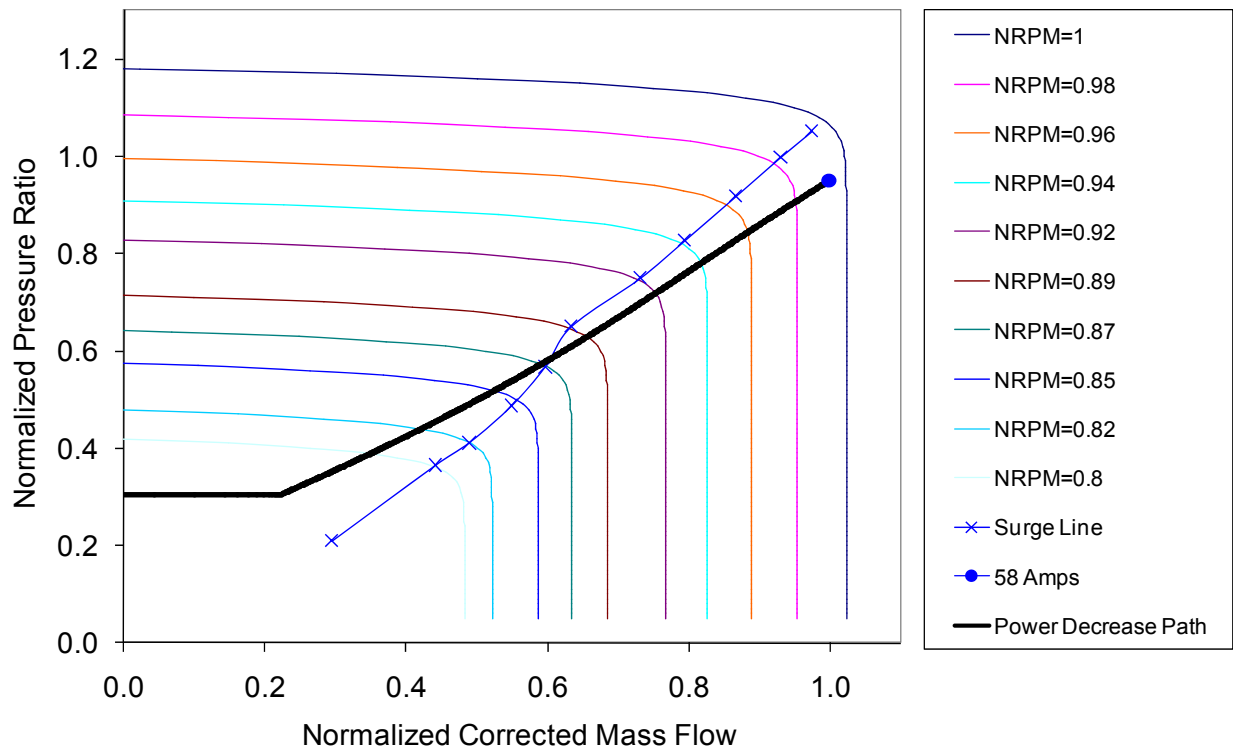


**Figure A2.2 - 133: Compressor dynamic response to a fuel cell shutdown over 8 days. Primary control of fuel cell temperature at 1,100 K and secondary control of gas turbine speed and primary control of blower/compressor mixture temperature at 800 K with secondary control of recycle blower speed.**

**Gas Turbine Moment of Inertia Doubled (Fuel Cell Subjected to a 25% Decrease in Current Demand)**

The moment of inertia for the gas turbine was increased twofold from its initial value and the hybrid system was subjected to a 25% drop in current demand shown in Figure A2.2 - 93 - Figure A2.2 - 98. No significant difference in results was seen compared to Figure A2.2 - 93 - Figure A2.2 - 98 for this perturbation and it will not be described further.

**Gas Turbine Moment of Inertia Halved (Fuel Cell Subjected to a 25% Decrease in Current Demand)**

The moment of inertia for the gas turbine was decreased twofold from its initial value and the hybrid system was subjected to a 25% drop in current demand shown in Figure A2.2 - 93 - Figure A2.2 - 98. No significant difference in results was seen compared to Figure A2.2 - 93 - Figure A2.2 - 98 for this perturbation and it will not be described further.

### **Blower Moment of Inertia Doubled (Fuel Cell Subjected to a 25% Decrease in Current Demand)**

The moment of inertia for the blower was increased twofold from its initial value and the hybrid system was subjected to a 25% drop in current demand shown in Figure A2.2 - 93 - Figure A2.2 - 98. No significant difference in results was seen compared to Figure A2.2 - 93 - Figure A2.2 - 98 for this perturbation and it will not be described further.

### **Blower Moment of Inertia Halved (Fuel Cell Subjected to a 25% Decrease in Current Demand)**

The moment of inertia for the blower was decreased twofold from its initial value and the hybrid system was subjected to a 25% drop in current demand shown in Figure A2.2 - 93 - Figure A2.2 - 98. No significant difference in results was seen compared to Figure A2.2 - 93 - Figure A2.2 - 98 for this perturbation and it will not be described further.

### **Comparison of Control Strategies #1 and #2**

Comparing the two control strategies reveals the very dramatic impact that control strategy has on compressor dynamics and surge avoidance. When control strategy #1 is used there is very little impact on the compressor steady state operating point and thus surge is relatively easily avoided. There are two main reasons for this. First, the fuel cell tri-layer temperature is allowed to vary during the dynamic and therefore the compressor is not required to respond in any way to changes in fuel cell operating temperature. However, large variations in fuel cell stack operating temperature can lead to stack degradation, which should be avoided. Second, the blower is primarily being used to control cathode inlet temperature by varying exhaust recycle ratios and this is done by using electrical power that is independent of the compressor. This is contrasted with the case when a cathode recycle ejector is used and cathode inlet temperature is controlled by the exhaust recycle ratio, which must be driven directly by the compressor. The ejector case thus leads to much more dynamic compressor response requirements to meet system operating conditions.

In contrast, there is a very strong impact on compressor dynamics and the potential for surge when control strategy #2 is used. This is because the compressor is being manipulated to maintain fuel cell tri-layer temperature at a constant and safe condition. This will likely be necessary to protect the high cost fuel cell stack in such hybrid systems. The trade off is that compressor surge can become difficult to avoid when the system is subjected to some of the more significant perturbations. It should be noted that there is very little difference in the initial and final states or the dynamic path of the compressor when a cathode blower is used instead of a cathode ejector in the case that fuel cell operating temperature is the primary control strategy (#2).

### **Strategies for Improved Dynamic Performance of Gas Turbines in Hybrid Systems**

One of the most damaging gas turbine responses to perturbations is compressor surge. Compressor surge is also challenging to avoid while maintaining the system within all operating constraints. This is especially the case when the turbo-machinery is integrated into a hybrid fuel

cell gas turbine system. As a result, the bulk of the dynamic system analyses conducted to-date have focused upon this formidable challenge to the dynamic operation and control of gas turbines as integrated into hybrid systems.

Many of strategies for avoiding compressor surge have been described in previous sections. This section of the current report outlines all of the major turbo-machinery design and control strategies investigated over the course of these studies to-date followed by a listing of some approaches that warrant further investigation.

### **Turbo-machinery Design and Control Strategies for Improved Dynamic Performance in Hybrid Systems Studied To-Date**

- Decrease the compressor's design mass flow. This allows operation in a region that avoids surge but is associated with a penalty in compressor efficiency.
- A similar means of moving operation away from surge is to increase the design pressure ratio but again this comes with an efficiency penalty.
- Surge avoidance is substantially improved with the combined effects of reducing design mass flow and increasing design pressure ratio.
- Minimizing the volume between the gas turbine and the compressor helps in avoiding surge. This approach has been suggested by others (e.g., Hill & Peterson, 1992).
- Minimizing gas turbine rotational moment of inertia was found to help avoid surge during load sheds.
- Operating the compressor in the vertical region of the speed line was found to help avoid surge since there is little mass flow dependence on pressure ratio in this region. This is especially true for systems being controlled to operate at constant speed. Steep speed lines are desired in general compressor design philosophy to enhance compressor flow distortion tolerance (Greitzer, 1980).
- In general, one should design the compressor such that mass flow will not decrease faster than the pressure ratio can decrease as suggested by Kurz & White, 2004.
- When a PID controller is used, careful tuning of the controller is necessary to avoid dynamic operation paths that can lead to surge. Assuming the PID controller is effective at reaching its set points, there is very little if any effect that tuning has on final and initial states of the transient response to perturbations that may occur in the region associated with surge.
- Surge was found to be much less of a concern when fuel cell temperature is not a control parameter than when it was. This is because the compressor mass flow is the main manipulated variable for controlling fuel cell temperature. The fuel cell temperature control strategy should be designed to accept some delays in mass flow response (which the fuel cell should be able to handle due to large thermal mass) so that the hybrid system will have better surge avoidance.
- When fuel cell temperature *is not* a control parameter, cathode recycle blowers were found to lead to less compressor operating point fluctuation than when an ejector is used for the same purpose. Thus, a blower is preferred for surge avoidance and superior dynamic response to perturbations with this control strategy.
- When fuel cell temperature *is* a control parameter, there was very little difference in surge avoidance between systems that used a cathode blower or an ejector.

- Lower fuel cell set point temperatures were found to aid in avoiding surge since higher mass flow rates are required to achieve the lower temperature. However, this control strategy incurs a system efficiency penalty.
- Some of the dynamics found to lead to surge, especially in the case when fuel cell temperature was a control parameter, were: (1) large decreases in fuel cell load current, and (2) decreases in syngas hydrogen content.
- In general, it was found that machines driving synchronous generators were less likely to experience surge but were unable to effectively control fuel cell temperature for all the perturbations studied. The converse of this is true for asynchronous machines.

### **Turbo-machinery Design and Control Strategies for Improved Dynamic Performance in Hybrid Systems that Merit Further Investigation**

- Compressor bleed and bypass flow
- Variable inlet guide vanes
- New control strategies and feedback/feedforward control loops
- Effect of compressor inlet area
- Effect of number of compressor stages
- Centrifugal vs. axial compressor design
- Impact of turbine inlet temperature
- Impact of turbine design size on compressor operating point
- Impact of the magnitude of various pressure drops within the cycle on compressor operating point
- Other dynamic perturbations that may lead to surge should also be investigated

## **CONCLUSIONS**

Two SOFC-GT hybrid cycles that meet DOE criteria were numerically modeled and their dynamic performance simulated as part of a perturbation and response analyses. The main difference between the two cycles is the means by which cathode recycle is accomplished; initially via an ejector and ultimately via a blower during the evolution of the study. Models of these two subsystems were built specifically to assist in these studies. The dynamic models of the entire system stem from the 220 kW Siemens Westinghouse hybrid system model that was developed at the National Fuel Cell Research Center and validated with experimental data. These correlations between the model and experiment have been described in numerous journal publications. The main changes to the 220 kW model were to scale up the power block to 100 MW, replace tubular fuel cell geometry with planar geometry, replace centrifugal turbo-machinery with axial design and adjust overpotential parameters in the SOFC to match SECA target performance goals of 500 mW/cm<sup>2</sup> at 80% fuel utilization. Since experimental data at the 100 MW system level is unavailable, model performance was compared and validated against ASPEN, industry standard software used in plant design. Very good correlation was found between the models described in this work and that of ASPEN.

These studies primary focused on the impact of perturbations to the steady state design operating point that led to gas turbine failure in the form of compressor surge and design and operational strategies to avoid this phenomenon. The pressure fluctuations associated with

compressor surge will likely damage if not destroy the fuel cell before the turbo-machinery if pressure regulators are not placed between the fuel cell stack and the turbo-machinery. The main perturbations investigated that lead to surge were load shed and dilution of syngas hydrogen content with nitrogen or steam. Fuel cell shutdowns also led to surge. The design strategies that were found to help in avoiding surge include designing the turbine and compressor to allow greater surge margin under steady state operation, minimizing the plenum volume between the fuel cell outlet and turbine inlet, minimizing gas turbine rotational moment of inertia and designing for compressor speed lines that are more vertical in nature. Modification of the turbo-machinery design pressure ratio and mass flow to achieve more stable dynamic response to load shed and fuel dilution perturbations usually comes with an efficiency penalty. But, the efficiency penalty associated with these design modifications may be worth the increase in stability. This argument is further supported if the gas turbine is mainly seen as a means of feeding air to the fuel cell.

The dynamic response of the fuel cell was studied for the above mentioned perturbations. These responses include anode-cathode inlet pressure difference, anode and cathode inlet-outlet temperature differences, average fuel cell cathode temperature, tri-layer (electrolyte) temperature and gas turbine shaft speed. In many cases the perturbation investigated did not lead to compressor surge but these other failure mechanisms were observed.

Two separate control strategies were employed in this study; the first controls gas turbine shaft speed at 3,600 RPM, assuming a synchronous generator and the second (cascade controller) primarily controls fuel cell temperature and secondarily controls gas turbine shaft speed, assuming an asynchronous generator. Careful tuning of the controls is necessary in order to avoid dynamic operational paths taken between initial and final steady state operating points that tend towards surge. The main difference between the two control strategies is that when RPM is the only control parameter, surge is more easily avoided but fuel cell temperature can vary dramatically. The cascade controller is very effective at controlling fuel cell temperature but because this parameter is controlled by varying gas turbine shaft speed, surge becomes a factor. The fuel cell temperature strategy should be designed to accept some delays in mass flow response (which the fuel cell should be able to handle due to its large thermal mass) so that the hybrid system will have better surge avoidance. When fuel cell temperature *is not* a control parameter, cathode recycle blowers were found to lead to less compressor operating point fluctuation than when an ejector is used for the same purpose. Thus, a blower is preferred for surge avoidance and superior dynamic response to perturbations with this control strategy. When fuel cell temperature *is* a control parameter, there was very little difference in surge avoidance between systems that used a cathode blower or an ejector. In general, it was found that machines driving synchronous generators were less likely to experience surge but were unable to effectively control fuel cell temperature for all the perturbations studied. The converse of this is true for asynchronous machines. Using the cathode blower in place of the ejector was found to increase steady state cycle efficiency by approximately three percentage points for the three different cycle pressure scenarios investigated. It is unknown whether currently available blowers can operate at the temperatures required or whether blowers could maintain the pressure ratios required in the current cycles.

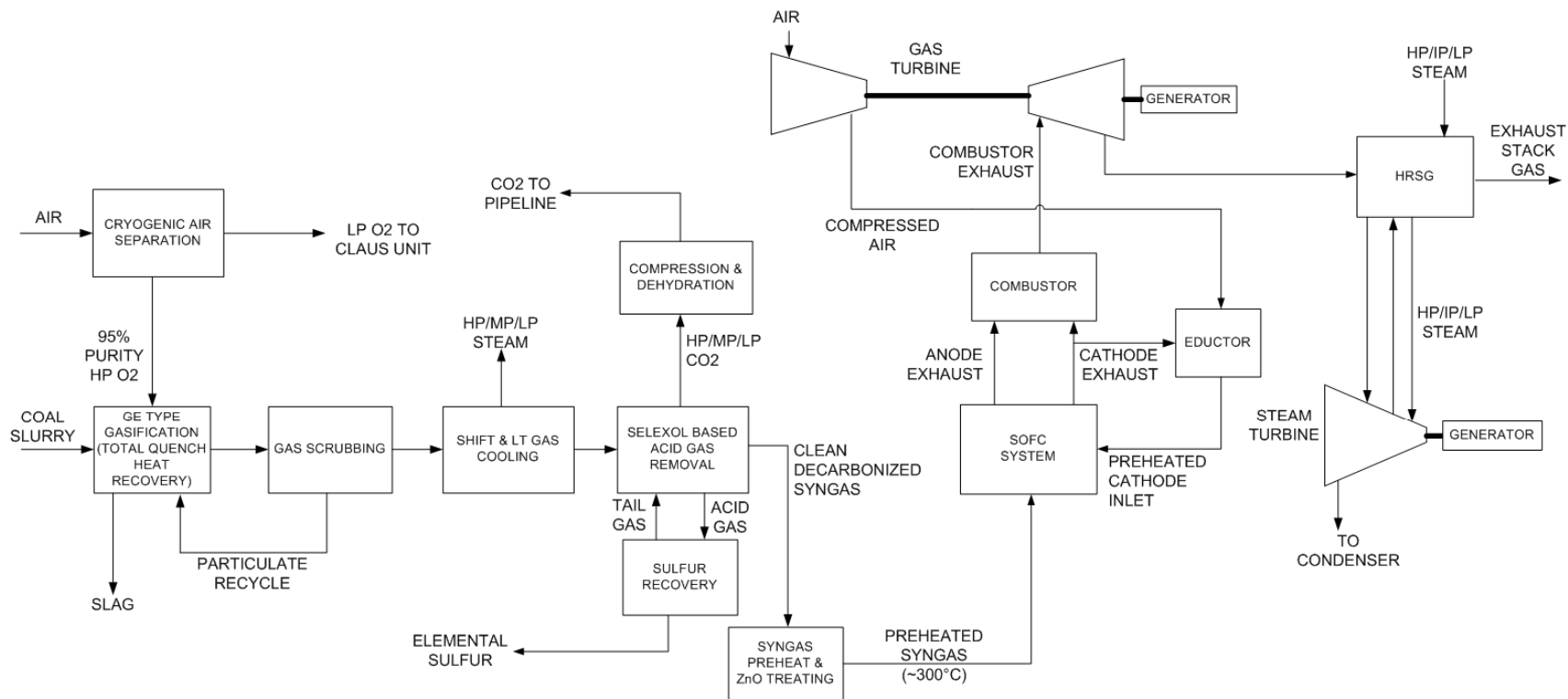
Many studies that merit further investigation are suggested.

## ATTACHMENT

This attachment contains the Design Guidelines and base power plant schematics for the complete IGFC power plant and the section of the power plant that will be used for dynamic simulations that have been negotiated with the U.S. Department of Energy.

### Design Guidelines

4. Overall Plant:
  - a. General Design Basis same as Baseline IGCC case for the Advanced Brayton Cycle study [CO<sub>2</sub> Capture = 90% of Gasified Carbon (leaving gasifier as gaseous components)]
  - b. Size of each FC / GT Power Block or Train = 100 MW (plant will consist of multiple 100 MW trains to take advantage of a larger gasification plant)
  - c. HRSG pressure drop for the dynamic simulations will be estimated by assuming flow through a non-choked orifice.
  
5. SOFC:
  - a. Planar SOFC
  - b. Non-Internal Reforming
  - c. Hydrocarbon Content of Syngas < 1%
  - d. Average Operating Temp = 750°C ( $\pm 25^\circ\text{C}$ ) or (998-1048 K)
  - e. Power Density = 500 mW/cm<sup>2</sup>
  - f. Fuel Utilization = 80%
  - g. Max Temp. Rise on Anode Side  $\leq 100^\circ\text{C}$
  - h. Max Temp. Rise on Cathode Side  $\leq 100^\circ\text{C}$
  - i. Air Preheat within Stack: 100 to 150°C Temperature Rise
  - j. Fuel Preheat within Stack: as required based on supplying the syngas to the power block at around 300°C
  - k. Operating pressure: 5 atm (two other pressures considered, steady-state only)
  - l. Syngas pressure at power block: 120 to 140 psi above SOFC Operating Pressure
  
6. Gas Turbine:
  - a. Dynamic simulations to aid in identifying and specifying the ideal (or optimal) turbine and compressor characteristics to accommodate the SOFC and allow for control during transient operation
  - b. Non-recuperated cycle with cathode recycle gas to preheat the cathode air
  - c. Simplified eductor model
    - i. Low design pressure drop that varies linearly with flow-rate squared
    - ii. Fixed eductant flow curve (function of pressure drop)
    - iii. Instantaneous dynamic response
    - iv. Ideal (“mixing cup”) temperature achieved with 3% heat loss



**NOTE:**  
 (1) PLANT INCLUDES ALL SUPPORT FACILITIES NOT SHOWN SUCH AS COAL HANDLING, SLURRY PREPARATION, WASTE WATER TREATMENT, BFW PREPARATION, COOLING WATER SYSTEM ETC.

**Figure A2.2 - 134: Integrated Gasification Fuel Cell Power Plant**

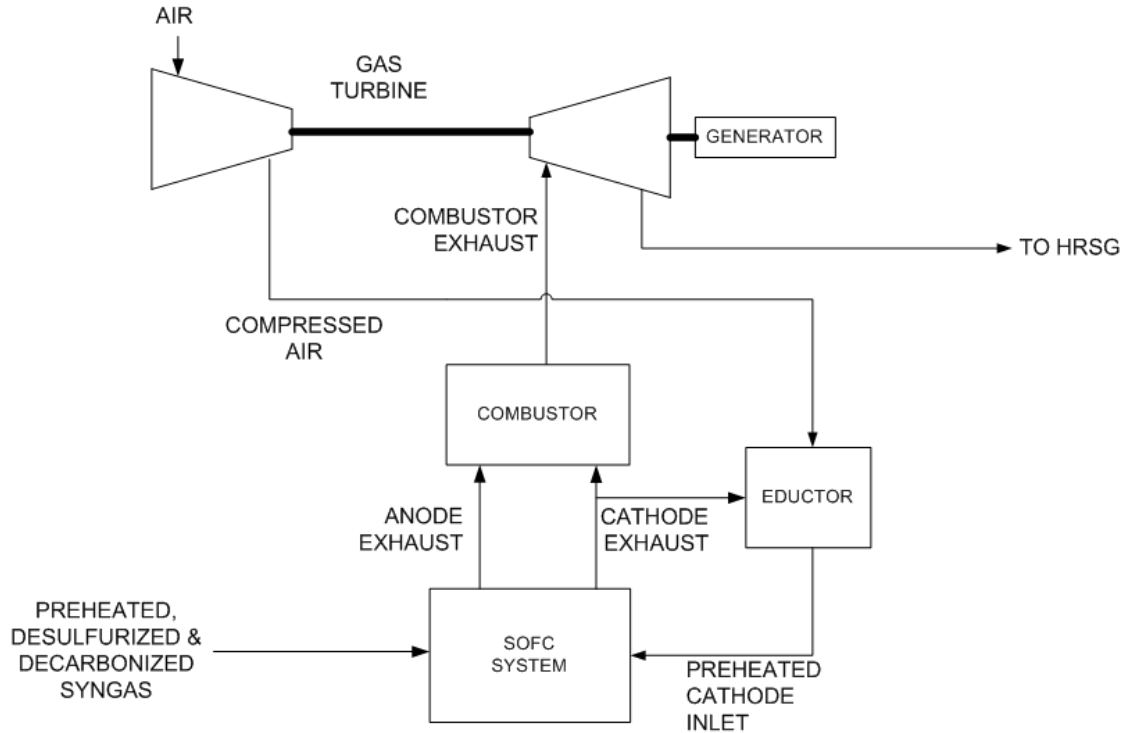


**Figure A2.2 - 135: Section of the Plant for Dynamic Analysis**

### USEFUL EQUATIONS

Some useful equations include Mach number  $M$ :

$$M = \frac{V}{a} = \frac{V}{\sqrt{\gamma RT}}$$

The ratio of specific heats for air which is the assumed working fluid throughout for cathode ejector analysis:

$$\gamma = \frac{c_p}{c_v} = \frac{1.005}{0.718} = 1.4 \text{ (For Air)}$$

And the specific gas constant for air:

$$R = c_p - c_v = (1.005 - 0.718) \frac{kJ}{kg * K} = 0.2870 \frac{kJ}{kg * K} = 287 \frac{J}{kg * K} \text{ (For Air)}$$

$$\text{Entrainment Ratio} = \omega = \frac{\dot{m}_2}{\dot{m}_1}$$

*Subscript (s) = Isentropic Case*

*Subscript (a) = Actual Case*

## REFERENCES

1. Cengel YA, Boles MA (2002). Thermodynamics: An Engineering Approach; USA: McGraw Hill.
2. Chunnanond K, Aphornratana S (2004). "Ejectors: applications in refrigeration technology." Renewable and Sustainable Energy Reviews; 8: 129-155.
3. Ferrari ML, Traverso A, Magistri L, Massardo AF (2005). "Influence of the anodic recirculation transient behaviour on the SOFC hybrid system performance." J. Power Sources; 149: 22-32.
4. Gas Turbine Simulation Program (GSP) <http://www.gspteam.com/main/main.shtml>
5. Greitzer, EM (1980). "Review-Axial Compressor Stall Phenomena." ASME J. Fluids Eng.; 102: 134-152.
6. Hill P, Peterson C (1992). Mechanics and Thermodynamics of Propulsion; New York: Addison-Wesley.
7. Keenan JH, Neumann EP (1942). "A simple air ejector" ASME Journal of Applied Mechanics; 9: A75-A81.
8. Keenan JH, Neumann EP, Lustwerk F (1950). "An investigation of ejector design by analysis and experiment" ASME Journal of Applied Mechanics; 72: 299-309.
9. Kurz R, White RC (2004). "Surge Avoidance in Gas Compression Systems." ASME Journal of Turbomachinery; 126: 501-506.
10. Marsano F, Magistri L, Massardo AF (2004). "Ejector performance influence on a solid oxide fuel cell anodic recirculation system." J. of Power Sources; 129: 216-228.
11. Pukrushpan JT, Stefanopoulou AG, Peng H (2005). Control of Fuel Cell Power Systems; London: Springer
12. Rao AD, Samuelson GS, Robson FL, Washom B, Berenyi SG (2006). "Advanced Power Plant Development and Analyses Methodologies." DOE Award No. DE-FC26-00NT40845.

13. Roberts RA, Brouwer J. (2006). "Dynamic Simulation of a 220kW Solid Oxide Fuel Cell Gas Turbine Hybrid System with Comparison to Data." ASME Journal of Fuel Cell Science and Technology; 3: 18-25.
14. Roberts RA, Brouwer J, Junker T, Ghezal-Ayagh H (2006). "Control Design of an Atmospheric Solid Oxide Fuel Cell/Gas Turbine Hybrid System: Variable versus Fixed Speed Gas Turbine Operation." Journal of Power Sources; 161: 484-491.
15. Saravanamuttoo HHH, Rogers GFC, Cohen H (2001). Gas Turbine Theory; Edinburgh Gate: Pearson Education Limited.
16. Sasaki K, Teraoka Y (2003). "Equilibria in fuel cell gases." Electrochemical Society Proceedings; 2003-07: 1225-1234.
17. SECA 2004 Annual Review:  
<http://www.netl.doe.gov/technologies/coalpower/fuelcells/seca/>
18. Sun DW, Eames IW, Aphornratana S (1996). "Evaluation of a novel combined ejector-absorption cycle- I: computer simulation." Int. J. Refrig.; 19: 172-180.
19. Wächter C, Lunderstädt R, Joos F (2006). "Dynamic model of a pressurized SOFC/gas turbine hybrid power plant for the development of control concepts." ASME Journal of Fuel Cell Science and Technology; 3: 271-279.
20. White FM (2003). Fluid Mechanics; USA: McGraw Hill.

## TASK 2.3: PERFORMANCE COMPARISON OF OXY-COMBUSTION AND IGCC PLANTS

### SUMMARY

This task consists of comparing the Oxy-combustion cycle being developed by Clean Energy Systems (CES) with the down-selected advanced Brayton cycle based combined cycle in integrated coal gasification plants. Pittsburgh No. 8 coal is utilized in both types of plants. In an IGCC system which consists of pre-combustion carbon capture, the percentage of CO<sub>2</sub> capture is limited by the thermodynamic penalty required to shift the raw syngas to a H<sub>2</sub> and CO<sub>2</sub> mixture and the performance of the acid gas removal unit to separate the CO<sub>2</sub>. As the percentage of carbon capture is pushed beyond 80 to 90%, a point of diminishing return can be reached. The oxy-fuel cycle may provide an advantage over the pre-combustion decarbonization cycle since the water gas shift reaction is not required, less duty is placed on the acid gas removal system (if pre-combustion desulfurization is utilized) while nearly 100% of the carbon (as CO<sub>2</sub>) is captured. Thus as a first step, a study is required to compare the thermal performance of the two types of plants. Maintaining consistency in the design basis with respect to coal characteristics, site conditions, mode of heat rejection, etc. between the two cases is essential to obtain meaningful results.

The following lists the appropriate gasifier and / or its operating pressure for each of the cycles:

- For the IGCC cases, General Electric slurry feed entrained bed type gasifiers with two alternate heat recovery options as specified in the Statement of Work with operating pressures of:
  - Operating pressure of < 8.7 MPa (1260 psia) for Total Quench (TQ) Heat Recovery option
  - Operating pressure of 5.62 MPa (815 psia) for Radiant Syngas Cooler Plus Quench (R+Q) Heat Recovery option
- For the oxy-combustion cycle, a gasifier of the E-STR type offered by Conoco Phillips also slurry fed while operating at a pressure of 8.38 MPa (1215 psia).

The following summarize the results and conclusions of this task:

- The calculated plant thermal efficiencies as summarized in Figures A2.3-1 and A2.3-2 show that the efficiency of the oxy-combustion cycle based cases is lower than both the Total Quench Heat Recovery option and the Radiant Syngas Cooler Plus Quench Heat Recovery option IGCC cases with the slightly lower CO<sub>2</sub> capture.
- Since the air separation unit is a major component of the total plant cost, the specific O<sub>2</sub> consumption expressed as total tones/hr O<sub>2</sub> per net MW produced by each plant is presented in Figures A2.3-3 and A2.3-4. As expected, the specific O<sub>2</sub> consumption is significantly higher for the oxy-combustion cycle based cases.
- The relative economic worth of capturing additional CO<sub>2</sub> is measured by subtracting the CO<sub>2</sub> emission penalty cost (assumed at \$30/tonne) from the revenue stream associated

with the sale of electricity (assumed at \$50/MWhr) for the various cases at constant throughput of 3,078 tonne/d of Pittsburgh No. 8 coal. These results as presented in Figures A2.3-5 and A2.3-6 show that there does not appear to be any advantage for the oxy-combustion based cases even with the assumed significantly high penalty of \$30/tonne for CO<sub>2</sub> emission and the assumed low sale price for electricity of \$50/MWhr, unless there is a substantial reduction in the plant cost for the oxy-combustion based cases. The significantly higher O<sub>2</sub> consumption per net MW produced for the oxy-combustion based cases, however, makes it quite improbable that the plant costs would be lower.

- Other inferences that may be drawn from these results are:
  - The Radiant Syngas Cooler Plus Quench Heat Recovery option IGCC is more efficient than the Total Quench Heat Recovery option IGCC even in applications where CO<sub>2</sub> capture is required. The total plant cost, however, for the IGCCs with the radiant syngas coolers will be significantly higher.
  - For the above set of assumptions with respect to CO<sub>2</sub> emission penalty and sale price of electricity, the “optimum” CO<sub>2</sub> capture for the Total Quench Heat Recovery option IGCC is about 90% while that for the Radiant Syngas Cooler Plus Quench Heat Recovery option IGCC is less than 80%.

## APPROACH

An advantage of the CES system which consists of post-combustion carbon capture is that it can capture essentially all the carbon entering with the coal without a significant incremental penalty to plant performance. To provide a valuable comparison, both the integrated gasification oxy-combustion system with the CES cycle and the IGCC system with the advanced Brayton cycle are modeled with a similar turbine firing temperature and balance of plant where appropriate. Both types of plants utilize cryogenic air separation technology. On the other hand the more suitable or appropriate gasifier and /or gasifier effluent heat recovery option is utilized for each case. For the oxy-combustion cases which do not require shifting of the CO in the syngas upstream of the power block, heat recovery in heat exchangers before the syngas is quenched in a scrubber is maximized.

Since the time-frame for the deployment of the Oxy-combustion cycle is uncertain, it is essential that the two approaches to carbon capture are compared at two different gas turbine firing temperatures:

- Rotor inlet temperature (RIT) of 1392°C, consistent with the Baseline Case (H Class turbine) of the Advanced Brayton Cycle Study representing the near term
- Rotor inlet temperature (RIT) of 1734°C, consistent with the advanced firing temperature identified in the Advanced Brayton Cycle Study.

Different degrees of carbon capture are investigated:

- IGCC cases: 80%, 90%, 95% and 99%+<sup>18</sup>
- Oxy-combustion cases: 99%+

Two different schemes for acid gas handling are addressed:

- The first consists of producing elemental sulfur from the acid gas utilizing a Claus plant.
- The second consists of combusting the acid gas with O<sub>2</sub> supplied by the ASU followed by co-sequestration of the SO<sub>2</sub> with the CO<sub>2</sub> stream.

The economic worth of reducing the CO<sub>2</sub> emissions is measured by the following methodology for this initial study phase (i.e., in the absence of plant costs required for a complete economic analysis of the various cases<sup>19</sup>):

- Assign a penalty for the emitted CO<sub>2</sub> (e.g., \$30/tonne)
- Determine the negative revenue stream due to the emitted CO<sub>2</sub> (\$/hr) for each case at an assumed plant capacity factor (85%).
- Select a certain sale price for electricity (\$50/MWhr)
- Based on the net power generated, determine \$/hr associated with the sale of electricity at the assumed plant capacity factor.
- Then reduce the above \$/hr associated with the sale of electricity by the \$/hr associated with the emitted CO<sub>2</sub> for each case to obtain the net revenue stream.

The method for CO<sub>2</sub> storage consists of over the fence remote geologic sequestration at a pressure of 152 bar (2200 psi) for both IGCC and Oxy-combustions cases. Composition of this CO<sub>2</sub> stream consistent with “Design Condition 3” of the NETL Technical Note No.10 (Ciferno, and Newby, 2007) is presented in Table A2.3-1.

The various cases for evaluation under this study task are presented in Table A2.3-2.

## **Process Configurations**

The over plant process schemes for the following cases are depicted in block flow diagrams:

- IGCCs with Gas Turbine Rotor Inlet Temperature of 1392°C
  - Total Quench Heat Recovery option IGCC cases with 80% and 90% CO<sub>2</sub> capture (Figure A2.3-7)
  - Total Quench Heat Recovery option IGCC cases with 90% and 99%+ CO<sub>2</sub> capture (Figure A2.3-8)
  - Radiant Syngas Cooler Plus Quench Heat Recovery option IGCC cases with 80% and 90% CO<sub>2</sub> capture (Figure A2.3-9)

<sup>18</sup> For the IGCC case with 99%+ carbon capture, the configuration consists of: PSA unit to further decarbonize the syngas leaving the acid gas removal unit while compressing the tail gas from the PSA for recycle to the shift unit. A purge stream is included to avoid building up of high concentrations of CH<sub>4</sub>, Ar, N<sub>2</sub> etc.

<sup>19</sup> Plant cost estimates and complete economic analysis are deferred to a future study, at the DOE’s discretion. The results of this initial “scoping study” provide justification for whether such a future study phase is warranted.

- Radiant Syngas Cooler Plus Quench Heat Recovery option IGCC cases with 90% and 99%+ CO<sub>2</sub> capture (Figure A2.3-10)
- IGCCs with Gas Turbine Rotor Inlet Temperature of 1734°C
  - Total Quench Heat Recovery option IGCC cases with 80% and 90% CO<sub>2</sub> capture (Figure A2.3-11)
  - Total Quench Heat Recovery option IGCC cases with 90% and 99%+ CO<sub>2</sub> capture (Figure A2.3-12)
  - Radiant Syngas Cooler Plus Quench Heat Recovery option IGCC cases with 80% and 90% CO<sub>2</sub> capture (Figure A2.3-13)
  - Radiant Syngas Cooler Plus Quench Heat Recovery option IGCC cases with 90% and 99%+ CO<sub>2</sub> capture (Figure A2.3-14)
- Oxy-combustion Cycle based Cases with Gas Turbine Rotor Inlet Temperature of 1392°C and 1734°C (Figure A2.3-15).
- SO<sub>2</sub> co-sequestration Cases
  - IGCC with Gas Turbine Rotor Inlet Temperature of 1392°C, Total Quench Heat Recovery option and 90% CO<sub>2</sub> capture (Figure A2.3-16)
  - Oxy-combustion Cycle with Gas Turbine Rotor Inlet Temperature of 1392°C, Total Quench Heat Recovery option and 90% CO<sub>2</sub> capture (Figure A2.3-17)

The following presents a discussion of the selection of the gasifier and / or its operating pressure for the IGCCs and the oxy-combustion cases. The number of shift reactors in series required for the IGCC cases with the various levels of carbon capture is also discussed in the following.

## IGCC Cases

The previous work conducted under this contract to identify advanced Brayton cycle is based on utilizing a General Electric type slurry feed high pressure entrained bed gasifier with Total Quench Heat Recovery. The justification for choosing this gasifier type is documented in a previous section of this report. In this new task, the heat recovery option consisting of a radiant syngas cooler is also included. A literature search was made as suggested by GE to arrive at the operating pressures for the two heat recovery options:

- For the Total Quench Heat Recovery option, an operating pressure of < 8.7 MPa or 1260 psia (Rigdon, 2007) is utilized.
  - The gasifier operating pressure required for the advanced firing temperature Brayton cycle which has a cycle pressure ratio of 50 is 7.67 MPa (1113 psia) without requiring syngas compression, consistent with previous cases developed under this contract (for gas turbine cycle pressure ratios of 50).
  - For the H class firing temperature Brayton cycle which has a cycle pressure ratio of 24, a lower gasifier pressure suffices. A gasifier operating pressure of 7.26 MPa (1053 psia) consistent with previous cases developed under this contract is utilized for the H class firing temperature Brayton, however. With this higher operating pressure for the gasifier, which is in excess of that required by the H

class gas turbine, benefits are realized in the Selexol™ acid gas removal unit by reducing the solvent circulation rate leading to lower utility consumptions and plant cost while the high pressure syngas is expanded in a turbo-expander to recover work before it is supplied to the gas turbine.

- For the Radiant Syngas Cooler Plus Quench Heat Recovery option, the gasifier operating pressure is limited to 5.62 MPa or 815 psia (Klara et. al., 2007). Syngas compression is included to provide the syngas at the appropriate pressure to the gas turbine in both the advanced and the H class firing temperature Brayton cycle cases.

The number of sour shift reactors in series (with intercooling) and type required for the Total Quench Heat Recovery IGCC cases and the Radiant Syngas Cooler Plus Quench Heat Recovery IGCC cases with the various levels of carbon capture are summarized in Tables A2.3-3 and A2.3-4. The number of reactors and operating temperature ranges selected for each level of carbon capture are based on minimizing the amount of CO shifted while at the same time keeping the level of CO<sub>2</sub> captured in the Selexol™ unit reasonable such that its utility consumptions and equipment sizes are not severely increased. By minimizing the amount of CO shifted, the amount of fuel bound energy contained in the syngas degraded to heat is minimized.

### **Oxy-combustion Cases**

The CES cycle requires about a third of the syngas at approximately 10.3 MPa (1500 psi) and two-thirds at approximately 4.8 MPa (700 psi). In order to minimize the parasitic syngas compression load, it is highly beneficial to operate the gasifier at the highest pressure practical for a given feed system and gasifier design.

High cold gas efficiency for the gasifier is always a desirable feature since a greater fraction of the chemically bound energy (as heating value) in the coal is conserved as chemically bound energy (as heating value) in the syngas while the syngas temperature leaving the gasifier is lower. Less coal bound energy by-passes the topping cycle resulting in a higher overall plant thermal efficiency while savings in the cost of the heat recovery equipment downstream of the gasifier are realized. Gasifiers with higher cold gas efficiency also have lower specific O<sub>2</sub> demand which in addition to further improving the overall plant thermal performance, reduces the plant cost by requiring a smaller air separation unit.

The CH<sub>4</sub> content of the syngas is typically increased as the temperature of the syngas leaving the gasifier is decreased. This becomes a disadvantage for cycles that utilize pre-combustion carbon capture such as the IGCC. In the case of oxy-combustion cycles, however, which utilize post-combustion carbon capture, high CH<sub>4</sub> content syngas is not a disadvantage at all but actually a benefit since the high CH<sub>4</sub> content is indicative of a high cold gas efficiency.

Thus, the two major desirable attributes for a gasifier suitable for the oxy-combustion cycle consisting of post-combustion capture of carbon (as CO<sub>2</sub>) are:

1. High cold gas efficiency
2. High operating pressure.

In addition to the above, a gasifier that produces a syngas (essentially) free of tars and oils is a very desirable feature. A gasifier projected to be demonstrated and commercially offered by 2015 is the E-STR gasifier which has these attributes. It is a next generation concept for Conoco Phillips, a cylindrical vessel which will accommodate higher pressures among other improvements. Conoco Phillips anticipates 7 to 8.38 MPa (1000 to 1200 psig) operating pressure. Conoco Phillips is still marketing the current “iron cross” or “inverted tee” gasifier as E-Gas but its operating pressure is limited to about 4.9 MPa (715 psia).

Thus, the gasifier recommended for the oxy-combustion cases is the E-STR type gasifier with the higher operating pressure of 8.38 MPa and a slurry feed system which maintains consistency with the gasifiers used in the IGCC cases which are also slurry fed. Syngas compression is included to provide the syngas at the appropriate pressure to the oxy-combustion power cycle.

## RESULTS AND DISCUSSIONS

The performance summaries for both the IGCC and the oxy-combustion cycle cases with gas turbine RIT of 1392°C and not involving SO<sub>2</sub> co-sequestration are presented in Table A2.3-5 while those for the corresponding higher RIT (1734°C) cases are presented in Table A2.3-6. The calculated data show that the oxy-combustion cycle based plants are less efficient than IGCC cases which have the slightly lower CO<sub>2</sub> capture at both firing temperatures studied and with the two heat recovery options used in the IGCC cases.

Table A2.3-7 summarizes the performances for the two SO<sub>2</sub> co-sequestration cases. Both the IGCC and the oxy-combustion cases do benefit but the reduction in heat rate is such that the IGCC continues to maintain a significant efficiency advantage over the oxy-combustion case.

The relative economic worth of capturing additional CO<sub>2</sub> as measured by subtracting the CO<sub>2</sub> emission penalty cost (assumed at \$30/tonne) from the revenue stream associated with the sale of electricity (assumed at \$50/MWhr) at constant coal throughput (3,078 tonne/d of Pittsburgh No. 8 coal) presented graphically in Figures A2.3-5 and A2.3-6 show that there does not appear to be any advantage for the oxy-combustion based cases even with the assumed significantly high penalty of \$30/tonne for CO<sub>2</sub> emission and the assumed low sale price for electricity of \$50/MWhr.

## CONCLUSIONS

- The calculated plant thermal efficiencies show that the efficiency of the oxy-combustion cycle based cases is lower than both the Total Quench Heat Recovery option and the Radiant Syngas Cooler Plus Quench Heat Recovery option IGCC cases with the slightly lower CO<sub>2</sub> capture.
- Unless there is a substantial reduction in the cost for the oxy-combustion based plant which appears to be unlikely due to its significantly higher O<sub>2</sub> consumption, the oxy-

combustion based cycle in coal gasification plants appears to show no efficiency nor economic advantage over the IGCC.

- Other inferences that may be drawn from these results are:
  - The Radiant Syngas Cooler Plus Quench Heat Recovery option IGCC is more efficient than the Total Quench Heat Recovery option IGCC even in applications where CO<sub>2</sub> capture is required. The total plant cost, however, for the IGCCs with the radiant syngas coolers will be significantly higher.
  - For the above set of assumptions with respect to CO<sub>2</sub> emission penalty and sale price of electricity, the “optimum” CO<sub>2</sub> capture for the Total Quench Heat Recovery option IGCC is about 90% while that for the Radiant Syngas Cooler Plus Quench Heat Recovery option IGCC is less than 80%.

## REFERENCES

1. Ciferno, J. and R. Newby, “Carbon Sequestration Systems Analysis,” DOE NETL Technical Note No. 10, Revised March 2007.
2. Klara, J. M. et. al., “Cost and Performance Baseline for Fossil Energy Plants,” Volume 1: Bituminous Coal and Natural Gas to Electricity, DOE/NETL Final Report -2007/1281, Revision 1, August 2007.
3. Rao, A. D., A. Verma and D. H. Cortez, Optimization of the Shift Conversion Unit in a gasification Plant,” presented at the Gasification Technologies Council conference, Washington, DC, October 1-4, 2006.
4. Rigdon, R, “Gasification Operational Success & Growth in China,” presented at the Gasification Technologies Council Conference, October 15, 2007.

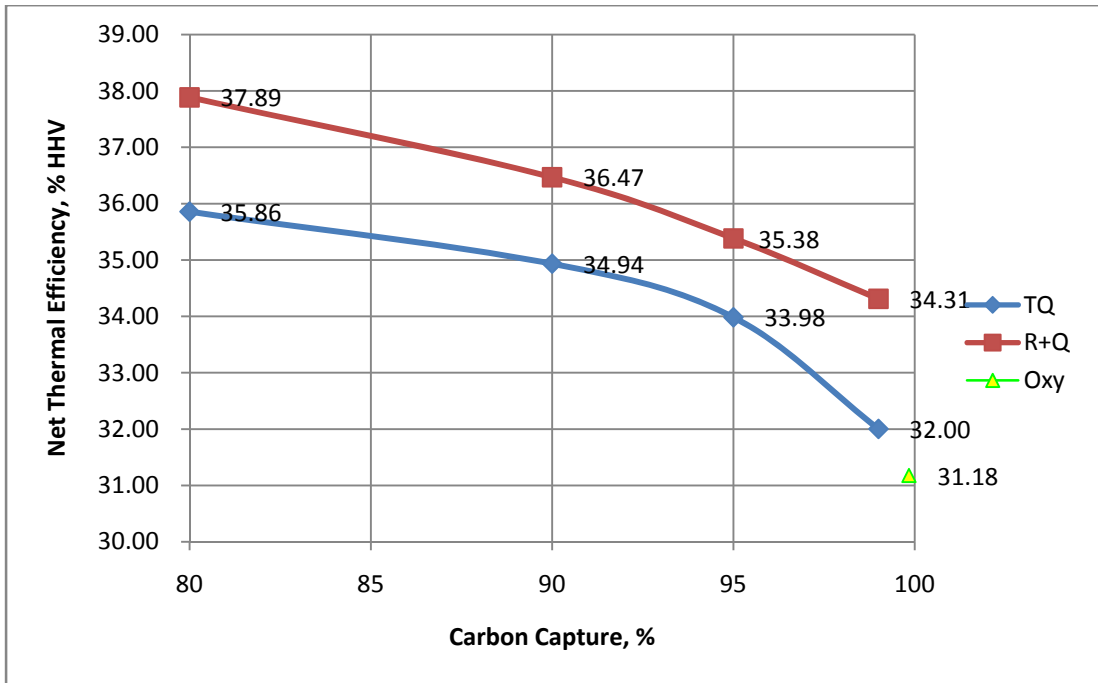


Figure A2.3- 1: Thermal Performance – H Class (1392°C RIT) GT Cases

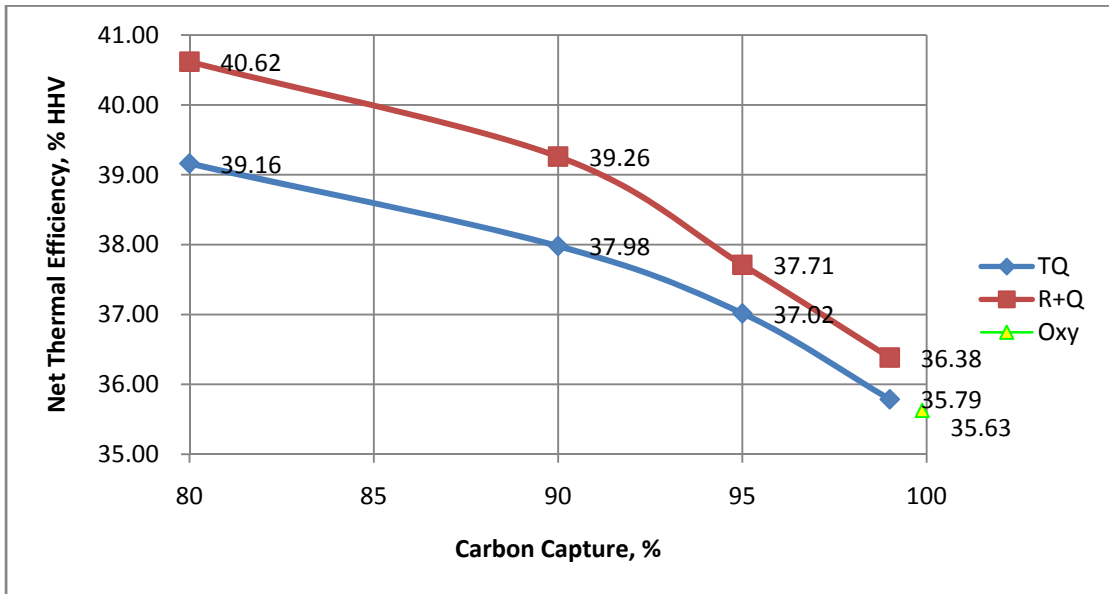


Figure A2.3- 2: Thermal Performance – Advanced (1734°C RIT) GT Cases

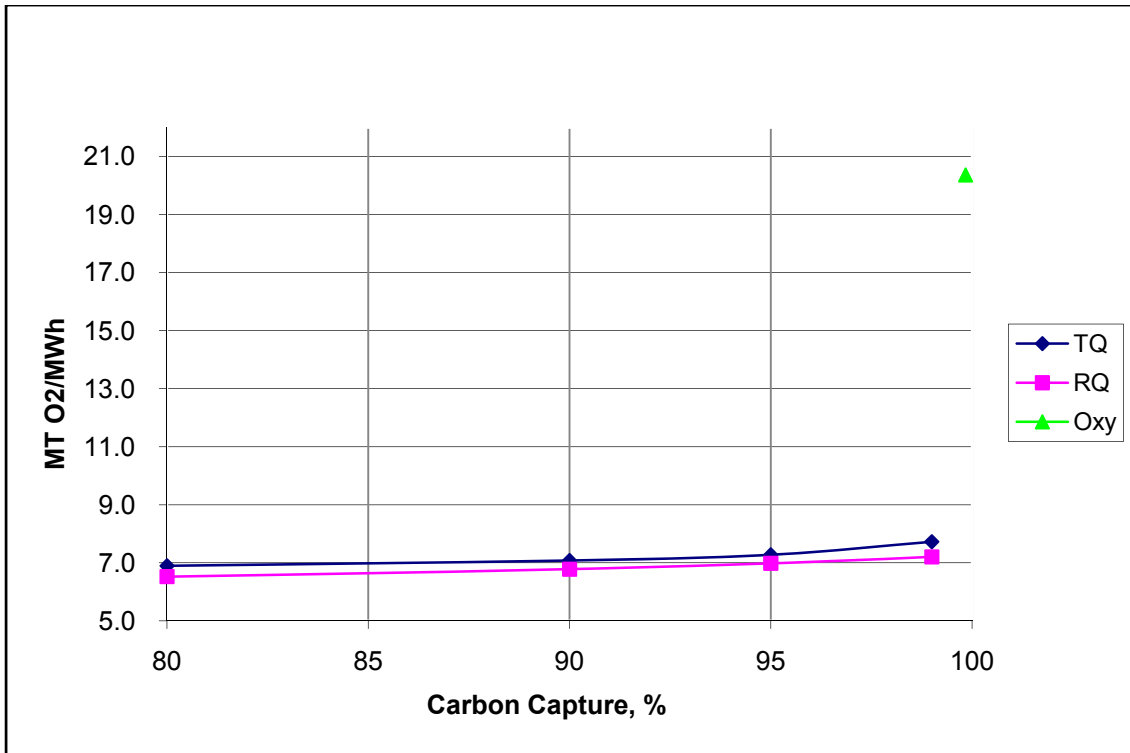


Figure A2.3- 3: Specific O<sub>2</sub> Consumption – H Class (1392°C RIT) GT Cases

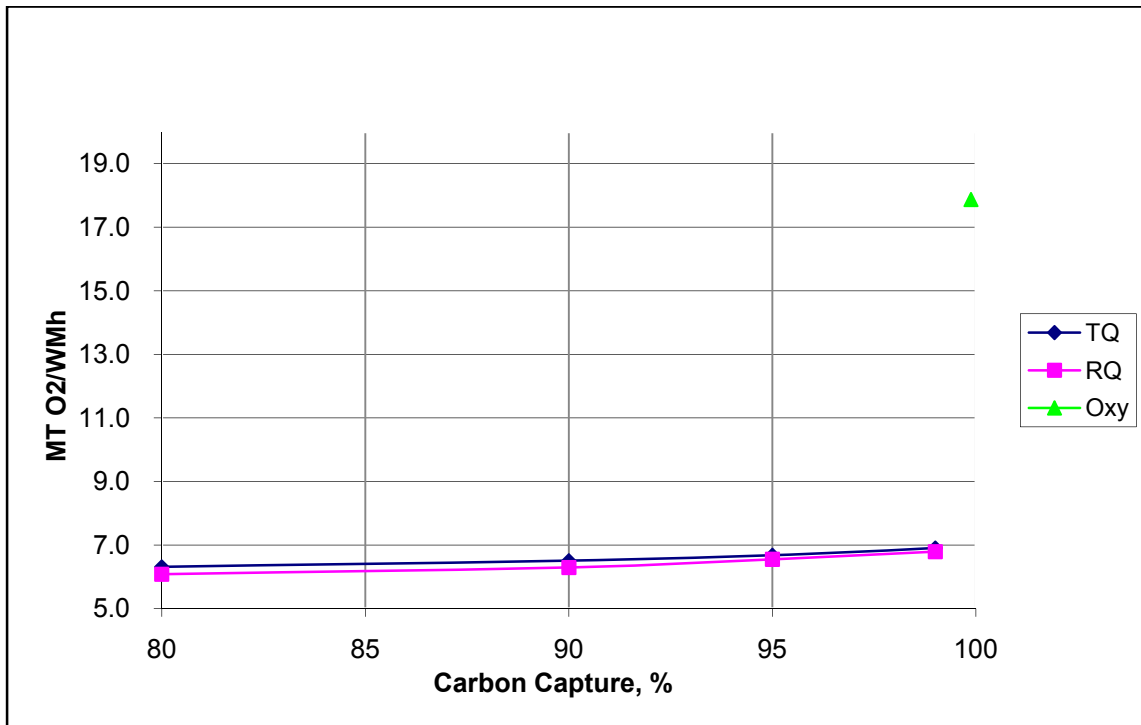


Figure A2.3- 4: Specific O<sub>2</sub> Consumption – Advanced (1734°C RIT) GT Cases

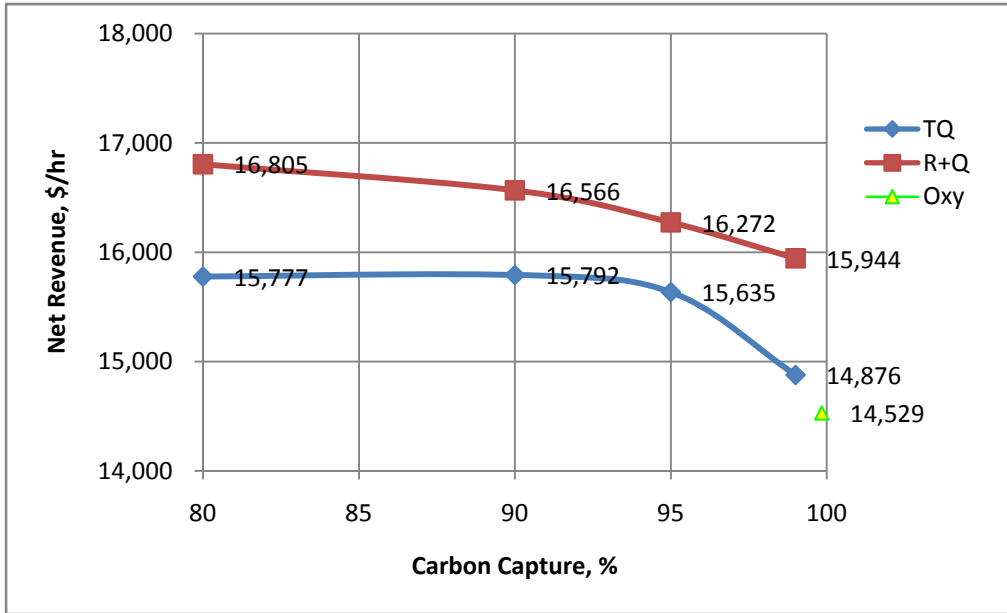


Figure A2.3- 5: Economic Worth of Additional CO<sub>2</sub> Capture – H Class (1392°C RIT) GT Cases

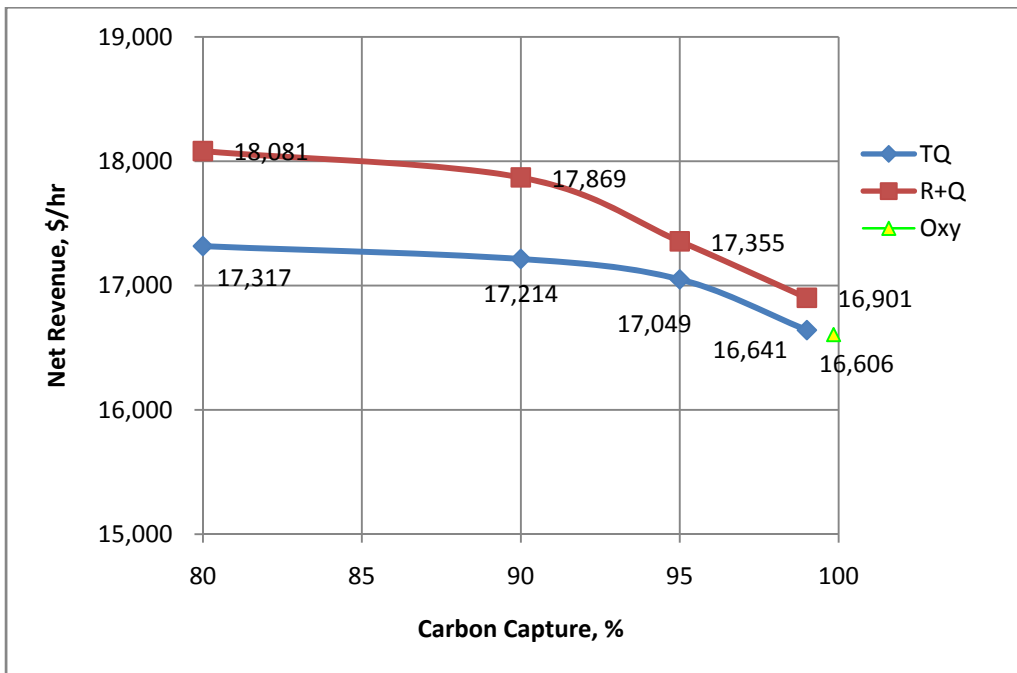


Figure A2.3- 6: Economic Worth of Additional CO<sub>2</sub> Capture – Advanced (1734°C RIT) GT Cases

**Table A2.3- 1: CO<sub>2</sub> Composition / Conditions<sup>20</sup>**

	<b>Design Condition 1</b>	<b>Design Condition 2</b>	<b>Design Condition 3</b>	<b>Design Condition 4</b>
	<b>Remote EOR</b>	<b>Adjacent EOR</b>	<b>Remote Geological</b>	<b>Adjacent Geological</b>
<b>Pipeline material</b>	carbon steel	carbon steel	carbon steel	304/316 SS
<b>Compression pressure (psia)</b>	2200	1600	2200	1600
<b>CO<sub>2</sub></b>	>95 vol%	>95 vol%	not limited <sup>a</sup>	not limited <sup>a</sup>
<b>Water</b>	dehydration <sup>b</sup> (0.015 vol%)	dehydration <sup>b</sup> (0.015 vol%)	dehydration <sup>b</sup> (0.015 vol%)	no dehydration <sup>c</sup> no free water
<b>N<sub>2</sub></b>	<4 vol%	<4 vol%	not limited <sup>1</sup>	not limited <sup>a</sup>
<b>O<sub>2</sub></b>	<40 ppmv	<40 ppmv	<100 ppmv	<100 ppmv
<b>Ar</b>	< 10 ppmv	< 10 ppmv	not limited	not limited
<b>NH<sub>3</sub></b>	<10 ppmv	<10 ppmv	not limited	not limited
<b>CO</b>	< 10 ppmv	< 10 ppmv	not limited	not limited
<b>Hydrocarbons</b>	<5 vol%	<5 vol%	<5 vol%	<5 vol%
<b>H<sub>2</sub>S</b>	<1.3 vol%	<1.3 vol%	<1.3 vol%	<75 vol%
<b>CH<sub>4</sub></b>	<0.8 vol%	<0.8 vol%	<0.8 vol%	<4.0 vol%
<b>H<sub>2</sub></b>	uncertain	uncertain	uncertain	uncertain
<b>SO<sub>2</sub></b>	<40 ppmv	<40 ppmv	<3 vol%	<3 vol%
<b>NO<sub>x</sub></b>	uncertain	uncertain	uncertain	uncertain

- a. These are not limited, but their impacts on compression power and equipment cost need to be considered.  
 b. Dehydration process, such as a glycol absorber, is required.  
 c. Dehydration process is not required, but no free water must occur in the gas

<sup>20</sup> J. Ciferno and R. Newby, 2007

**Table A2.3- 2: Case Matrix**

(yes = to be evaluated)

	IGCC Cases				Oxy-combustion Cases	
Gasifier	GE Type with Radiant Syngas Cooler + Water Quench (R+Q)		GE Type with Water Quench Only (TQ)		CoP E-STR Type	
Gas Turbine RIT (°C)	1392	1734	1392	1734	1392	1734
Gasifier Pressure, MPa	5.62	5.62	7.26	7.67	8.38	8.38
99%+ Carbon Capture	yes	yes	yes	yes	yes	yes
95% Carbon Capture	yes	yes	yes	yes		
90% Carbon Capture	yes	yes	yes	yes		
80% Carbon Capture	yes	yes	yes	yes		
Co-sequestration of Sulfur Compounds			yes (at 90% Carbon Capture)		yes (at 99%+ Carbon Capture)	

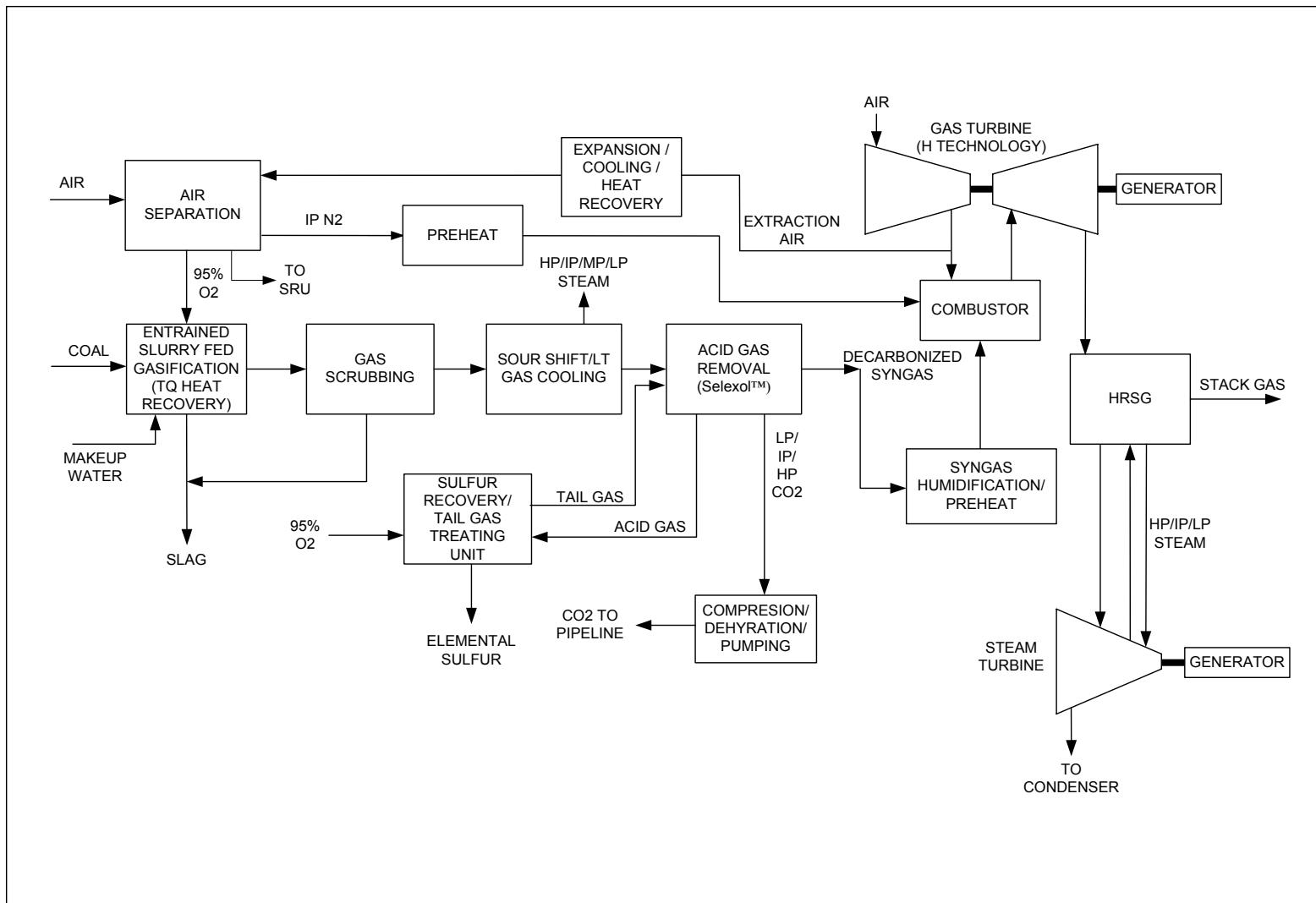


Figure A2.3- 7: Block Flow Diagram - TQ IGCC Cases with 80% and 90% CO<sub>2</sub> Capture, GT RIT = 1392°C

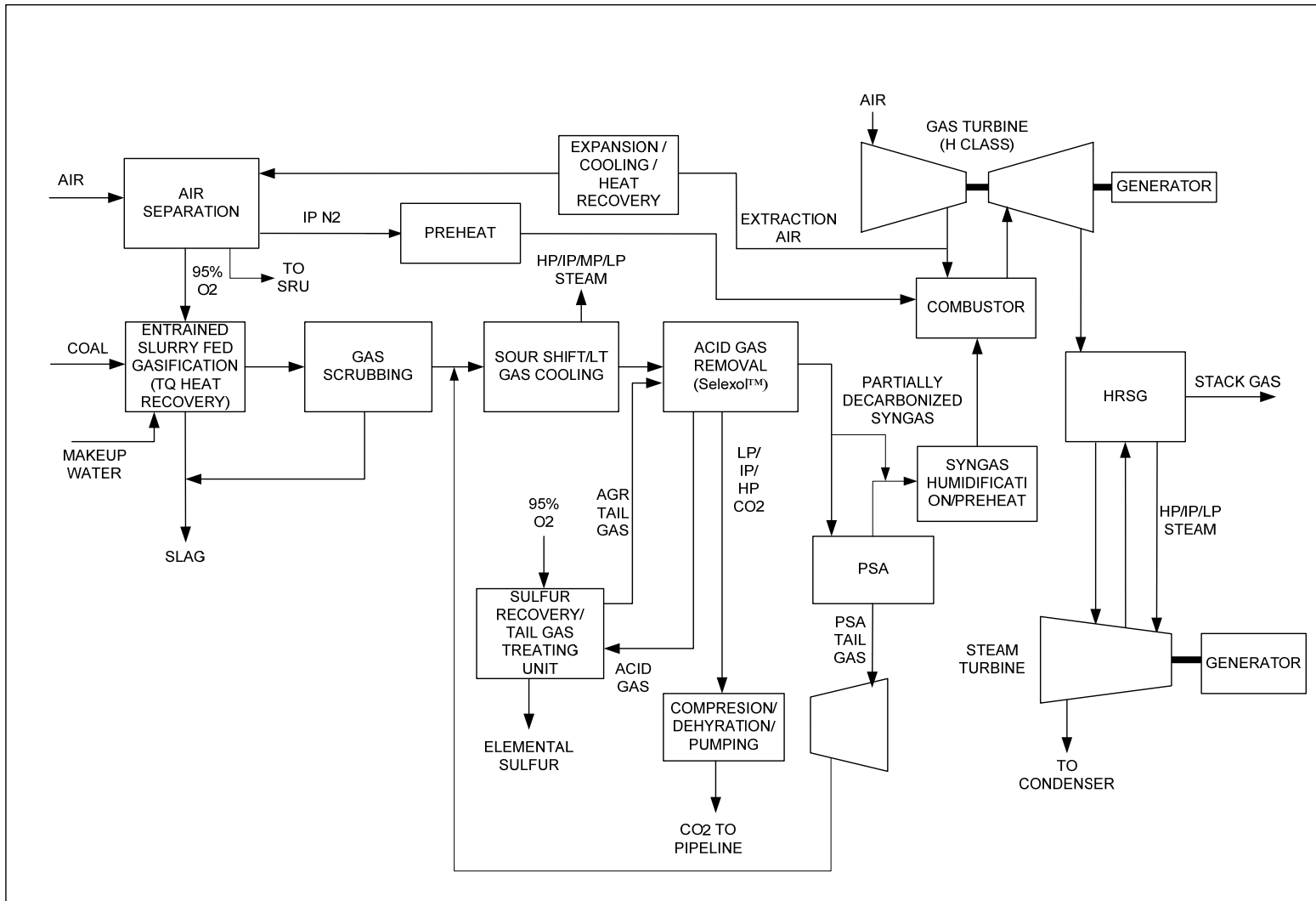


Figure A2.3- 8: Block Flow Diagram - TQ IGCC Cases with 90% and 99%+ CO<sub>2</sub> Capture, GT RIT = 1392°C

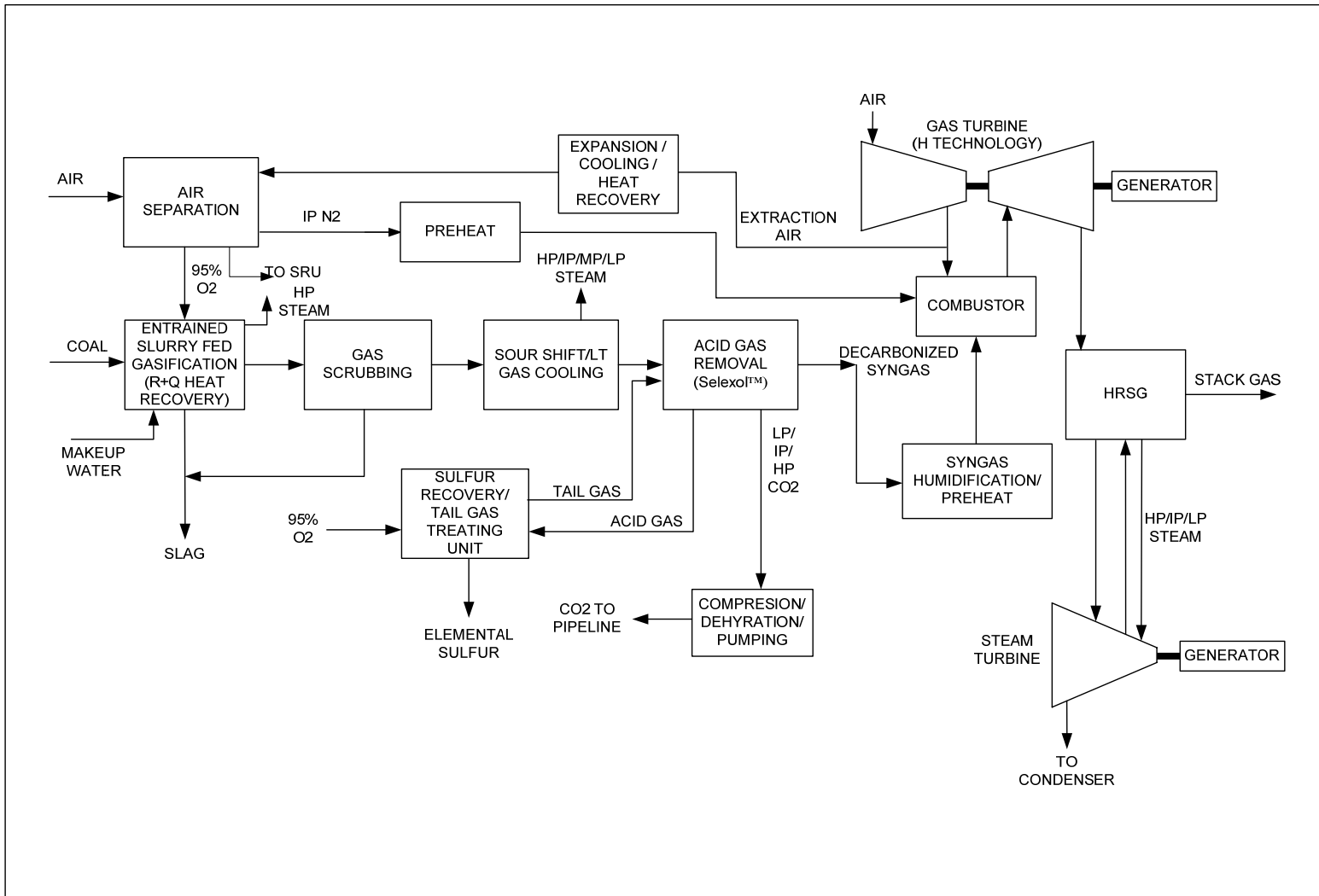


Figure A2.3- 9: Block Flow Diagram – R+Q IGCC Cases with 80% and 90% CO<sub>2</sub> Capture, GT RIT = 1392°C

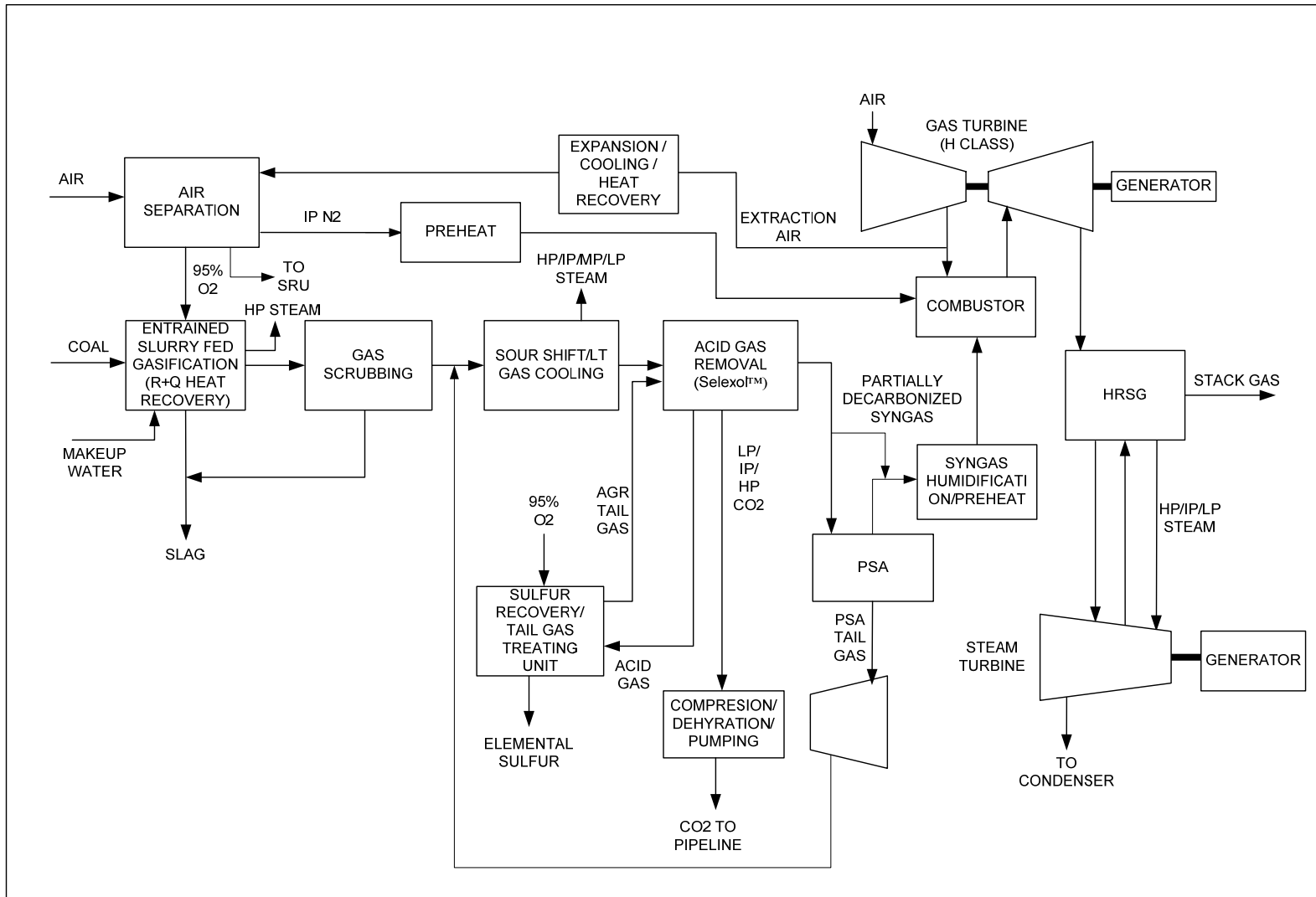


Figure A2.3- 10: Block Flow Diagram – R+Q IGCC Cases with 90% and 99%+ CO<sub>2</sub> Capture, GT RIT = 1392°C

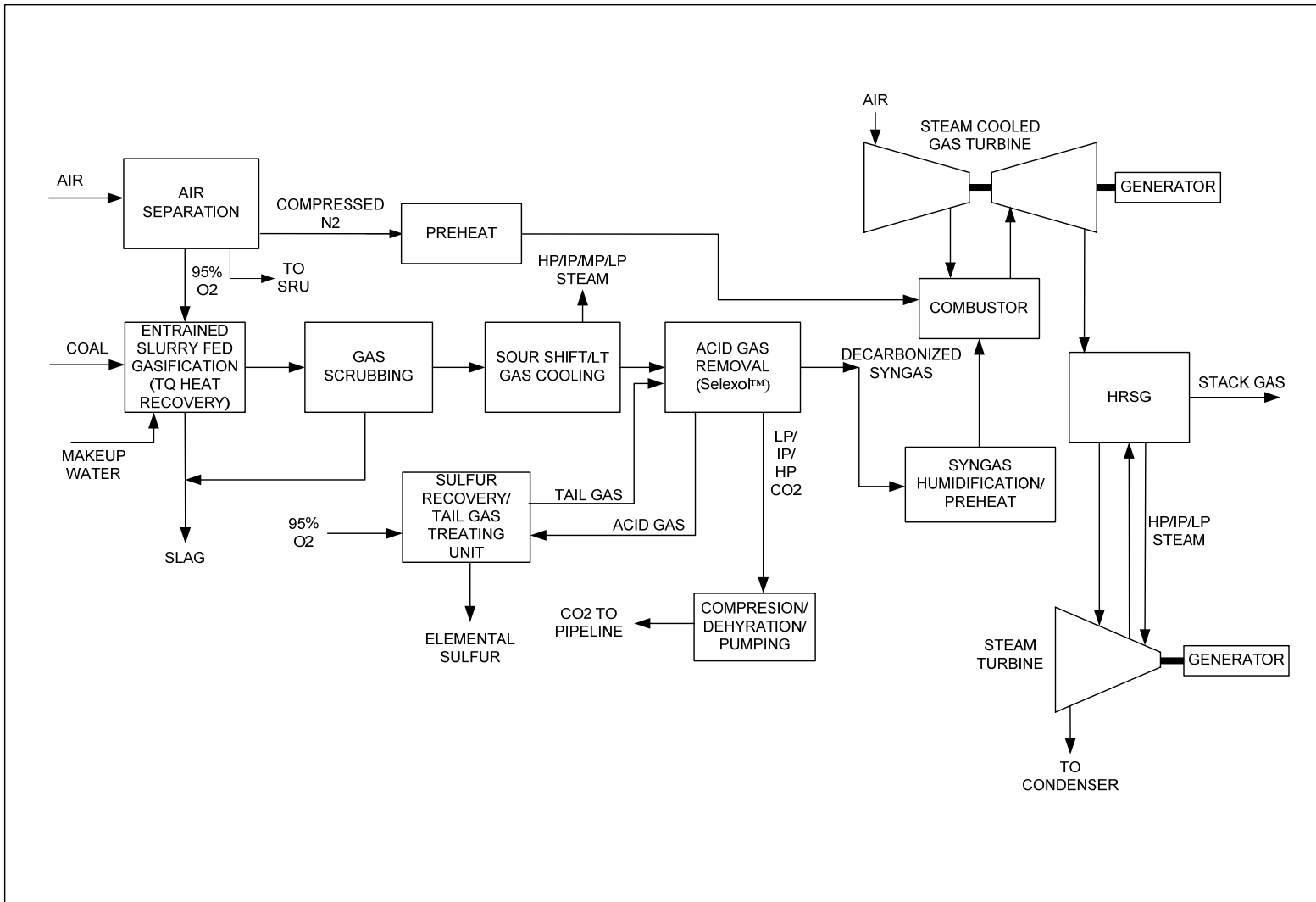


Figure A2.3- 11: Block Flow Diagram - TQ IGCC Cases with 80% and 90% CO<sub>2</sub> Capture, GT RIT = 1734°C

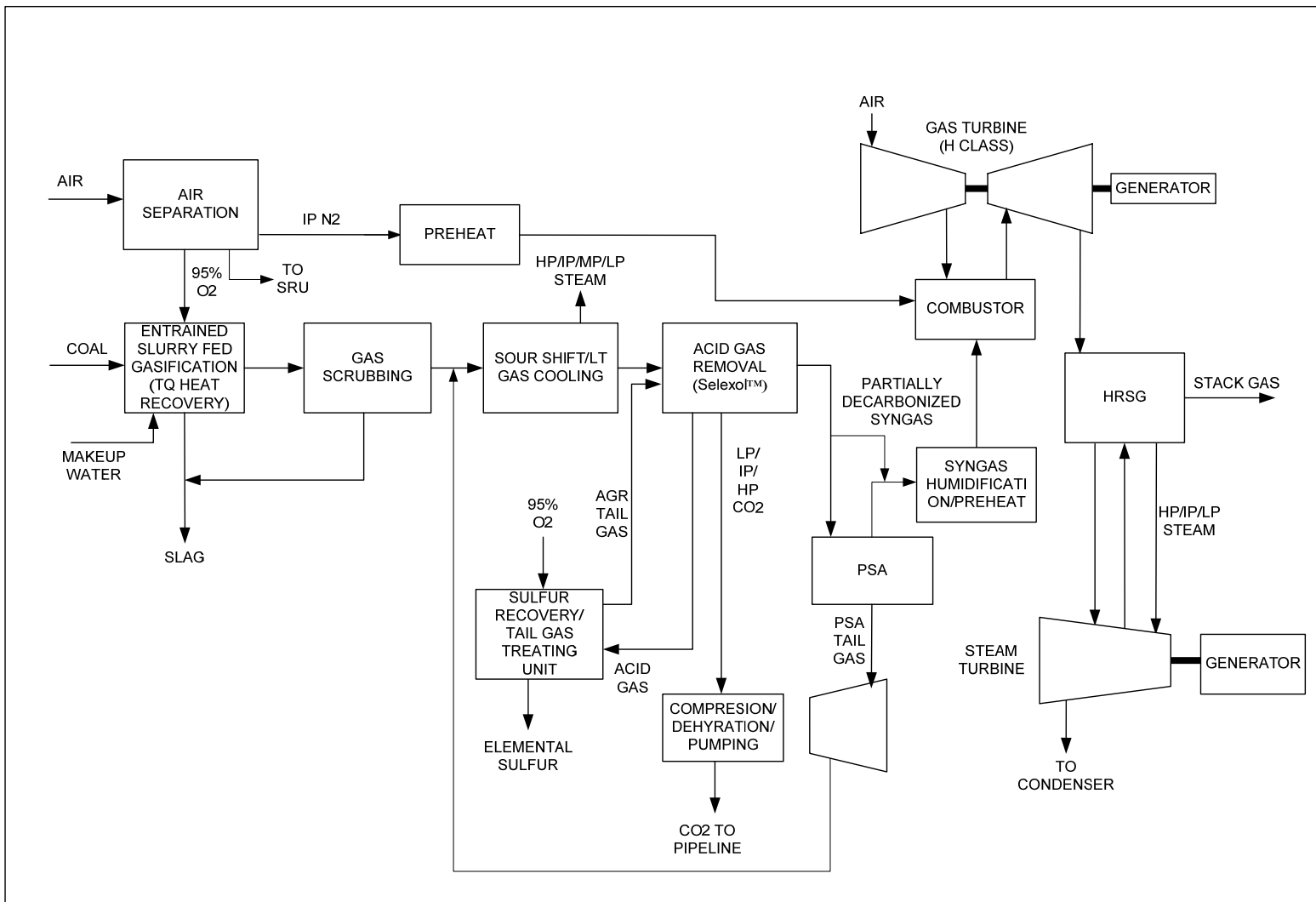


Figure A2.3- 12: Block Flow Diagram - TQ IGCC Cases with 90% and 99%+ CO<sub>2</sub> Capture, GT RIT = 1734°C

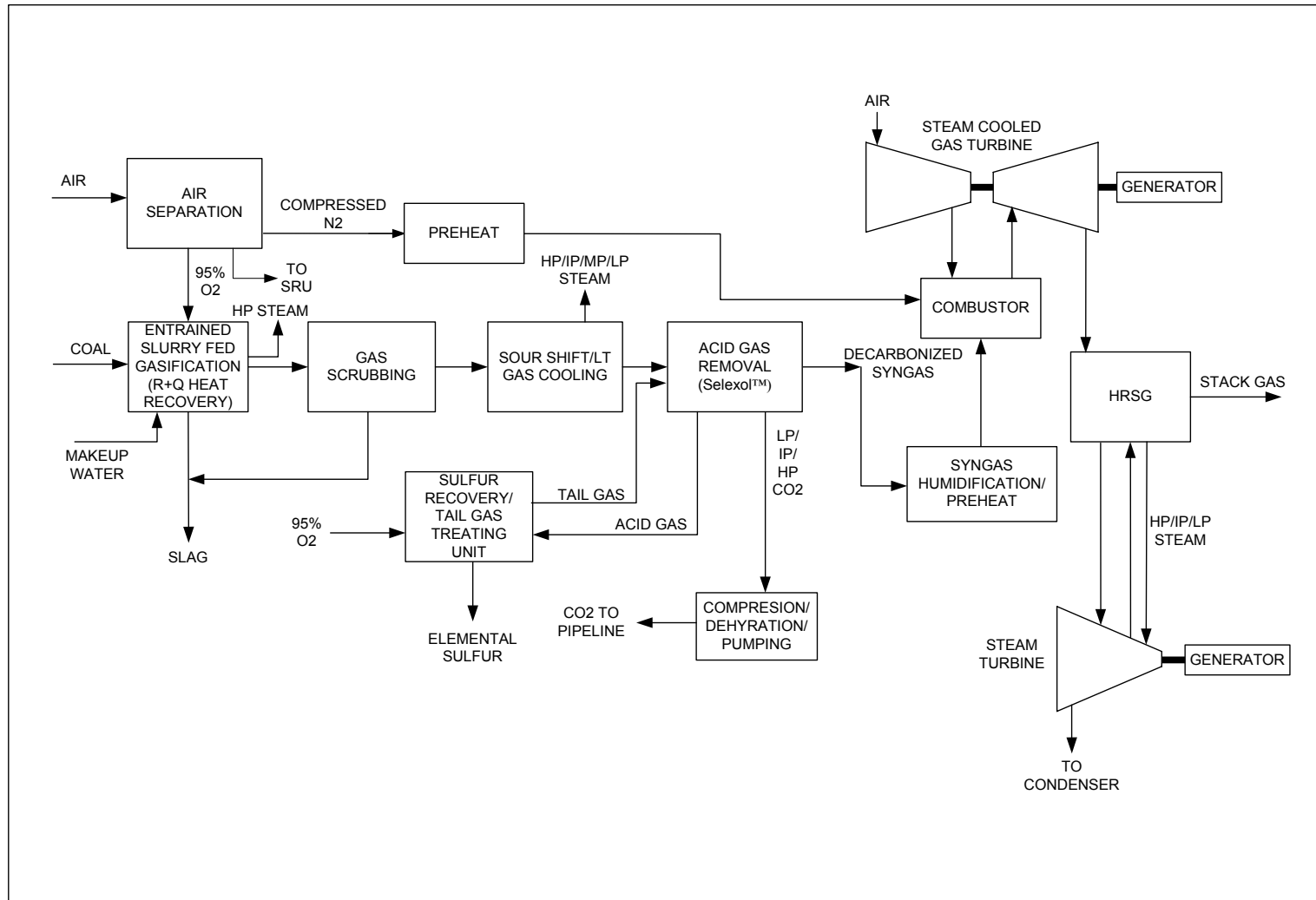


Figure A2.3- 13: Block Flow Diagram – R+Q IGCC Cases with 80% and 90% CO<sub>2</sub> Capture, GT RIT = 1734°C

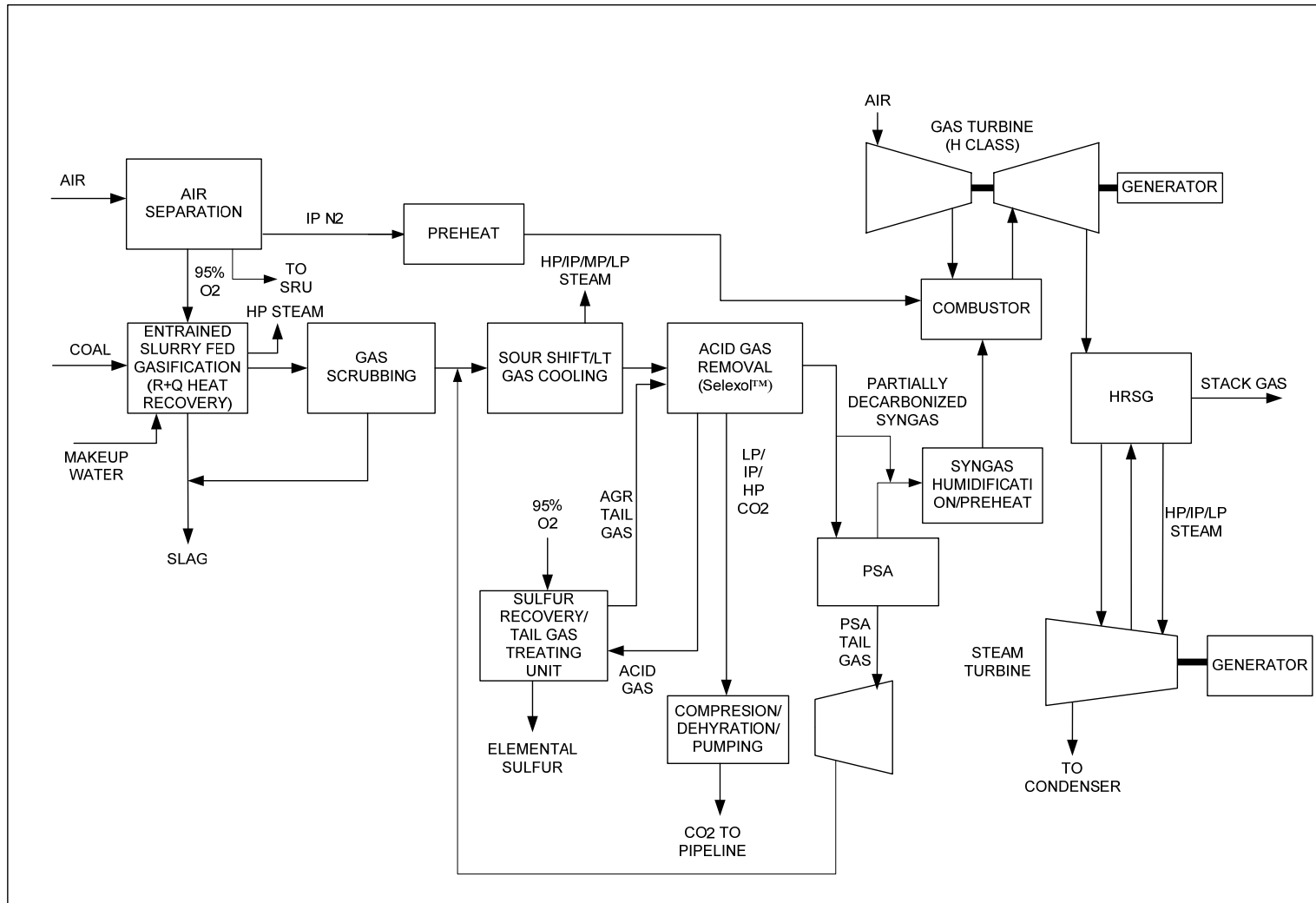


Figure A2.3- 14: Block Flow Diagram – R+Q IGCC Cases with 90% and 99%+ CO<sub>2</sub> Capture, GT RIT = 1734°C

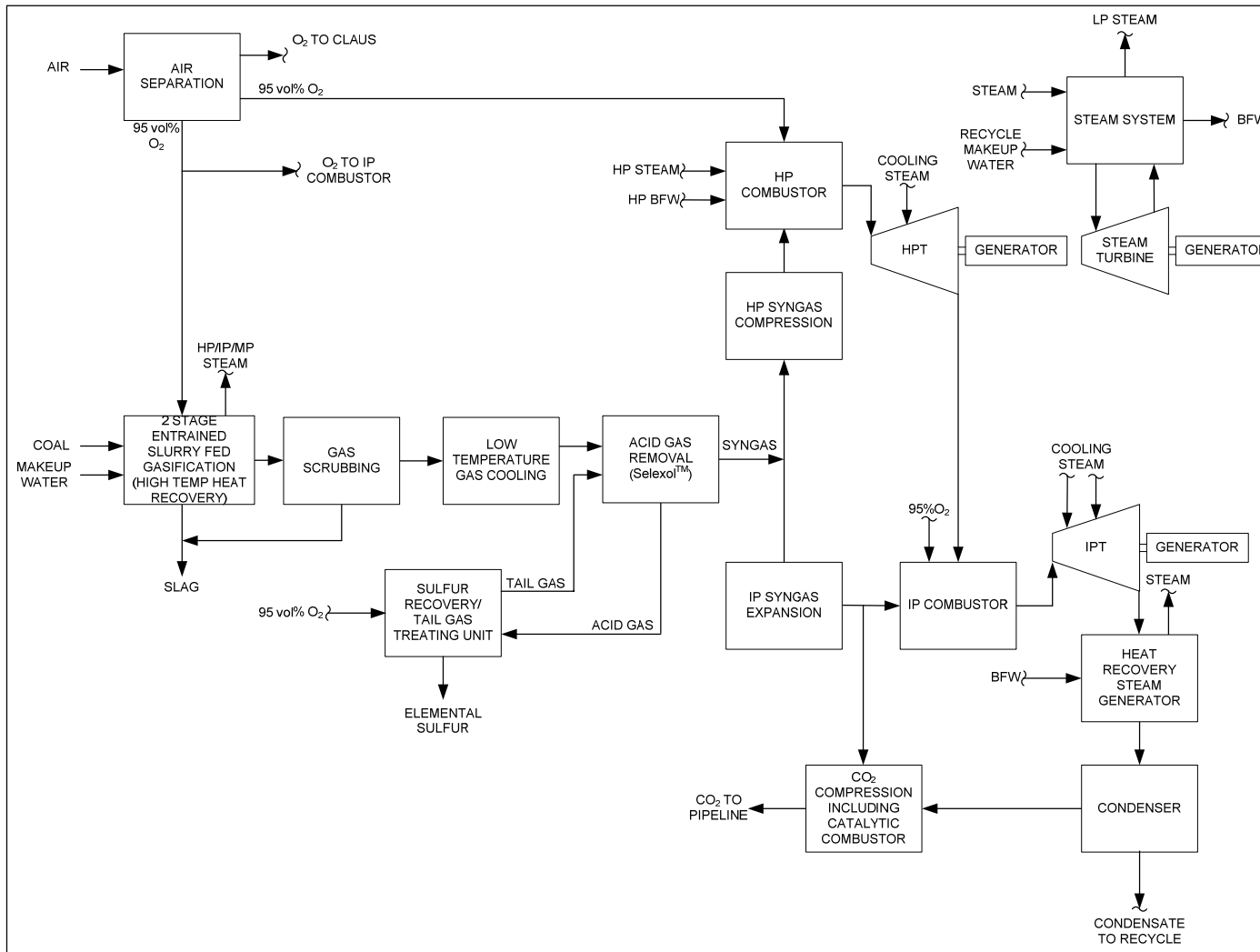


Figure A2.3- 15: Block Flow Diagram - Oxy-combustion Cycle based Cases

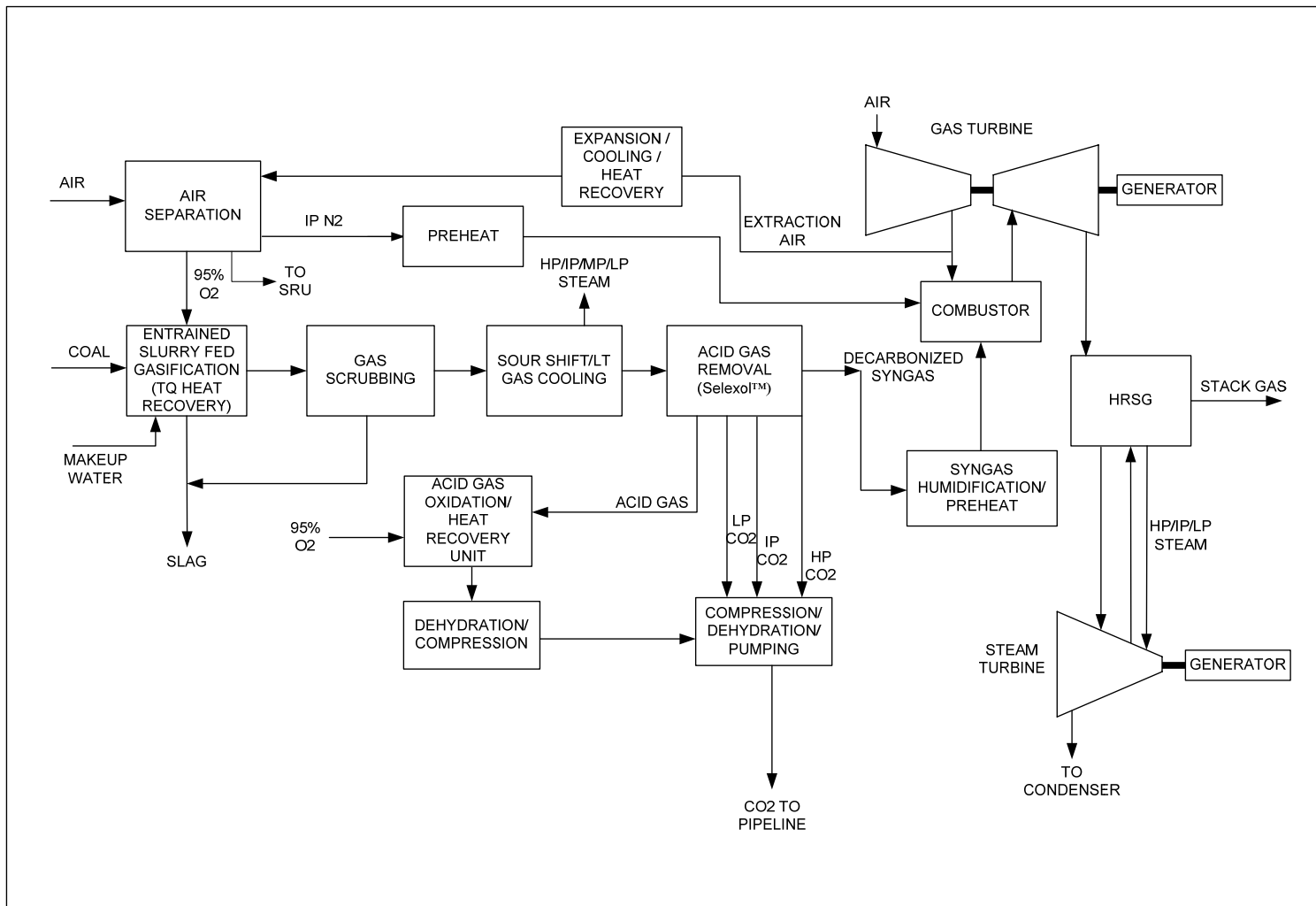


Figure A2.3- 16: Block Flow Diagram - TQ IGCC SO<sub>2</sub> Co-sequestration Case with 90% CO<sub>2</sub> Capture, GT RIT = 1392°C

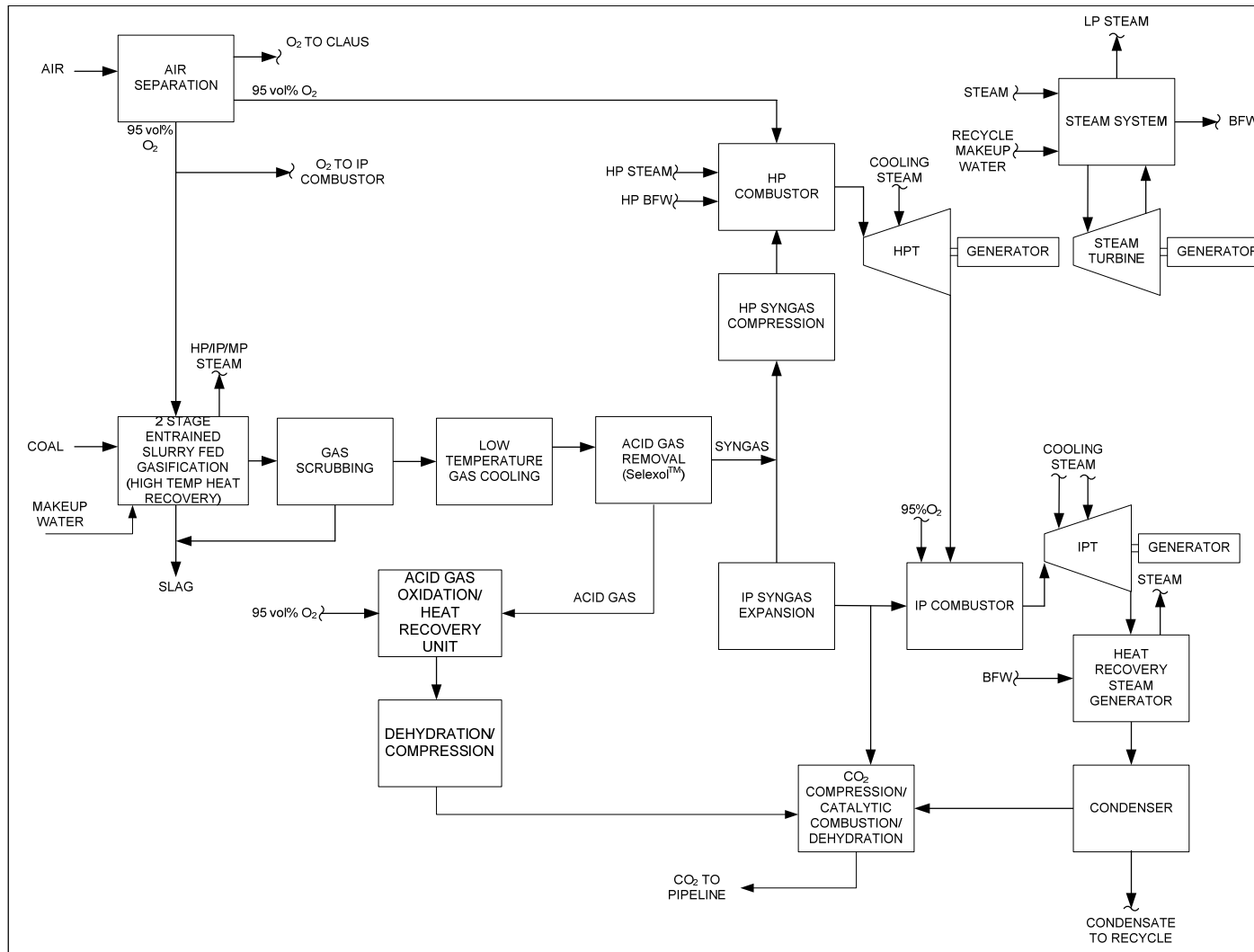


Figure A2.3- 17: Block Flow Diagram - Oxy-combustion Cycle based SO<sub>2</sub> Co-sequestration Case, GT RIT = 1392°C

**Table A2.3- 3: Shift Reactors in IGCC Cases with Total Quench Heat Recovery**

<b>Degree of Carbon Capture</b>	<b>Sour Shift Reactors in Series</b>	<b>Comments</b>
<b>80%</b>	1 High Temperature Reactor	92% capture of the CO <sub>2</sub> entering the Selexol™ unit is required which is achievable with Selexol™ without severely increasing utility consumptions and equipment sizes.
<b>90%</b>	2 High Temperature Reactors	92% capture of the CO <sub>2</sub> entering the Selexol™ unit is required which is achievable with Selexol™ without severely increasing utility consumptions and equipment sizes.
<b>95%</b>	2 Low Temperature Reactors	In addition to the low temperature shift reactors, a PSA with tail gas recycle is required.
<b>99%+</b>	2 Low Temperature Reactors	In addition to the low temperature shift reactors, a PSA with tail gas recycle is required.

**Table A2.3- 4: Shift Reactors in IGCC Cases with Radiant Quench Heat Recovery**

<b>Degree of Carbon Capture</b>	<b>Sour Shift Reactors in Series</b>	<b>Comments</b>
<b>80%</b>	2 Low Temperature Reactors with 32% By-pass around 1 <sup>st</sup> Reactor <sup>21</sup>	Reduces amount of steam injection required. 95% capture of the CO <sub>2</sub> entering the Selexol™ unit is required which is achievable with Selexol™ without severely increasing utility consumptions and equipment sizes.
<b>90%</b>	2 Low Temperature Reactors	If both low temperature shift reactors are not used, 95% carbon capture may not be possible even if 100% of the incoming CO <sub>2</sub> is separated in the Selexol™ unit. About 95% capture of the CO <sub>2</sub> entering the Selexol™ unit is required which is achievable with Selexol™ without severely increasing utility consumptions and equipment sizes.
<b>95%</b>	2 Low Temperature Reactors	In addition to the low temperature shift reactors and steam injection into the syngas upstream of the shift reactors, a PSA with tail gas recycle is required.
<b>99%+</b>	2 Low Temperature Reactors	In addition to the low temperature shift reactors and steam injection into the syngas upstream of the shift reactors, a PSA with tail gas recycle is required.

<sup>21</sup> The bypass around the 1<sup>st</sup> reactor reduces the required amount of steam injection (Rao, Verma and Cortez, 2006).

**Table A2.3- 5: Overall Plant Performance Summaries - GT RIT = 1392°C**

Gasifier Heat Recovery	TQ				R+Q				Oxy
	80	90	95	99	80	90	95	99	99.8
Carbon Capture, %									
Fuel Feed Rate, ST/D (MF)	3,392	3,392	3,392	3,392	3,392	3,392	3,392	3,392	3,392
MMBtu/hr (HHV)	3,744	3,744	3,744	3,744	3,744	3,744	3,744	3,744	3,744
Fuel Feed Rate, MT/D (MF)	3,078	3,078	3,078	3,078	3,078	3,078	3,078	3,078	3,078
GJ/hr (HHV)	3,949	3,949	3,949	3,949	3,949	3,949	3,949	3,949	3,949
Power Generation, kWe									
Gas Turbine	325,999	318,378	316,807	312,953	325,788	319,676	316,846	311,932	504,794
Steam Turbine	162,431	157,600	151,492	141,754	184,792	176,164	173,304	172,913	8,834
Clean Syngas Expander	2,348	2,320	2,303	2,264	1,107	1,112	1,228	1,364	1,246
Gas Turbine Extraction Air Expander	4,745	4,745	4,739	4,515	5,305	4,819	4,744	4,704	-
Auxiliary Power Consumption, kWe	102,141	99,795	102,535	110,412	101,356	101,682	107,949	114,507	172,856
Net Plant Output, kWe	393,382	383,247	372,806	351,074	415,636	400,088	388,174	376,405	342,019
Generation Efficiency (HHV)									
Net Heat Rate, Btu/kWh	9,518	9,769	10,043	10,665	9,008	9,358	9,645	9,947	10,947
Net Heat Rate, kJ/kWh	10,039	10,305	10,593	11,249	9,502	9,871	10,174	10,492	11,547
% Fuel to Power	35.86	34.94	33.98	32.00	37.89	36.47	35.38	34.31	31.18

**Table A2.3- 6: Overall Plant Performance Summaries - GT RIT = 1734°C**

Gasifier Heat Recovery	TQ				R+Q				Oxy
	80	90	95	99	80	90	95	99	99.9
Carbon Capture, %									
Fuel Feed Rate, ST/D (MF)	3,392	3,392	3,392	3,392	3,392	3,392	3,392	3,392	3,392
MMBtu/hr (HHV)	3,744	3,744	3,744	3,744	3,744	3,744	3,744	3,744	3,744
Fuel Feed Rate, MT/D (MF)	3,078	3,078	3,078	3,078	3,078	3,078	3,078	3,078	3,078
GJ/hr (HHV)	3,949	3,949	3,949	3,949	3,949	3,949	3,949	3,949	3,949
Power Generation, kWe									
Gas Turbine	419,467	414,531	412,311	408,733	419,659	414,683	412,230	408,057	564,846
Steam Turbine	139,994	129,254	124,447	121,667	162,248	150,023	142,278	136,545	13,806
Clean Syngas Expander	0	-	0	0	0	0	0	0	1,536
Gas Turbine Extraction Air Expander	0	-	-	-	0	0	0	0	-
Auxiliary Power Consumption, kWe	129,845	127,121	130,667	137,799	136,302	134,006	140,800	145,452	189,341
Net Plant Output, kWe	429,616	416,665	406,090	392,601	445,605	430,700	413,709	399,150	390,846
Generation Efficiency (HHV)									
Net Heat Rate, Btu/kWh	8,715	8,986	9,220	9,537	8,402	8,693	9,050	9,380	9,579
Net Heat Rate, kJ/kWh	9,193	9,478	9,725	10,059	8,863	9,169	9,546	9,894	10,104
% Fuel to Power	39.16	37.98	37.02	35.79	40.62	39.26	37.71	36.38	35.63

**Table A2.3- 7: Overall Plant Performance Summaries - SO<sub>2</sub> Co-sequestration - GT  
RIT = 1392°C**

	<b>IGCC</b>	<b>Oxy</b>
Carbon Capture, %	90	99.8
Fuel Feed Rate, ST/D (MF)	3,392	3,392
MMBtu/hr (HHV)	3,744	3,744
Fuel Feed Rate, MT/D (MF)	3,078	3,078
GJ/hr (HHV)	3,949	3,949
Power Generation, kWe		
Gas Turbine	315,437	506,607
Steam Turbine	163,024	10,183
Clean Syngas Expander	2,314	1,209
Gas Turbine Extraction Air Expander	4,710	-
Auxiliary Power Consumption, kWe	99,533	170,743
Net Plant Output, kWe	385,951	347,257
Generation Efficiency (HHV)		
Net Heat Rate, Btu/kWh	9,701	10,782
Net Heat Rate, kJ/kWh	10,233	11,373
% Fuel to Power	35.18	31.65